The influence of macrofauna on intertidal sediment stability and biogeochemical properties.

Rachel Hale

A thesis submitted in partial fulfilment of the requirements for the degree of Doctor of Philosophy to the School of Environmental Sciences,

University of East Anglia

November 2013

Abstract

Macrofauna are known to have a significant effect on intertidal sediment stability and biogeochemical properties. A series of manipulative *in situ* mudflat studies at Breydon Water, Great Yarmouth, UK investigated the effect of biodiversity on selected biogeochemical sedimentary properties related to mudflat sediment stability including the sediment erosion threshold and relative erosion rate, microphytobenthos biomass and health, sediment particle size and size distribution, sediment water content, chlorophyll *a* and *b* concentration, and colloidal carbohydrate concentration. Mudflat sediment macrofaunal biomass was removed using cryo-defaunation and the abundances of three common mudflat species *Hediste diversicolor*, *Hydrobia ulvae* and *Corophium volutator* manipulated to examine different aspects of macrofaunal biodiversity including species identity, density, biomass distribution, and richness. An additional laboratory study enabled two and three dimensional high resolution visualisation of fluid and particle mixing as a result of organism sediment bioturbation.

Species identity was found to have a significant effect on sediment properties. The three species have distinct bioturbatory actions with consequences for sediment stability. In some circumstances a single organism was found to have as great an effect on selected ecosystem processes as a whole community. Variations in species density significantly changed the effect of the species on the measured sedimentary processes. Species richness effects were negatively interactive, with species mixtures underyielding in comparison to their monoculture counterparts. Changes in species biomass distribution and richness resulted in significant context dependent changes to sediment properties, moderated by inter- and intra-specific interactions. Species were also observed to exhibit a functional abundance threshold, below which they did not contribute significantly to ecosystem processes. Temporal and spatial variability observed in the experiments emphasised the potential of environmental and abiotic factors to also influence ecosystem processes. Investigating these subtle aspects of biodiversity will be key in the determination of the relationship between biodiversity and ecosystem processes.

List of Contents

List of Tables

List of Illustrations

Acknowledgements

Supervisors

Thank you to Trevor Tolhurst for help with all things fieldwork, labwork and writing. Thanks to Alastair Grant for comments on the draft.

At UEA

Thank you to Andy MacDonald, Stephen Humphries, Paul Disdle, John Brindle, Jenny Stevenson all without whom this thesis would not have been possible. Special thanks to Judith Mayne for her constant patience and help in the lab.

In Southampton

Thank you to Martin Solan and Jasmin Godbold at the National Oceanography Centre for trusting me with their laboratory and equipment and their help with statistics and R. Thank you to Ashleigh Currie and Carmen B de los Santos for their help with the experimental setup. Thank you to Mark Mavrogordato, Richard Boardman and Ian Sinclair at μ-VIS at the University of Southampton for allowing me to take my sloppy mud into their extremely expensive computed tomography suite and allowing me to monopolise all their computing equipment.

Field helpers

Thanks to my fieldwork volunteers including Melanie Froude, Amy Vigrass, James Booty, Joey Innes-Hopkins and Kat Bruce.

Special wet and muddy thanks to Richard Jacques and Susan Hale, who didn't volunteer - attendance was compulsory, for enduring repeated visits to the mud come rain or shine.

Thanks to Anne Gallagher, Ben Locke and others in the BBC Autumnwatch crew for selecting a video of a 3D Hediste burrow reconstruction to be shown on Autumnwatch Extra.

Thanks to the rowing team and my friends for providing ample distractions from actually working. Thanks to Peter Hale for always providing 'constructive criticism' and providing funding when the official funding ran out.

Conference Funding

Thanks to the European Sciences fund for allowing me the opportunity to attend and to present my work at 'The effects of climate change on vulnerable life traits of aquatic ectotherms: towards an integrated approach' workshop at the Alfred Wegener Institute, Bremerhaven, Germany, 18th - 21st September 2011. Thanks to the Gordon and Betty Moore Foundation for allowing me to attend and to present my work at the 'Third Symposium on the Ocean in a High-CO_2 World' in Monterey, California, 24th - 27th September 2012. Thanks to the University of East Anglia for giving me the opportunities to attend and present my work at the 'World Conference on Marine Biodiversity', in Aberdeen, Scotland, 26th - 30th September 2011, the '15th Biennial Challenger Conference for Marine Sciences' at UEA, 3rd - 6th September 2012, and the chance to attend the '2014 Ocean Sciences Meeting' in Honolulu, Hawaii, 23rd - 28th February 2014.

Abbreviations

AIC	Akaike Information Criteria
$\triangle[Br^-]$	Change in bromide concentration
$Carb_{CC}$	Contact core sediment carbohydrate concentration (μgcm^{-3})
Chl a_{CC}	Contact core sediment chlorophyll *a* concentration (μgcm^{-3})
CSM	Cohesive Strength Meter
$^{CT}B_{max}$	X-CT calculated maximum burrow depth (cm)
$^{CT}B_{SA}$	X-CT calculated burrow surface area (cm^2)
$^{CT}B_{Vol}$	X-CT calculated burrow volume (cm^3)
CV	*Corophium volutator*
D_{10}	Particle size below which 10 % of the sample volume exists (µm)
D_{10CC}	Contact core sediment D_{10} (µm)
D_{10MC}	Minicore sediment D_{10} (µm)
D_{max}	Trangressive species richness overyielding to maximum
D_{min}	Trangressive species richness overyielding to minimum
D_{sp}	Non-trangressive species density overyielding
D_T	Non-trangressive species richness overyielding
ET	Erosion threshold (Nm^{-2})
F_o	Microphytobenthos minimum fluorescence
f-SPI	Florescent sediment profile imaging
$^{f\text{-}SPI}L_{max}$	f-SPI calculated maximum mixed depth (cm)
$^{f\text{-}SPI}L_{mean}$	f-SPI calculated mean maximum mixed depth (cm)
$^{f\text{-}SPI}L_{med}$	f-SPI calculated median maximum mixed depth (cm)
HD	*Hediste diversicolor*
HU	*Hydrobia ulvae*
$Mean_{CC}$	Contact core sediment mean particle size (µm)
$Mean_{MC}$	Minicore sediment mean particle size
ML	Maximum likelihood
Mud_{CC}	Contact core sediment mud content (%)
Mud_{MC}	Minicore sediment mud content (%)
nlme	Nonlinear mixed effects package
PAM	Pulse Amplitude Modulated Fluorometer
REML	Restricted maximum likelihood
SBR	f-SPI calculated surface boundary roughness (cm)
S_i	Suspension index
$Water_{CC}$	Contact core sediment water concentration (gcm^{-3})
$Water_{MC}$	Minicore sediment water content
X-CT	X-ray computed tomography
Y	Microphytobenthos maximum quantum yield

Chapter 1 | Introduction

1.1 | Background

This thesis uses multidisciplinary techniques and manipulative experiments in the field and the laboratory to investigate the effects of biodiversity, species identity, richness, abundance and biomass distribution on a number of physical, chemical and biological properties of a mudflat with particular regard to sediment stability.

1.1.1 | Why biodiversity?

The concept of biodiversity, as we currently understand it, was born at the National Forum on BioDiversity, held in Washington, D.C., in 1986 (Reaka-Kudla et al. 1997). While not only important in its own right, biodiversity has been frequently cited as an key factor in human health (Reaka-Kudla et al. 1997) and well-being, through access to medicines, crops, fibres, clean water, and fresh air (Diaz et al. 2006). The current period of global disturbance, causing changes to ocean acidity (Caldeira and Wickett 2003), temperature, and salinity (Feely et al. 2004, Solomon et al. 2007), has resulted in a dramatic alteration in the distribution (Parmesan et al. 1999, Davis and Shaw 2001, Walther et al. 2002), abundance (Condit et al. 1996, Thomas et al. 2004, Mieszkowska et al. 2006) and interactions (Portner 2008) of many species. The consequences of these changes are, currently, at best poorly understood, and predicting the effects of these species changes is complicated (Chapin et al. 2000). The resulting potential changes in ecosystem functioning is a controversial topic (Tilman 1999, Waide et al. 1999, Schwartz et al. 2000), which has become an important ecological (Chapin et al. 2000, Naeem et al. 2002, Baumgartner 2007), economic (Perrings et al. 1995, Duncan 2013), and social issue (Nunes et al. 2011, Nature Editorial 2012, Turnhout et al. 2012).

1.1.2 | Why mudflats?

About two thirds of the Earth's surface is covered with intertidal and subtidal soft marine sediments (Rosenberg et al. 2007). In the intertidal

zone these sediments are known as mudflats, and are coastal wetlands formed when tides or rivers lose flow energy and deposit sediment particles (Frey and Basan 1985). These gravel, sand and mud particles build up to form a mudflat. The mud content of these sediments makes them cohesive. These sediments provide a valuable habitat, not only directly for the benthic organisms that inhabit them, but also indirectly for pelagic organisms in the waters above (Marcus and Boero 1998, Kirby et al. 2007) and other linked ecosystems, including terrestrial organisms and humans, through provision of nutrients and resources (Diaz et al. 2006). Fluxes of materials occurring in soft sediments, across the sediment-water interface, and actions of the organisms and mechanisms that control those fluxes are likely to have an important global significance (Raffaelli et al. 2003a).

The estuarine and coastal environment is one of the most ecologically diverse and productive in the world (Nixon et al. 1986) and of a high economic value to human society for the services it provides (Costanza et al. 1997, Arkema et al. 2013, Barbier et al. 2013). These are services such as sediment and nutrient storage and flux, food provision, waste disposal (Crooks and Turner 1999), flood defence and storm protection (Bale et al. 2007, Arkema et al. 2013, Barbier et al. 2013, Liquete et al. 2013).

Damaging influences on estuaries as a result of anthropogenic activities, such as over-fishing, habitat degradation and destruction, and pollution are affecting the contributions of these habitats to society (Worm et al. 2006). As such, it is important to understand the changes that these influences may cause by investigating the relationships between biodiversity and the mudflat ecosystem (Boogert et al. 2006, Naeem 2006). Additionally, the strength of inter-habitat coupling in an estuarine system means that when considering the implications of local species loss the consequences may reach further than just the local estuary, propagating into other linked ecosystems (Covich et al. 2004).

Estuarine systems are already heavily studied for their biological, chemical and physical properties. Much information has been obtained on the basic functioning of these important habitats and the patterns of abundance and actions of many common macrofauna species are well documented

(Solan et al. 2006). This is an advantage when studying them, in that further knowledge can build on previous investigations. Estuaries are relatively species poor when compared to other habitats, such as rainforests and coral reefs, which makes studying interactions among species easier (Emmerson et al. 2001). Their productivity, however, can be disproportionately large (Lawton 1994, Tilman and Downing 1994). Using this knowledge, simple manipulative experiments can be designed and carried out to enable the examination of complex ecological questions.

1.1.3 | Why sediment stability?

At a basic level, sediment stability is important in maintaining the presence of the mudflat habitat, through preventing erosion. Sediment stability is also important in maintaining the functions of the mudflat and allows the provision of a habitat for a wide range of fauna, from microphytobenthos, to macrofauna such as worms and shrimp, and megafauna, such as birds and fish. The mudflats themselves are shaped to a great degree by the overlying fluid which induces a shear stress at the sediment-water interface (Kling et al. 2000, Gooday 2002), literally shaping the habitat by affecting the type and structure of the substrate, the location of habitat patches, the distribution of resources and the structure of biotic communities (Austen et al. 2002). Sediment supply from the terrestrial landscape and the dynamic properties of the mudflat, such as the constant sediment destabilisation, erosion, transport, deposition and sediment stabilisation, enable this unique habitat to fulfil its important role as a transitional area between the terrestrial and shallow-marine environments (Mwamba and Torres 2002).

1.1.4 | Biogeochemical processes measured

Other physical, chemical and biological properties of the mudflat were measured to provide a holistic picture of how sediment stability is directly and indirectly affected by species biodiversity. These properties included microphytobenthos biomass and health, sediment water content and particle size distribution and colloidal carbohydrate and chlorophyll concentrations.

1.2 | Sediment Erosion

Natural sediment deposits consist of individual grains held together in non-cohesive sediments by friction and in cohesive sediments by electrochemical forces (Jones and Jago 1993). Biota and their products often add cohesion to sediment (Black et al. 2002), although their net effect may be stabilising or destabilising (Widdows and Brinsley 2002). Sediment erosion potential or sediment erodibility can be defined using the erosion threshold (ET), or the critical shear stress, sometimes represented as τ_{crit}. This is the shear stress or force below which little or no erosion occurs, whereas once this value is exceeded significant erosion will occur (Teisson et al. 1993). There are a number of other ways that have historically been used to describe erosion. An accurate numerical description of the erodibility of cohesive sediments is usually comprised of a measure of the force per area required to erode a certain mass of the sediment, such as the erosion rate (Tolhurst et al. 2009). Another measure that may be provided is the mass of sediment eroded at a particular shear stress over a period of time (Widdows and Brinsley 2002, Torres et al. 2003). The indices used to characterise sediment erosion can vary from researcher to researcher and with the methodology used, with those studies using laboratory or annular flumes presenting different indices to those using smaller portable devices *in situ*.

The critical shear values required for sediment erosion on a mudflat range from 0.02 Nm^{-2} for a 'fluffy top layer' (Gust and Morris 1989, Ruddy et al. 1998), to 0.2 to 0.74 Nm^{-2} for recently air exposed natural muds (Amos et al. 1992, Schunemann and Kuhl 1993, Amos et al. 1997, Widdows et al. 1998b), to in excess of 8 Nm^{-2} for dewatered biostabilised sediments (Defew et al. 2002). Tidal flows can often be below critical shear value (Shi et al. 1996, Christiansen et al. 2000) with shear stresses of <1 Nm^{-2} (Mimura 1993). However, cohesive sediment mudflats can have a highly dynamic surface 'fluff' layer (Ruddy et al. 1998) of approximately 500 µm which may have much lower critical shear values and be constantly resuspended and deposited under low erosive forces, such as tides or other disturbance actions. This has led to the classification of two types of erosion based on erosion rate that may occur on intertidal mudflats (Amos et al. 1992). Type 1 erosion is surface erosion, the erosion of the highly dynamic surface layer, and Type 2

erosion is mass or bulk erosion (Tolhurst et al. 2000a, Tolhurst et al. 2009). Due to the different nature of these erosion thresholds and changes in sediment properties with depth, a mudflat sediment may exhibit more than one type of erosion, with erosion of a fine surface 'fluff' layer occurring rapidly, before steady bulk erosion of underlying sediments occurs (Amos et al. 1992).

A variety of factors influence sediment erodibility, interacting in a complex manner (Austen et al. 1999). These include a wide range of physical (Verreet et al. 1986, Mehta et al. 1989, Berlamont et al. 1993, Mimura 1993, Defew et al. 2002, Mwamba and Torres 2002, Torres et al. 2003, Neumeier et al. 2006, Tolhurst et al. 2006a, Tolhurst et al. 2006c, Tolhurst et al. 2008b), chemical (Tolhurst et al. 2002, Perkins et al. 2003, Noyes et al. 2009), and biological processes (Montague 1986, Grant and Daborn 1994, Widdows et al. 2000a, de Deckere et al. 2001, Tolhurst et al. 2003, Tolhurst et al. 2008a, Murphy and Tolhurst 2009, Chapman et al. 2010). Some of these factors are discussed below.

1.3 | Faunal influence on sediment stability

In areas of rapid change, such as coastal areas at threat of rising sea level, species loss, temperature changes, salinity changes and ocean acidification, predicting the response of the ecosystem to these changes requires consideration of the ability of biological processes and species actions to modify their surrounding environment (Kirwan et al. 2010). With respect to sediment stability, the organisms found on a mudflat are usually split into two groups: stabilisers and destabilisers (Black et al. 2002, Widdows and Brinsley 2002), however some species may fall into both categories over spatial or temporal scales (Table 1.1).

Stabilising organisms can influence the hydrodynamics in the benthic boundary layer by altering tidal currents and wave action by providing physical protection to the bed, such as mussel beds, macro-algae and salt marsh, or can enhance cohesiveness and alter the critical erosion threshold, such as microphytobenthos (Black et al. 2002, Widdows and Brinsley 2002). Destabilising organisms can increase sediment erosion and resuspension

through increasing surface roughness, sediment water content, producing faecal pellets, and grazing or removing bio-stabilisers (Black et al. 2002, Widdows and Brinsley 2002). It is important to distinguish between stabilising and destabilising effects and their impact on sediment flux. For example, an organism may act to stabilise the sediment bed through burrow construction but also increase the flux of sediment from the bed through burrow cleaning. In this case, sediment stability is increased but 'erosion' of sediment from the bed is also increased. This ejection of sediment from burrows may however result in deposition of loose grains on the surface of the sediment, decreasing the sediment erosion threshold.

Table 1.1 | The stabilising and destabilising effects of some common mudflat flora and fauna actions.

Action	Stabilising / enhanced deposition	Destabilising / increased erosion
Biofilm creation	Extracellular polymeric substances (EPS) secretion enhances cohesion and promotes particle flocculation, settling and adhesion	During photosynthesis, oxygen bubbles may be trapped within the biofilm, increasing buoyancy and layers of sediment may pull away from the surface An over stabilised top layer may detach from the underlying sediment
Burrowing	Sediment compaction increases sediment density and stability Increased drainage promotes dewatering and stability during low tide Secretion of EPS by the burrower and by bacterial communities in the burrow wall can stabilise sediment	Bioturbation breaks up the sediment Burrow cleaning ejects sediment from the bed
Network growth	Filamentous biota bind sediment particles together	
Filter feeding	Removal of particles from the overlying water, and species may biodeposit	Biodeposited particles may be easily eroded at low current speeds
Bed over growth	Provides physical protection of the bed from overlying water currents	Scouring may occur around clumps of organisms as local bed roughness is increased
Production of mounds	Creation of higher areas may increase sediment dewatering and stability at low tide	Increased bed roughness provides a focal point for erosion by water currents Overdrying of high areas during low tide may reduce attachment to the underlying sediment and enhance erosion once covered at high tide
Production of pits	Pits provide low flow areas encouraging the deposition of particles	Increased bed roughness provides a focal point for erosion by water currents
Movement	Organisms may leave EPS in tracks, stabilising the sediment	Organisms disrupt the sediment bed, dislodging particles, creating tracks, increasing water content and bed roughness
Pelletisation	Faecal pellets may be sticky with EPS and enhance sediment flocculation and bed stability	Production of faecal pellets, pseudofaeces or ejection of filtered sediment enhances erosion
Grazing	Organisms may leave EPS in tracks, stabilising the sediment	Movement destabilises the sediment (see above) Grazing of MPB and EPS reduces stabilising effects (see above)

Sediment permeability and water content affect erodibility. Meadows and Tait (1989) examined the effects of *Corophium volutator* and *Hediste diversicolor* on sediment permeability, water content and shear strength in a laboratory experiment. Sediment permeability decreased with increased *Corophium* density (58 % for density 22,500 individuals m^{-2}) and greatly increased with increased *Hediste* density (123 % for a density of 9,000 individuals m^{-2}) compared to sediments containing low species densities (2,500 individuals m^{-2} for *Corophium volutator* and 1,000 individuals m^{-2} for *Hediste diversicolor*). Both species increased the shear strengths of the sediments; *Corophium* increased shear strengths by approximately 50% at 7,500 individuals m^{-2} and 180 % at 22,500 individuals m^{-2}, while *Hediste* increased shear strength by approximately 59% at 3,000 individuals m^{-2} and 80% at 9,000 individuals m^{-2} compared to sediments containing low species densities. Both species reduced the water content of the surface sediment with the addition of *Corophium* reducing water content by over 78 % and the addition of *Hediste* reducing water content by over 69 % at densities above 7,500 individuals m^{-2} and 3,000 individuals m^{-2} respectively compared to the low density treatments. However, effects of the two species in combination were not additive.

Macrofauna may build structures, such as tubes and stabilised burrows, which can enhance sediment stability. Box cores seeded with the capitellid *Heteromastus filiformis* showed an 80 % increase in the sediment critical rolling velocity in a flume experiment, and a doubling of the sediment suspension velocity due to dense tube aggregations (Rhoads et al. 1978b). Lower water velocities were measured within tube clumps when tubes of the polychaete *Owenia fusiformis* were inserted into wetted foundry sand (Eckman et al. 1981). Grant and Daborn (1994) noted no change in the critical shear velocity for erosion of intact cores held in a laboratory flume in relation to *Corophium volutator* density. However bedload trap measured sediment erosion rates were negatively correlated with *Corophium* density, meaning that while *Corophium* did not cause a change in the sediment stability it did cause net loss of sediment from the substrate, possibly due to ejection from burrows or production of faecal pellets. Luckenbach (1986) showed 46 % lower critical entrainment velocities in sediment cores with 8 individuals of the tube-building worm *Diopatra cuprea* per 0.01 m^2 than in

cores with 1 individuals per 0.01 m^2. Deposition occurring due to the presence of mats of the tube-building polychaetes *Polydora* was found to be caused equally by direct acquisition of the particles by species themselves and by particle settlement between the tubes (Rhoads et al. 1978b). Frithsen and Doering (1986) used radiolabeled 16 µm diameter particles to determine the rate of particle removal from the overlying water by organisms. Removal rates increased in the presence of high densities of the tube-building polychaetes *Streblospio benedicti* and *Polydora ligni* with deposition occurring between the tubes. Conversely, Eckman and Nowell (1984) and Carey (1983) observed increased sediment entrainment at the base of an animal-tube mimic of the sandmason worm *Lanice conchilega* but reduced overlying current velocities (Carey 1983) and increased sediment deposition downstream of the tube (Eckman and Nowell 1984).

The mud shrimp *Corophium volutator* was shown to stabilise mudflats and maintain the mudflat habitat in the Danish Wadden Sea, where the mudflat was characterised at low tide by emergent plateaux and small pools (Mouritsen et al. 1998). A parasite induced mass-mortality of the *Corophium* population in the summer of 1990 resulted in a large amount of sediment erosion. The plateaux and pool structure was eroded and the sediment particle size shifted, decreasing in silt content and increasing the median particle diameter (Mouritsen et al. 1998). The chlorophyll *a* concentration of the sediment increased. This suggested the *Corophium* were stabilising the sediment with their activities and burrows which extend into the deeper sediment, the effects of which outweigh destabilisation due to diatom grazing (Mouritsen et al. 1998).

Pits or wide burrows can benefit sediment deposition. The burrows of the crab *Neohelice granulata* were found to act as passive traps of sediment (Escapa et al. 2008). Yager et al. (1993) observed enhanced deposition to mimicked biogenous pits under certain flow regimes, such as transitional flow (Reynolds number = 60, where smooth flow has a Reynolds number of 0). However, the mounds caused by excavation of these burrows by the crab were found to enhance erosion as a result of erosion of the mounds while submerged due to tidal flow and mound dessication and degradation while exposed with later mobilisation by the tide (Escapa et al. 2008). The crab

therefore contributed to both erosion (between 10 and 500 gm^{-2} per day) and deposition occurring on the mudflat (between 380 and 1,200 gm^{-2} per day). Increasing bed roughness by the creation of mounds, therefore, enhances the erodibility of sediment. The burrowing ghost shrimp, *Callianassa subterraneana*, was found to increase the roughness of the North Sea bottom sediment surface by a factor of over 1000 due to the production of large mounds, causing a resuspension of 11 kgm^{-2} dry weight of sediment per year (Rowden and Jones 1994). There was, however, also a limiting effect observed in that the effect of the species was self-inhibiting as burrows produced were smaller when the species was present in high densities (Rowden and Jones 1995).

Species movement, creating sediment disruption, has been found to decrease the erosion threshold of sediments. The presence of the bivalve *Nucula* in an annular flume increased resuspension by 2 - 10 fold under low to high current velocities compared to abiotic sediments, due to sediment reworking and increased bed roughness (Davis 1993). Tracks of the motile bivalve *Transenella tanilla* were shown to reduce critical entrainment velocity of sediment in a flume by 20 % from 1.74 cms^{-1} to 1.39 cms^{-1}, even at low densities, through increased bed surface roughness (Nowell et al. 1981). The tracks were up to 2 mm deep with steep sides resulting in small levees along the tracks, causing sediment entrainment to occur at the crest of the levees. In this way, surface activity can cause disruption of the surface sediment and particle erosion. The hermit crab *Pagurus* sp. produced an arrhythmic pattern of almost continuous resuspension of sediment as a result of surface browsing. Under these conditions low levels of shear stress (less than 0.002 Nm^{-2}) were required to suspend this disrupted sedimentary surface material into the water column (Davis 1993). Surface tracking of *Hydrobia ulvae* held in a racetrack flume caused an increase in sediment and microbial suspension and a decrease in critical shear velocity (Blanchard et al. 1997).

Species activity (bioturbation) can also physically disrupt sediment by dislodging particles into suspension and can destabilise sediment, making it more easily erodible under low current speeds by reducing sediment cohesion. Increased biomass of *Corophium volutator*, a burrowing amphipod, was observed to increase the amount of sediment put into suspension whereas

increased biomass of the cockle *Cerastoderma edule* and the mussel *Mytilus edulis*, which are filter feeders and are not as active as *C. volutator*, reduced the amount of sediment put into suspension (Biles et al. 2002).

Frozen discs of sediment containing luminophores can be used to determine the movement of particles within sediment (Biles et al. 2002). Behaviour differences in fauna may explain the variation in luminophore burial rates, with sites dominated by polychaetes and oligochaetes showing a larger percentage of subducted luminophores than sites dominated by *Hydrobia ulvae*, a surface dwelling mollusc (Biles et al. 2002).

Bioturbation caused by the Manila clam *Ruditapes philippinarum* was found to increase sediment erosion in a laboratory benthic annular flume, decreasing the critical erosion velocity from 32 cms^{-1} in sediment containing no clams to 20 cms^{-1} at clam densities of 206 individuals per m^2 and an increase in the sediment erosion rate at higher clam densities (Sgro et al. 2005). *Macoma balthica* was found to be a sediment destabiliser by Widdows et al. (2000b). Three hours of bioturbation by the clam *Macoma balthica* at a density of 1200 individuals m^{-2} approximately doubled the mass of sediment eroded at current velocities above 20 cms^{-1} in an annular flume experiment on the Skeffling mudflats. Temporal changes in the erosion threshold on the Skeffling mudflat, UK were not correlated with the relatively small differences in the physical properties of the surficial sediments (Widdows et al. 2000b). These changes were, however, correlated with *Macoma balthica* densities with a decrease in the erosion threshold and an increase in the mass of sediment eroded correlated with an increasing density of *Macoma balthica* (Widdows et al. 2000b). This was also observed by Widdows et al. (2000a) in the Westerschelde and Humber estuaries. Spatial and temporal variation in sediment erodibility on the mid to upper shores of the Humber and Westerschelde estuaries was attributed to changes in abundance of biostabilising microphytobenthos and destabilising *Macoma balthica* (Widdows et al. 2000a, Widdows et al. 2000b). The erosion rate and the sediment mass eroded was increased by the activities of *Macoma balthica* and found to be density dependent (Widdows et al. 1998c). Widdows et al. (1998a) found the suspension feeding bivalves *Cerastoderma edule* and *Macoma balthica* decreased the erosion threshold and increased the erosion rate in an annular

flume study on the Skeffling mudflat. *Cerastoderma edule* has also been found to increase suspended sediment concentrations up to 5-fold and sediment erosion by up to 10-fold when increasing *Cerastoderma* density from 0 to 141 individuals per m^2 (Ciutat et al. 2006), and reduce the sediment erosion threshold by 50 – 75 % compared to sediments with a biofilm (Neumeier et al. 2006). This was attributed to surface disturbance (Ciutat et al. 2006, Neumeier et al. 2006).

Experiments using sediment beds in a flume showed bioturbation by *Hydrobia ulvae* caused surface layer erosion relative to species density and that increased sediment moisture content also increased sediment erosion (Orvain et al. 2006). *Hediste diversicolor* was shown to have a strong effect on erodibility of muddy sediments when different densities of individuals were tested in a laboratory annular flume (Widdows et al. 2009). High densities of individuals, 1,000 and 3,000 individuals m^{-2}, showed active sediment resuspension at low current speeds (0.05 ms^{-1}). There was also a density dependent effect of *Hediste* as current speeds were increased, with a 37-fold increase in sediment erosion from the control (no *Hediste*) at 3,000 individuals m^{-2} (current speed 0.4 ms^{-1}). However, at low densities of *Hediste*, there was little bed erosion until current speeds of 0.4 to 0.45 ms^{-1} were reached. In both flume and aquaria based experiments to which known densities of *Corophium volutator* were added, de Deckere et al. (2000) showed the concentration of suspended solids in the overlying water increased with increasing *Corophium volutator* density. The presence of *Corophium volutator* also decreased the critical erosion threshold of the sediments.

Conversely, sediment agitation and disruption by burrowing tubificid oligochaetes facilitated particle settlement due to the creation of a loosely bound, porous layer. Stolzenbach et al. (1992) suggested that organismal activity caused suspended fine particles to collide with and adhere to the fluffy layer on the sediment surface, increasing particle deposition rates. Bioturbation and herbivory by the ragworm *Hediste diversicolor* has been suggested to exacerbate internal creek erosion of salt marshes (Hughes and Paramor 2004, Paramor and Hughes 2004) and sediment destabilisation by

infauna may be a major cause in the reduction in saltmarsh area observed in the south-east of England (Paramor and Hughes 2004).

Some species contribute to sediment resuspension directly by expelling sediment into the water column. The surface and sub-surface deposit feeding bivalve *Yoldia limatula* ejects fluidised pellets and pseudo pellets several centimetres into the benthic boundary layer (Bender and Davis 1984). Under high species densities up to 24.6 kg of dry sediment may be input into the water column per metre squared per year, with an increase in overall grain size in the area (Bender and Davis 1984). Davis (1993) found that the deposit feeders *Macoma tenta* and *Yoldia limatula*, both bivalves, and the polychaete *Pectinaria gouldi* ejected watery sediment into overlying water, observing a temporal pattern of increased turbidity of the seawater passing over the fauna in small single species flow-through mesocosms. *Macoma* was observed to eject a thick slurry every 15 – 20 minutes, *Pectinaria* ejected a plume of watery sediment every 25 – 35 minutes and *Yoldia* ejected a cloud of watery sediment every 20 – 25 seconds. The bivalve *Macoma nasuta* has been observed to eject a jet of material that reached 3 cm above the sediment bed (Nowell et al. 1981). In the Danish Wadden Sea the erosion rate was dependent on the faecal pellet content of the bed material (Andersen 2001). *Hydrobia* faecal pellets behave non-cohesively and are therefore easily erodible. In particular, *Hydrobia ulvae*'s increased production of faecal pellets at higher temperatures and increased grazing on benthic diatoms controlled the seasonal variability of the erosion threshold (Andersen 2001). Conversely, faecal coils of the tube worm *Hobsonia florida* and the spionid polychaete *Pseudopolydora kempi japonica* have been observed to have an increased critical erosion threshold than the surrounding sediment due to their adhesion to each other and the bed sediment (Nowell et al. 1981).

Some species provide physical protection for the bed by growing over it. Mussels in particular can cover the sediment bed material and protect it from erosion by overlying water flow. Sediment resuspension was determined to decline in an exponential manner with increasing mussel density, with mussels reducing sediment erosion by up to 10-fold at their highest densities, in a flume study based in the Humber Estuary (Widdows et

al. 1998c). However, a later study found sediment resuspension was five and four times higher for 25 % and 50 % mussel cover, respectively due to increased turbulence and scouring around mussel clumps, but at 100 % mussel cover sediment resuspension was three times lower than 0 % cover as the sediment bed was more protected (Widdows et al. 2002).

Many benthic in- and epi-fauna are specialised in filter feeding and selective removal of particles from the water column, which they then biodeposit, causing a net deposition effect. In the Dutch Wadden Sea the filter feeding bivalve *Cerastoderma edule* was estimated to deposit 100,000 tons of sediment (dry weight) per year, and the blue mussel, *Mytilus edulis*, was shown to remove 175,000 tons of sediment (dry weight) from the water column per year (Verwey 1952). *Mytilus edulis* can form extensive biogenic reefs within estuaries and on lower sediment shores in areas of high tidal flow (Widdows and Brinsley 2002) and remove up to 20 % of the water seston load depending on the carbon content of the seston (Asmus and Asmus 1991, Muschenheim and Newell 1992). Filter feeding by *Mytilus edulis* can biodeposit 1-70 g of carbon per square metre every day (Muschenheim and Newell 1992), equivalent to 40 times the natural sedimentation rate (Widdows et al. 1998c), however, these biodeposits have a low threshold for resuspension. Widdows et al. (1998c) suggest that the majority of these biodeposits are resuspended, even at low current speeds, however, Loo and Rosenberg (1989) estimated that 80 $mgCm^{-2}$ of 200 $mgCm^{-2}$ ingested by the bivalve species *Cerastoderma edule* and *Mya arenaria* remained deposited.

Macrofauna can therefore have a significant effect on the stability, erosion and resuspension of intertidal and subtidal sediments through a range of activities and behaviours. Another group of organisms, much smaller than the macrofauna, the microphytobenthos, also have a vital role to play in sedimentary processes.

1.4 | Microphytobenthos influence on sediment stability

The microphytobenthos are microscopic, photosynthetic organisms, including eukaryotic algae and cyanobacteria that live on and within the upper millimetres of intertidal and subtidal sediments in the euphotic zone

(MacIntyre et al. 1996). On European mudflats, these benthic microalgae are predominantly composed of diatoms, which may either be epipsammic, closely attached to particle grains, or epipelic, free and motile (Blanchard et al. 2003). Diatoms can secrete large amounts of extracellular polymeric substances (EPS) (Dade et al., 1990, Hoagland et al., 1993, Decho, 2000, Stal, 2003) producing a matrix of diatoms and EPS known as diatom mats or biofilms (de Brouwer et al. 2003). This EPS performs a variety of functions, including locomotion (Edgar and Pickettheaps 1984), as part of unbalanced growth and as a food source for later use (de Brouwer and Stal 2002), and protection against toxins and desiccation during periods of air exposure (Widdows and Brinsley 2002). One vital function of EPS is in stabilising sediments, acting as a kind of glue, that increases sediment particle cohesion and reduces erosion (Montague 1986, Grant 1988, Paterson 1989, Dade et al. 1990, Paterson et al. 1990, Paterson 1997, Tolhurst et al. 2002).

Biofilms may also provide sticky surfaces which adhere settled material that may otherwise be resuspended (Stolzenbach 1989, Graf and Rosenberg 1997), reducing the resuspension of sediments (De Jonge and Van Den Berg 1987, Grant and Bathmann 1987, Paterson 1989, Self et al. 1989, Delgado et al. 1991, Dade et al. 1992). Where macrofauna populations were dominant in the Danish Wadden Sea biofilms were absent, resulting in low erosion thresholds (Andersen 2001). The role of the microphytobenthos in mediating erosion of sediments has been well documented (Paterson 1989, Underwood and Paterson 1993, Sutherland et al. 1998, Paterson and Black 1999, Riethmuller et al. 2000, Yallop et al. 2000, Black et al. 2002, Wood and Widdows 2002, de Brouwer et al. 2003, Friend et al. 2003b, Lucas et al. 2003, Stal 2003). Whilst the relationship is complex, the critical erosion threshold of sediments covered by a biofilm has been shown to be correlated with microphytobenthos density measured via colloidal carbohydrate, chlorophyll *a* concentrations (Sutherland et al. 1998, Paterson et al. 2000, Tolhurst et al. 2006b, Tolhurst et al. 2008a), pulse amplitude modulated fluorometry (PAM) (Tolhurst et al. 2006b), and spectroradiometry (Murphy et al. 2008). There is often a significant increase in the critical shear stress at which erosion occurs and a reduction in the erosion rate at greater microphytobenthos densities. Much of the spatial and temporal variation in sediment erodibility can be attributed to the establishment and loss of algal or microphytobenthos

biofilms, as shown by multidisciplinary field studies in the Humber Estuary, England (Amos et al. 1998, Widdows et al. 2000b) the Westerschelde, Netherlands (de Brouwer et al. 2000, Widdows et al. 2000a), the Tagus Estuary, Portugal (Tolhurst et al. 2003) and the Wadden Sea, Germany (Riethmuller et al. 2000, Andersen 2001). Low erosion thresholds measured in the Danish Wadden Sea were hypothesised to be as a result of the absence of algal biofilms (Andersen 2001). Additionally, diatoms can have an effect on other sediment properties and the development of a diatom biofilm over a period of 45 days in the laboratory resulted in an increase in the sediment water content, chlorophyll *a* concentration, colloidal carbohydrate concentration and the erosion threshold (Tolhurst et al. 2008a). However, under some conditions diatom biofilms can enhance sediment erosion. Orvain et al. (2004) and Tolhurst et al. (2008a) found that during the diatom senescent phase, after the exponential growth phase, increased bed roughness and water content increased sediment erosion due to increased biofilm fragility and breakage.

Microphytobenthos also provide an important food source for the macrofauna and a number of studies have found it is the interaction in abundance between these two mudflat inhabitants that predominantly controls sediment stability (Austen et al. 1999, Andersen 2001, Orvain et al. 2004).

1.5 | Faunal influence on microphytobenthos

Removal of macrofauna from sediments has been shown to cause an increase in sediment microphytobenthos biomass (Smith et al. 1996) and a corresponding increase in sediment stability (Davis and Lee 1983). Smith et al. (1996) showed that sediment cores held in the laboratory without macrofauna had significantly greater densities of diatoms after 8 days than cores containing *Corophium volutator* and *Hediste diversicolor*, due to the grazing effects of *Corophium* and *Hediste*. In field removal experiments, densities of diatoms increased when *Corophium volutator* was removed by spraying with insecticide and when *Hediste diversicolor* was prevented from surface deposit feeding, i.e. feeding on surface dwelling diatoms (Smith et al. 1996). In a laboratory experiment, 40 days after sediment defaunation

mudflat sediment had a four times greater chlorophyll *a* concentration and gross primary production had doubled (Davis and Lee, 1983). Grazing of microalgae by macrofauna was determined to be the mechanism of control of microphytobenthos biomass and production (Davis and Lee 1983).

Daborn et al. (1993) noted that the predation of epi- and in-fauna by birds promoted sediment stability by removal of grazing pressure from macrofaunal species such as *Corophium volutator*, also resulting in an increased biomass of microphytobenthos. Sediment stability has been observed to decrease with increased distance from the upper shore salt marsh due to changes in microphytobenthos biomass, with areas close to the saltmarsh dominated by microphytobenthos and areas offshore dominated by *Hydrobia ulvae* with lower microphytobenthos biomass due to grazing (Austen et al. 1999). Surface layer erosion caused by *Hydrobia ulvae* density and bioturbation was found to be correlated with the growth stage of a diatom biofilm, with the greatest erosion occurring during the diatom exponential growth phase due to increased bioturbation during this period (Orvain et al. 2004).

Macrofauna may have positive effects on the microphytobenthos. *Corophium volutator* has been shown to preferentially consume dominant diatom taxa, increasing the species richness, evenness and diversity of epipelic diatom assemblages (Hagerthey et al. 2002). A range of macrofaunal species, including nereid polychaetes (Woodin 1977) and limpets (Stimson 1973, Mcquaid and Froneman 1993, Plaganyi and Branch 2000) have been shown to 'garden' algae. The nereid polychaetes *Nereis vexillosa* and *Platynereis bicanaliculata* can attach pieces of algae to their tubes (Woodin 1977). The attached algae provide food for the nereids, and other local grazers and deposit feeders, and increases the dispersal ability of the algae. Grazing macrofauna can positively affect the supply of nutrients to algae, either by grazing and removal of overlying cells allowing nutrient diffusion (Mccormick and Stevenson 1991) or through the fertilisation of the sediment via excretion (Williams and Carpenter 1988). During low tide, nitrogenous excretions that accumulated under the shell of the limpet *Patella cochlear* were found to comprise 30 % of the adjacent algae's daily nitrogen growth requirements (Plaganyi and Branch 2000). The algae demonstrated

an ability to increase their uptake rate to take advantage of the increased concentration of nitrogenous compounds surrounding them (Plaganyi and Branch 2000).

However, the grazer-microphytobenthos interaction is not the only interaction occurring on the mudflat and many direct and indirect species interactions within macrofaunal communities can cause changes to sediment stability.

1.6 | Species interactions and diversity effects

Species interactions can influence the effects organisms and the microphytobenthos have on sediment stability in a number of ways. Increased predator-prey interactions can directly or indirectly influence the species abundance or richness of sediment stabilisers or destabilisers or result in a change in behaviour, altering the effect an organism has on sediment stability, however few studies have looked at this directly.

As discussed above, Daborn et al. (1993) noted the indirect effects on mudflat stability caused by birds. The arrival of a large number of predatory, migratory birds resulted in a reduction in abundance of *Corophium* due to grazing and a change in *Corophium* behaviour, increasing predator avoidance behaviour and reducing the amount of time spent grazing on the surface of the sediment. This, in turn, had an effect on the number of diatoms in the sediment which would normally be kept low due to grazing pressure. As a result of the arrival of the birds, diatom biomass increased, causing an increase in the stability of the sediments (Daborn et al. 1993).

De Deckere et al. (2001) reduced sediment infaunal abundance *in situ* by spraying with insecticide. Macrofaunal and meiofaunal density was reduced, especially that of *Hediste diversicolor* and the oligochaetes. Diatom biomass was not observed to increase as a result of the reduction of infauna, however, the treated plots had a significantly higher erosion threshold and a lower suspension index.

Symbiosis between two species can have a stabilising effect on sediments. Fager (1964) found that the tube worm *Owenia fusiformis* and a small anemone can act together to stabilise the sediment surface against erosion resulting in the formation of areas of stabilised substrate, encouraging the settlement of additional flora and fauna. Solan et al. (2008) reported a clear positive effect of species richness on bioturbation intensity of the species *Hediste diversicolor*, *Hydrobia ulvae* and *Cerastoderma edule* in monoculture and mixture. Bioturbation intensity was greatest in those treatments containing a mixture of two of the species. Saunders et al. (2005) used fine mesh buried 10 cm deep in the sediment to exclude the lugworm *Arenicola marina* by preventing establishment of the U-shaped burrows they live in. The exclusion of *A. marina* caused a small increase in biodiversity due to increased numbers of smaller worms, however exclusion of *A. marina* or the increase in biodiversity was not shown to affect sediment stability. Allen and Vaughn (2011) investigated the effect of species diversity on physical processes in artificial streams, showing that increased mussel biodiversity, and functional trait diversity, such as size, shell morphology and burrowing behaviour, led to increased erosion at both low and high densities. Erosion observed at low densities was additive with increasing species diversity, however at high densities certain combinations of species showed non-additive effects on erosion.

Indirect effects of increased sediment resuspension caused by the activities of some species can have important implications for habitat maintenance, controlling the presence and abundance of other species within the habitat. The presence of the tadpole shrimp *Lepidurus packardi* was found to be the most important factor in reducing total macrophyte cover, increasing crustacean species richness and varying macrophyte community composition in aquaria mesocosms due to changes caused in water turbidity and physicochemistry (Croel and Kneitel 2011). Therefore, reduction of local species richness is likely to have unpredictable effects. Solan et al. (2004a) surveyed 139 benthic invertebrate species inhabiting Inner Galway Bay, Ireland and parameterised models to predict how species extinction would affect the biogenic mixing depth, an indicator of bioturbation measured using sediment profile images. They concluded that species extinction would result in a reduction of the biogenic mixing depth and that changes in bioturbation

may depend on the order in which species are lost, as extinction risk is correlated with life-history traits, which determine the intensity of bioturbation.

Murphy and Tolhurst (2009) observed that reducing numbers of some groups of animals, such as nereids, did not significantly affect any of the measured sediment properties, which included grain size, water concentration, colloidal and total carbohydrate concentration, chlorophyll *a* concentration, and organic matter, except for colloidal carbohydrate concentration which increased. Removal of the algae using an algaecide reduced the number of individuals of a range of macrofauna taxa, including the nereids, capitellids, sabellids, oligochaetes, nematodes, opisthobranch molluscs and the snail *Salinator*, resulting in changes to the sediment properties, such as an increase in sediments grains greater than 63 μm, and a decrease in the colloidal and total carbohydrate concentration, organic matter, water concentration and chlorophyll *a* concentration. They concluded that the microphytobenthos were key in structuring the macrofaunal community.

A caged field experiment was used to observe the effects of species richness and biomass on benthic respiration rates. These were driven by the presence of *Nepthys hombergii*, a large catworm, in the cages (Bolam et al. 2002). Sediment water content, percentage carbon, percentage silt, redox potential, sediment shear strengths (measured using a Geonor H-60 Vane Borer), benthic respiration rate and nutrient fluxes showed no change with species richness or biomass.

Emmerson et al. (2001) used mesocosms containing a gradient of species richness and biomass from three sites in northeast Scotland, southwest Sweden and central south Australia to investigate the effects of species diversity on nutrient flux at a global level. They also transferred whole communities to a mesocosm system to determine the effects of rarer species not manipulated in the species richness mesocosms. No consistent effect of species richness or functional group was observed on a global scale, probably resulting from inherent site differences. The data showed reduced variability in the nutrient fluxes observed as diversity increased and some species had a greater effect on nutrient flux rates than others, showing rare

species have the potential to contribute disproportionately to ecosystem function (Emmerson et al. 2001).

Species-specific traits associated with bioturbation were shown to be more important in determining nutrient generation in a laboratory mesocosm experiment (Ieno et al. 2006). Raffaelli et al. (2003b) manipulated the fauna in mesocosms adding up to 10 species per tank, also varying species biomass. Single species treatments for some species, including *Hediste diversicolor* and *Corophium volutator*, were observed to have high ammonium concentrations correlated with the species biomass present. The presence of suspension feeders, such as *Cerastoderma edule* and *Mytilus edulis*, reduced ammonium concentrations due to their ability to remove suspended particles from the water column. The effects of biodiversity were shown to be inconsistent, with the sum of ammonium measured after the experiment in tanks with each species in isolation unequal to the ammonium measured after the experiment in multispecies tanks. Increased ammonium concentrations with increased biodiversity were put down to functional trait richness rather than species richness (Raffaelli et al. 2003b). Additionally, environmental conditions can have a feedback effect on biodiversity effects. Current flow was shown to be an important factor with modifying effects, causing changes in organism behaviour with significant effects on nutrient fluxes (Raffaelli et al. 2003b). Current flow on a marine intertidal mudflat also affected nutrient fluxes in both natural and assembled macrofaunal communities but had no effect on nutrient flow in the control systems that were free of macrofauna (Biles et al. 2003). Currents may, therefore, generate a positive effect on nutrient fluxes by promoting changes in the bioturbatory, feeding and behavioural activity of the infauna (Biles et al. 2003, Raffaelli et al. 2003b).

Faunal movement between algal enriched mesocosm patches of sediment differs with species identity, density and habitat composition (Bulling et al. 2008). These factors combined resulted in changes in nutrient release, with ammonium release affected by species identity and phosphate release affected by species density. This increase in species movement could cause an increase in sediment disruption, destabilising sediments and decreasing the erosion threshold. *Hediste diversicolor* and *Hydrobia ulvae* both moved towards enriched sediment patches, whereas *Macoma balthica*

and *Corophium volutator* moved away. *Hediste diversicolor*, *Hydrobia ulvae* and *Corophium volutator* all showed strong movement responses to starting density difference and sediment interface type (whether the interface was enriched sediment next to enriched sediment, enriched sediment next to un-enriched sediment or un-enriched sediment next to un-enriched sediment). *Hediste* and *Hydrobia* were observed to move away from the higher starting density areas. *Hediste* was observed to cause the greatest change in nutrient concentrations between different sediment interfaces due to greater movement in general, while *Macoma* was observed to cause the least, due to less movement in general.

The effects of species interactions on sediment stability can be direct, indirect and complex, requiring careful interpretation. Statzner and Sagnes (2008) examined the combined effects of bioturbation by pairing the barbel, *Barbus barbus*, and the gudgeon, *Gobio gobio*, or the gudgeon and male crayfish of the species *Orconectes limosus*. These three species show different mechanistic effects on the transport of sediments, sediment surface characteristics and sediment surface critical shear stress, in experimental streams. Species pairs were observed to show negative interactive combined effects on the sediment variables measured, i.e. lower than would be expected by summing the effects of the species in isolation, moderated by physical interactions among bioturbator-induced sediment surface modifications. The change observed in the critical shear stress of the sediments was proposed to be as a direct result of the effect of the species on algal cover.

With regard to the effect of biodiversity on ecosystem processes a number of models have been posited so far. The null model states that ecosystem functions will be unaffected by the addition or subtraction of species within the ecosystem. This hypothesis is not supported by experimental evidence and it is widely accepted that there is a relationship between biodiversity and the delivery of ecosystem processes and services. A linear relationship in which trophic groups, along with species, increase the stability of the ecosystem was suggested by MacArthur (1955). This model is too simplistic and does not take into account any variation in species importance to ecosystem processes or species interactions. The rivet

hypothesis (Ehrlich and Ehrlich 1981) considers all species to play an important role in ecosystem functioning, however individual species are likened to the rivets on an aeroplane wing. The rivets hold the aeroplane wing together, but a few rivets may be lost before the aeroplane wing falls apart. Under this hypothesis a few species extinctions may not affect ecosystem processes and services as the actions of different species may overlap and those species left can compensate. The redundant species hypothesis (Walker 1992) suggested that relatively few species are needed to sustain ecosystem processes and any additional species will have little measurable effect on ecosystem processes. This model identifies that some species are more important than others and that species can be classified into functional groups. Extinction within a group is not detrimental until the extinction of the whole group. The rivet and redundancy models do not take into account the subtleties of species-environment interactions and are too simplistic. While the concepts introduced by these models may be useful, their explanatory power is low. For example, these models do not take into account that loss of these redundant species may result in decreased resilience of the system to environmental change as and that these species provide a level of insurance in the system as they may be able to fill gaps if species extinctions were to occur (Naeem 1998, Yachi and Loreau 1999). The keystone species model identifies that some important species may provide a greater function within the community than others (Mills et al., 1993). A discontinuous model suggests that functional diversity may have a discontinuous effect on ecosystem processes (Wedin and Tilman 1996) due to powerful feed-back and feed-forward processes (Grigulis et al. 2005).

The idiosyncratic model (Lawton 1994) suggests that the delivery of ecosystem processes will change as the number and identity of species present changes, however the magnitude and direction (increased or decreased functioning) is unpredictable due to the complex and varied interacting roles of individual species, therefore the effect of losing each species depends on the identity and services of that species and the current environmental conditions (Naeem et al. 2002). Recently it has been suggested that other aspects of biodiversity, other than species identity and richness, such as species density (Polley et al. 2003), species evenness (Wilsey and Potvin 2000, Wilsey and Polley 2004, Maestre et al. 2012),

spatial heterogeneity of species (Maestre et al. 2012) and resources (Dyson et al. 2007, Bulling et al. 2008), abiotic conditions (Biles et al. 2002, Biles et al. 2003, Raffaelli et al. 2003b), and order of species extinction (Solan et al. 2004a) will have significant effects on ecosystem functioning.

The implied assumption of the idiosyncratic hypothesis is that with total knowledge of the species, the environment and their interactions robust predictions of the effect of species loss and biodiversity could be calculated (Lawton 1994, Naeem et al. 2002). Improved quantification and understanding is needed to improve modelling of the role of biota and biological processes and their interaction with the physical and chemical processes occurring on mudflats. This will enable improved forecasting of changes that may occur in sediment dynamics and estuarine morphology in response to global climate change and its consequences, such as sea level rise (Widdows and Brinsley 2002). Ruddy et al. (1998) highlighted the need for an integrated approach to interpreting mudflat processes and variables due to the interdependence of the sediment-water system. Experiments examining a wide range of variables may be able to tease out the particulars of how each species, and the species in mixtures, are affecting the erosion threshold, by looking at the different interdependent variables. Examining the changes caused to microphytobenthos related variables, sediment water content, and particle size when different species combinations are present on the mudflat may help determine the reasons why different species have different effects on the sediment erosion threshold.

One conclusion that stands out in the experiments and studies dealing with multiple species and environmental interactions is the complexity of the relationships occurring (Menge 1995), even within a relatively species poor system such as a mudflat. With so many interactions occurring, influencing species activities and behaviours, overlain with physical processes and spatial and temporal variability, it can be extremely difficult to determine how and why sediment stability and other mudflat characteristics are changing.

1.7 | This study

The aim of this study was to develop a series of experiments that would build on each other to examine the effects of single species and species combinations on selected physical, chemical and biological aspects of a mudflat habitat that contribute to the functioning of this particular habitat. Conducting experiments such as this in the field allows for the influence of real world factors on the experimental treatments, such as temporal and spatial resource heterogeneity and environmental fluctuation (Fridley 2001). The use of experiments where biodiversity is manipulated in a combinatorial design, with the response of specific ecosystem functions measured to determine the effect, has become an important and powerful tool in investigating the effects of biodiversity changes on the natural world (Naeem et al. 1995, Naeem et al. 1996, Tilman et al. 1996, Hector et al. 1999). Conducting experiments such as these *in situ* on the mudflat increases the relevance of the results to the natural world (Fridley 2001).

Collecting data on a range of biogeochemical variables, including microphytobenthos biomass and health, sediment particle size and size distribution, sediment water content and concentration, chlorophyll *a* and *b* concentration, and colloidal carbohydrate concentration, provides a comprehensive examination of the effects of macrofaunal biodiversity changes on an intertidal Norfolk mudflat. Using a multidisciplinary field and laboratory based approach, manipulating the abundances of three key mudflat species, *Hediste diversicolor*, *Hydrobia ulvae* and *Corophium volutator*, this study aims to determine the effects of changes in mudflat biodiversity on sediment stability. These experiments will specifically address the following objectives:

Objective 1 | Investigate the effect of individual macrofauna species on mudflat sediment stability and biogeochemical properties *in situ*.

Objective 2 | Investigate the effect of macrofaunal species density on mudflat sediment stability and biogeochemical properties *in situ*.

Objective 3 | Investigate the effect of macrofaunal species richness on mudflat sediment stability and biogeochemical properties *in situ*.

Objective 4 | Investigate the effect of macrofaunal species biomass distribution on mudflat sediment stability and biogeochemical properties *in situ*.

Objective 5 | Investigate the effect of a macrofaunal species community on mudflat sediment stability and biogeochemical properties.

Objective 6 | Visualise the effect of *Hediste diversicolor*, *Hydrobia ulvae* and *Corophium volutator* on sediment particle mixing.

In this thesis, Chapter 2 describes the methodologies by which these objectives were investigated and details the sediment properties that were examined. Chapter 3 describes and validates an *in situ* defaunation method that was designed specifically to enable experimental investigation of the above objectives in the field. Chapter 4 examines the effects of three common macrofauna species on mudflat sediment properties in isolation and combination. The presence and abundance of the species *Hediste diversicolor*, *Hydrobia ulvae,* and *Corophium volutator* were manipulated to determine the effects of species identity, species density and species richness on mudflat stability and biogeochemical properties, addressing Objectives 1, 2 and 3. Chapter 5, using the same methodology as Chapter 4, examines how species combinations containing 2 and 3 species, with varying species densities and biomass distribution, affect the properties of the mudflat. This chapter addresses Objectives 1, 2, 3 and 4. Chapter 6 investigates how changes in species biomass distribution in natural communities has the potential to alter the properties of the mudflat and addresses Objectives 1, 2, 4 and 5. The use of field mesocosms in these experiments allows the inclusion of temporal and spatial resource heterogeneity and environmental fluctuation, increasing the relevance of the results to the natural world (Fridley 2001). The final results chapter, Chapter 7, uses a laboratory experiment with a two and three dimensional approach to investigate how the three species interactions affect bioturbation and bioirrigation in a three dimensional environment within a mud core. This chapter addresses Objectives 1, 3 and 6.

Introducing the use of established technologies, such as computed tomography, into new disciplines allows the production of revealing datasets which can lead to new perspectives on biodiversity research. Chapter 8 provides a final discussion and an overall synthesis of the data.

Chapter 2 | Materials and Methods

2.1 | Study description

This study uses a multidisciplinary field and laboratory based approach manipulating the abundances of three key mudflat species, *Hediste diversicolor*, *Hydrobia ulvae* and *Corophium volutator* to determine the effects of changes in mudflat biodiversity on sediment stability and other mudflat biogeochemical properties. The measurement of microphytobenthos biomass and health, sediment particle size and size distribution, sediment water content and concentration, chlorophyll *a* and *b* concentration, and colloidal carbohydrate concentration, provides a comprehensive examination of the effects of biodiversity changes on an intertidal Norfolk mudflat.

Sediment erosion is vulnerable to change caused by sampling disturbance (Tolhurst et al. 2000b), a property that limits the usefulness of measurements made in laboratory cores (Jones and Jago 1993). Jones and Jago (1993) go on to suggest that these difficulties necessitate that methods of measurement of sediment stability be carried out *in situ*. Conducting experiments in the field also allows for the influence of real world factors on the experimental treatments, such as temporal and spatial resource heterogeneity and environmental fluctuation, increasing the relevance of the results to the natural world (Fridley 2001). Natural variability however decreases the chance of identifying variation due to the experimental treatments. By using a laboratory experiment to examine species bioturbation and bioirrigation in a controlled environment the effects of individual organisms on sedimentary processes can be identified. This knowledge can then be applied during the interpretation of the data obtained from the field experiments; however a laboratory experiment can never fully replicate conditions in the field.

As a result of this it was decided that the majority of the experiments undertaken for this thesis would be carried out *in situ* using three common species found on a local mudflat located at Breydon Water, Norfolk, UK. A final experiment, examining more closely the bioturbation and bioirrigation

caused by the three species in isolation and in mixture, was carried out in a laboratory.

2.1.1 | Species manipulated

Three common mudflat species were selected for use in these investigations on the basis of their abundance at the experimental site, ease of collection *in situ*, and contrasting feeding and burrowing behaviours. The species selected were *Hediste diversicolor*, *Hydrobia ulvae* and *Corophium volutator*. An additional advantage of using these species is that many studies have already investigated their behaviours in the laboratory and *in situ*, so that the effect of these species on sediment stability, microphytobenthos biomass and sediment particle size can be attributed to species activities and behaviours already observed and studied.

Hediste diversicolor, Annelida, Polychaeta (O.F. Muller, 1776)

Hediste diversicolor is a small polychaete annelid, also known as a ragworm, which can grow up to 10 cm in length. It is found along all British coasts in brackish water, where suitable soft sediment habitat exists, in permanent or semi-permanent burrows (Budd 2008). *Hediste diversicolor* exhibits a range of feeding methods including surface deposit feeder, omnivore, scavenger, sub-surface deposit feeder and passive suspension feeder (Barnes 1994). Filter feeding occurs when high numbers of algal cells are present in the overlying water column (Riisgard 1991). A funnel shaped net is produced, composed of fine mucous threads, through which a water current is driven by undulating body movements (Fauchald and Jumars 1979). When a sufficient amount of particles have been trapped by the net the whole structure is ingested and replaced (Fauchald and Jumars 1979). Deposit feeding can occur in one of two ways: by actively hunting for food on the sediment surface, or by depositing a string of mucous on either side of its body on the sediment surface which is then gathered back to the burrow when the worm retreats, and can be either consumed or stored as a pellet for later consumption (Esnault et al. 1990). Olivier et al. (1995) discovered that juvenile *Hediste diversicolor* could select detritus from the sediment surface and accumulate it in the burrow so that they could stimulate bacterial growth, also known as gardening, to feed upon. *Hediste diversicolor* is very common

at the field site and can be easily collected from the mud by digging and teasing out individuals from the mud.

Hydrobia ulvae, Mollusca, Gastropoda (Pennant, 1777)

Also known as the Laver spire shell or mud shell, *Hydrobia ulvae* is a small gastropod snail, reaching up to 6 mm in length. *Hydrobia ulvae* is often a dominant inhabitant of intertidal mudflats (Barnes 1981, Reise 1985) and can be found at high densities (up to 42,000 per square metre; Green, 1968). It is a surface and sub-surface deposit feeder (Sauriau et al. 1989) feeding on the microphytobenthos (Gall and Blanchard 1995), small organic particles, and bacteria (Green 1968). *Hydrobia ulvae* will also eat its own fecal pellets (Lopezfigueroa and Niell 1987). When the mudflat is submerged *Hydrobia* can float on the water surface (Little and Nix 1976) using a mucus raft which allows it to trap diatoms (Newell 1962) and disperse using tidal flows (Anderson 1971). This species is also very common at the field site and can be picked off the sediment surface or scooped up in large numbers at the edges of the adjacent salt marsh.

Corophium volutator, Crustacea Amphipoda (Pallas 1766)

The mud shrimp, *Corophium volutator*, is a small crustacean identifiable by its enlarged second antenna. *Corophium volutator* frequently found at high densities (up to 140,000 per square metre in southeast England saltmarshes) (Gerdol and Hughes, 1994). *Corophium* is an important food source for many species of birds and fish, especially at Breydon Water as it is an overwintering ground for internationally important bird species (Joint Nature Conservation Committee 2001). *Corophium* have been shown to suspension feed by creating a current using their pleopods (Hughes 1988), deposit feed by scraping surface detritus and microorganisms into the burrow with their antennae and using the current created by the pleopods to pass this material to the mouth (Hart 1930, Hughes 1988), and to graze by scraping the microbial biofilm off individual sediment grains (Meadows and Reid 1966, Gerdol and Hughes 1994). *Corophium volutator* were numerous at the field site and could be easily collected by sieving the water at high tide to collect them while swimming or picking individuals off the sediment surface when they emerged to graze at low tide.

2.1.2 | Study Site

Breydon Water is a 5km long and up to 1.5km wide inland tidal estuary located at Great Yarmouth in Norfolk at N52° 37.030', E01° 41.390' (Figure 2.1). The western end of Breydon Water consists of the confluence of the Rivers Yare and Waveney, with the eastern end becoming a channel, where the River Bure also enters, that flows through Yarmouth and Gorleston to enter the North Sea. The estuary is very turbid, well mixed and relatively shallow (Sabri 1977). The area has a tidal range of approximately 1.5 metres, and is therefore a microtidal to mesotidal estuary, with little semi-diurnal tidal variability (Baban 1997). The area of Breydon Water at high tide is approximately 7 km^2, however at low tide the area drains to a distinct channel (Figure 2.1) approximately 10-12 m in width (Baban 1997). The residence time of tidal waters in the estuary is estimated to be no more than 1-2 days and most is flushed every tide (Sabri 1977).

The site was chosen for its diversity, macrofaunal abundance and vehicular accessibility. The sediment is typically muddy sand (mean particle size = 54.80 µm, sediment mud content = 55.93 %; data based on minicores taken from the control treatments in the experiment presented in Chapter 3). The experimental site has been shown to have suspended solid concentrations between 136 and 151 μgl^{-1} and a salinity of 34.8 (Baban 1997).

The site is a designated nature reserve and environmentally sensitive area in the care of the Royal Society for the Protection of Birds (Royal Society for the Protection of Birds 2013). It is also a Ramsar site (Joint Nature Conservation Committee 2004), a site of special scientific interest (Natural England 2013) and a Special Protection Area (Joint Nature Conservation Committee 2001). It is an internationally important area for wintering waterbirds and regularly supports at least 20,000 waterfowl and waders including the Avocet *Recurvirostra avosetta*, Bewick's Swan *Cygnus columbianus bewickii* and the Golden Plover *Pluvialis apricaria* (Joint Nature Conservation Committee 2001). Breydon Water is of local significance with long distance walking paths forming part of the Wherryman's Way and the Weaver's Way following the northern bank of the estuary (Countryside Access

2013, The Wherryman's Way 2013). These also provide popular bird-watching routes. In addition to this, the area is an historically important UK tourism destination with many nearby holiday parks and attractions.

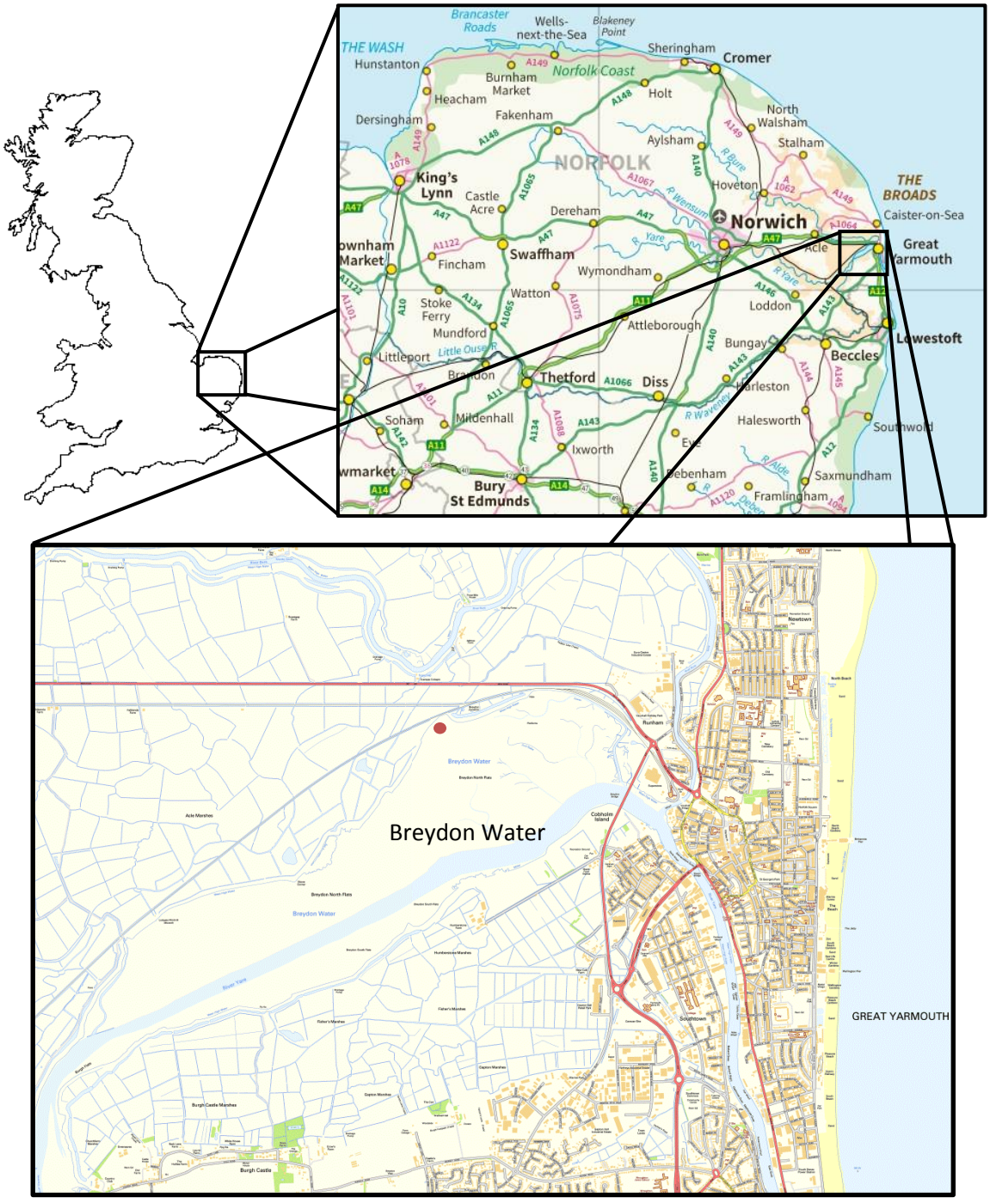

Figure 2.1 | The British, Norfolk and local location of the experimental area (red dot; at N52° 37.030', E01° 41.390') at Breydon Water, Great Yarmouth, UK. Ordnance survey maps from OS OpenData (Ordnance Survey 2013).

The experiments carried out were spread across the experimental area (Figure 2.1) in blocks (Figure 2.2). Each experiment presented in the following chapters was carried out in a separate block. Where experimental setup and data collection was split over two days, in Chapters 4 and 5, each days experimental treatments were in adjacent blocks to reduce any disturbance caused by experimental setup and data collection between the treatments.

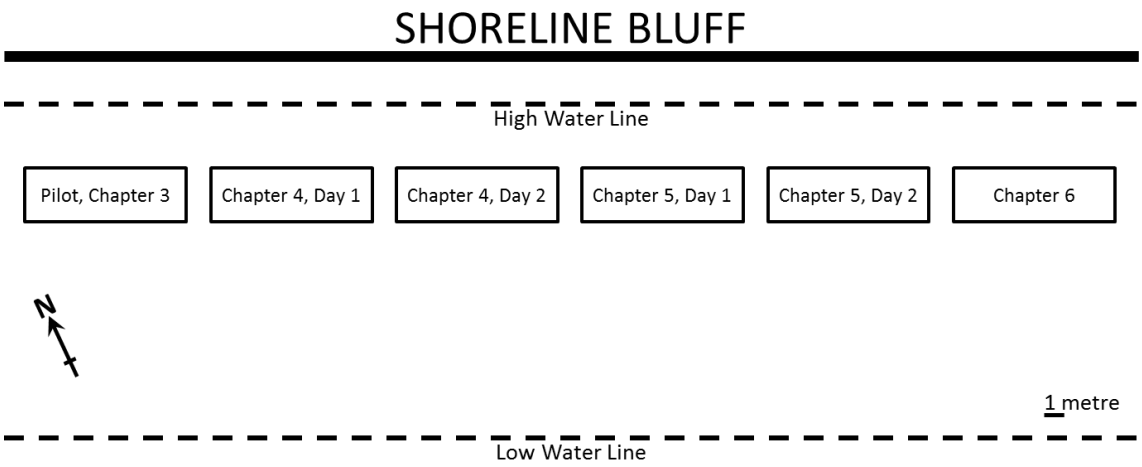

Figure 2.2 | The location of the blocks of experimental treatments on the mudflat at Breydon Water. Each block consists of between 30 to 35 experimental treatments in 3 or 4 rows.

2.2 | *In situ* mesocosm design

The *in situ* mesocosms consisted of a 160 mm diameter plastic drainage pipe, of height 150 mm, with six 45 mm diameter circles cut out equal distances around the top of the pipe such that the tip of the circles were 5 mm from the top (Figure 2.3). Nylon mesh (300 µm) was glued around the top of the pipe using non-toxic aquarium sealant to cover the holes and prevent the unwanted entrance and exit of the organisms being studied. A shaped mesh 'cap' was held on to the top of the mesocosm using cable ties. To collect a sediment core for the experiment, the mesocosm was pushed into the sediment up to the lower edge of the cut-out holes and an intact sediment core removed from the area of mudflat held within the mesocosm. Once allocated to a treatment, movement of species through the bottom of the pipe was prevented by using a layer of 40 µm thick florists cellophane. When returned to the sediment, the mesocosms were pushed

into the sediment with the cellophane still underneath to a depth of 10cm so that the bottom of the 5 cm holes was flush with the sediment surface. When replaced onto the mudflat the cellophane is held against the core by the mud that surrounds it. A more detailed description of how the *in situ* mesocosms were assembled during and after the defaunation procedure is provided in Chapter 3.

Figure 2.3 | The field mesocosms a) before assembly and b) once placed into the mud after fauna manipulation.

To determine species numbers and biomass addition for the different experimental treatments, a few days prior to mesocosm deployment biomass cores of the same size as the sediment cores to be used in the experiments (160 mm in diameter and 70 mm deep), were taken and the species abundance and biomass obtained by weighing the total abundance of each species found in the core. The average total biomass calculated from these samples was used to determine the species biomass to be added during the experiments.

The defaunation procedure and species addition is described in detail in Chapter 3. Once the defaunation or species addition treatments had been applied, the mesocosms were left in the field for up to 2 weeks, depending on the weather conditions. Due to the large effect of rainfall on sediment stability (Torres et al. 2003, Tolhurst et al. 2006c, Pilditch et al. 2008, Tolhurst et al. 2008b), if on the determined day for fieldwork rain was forecast, data collection was delayed.

2.3 | Field measurement and sediment sample collection

The pipe mesocosms were located on the high-shore to enable low tide access to the mesocosms with enough time to take field measurements and collect sediment samples, but also ensure full coverage for a period of at least 3 hours at high tide. On a dry day, the field measurements and sediment samples were collected for each experimental treatment. Two field measurements and two sediment sample types were collected.

2.3.1 | Field measurement 1: The cohesive strength meter

The cohesive strength meter (CSM; Mark IV, Sediment Services, Sussex, UK) is a device used to determine the critical erosion shear stress and the suspension index of surface sediments *in situ* (Tolhurst et al. 1999). The CSM uses a vertical jet of water to measure the force required to erode the sediment surface. The device consists of three parts; a computer and associated electronics held within a watertight case for easy and safe transport to the mudflat that controls the testing process, a pressurised air tank and high pressure hose (Figure 2.4), and a detachable sense head consisting of an inner chamber of 29 mm diameter and a protective outer cylinder of 56 mm diameter (Figure 2.5).

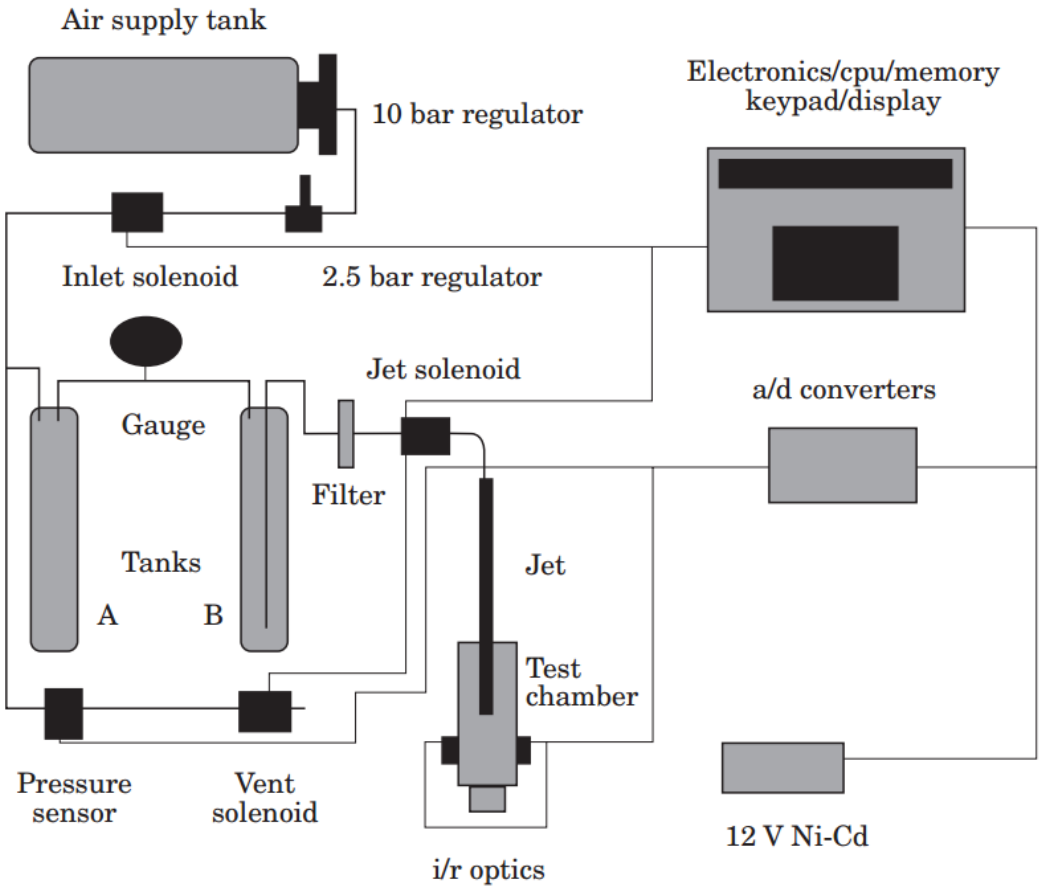

Figure 2.4 | Schematic diagram of the cohesive strength meter (CSM) showing the computer and electronic apparatus making up the main body of the CSM held within the case and the attached air supply tank and test chamber (from Tolhurst et al., 1999).

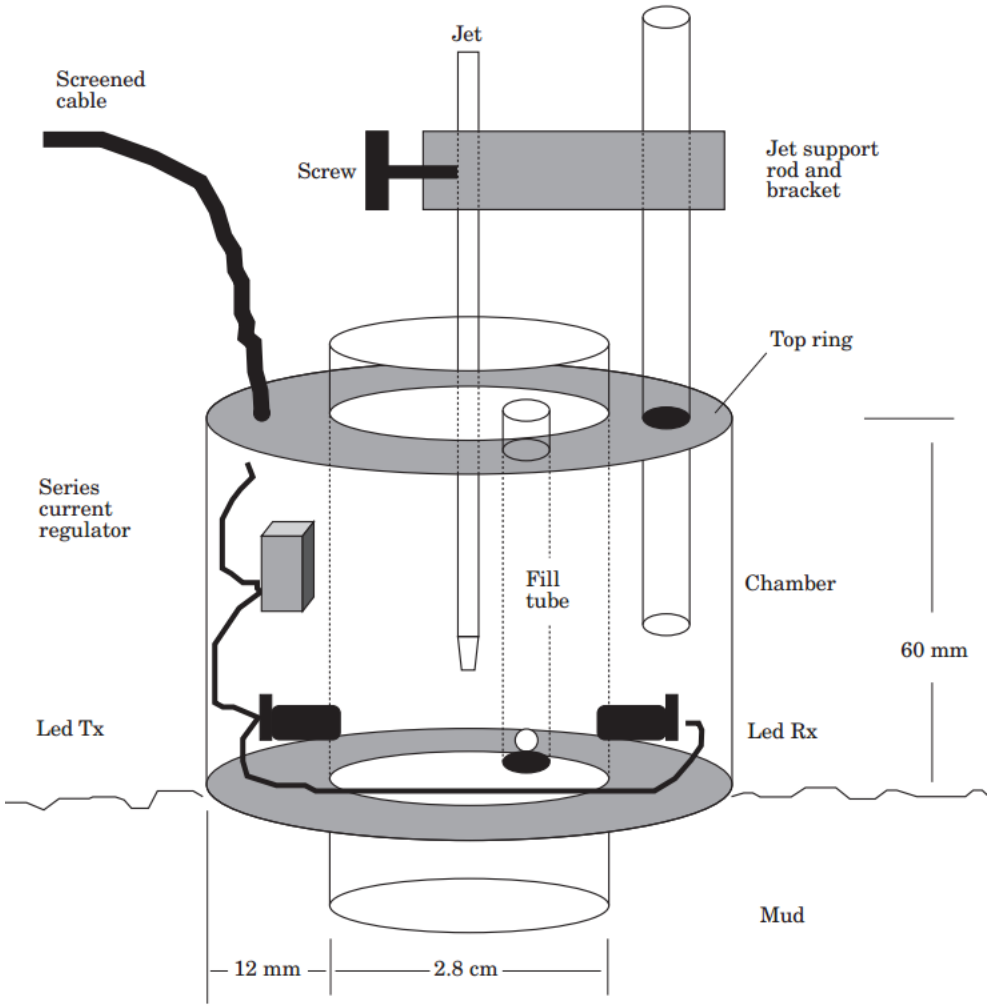

Figure 2.5 | The sense head, chamber and jet apparatus that is pushed into the sediment and fires the jet of water (from Tolhurst et al., 1999).

Prior to running a test, the CSM is set up by attaching the air tank to the body of the CSM via the pressure hose and attaching the sense head via a tube that carries the water to the jet nozzle and an electronic cable for the headlamp and sensor. The test chamber is pushed into undisturbed sediment up to the lower lip (Figure 2.6) and filled by hand with clear ambient estuary water in which the suspended sediment has been allowed to settle out. The jet of water comes from a downward directed nozzle in the chamber located 20 mm above the surface of the sediment. Clear ambient seawater from a reservoir tank within the CSM case is fired out the nozzle at predetermined regulated pressures via the connection of the system to a tank of pressurised air. An erosion test consists of gradually increasing the pressure of the jet of water until the surface particles of the sediment are disturbed and suspended into the chamber. The erosion point is determined by measurement of the transmission of an infra-red beam (known as the headlamp, wavelength 940

nm) across the chamber. This beam is located 10 mm above the sediment surface. Attenuation of the beam is detected by measuring the transmission across the eroding chamber using a spectrally matched receiver on the other side of the chamber (Tolhurst et al. 1999). There are a variety of pre-programmed sediment erosion tests that can be run using the CSM, which have different jet durations and pressure increments. All the tests in this thesis were carried out using the 'Fine 1' test, a test specifically designed for fine sediments that commences the test at a very low jet force and initially raises the jet force in small increments in anticipation of a low erosion threshold, then increasing in large increments at higher pressures. Both personal experience and prior testing at the experimental site determined this to be the most appropriate test type to use.

Figure 2.6 | The cohesive strength meter on the mudflat with the test chamber located in the sediment ready to be filled to run a test.

Once the test chamber is filled with ambient seawater the headlamp is switched on to examine whether emplacing and/or filling of the test chamber resulted in any sediment disturbance. If this is the case, the headlamp transmission value will be low (below 80) and it may be necessary to pick another undisturbed area of sediment nearby and relocate the chamber. If the headlamp reads a suitable value the appropriate test can be selected on the visual display and started. While running the test, the visual display on the main body of the CSM tells the user when the headlamp turns on and

turns off and the strength of the beam being transmitted across the chamber. When the strength of the beam has dropped by at least 10% from the starting transmission value, the point at which the critical erosion threshold of the sediment has been reached (Vardy et al. 2007), the test is complete. The chamber should then be removed from the sediment and rinsed with clear ambient seawater before commencing the next measurement.

2.3.2 | Field measurement 2: The pulse amplitude modulated fluorometer

The pulse amplitude modulated fluorometer (PAM; Diving-PAM, Walz, Effeltrich, Germany; Figure 2.7) provides a quick and reliable assessment of the microphytobenthos minimum fluorescence and the maximum quantum yield of photochemical energy conversion in photosynthesis by applying pulse-modulated light for selective detection of chlorophyll fluorescence yield (Heinz Walz GmbH 1998). These are measured by application of a saturating light pulse, briefly suppressing photochemical yield (Schreiber et al. 1986), which is then calculated and stored by the PAM (Heinz Walz GmbH 1998). The measurement of the minimum fluorescence can be used as a proxy for microphytobenthos biomass on the sediment surface (Honeywill et al. 2002, Eggert et al. 2006, Jesus et al. 2006), while the calculated maximum quantum yield is an indicator of photosynthetic efficiency and health (Maxwell and Johnson 2000).

Figure 2.7 | The Diving-PAM showing the probe sense head and visual display.

To take PAM measurements in the field, custom chambers must be placed over the area of interest to dark adapt the microphytobenthos on the sediment surface for 15 minutes. After dark adaption the probe head is placed against the sediment surface and the measurement button on the PAM used to take a reading. Taking PAM measurements is non-destructive, so these were the first readings to be taken during fieldwork at the experimental site. Three readings, on separate patches of sediment, were taken per replicate in the field (see Figure 2.10). To prevent any chance of data loss readings were noted down in the field from the visual display as a backup. The logged measurements were downloaded from the PAM memory upon return to the laboratory.

The distance between the fibre optic tip of the probe and the surface of the biofilm was kept constant by resting the tip on the sediment surface. This is essential to compare absolute values of fluorescence yields as variations of small distances can cause large variations in the measured values (Jesus et al. 2006). The PAM data are taken in parallel with other

microphytobenthos measurements such as chlorophyll *a* and *b* concentration, which can obtained from the contact cores and are discussed below.

2.3.3 | Sediment sample 1: Minicores

After the PAM measurements had been taken minicores were collected using a 2 cm diameter syringe with the base tip cut off and marked at 1 cm (Figure 2.8) to allow a core of approximate known size to be taken (Underwood et al. 1995). Excess sediment picked up below the depth of 1 cm was scraped away before being transferred to a labelled small plastic bag in the field and frozen at -20°C upon return to the laboratory. These cores were used to determine sediment particle size in the surface sediment to 1 cm depth.

Figure 2.8 | Taking a minicore sample of the mudflat sediment.

2.3.4 | Sediment sample 2: Contact cores

Contact cores were collected using a custom metal disc core after Anderson and Black (1980), and Honeywill et al. (2002). The top part consists of a 'cup' that can hold approximately 30 ml of liquid nitrogen and the bottom part consists of a flat base that rests on the sediment surface with a lip that extends 2 mm into the top layer of the sediment (Figure 2.9). In this way a thin surface core of sediment can be extracted (obtained samples ranged from 1.7 mm to 2.59 mm thick). Upon placement of the sediment core on the sediment surface, liquid nitrogen is poured into the cup and the top layer of sediment freezes and sticks to the corer. The time needed to freeze 2-3 mm of sediment is dependent on the sediment type, water content

and environmental conditions, such as temperature and wind (Honeywill et al. 2002). In these experiments, 45 to 60 seconds was the time required. The core and the frozen sediment was then removed from the sediment surface (while wearing gloves to prevent freezing burns) and the excess sediment frozen to the core from below a depth of approximately 2mm was scraped away until the lower sediment surface was flush with the core lip. The frozen disc can then be removed using a slit to provide a knife access to the base of the core, taking care not to snap the brittle, frozen disc of mud. This disc was then placed into a square of labelled aluminium foil and transferred to a dewar of liquid nitrogen (-196°C). These cores were stored in darkness at -80°C until ready for analysis for biogeochemical properties of the sediment.

Figure 2.9 | A contact core in place on the sediment surface, ready for liquid nitrogen to be poured in to take a core.

2.4 | Layout of field tests and sediment samples

The tests and sediment samples taken for each replicate during an experiment were always carried out in the same order and in the same way. The PAM readings were taken first, with three readings taken in an equilateral triangle, the readings taken at the tips, on both the natural sediment treatments and the mesocosm contained treatments. The seaward most tip of the triangle reading was always taken first followed by the left-hand bottom tip and finally the right hand tip (Figure 2.10). The sediment minicores were then taken from the location of the bottom right PAM reading. The contact core was then taken from the top location of the PAM measurement. Finally, as the CSM measurement has to be taken on

undisturbed sediment, this was taken in approximately the centre of the core depending on where in the core the sediment was flat, undisturbed and without any obvious burrow holes which can confound the test. This was taken last as the removal of the chamber from the test site results in the flooding of the surrounding area with ambient seawater, which could affect any measurements taken later.

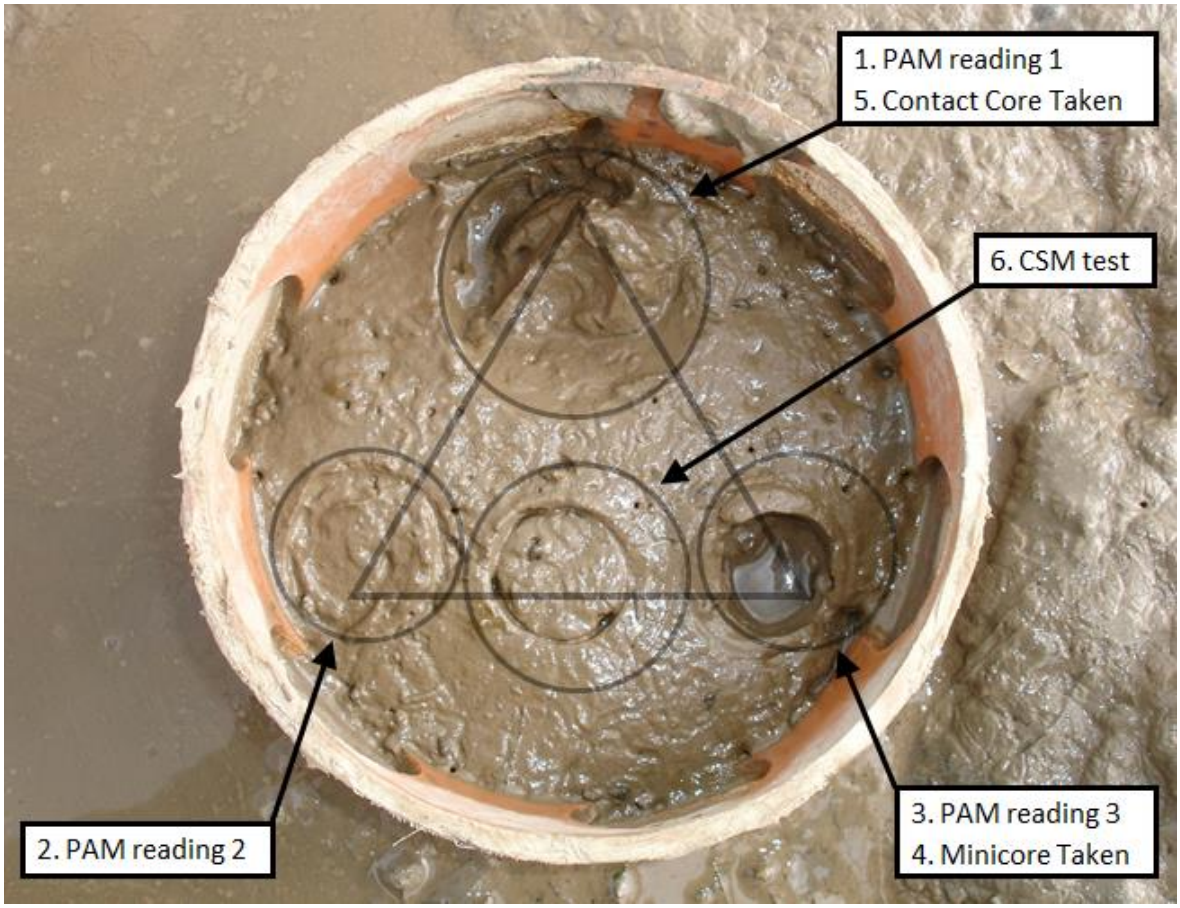

Figure 2.10 | The location of all readings and samples taken during fieldwork within a mesocosm and the order in which they were taken. The top of the picture is seaward.

2.5 | Community composition cores

On the final day of each experiment to ensure successful maintenance of suitable defaunation and monitor community species abundances and/or recovery, samples were collected for benthic macrofauna analysis. Cores were collected using the core mesocosms. Where the treatment was held in a mesocosm the entirety of the sediment bordered by the pipe and the cellophane sheet was transferred to a strong plastic bag containing a label identifier. In the natural sediment treatments (with no mesocosm), a spare

mesocosm was used to take out a sediment core of 16 cm diameter and 7 cm depth.

2.6 | Field data and sediment sample analysis

2.6.1 | CSM data processing

The erosion threshold (ET) is the force of the water jet (in equivalent Nm^2) required to cause enough resuspension of surface sediment to cause a 10% drop in transmission of the infra-red beam across the CSM chamber (Tolhurst et al. 1999, Tolhurst et al. 2000a). The suspension index (S_i) measures the rapidity of the erosion, i.e. the rate of decrease in headlamp transmission with time, using a post processing graphical method (Tolhurst et al. 1999). It provides a semi-quantitative measure of the erosion rate, giving a 'relative erosion rate'. The jet force (Nm^{-2}) applied by the CSM is plotted against the light transmission (Figure 2.11). The gradient of the drop at the point of a 10 % decrease in transmission is the S_i. The infra-red beam transmission across the CSM chamber (after filling with seawater and prior to beginning an erosion data set measurement) can also be used as an indication of sediment erodibility. If this transmission level (known as the starting transmission) is low, then it can be inferred that the sediment surface is loose and has already been suspended. The sediment is therefore erodible at a very low shear stress. This initial suspension of particles is not taken into account in the later ET and S_i calculations as the CSM uses the starting transmission to normalise the data to 100 % and the 10 % drop in transmission is calculated from this 100 % value. Starting transmissions above 80 generally indicate that the chamber has been emplaced and filled without too much disturbance of the sediment surface.

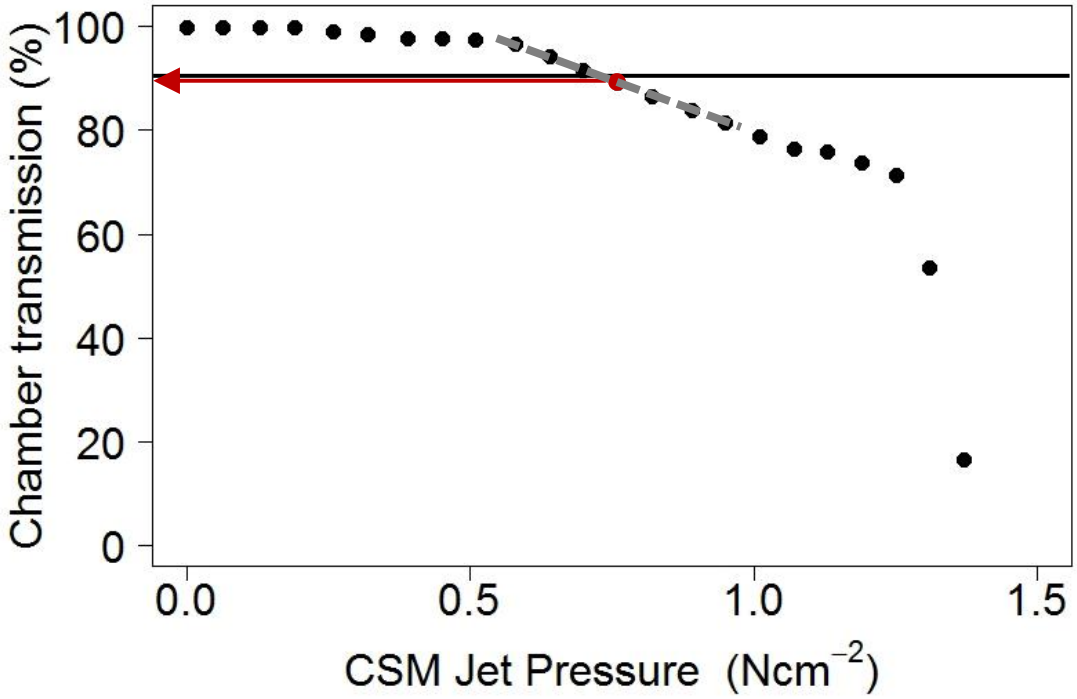

Figure 2.11 | A typical erosion dataset with the erosion threshold and suspension index presented graphically. The solid black line shows the 90% transmission level. The jet pulse at which the transmission value is below this (the red data point) is the erosion threshold. This can be read from the processed CSM data. The suspension index is the gradient of the drop in transmission as the erosion threshold is passed (grey dashed line).

2.6.2 | PAM data processing

The Diving-PAM measures and calculates a range of statistics when taking a reading. For the purpose of microphytobenthos characterisation, this study uses the microphytobenthos minimum fluorescence (F_o), the fluorescence in the absence of photosynthetic light (Maxwell and Johnson 2000), which can be used as a proxy for microphytobenthos biomass (Honeywill et al. 2002), and the maximum quantum yield (Y), the ratio of the variable fluorescence to the maximum fluorescence, a measure of photosystem II efficiency (Heinz Walz GmbH 1998). These measurements were downloaded from the PAM upon return to the laboratory. The three repeated measurements for each of the variables were averaged before statistical analysis.

2.6.3 | Minicore analysis

Sediment minicores were weighed frozen (wet), lyophilised and weighed again (dry) to obtain water content. Sediment water content was calculated using Equation 2.1.

$$\text{Equation 2.1} \qquad \text{Water Content } (\%) = \frac{\text{Weight wet-Weight dry}}{\text{Weight wet} \times 100}$$

The dry sediment was then used for particle size analysis, carried out by laser diffraction using a Mastersizer particle size analyser (Mastersizer 2000, Malvern, Worcestershire, UK). Resulting particle size data were processed using the GRADISTAT program (Version 6; Blott and Pye, 2001) and a geometric method of moments technique to obtain the mean particle size (μm), the mode particle size (μm), sample sorting, the sample skewness, the sample kurtosis, and the particle size which 10 % of the sample is below, known as D_{10} (μm). The geometric method of moments technique uses a log-normal distribution with metric size values following the terminology and formulae specified in Krumbein and Pettijohn (1938). This method is less affected by outliers and is recommended for use in characterising sediments (Blott and Pye 2001). Sample sorting describes the spread of the particle sizes around the average particle size, where well sorted samples have low sorting values due to a low spread of the particle sizes around the average. Sample skewness describes the symmetry or preferential spread to one side of the average, where a log normally distributed sample has a skewness value of 0. Sample kurtosis describes the degree of concentration of the grains relative to the average where a log normally distributed sample has a kurtosis value of 3. Values higher than 3 indicate a leptokurtic distribution, which when presented graphically appears strongly peaked, and smaller values indicate a platykurtic distribution, which appears relatively flat when presented graphically (Blott and Pye 2001). By using a range of statistical analyses, the full effects of the changes in biodiversity and species abundances on the physical sediment characteristics can be examined.

Following the National Marine Biological Analytical Quality Control Scheme Best Practice Guidance for particle size analysis for supporting

biological analysis (Mason 2011) no additional pre-treatment was applied to the samples before particle size analysis.

2.6.4 | Contact core analysis

Before sediment analysis, the contact core depths were measured in three different areas of the contact core using digital callipers (Mitutoyo 500 196-20 Absolute Digimatic Digital Electronic Vernier, Kawasaki, Japan) to calculate a mean depth. The cores were wet weighed, still frozen, then lyophilised and the dry weight measured. These data were used to calculate the sediment water content using Equation 2.1.

The sediment was then subsampled for analysis of chlorophyll *a*, chlorophyll *b*, colloidal carbohydrate and particle size. Chlorophyll analysis was carried out using the N,N-dimethylformamide (DMF) method (Porra et al. 1989). 1.5 ml of DMF was added to between 1.5 and 2.0 g of lyophilised sediment in a small capped vial and swirled gently to mix the sediment and liquid together. The vials were then covered in aluminium foil and left to stand at room temperature for approximately 12 hours. The supernatant was transferred to eppendorf tubes and microcentrifuged for 20 minutes at 9000 rpm before transfer to a 1 ml glass cuvette and measurement of the absorbance of the liquid at the wavelengths 647 and 664 nm. Measurement of the absorbance of the liquid at the wavelength 750 nm provides a turbidity calibration value. Once calibrated for turbidity, chlorophyll *a* and *b* concentrations were calculated in $\mu g ml^{-1}$ using equations 2.2 a, b and c (Porra et al. 1989).

Equation 2.2

a) $$Chl\ a = 12.00\ A^{664} - 3.11\ A^{647}$$

b) $$Chl\ b = 20.78\ A^{647} - 4.88\ A^{664}$$

c) $$Chl\ a + b = 17.67\ A^{647} + 7.12\ A^{664}$$

A number of studies have shown colloidal carbohydrate to be a good biochemical predictor of sediment stabilisation (Underwood and Paterson 1993, Yallop et al. 2000, Friend et al. 2003a). Colloidal carbohydrate was extracted following Underwood et al. (1995) and quantified using the Dubois assay (Dubois 1956). One ml of distilled water was added to 5 mg of

lyophilised sediment and vortexed. After centrifugation at 2500 rpm for 15 minutes, 0.5 ml of supernatant was decanted into a glass boiling test tube. Following the phenol-sulphuric acid assay, 0.5 ml of 5 % phenol and 2.5 ml of 98 % analytical grade sulphuric acid was added, the sample was vortexed, and left for 35 minutes for the reaction colour to develop (after Taylor and Paterson, 1998). If carbohydrates are present a straw like colour develops. The supernatant was then decanted into a 1 ml cuvette and a spectrophotometer used to measure the absorbance at 485 nm. This absorbance value is then converted into a colloidal carbohydrate concentration of μg glucose equivalents ml^{-1} using a standard curve. The resulting value can then be expressed as a mass of glucose equivalents per mass of dry sediment (μg mg^{-1}).

The chlorophyll, carbohydrate and water contents were converted to a mass per volume using Equation 2.3. Data were expressed in this way to avoid to problems of expressing data as a mass per grams of dry sediment (Flemming and Delafontaine 2000, Perkins et al. 2003, Tolhurst et al. 2005).

Equation 2.3

$$\text{Concentration per volume} = \frac{\text{Content per gram of dry sediment}}{\text{Contact core volume}}$$

Particle size analysis for the contact cores was carried out with the remaining sediment as described above for the minicore analysis.

2.6.5 | Community composition core analysis

To determine species abundances on the last day of each experiment, the whole of the mesocosm core was collected for each treatment measured that day and taken back to the laboratory. These cores were sieved immediately through a 5 mm sieve used to break up the sediment, and a 500 μm sieve to retain the macrofauna. The macrofauna and sieve residue was then preserved using 10 % buffered formalin solution and left for at least 24 hours. This residue was then washed and picked for macrofauna and the macrofauna enumerated, weighed damp, and preserved in alcohol. These data were used to check the experimental control treatments for sufficient

defaunation and to determine the final species composition of the experimental cores.

2.7 | Statistical analysis

Statistical models were developed to assess the effects of species identity, species richness, and species biomass distribution on the measured sedimentary variables. Contributions of species mixtures were assumed to be synergistic rather than additive (Ieno et al. 2006) and each species combination, whether monoculture, single species dominated or mixed, was treated as a unique identity (Solan et al. 2008). Initially a linear regression model was fitted and assessed for homogeneity of variance and outlying values (Cook's distance) following Zuur et al. (2009a). Exploratory plots (Q-Q plots) revealed much of the data showed different residual spread per treatment for many of the variables, violating the homogeneity of variance assumption, one of the most important assumptions of linear regression (Zuur et al. 2009b). The linear model approach is therefore not suitable for analysis of much of the data. One solution to this would be data transformation to restore the homogeneity of variance, however this was avoided due to the fact that heterogeneity is a characteristic of the data that can also provide interesting ecological information, which, using a nonlinear mixed modelling technique, can be incorporated into the statistical analysis of the data (Zuur et al. 2009b). When heterogeneity of variance was identified in the data, a generalised least squares estimation procedure using a VarIdent variance-covariance structure was used (Pinheiro and Bates 2000, West et al. 2006, Zuur et al. 2007) that allows the residual spread to vary with individual explanatory variables.

The most appropriate model was determined using manual backwards stepwise selection of model terms using maximum likelihood methods informed by Akaike Information Criteria (AIC) and inspection of model residual patterns. The optimal variance covariate structure was determined by comparing the initial analysis of variance model without variance structure to the equivalent generalised least squares model incorporating specific variance structures using AIC and visualisation of model residuals obtained by restricted maximum likelihood (REML) estimation. The optimal fixed

structure was then determined by applying backward selection using the likelihood ratio test obtained using maximum likelihood (ML) estimation (Diggle et al. 2002, West et al. 2006). These analyses were performed in R (Version 2.15.13; R Core Team, 2013) using the mixed modelling and nonlinear mixed effects package (nlme) (Pinheiro et al., 2013).

To determine how the changes in species biomass and diversity of the species mixtures influenced species activity, and consequently the changes in the sediment properties measured, the principles of both transgressive and non-transgressive overyielding were used (Loreau 1998, Fridley 2001, Petchey 2003, Griffin et al. 2009) to compare species performances at low and high densities and in monoculture and mixture (Figure 2.12). Overyielding (calculated value > 0) occurs when a mixture outperforms the corresponding monocultures. The specific statistics calculated and comparisons made are detailed in the relevant chapters.

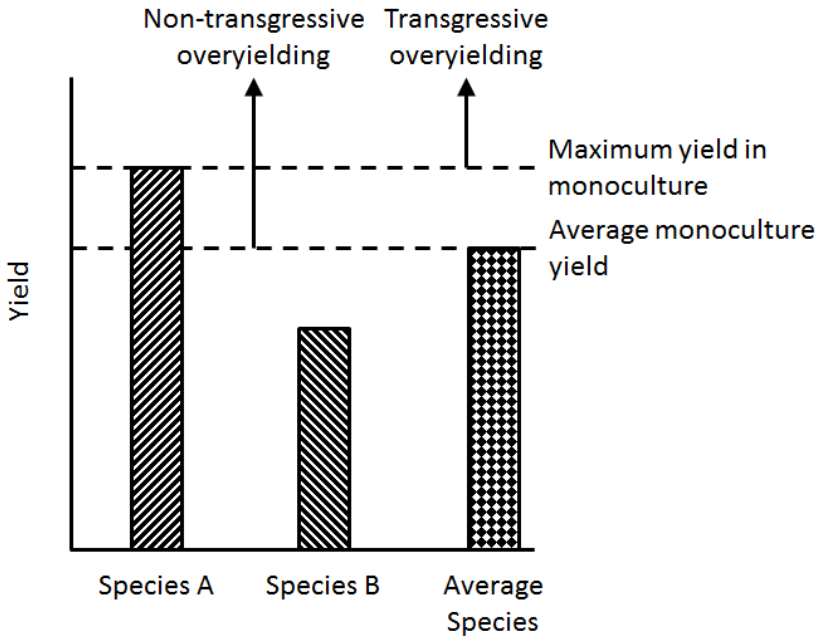

Figure 2.12 | A schematic diagram of the two types of overyielding. Two monocultures (Species A and Species B) and their average yield (Average Species) are shown. If the species mixture yield is greater than the average monoculture yield the species mixture overyields non-transgressively. If the species mixture yield is greater than the maximum yield in monoculture the species mixture overyields transgressively. (After Fridley, 2001)

For more details on the rationale and statistical methods used in this thesis please refer to the retrospective reflection section on page 301.

Chapter 3 | Development of a New Defaunation Technique

3.1 | Introduction

To determine the effects of single species in isolation and multiple species combinations on sediment erodibility and biogeochemical properties with any accuracy, first the total or majority of the ambient fauna must be removed. Previous studies looking at the effects of single species and multiple species combinations on mudflats in both the laboratory and *in situ* have predominantly used disruptive methods of defaunation (see Table 3.1). This disruption can cause significant changes to the sediment properties and to biota other than macrofauna (Tolhurst et al. 2012). Choosing the appropriate method of defaunation is very important if experimental interpretations are not to be confounded by the effects of the disturbance caused by the defaunation (Tolhurst et al. 2012). Disruptive methods of defaunation include sieving through various sieve sizes from 300 μm to 2 mm, removal and freezing of sediment, commercially purchasing an experimental material, baking and drying in an oven, air drying for various periods of time, sediment agitation, and washing with fresh or distilled water. Non-disruptive methods can include removal and freezing as whole cores, picking out the larger conspicuous animals, purging the overlying water with nitrogen to induce anoxia which kills the animals or forces them up to the surface, covering with material for various amounts of time to induce anoxia, addition of 30 % sodium chloride solution into the overlying water, and addition of formalin *in situ*. There appears to be no standardised method of defaunation (Tolhurst et al. 2012), with many studies using a combination of methods (Table 3.1). Freezing, in isolation or in combination with other techniques, is by far the most popular method.

Table 3.1 | Some of the various different approaches used to defaunate sediments historically.

Reference	Defaunation Method															Details
	Sieving	Air Drying	Heating	Combustion	Freshwater	Saltwater	Formalin	Refridgeration	Freezing	Fauna Picked	Covering	Anoxia	Agitation	Substitution	Pestcide	
Bell and Devlin, 1983			●													Heated at 121°C for 15 min
Bell and Devlin, 1983													●			Stirred with wire brush
Chandler and Fleeger, 1983									●							Frozen at -20°C 3+ times
Gallagher et al., 1983														●		Used commercially purchased sand
Levin, 1984		●											●			Air dried
Whitlach and Zajac, 1985		●														Air dried for 1 week
Crowe et al., 1987					●											Freshwater for 5 days
Service and Bell, 1987													●			Raking for 20 minutes
Fegley, 1988			●		●											Freshwater, heating at 50°C
Savidge and Taghon, 1988	●								●							300 µm sieved, frozen
Thrush and Roper, 1988									●							Frozen for 10 days
Berge,1990									●							Frozen
Kern, 1990			●													Heating at 200°C for 3 hours
Olafsson and Moore, 1990									●	●						Large organisms picked out, frozen
Hansen and Blackburn, 1991										●	●	●				Covered for 24 hours, anoxia, organisms removed
Pechenik and Cerulli, 1991	●								●							Sieved, frozen
Olafsson and Moore, 1992									●							Frozen
Snelgrove et al., 1992					●				●							Frozen, freshwater
Thrush et al., 1992	●								●							2mm sieved, frozen
Flemer et al.,1993								●			●					Covered for 6 weeks at 4°C
Ruth et al., 1994									●							Frozen for 3 days
Gamenick et al., 1996											●					Covered with PVC foil for 1 month
Gilbert et al, 1996												●				N_2 purged to anoxia
Thrush et al., 1996											●					Covered with black plastic and concrete slabs for 3 weeks
Hall and Frid, 1997									●							Frozen at -18°C for 48 hours
Hansen and Kristensen, 1997												●				N_2 purged to anoxia
Schaffner et al., 1997										●		●				N_2 purged to anoxia, organisms removed
Turner et al., 1997									●							Frozen
Wu and Shinn, 1997		●														Air dried for 1 month
Beukema et al., 1999											●					Covered with synthetic material for 3 months
Ford et al., 1999									●							Frozen at -18°C for 12 hours
Hsieh and Hsu, 1999									●							Frozen at -70°C for 7 days twice
Lee, 1999		●														Air dried for several weeks
Bostrom and Bonsdorff, 2000														●		Used commercially purchased sand
Christensen et al., 2000	●															Sieved
Lu and Wu, 2000		●														Air dried for 1 month
Sandnes et al., 2000						●										30% NaCl solution
De Deckere et al., 2001															●	Sprayed with insecticide over four days
Emmerson et al., 2001	●								●							Frozen at -18°C for 2 weeks, thawed, refrozen
Heilskov and Holmer, 2001												●				N_2 purged to anoxia
Kline and Stekoll, 2001					●	●		●	●							Frozen at -20°C for 1 week, room temperature 1 week, freshwater, saltwater, refrigeration at 4°C for 6 weeks, 0°C 1 day
Stocks and Grassle, 2001											●					Sediment enclosed in plastic bags for 2-3 weeks
Zhou, 2001				●												Combustion at 500°C for 3 hours
Biles et al., 2002	●								●							Frozen at -18°C for 6 days, thawed, homogenised
Bolam et al., 2002											●					Covered with wooden boards
Flemer et al., 2002		●							●							Frozen, air dried
Raffaelli et al., 2003									●							Frozen at -18°C for 6 days, thawed, homogenised
Faraco and Lana, 2003			●													Heated at 80°C for 2 days
Biles et al., 2003	●															500 µm sieved
Bolam et al., 2004									●							Frozen at -20°C for 3 days, thawed, refrozen three times
Mermillod-Blondin et al.,2005	●															1 mm sieved
Negrello Filho et al., 2006							●									40% formalin
Arroyo et al., 2006	●								●							500µm sieved, frozen at -18°C for 48h
Guerra-Garcia and Garcia-Gomez, 2006		●	●						●		●					Frozen at -20°C, thawed at 40°C, air dried for 2 months, stored in dark
Ieno et al., 2006	●															500 micron sieved
Norkko et al., 2006											●					Covered with polyethylene
Dyson et al., 2007	●															500 micron sieved
Bulling et al., 2008	●															500 micron sieved
Montserrat et al., 2008											●					Covered with polyethylene sheet for 40 days
Van Colen et al., 2008											●					Covered with polyethylene sheet for 40 days
Godbold et al., 2009	●															500 micron sieved
Guerra-Garcia and Garcia-Gomez, 2009			●						●							Frozen for 3 days, heated at 40°C three times
Murphy and Tolhurst, 2009															●	Sprayed with pesticide on days 1, 10 and 16
Braeckman et al., 2010	●								●							1 mm sieved, frozen at -20°C for 6 weeks
Botter-Carvalho et al., 2011											●					Covered with polyethylene

Tolhurst et al. (2012) carried out an experimental review of five different defaunation methods, examining the efficiency of defaunation and how these methods affected the properties of the sediments being studied. Changing the properties of the sediments may cause secondary changes in the macrofauna or microphytobenthos independently of the hypotheses being tested (Tolhurst et al., 2012). The methods tested were: removal and laboratory freezing of sediment, removal and oven-heating, freezing *in situ* with liquid N_2, spraying with formalin *in situ* and spraying with hydrogen peroxide *in situ*. The following properties of the sediment were measured after defaunation: erosion threshold, suspension index (relative erosion rate), minimal fluorescence (F_o), photosynthetic yield (F_v/F_m), water content, grains greater and less than 63 µm, chlorophyll *a* and *b* concentration, total carbohydrate concentration, and colloidal carbohydrate concentration. There were no significant effects of any defaunation treatment on water content, grain size, total carbohydrate and suspension index (Tolhurst et al. 2012). Removal of the sediment for freezing and heating caused major changes to the sediment because of the disturbance involved (Tolhurst et al. 2012). *In situ* use of formalin and hydrogen peroxide caused persistent changes after 4 days in some sediment properties, such as chlorophyll *a* and *b* concentration and sediment mud content. *In situ* freezing with liquid nitrogen showed no persistent effects and this method was deemed the least destructive method that caused the least persistent and smallest changes to sediment properties. However, the method of freezing, using a metal frame pushed 1 cm into the mud and pouring 4 litres of liquid nitrogen onto the surface of the sediment, was not a very effective defaunator with only 52 ± 10 % (n = 6) of the sediment fauna killed (Tolhurst et al. 2012). This is at least partly due to the fact that only the surface sediment is frozen, allowing certain macrofauna to retreat deeper into the sediment to survive.

3.2 | Methodology development

To complete the experiments addressing the objectives outlined in Section 1.7 and enable the manipulation of macrofaunal biodiversity, an effective method of defaunation was needed that was easily replicated in the field, would minimise disturbance to the sediment and keep the natural sediment structure intact. Properties such as particle size distribution and

the presence of burrow holes can affect a number of sediment processes such as nutrient flux, the erosion threshold and rate, and sediment permeability, which in turn can alter other sediment properties and processes. Thus, it was important to minimise any effects of defaunation upon these properties in my experiments. Freezing *in situ* was chosen as a suitable method to trial for effective defaunation.

3.2.1 | Methodology 1 testing

The first protocol trialled involved using a 30 cm square, plastic, 7 cm deep walled quadrat, gently pushed into the top 2 cm of the sediment to hold the liquid nitrogen in a small area enabling localised freezing. Volumes of either 1.5 L or 3 L of liquid nitrogen were poured onto the surface of the sediment (n = 3). While trialling this method visual observations in the field indicated that with the volumes used (16.6 to 33.3 litres per m^2) only the top 2 to 4 cm of sediment were frozen, so any organisms present deeper in the sediment were less likely to be killed, or suffer any effects of freezing. No effort was made to prevent organismal migration into or out of the frozen area.

Defaunation efficacy was then tested by taking round sediment cores of 10 cm diameter and 10 cm deep and comparing the frozen cores to natural, unfrozen sediment cores. The frozen cores were compared to control cores 1 and 7 days after the freezing treatment. One day after freezing, species abundance had been reduced by an average of 2 % in the cores treated with 1.5 litres and 45 % in the cores treated with 3 litres compared to the control cores (Table 3.2). By day seven this had increased to a reduction of 7 % in the cores treated with 1.5 litres and 61 % in the cores treated with 3 litres. It can be seen that the use of 3 litres of liquid nitrogen for defaunation of the cores was much more effective than just 1.5 litres. After 1 day the cores treated with 1.5 litres of liquid nitrogen had only a 0.08 Bray-Curtis dissimilarity index, and after 7 days only a 0.11 Bray-Curtis dissimilarity index. The cores treated with 3 litres of liquid nitrogen had a 0.31 Bray-Curtis dissimilarity index after 1 day and a 0.44 Bray-Curtis dissimilarity index after 7 days (see Appendix 1). However, this defaunation was not deemed sufficient, particularly in the case of the species *Hediste diversicolor*.

Table 3.2 | Average species abundance reduction caused by defaunation using methodology 1 compared to natural, undisturbed sediments (n = 3). All average fractions of fauna have been rounded up to the nearest whole integer.

	Control cores	Day 1				Day 7			
		1.5 litres	Average Difference	3 litres	Average Difference	1.5 litres	Average Difference	3 litres	Average Difference
Total abundance	176 ± 6.72	172 ± 5.21	-2 %	96 ± 9.90	-45 %	164 ± 6.13	-7 %	68 ± 11.7	-61 %
Total species	9 ± 0.71	7 ± 0.47	-22 %	8 ± 0.71	-11 %	6 ± 0.27	-33 %	5 ± 0.71	-44 %
Hediste diversicolor	9 ± 0.71	7 ± 1.25	-22 %	9 ± 2.47	0 %	5 ± 0.27	-44 %	9 ± 0.71	0 %
Hydrobia ulvae	2 ± 1.06	0 ± 0	-100 %	1 ± 0.35	-50 %	0 ± 0	-100 %	1 ± 0.35	-50 %
Corophium volutator	131 ± 1.77	141 ± 14.06	+8 %	69 ± 15.9	-47 %	139 ± 13.37	+65 %	54 ± 12.4	-59 %
Macoma balthica	20 ± 2.47	14 ± 0.72	-30 %	6 ± 1.41	-70 %	10 ± 1.52	-50 %	1 ± 0.35	-95 %
Spionidae spp.	5 ± 3.54	3 ± 1.19	-40 %	1 ± 0.71	-80 %	0 ± 0	-100 %	0 ± 0	-100 %
Tubificidae spp.	4 ± 1.77	1 ± 0.27	-75 %	4 ± 1.77	0 %	1 ± 0.27	-75 %	0 ± 0	-100 %
Tubificoides benedii	1 ± 0.71	3 ± 0.72	+ 200 %	4 ± 0.71	+300 %	6 ± 0.98	+500 %	0 ± 0	-100 %
Ampharete sp.	1 ± 0.35	0 ± 0	-100 %	0 ± 0	-100 %	0 ± 0	-100 %	0 ± 0	-100 %
Philine sp.	3 ± 0	3 ± 0.27	0 %	2 ± 0	-33 %	3 ± 0.27	0 %	3 ± 0.71	0 %

There were a number of other drawbacks to this method, including the necessity to carry a 4 litre dewar of liquid nitrogen across the mud while wearing enough personal protective equipment. The physical act of pouring the liquid nitrogen onto the sediment often resulted in a high level of disruption to the sediment surface, the area of interest when determining sediment erosion threshold and relative erosion rate. For the larger manipulative experiments being planned using 3 litres or more of liquid nitrogen per replicate would be prohibitive for a PhD thesis. For an experiment of 30 replicates it would be necessary to take 90 litres of liquid nitrogen into the field. It was hypothesised that if the depth of freezing could be increased and if the method of freezing could be altered so that less liquid nitrogen was needed, this methodology could be more effective at defaunation and thus more useful for experiments manipulating fauna, therefore an improved methodology was designed and trialled.

3.2.2 | Methodology 2 testing - Cryo-defaunation

The second methodology involved a different approach using constructed mesocosms (described in Section 2.2). The mesocosms were used carefully to remove a 7 cm deep sediment core from the mudflat which was then transferred to a custom built 16.5 cm^2 polystyrene cryochamber. A cellophane base was placed under the pipe mesocosm to hold in the core and the cellophane, pipe and sediment core placed within a holder caddy to keep the structure together while freezing. The caddy consisted of a thin 1 cm deep base made from the same material as the pipe mesocosm, and therefore held the cellophane onto the base of the pipe snugly, with two wires looped over to form handles. This enabled the whole assemblage to be lowered into and out of the freezing apparatus ensuring no contact between the operator and the liquid nitrogen. Once the sediment core was placed in the caddy the core was lowered into the cryochamber which was then filled with 2 litres of liquid nitrogen (Figure 3.1). To assist freezing the centre of the sediment core, the part most insulated by the mud, a thin metal rod was inserted into the centre of the core to conduct heat away from the centre of the core, with minimum sediment disturbance. Personal protective equipment and clothing was worn by the operator at all times.

Figure 3.1 | The cryochamber used to enable freezing of a whole core of sediment. A lid is placed on top after the liquid nitrogen is added to retain the cold in the chamber.

As the liquid nitrogen is allowed to flow around the bottom of the core, ensured by the 1 cm deep caddy base, and around the side in the cryochamber the cold from the liquid nitrogen can penetrate the core from all directions, enabling the whole core of sediment to freeze. The lid was then placed on the cryochamber and the core left for 5 minutes. After 5 minutes the core is taken out and physically inspected to determine effectiveness of freezing. Cores usually came out of the cryochamber covered in a thin layer of frost. Once removed, the cores were left for an additional 15 minutes to ensure effective freezing, as upon return to the mud defrosting occurred quickly due to equilibration of the core temperature with the surrounding warmer mud.

The cores were then replaced onto the mudflat with the cellophane still underneath. The core was placed to ensure the base of the round holes was at the sediment surface, with the sediment within the core at the same level as that outside the core and the surrounding sediment pushed back up

against the core to fill the gap created during core removal and replacement. Pushing the sediment against the core prevented loosening of the core and it being lost due to scouring and washing away. The mesh lid was then cable tied onto the top of the core *in situ*.

Preliminary trials of this method indicated that upon examination of the cores after 5 minutes in the cryochamber and 15 minutes rest, the sediment was effectively frozen throughout. To test the efficacy of defaunation, five cores were taken back to laboratory and passed carefully through a 500 µm sieve to retain any macrofauna. All macrofauna were counted and scored as either living or dead after observation of the sieving residue (Table 3.3). It can be seen that this cryo-defaunation method is more effective at reducing the majority of the individuals of all the species present except for *Hediste diversicolor*, of which an average of 71 % are killed.

Table 3.3 | Macrofauna live or dead counts after defaunation with liquid nitrogen using the custom cryochamber.

Species	Core 1		Core 2		Core 3		Core 4		Core 5	
	Live	Dead	Live	Dead	Live	Dead	Live	Dead	Live	Dead
Hediste diversicolor	7	12	5	18	7	14	4	16	6	13
Hydrobia ulvae	0	41	0	32	0	48	0	31	0	61
Corophium volutator	0	252	0	190	2	229	0	224	1	250
Macoma balthica	0	20	0	12	0	12	0	14	0	15
Spionidae spp.	0	0	0	0	0	0	0	0	0	1
Tubificidae spp.	0	2	0	10	0	9	1	13	0	10
Tubificoides benedii	0	0	0	0	0	0	0	1	0	3
Tanaidacea sp.	0	0	0	0	0	0	0	0	0	1

A further test of the cryochamber freezing protocol was carried out by examining the defaunation efficacy under conditions similar to that of the proposed manipulative experiments. Undisturbed natural sediment cores were compared with both natural sediment cores held within one of the mesocosms and cryo-defaunated sediment held within the mesocosms after two weeks in the field, the proposed length of time after which the sediment properties of the experimental treatment plots would be examined for any changes to sedimentary properties, to determine the effects of both the mesocosms and the freezing. Defaunation in this method was shown to greatly reduce the faunal abundance within the cores, especially the three species of interest (Table 3.4). There was an overall reduction in species abundance of 78% and a reduction of the three species of interest of greater than 72%. The frozen sediments showed a 0.65 Bray-Curtis dissimilarity index from the control cores and a 0.54 Bray-Curtis dissimilarity index from the mesocosm sediments (Appendix 1).

Table 3.4 | Average species abundance reduction caused by cryo-defaunation and mesocosm presence compared to natural, undisturbed sediments 2 weeks after cryo-defaunation (n = 6). All average fractions of fauna have been rounded up to the nearest whole integer.

	Control cores	Mesocosm only	Average Difference	Cryo-defaunated	Average Difference (control cores)	Average Difference (mesocosm cores)
Total abundance	336	245	-27 %	74	-78 %	-70 %
Total species	8	8	0 %	7	-13 %	-13 %
Hediste diversicolor	18	14	-22 %	5	-72 %	-64 %
Hydrobia ulvae	42	25	-40 %	8	-81 %	-68 %
Corophium volutator	205	144	-30 %	32	-84 %	-78 %
Macoma balthica	38	29	-24 %	9	-76 %	-69 %
Spionidae spp.	6	10	+66 %	3	-50 %	-70 %
Tubificidae spp.	16	13	-19 %	14	-13 %	+8 %
Tubificoides benedii	1	3	+200 %	3	+200 %	0 %
Ampharete sp.	10	7	-30 %	0	-100 %	-100 %

The cryo-chamber defaunation method is good at removing the sediment surface based fauna, such as *Hydrobia ulvae* and *Corophium volutator*, however it is not as good at removing the deeper living species such as *Hediste diversicolor*.

This method is more disruptive than pouring the liquid nitrogen directly onto the mudflat as it requires the removal of a core to freeze it in the cryo-defaunation chamber, however sediment disturbance during this process was kept to a minimum. Using the cryo-chamber actually causes less disruption of the sediment surface, the area of interest for studies concerned with sediment erosion, as it does not require the liquid nitrogen to be poured directly on the sediment surface, which usually caused dislodgement of some sediment particles. This cryo-defaunation method allows the liquid nitrogen to flow over the sediment surface gently as the liquid nitrogen is initially poured down the edge of the cryo-chamber. This method is also better than transporting sediment back to the laboratory for freezing, where vibration during transport can disrupt the sediment structure and, in extreme cases, cause liquefaction (Tolhurst et al. 2000b).

When examined during the live or dead analysis the sediment was frozen throughout the whole core, therefore any organisms that have survived the cryo-defaunation process have survived freezing temperatures. A more efficient method of defaunation may have been to disturb the sediment more. It is possible that longer or repeated freezing may further reduce the numbers of *Hediste*, however this would require the transport of more liquid nitrogen into the field and repeated freezing effort. As with any methodology used for defaunation, there is a trade-off between experimental effort, method efficacy, disturbance minimisation and cost, therefore a compromise must be made. After two weeks in the field the reduction in abundance of the species of interest is still significant, and this method was deemed suitable to provide a defaunation method for the thesis. After completion of the experiment, the treatment sediment cores were collected for species enumeration to monitor species defaunation and addition efficacy.

Using this method of cryo-defaunation, a pilot experiment was carried out to examine the feasibility of doing a large scale experiment with

replicates in the field to examine the effects of two mudflat species on sediment stability and a subset of biogeochemical properties. An experiment designed to determine the effects of two mudflat species in single species dominant communities, *Hediste diversicolor* and *Hydrobia ulvae*, was selected.

3.3 | Pilot experiment

The pilot study was carried out on the tidal mudflats at Breydon Water, Great Yarmouth between the 13th of April and the 5th of May 2012. Five treatments with 7 replicates each were representatively allocated to 35 plots or mesocosms on the mudflat high shore in a 3 by 28 m area. Due to the loss of a number of replicates during the experiment the total number of experimental plots was reduced to 22. Treatments consisted of control treatment (n = 6), two procedural control treatments and two fauna manipulations (all other treatments n = 4). The control treatment (N) was natural undisturbed sediment not held within a mesocosm. The procedural control treatments were one of cryo-defaunated sediment held within a mesocosm (PD) and one where sediment was defaunated but was placed back onto the mudflat without a surrounding pipe mesocosm (D) so movement of species into the defaunated sediments was not prevented and species recolonisation could occur. The two fauna manipulation treatments consisted of defaunated sediment with the total biomass replaced by an equal biomass of either *Hediste diversicolor* (HD) or *Hydrobia ulvae* (HU), held within a mesocosm. Total macrofauna species biomass was determined by collecting four cores of the same size as those used for the experimental treatments and weighing the species present in the sample. These cores contained 0.44 ± 0.20 g of macrofaunal biomass, equivalent to 21.83 ± 9.90 g per m^2, consisting of predominantly *Hediste diversicolor*, *Corophium volutator* and *Hydrobia ulvae*.

3.3.1 | Experimental setup and data collection

Experimental setup was carried out following the cryo-defaunation method, as described in Section 3.2.2, however the sediment cores frozen in this experiment were of a depth of 10 cm. This was later reduced to 7 cm for the set of experiments presented in this thesis due to low efficacy of

defaunation (see Section 3.3.2). *Hediste diversicolor* and *Hydrobia ulvae* collected adjacent to the experimental site were added to the appropriate treatment mesocosms by removing the mesh lids, placing the organisms on the surface of the sediment and replacing the lids again.

After 14 days, sediment characteristics were measured using the CSM and PAM and minicore samples taken following the procedures laid out in Sections 2.3.1, 2.2.2 and 2.3.3 respectively. Data analysis was carried out following Sections 2.6.1 (CSM data), 2.6.2 (PAM data), and 2.6.3 (minicore analysis). For minicore analysis, the mean particle size (μm) and D_{10} (μm) were selected as sample measures to analyse for the pilot experiment. Statistical analysis was carried out using a generalised least squares approach in R following Section 2.7.

3.3.2 | Results

To test the efficacy of the cryo-defaunation method used in this experiment the species abundances of the control cores were compared to those of the defaunated control cores. The defaunation method caused an average 49 % drop in the abundance of *Hediste diversicolor*, an average 47 % drop in the abundance of *Hydrobia ulvae*, an average 45 % drop in the abundance of *Corophium volutator* and an average total drop in species abundance of 47 %. The cryo-defaunation method used in this pilot study is slightly different from the refined method described in Section 3.2.2 in that sediment cores of 10 cm were frozen in the cryochamber. This was later deemed to be too large a sediment core for effective freezing throughout the core and the depth of sediment core used was changed to 7 cm for all further experiments.

The pilot study was also used to determine whether there would be temporal effects of measuring a range of variables on the mudflat over the low tide period would significantly affect the results obtained as a number of previous studies have shown measurements taken with the CSM and PAM to vary over the tidal cycle. Diatom migrations that occur in the upper surface layers over the tidal cycle can affect PAM fluorescence measurements (Consalvey et al. 2004a, Consalvey et al. 2004b, Jesus et al. 2005) and

sediment stability (Paterson 1989, Tolhurst et al. 2003, Tolhurst et al. 2006a) and sediment water draining as the tide recedes can affect sediment stability (Paterson et al. 1990, Tolhurst et al. 2006a).

In this study the starting transmission was not found to vary significantly over time due to tidal or other influences (Figure 3.2; Linear regression; Adj-R^2 = 0.09, p = 0.097).

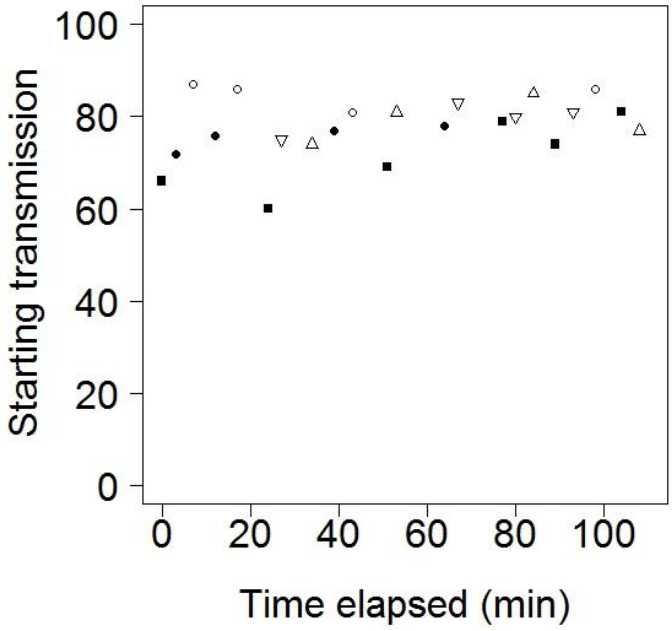

Figure 3.2 | Cohesive strength meter (CSM) starting transmission variation with time elapsed (min) since data collection commencement where the first measurement was taken at time 0 minutes (n = 22). Where ■ represents the natural core, ● represents the defaunated core, ○ represents the defaunated core held in a mesocosm, △ represents the core with biomass replaced by *Hediste diversicolor* and ▽ represents the core with biomass replaced by *Hydrobia ulvae*.

Visually, the erosion threshold showed a reduction in variability over the period of the experiment, with the highest erosion thresholds (i.e. the sediments which were more stable and required a greater force of the jet to erode) found within the first hour of the data collection (Figure 3.3; Linear regression; Adj-R^2 = 0.08, P = 0.1149), suggesting that unequal drainage of the mudflats is causing variations in sediment stability over the initial period of the measurements. Measurements in future experiments were taken longer after site exposure as the sediment showed less variation in erosion threshold after 45 minutes (Figure 3.3). It should be noted that all the erosion thresholds measured are within usual ranges for natural sediment where erosion thresholds of 2 Nm^{-2} and below are considered the normal range (Amos et al. 1992, Amos et al. 1997, Defew et al. 2002).

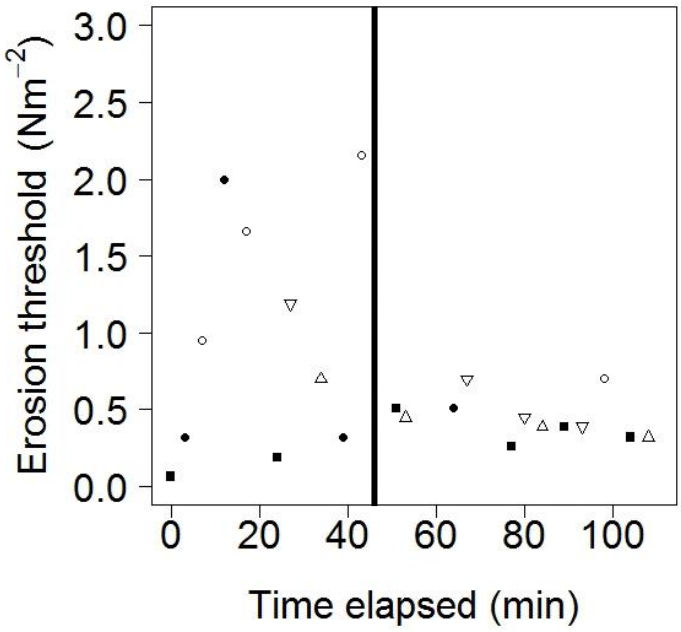

Figure 3.3 | Erosion threshold measurement (Nm^{-2}) variation with time elapsed (min) since data collection commencement where the first measurement was taken at time 0 minutes (n = 22). Where ■ represents the natural core, ● represents the defaunated core, ○ represents the defaunated core held in a mesocosm, △ represents the core with biomass replaced by *Hediste diversicolor* and ▽ represents the core with biomass replaced by *Hydrobia ulvae*. The line indicates when data collection commenced in the later experiments in Chapters 4, 5 and 6, after which the erosion threshold had stabilised after mudflat tidal dewatering.

The suspension index did not vary throughout the duration of the experiment (Figure 3.4; Linear regression; Adj-R^2 = 0.01, P = 0.2904), indicating that the suspension index, while quite variable, does not have any temporal trends.

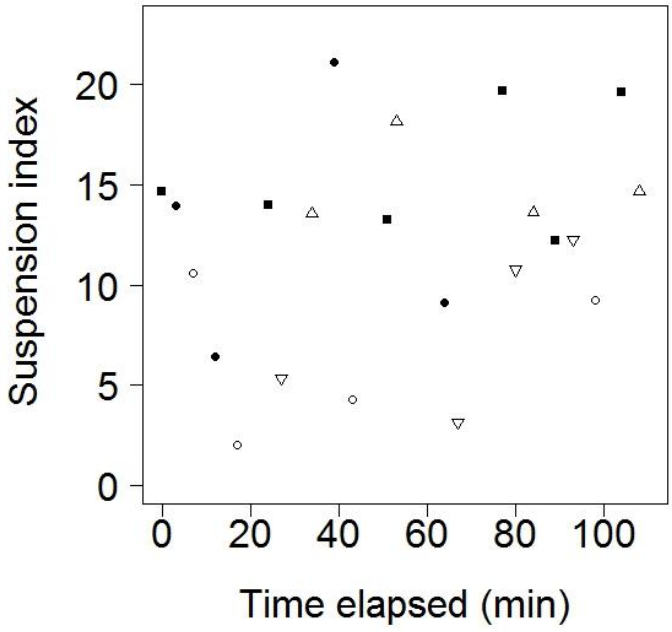

Figure 3.4 | Suspension index variation with time elapsed (min) since data collection commencement where the first measurement was taken at time 0 minutes (n = 22). Where ■ represents the natural core, ● represents the defaunated core, ○ represents the defaunated core held in a mesocosm, △ represents the core with biomass replaced by *Hediste diversicolor* and ▽ represents the core with biomass replaced by *Hydrobia ulvae*.

The pulse amplitude modulation measured minimum fluorescence did not vary throughout the duration of the experiment (Figure 3.5; Linear regression; Adj-R^2 = -0.008, p = 0.3697), indicating that the behaviour or photosynthetic activity of the microphytobenthos present on the sediment surface does not change over the period of data measurement. The minimum fluorescence values appear to be more controlled by sediment or species treatment than the time when they were measured.

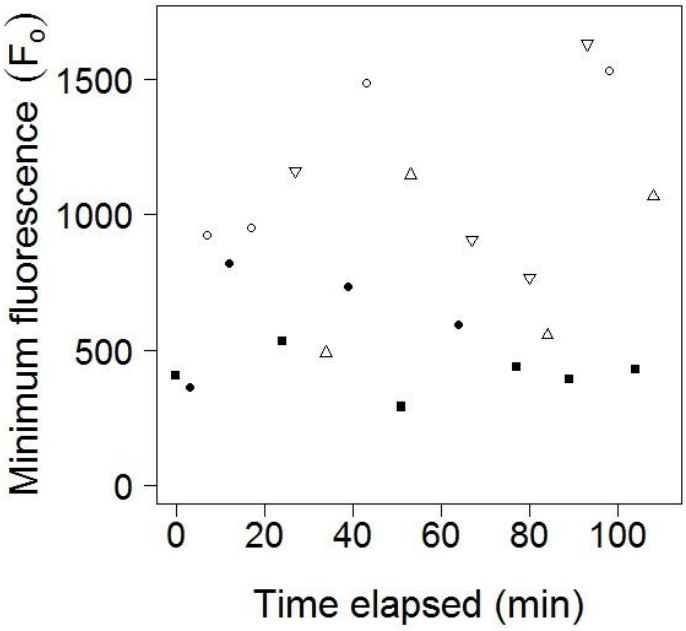

Figure 3.5 | Minimum fluorescence (F_o) of the microphytobenthos variation with time elapsed (min) since data collection commencement where the first measurement was taken at time 0 minutes (n = 22). Where ■ represents the natural core, ● represents the defaunated core, ○ represents the defaunated core held in a mesocosm, △ represents the core with biomass replaced by *Hediste diversicolor* and ▽ represents the core with biomass replaced by *Hydrobia ulvae*.

The pulse amplitude modulation measured maximum quantum yield did not vary throughout the duration of the experiment (Figure 3.6; Linear regression; Adj-R^2 = 0.07, p = 0.1313), indicating that the photosynthetic efficiency of the microphytobenthos present on the sediment surface does not change over the period of data measurement.

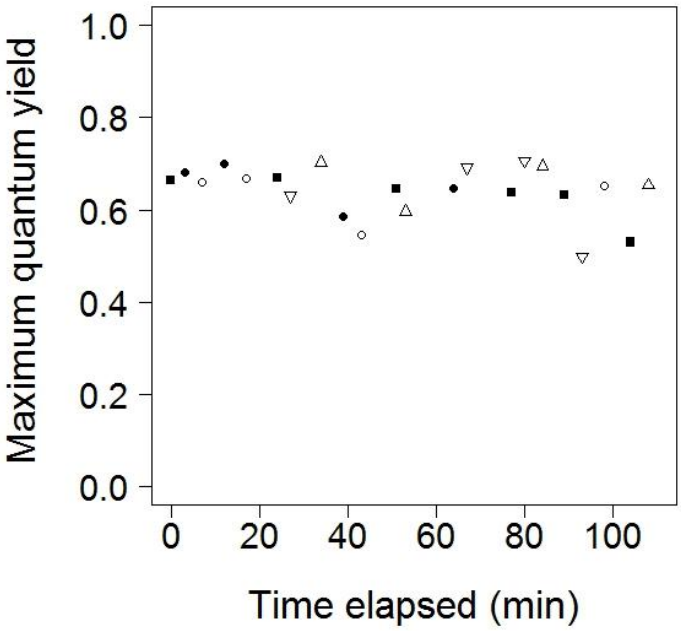

Figure 3.6 | Photosynthetic maximum quantum yield value of the microphytobenthos variation with time elapsed (min) since data collection commencement where the first measurement was taken at time 0 minutes (n = 22). Where ■ represents the natural core, ● represents the defaunated core, ○ represents the defaunated core held in a mesocosm, △ represents the core with biomass replaced by *Hediste diversicolor* and ▽ represents the core with biomass replaced by *Hydrobia ulvae*.

The sediment mean particle size (µm) did not vary throughout the duration of the experiment (Figure 3.7; Linear regression; Adj-R^2 = -0.042, p = 0.7032), indicating that there is no change in particle size over the duration of the data collection caused by tidal retreat or sediment water draining.

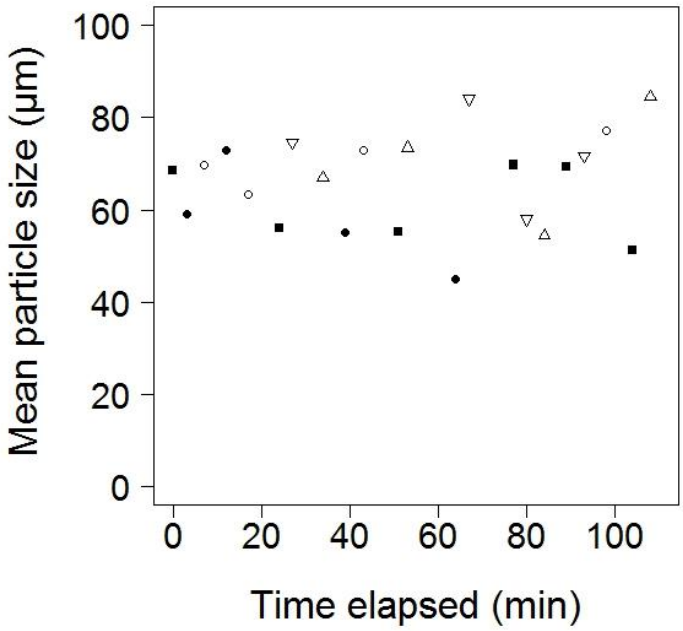

Figure 3.7 | Mean particle size (µm) variation with time elapsed (min) since data collection commencement where the first measurement was taken at time 0 minutes (n = 22). Where ■ represents the natural core, ● represents the defaunated core, ○ represents the defaunated core held in a mesocosm, △ represents the core with biomass replaced by *Hediste diversicolor* and ▽ represents the core with biomass replaced by *Hydrobia ulvae*.

The sediment particle D_{10} (µm) did not vary throughout the duration of the experiment (Figure 3.8; Linear regression; Adj-R^2 = -0.043, p = 0.7253), indicating that there is no shift in particle size to the coarse or fine fraction over the duration of the data collection caused by tidal retreat or sediment water draining.

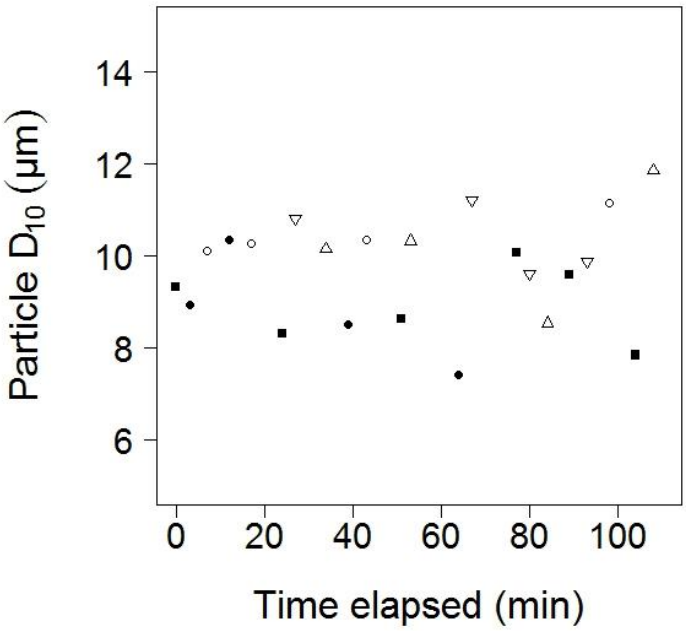

Figure 3.8 | Particle D_{10} (µm) variation with time elapsed (min) since data collection commencement where the first measurement was taken at time 0 minutes (n = 22). Where ■ represents the natural core, ● represents the defaunated core, ○ represents the defaunated core held in a mesocosm, △ represents the core with biomass replaced by *Hediste diversicolor* and ▽ represents the core with biomass replaced by *Hydrobia ulvae*.

The sediment mud content (%) did not vary throughout the duration of the experiment (Figure 3.9; Linear regression; Adj-R^2 =-0.045, p = 0.7708), indicating that there is no shift in particle size to the fine fraction or loss of smaller mud particles over the duration of the data collection caused by tidal retreat or sediment water draining.

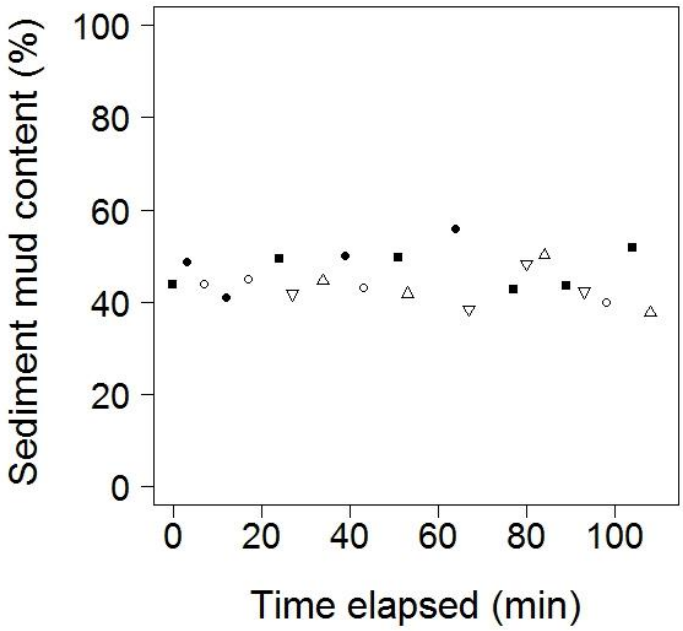

Figure 3.9 | Sediment mud content (%) variation with time elapsed (min) since data collection commencement where the first measurement was taken at time 0 minutes (n = 22). Where ■ represents the natural core, ● represents the defaunated core, ○ represents the defaunated core held in a mesocosm, △ represents the core with biomass replaced by *Hediste diversicolor* and ▽ represents the core with biomass replaced by *Hydrobia ulvae*.

As previous studies have identified a relationship between species abundances and sediment properties and shore height (Paterson et al. 2000, Davidson et al. 2004) the effect of 'Row' was examined (where Row 3 was highest on the shore and Row 1 lowest). The effect of row location (n = 6) was tested against three variables; the erosion threshold (ET, Nm^{-2}), the PAM measured minimum fluorescence (F_o) and the minicore sediment particle size D_{10} (µm). All three variables showed no significant variation with row location of mesocosm (ET: Figure 3.10; L-ratio = 2.36, d.f. = 6, p = 0.3067, F_o: Figure 3.11; L-ratio = 0.17, d.f. = 6, p = 0.9185; D_{10}: Figure 3.12; L-ratio = 0.69, d.f. = 6, p = 0.7072).

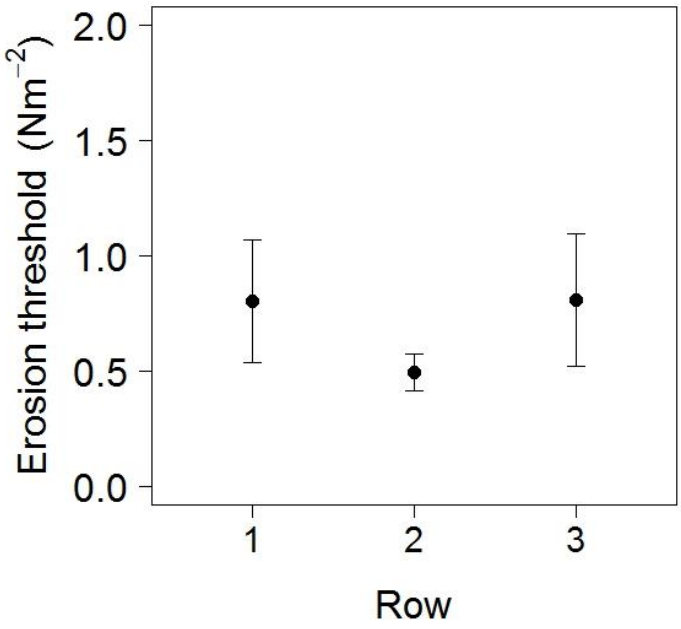

Figure 3.10 | Effect of row of mesocosm location on the sediment erosion threshold (Nm^{-2}; n = 6). Error bars are standard error. 1, Row 1; 2, Row 2; 3, Row 3; where Row 1 was highest on the shoreline.

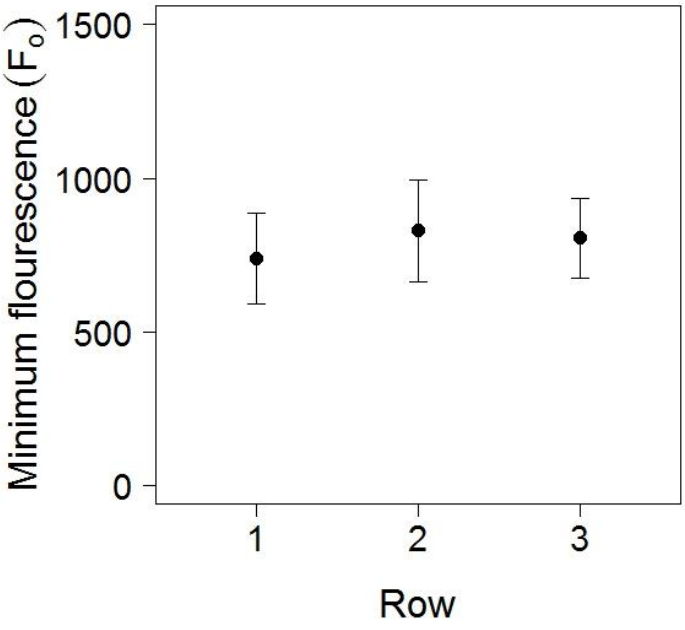

Figure 3.11 | Effect of row of mesocosm location on the pulse amplitude modulated measured minimum fluorescence (F_o; n = 6). Error bars are standard error. 1, Row 1; 2, Row 2; 3, Row 3; where Row 1 was highest on the shoreline.

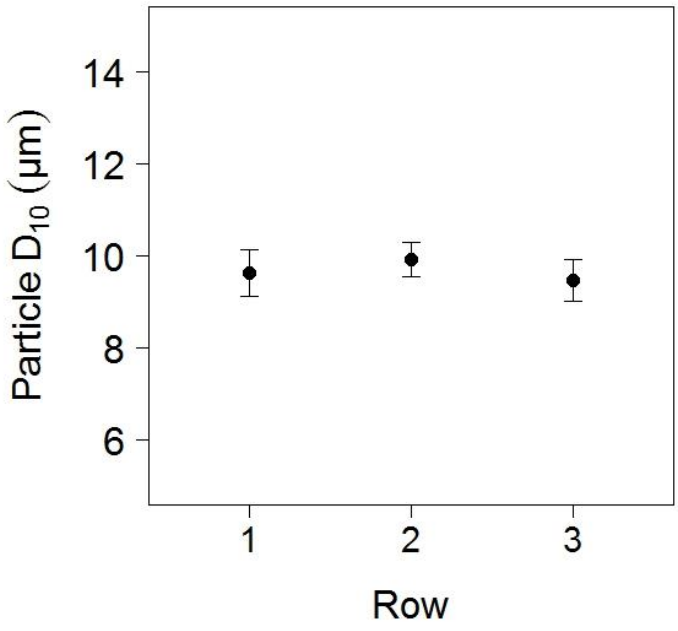

Figure 3.12 | Effect of row of mesocosm location on minicore particle size D_{10} (µm; n = 6). Error bars are standard error. 1, Row 1; 2, Row 2; 3, Row 3; where Row 1 was highest on the shoreline.

As there was no effect of treatment row location on three of the main variables the data were analysed together regardless of 'Row'. It was not possible to undertake a two-way analysis of treatment and row due to the fact this would have reduced the replicates (degrees of freedom) for the interaction terms too much.

The mudflat at Breydon Water had a small erosion threshold (Figure 3.13; N; meaning it is easily erodible under low current speeds. Sediment defaunation and species re-addition had a significant effect on sediment erodibility (Nm^{-2}; L-ratio = 12.35, d.f. = 10, p = 0.0149). The cryo-defaunated treatment held inside a mesocosm (PD) had a larger mean (± 95 % CI, n = 4) erosion threshold (1.37 ± 1.06 Nm^{-2}) than the natural mudflat sediments (N; n = 6; 0.29 ± 0.16 Nm^{-2}; t = 3.18, p = 0.0055) and the sediments that had been defaunated with the total species biomass replaced by *Hediste diversicolor* (HD; 0.47 ± 0.26 Nm^{-2}; t = 2.63, p = 0.0176).

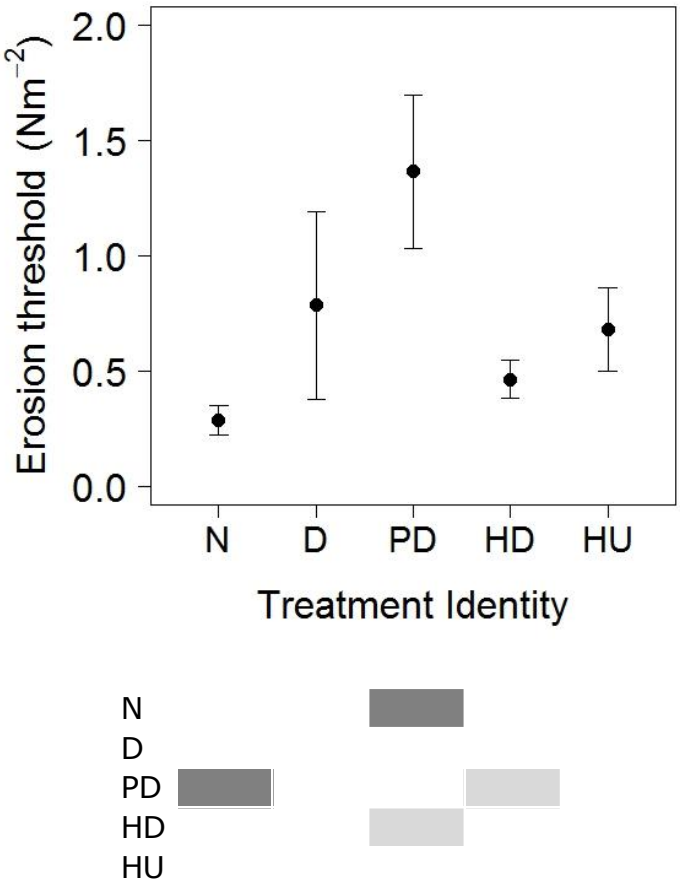

Figure 3.13 | Effect of sediment defaunation, mesocosm presence and species identity on the sediment erosion threshold (Nm^{-2}; n = 4). Error bars are standard error. The species composition of each mixture is indicated on the x-axis, where treatment identity corresponds to: N, natural sediment as a mudflat baseline; D, cryo-defaunated sediment replaced onto the mudflat without a mesocosm; PD, cryo-defaunated sediment replaced onto the mudflat in a mesocosm as an experimental control; HD, sediment cryo-defaunated with the original species biomass replaced with *Hediste diversicolor*; HU, sediment cryo-defaunated with the original species biomass replaced with *Hydrobia ulvae*. Significant differences are indicated in the accompanying table where darker shading indicates greater significant difference: 0.01 < p < 0.05; 0.0001 < p < 0.01; p < 0.0001.

Sediment defaunation and species re-addition had a significant effect on sediment erosion rate (L-ratio = 14.34, d.f. = 10, p = 0.0063). The mean (± 95 % CI, n = 6) suspension index of the natural sediments at Breydon Water was the largest (Figure 3.14; N; 15.57 ± 3.43), meaning it erodes at the fastest rate of all the treatments, and was greater than the mean (± 95 % CI, n = 4) suspension index of the cryo-defaunated treatment held inside a mesocosm (PD; 6.54 ± 6.45; t = 3.72, p = 0.0017) and the sediment that

was cryo-defaunated with the original species biomass replaced with *Hydrobia ulvae* (HU; 7.88 ± 6.88; t = 3.02, p = 0.0077). The cryo-defaunated sediment held inside a mesocosm (PD) also had a smaller mean (± 95 % CI, n = 4) suspension index than the sediment that was cryo-defaunated with the original species biomass replaced with *Hediste diversicolor* (HD; 15.01 ± 3.43; t = -3.69, p = 0.0018).

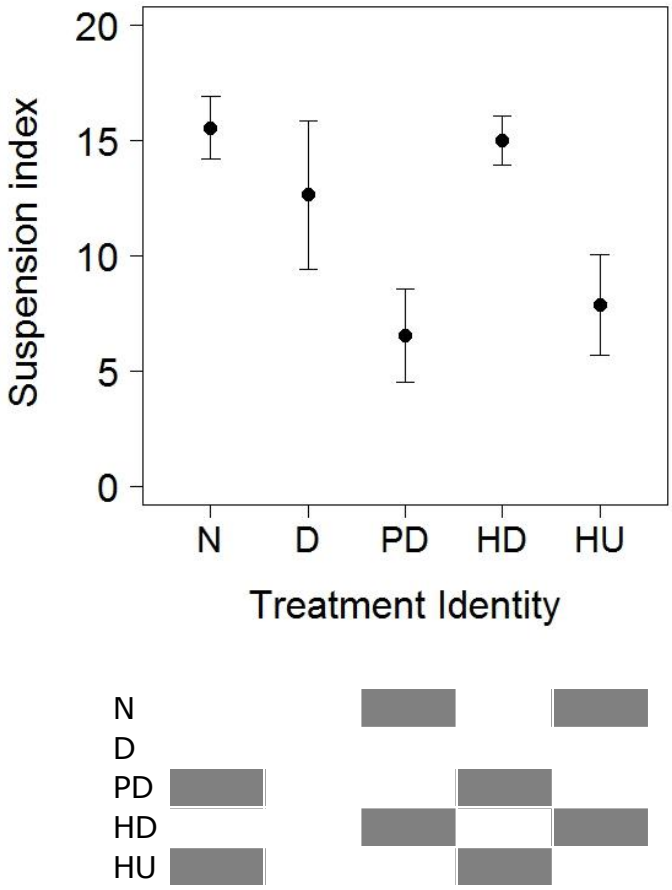

Figure 3.14 | Effect of sediment defaunation, mesocosm presence and species identity on the sediment suspension index (n = 4). Error bars are standard error. Treatment identity as in Figure 3.13. Significant differences are indicated in the accompanying table where darker shading indicates greater significant difference: 0.01 < p < 0.05; 0.0001 < p < 0.01; p < 0.0001.

Sediment defaunation and species re-addition had a significant effect on sediment microphytobenthos biomass (F_o; L-ratio = 22.92, d.f. = 10, p < 0.0001). The natural sediments had a small mean (± 95 % CI, n = 6) pulse amplitude modulated measured minimum fluorescence (Figure 3.15; N; 413.94 ± 82.19), smaller than that of the cryo-defaunated sediment held inside a mesocosm (PD; 1222.00 ± 523.37; t = -4.82, p = 0.0002), the sediment that was cryo-defaunated with the original species biomass

replaced with *Hediste diversicolor* (HD; 813.91 ± 538.77; t = -2.32, p = 0.0329) and the sediment that was cryo-defaunated with the original species biomass replaced with *Hydrobia ulvae* (HU; 1115.58 ± 603.69; t = -3.65, p = 0.0020). The defaunated sediments returned to the mudflat without a mesocosm (D; 627.08 ± 316.17) had a smaller mean (± 95 % CI, n = 4) minimum fluorescence than the defaunated sediments held within a mesocosm (PD; t = -3.10, p = 0.0066) and the sediment that was cryo-defaunated with the original species biomass replaced with *Hydrobia ulvae* (HU; t = -2.28, p = 0.0357).

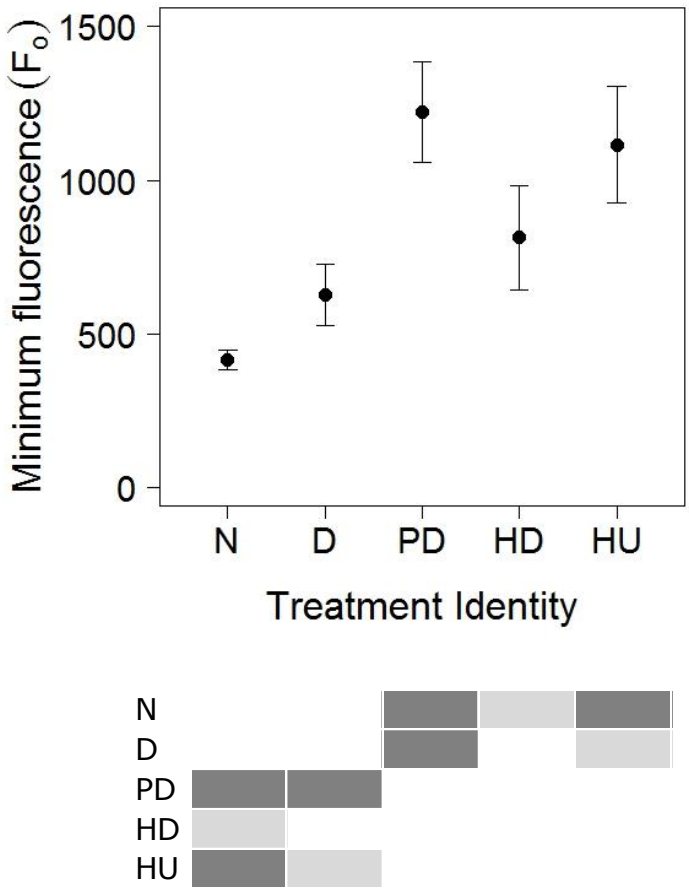

Figure 3.15 | Effect of sediment defaunation, mesocosm presence and species identity on the pulse amplitude modulated measured minimum fluorescence (n = 4). Error bars are standard error. Treatment identity as in Figure 3.13. Significant differences are indicated in the accompanying table where darker shading indicates greater significant difference: ▒ 0.01 < p < 0.05; ▓ 0.0001 < p < 0.01; ■ p < 0.0001.

There was no effect of sediment defaunation, mesocosm presence or the replacement of the natural species biomass with *Hediste diversicolor* or *Hydrobia ulvae* on the pulse amplitude modulated measured maximum quantum yield (Figure 3.16; L-ratio = 1.77, d.f. = 10, p = 0.7777).

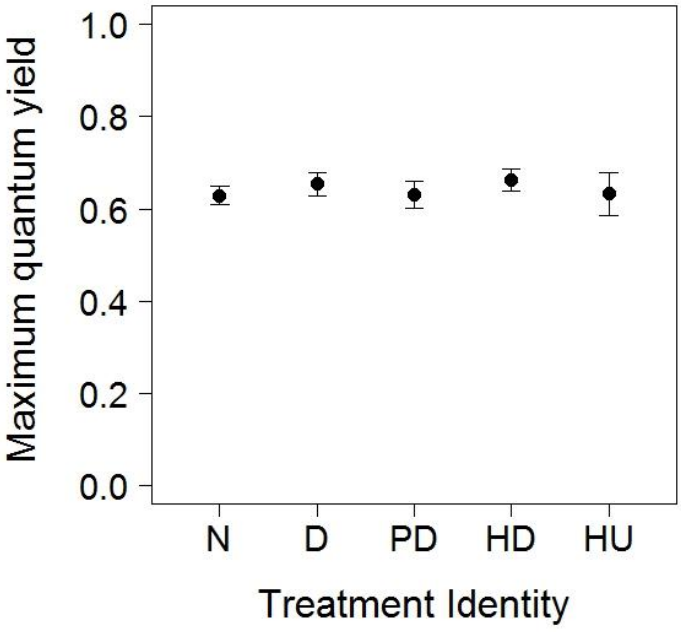

Figure 3.16 | Effect of sediment defaunation, mesocosm presence and species identity on the pulse amplitude modulated measured maximum quantum yield (n = 4). Error bars are standard error. Treatment identity as in Figure 3.13.

The minicore sediments were classified as either very fine sand or very coarse silt under the GRADISTAT program scale (Blott and Pye 2001). There was no effect of sediment defaunation, mesocosm presence or the replacement of the natural species biomass with *Hediste diversicolor* or *Hydrobia ulvae* on the minicore sediment mean particle size (μm; Figure 3.17; L-ratio = 7.77, d.f. = 10, p = 0.1003).

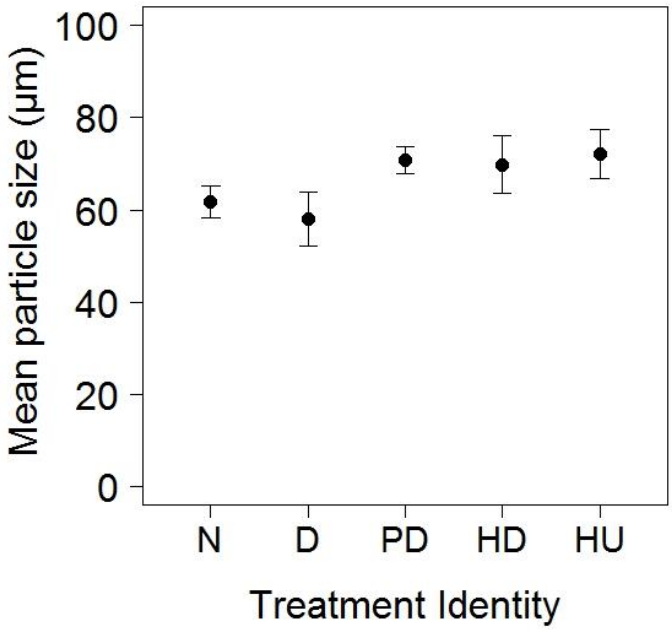

Figure 3.17 | Effect of sediment defaunation, mesocosm presence and species identity on the minicore sediment mean particle size (μm; n = 4). Error bars are standard error. Treatment identity as in Figure 3.13.

Sediment defaunation and species re-addition had a significant effect on minicore sediment particle D_{10} (µm) (L-ratio =13.45, d.f. = 10, p = 0.0093). Minicore sediment particle size D_{10} (µm) did not vary greatly among treatments, however the cryo-defaunated sediment held inside a mesocosm (PD; 10.47 ± 0.74 µm) had a larger mean (± 95 % CI, n = 4) particle D_{10} than the natural sediments (Figure 3.18; N; n = 6; 8.96 ± 0.88 µm; t = 3.63, p = 0.0021) and the defaunated sediments returned to the mudflat without a mesocosm (D; 627.08 ± 316.17 µm; t = 2.56, p = 0.0204). The sediment that was cryo-defaunated with the original species biomass replaced with *Hydrobia ulvae* (HU; 10.38 ± 1.20 µm) had a larger mean (± 95 % CI, n = 4) particle D_{10} than the natural sediments (N; n = 6; t = 2.78, p = 0.0128) and the defaunated sediments returned to the mudflat without a mesocosm (D; t = 2.20, p = 0.0416).

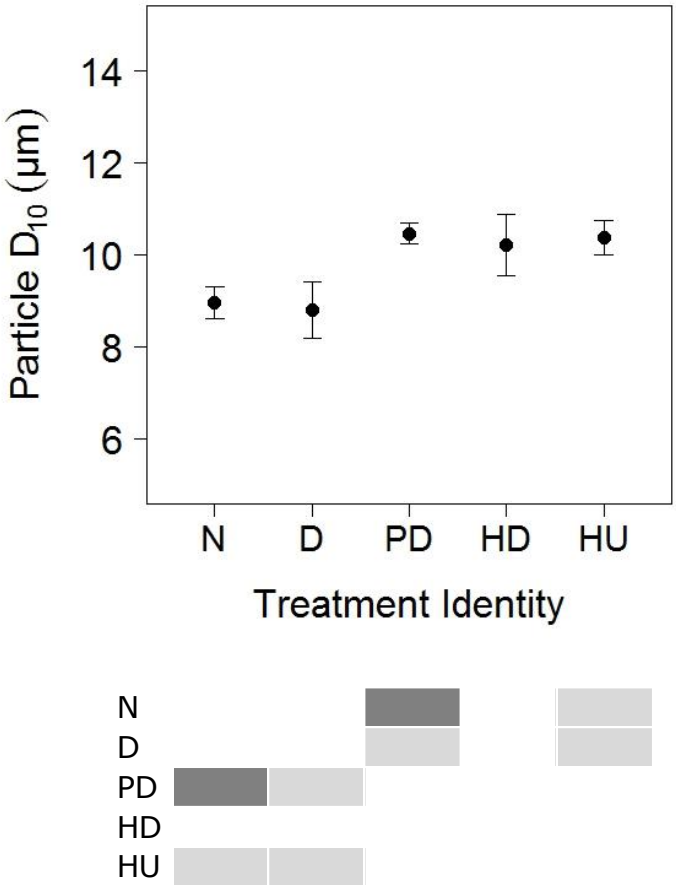

Figure 3.18 | Effect of sediment defaunation, mesocosm presence and species identity on the minicore sediment particle size D_{10} (µm; n = 4). Error bars are standard error. Treatment identity as in Figure 3.13. Significant differences are indicated in the accompanying table where darker shading indicates greater significant difference: 0.01 < p < 0.05; 0.0001 < p < 0.01; p < 0.0001.

There was no effect of sediment defaunation, mesocosm presence or the replacement of the natural species biomass with *Hediste diversicolor* or *Hydrobia ulvae* on the minicore sediment mud content (%; Figure 3.19; L-ratio = 6.84, d.f. = 6, p = 0.1445).

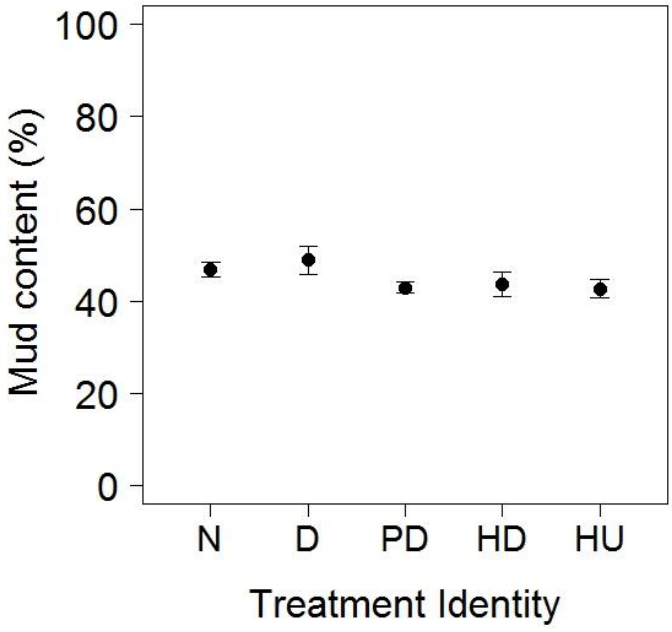

Figure 3.19 | Effect of sediment defaunation, mesocosm presence and species identity on the minicore sediment mud content (%; n = 4). Error bars are standard error. Treatment identity as in Figure 3.13.

In summary:

1 | The defaunation procedure removed only 49 % of the fauna.

2 | There were no temporal trends in the sediment measurements over the low tide period examined.

3 | Freezing had effects on the sediment (treatment N vs D), increasing the sediment erosion threshold and the microphytobenthos minimum fluorescence. There was no effect on sediment particle size.

4 | Mesocosm presence had effects on the sediment (treatment D vs PD) on the sediment, also increasing the sediment erosion threshold, the microphytobenthos minimum fluorescence and the sediment particle D_{10}.

Sediment suspension index decreased in the treatments with a mesocosm.

4 | *Hediste diversicolor* had an effect on the sediment (PD vs HD). Treatments containing *Hediste diversicolor* had a smaller erosion threshold and minimum fluorescence and a larger suspension index.

5 | *Hydrobia ulvae* had no significant effect on the sediment (PD vs HU).

3.3.3 | Discussion

1 | Defaunation efficacy of *in situ* liquid nitrogen freezing

Sediment defaunation was not complete, however the cryo-defaunation method resulted in a partial reduction (47 %) in sediment macrofaunal abundance. Freezing of sediment to achieve defaunation may also result in the loss of meiofauna (Raffaelli et al. 2003b), microphytobenthos, and other unmeasured faunal groups e.g. bacteria, fungi, and changes in sediment properties (Tolhurst et al. 2012). In this study the meiofauna and microphytobenthos may recolonise the defaunated sediments through the mesocosm mesh and any changes in nutrients, caused by sediment disruption and breakdown of killed fauna, will hopefully be equilibrated with the overlying seawater. Tolhurst et al. (2012) noted no persistent effects on microphytobenthos properties when testing the effect of pouring liquid nitrogen on the surface of intertidal sediments. Cryo-defaunation, therefore, provides a suitable method for use *in situ* to decrease the abundance of the dominant macrofauna and assess the effects of *Hediste diversicolor* and *Hydrobia ulvae* on the stability, microphytobenthos and sediment particle size distribution in the field especially if the sediment core volume defaunated is reduced in future experiments.

2 | Spatial and temporal effects on sediment properties

The row location of the mesocosms did not affect the measured sediment stability or microphytobenthos characteristics, and there were no significant temporal trends. This contrasts with previous studies that have

observed temporal changes in microphytobenthos and sediment properties due to diatom migration in the sediment surface layers (Paterson 1989, Tolhurst et al. 2003, Consalvey et al. 2004b, Tolhurst and Chapman 2005, Tolhurst et al. 2006b) and sediment compaction and dewatering (Perkins et al. 2003) during tidal exposure. This was probably because the mudflat surface remained moist throughout the tidal exposure and did not dry out. No obvious migrating diatom biofilm was observed. The only sediment property that seemed to change during the experiment was the variability in the erosion threshold, which reduced as the experiment progressed. Erosion threshold was variable for approximately the first 45 minutes of the experiment. Even with changes that may be occurring due to tidal retreat or diatom migration, it appears that a successful statistically robust investigation may be carried out during low tide on the mudflat at Breydon Water. Future experiments, however, should wait longer after mudflat exposure before commencing measurements of the erosion threshold to reduce erosion threshold variation between replicates. Mudflat sediment properties have also been shown to be significantly spatially variable (Paterson et al. 2000, Tolhurst and Chapman 2005, Tolhurst et al. 2006b) at small scales, however visually the mudflat area at Breydon Water used for this experiment appears very similar and no significant spatial variation was observed.

3 | Effect of defaunation on sediment properties

All the erosion thresholds measured were under 2 Nm^{-2}, which would be considered normal for a mudflat area such as Breydon Water (Amos et al. 1992, Amos et al. 1997, Defew et al. 2002). Defaunation of the sediment increases the erosion threshold and decreases the suspension index. De Deckere (2001) attributed a similar effect after the removal of sediment infauna to a reduction in bioturbation and grazing. This finding is in contrast to Murphy and Tolhurst (2009) who showed that the removal of some fauna, predominantly Nereidae, the family to which *Hediste diversicolor* belongs, did not significantly affect any sediment property except sediment colloidal carbohydrate concentrations, a variable that was not measured in this pilot study.

The defaunated sediments had a significantly larger microphytobenthos biomass than the natural sediments and the increased sediment stability observed may be an indirect effect caused by the loss of the majority of grazers, such as *Hydrobia ulvae* and *Corophium volutator*. Defaunated sediment has been shown to be rapidly colonised by microalgae in the laboratory (Tolhurst et al. 2008a) and in the field (Davis and Lee 1983) leading to sediment stabilisation through the production of extracellular polymeric substances (EPS) causing a stable biofilm (Paterson 1989, Stolzenbach 1989, Paterson 1997, Tolhurst et al. 2002). This indirect effect of macrofaunal species abundance on sediment stability has also been observed by Daborn et al. (1993), Smith et al. (1996), Austen et al. (1999), and Andersen et al. (2001).

There was also a shift in particle size to a slightly, but not significantly, larger grain size in the defaunated cores, shown by a larger mean particle size, an increased particle size D_{10}, and a slight decrease in sediment mud content, indicating there are less small particles present in the sediment samples, an effect also observed after defaunation by Murphy and Tolhurst (2009).

The sediment treatment that was cryo-defaunated and replaced onto the mudflat without a mesocosm to prevent species ingress (treatment D) showed no significant change in the erosion threshold compared to either the natural sediments (N) or the defaunated sediments held in a mesocosm (PD). This treatment, however, did have an erosion threshold larger than that of the natural mudflat sediments, but lower than that of the defaunated sediments held in a mesocosm indicating that the partial recovery of macrofauna from the cryo-defaunated state is reducing the erosion threshold. Treatment D had a significantly smaller minimum fluorescence value than treatment PD indicating that the prevention of macrofaunal recovery keeps grazing pressure low and when macrofauna are allowed to recolonize the sediment, grazing keeps the microphytobenthos biomass from increasing to that observed in the defaunated treatment held within a mesocosm.

When the species biomass is replaced with *Hediste diversicolor* (HD treatment) the erosion threshold is significantly smaller than that of the defaunated mesocosm treatment (PD). In this study the erosion threshold of the sediments containing only *Hediste diversicolor* is not much greater than that of the natural mudflat sediments. This suggests that the activity of *Hediste* on sediment stability is able to compensate for the loss of the majority of the rest of the macrofauna, suggesting a degree of functional redundancy or functional compensation in relation to the sediment erosion threshold in the mudflat system. The addition of *Hediste diversicolor* to defaunated cores also resulted in a significant increase in sediment erosion rate compared to the defaunated mesocosm treatment. *Hediste diversicolor* has been suggested to have a destabilising effect on sediments due to bioturbation (de Deckere et al. 2001, Widdows et al. 2009), an activity that will affect both the sediment surface erosion, increasing the erosion threshold, and the stability of lower layers of the sediment, increasing the sediment erosion rate. *Hediste diversicolor* also caused a significant reduction in the microphytobenthos minimum fluorescence, a proxy for microphytobenthos biomass (Jesus et al. 2006) and therefore may also have an indirect destabilising effect due to grazing removal of microphytobenthos (Smith et al. 1996, de Deckere et al. 2001). This suggests that at least some of the reduction in the erosion threshold can be attributed to either increased grazing or suppressed growth of microphytobenthos, resulting in a reduction in sediment cohesion provided by the secretion of EPS (Montague 1986, Grant 1988, Paterson 1989, Paterson et al. 1990, Paterson 1997, Tolhurst et al. 2002, Tolhurst et al. 2008a)

In previous studies, *Hydrobia ulvae* has been found to have a predominantly destabilising effect, through removal of microphytobenthos by grazing (Smith et al. 1996, Austen et al. 1999, Andersen 2001, Orvain et al. 2004), surface disruption (Blanchard et al. 1997, Orvain et al. 2004), bioturbation (Orvain et al. 2006) and increased sediment moisture content (Orvain et al. 2006). While the addition of *Hydrobia ulvae* causes a reduction in the erosion threshold compared to the defaunated mesocosm treatment, this difference was not significant in this study. The addition of *Hydrobia*

caused no change in the suspension index or the minimum fluorescence of the sediments from that of the defaunated mesocosm sediments either. The erosion rate observed was relatively slow, indicating that while the erosion threshold may have been reached at a relatively low shear stress, the underlying sediments were relatively stable. The small mean erosion threshold observed is possibly as a result of type 1 erosion of a loose surface layer (Amos et al. 1992, Tolhurst et al. 2000a). This may be because the destabilising influence of *Hydrobia* does not extend down into the sediment, as they are not found to burrow extensively if the sediment is too hard (Little and Nix 1976), which may be the case in the defaunated sediment where no bioturbation is occurring. They also do not burrow if the sediment remains wet during low tide periods (Linke 1939, Little and Nix 1976), which the sediment at the experimental site usually does.

The relatively small and insignificant reduction in the microphytobenthos minimum fluorescence compared to the defaunation mesocosm treatment indicates that destabilising actions caused by *Hediste* and *Hydrobia*, other than that of the indirect effect of microphytobenthos grazing, are also important in causing the reduction in sediment erosion threshold. These may include surface disruption by grazing trails (Nowell et al. 1981, Blanchard et al. 1997), the creation of faecal pellets (Andersen 2001), bioturbation (de Deckere et al. 2001, Orvain et al. 2004, Widdows et al. 2009), and increasing sediment water content (Orvain et al. 2006).

5 | Experimental limitations and implications for further experiments

There were a number of issues with the methodology used that were raised by this experiment. As this experiment was carried out using *in situ* mesocosms it is potentially affected by a number of experimental artefacts, however the use of mesocosms to prevent colonisation of defaunated sediments and maintain the species biomass was necessary. The inclusion of a mesocosm only treatment as a procedural control, with which all other mesocosm treatments could be compared should be included in future experiments.

As discussed in Section 3.3.1, the depth of the cores attempted to be frozen in this experiment was 10 cm. The defaunation that occurred in this experiment was less than required. This was estimated to be due to a lack of penetration of the cold into the centre of the sediment core. The use of a shallower core depth would provide a better freezing efficacy. Another problem with the pilot experiment was that a number of replicates were lost due to scouring around the pipes and erosion of the surrounding mud. Further experiments ensured that the cores were secured upon placement back on to the mudflat by carefully replacing disturbed sediment from around the core. A number of mesh lids were also lost during the experimental period and in future experiments the setup was monitored every few days to re-secure the cable ties holding the lids.

As discussed above, many of the observations made in this experiment may be explained by changes in sediment water or EPS concentrations. Measurement of additional sediment properties related to sediment stability and microphytobenthos biomass, such as sediment water, chlorophyll and colloidal carbohydrate concentrations should provide a greater understanding of the processes occurring on the mudflat that affect sediment stability. Later experiments, in Chapters 4, 5 and 6, measured these variables to attain a more comprehensive picture of the mudflat.

In conclusion, this method of sediment defaunation and species addition using *in situ* mesocosms provides a suitable method by which the species abundance and diversity can be reduced and manipulated. Single species re-addition can allow the effects of species identity to be examined and addition of multiple species combinations will allow the effects of richness and biomass distribution to be studied. The successful setup and collection of data from this pilot experiment indicates that this method is suitable for larger scale experiments using multiple treatments and replications.

Chapter 4 | Effect of Single Species Dominated Communities and Species Combinations on Biogeochemical Mudflat Properties

4.1 | Introduction

This chapter expands on the work presented in the pilot experiment and examines the effects of common macrofauna species on mudflat sediment properties when dominant and in combination. The presence and abundance of the species *Hediste diversicolor*, *Hydrobia ulvae* and *Corophium volutator*, were manipulated to determine the effects of species identity, species density and species richness on mudflat stability and biogeochemical properties, specifically addressing Objectives 1, 2 and 3 presented in Section 1.7:

Objective 1 | Investigate the effect of individual macrofauna species on mudflat sediment stability and biogeochemical properties *in situ*.

Objective 2 | Investigate the effect of macrofaunal species density on mudflat sediment stability and biogeochemical properties *in situ*.

Objective 3 | Investigate the effect of macrofaunal species richness on mudflat sediment stability and biogeochemical properties *in situ*.

4.1.1 | Rationale

The estuarine and coastal environment is one of the most ecologically diverse and productive in the world (Nixon et al. 1986). Current and predicted environmental change will inevitably have an effect on these important habitats (Covich et al. 2004, Worm et al. 2006). In recent years, this impetus has resulted in the development of an area of science identifying the effects of biodiversity loss on mudflat ecological processes and functioning (Solan et al. 2008). An informative approach has been to use simple model communities to allow the determination of the mechanisms by which intertidal species and communities affect the important ecosystem

functions of the mudflat (Raffaelli et al. 2003b, Solan et al. 2008). Few studies thus far have used this experimental approach to look at biodiversity effects on ecosystem processes in the field. Conducting experiments in the field allows for the influence of real world factors on the experimental treatments, such as temporal and spatial resource heterogeneity and environmental fluctuation, increasing the relevance of the results to the natural world (Fridley 2001). Additionally, by collecting data on a range of biogeochemical variables, including sediment stability, microphytobenthos biomass and health, sediment particle size and size distribution, sediment water content, and colloidal carbohydrate and chlorophyll *a* and *b* concentration, this study hopes to examine the effect of species and biodiversity on the biogeochemical properties an intertidal Norfolk mudflat.

4.2 | Materials and methods

Fieldwork was carried out at Breydon Water, Great Yarmouth, UK over the period 20th of August to 13th of September 2012, adjacent to the area where the pilot experiment was carried out. Five sediment cores to determine core species biomass were taken on the 20th of August 2012 following the method given in Section 2.2 for measurement of the macrofaunal biomass. These biomass measurements were used to determine the biomass required for the experimental treatments. Biomass cores contained an average (± SE) of 0.48 ± 0.03 g of macrofaunal biomass, equivalent to 23.75 ± 1.73 g per m^2, consisting of predominantly *Hediste diversicolor*, *Corophium volutator* and *Hydrobia ulvae*. The experiment was set up over four days from the 29th of August to the 2nd of September 2012.

4.2.1 | Experimental design

The experimental design consisted of 11 treatments (Figure 4.1; n = 6). There were three control treatments; natural sediment as a control baseline (N), a pipe mesocosm only treatment as a procedural control (P) and a defaunated mesocosm treatment as an experimental control (PD).

Treatments consisting of each species in single species dominant mixtures were designed to examine how species identity affects sediment

properties. For each species, there was a high biomass treatment, where the whole of the total original biomass of the sediment (determined using the macrofaunal biomass value obtained from the five sediment cores taken on the 20th of August) was replaced after defaunation of the majority of the present species to create a single species dominant community, and a low biomass treatment, where one third of the total original biomass of the sediment was replaced by the single species. This would enable the determination of how species biomass and density affects sediment properties and the comparison of how each species affects the sediment when in the single species dominant treatment and when all three species are combined using the overyielding statistic. The single species dominant treatments consisted of defaunated mesocosms with the total original biomass replaced with *Hediste diversicolor* (HD_1); the original biomass replaced with *Hediste diversicolor* equal to $^1/_3$ of the original biomass (HD_2); the total original biomass replaced with *Hydrobia ulvae* (HU_1); the original biomass replaced with *Hydrobia ulvae* equal to $^1/_3$ of the original biomass (HU_2); the total original biomass replaced with *Corophium volutator* (CV_1); and the original biomass replaced with *Corophium volutator* equal to $^1/_3$ of the original biomass (CV_2).

To examine how species community composition affects sediment properties, two treatments consisting of species mixtures were also included; one consisting of defaunated cores with the whole biomass replaced with an equal mix of *Hediste diversicolor*, *Hydrobia ulvae* and *Corophium volutator* to three times the original biomass (Mix_1) and another consisting of defaunated cores with the total biomass replaced with an equal mix of *Hediste diversicolor*, *Hydrobia ulvae* and *Corophium volutator* to the original biomass (Mix_2).

The first two days of experimental setup consisted of laying out the 66 experimental plots as detailed in Section 2.2 and defaunation of the mesocosms allocated to species biomass replacement treatments and the experimental control following the cryo-defaunation methodology given in Section 3.2.2. On the following two days, treatments were representatively allocated to the treatment areas ensuring even allocation to day (n = 33;

Day1, Day2) and row (n = 16 or 17; Row1, Row2, Row3, Row4; where Row1 was highest on the shore).

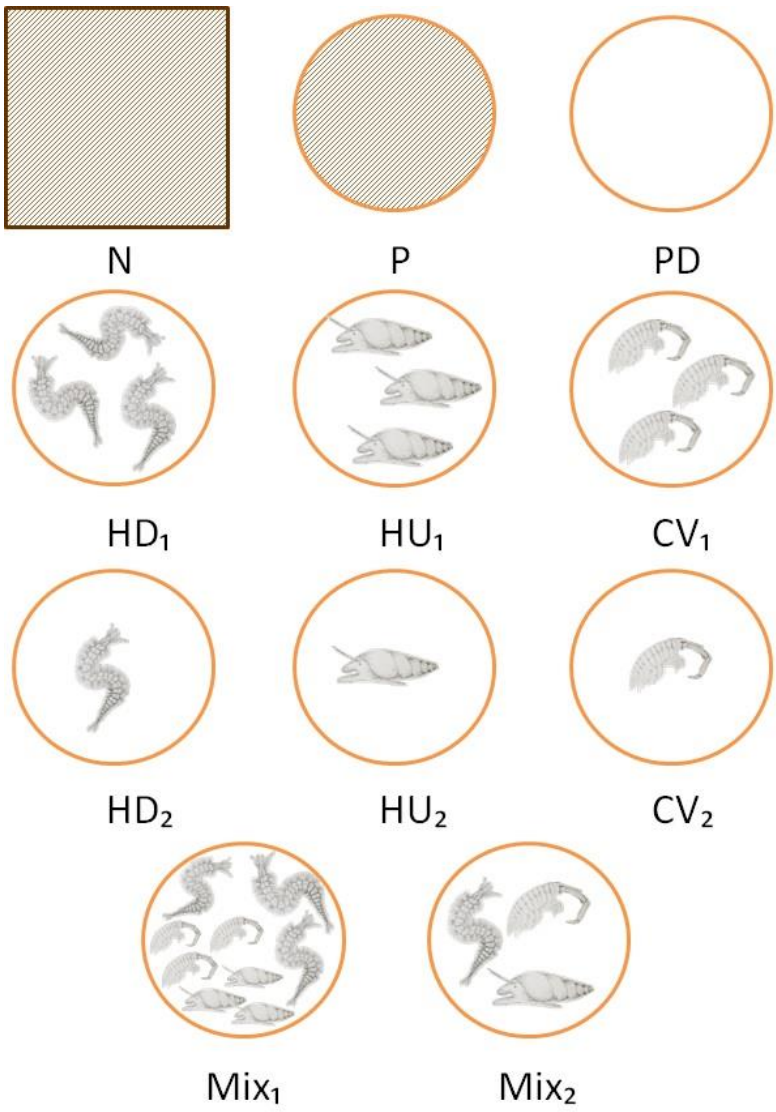

Figure 4.1 | The eleven experimental treatments represented visually. Shading represents the natural sediment. Each diagrammatic organism represents $^{1}/_{3}$ of the total core biomass. Where N contains natural sediment as a mudflat baseline, P is a pipe mesocosm only treatment as a procedural control, PD is a defaunated mesocosm treatment as an experimental control. The species treatments are defaunated cores where HD_1 contains the original biomass replaced with *Hediste diversicolor*, HD_2 contains $^{1}/_{3}$ of the original biomass replaced with *Hediste diversicolor*, HU_1 contains the original biomass replaced with *Hydrobia ulvae*, HU_2 contains $^{1}/_{3}$ of the original biomass replaced with *Hydrobia ulvae*, CV_1 contains the original biomass replaced with *Corophium volutator*, CV_2 contains $^{1}/_{3}$ of the original biomass replaced with *Corophium volutator*, Mix_1 contains the biomass replaced with an equal mix of *Hediste diversicolor*, *Hydrobia ulvae* and *Corophium volutator* to three times the original biomass and Mix_2 contains the biomass replaced with an equal mix of *Hediste diversicolor*, *Hydrobia ulvae* and *Corophium volutator* to the original biomass.

4.2.2 | Experimental data collection

Field measurements and sediment samples were collected on the 12th and 13th of September 2012 as described in Section 2.3. In the field, data were collected using a Cohesive Strength Meter (CSM; Section 2.3.1) and a Pulse Amplitude Modulated fluorometer (PAM; Section 2.3.2). Minicores (Section 2.3.3) were collected and analysed for water content and particle size properties in the laboratory, following the procedures presented in Section 2.6.3. Contact cores (Section 2.3.4) were collected and analysed for water concentration, carbohydrates, chlorophyll *a* and *b* and particle size properties in the laboratory, following the procedures presented in Section 2.6.4. Community composition cores were taken on the final day of the experiment, the 13th of September 2012, and analysed to determine species biomass in the cores at the end of the experiment, following the methods presented in Section 2.6.5.

4.2.3 | Data analysis

Data were analysed using a generalised least squares approach and non-trangressive and trangressive overyielding, as described in Section 2.7, to compare the single and mixed species treatments and the procedural and experimental controls. All generalised least squares initial and final models used are presented in Appendix 2. Non-transgressive and transgressive overyielding techniques were used to examine species density and richness effects.

The principles of non-transgressive over-yielding (Loreau 1998, Fridley 2001, Petchey 2003, Griffin et al. 2009) were used to compare the effect of each species, *Hediste diversicolor*, *Hydrobia ulvae* or *Corophium volutator*, when present at a high (whole of the sediment species biomass replaced by the single species) and low (whole of the sediment species biomass replaced by a single species at $^1/_3$ of the original biomass) biomass. The average effect of each species when only $^1/_3$ of the biomass was added to defaunated sediments was determined by calculating the difference between this treatment and the defaunated control treatment. This difference was extrapolated to three times the value to estimate the effect that should be

observed in the whole biomass replacement species treatment if no density dependent species effects are occurring ('$V_{high}(E)$'). This value was then compared to the actual measurement taken on the whole biomass replacement treatment ('$V_{high}(O)$') using the non-transgressive over-yielding equation, Equation 4.1.

Equation 4.1 $$D_{sp} = \frac{V_{high}(O) - V_{high}(E)}{V_{high}(E)}$$

Where D_{sp} is negative, the values observed in the whole biomass treatment are smaller than would be expected and where D_{sp} is positive, the values observed in the whole biomass treatment are larger than would be expected.

Trangressive overyielding was used to compare the effects of the species in the single species dominant communities (HD_1, HU_1 and CV_1) with the observed values in the species mixture (Mix_2; V_{mix}) at a constant biomass. As the directionality of the change in each variable was unknown both the maximum ('$V_{maximum\ in\ dominant\ community}$') and minimum ('$V_{minimum\ in\ dominant\ community}$') effects of the species when dominant was calculated to determine a D_{max} (Equation 4.2) and a D_{min} (Equation 4.3). For example, a change in erosion threshold can be interesting if it is larger, and the sediment more stable, or if it is smaller, and the sediment less stable; it is not a variable such as productivity where more productivity would be of interest (e.g. in Griffin et al., 2009). In fact, even microphytobenthos minimum fluorescence increase and decrease is of interest in this study as it can indicate more or less activity or effect of the macrofauna. To adapt the traditional transgressive overyielding formula to analyse a reduction in the variables the inverse (Inv) of the observed value of the variable and the minimum measured value in the single species dominant communities was used to determine D_{min} (Equation 4.3).

Equation 4.2 $$D_{max} = \frac{V_{mix} - V_{maximum\ in\ dominant\ community}}{V_{maximum\ in\ dominant\ community}}$$

Equation 4.3 $$D_{min} = \frac{Inv\,V_{mix} - Inv\,V_{minimum\ in\ dominant\ community}}{Inv\,V_{minium\ in\ dominant\ community}}$$

Non-transgressive overyielding techniques were used to determine whether the mixed species treatments had a greater effect on the variables than the species in single species dominant communities in an additive model for the low biomass treatments (HD_2, HU_2, CV_2) and the corresponding mixed species treatment (Mix_2) and the high biomass treatments (HD_1, HU_1, CV_1) and the corresponding mixed species treatment (Mix_1). The effect of each species in when dominant was determined by calculating the difference between the single species dominant treatments and the defaunated control treatment. These effects were summed to produce an expected mixed species effect ('$V_{mix}(E)$'). This was compared to the observed effect in the corresponding additive mixed species treatment ('$V_{mix}(O)$') using Equation 4.4.

Equation 4.4 $$D_T = \frac{V_{mix}(O) - V_{mix}(E)}{V_{mix}\ (E)}$$

Where D_T is negative, the values observed in the mixed species treatments are smaller than would be expected and where D_T is positive, the values observed in the mixed species treatment are larger than would be expected.

Additionally, these techniques were also used to determine whether the mixed species treatments had a greater effect on the variables than the species in single species dominant communities in a substitutive model using the high biomass single species dominant treatments (HD_1, HU_1 and CV_1) and the low biomass mixed species treatment (Mix_2).

4.3 | Results

From analysis of the community composition cores taken on day two of the experiment (Section 2.6.5), cryo-defaunation of the cores resulted in a 78 % reduction in species abundance in the defaunation control cores compared to the procedural control cores (see Section 3.2.2). The three species were reintroduced into the defaunated cores resulting in the

successful creation of high and low biomass treatments of the three species and high and low mixed species treatments (Table 4.1). The abundance values presented in Table 4.1 show the abundance of each species in the mesocosms (201.06 cm^2) after two weeks in the field. Species biomasses and abundances are expected to have changed slightly from what was originally put into the mesocosms due to normal ecological processes and species interactions. It is therefore worth noting that the reduction in *Corophium* numbers is not as high as would be expected from the efficacy of the cryo-defaunation method. This could be as a result of the mobility of the *Corophium* juveniles and their potential ability to recolonize through the 300 µm mesh surrounding the mesocosms. Additionally, the low biomass *Hediste diversicolor* treatment contains a higher number of *Hediste* individuals than expected, as do the high *Corophium* treatments. This could be due to a net settlement of *Hediste* larvae or small adults, which could pass through the mesh, into the mesocosms as a result of increased prey availability and reduced competition as a result of *Hediste* removal through cryo-defaunation. Many of the *Hediste* individuals recorded in the non-*Hediste* treatments were small and could be classified as juveniles of the species. It is probable that this is a relatively small increase in biomass over what was expected and does not significantly affect the overall experimental results, however, biomass was not quantified. To determine this in later experiments the species biomass was determined for each replicate in addition to species abundance. These extra data in the later experiments showed no large change in biomass from expected values, indicating the increase in species abundance in this experiment is not matched by an increase in species biomass.

Table 4.1 | The abundance per mesocosm (mean ± standard error in 201.06 cm^2) of the three species of interest, *Hediste diversicolor*, *Hydrobia ulvae* and *Corophium volutator*, in the community composition cores taken after the experimental cores had been in the field for two weeks. Mean abundance and standard error values have been rounded to whole individuals.

Treatment	*Hediste*	*Hydrobia*	*Corophium*
Natural Sediments (N)	16 ± 1	34 ± 4	188 ± 11
Mesocosm Control (P)	14 ± 2	24 ± 3	144 ± 13
Defaunated Sediments (PD)	5 ± 1	7 ± 3	32 ± 7
High *Hediste* Biomass (HD_1)	16 ± 1	3 ± 1	16 ± 4
Low *Hediste* Biomass (HD_2)	13 ± 0	4 ± 1	26 ± 11
High *Hydrobia* Biomass (HU_1)	3 ± 1	34 ± 6	23 ± 10
Low *Hydrobia* Biomass (HU_2)	6 ± 1	16 ± 2	36 ± 11
High *Corophium* Biomass (CV_1)	10 ± 2	4 ± 1	73 ± 5
Low *Corophium* Biomass (CV_2)	8 ± 2	5 ± 0	58 ± 12
High Mixed Biomass (Mix_1)	17 ± 1	36 ± 1	50 ± 7
Low Mixed Biomass (Mix_2)	14 ± 2	14 ± 2	34 ± 6

4.3.1 | Day and row effects

The effects of the day the data were collected (n=33, Day1, Day2) and the row the treatment was located in (n = 16 or 17; Row1, Row2, Row3, Row4; where Row1 was highest on the shoreline) were tested against two variables; the erosion threshold (ET, Nm^{-2}) and the PAM measured minimum fluorescence (F_o). Both the mean erosion threshold and the mean PAM F_o value did not vary significantly with day of data collection (ET: Figure 4.2; L-ratio = 1.51, d.f. = 3, p = 0.2189, F_o: Figure 4.3; L-ratio = 3.78, d.f. = 2, p = 0.0517) or row location (ET: Figure 4.4; L-ratio = 3.86, d.f. = 8, p = 0.2766, F_o: Figure 4.5; L-ratio = 5.63, d.f. = 8, p = 0.1311).

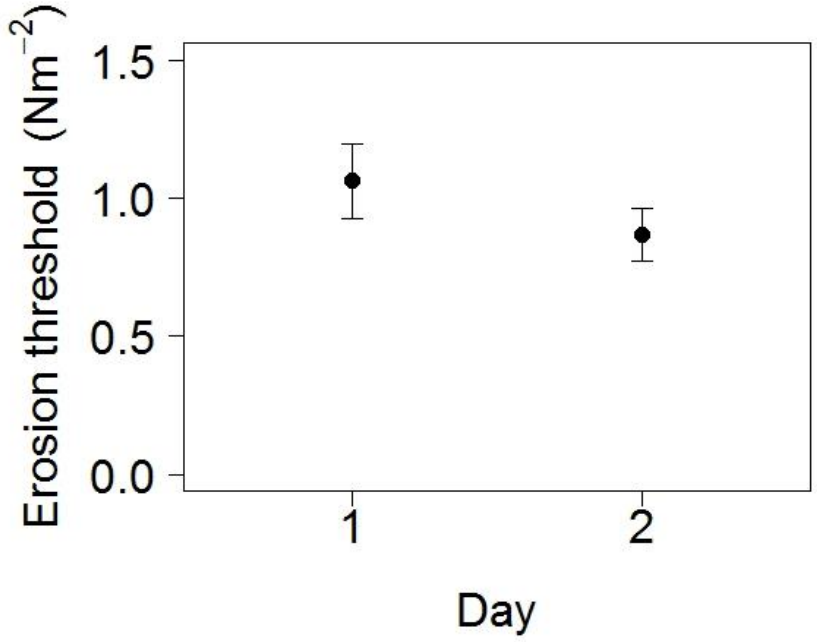

Figure 4.2 | Effect of day of data collection on the sediment erosion threshold (Nm^{-2}; n = 33). Error bars are standard error. 1, Day 1; 2, Day 2.

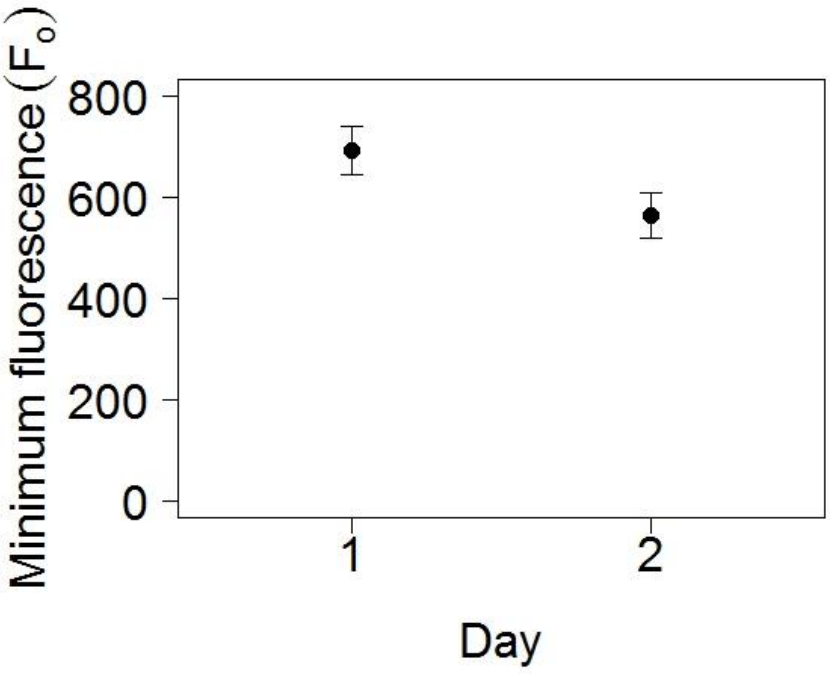

Figure 4.3 | Effect of day of data collection on the pulse amplitude modulated measured minimum fluorescence (F_o; n = 33). Error bars are standard error. 1, Day 1; 2, Day 2.

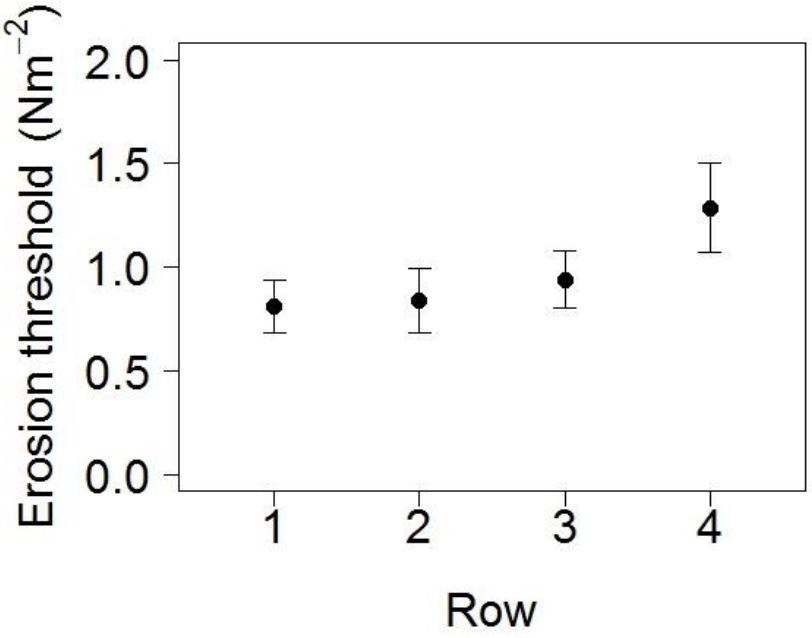

Figure 4.4 | Effect of row of mesocosm location on the sediment erosion threshold (Nm^{-2}; n = 16). Error bars are standard error. 1, Row 1; 2, Row 2; 3, Row 3; 4, Row 4, where Row 1 was highest on the shoreline.

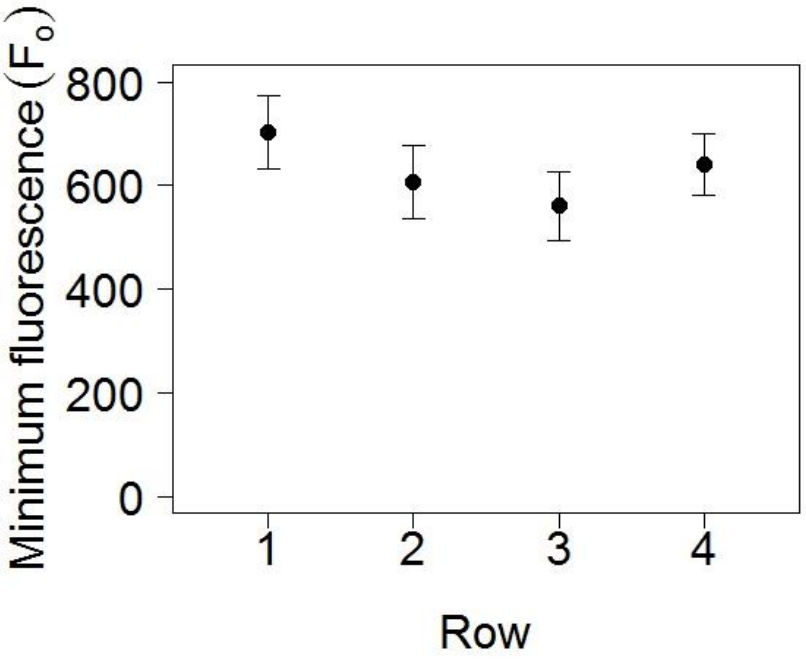

Figure 4.5 | Effect of row of mesocosm location on the pulse amplitude modulated measured minimum fluorescence (F_o; n = 16). Error bars are standard error. 1, Row 1; 2, Row 2; 3, Row 3; 4, Row 4, where Row 1 was highest on the shoreline.

Splitting the experimental treatments between two days was necessary to enable the collection of suitable data with enough replication. Treatments were split between rows to reduce their spread along the shore and reduce variation due to the different hydrodynamic regimes along the coast. Four rows enabled all the replicates to be placed within an embayment in the estuary. As there was no effect of treatment row location or day of data collection on two of the main variables all the data were analysed together regardless of 'Day' or 'Row'. It was not possible to undertake a two-way analysis of treatment and either day or row due to the fact this would have reduced the replicates (degrees of freedom) for the interaction terms too much as there were 2 days, 4 rows and 6 replicates of each treatment.

Many of the procedural control treatments (those sediments enclosed in a mesocosm on the mudflat but not defaunated; P) differed significantly from the natural sediments (no mesocosm; N). Thus, during the data statistical analysis and discussion all experimental treatments will be compared to the procedural (P) and experimental (defaunated sediment enclosed within a mesocosm; PD) controls. The measurement of a natural mudflat baseline is interesting in its own right, but as the presence of the pipe mesocosm has a significant effect on some of the sediment properties the correct approach is to compare all species treatments with the procedural control. This approach will be adopted for all the following analyses in this chapter. See Appendix 2 for coefficients tables containing all p-values discussed in this chapter.

4.3.2 | Sediment erosion effects

The mudflat at Breydon Water has a small mean (± 95 % CI, n = 6) erosion threshold (Figure 4.6; treatment N; 0.23 ± 0.13 Nm^{-2}) meaning it is easily erodible under low current speeds. There was a significant effect of sediment treatment on the erosion threshold (L-ratio = 36.90, d.f. = 22, $p < 0.0001$). The procedural control (treatment P) had a larger mean (± 95 % CI, n = 6) erosion threshold (0.69 ± 0.45 Nm^{-2}; t = 2.51, p = 0.0151) and the defaunated sediments (PD) had a much larger mean (± 95 % CI, n = 6) erosion threshold (1.33 ± 0.61 Nm^{-2}; t = 2.17, p = 0.0340) than the natural sediments (N). Compared to the defaunated sediments the low biomass

Hydrobia treatment had a smaller mean (± 95 % CI, n = 6) erosion threshold (0.66 ± 0.34 Nm^{-2}; t = 2.45, p = 0.0176).

Among the species treatments, the high biomass *Corophium* treatment (CV_1) had a smaller mean (± 95 % CI, n = 6) erosion threshold (0.77 ± 0.44 Nm^{-2}) than the low biomass *Corophium* treatment (CV_2; 1.62 ± 0.89 Nm^{-2}; t = 2.19, p = 0.0327). The low biomass *Corophium* treatment had a much larger mean (± 95 % CI, n = 6) erosion threshold than the high biomass *Hydrobia* treatment (HU_1; 0.76 ± 0.43 Nm^{-2}; t = 2.23, p = 0.0302) and the low biomass *Hydrobia* treatment (HU_2; 0.66 ± 0.34 Nm^{-2}; t = 2.19, p = 0.0327).

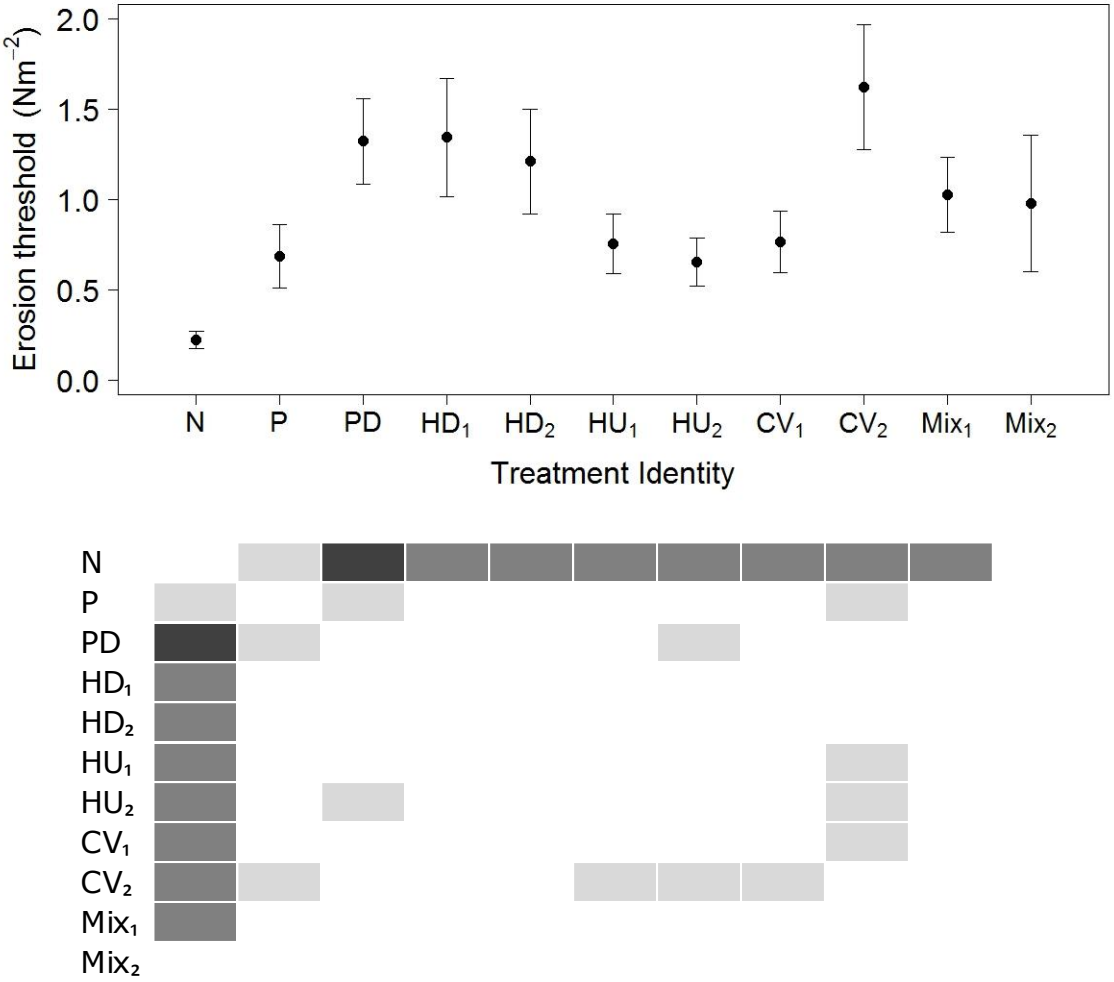

Figure 4.6 | Effect of sediment defaunation, species identity and richness on the sediment erosion threshold (Nm^{-2}; n=6). Error bars are standard error. The species composition of each mixture is indicated on the x-axis, where treatment identity corresponds to: N, natural sediment as a mudflat baseline; P, pipe mesocosm only treatment as a procedural control; PD, defaunated mesocosm treatment as an experimental control; HD_1, original biomass replaced with *Hediste diversicolor*; HD_2, $^1/_3$ original biomass replaced with *Hediste diversicolor*; HU_1, original biomass replaced with *Hydrobia ulvae*; HU_2, $^1/_3$ original biomass replaced with *Hydrobia ulvae*; CV_1, original biomass replaced with *Corophium volutator*; CV_2, $^1/_3$ original biomass replaced with *Corophium volutator*; Mix_1, biomass replaced with an equal mix of HD, HU and CV to three times the original biomass; Mix_2, biomass replaced with an equal mix of HD, HU and CV to the original biomass. Significant differences are indicated in the accompanying table where darker shading indicates greater significant difference: 0.01 < p < 0.05; 0.0001 < p < 0.01; p < 0.0001.

There was a significant effect of experimental treatment on the sediment suspension index (L-ratio = 27.75, d.f. = 22, p = 0.0020). The mean (± SE, n =6) suspension index of the natural sediments at Breydon Water was the largest (Figure 4.7; N; 21.19 ± 1.35), meaning it erodes at a rapid rate, and was significantly larger than the mean (± 95 % CI, n = 6) suspension index of the mesocosm only treatment (P; 10.40 ± 5.00; t = 2.09, p = 0.0411). The high *Corophium* biomass treatment had a larger mean (± 95 % CI, n = 6) erosion rate (CV_1; 7.81 ± 4.95) than the low *Corophium* biomass treatment (CV_2; 2.89 ± 1.65; t = 2.42, p = 0.0188. The low *Corophium* biomass treatment also had a smaller mean (± 95 % CI, n = 6) suspension index than the low *Hydrobia* biomass treatment (HU_2; 5.35 ± 2.63; t = 2.04, p = 0.0466).

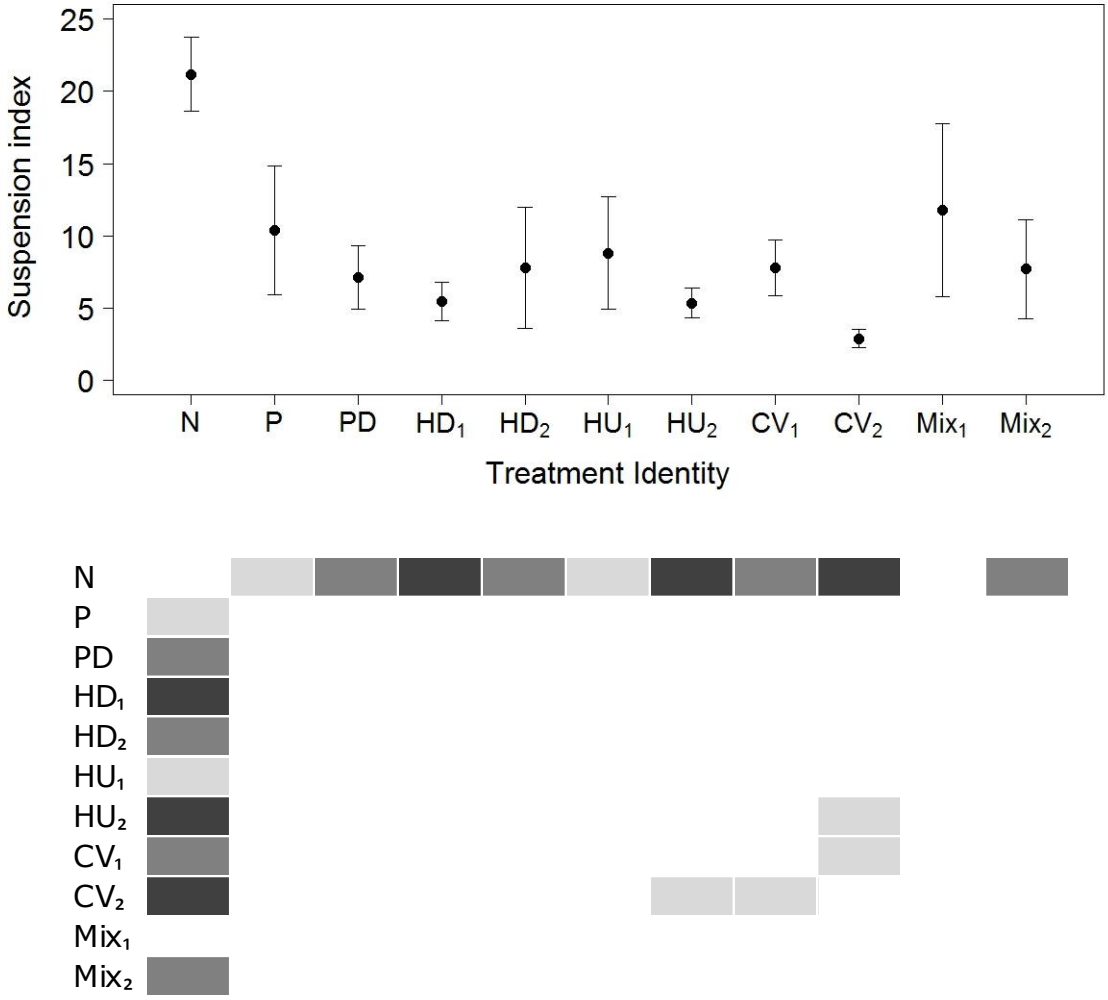

Figure 4.7 | Effect of sediment defaunation, species identity and richness on the sediment suspension index (n = 6). Error bars are standard error. Treatment identity as in Figure 4.6. Significant differences are indicated in the accompanying table where darker shading indicates greater significant difference: 0.01 < p < 0.05; 0.0001 < p < 0.01; p < 0.0001.

4.3.3 | Microphytobenthos biomass

There was a significant effect of experimental treatment on the sediment pulse amplitude modulated fluorometer (PAM) measured minimum fluorescence (L-ratio = 54.30, d.f. = 22, $p < 0.0001$). The natural sediments showed a small mean (± 95 % CI, n = 6) minimum fluorescence (Figure 4.8; N; 230 ± 53.79), smaller than the mesocosm treatment (P; 444 ± 173.07; t = 3.04, p = 0.0037), which also had a smaller minimum fluorescence than the defaunated treatment (PD; 862.22 ± 213.5468; t = 3.91, p = 0.0003). The high biomass *Hediste* (HD_1; 649.22 ± 192.29), the low biomass *Hediste* (HD_2; 802.11 ± 399.88), the low biomass *Hydrobia* (HU_2; 781.94 ± 364.71), the low biomass *Corophium* (CV_2; 789.78 ± 141.50), and the low biomass mixed species (Mix_2; 644.56 ± 187.03) treatments all had larger mean (± 95 % CI, n = 6) minimum fluorescence than the mesocosm treatment (t = 2.04, p = 0.0463; t = 2.11, p = 0.0392; t = 2.15, p = 0.0358; t = 3.98, p = 0.0002, and t = 2.02, p = 0.0479 respectively). Only the high biomass mixed species treatment (Mix_1) had a significantly smaller mean (± 95 % CI, n = 6) minimum fluorescence (451.28 ± 132.06) than the defaunated treatment (t = 4.21, p = 0.0001). The high biomass mixed treatment also had a smaller mean (± 95 % CI, n = 6) minimum fluorescence than the high biomass *Hediste* (HD_1; 649.22 ± 192.29), the low biomass *Hediste* (HD_2; 802.11 ± 399.88), the low biomass *Hydrobia* (HU_2; 781.94 ± 364.71), the low biomass *Corophium* (CV_2; 789.78 ± 141.50), and the low biomass mixed species (Mix_2; 644.56 ± 187.03) treatments (t = 2.18, p = 0.0335; t = 2.14, p = 0.0367; t = 2.1914, p = 0.0327; t = 4.50, $p < 0.0001$, and t = 2.17, p = 0.0343 respectively).

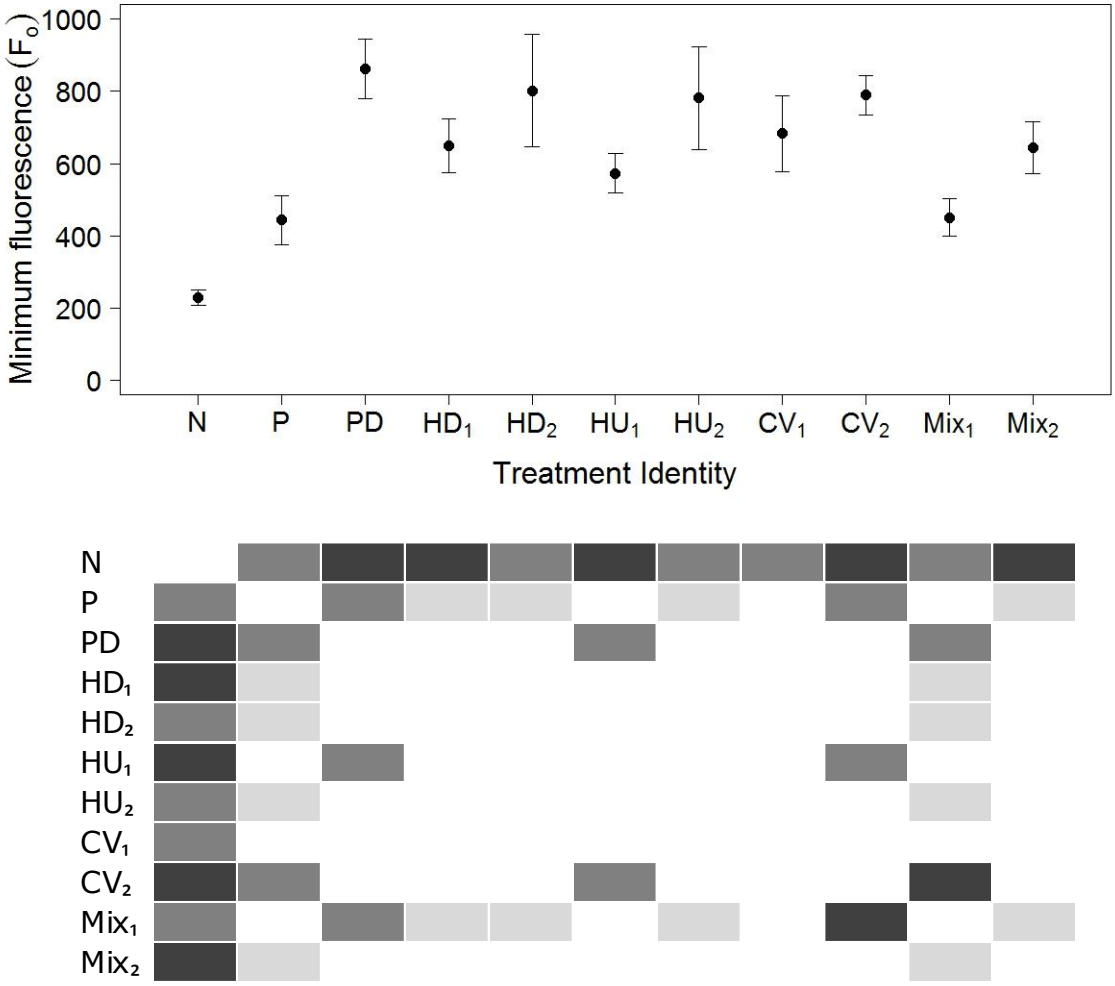

Figure 4.8 | Effect of sediment defaunation, species identity and richness on the pulse amplitude modulated fluorometer measured minimum fluorescence (F_o; n = 6). Error bars are standard error. Treatment identity as in Figure 4.6. Significant differences are indicated in the accompanying table where darker shading indicates greater significant difference: 0.01 < p < 0.05; 0.0001 < p < 0.01; p < 0.0001.

There was a significant effect of experimental treatment on the sediment PAM measured minimum fluorescence (L-ratio = 20.39, d.f. = 12, p = 0.0258). Defaunation of the sediments reduced the mean (± 95 % CI, n = 6) maximum quantum yield (0.50 ± 0.04) relative to the natural sediment (Figure 4.9; N; 0.58 ± 0.06; t = 2.73, p = 0.0086) and the mesocosm treatment (P; 0.56 ± 0.03; t = 2.71, p = 0.0090). Only the high biomass *Hydrobia* (HU_1; 0.56 ± 0.05) and the high biomass mixed species (Mix_1; 0.58 ± 0.03) treatments had a larger mean (± 95 % CI, n = 6) maximum quantum yield than the defaunated treatment (t = 2.01, p = 0.0491; t = 3.56, p = 0.0008 respectively). The high biomass mixed species treatment also had a larger mean (± 95 % CI, n = 6) maximum quantum yield than the low biomass mixed species treatment (Mix_2; 0.54 ± 0.04; t = 2.33, p = 0.0234).

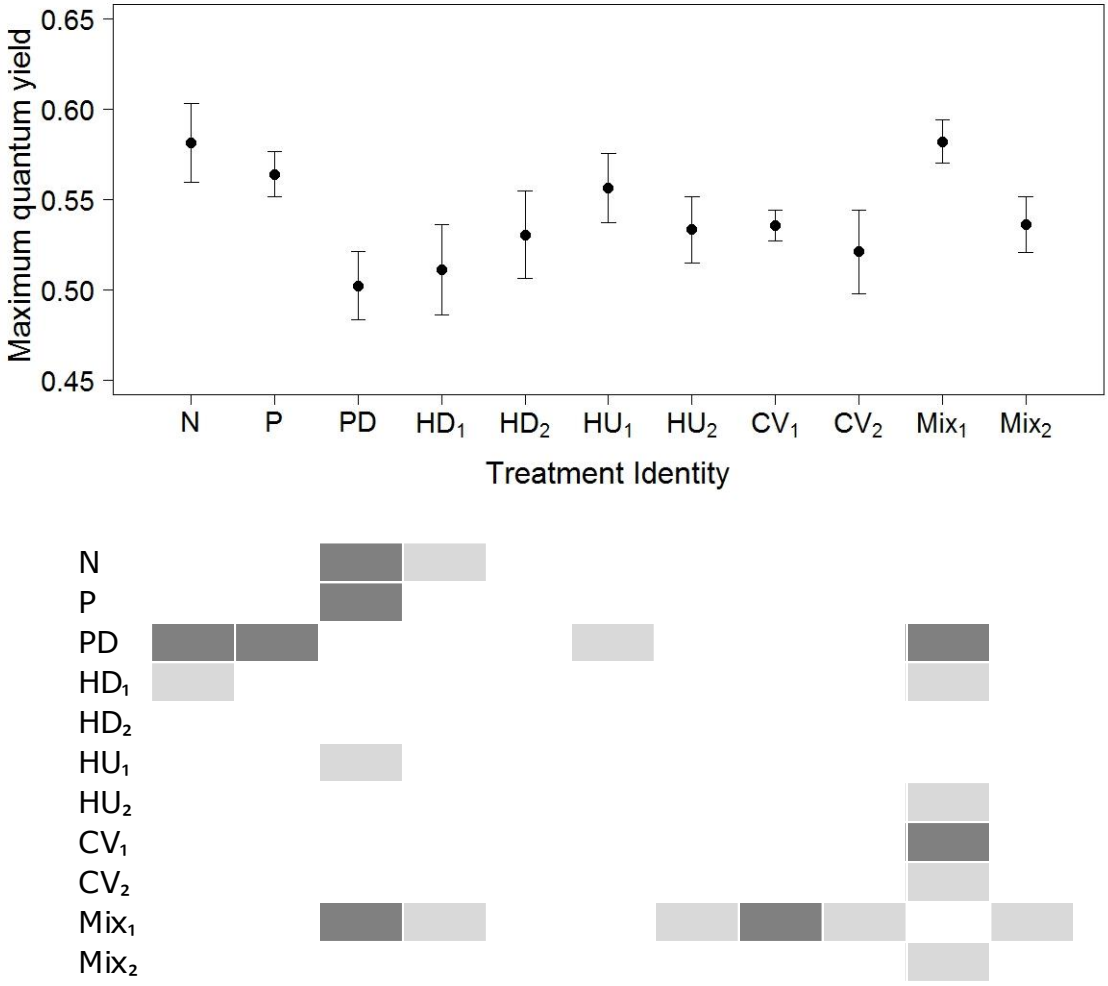

Figure 4.9 | Effect of sediment defaunation, species identity and richness on the pulse amplitude modulated fluorometer measured maximum quantum yield (n = 6). Error bars are standard error. Treatment identity as in Figure 4.6. Significant differences are indicated in the accompanying table where darker shading indicates greater significant difference: 0.01 < p < 0.05; 0.0001 < p < 0.01; p < 0.0001.

4.3.4 | Minicore sediment properties

Minicore water content ranged between 59.18 and 69.18 %, however, there was no effect of mesocosm presence, defaunation or species treatment on minicore water content (%; Figure 4.10; L-ratio = 12.35, d.f. = 22, p = 0.2620).

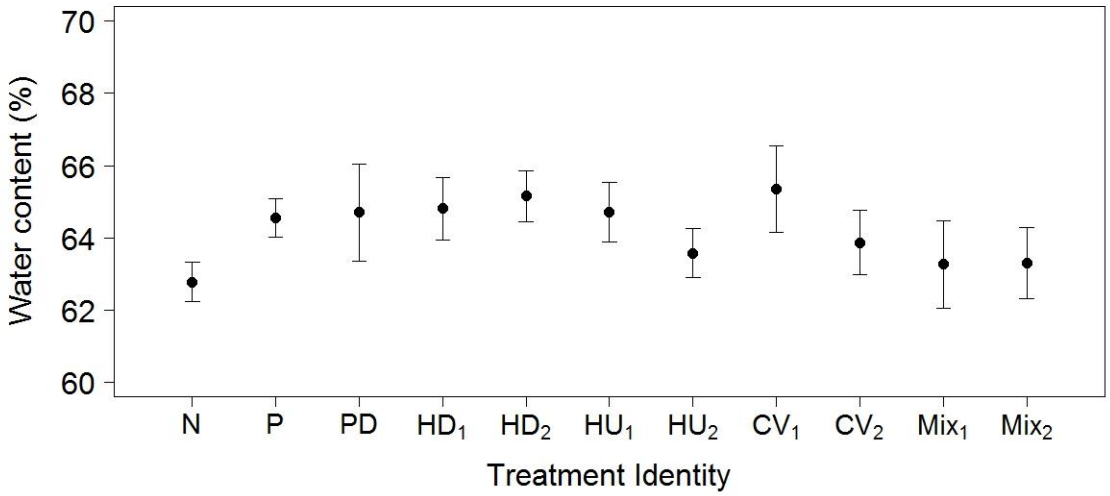

Figure 4.10 | Effect of sediment defaunation, species identity and richness on minicore sediment water content (%; n = 6). Error bars are standard error. Treatment identity as in Figure 4.6.

The minicore sediments were classified as either very fine sand or very coarse silt under the GRADISTAT program scale (Blott and Pye 2001). Minicore mean particle size showed great variability within and between treatments and there was no effect of mesocosm presence, defaunation or species treatment on minicore mean particle size (μm; Figure 4.11; L-ratio = 6.71, d.f. = 22, p = 0.7529).

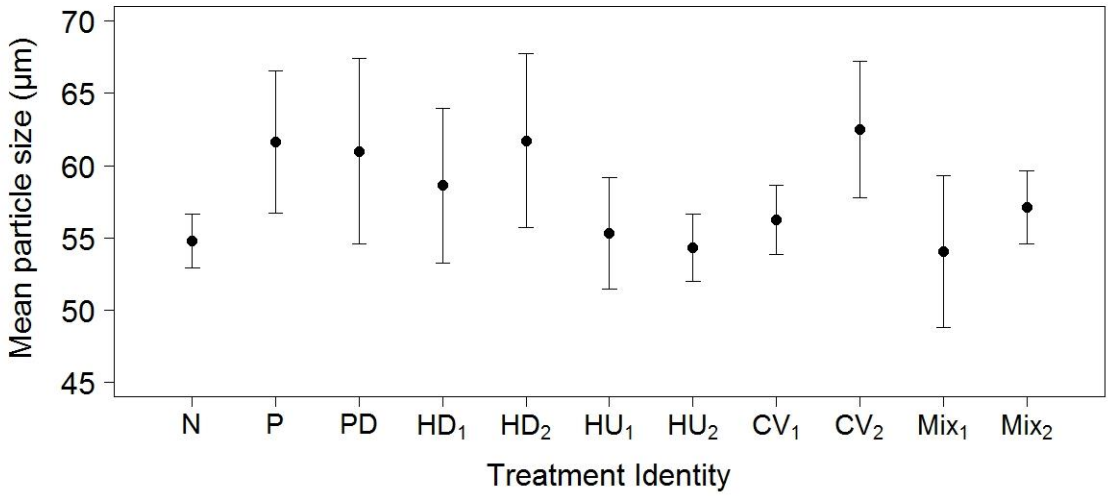

Figure 4.11 | Effect of sediment defaunation, species identity and richness on minicore sediment mean particle size (μm; n = 6). Error bars are standard error. Treatment identity as in Figure 4.6.

Minicore mode particle size (μm) did not change between treatments and there was no effect of mesocosm presence or defaunation (Figure 4.12; F = 0.4533, d.f. = 10, p = 0.9124).

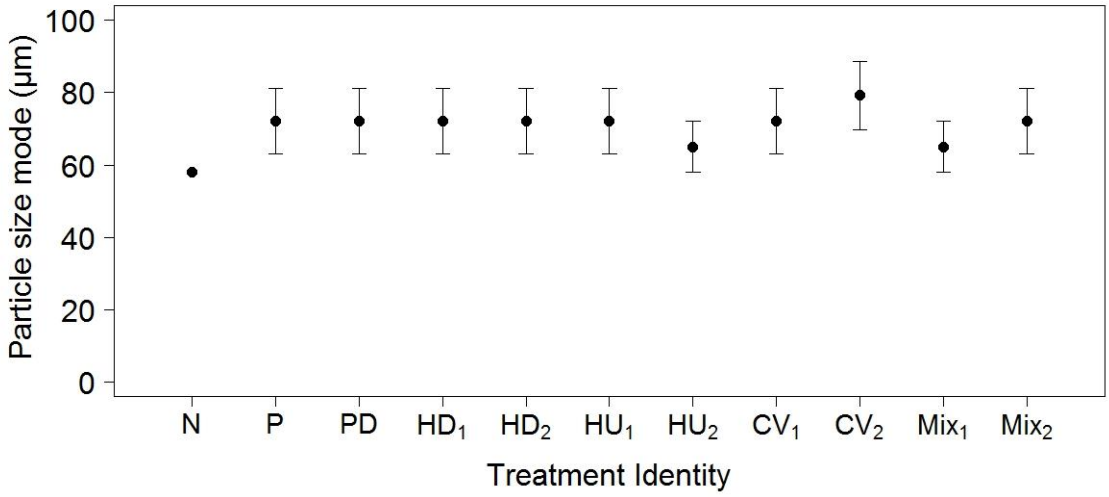

Figure 4.12 | Effect of sediment defaunation, species identity and richness on minicore sediment particle size mode (μm; n = 6). Error bars are standard error. Treatment identity as in Figure 4.6.

The minicore sediments were poorly sorted. Minicore particle sorting only ranged between 2.02 and 2.86 for all treatments and there was no effect of mesocosm presence, defaunation or species treatment on minicore particle sorting (Figure 4.13; L-ratio = 17.57, d.f. = 22, p = 0.0626).

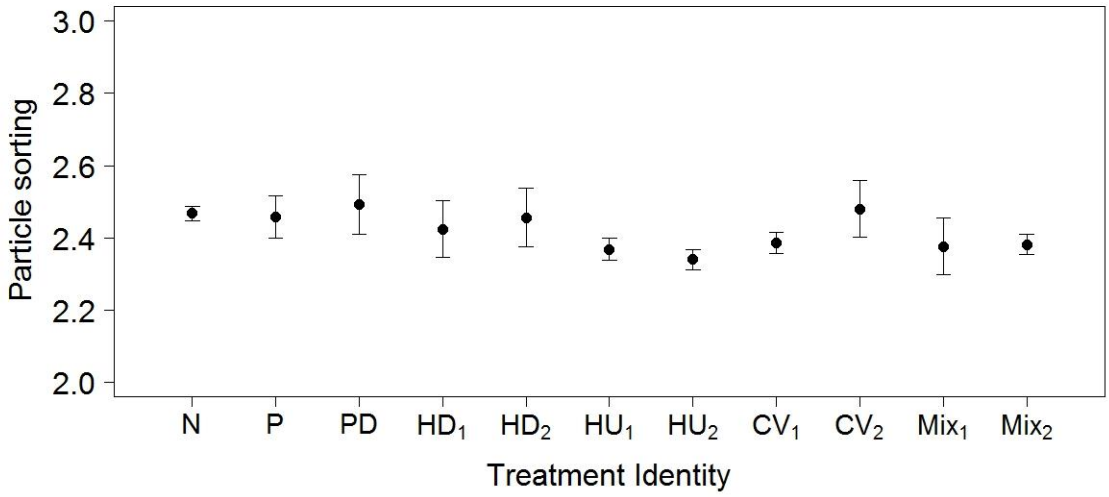

Figure 4.13 | Effect of sediment defaunation, species identity and richness on minicore sediment particle sorting (n = 6). Error bars are standard error. Treatment identity as in Figure 4.6.

The minicore sediments were either fine skewed or very fine skewed. Minicore particle skewness ranged between -1.32 and -0.14 for all treatments and there was no effect of mesocosm presence, defaunation or species treatment on minicore particle skewness (Figure 4.14; L-ratio = 17.52, d.f. = 22, p = 0.0635).

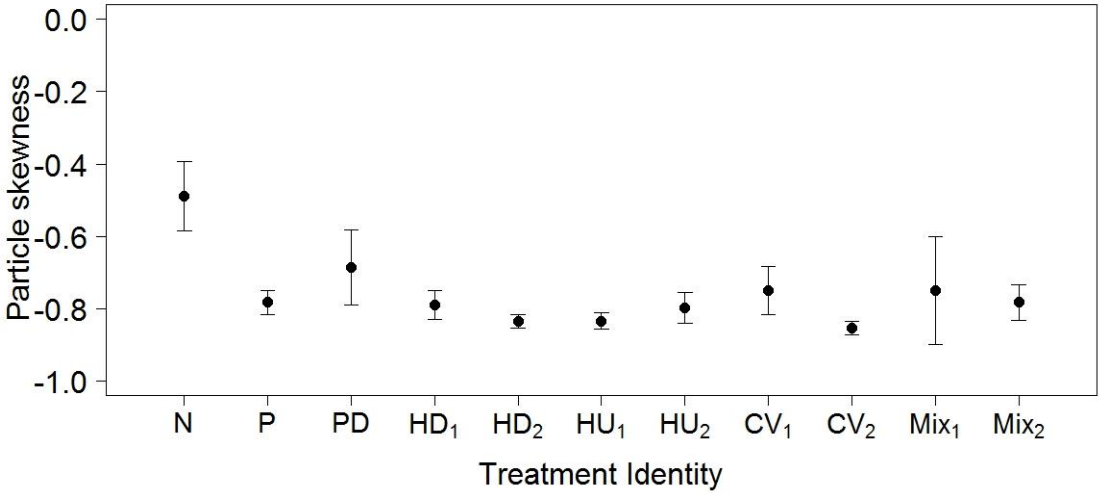

Figure 4.14 | Effect of sediment defaunation, species identity and richness on minicore sediment particle skewness (n = 6). Negative values indicate a fine skew. Error bars are standard error. Treatment identity as in Figure 4.6.

The minicore sediments showed either meso-kurtosis or lepto-kurtosis, meaning there was little spread of particle size compared to the peaked-ness of the distribution curve in the samples. There was a significant effect of sediment treatment on sediment particle kurtosis (L-ratio = 24.89, d.f. = 22, p = 0.0056). Particle kurtosis was not affected by the presence of the mesocosm or defaunation. The high biomass mixed species treatment, however had a large mean (± 95 % CI, n = 6) particle kurtosis (3.93 ± 0.35), larger than the mesocosm treatment (Figure 4.15; P; 3.16 ± 0.13; t = 2.17, p = 0.0341), the high biomass *Hediste* treatment (HD_1; 3.63 ± 0.13; t = 2.05, p = 0.0447), the low biomass *Hediste* treatment (HD_2; 3.58 ± 0.11; t = 2.45, p = 0.0175), the high biomass *Hydrobia* treatment (HU_1; 3.61 ± 0.08; t = 2.27, p = 0.0269), and the low biomass *Corophium* treatment (CV_2; 3.57 ± 0.16; t = 2.43, p = 0.0185). The low biomass *Hydrobia* treatment (HU_2; 3.72 ± 0.03) had a larger mean (± 95 % CI, n = 6) particle kurtosis relative to the high biomass *Hydrobia* treatment (HD_1; 3.63 ± 0.13; t = 3.19, p = 0.0024), however this may have been influenced by the low variation in

these treatments as the actual kurtosis values did not differ greatly. Minicore particle kurtosis only ranged between 3.35 and 4.43 for all treatments, therefore while the differences in particle kurtosis observed between treatments may be significant the actual changes occurring are only small.

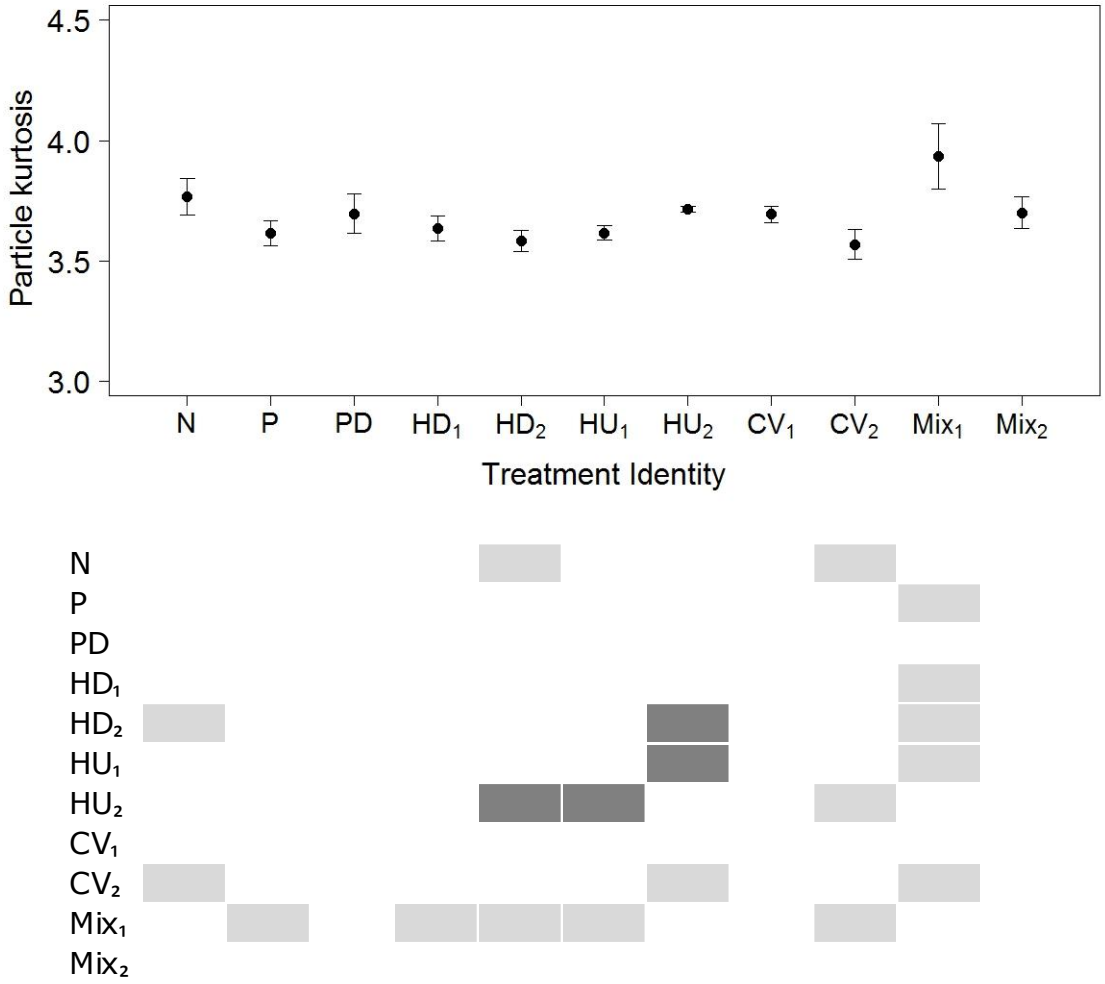

Figure 4.15 | Effect of sediment defaunation, species identity and richness on minicore sediment particle kurtosis (n = 6). Error bars are standard error. Treatment identity as in Figure 4.6. Significant differences are indicated in the accompanying table where darker shading indicates greater significant difference: 0.01 < p < 0.05; 0.0001 < p < 0.01; p < 0.0001.

Minicore particle D_{10} ranged between 10.75 and 20.45 µm for all treatments. There was no effect of mesocosm presence, defaunation or species treatment on minicore particle D_{10} (µm; Figure 4.16; L-ratio = 7.70, d.f. = 22, p = 0.6578).

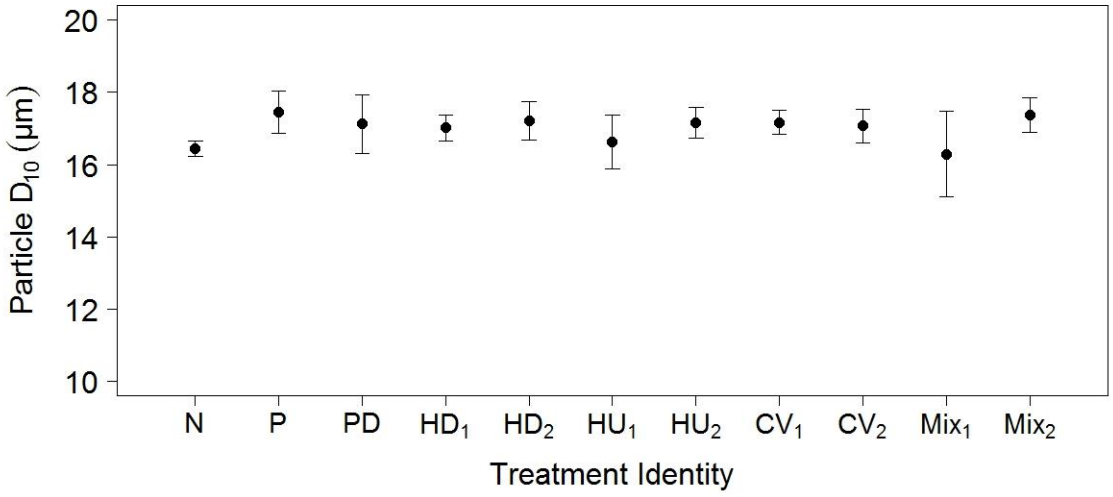

Figure 4.16 | Effect of sediment defaunation, species identity and richness on minicore sediment particle D_{10} (µm; n = 6). Error bars are standard error. Treatment identity as in Figure 4.6.

There was no effect of mesocosm presence, defaunation or species treatment on minicore mud content (%; Figure 4.17; L-ratio = 6.23, d.f. = 22, p = 0.7958).

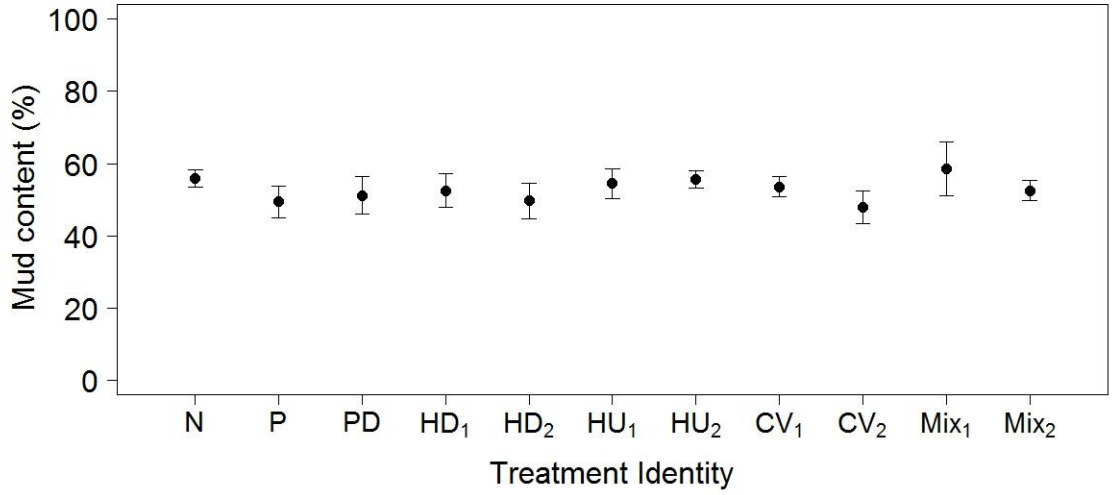

Figure 4.17 | Effect of sediment defaunation, species identity and richness on minicore sediment mud content (%; n = 6). Error bars are standard error. Treatment identity as in Figure 4.6.

4.3.5 | Contact core sediment properties

Only small changes in contact core water concentration (Figure 4.18) were observed in response to the sediment treatments, with water concentration ranging from 0.66 to 0.82 gcm^{-3}, however these changes were significant (L-ratio = 30.61, d.f. = 12, $p < 0.0001$).

Addition of the mesocosm (P; 0.72 ± 0.04 gcm^{-3}) and defaunation (PD; 0.72 ± 0.03 gcm^{-3}) reduced the mean (± 95 % CI, n = 6) contact core water concentration ($t = 2.70$, $p= 0.0091$; $t = 2.75$, $p = 0.0081$ respectively) relative to the natural sediments (N; 0.77 ± 0.03 gcm^{-3}). The high biomass *Hediste* treatment (HD_1; 0.77 ± 0.03 gcm^{-3}) and the low biomass *Corophium* treatment (CV_2; 0.77 ± 0.03 gcm^{-3}) had larger mean (± 95 % CI, n = 6) water concentrations than the mesocosm treatment (HD_1: $t = 2.42$, $p = 0.0191$; CV_2: $t = 2.62$, $p = 0.0114$) and the defaunated treatment (HD_1: $t = 2.45$, $p = 0.0173$; CV_2: $t = 2.66$, $p = 0.0101$). The high biomass *Hediste* treatment also had a larger mean (± 95 % CI, n = 6) water concentration than the high biomass *Hydrobia* treatment (HU_1; 0.72 ± 0.02 gcm^{-3}; $t = 3.15$, $p = 0.0027$).

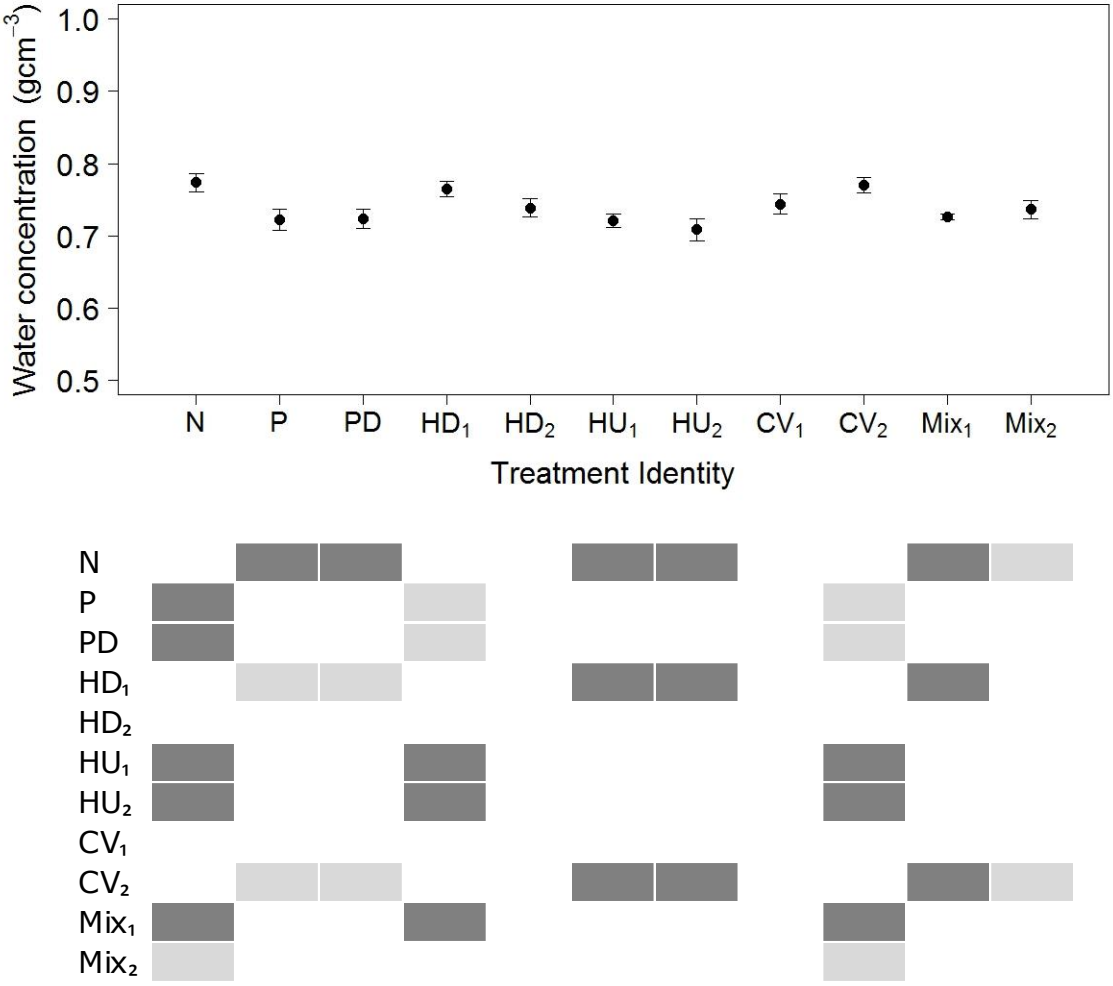

Figure 4.18 | Effect of sediment defaunation, species identity and richness on contact core sediment water concentration (gcm^{-3}; n = 6). Error bars are standard error. Treatment identity as in Figure 4.6. Significant differences are indicated in the accompanying table where darker shading indicates greater significant difference: 0.01 < p < 0.05; 0.0001 < p < 0.01; p < 0.0001.

Contact core colloidal carbohydrate concentration (µgcm^{-3}) varied between the treatments (Figure 4.19) significantly (L-ratio = 41.87, d.f. = 22, p < 0.0001). Addition of the mesocosm (P; 965.22 ± 319.60 µgcm^{-3}) and defaunation (PD; 1087.33 ± 434.90 µgcm^{-3}) greatly increased the mean (± 95 % CI, n = 6) contact core colloidal carbohydrate concentration (t = 3.19, p= 0.0024; t = 3.08, p = 0.0033 respectively) relative to the natural sediments (N; 561.84 ± 61.28 µgcm^{-3}). The low biomass *Hediste* treatment (HD$_2$; 634.86 ± 218.16 µgcm^{-3}) had a smaller mean (± 95 % CI, n = 6) colloidal carbohydrate concentration than the high biomass *Hediste* treatment (HD$_1$; 1093.32 ± 410.75 µgcm^{-3}; t = 2.19, p = 0.0325), the mesocosm

treatment (t = 2.19, p = 0.0324) and the defaunated treatment (t = 2.39, p = 0.0203).

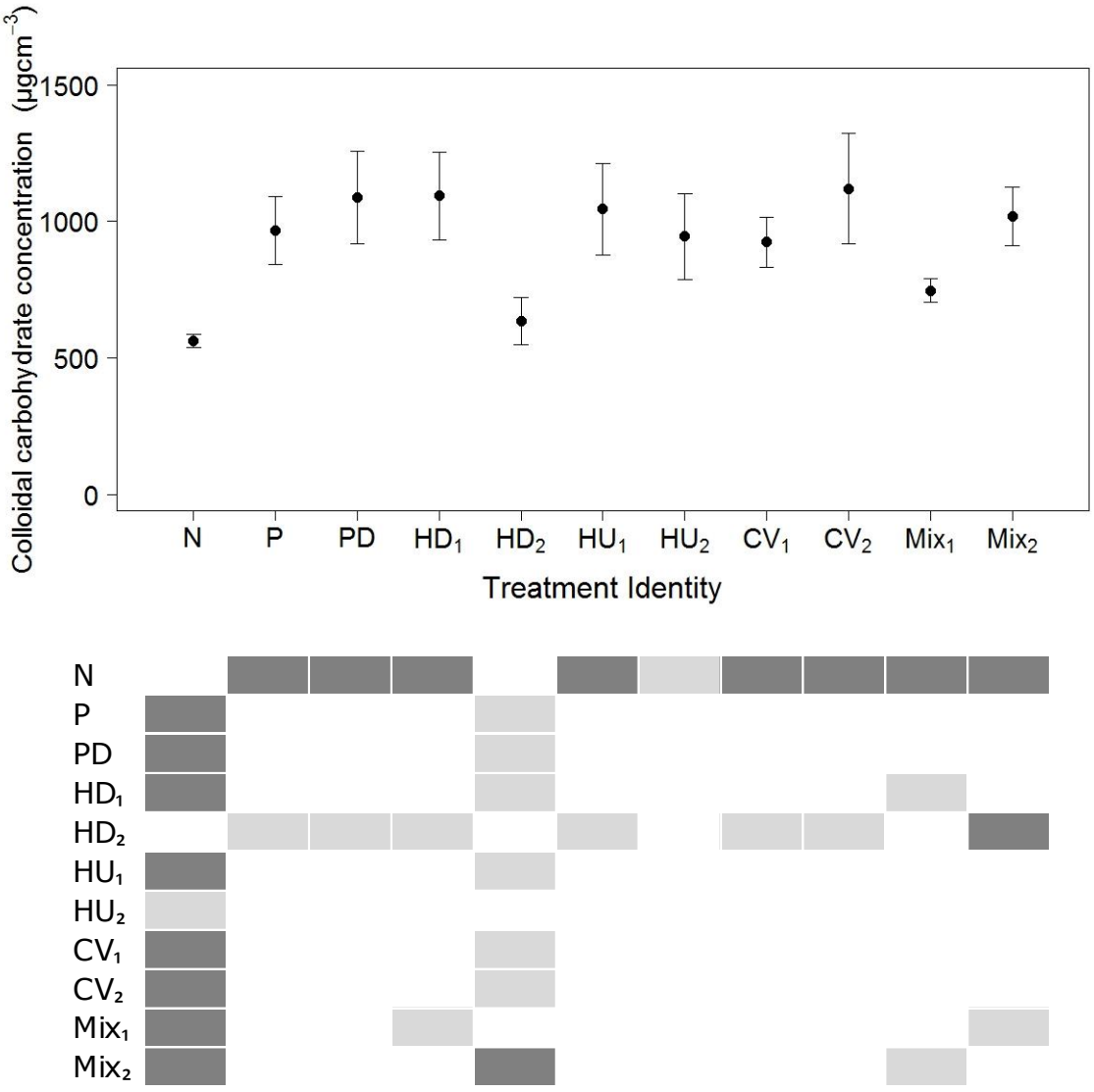

Figure 4.19 | Effect of sediment defaunation, species identity and richness on contact core colloidal sediment carbohydrate concentration (µgcm^{-3}; n = 6). Error bars are standard error. Treatment identity as in Figure 4.6. Significant differences are indicated in the accompanying table where darker shading indicates greater significant difference: ▒ 0.01 < p < 0.05; ▓ 0.0001 < p < 0.01; ■ p < 0.0001.

Contact core chlorophyll *a* content varied significantly between treatments (μgcm^{-3}; Figure 4.20; L-ratio = 36.73, d.f. = 22, p < 0.0001). Addition of the mesocosm (P; 22.34 ± 3.23 μgcm^{-3}) and defaunation (PD; 27.73 ± 4.20 μgcm^{-3}) increased the contact core mean (± 95 % CI, n = 6) chlorophyll *a* concentration (t = 3.01, p= 0.0039; t = 5.47, p < 0.0001 respectively) relative to the natural sediments (N; 18.05 ± 1.74 μgcm^{-3}). The mesocosm treatment sediment (P) had a smaller mean (± 95 % CI, n = 6) chlorophyll *a* concentration than the high biomass *Hediste* (HD_1; 30.50 ± 6.72 μgcm^{-3}; t = 2.81, p = 0.0068), the low biomass *Hediste* (HD_2; 28.30 ± 6.69 μgcm^{-3}; t = 2.06, p = 0.0441), the low biomass *Hydrobia* (HU_2; 26.62 ± 4.26 μgcm^{-3}; t = 2.06, p = 0.0446), and the low biomass *Corophium* (CV_2; 29.40 ± 5.76 μgcm^{-3}; t = 2.75, p = 0.0081) treatments. Only the high biomass *Hydrobia* treatment sediment (HD_1; 30.50 ± 6.72 μgcm^{-3}) had a smaller mean (± 95 % CI, n = 6) chlorophyll *a* concentration than the defaunated treatment sediments (PD; t = 2.02, p = 0.0488).

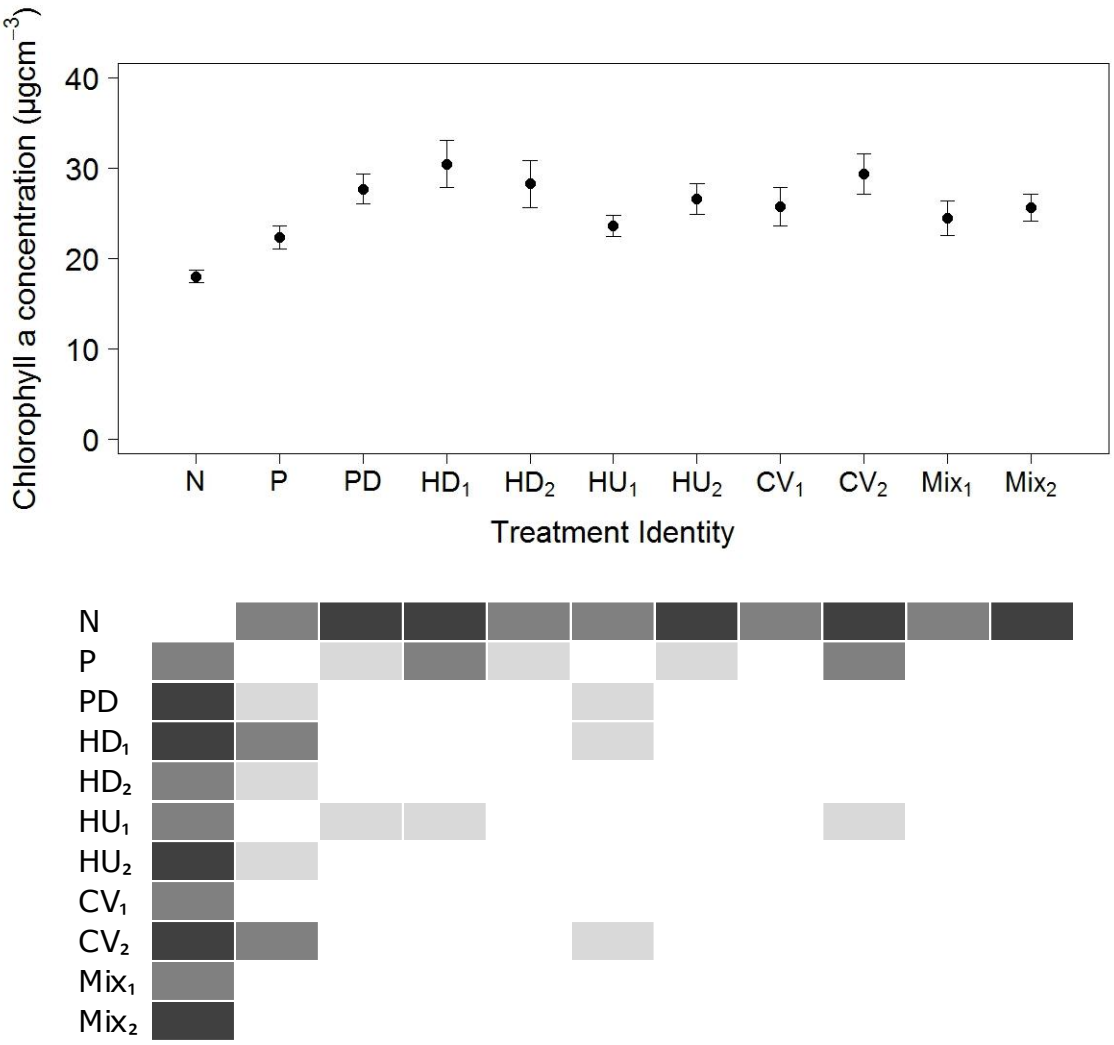

Figure 4.20 | Effect of sediment defaunation, species identity and richness on contact core sediment chlorophyll *a* concentration (µgcm^{-3}; n = 6). Error bars are standard error. Treatment identity as in Figure 4.6. Significant differences are indicated in the accompanying table where darker shading indicates greater significant difference: ▒ 0.01 < p < 0.05; ▓ 0.0001 < p < 0.01; ■ p < 0.0001.

The effect of the addition of the mesocosm, defaunation and species readdition had a very similar significant effect on sediment chlorophyll *b* concentration to that of chlorophyll *a* concentration (Figure 4.21; L-ratio = 43.97, d.f. = 22, p < 0.0001). Addition of the mesocosm (P; 5.04 ± 0.56) and defaunation (PD; 6.69 ± 1.41 µgcm^{-3}) increased the mean (± 95 % CI, n = 6) contact core chlorophyll *b* concentration (t = 4.05, p= 0.0002; t = 4.87, p < 0.0001 respectively) relative to the natural sediments (N; 3.87 ± 0.49 µgcm^{-3}). The high biomass *Hediste* (HD$_1$; 7.40 ± 2.19 µgcm^{-3}), the low biomass *Hediste* (HD$_2$; 7.19 ± 2.09 µgcm^{-3}), the low biomass *Hydrobia* (HU$_1$; 5.82 ± 1.10 µgcm^{-3}), and the low biomass *Corophium* (CV$_1$; 6.25 ± 1.61 µgcm^{-3}) had larger mean (± 95 % CI, n = 6) chlorophyll *b* sediment

concentrations than the mesocosm treatment (t = 2.68, p = 0.0097; t = 2.56, p = 0.0133; t = 2.85, p = 0.0062; t = 4.45, p < 0.0001 respectively). No species treatments were significantly different from the defaunation treatment.

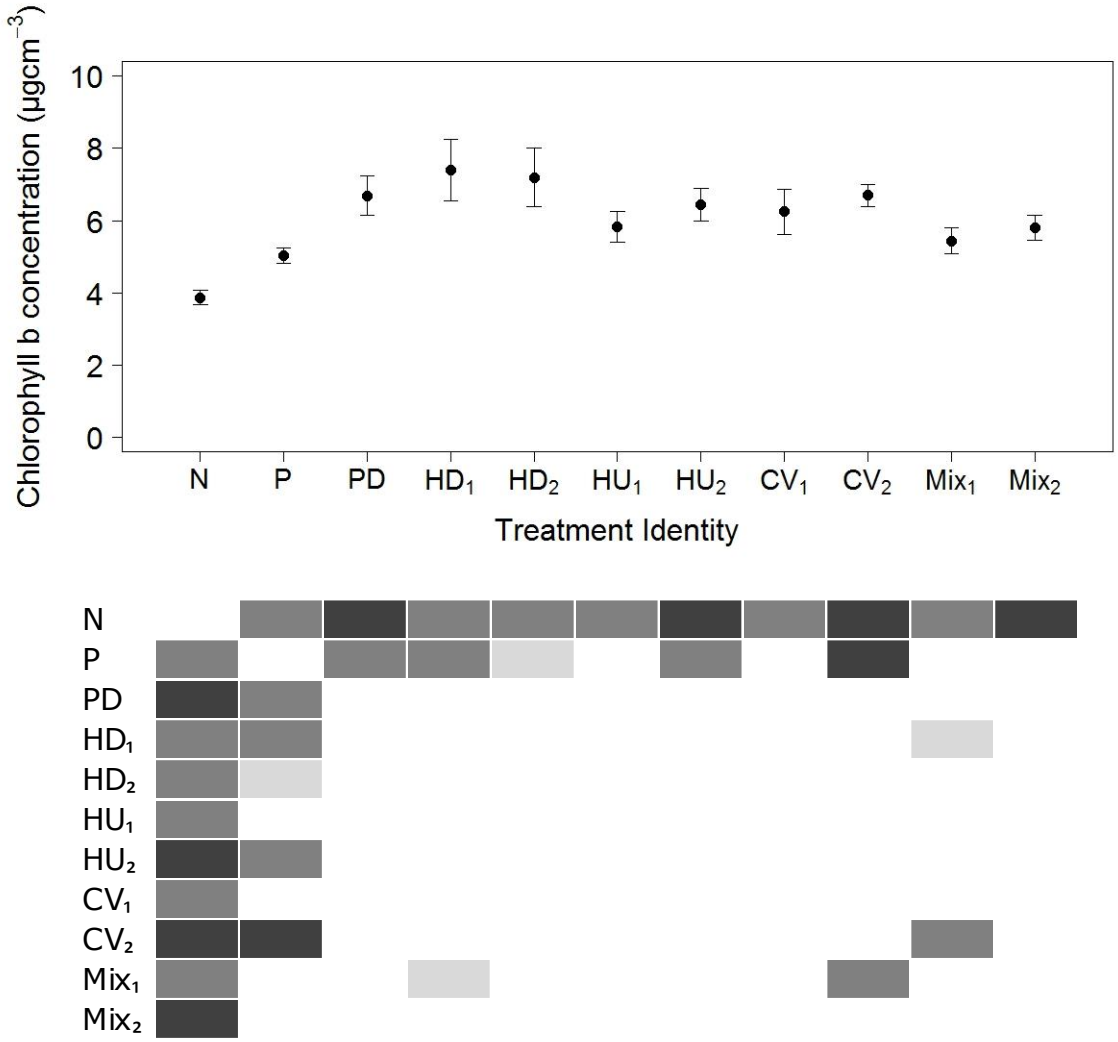

Figure 4.21 | Effect of sediment defaunation, species identity and richness on contact core sediment chlorophyll *b* concentration (µgcm^{-3}; n = 6). Error bars are standard error. Treatment identity as in Figure 4.6. Significant differences are indicated in the accompanying table where darker shading indicates greater significant difference: 0.01 < p < 0.05; 0.0001 < p < 0.01; p < 0.0001.

The contact core sediments were classified as either very coarse silt or coarse silt under the GRADISTAT program scale (Blott and Pye 2001). Contact core sediment mean particle size (all treatments, 36.66 ± 0.89 μm) was smaller than that of the minicores (all treatments, 57.94 ± 2.57 μm). There was no effect of mesocosm presence, defaunation or species treatment on contact core mean particle size (μm; Figure 4.22; L-ratio = 6.31, d.f. = 22, p = 0.7887).

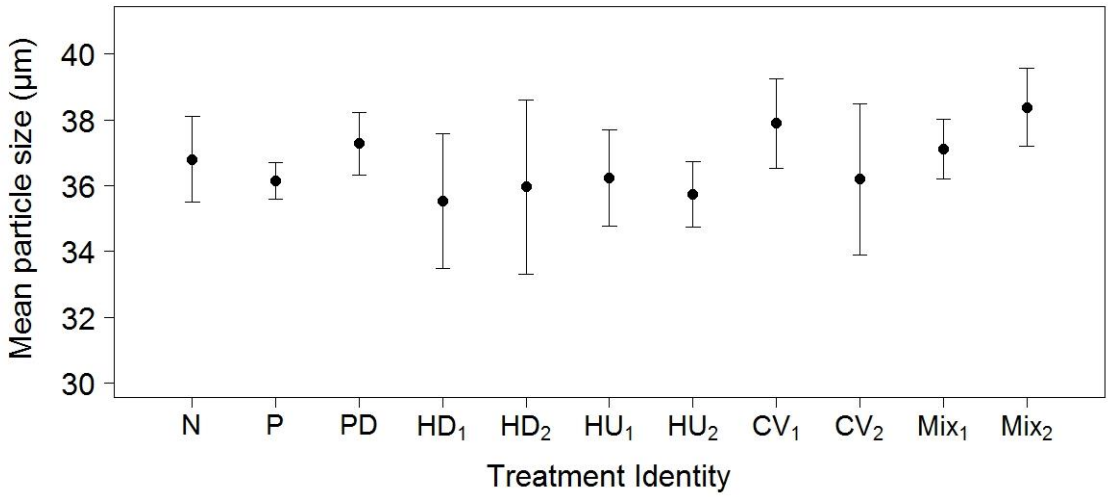

Figure 4.22 | Effect of sediment defaunation, species identity and richness on contact core sediment mean particle size (μm; n = 6). Error bars are standard error. Treatment identity as in Figure 4.6.

Contact core mode particle size (μm) did not change between treatments and there was no effect of mesocosm presence or defaunation (Figure 4.23; F = 0.8261, d.f. = 10, p = 0.6054).

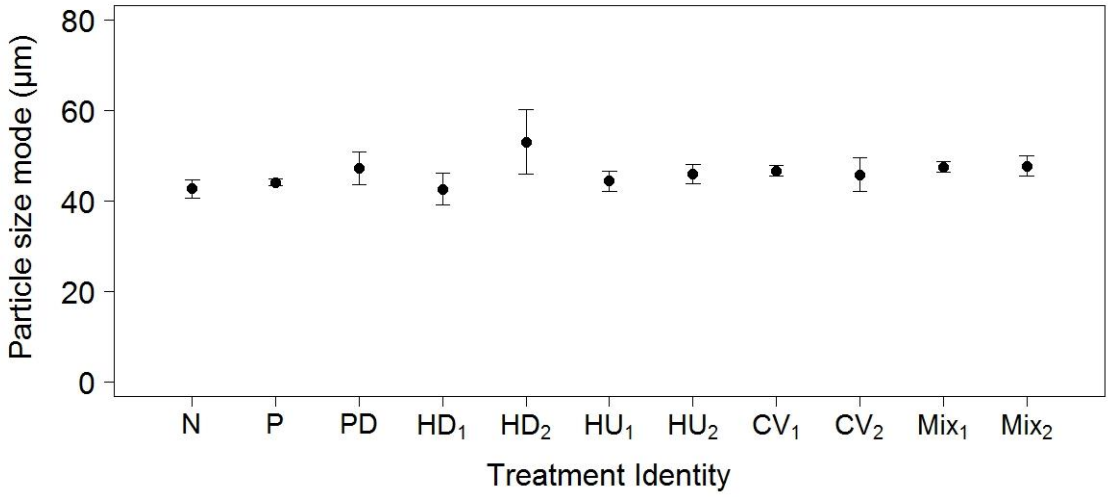

Figure 4.23 | Effect of sediment defaunation, species identity and richness on contact core sediment particle size mode (μm; n = 6). Error bars are standard error. Treatment identity as in Figure 4.6.

The contact core sediments were poorly sorted. Contact core particle sorting ranged between 2.24 and 3.08 for all treatments and there was no effect of mesocosm presence, defaunation or species treatment (Figure 4.24; L-ratio = 16.51, d.f. = 22, p = 0.0859).

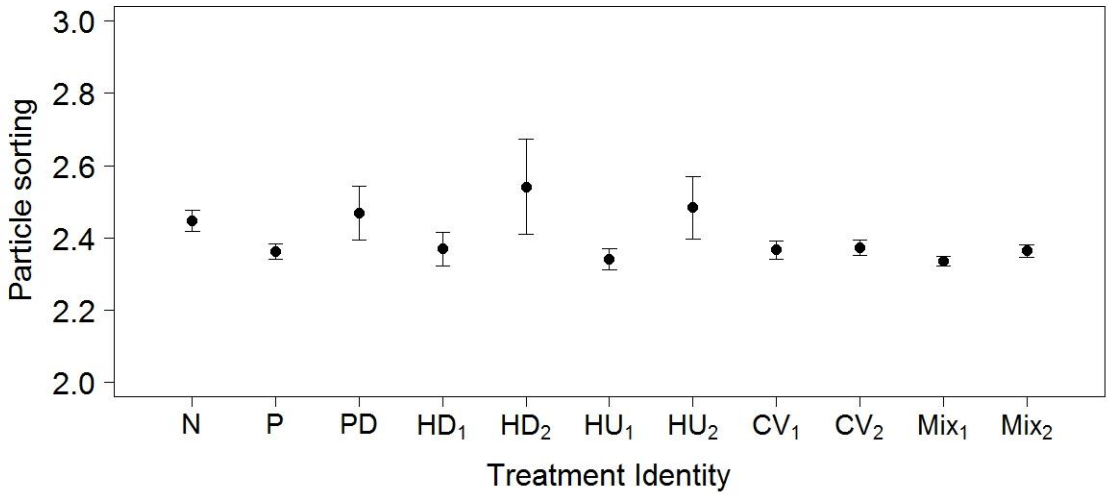

Figure 4.24 | Effect of sediment defaunation, species identity and richness on contact core particle sorting (n = 6). Error bars are standard error. Treatment identity as in Figure 4.6.

The contact core sediments were either finely skewed or symmetrical. Contact core skewness ranged between -0.76 and 0.35 for all treatments and there was no effect of mesocosm presence, defaunation or species treatment on contact core sediment particle skewness (Figure 4.25; L-ratio = 18.01, d.f. = 22, p = 0.0549).

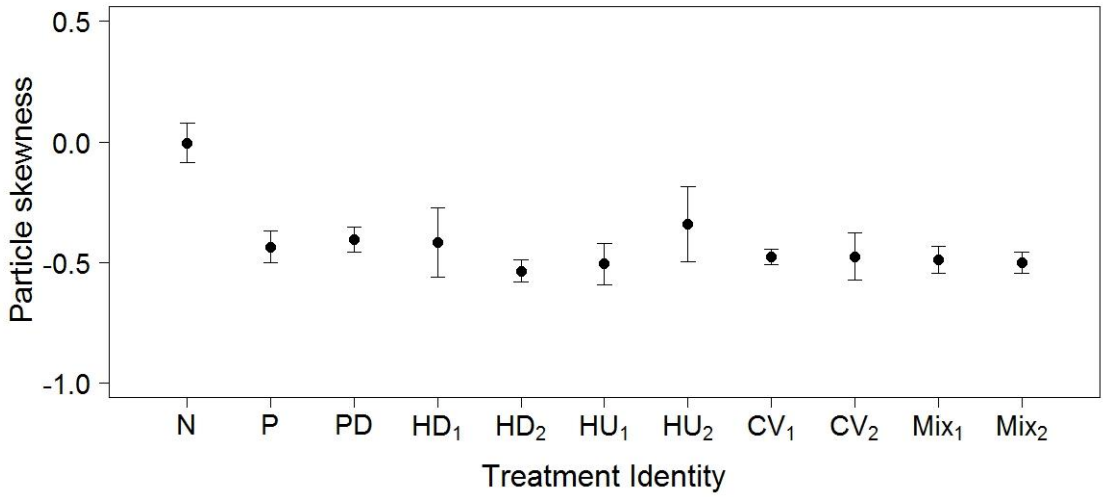

Figure 4.25 | Effect of sediment defaunation, species identity and richness on contact core particle skewness (n = 6). Error bars are standard error. Treatment identity as in Figure 4.6.

The contact core sediments showed either meso-kurtosis or lepto-kurtosis. There was a significant effect of sediment treatment on sediment particle kurtosis (L-ratio = 23.97, d.f. = 22, p = 0.0077). Addition of the mesocosm (P; 3.70 ± 0.16) and defaunation (PD; 3.47 ± 0.40) decreased the contact core mean (± 95 % CI, n = 6) particle kurtosis (Figure 4.26; t = 3.99, p= 0.0002; t = 4.07, p = 0.0002 respectively) relative to the natural sediments (N; 4.35 ± 0.39). The low biomass *Hediste* treatment had a smaller mean (± 95 % CI, n = 6) particle kurtosis (HD_2; 3.09 ± 0.41) than the mesocosm treatment (t = 3.58, p = 0.0007). The low biomass *Hediste* treatment also had a smaller mean (± 95 % CI, n = 6) particle kurtosis relative to the high biomass *Hediste* treatment (HD_1; 3.65 ± 0.21; t = 3.13, p = 0.0028). No species treatment changed the measured particle kurtosis relative to the defaunated treatment.

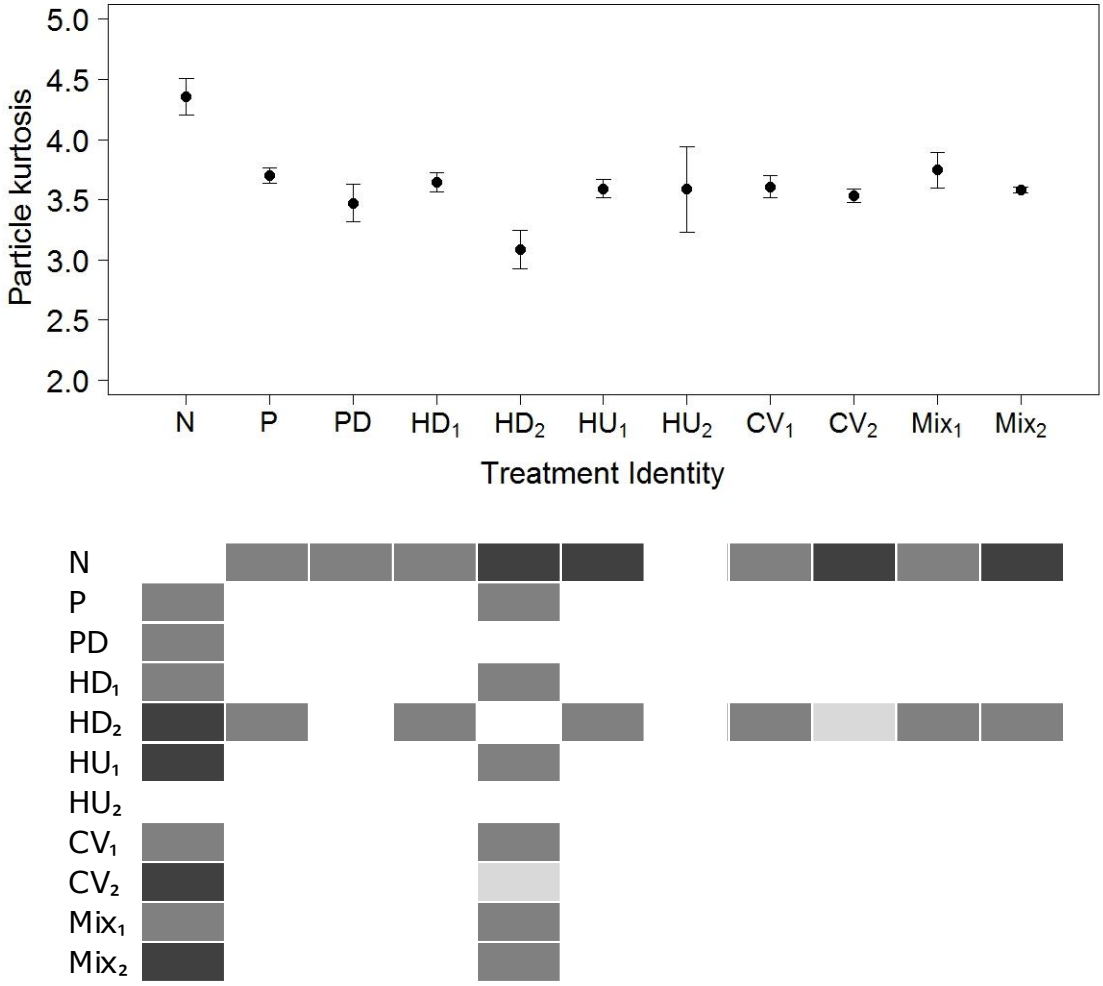

Figure 4.26 | Effect of sediment defaunation, species identity and richness on contact core particle kurtosis (n = 6). Error bars are standard error. Treatment identity as in Figure 4.6. Significant differences are indicated in the accompanying table where darker shading indicates greater significant difference: ▒ 0.01 < p < 0.05; ▓ 0.0001 < p < 0.01; ■ p < 0.0001.

Contact core particle D_{10} ranged between 7.63 and 14.17 µm for all treatments and was smaller than the minicore D_{10}. There was no effect of mesocosm presence, defaunation or species treatment on contact core particle D_{10} (µm; Figure 4.27; L-ratio = 13.61, d.f. =22, p = 0.1913).

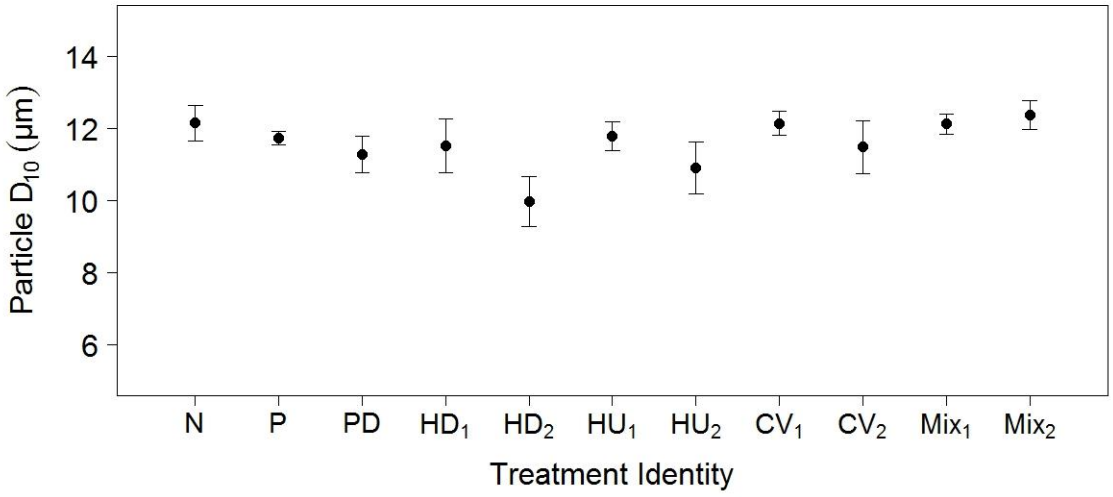

Figure 4.27 | Effect of sediment defaunation, species identity and richness on contact core particle D_{10} (µm; n = 6). Error bars are standard error. Treatment identity as in Figure 4.6.

The contact core sediment mud content was larger than that of the minicores. There was no effect of mesocosm presence, defaunation or species treatment on contact core mud content (%; Figure 4.28; L-ratio = 7.81, d.f. = 22, p = 0.6469).

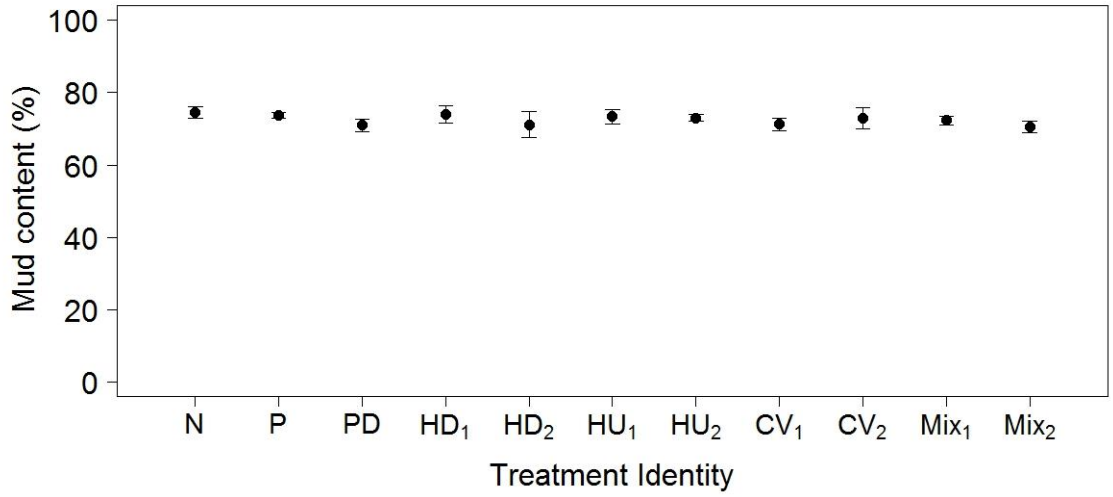

Figure 4.28 | Effect of sediment defaunation, species identity and richness on contact core mud content (%; n = 6). Error bars are standard error. Treatment identity as in Figure 4.6.

Table 4.2 | Summary table of effects of manipulating the density of benthic fauna on sediment characteristics compared with the control defaunated mesocosm (treatment PD). **+** or **–** indicate the direction of the effect where + represents a positive effect and – represents a negative effect compared to the control defaunated mesocosm. A single symbol indicates significance with $p < 0.05$, and a double symbol indicates significance with $p < 0.01$.

		HEDISTE DIVERSICOLOR		*HYDROBIA ULVAE*		*COROPHIUM VOLUTATOR*		MIXED SPECIES	
	Sediment Characteristic	1/3 total natural biomass	full equivalent of natural biomass	1/3 total natural biomass	full equivalent of natural biomass	1/3 total natural biomass	full equivalent of natural biomass	1/3 natural biomass of all three species	Full equivalent of natural biomass of all three species
Erosive properties	Erosion threshold			-					
	Suspension index								
MPB properties	Minimum fluorescence				--				--
	Maxmimum quantum yield				+				++
Mini core sediment properties	Water content								
	Mean particle size								
	Mode particle size								
	Particle sorting								
	Particle skewness								
	Particle kurtosis								
	Particle D10								
	Mud content								
Contact core sediment properties	Water concentration		+			+			
	Colloidal carbohydrate concentration	-							
	Chlorophyll a concentration				-				
	Chlorophyll b concentration								
	Mean particle size								
	Mode particle size								
	Particle sorting								
	Particle skewness								
	Particle kurtosis								
	Particle D10								
	Mud content								

4.3.6 | Species density effects

For *Hediste diversicolor*, the contact core sediment colloidal carbohydrate concentration was much larger in the whole biomass replacement treatment (the high biomass treatment: HD_1) than would be expected (Figure 4.29; the D_{sp} values are > 0) if the effect of this treatment was equivalent to three times the effect of a third of the biomass replacement treatment (the low biomass treatment: HD_2). It would be expected, based on the small colloidal carbohydrate concentrations found in the low biomass *Hediste* treatments that the high biomass treatments would have an extremely small concentration or no colloidal carbohydrate in the contact core sediment, however the concentration observed is not significantly different from those treatments containing no fauna (Figure 4.19). Additionally, the erosion threshold is larger than expected, and therefore the sediment more stable than would be expected, and the contact core particle D_{10} is larger than expected. For the remaining variables, values were spread about 0 and therefore did not show deviation from what may be expected.

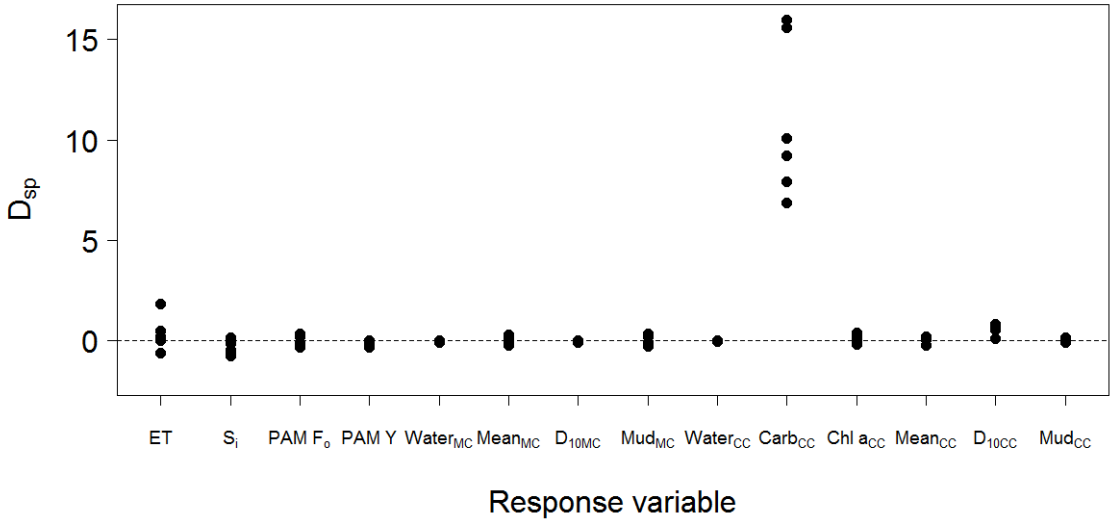

Figure 4.29 | The species biomass effect of *Hediste diversicolor* (n = 6). Where $D_{sp} < 0$, the values observed in the whole biomass treatment are smaller than would be expected and where $D_{sp} > 0$, the values observed in the whole biomass treatment are larger than would be expected compared to three times the effect of a third of the biomass replacement treatment. Response variables are: ET = erosion threshold (Nm^{-2}), S_i = suspension index or relative erosion rate, PAM F_o = pulse amplitude modulated measured minimum fluorescence, PAM Y = pulse amplitude modulation measured maximum quantum yield, $Water_{MC}$ = minicore water content (%), $Mean_{MC}$ = minicore mean particle size (µm), D_{10MC} = minicore particle D_{10} (µm), Mud_{MC} = minicore mud content (%), $Water_{CC}$ = contact core water concentration (gcm^{-3}), $Carb_{CC}$ = contact core carbohydrate concentration (μgcm^{-3}), Chl a_{CC} = contact core chlorophyll *a* concentration (μgcm^{-3}), $Mean_{CC}$ = contact core mean particle size (µm), D_{10CC} = contact core particle D_{10} (µm), Mud_{CC} = contact core mud content (%)) To allow suitable presentation of this figure, D_{sp} obtained for $Carb_{CC}$ has been reduced by a factor of 100.

For *Hydrobia ulvae*, again, many of the observed values were close to those that would be expected if the effect of whole biomass replacement treatment (the high biomass treatment: HU_1) was equivalent to the three times the effect of a third of the biomass replacement treatment (the low biomass treatment: HU_2). However, the high biomass *Hydrobia* treatments had a larger erosion threshold and a larger suspension index than expected, meaning the sediment is more stable than expected but it erodes at a faster rate once the erosion threshold is reached (Figure 4.30). Additionally, compared to the carbohydrate reduction (from the defaunated treatment) caused by addition of a low biomass of *Hydrobia*, the contact core carbohydrate concentration should be much smaller in the high *Hydrobia* biomass treatments. The mean particle size of the minicore sediment samples is also larger than would be expected.

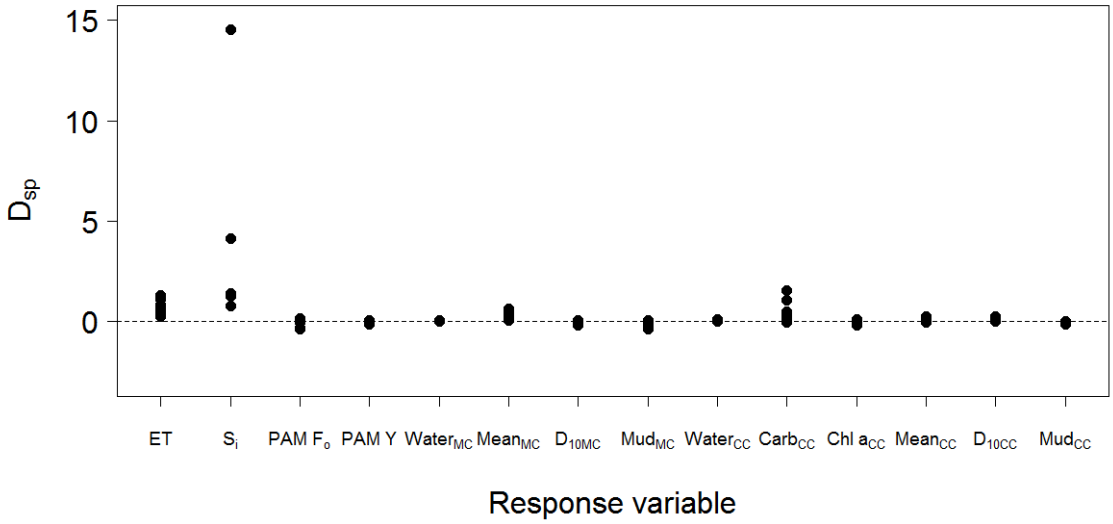

Figure 4.30 | The species biomass effect of *Hydrobia ulvae* (n = 6). Where $D_{sp} < 0$, the values observed in the whole biomass treatment are smaller than would be expected and where $D_{sp} > 0$, the values observed in the whole biomass treatment are larger than would be expected compared to three times the effect of a third of the biomass replacement treatment. Response variables as in Figure 4.29.

For *Corophium volutator*, the erosion threshold in the whole biomass replacement *Corophium volutator* treatment (the high biomass treatment: CV_1) was smaller than would be expected based on the treatment in which only a third of the total biomass was added as *Corophium volutator* (the low biomass treatment: CV_2). Correspondingly, the suspension index was larger than would be expected, meaning the sediment is less stable and erodes more rapidly than expected at the erosion threshold, indicating the sediment is greatly destabilised by the addition of *Corophium*. The pulse amplitude modulation measured minimum fluorescence in the high biomass treatments was also smaller than that which would be predicted based upon the low biomass treatment, as were the contact core water concentration and carbohydrate concentration. The mud content of the high biomass treatment was larger than would be expected based on the mud content of the low biomass treatment.

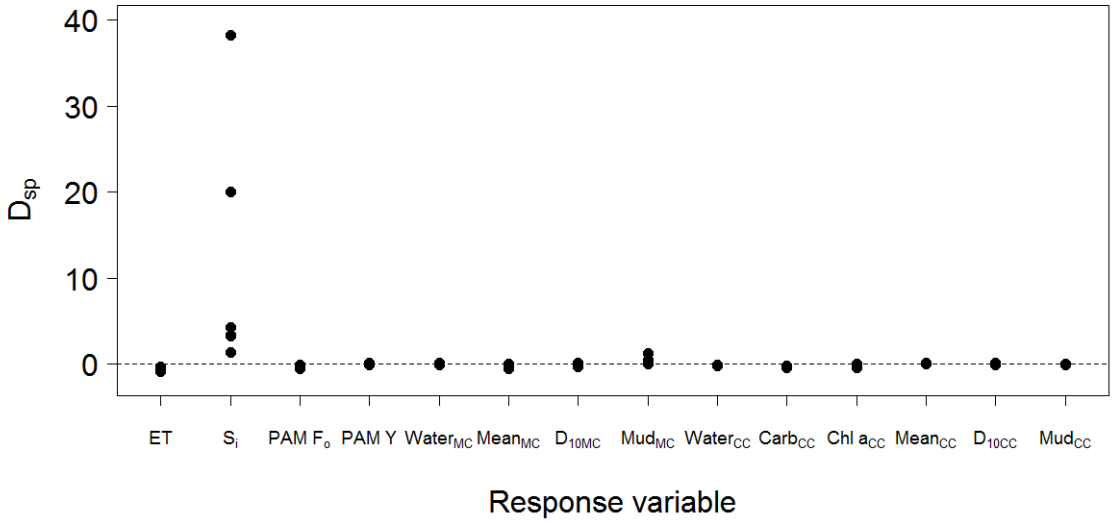

Figure 4.31 | The species biomass effect of *Corophium volutator* (n = 6). Where $D_{sp} < 0$, the values observed in the whole biomass treatment are smaller than would be expected and where $D_{sp} > 0$, the values observed in the whole biomass treatment are larger than would be expected compared to three times the effect of a third of the biomass replacement treatment. Response variables as in Figure 4.29.

4.3.7 | Species richness effects

When examining species richness using trangressive overyielding, for all variables analysed (the erosion threshold, the suspension index, the microphytobenthos minimum fluorescence and maximum quantum yield, the syringe core mean particle size, D_{10} and mud content and the contact core water concentration, carbohydrate concentration and chlorophyll *a* concentration, mean particle size, D_{10} and mud content), the maximum and minimum effect of the species in the single species dominant treatments was greater than the effect of the species mixture (Figures 4.32 and 4.33)

Non-trangressive overyielding revealed that the whole biomass replacement mixed species treatment had a greater suspension index, therefore was more readily erodible, than would be expected based on the additive effects of the three species in the single species dominant communities, and also had a greater surface sediment colloidal carbohydrate concentration and a very slightly larger particle D_{10} than would be expected (Figure 4.34).

Non-trangressive overyielding applied to the high biomass treatments revealed that the high biomass mixed species treatment (Mix_1), was more stable than expected, shown by the larger erosion threshold than expected (Figure 4.35). The mixed species treatment also had a larger minimum fluorescence than expected.

In the substitutive model, again the erosion threshold and the minimum fluorescence were larger than expected (Figure 4.36).

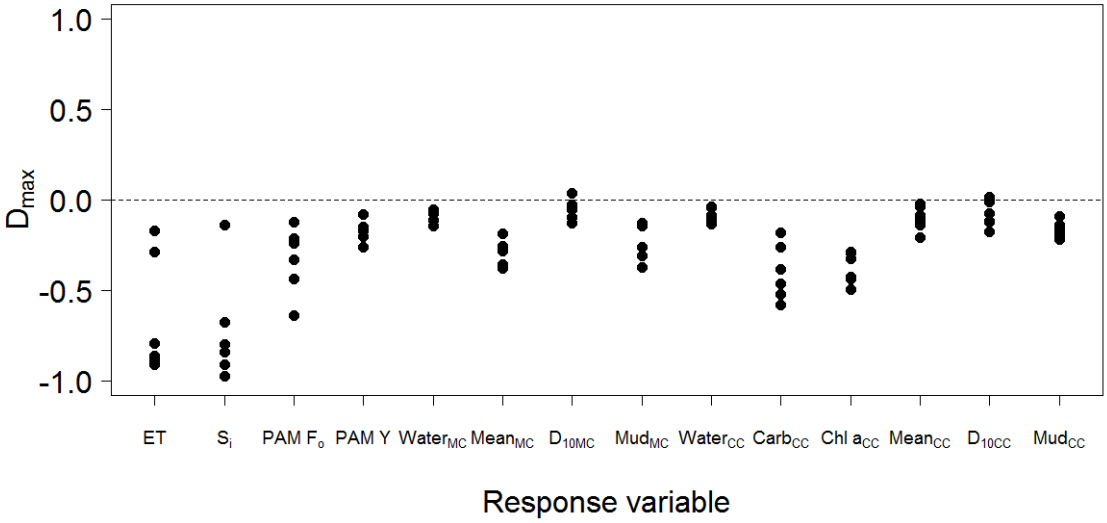

Figure 4.32 | The maximum species effect in the single species dominant communities compared to that in the species mixtures (n = 6). Where $D_{max} < 0$, the values observed in the mixed species treatment are smaller than would be expected and where $D_{max} > 0$, the values observed in the mixed species are larger than would be expected compared to the maximum species effect in the single species dominant communities. Response variables as in Figure 4.29.

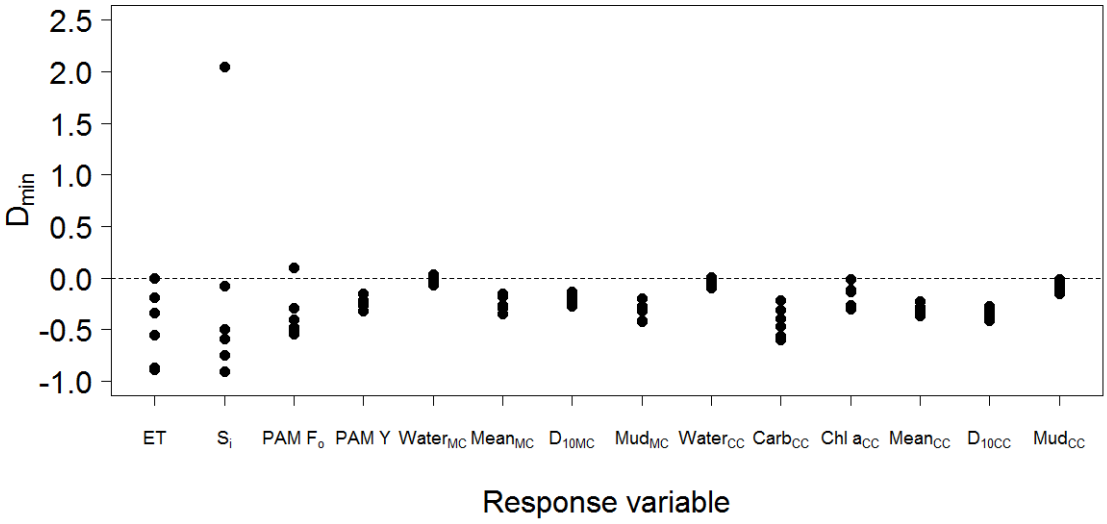

Figure 4.33 | The minimum species effect in the single species dominant communities compared to that in the species mixtures (n = 6). Where $D_{min} < 0$, the values observed in the mixed species treatment are larger than would be expected and where $D_{min} > 0$, the values observed in the mixed species are smaller than would be expected compared to the minimum species effect in the single species dominant communities. Response variables as in Figure 4.29.

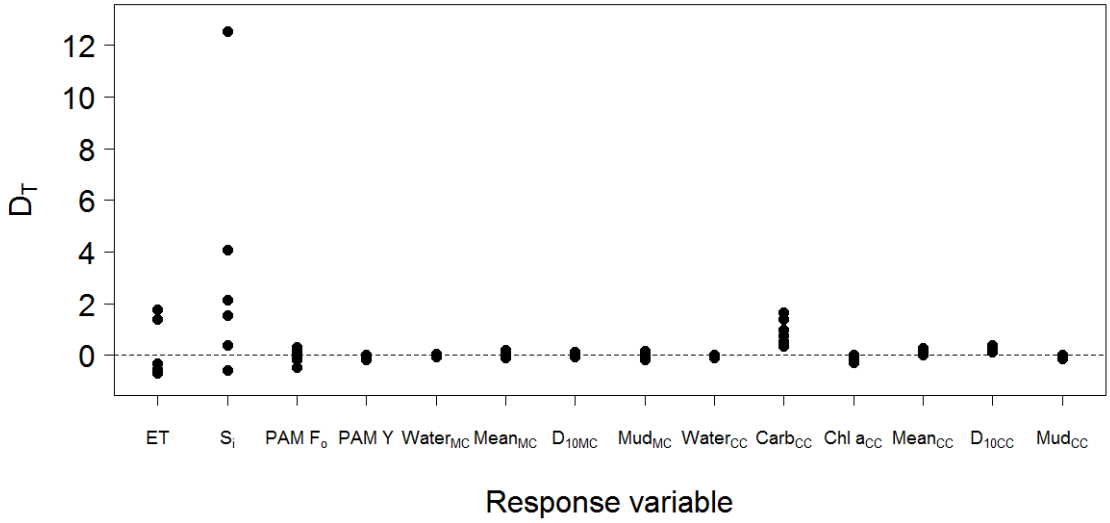

Figure 4.34 | The additive species effects in the single species dominant communities compared to the mixed species treatment for the low biomass treatments (n = 6). Where $D_T < 0$, the values observed in the mixed species treatment are smaller than would be expected and where $D_T > 0$, the values observed in the mixed species are larger than would be expected compared to the species effects in the single species dominant communities. Response variables as in Figure 4.29.

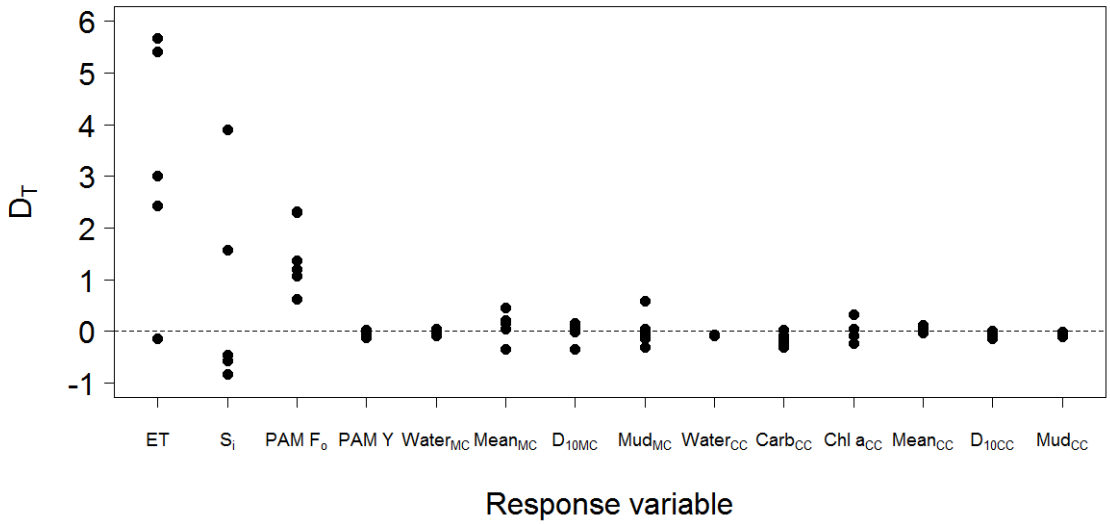

Figure 4.35 | The additive species effects in the single species dominant communities compared to the mixed species treatment for the high biomass treatments (n = 6). Where $D_T < 0$, the values observed in the mixed species treatment are smaller than would be expected and where $D_T > 0$, the values observed in the mixed species are larger than would be expected compared to the species effects in the single species dominant communities. Response variables as in Figure 4.29.

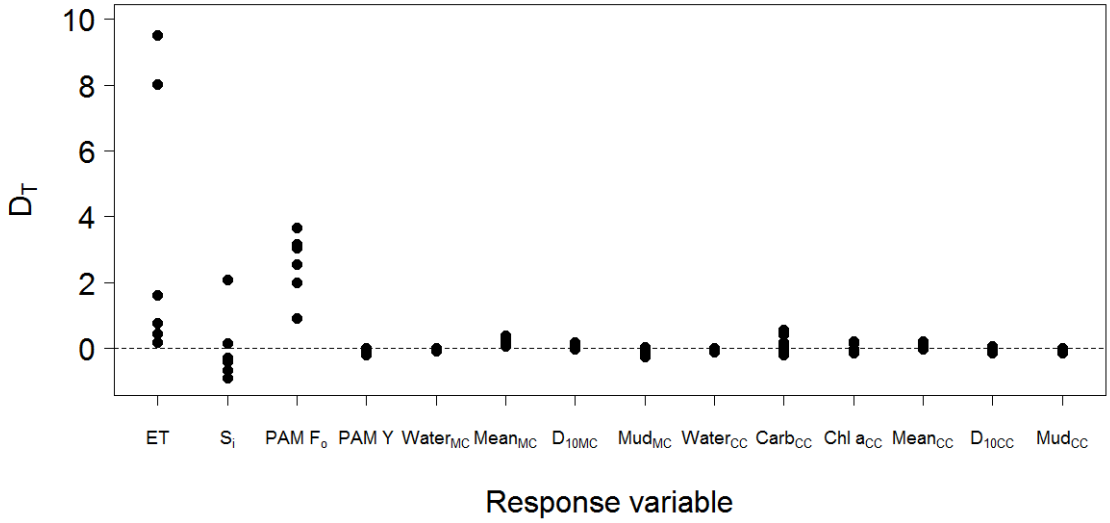

Figure 4.36 | The substitutive species effects in the single species dominant communities compared to the mixed species treatment for the high biomass single species dominant communities treatments compared to the low biomass mixed species treatment, providing a comparison across a constant biomass (n = 6). Where $D_T < 0$, the values observed in the mixed species treatment are smaller than would be expected and where $D_T > 0$, the values observed in the mixed species are larger than would be expected compared to the species effects in the single species dominant communities. Response variables as in Figure 4.29.

4.4 | Discussion

This experiment examined whether species identity, species density or species richness affected mudflat stability and sediment biogeochemical properties. The cryo-defaunation method resulted in a sufficient reduction (78 %) in the abundance of the three species of interest, *Hediste diversicolor*, *Hydrobia ulvae*, and *Corophium volutator*, to provide a suitable method for assessing the effects of the individual species and the species mixtures on the stability and biogeochemistry of the sediment in the field.

4.4.1 | Use of mesocosms in the field

The mesocosms provided an effective way to ensure that sediment defaunation and manipulations in species abundances were maintained for the length of the experiment. They were not observed to cause increased sedimentation over the short timescale of the experiment, a common problem in caging experiments (Virnstein 1978, Raffaelli et al. 1989, Hall et

al. 1990). There were, however, some experimental artefacts caused by the addition of the mesocosm. Sediment held within the mesocosm had reduced species numbers of the three species of interest compared to the natural sediments, and there was a significant increase in the erosion threshold, the microphytobenthos minimum fluorescence, contact core carbohydrate concentration and contact core chlorophyll *a* and *b* concentration. There was also a significant decrease in the sediment suspension index, contact core water concentration and contact core particle size distribution (kurtosis). There are therefore a number of experimental artefacts associated with using these mesocosms. It is difficult to separate the effects of the mesocosm on the sediment from the effect of the change in species abundance caused by the mesocosm (Reise 1978) because there were similar effects caused by defaunation (see Section 4.4.2). The inclusion of a mesocosm only treatment as a procedural control, however, as well as a defaunation control ensures there are comparable control treatments.

4.4.2 | The effect of defaunation

Defaunation resulted in a significant increase in the erosion threshold, the microphytobenthos minimum fluorescence, contact core carbohydrate concentration, and contact core chlorophyll a and b concentration. There was also a significant decrease in the suspension index, microphytobenthos maximum quantum yield, contact core water concentration, contact core particle size distribution (kurtosis). Defaunation has previously been shown to increase sediment erosion threshold through the reduction of macrofaunal bioturbation (de Deckere et al. 2001) and increased microphytobenthos biomass (Davis and Lee 1983). The increased microphytobenthos biomass is likely caused by the removal of the majority of the macrofauna resulting in reduced grazing pressure (Smith et al. 1996). This increase in sediment stability could also be caused by nutrient release as a result of defaunation leading to an increase in colloidal carbohydrate concentration and possibly bacterial biomass (Murphy and Tolhurst 2009). However, as the chlorophyll concentration of the sediments was also determined to have increased after defaunation, this rise in sediment stability can be predominantly attributed to increased microphytobenthos biomass (Paterson 1989, Underwood and

Paterson 1993, Sutherland et al. 1998, Paterson and Black 1999, Black et al. 2002).

4.4.3 | Single species and species density effects: *Hediste diversicolor*

The addition of *Hediste diversicolor* of either high or low density to the defaunated sediments does not result in a significant change in the sediment erosion or microphytobenthos related properties from that observed in the defaunated sediments. The *Hediste* do appear to be grazing on the microphytobenthos, resulting in a reduction of the observed minimum fluorescence when a larger biomass of *Hediste* is added, however this reduction in microphytobenthos biomass is not significant and does not result in a corresponding reduction in the erosion threshold. *Hediste diversicolor* has been observed to undertake a number of contrasting activities that act to both stabilise and destabilise the sediment. These activities include the reduction of sediment water content (Meadows and Tait 1989) resulting in sediment stabilisation, bioturbation (Widdows et al. 2009) resulting in net destabilisation, and microphytobenthos grazing (Smith et al. 1996), resulting in indirect destabilisation through loss of stabilising microphytobenthos. *Hediste diversicolor* has also been shown to stimulate biofilm development, even when feeding on diatoms (Passarelli et al. 2012), and enhance sediment cohesion. The undertaking of these contrasting activities may have led to no net effect of *Hediste diversicolor* on sediment erosive or microphytobenthos properties in this experiment.

High densities of *Hediste diversicolor* were shown to increase the sediment water concentration at the surface of the sediment (top 2 mm, as measured by contact core samples) compared to defaunated sediments, in contrast to the observations made by Meadows and Tait (1989) who found that the water content of the upper 1 cm of the sediment decreased when *Hediste diversicolor* was present. Low densities of *Hediste diversicolor* were observed to cause a significant decrease in sediment colloidal carbohydrate concentration compared to defaunated sediment, whereas high densities of *Hediste* did not. This is possibly as a result of selective grazing or the influence of *Hediste diversicolor* grazing on the growth phase of the

microphytobenthos, resulting in a reduction in colloidal carbohydrate production (Orvain et al. 2003).

4.4.4 | Single species and species density effects: *Hydrobia ulvae*

The addition of both high and low biomasses of *Hydrobia ulvae* caused a net destabilisation of the mudflat sediments compared to the defaunated sediments (however this effect was only significant for the low biomass *Hydrobia* treatment). Re-addition of the total or partial biomass of sediment with just *Hydrobia* resulted in similar erosion thresholds to that of the procedural control. *Hydrobia* has been shown to destabilise sediments in the field previously (Austen et al. 1999, Andersen 2001), which has been attributed to a number of activities. Surface browsing (Blanchard et al. 1997) and bioturbation (Orvain et al. 2006) can cause surface disruption allowing particle dislodgement by currents, and the creation of tracks across the sediment surface increases sediment surface roughness, creating erosion focal points at the tip of the ridges left either side of the tracks (Nowell et al. 1981). *Hydrobia ulvae* has also been observed to excrete fecal pellets (Andersen 2001), which at low tide may be deposited on the surface of the sediment and are then easily erodible by the next flood tide. Increased sediment moisture caused by *Hydrobia ulvae* has been shown to destabilise sediment (Orvain et al. 2006), however, increased moisture was not observed in this experiment in the surface sediment (the top 2 mm sampled using the contact core) or the syringe cores (top 1 cm).

At high densities *Hydrobia* caused a significant reduction in the minimum fluorescence and the chlorophyll *a* concentration compared to the defaunated sediment treatments. This indicates that *Hydrobia* is grazing on the microphytobenthos, also observed by (Blanchard et al. 1997, Austen et al. 1999), which could have indirectly resulted in the decrease in the erosion threshold observed.

The microphytobenthos maximum quantum yield (a measure of 'health') increased significantly when *Hydrobia* was at high densities. *Hydrobia* has been shown to be a general consumer of epipelic diatoms

(Hagerthey et al. 2002), grazing on all species, causing a general reduction in epipelic microphytobenthos biomass, but not affecting species richness or evenness. However, *Hydrobia* have also been shown to graze preferentially upon larger particle sizes of 20 to 300 µm (Fenchel et al. 1975), and may therefore cause a greater grazing pressure on the larger motile epipelic diatoms (Reise 1992). This may cause a relative increase in the particle attached epipsammic diatoms, which have been shown to have enhanced growth rates and light absorption compared to larger diatoms (Geider et al. 1986), which may result in the increased microphytobenthos 'health' observed.

At low *Hydrobia* densities, the grazing appears to result in a significant reduction in sediment colloidal carbohydrate content, the reduction of which could account for the significant reduction in the erosion threshold observed, because carbohydrate based extra-cellular polymeric substances (EPS) have been shown to increase sediment stability significantly (Montague 1986, Grant 1988, Paterson 1989, Dade et al. 1990, Paterson et al. 1990, Paterson 1997, Tolhurst et al. 2002). Epipelic diatom biomass has been shown to be correlated with sediment colloidal carbohydrate concentration, but not epipsammic diatom biomass (Madsen et al. 1993). Perhaps the decrease in carbohydrate concentration of the sediment reflects a reduction in epipelic diatoms, while it is an increase in epipsammic diatoms that maintains sediment chlorophyll concentrations, microphytobenthos biomass and photosynthetic productivity.

The greater density of *Hydrobia* does not decrease the erosion threshold correspondingly, as would be expected if the effects of *Hydrobia* in low densities were additive at high densities, indicating an intra-specific species density effect occurring. This could be due to a number of previously observed effects. At high *Hydrobia* abundances, fecal excretions may play a role in enriching and fertilising diatom populations (Lopezfigueroa and Niell 1987, Plaganyi and Branch 2000) resulting in the maintenance of microphytobenthic biomass and stabilisation, even under increased grazing pressure. Levinton (1979) noted that movement and feeding of the closely related species *Hydrobia ventrosa* was reduced at increased densities, which may reduce the sediment destabilisation caused by *Hydrobia* surface crawling.

Blanchard et al. (2000) also showed that the individual ingestion rate of *Hydrobia ulvae* decreased at high species density.

4.4.5 | Single species and species density effects: *Corophium volutator*

The addition of a high or low density of *Corophium volutator* to defaunated sediments did not result in a significantly lower erosion threshold compared to the defaunated sediments, however the addition of a high biomass of *Corophium* resulted in sediment with an erosion threshold similar (i.e. not significantly different) to those of the procedural control. This increased sediment erodibility at high *Corophium* densities is probably due to the high level of bioturbation caused by *Corophium* and their burrow creation (de Deckere et al. 2000), the ejection of sediment while creating burrows (Grant and Daborn 1994) and grazing (Smith et al. 1996, Mouritsen et al. 1998). *Corophium* has been shown to exhibit a higher bioturbation rate at higher densities (De Backer et al. 2011). At low densities, the bioturbatory and grazing effect of the *Corophium* may be too low to exert a destabilising effect on the sediments.

Low densities of *Corophium* were shown to significantly increase the water concentration of the sediment surface (as measured using contact cores) over that of both the procedural control treatments and the defaunated treatments. This is possibly due to increased activity or grazing on the sediment surface. This increase in sediment surface water concentration was not observed at high densities of *Corophium*, possibly as a result of reduced sediment surface activity due to an increase in sub-surface activity and bioturbation at high densities as found by De Backer et al. (2011). The average water content of the top 1 cm of the sediment (as measured using syringe cores) was shown to be larger in the high density *Corophium* treatments than the low density *Corophium* treatments, the defaunated treatments, the procedural control treatments, and all the other species treatments, however not significantly so. This could be because the *Corophium* burrows contain water in these saturated sediments, so increased bioturbation and burrow creation results in increased sub-surface sediment water content.

Corophium volutator has been shown to reduce microphytobenthos biomass through grazing in previous studies (Smith et al. 1996, Mouritsen et al. 1998, de Deckere et al. 2002), however no significant effect of *Corophium* on microphytobenthos minimum fluorescence, maximum quantum yield, or sediment chlorophyll concentration compared to the defaunated sediment treatment was observed in this study. *Corophium* has been shown to exhibit both deposit feeding and filter feeding (Hart 1930, Meadows and Reid 1966, Hughes 1988, Gerdol and Hughes 1994, Riisgard and Schotge 2007), switching to filter feeding when water column algal cell concentration is high (Riisgard and Schotge 2007). It is possible that at low densities, low total grazing means that the microphytobenthos biomass is not significantly affected and at high densities, increased sub-surface activity and filter feeding means that the sediment surface layer microphytobenthos are not significantly affected.

4.4.6 | Species richness effects

There was no significant effect of the mixed species treatments on the sediment erosion properties compared to the defaunation treatment. The high biomass mixed treatment, however showed a significant reduction in microphytobenthos biomass and a significant increase in microphytobenthos health. It is surprising that at what is potentially three times the grazing pressure (the high biomass mixed species treatment consists of defaunated sediment with the equivalent of the three times the biomass of the natural sediment added) the microphytobenthos is actually healthier than in the other species treatments. This may be due to a regulatory effect occurring due to high levels of grazing occurring, as has been shown for *Corophium volutator* (Hagerthey et al. 2002), in which grazing of the dominant diatom taxa promotes diatom species richness, evenness and overall diversity.

The action of individual organisms on the sediment and the sediment properties can affect marine ecosystems through a number of diverse mechanisms, including those discussed above for *Hediste diversicolor*, *Hydrobia ulvae* and *Corophium volutator*; however, the combined effects of such species in mixture have more relevant implications for real ecosystems, in which species are rarely found in monoculture. Mixed species effects can

be additive, i.e. the sum of the individual effect of each species, or they can be positively or negatively interactive, being greater or smaller than the sum of the individual effects (Statzner and Sagnes 2008). In this experiment, the effect of the species in mixture is a negative interactive effect. While the species mixture treatments had a smaller average erosion threshold and microphytobenthos biomass there was no significant reduction in these variables compared to the defaunated sediment treatments. The effect of the three species in mixture on sediment erodibility and microphytobenthos biomass was less than that predicted based on the effects of the species in single species dominant communities for both the additive and substitutive models.

These species have been found to act interactively in combination in other studies as well. Meadows and Tait (1989) found that in a laboratory experiment the sediment stabilising effects of *Corophium volutator* and *Hediste diversicolor* were additive in combination compared to in monoculture, however, some of the treatments had a smaller sediment permeability than predicted suggesting a negative interaction between the species.

Hediste has a range of feeding strategies (Barnes 1994), the use of which may depend on the surrounding species and food availability. *Hydrobia* and *Corophium* have also been shown to select different diatom species and particle sizes depending upon grazing competition and availability (Hagerthey et al. 2002). Species activities undertaken when in multispecies assemblages may therefore be different from those undertaken in monoculture or single species dominant communities due to context dependent effects of biodiversity (Petchey and Gaston 2002) conditional on physical and biological interactions occurring within the environment.

4.4.7 | Experimental limitations

As this experiment was carried out using *in situ* mesocosms it is affected by a number of potential experimental artefacts, however the use of mesocosms to prevent colonisation of defaunated sediments and maintain the species biomass was necessary. The inclusion of a mesocosm only

treatment ensured that the changes observed in the defaunated and the species treatments could be compared to a procedural control.

The mesocosms may not have prevented the ingress of small individuals of *Corophium volutator* or *Hediste diversicolor* into the cores. The abundance recorded of each of these species in the community composition cores was larger than those added, however many of the individuals recorded were small in size. Further experiments using *in situ* mesocosms in this thesis will assess species biomass at the end of the experiment to account for ingress of low biomass juveniles through the mesocosm mesh.

4.4.8 | Future work

Future experiments should investigate the mechanism of how changes in species behaviour and activities, such as bioturbation and bioirrigation, may change between species held in monoculture and in mixture to determine why the effects of the species in mixture vary from what might be expected based on the species activities in monoculture. Biological context dependence could be investigated further using experimental treatments with varying species evenness and biomass allocation, whereas physical context dependence could be investigated under different temporal, spatial and environmental variable regimes.

4.4.9 | Chapter conclusions

1 | Defaunation of the sediment results in increased sediment stability and increased microphytobenthos biomass.

2 | Species identity has a significant effect on sediment stability and biogeochemical properties. *Hediste diversicolor*, *Hydrobia ulvae* and *Corophium volutator* have different functional traits that affect the sediment in distinct ways, resulting in the different patterns seen in the sediment biogeochemical properties.

3 | Species density has a significant effect on sediment stability and biogeochemical properties. At high species densities, density dependent intra-specific effects become important in structuring sediment properties, whereas at low species densities, species activity may be too low to result in any discernible effect.

4 | Species richness effects are negatively interactive. The individual effects of species observed in single species dominant communities are reduced by species interactions indicating species effects may be ecologically context dependent.

Chapter 5 | Effects of Multiple Species Combinations on Mudflat Biogeochemical Properties

5.1 | Introduction

This chapter examines how species combinations containing 2 and 3 species, with varying species richness and biomass densities, affect the properties of the mudflat. The abundance and biomass distribution of the species *Hediste diversicolor*, *Hydrobia ulvae* and *Corophium volutator*, were manipulated in two and three species combinations to determine the effects on mudflat stability and biogeochemical properties, specifically addressing Objectives 1, 2, 3 and 4 presented in Section 1.7:

Objective 1 | Investigate the effect of individual macrofauna species on mudflat sediment stability and biogeochemical properties *in situ*.

Objective 2 | Investigate the effect of macrofaunal species density on mudflat sediment stability and biogeochemical properties *in situ*.

Objective 3 | Investigate the effect of macrofaunal species richness on mudflat sediment stability and biogeochemical properties *in situ*.

Objective 4 | Investigate the effect of macrofaunal species biomass distribution on mudflat sediment stability and biogeochemical properties *in situ*.

5.1.1 | Rationale

Many recent studies have established that species richness is important in maintaining ecosystem processes (Emmerson et al. 2001, Bolam et al. 2002, Biles et al. 2003, Raffaelli et al. 2003b), however other ecosystem attributes such as spatial patterns and species evenness have been little studied (Maestre et al. 2012). This chapter aims to investigate how various scenarios of extinction, approximated by creating marked reductions in species density, affect sediment stability and biogeochemical

processes. Recent work has suggested that extinction is a non-random process (Solan et al. 2004a, Gross and Cardinale 2005). Extinction risk is determined by species population size (Tracy and George 1992), body size (McKinney 1997), trophic level (Petchey et al. 1999) and sensitivity to stressors (Thomas et al. 2004), however in the real world it is unknown how, why and in what order species may potentially go extinct and how these extinctions will affect the remaining species and biogeochemical properties of the sediment. Three sets of treatments were devised where *Hediste diversicolor*, *Hydrobia ulvae* or *Corophium volutator* was selected for extinction and not re-added to the sediment after defaunation. Within each two species treatment the species biomass distribution of each species was varied to simulate the biomass changes which may occur after species extinction. Dominance of one species over the other may occur as a result of species expansion due to decreased competition or a reduction in species abundance due to decreased facilitation, or species biomass distribution may be equal.

5.2 | Materials and methods

Fieldwork was carried out at Breydon Water, Great Yarmouth, UK over the period 21st of May to 14th of June, 2012 adjacent to the area where the pilot experiment and the experiment presented in Chapter 4 were carried out. Five sediment cores to determine core species biomass were taken on the 21st of May 2012 following the method given in Section 2.2 for measurement of the macrofaunal biomass. These biomass measurements were used to determine the biomass required for the experimental treatments. Biomass cores contained an average (± SE) of 0.90 ± 0.11 g of macrofaunal biomass, equivalent to 44.67 ± 5.65 g per m^2, consisting of predominantly *Hediste diversicolor*, *Corophium volutator* and *Hydrobia ulvae*. The experiment was setup over two days from the 30th to the 31st of May, 2012.

5.2.1 | Experimental design

The experimental design consisted of 13 treatments (Figure 5.1; n = 4); natural sediment as a control baseline (N), a pipe mesocosm only

treatment as a procedural control (P), a defaunated mesocosm treatment as an experimental control (PD), and 10 experimental treatments in mesocosms.

Treatments consisting of two species were designed to examine how species biomass distribution affects sediment properties, and the species biomass was split between two species in ratios of 1:2, 1:1 or 2:1. The two species treatments consisted of defaunated mesocosms with $^2/_3$ of the original biomass replaced with *Hediste diversicolor* and $^1/_3$ original biomass replaced with *Hydrobia ulvae* (HD_1HU_2); $^1/_2$ of the original biomass replaced with *Hediste diversicolor* and $^1/_2$ of the original biomass replaced with *Hydrobia ulvae* (HDHU); $^2/_3$ of the original biomass replaced with *Hydrobia ulvae* and $^1/_3$ of the original biomass replaced with *Hediste diversicolor* (HU_1HD_2); $^2/_3$ of the original biomass replaced with *Hediste diversicolor* and $^1/_3$ of the original biomass replaced with *Corophium volutator* (HD_1CV_2); $^1/_2$ of the original biomass replaced with *Hediste diversicolor* and $^1/_2$ of the original biomass replaced with *Corophium volutator* (HDCV); $^2/_3$ of the original biomass replaced with *Corophium volutator* and $^1/_3$ of the original biomass replaced with *Hediste diversicolor* (CV_1HD_2); $^2/_3$ of the original biomass replaced with *Hydrobia ulvae* and $^1/_3$ of the original biomass replaced with *Corophium volutator* (HU_1CV_2); $^1/_2$ of the original biomass replaced with *Hydrobia ulvae* and $^1/_2$ of the original biomass replaced with *Corophium volutator* (HUCV); $^2/_3$ of the original biomass replaced with *Corophium volutator* and $^1/_3$ of the original biomass replaced with *Hydrobia ulvae* (CV_1HU_2).

A final three species treatment was added to compare the effect of two species to three species and to enable the comparison of a similar treatment included in the experiment presented in Chapter 4. The three species treatment consisted of a mix of *Hediste diversicolor*, *Hydrobia ulvae* and *Corophium volutator*, each species replacing a $^1/_3$ of the original biomass, as in Chapter 4 (Mix_2). The 52 mesocosms were set up as detailed in Section 2.2 and the cryo-defaunation methodology carried out as detailed in Section 3.2.2. Data collection occurred on the 13th and 14th of June 2012 following the protocols detailed in Section 2.3.

This experiment was originally meant to consist of 96 replicates (n = 6 for each treatment), however during data collection on what would have been Day 1 a heavy rain storm occurred approximately two thirds of the way through the data collection period. The rain storm significantly disturbed the sediment surface of the remaining treatments. This would have had a significant effect on the sediment properties, particularly the erodibility (see for example Torres et al., 2003, Tolhurst et al., 2006, Pilditch et al., 2008, Tolhurst et al., 2008) so data collection was halted. Weather forecasts for the following days also predicted rain so further data collection was delayed. As the remaining treatments still provided four replicates for each experimental treatment, the experimental data were still collected; however the statistical power of this experiment is reduced (Button et al. 2013).

The first two days of experimental setup, 30th to the 31st of May 2012, consisted of laying out the experimental mesocosms and defaunation of the mesocosms allocated to species biomass replacement treatments and the experimental control. On the following two days, treatments were representatively allocated to the treatment areas ensuring even allocation to day (n = 26; Day1, Day2) and row (n = 13; Row1, Row2, Row3, Row4; where Row1 was highest on the shore).

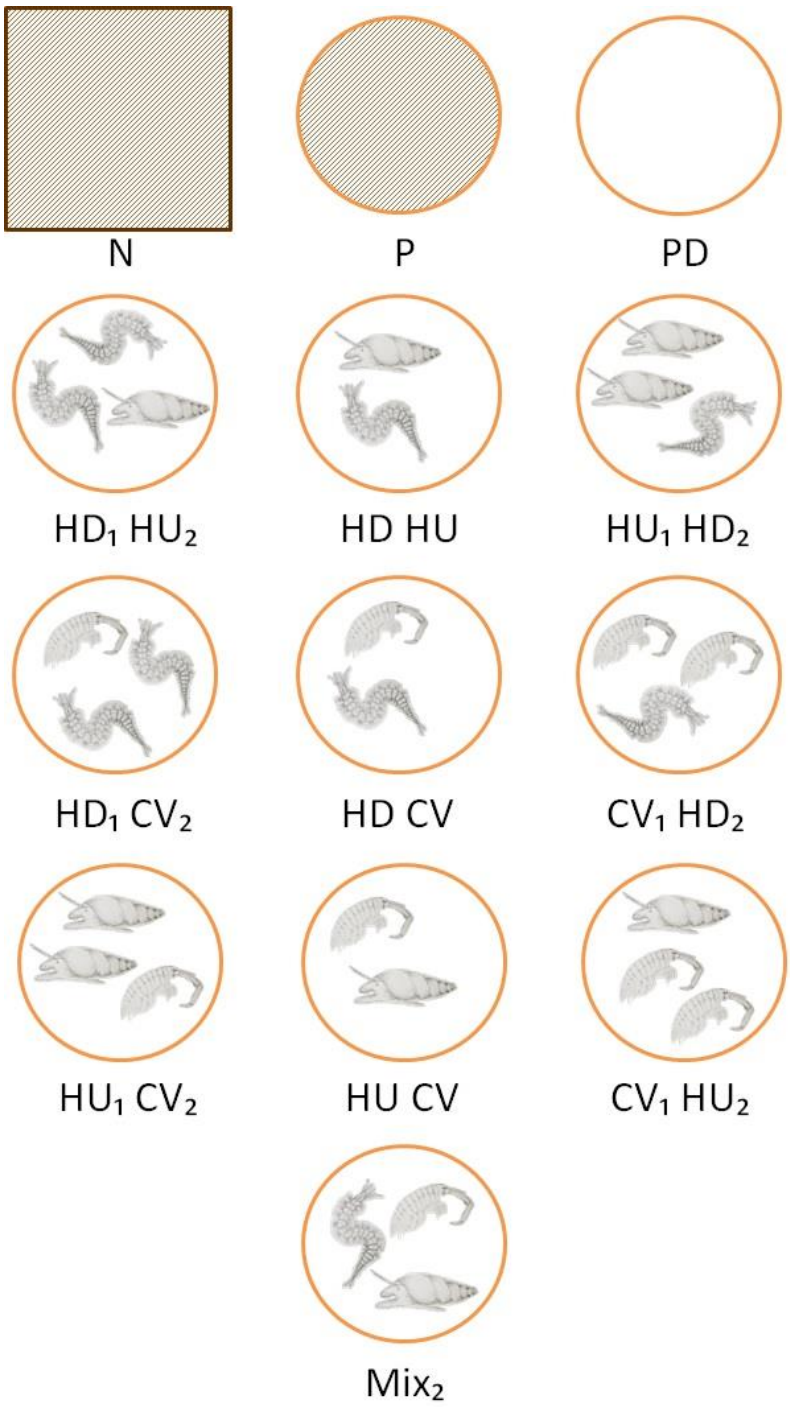

Figure 5.1 | The thirteen experimental treatments represented visually. Shading represents the natural sediment. Each core containing species addition treatment contains the same biomass as the average of a natural core. The ratio of diagrammatic organisms in the cores represent the ratios in the species treatments. Where N is natural sediment as a mudflat baseline, P is a pipe mesocosm only treatment as a procedural control, PD is a defaunated mesocosm treatment as an experimental control. The species treatments are defaunated cores where HD_1HU_2 contains $^2/_3$ of the original biomass replaced with *Hediste diversicolor* and $^1/_3$ of the original biomass replaced with *Hydrobia ulvae*, HDHU contains $^1/_2$ of the original biomass replaced with *Hediste diversicolor* and $^1/_2$ of the original biomass replaced with *Hydrobia ulvae*, HU_1HD_2 contains $^2/_3$ of the original biomass replaced
(Continued overleaf…)

with *Hydrobia ulvae* and $^1/_3$ of the original biomass replaced with *Hediste diversicolor*, HD_1CV_2 contains $^2/_3$ of the original biomass replaced with *Hediste diversicolor* and $^1/_3$ of the original biomass replaced with *Corophium volutator*, HDCV contains $^1/_2$ of the original biomass replaced with *Hediste diversicolor* and $^1/_2$ of the original biomass replaced with *Corophium volutator*, CV_1HD_2 contains $^2/_3$ of the original biomass replaced with *Corophium volutator* and $^1/_3$ of the original biomass replaced with *Hediste diversicolor*, HU_1CV_2 contains $^2/_3$ of the original biomass replaced with *Hydrobia ulvae* and $^1/_3$ of the original biomass replaced with *Corophium volutator*, HUCV contains $^1/_2$ of the original biomass replaced with *Hydrobia ulvae* and $^1/_2$ of the original biomass replaced with *Corophium volutator*, CV_1HU_2 contains $^2/_3$ of the original biomass replaced with *Corophium volutator* and $^1/_3$ of the original biomass replaced with *Hydrobia ulvae*, and Mix_2 contains a mix of HD, HU and CV, each species replacing a $^1/_3$ of the original biomass.

5.2.2 | Experimental data collection

Field measurements and sediment samples were collected as described in Section 2.3. In the field, data were collected using a cohesive strength meter (CSM; Section 2.3.1) and a pulse amplitude modulated fluorometer (PAM; Section 2.3.2). Minicores (Section 2.3.3) were collected and analysed for water content and particle size properties in the laboratory following the procedures presented in Section 2.6.3. Contact cores (Section 2.3.4) were collected and analysed for water concentration, carbohydrates, chlorophyll *a* and *b* and particle size properties in the laboratory following the procedures presented in Section 2.6.4. Community composition cores were taken on the final day of the experiment, the 14th of June, and analysed to determine species biomass in the cores at the end of the experiment, following the methods presented in Section 2.6.5.

5.2.3 | Data analysis

Data obtained from the CSM was processed to obtain the sediment erosion threshold and suspension index following the procedures given in Section 2.6.1. Data obtained from the PAM provided the microphytobenthos minimum fluorescence and the maximum quantum yield (see Section 2.6.2). All the resulting data were analysed using a generalised least squares approach, as described in Section 2.7, to compare mixed species treatments and the procedural and experimental controls. All initial and final models used are presented in Appendix 3.

5.3 | Results

From analysis of the community composition cores taken on day two of the experiment, cryo-defaunation of the cores resulted in an 85 % average reduction in species abundance in the defaunation control cores compared to the procedural control cores. After two weeks in the field, due to the variable efficacy of defaunation and changes in species abundance or biomass throughout the duration of the experiment, there were variations in the species biomass expected in the species treatment cores (Table 5.1). These variations are addressed in the discussion.

Table 5.1 | The biomass (g; n = 5; mean ± standard error) of the three species of interest, *Hediste diversicolor*, *Hydrobia ulvae* and *Corophium volutator*, in the community composition cores taken after the experimental cores had been in the field for two weeks. Mean abundance and standard error values have been rounded to whole individuals. Fill bars represent the relative biomass of each core.

Treatment	*Hediste*	*Hydrobia*	*Corophium*
N	0.098 ± 0.063	0.218 ± 0.006	0.186 ± 0.056
P	0.085 ± 0.014	0.074 ± 0.002	0.088 ± 0.034
PD	0.038 ± 0.016	0.034 ± 0.003	0.012 ± 0.004
HD_1HU_2	0.350 ± 0.015	0.291 ± 0.053	0.007 ± 0.000
HDHU	0.261 ± 0.021	0.414 ± 0.084	0.015 ± 0.001
HU_1HD_2	0.169 ± 0.026	0.430 ± 0.118	0.022 ± 0.003
HD_1CV_2	0.424 ± 0.027	0.052 ± 0.019	0.025 ± 0.004
HDCV	0.215 ± 0.021	0.031 ± 0.001	0.025 ± 0.016
CV_1HD_2	0.374 ± 0.012	0.067 ± 0.029	0.100 ± 0.053
HU_1CV_2	0.116 ± 0.022	0.501 ± 0.038	0.041 ± 0.005
HUCV	0.148 ± 0.049	0.295 ± 0.023	0.076 ± 0.003
CV_1HU_2	0.133 ± 0.000	0.301 ± 0.066	0.134 ± 0.059
Mix_2	0.163 ± 0.000	0.294 ± 0.052	0.099 ± 0.007

5.3.1 | Day and row effects

The effects of the day the data were collected (n = 26, Day1, Day2) and the row the treatment was located in (n = 13; Row1, Row2, Row3, Row4; where Row1 was highest on the shoreline) were tested against two variables; the erosion threshold (ET, Nm^{-2}; Figure 5.2 and Figure 5.3) and the pulse amplitude modulation (PAM) measured minimum fluorescence (F_o; Figure 5.4 and Figure 5.5). The day of data collection (Day; L-ratio = 1.52, d.f = 4, p =

0.2171) and the row of mesocosm location (Row; L-ratio = 0.17, d.f. = 5, p = 0.9827) did not affect the erosion threshold (Nm^{-2}).

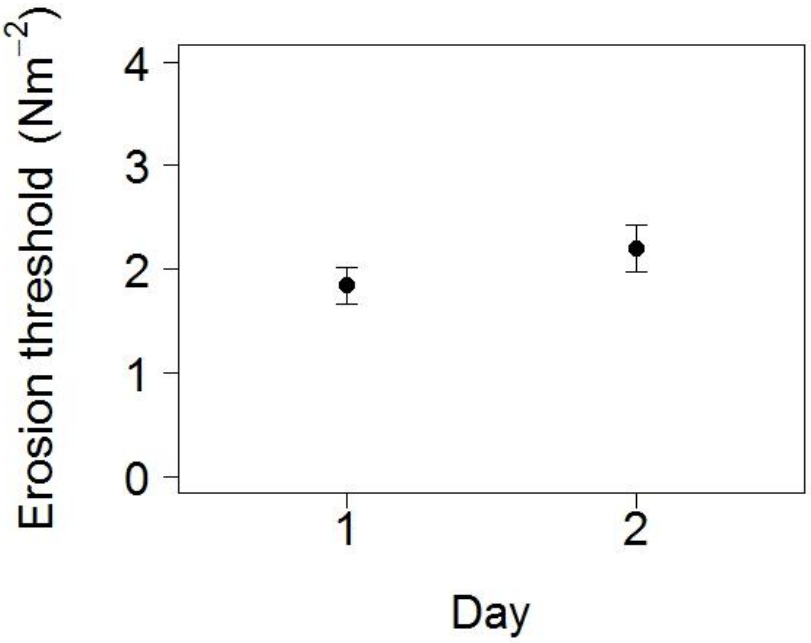

Figure 5.2 | Effect of day of data collection on the sediment erosion threshold (Nm^{-2}; n = 26). Error bars are standard error. 1, Day 1; 2, Day 2.

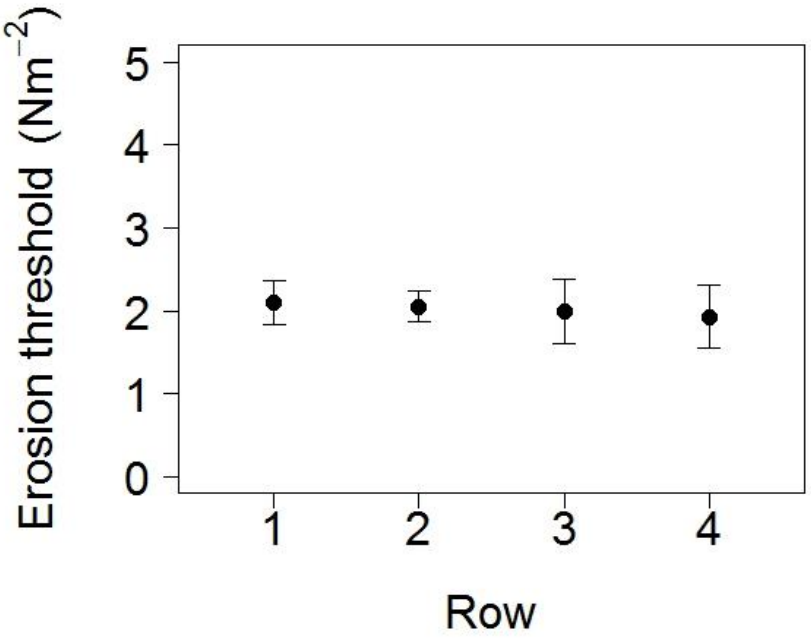

Figure 5.3 | Effect of row of mesocosm location on the sediment erosion threshold (Nm^{-2}; n = 13). Error bars are standard error. 1, Row 1; 2, Row 2; 3, Row 3; 4, Row 4, where Row 1 was highest on the shoreline.

The pulse amplitude modulated measured minimum fluorescence did, however, vary significantly with both the day of data collection (L-ratio = 10.10, d.f. = 3, p = 0.0015) and the row of mesocosm location (L-ratio = 9.71, d.f. = 8, p = 0.0212). The mean (±95 % CI, n = 26) minimum fluorescence values measured on day two (554.38 ± 88.97) were higher than those measured on day one (368.54 ± 75.84; Figure 4.4; t = 3.27, p = 0.0019).

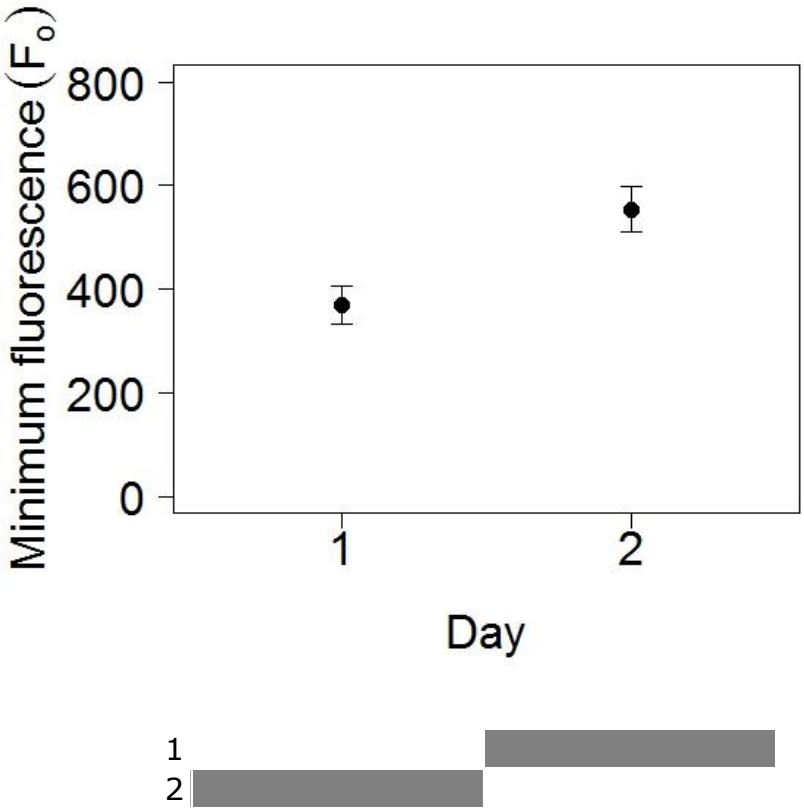

Figure 5.4 | Effect of day of data collection on the pulse amplitude modulated measured minimum fluorescence (F_o; n = 26). Error bars are standard error. 1, Day 1; 2, Day 2. Significant differences are indicated in the accompanying table where darker shading indicates greater significant difference: 0.01 < p < 0.05; 0.0001 < p < 0.01; p < 0.0001.

The mean (± 95 % CI, n = 13) minimum fluorescence values measured in mesocosms located on rows 3 (371.83 ± 114.56) and 4 (361.56 ± 80.80) were higher than those measured in mesocosms on row 1 (613.38 ± 173.41; Figure 4.5; Row 3: t = -2.56, p = 0.0137; Row 4: t = -2.87, p = 0.0061).

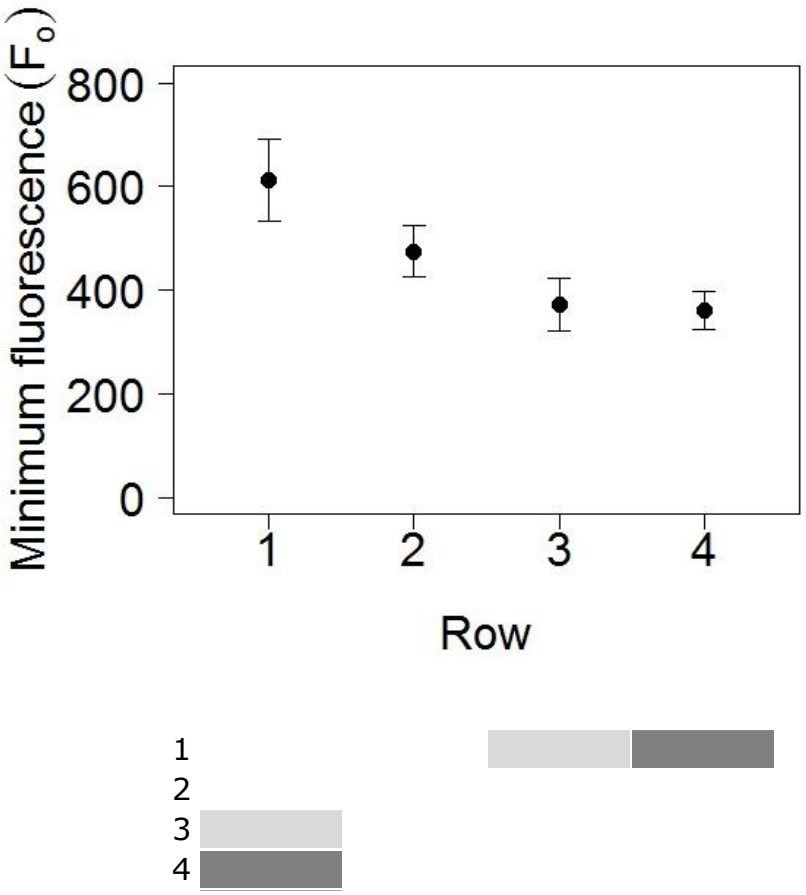

Figure 5.5 | Effect of row of mesocosm location on the pulse amplitude modulated measured minimum fluorescence (F_o; n = 13). Error bars are standard error. 1, Row 1; 2, Row 2; 3, Row 3; 4, Row 4, where Row 1 was highest on the shoreline. Significant differences are indicated in the accompanying table where darker shading indicates greater significant difference: 0.01 < p < 0.05; 0.0001 < p < 0.01; p < 0.0001.

Splitting the experimental treatments between two days was necessary to enable the collection of suitable data with enough replication. Treatments were split between rows to reduce their spread along the shore and reduce variation due to the different hydrodynamic regimes along the coast. Four rows enabled all the replicates to be placed within an embayment within the estuary. Even though there was an effect of 'Day' and 'Row' on the measured minimum fluorescence, because there was an equal number of each treatment spread between each day and an equal number of each treatment spread between each row the data were analysed together regardless of 'Day' or 'Row'. Unfortunately it was not possible to undertake a two-way analysis of treatment and either day or row due to the fact this would have reduced the replicates (degrees of freedom) for the interaction terms too much (see Section 4.3.1), especially as the total number of

replicates for the experiment was already reduced due the unexpected extreme weather.

Many of the procedural control treatments (those sediments enclosed in a mesocosm on the mudflat but not defaunated; P) differed significantly from the natural sediments (no mesocosm; N). Thus, during the data statistical analysis and discussion all experimental treatments will be compared to the procedural (P) and experimental (defaunated sediment enclosed within a mesocosm; PD) controls. The measurement of a natural mudflat baseline is interesting in its own right, but as the presence of the pipe mesocosm has a significant effect on some of the sediment properties the correct approach is to compare all species treatments with the procedural control. This approach will be adopted for all the following analyses in this chapter. See Appendix 3 for coefficients tables containing all p-values discussed in this chapter.

5.3.2 | Sediment erosion effects

Similarly to the results presented in Section 4.3.2, the mudflat at Breydon Water was found to have a small mean (± 95 % CI, n = 4) erosion threshold (Figure 5.6; treatment N; 0.32 ± 0.14 Nm^{-2}) meaning it is erodible under low current speeds. There was a significant effect of sediment treatment on the erosion threshold (Nm^{-2}; L-ratio = 45.50, d.f. = 26, $p < 0.0001$). The procedural control (treatment P; 1.71 ± 0.68 Nm^{-2}; $t = 6.30$, $p < 0.0001$) and the defaunated sediments (PD; 2.99 ± 2.51 Nm^{-2}; $t = 3.37$, $p = 0.0017$) had a larger mean (± 95 % CI, n = 4) erosion threshold than the natural sediments. The high biomass *Hediste* and low biomass *Corophium* treatment (HD_1CV_2; 2.76 ± 0.86 Nm^{-2}) and the high biomass *Hydrobia* and low biomass *Corophium* treatment (HU_1CV_2; 2.64 ± 0.70 Nm^{-2}) had larger mean (± 95 % CI, n = 4) erosion thresholds than the procedural control (P; $t = 3.05$, $p = 0.0041$; $t = 3.4$, $p = 0.0042$ respectively). The high biomass *Hediste* and low biomass *Corophium* treatment (HD_1CV_2) also had a larger mean (± 95 % CI, n = 4) erosion threshold than the equal biomass *Hediste* and *Hydrobia* treatment (HDHU; 1.33 ± 1.11 Nm^{-2}) and the high biomass *Hydrobia* and low biomass *Hediste* treatment (HU_1HD_2; 1.81 ± 0.92 Nm^{-2}). The high *Hediste* and low *Corophium* biomass treatment (HD_1CV_2) also had a

larger mean (± 95 % CI, n = 4) erosion threshold than the other *Hediste* and *Corophium* mixtures (HDCV; 1.92 ± 0.80 Nm^{-2}; t = -2.27, p = 0.0289 and CV_1HD_2; 1.78 ± 0.82 Nm^{-2}; t = -2.62, p = 0.0124). The high *Hydrobia* and low *Corophium* biomass treatment (HU_1CV_2; 2.64 ± 0.70 Nm^{-2}) had a larger mean (± 95 % CI, n = 4) erosion threshold than the equal *Hediste* and *Hydrobia* biomass treatment (HDHU; 1.33 ± 1.11 Nm^{-2}; t = 3.21, p = 0.0027), the high *Hydrobia* and low *Hediste* biomass treatment (HU_1HD_2; 1.81 ± 0.92 Nm^{-2}; t = 2.30, p = 0.0267), the equal *Hediste* and Corophium biomass treatment (HDCV; 1.92 ± 0.80 Nm^{-2}; t = 2.16, p = 0.0369) and the high *Corophium* and low *Hediste* biomass treatment (CV_1HD_2; 1.78 ± 0.82 Nm^{-2}; t = 2.55, p = 0.0148).

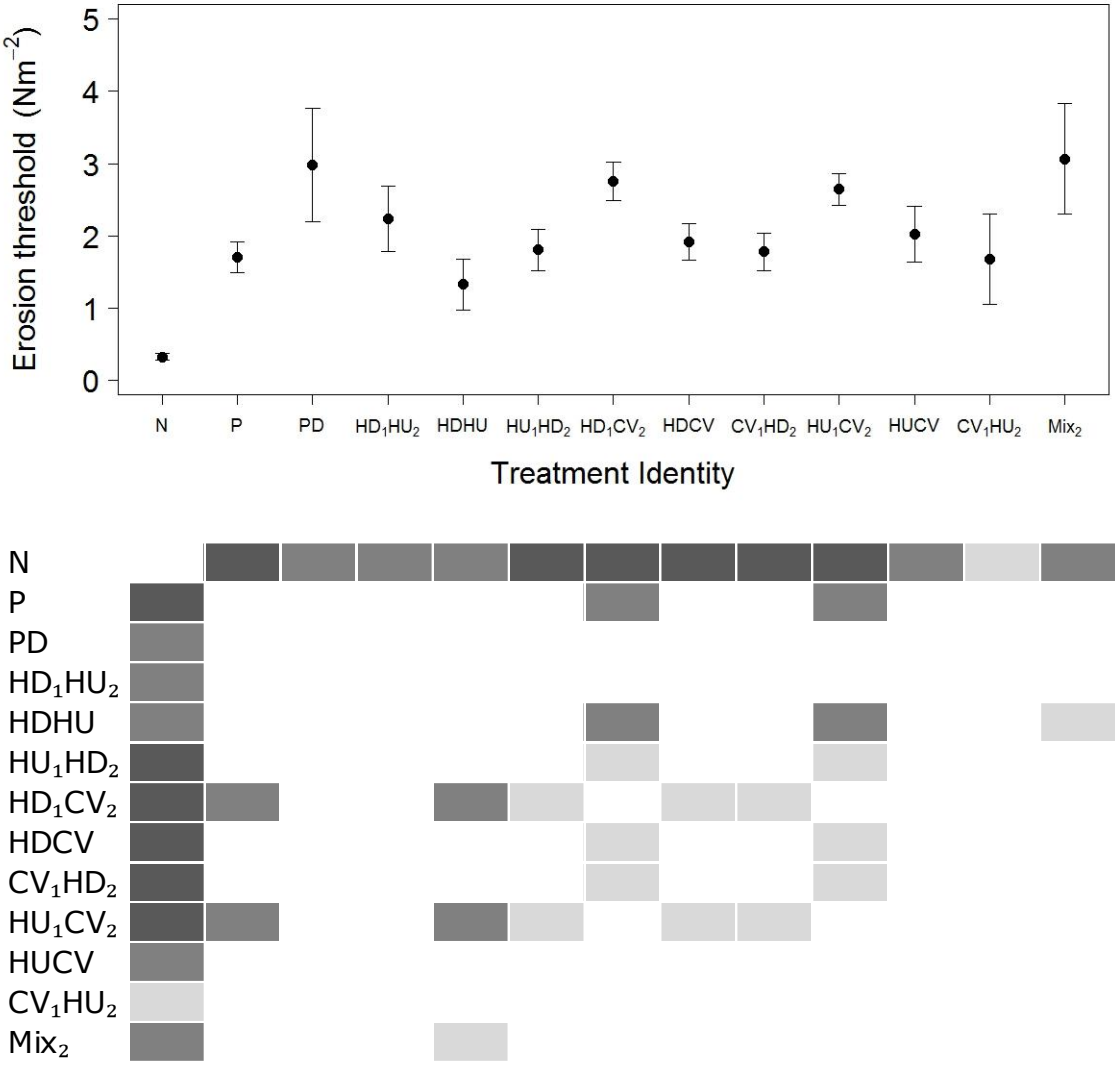

Figure 5.6 | Effect of defaunation, mesocosm presence and species biomass distribution on sediment erosion threshold (Nm^{-2}; n = 4). Error bars are standard error. The species composition of each mixture is indicated on the x-axis, where treatment identity corresponds to: N, natural sediment as a mudflat baseline; P, pipe mesocosm only treatment as a procedural control; PD, defaunated mesocosm treatment as an experimental control; HD_1HU_2 $^2/_3$ original biomass replaced with *Hediste diversicolor*, $^1/_3$ original biomass replaced with *Hydrobia ulvae*; HDHU, $^1/_2$ original biomass replaced with *Hediste diversicolor*, $^1/_2$ original biomass replaced with *Hydrobia ulvae*; HU_1HD_2, $^2/_3$ original biomass replaced with *Hydrobia ulvae*, $^1/_3$ original biomass replaced with *Hediste diversicolor*; HD_1CV_2 $^2/_3$ original biomass replaced with *Hediste diversicolor*, $^1/_3$ original biomass replaced with *Corophium volutator*; HDCV, $^1/_2$ original biomass replaced with *Hediste diversicolor*, $^1/_2$ original biomass replaced with *Corophium volutator*; CV_1HD_2, $^2/_3$ original biomass replaced with *Corophium volutator*, $^1/_3$ original biomass replaced with *Hediste diversicolor*; HU_1CV_2 $^2/_3$ original biomass replaced with *Hydrobia ulvae*, $^1/_3$ original biomass replaced with *Corophium volutator*; HUCV, $^1/_2$ original biomass replaced with *Hydrobia ulvae*, $^1/_2$ original biomass replaced with *Corophium volutator*; CV_1HU_2, $^2/_3$ original biomass (Continued overleaf…)

replaced with *Corophium volutator*, $^1/_3$ original biomass replaced with *Hydrobia ulvae*; Mix_2, mix of HD, HU and CV, each species replacing a $^1/_3$ of the original biomass. Significant differences are indicated in the accompanying table where darker shading indicates greater significant difference: ▒ $0.01 < p < 0.05$; ▓ $0.0001 < p < 0.01$; ■ $p < 0.0001$.

There was a significant effect of sediment treatment on the suspension index (L-ratio = 21.90, d.f. = 26, p = 0.0387). The mean (± 95 % CI, n = 4) suspension index of the natural sediments (N; 10.40 ± 5.75) was larger than that of the procedural control treatment (P; 2.05 ± 3.95; t = -3.81, p = 0.0005) and the defaunated sediments (Figure 5.7; PD; 2.07 ± 2.26; t = -4.30, p= 0.0001). The suspension index of high *Corophium* and low *Hydrobia* biomass treatment (CV_1HU_2; 10.88 ± 15.01) was very similar to the natural sediments. The high *Corophium* and low *Hydrobia* biomass treatment (CV_1HU_2) had a larger mean (± 95 % CI, n = 4) suspension index than the high *Hydrobia* and low *Hediste* treatment (HU_2HD_1; 0.91 ± 0.71; t = 2.11, p = 0.0413) and the equal *Hediste* and *Corophium* biomass treatment (HDCV; 1.28 ±1.16; t = 2.03, p = 0.0493). Apart from the natural sediments and the high *Corophium* and low *Hydrobia* biomass treatment, all the other treatments showed a very similar mean suspension index (Figure 5.7).

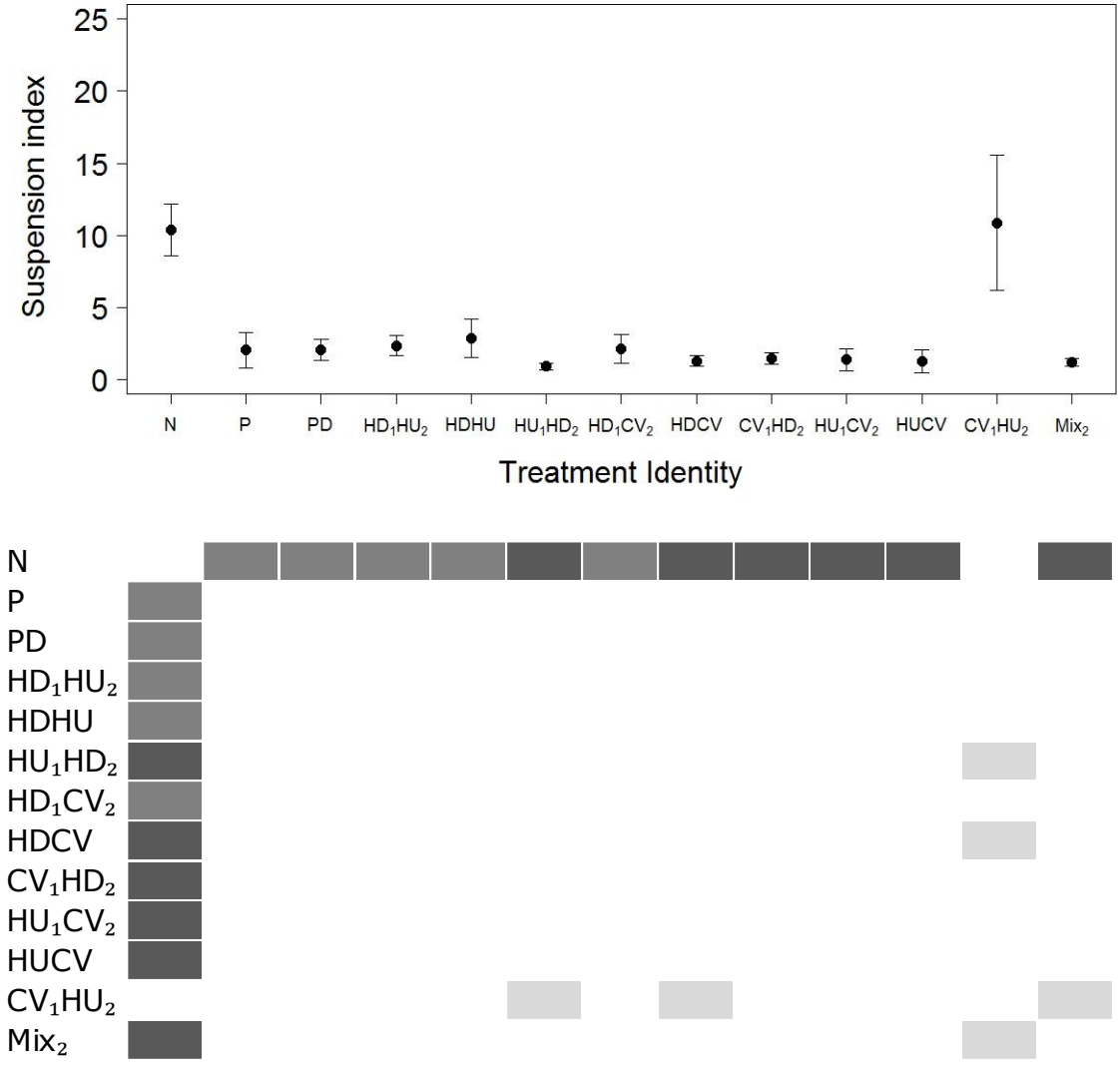

Figure 5.7 | Effect of defaunation, mesocosm presence and species biomass distribution on sediment suspension index (n = 4). Error bars are standard error. Treatment identity as in Figure 5.6. Significant differences are indicated in the accompanying table where darker shading indicates greater significant difference: 0.01 < p < 0.05; 0.0001 < p < 0.01; p < 0.0001.

5.3.3 | Microphytobenthos biomass

There was a significant effect of sediment treatment on the pulse amplitude modulated fluorometer (PAM) measured minimum fluorescence (F_o; Figure 5.8; L-ratio = 60.55, d.f. = 26, $p < 0.0001$). The mean (± 95 % CI, n = 4) minimum fluorescence of the natural sediments (N; 195.50 ± 25.61) was lower than that of the procedural control treatment (Figure 5.8; P; 245.17 ± 14.41; t = 5.38, $p < 0.0001$) and the defaunated sediments (PD; 416.00 ± 264.71; t = 2.64, p= 0.0119). The procedural control treatment had a lower mean (± 95 % CI, n = 4) minimum fluorescence than the defaunated sediments (t = 2.05, p = 0.0470), the high *Hediste* and low *Hydrobia* biomass treatment (HD_1HU_2; 529.42 ± 399.67; t = 2.26, p = 0.0294), the high *Hydrobia* and low *Hediste* treatment (HU_1HD_2; 617.75 ± 282.84; t = 4.19, p = 0.0002), the equal biomass *Hediste* and *Corophium* treatment (HDCV; 697.58 ± 481.62; t = 2.99, p = 0.0048), the high *Corophium* and low *Hediste* biomass treatment (CV_1HD_2; 384.75 ± 146.01; t = 3.03, p = 0.0044), the high *Hydrobia* and low *Corophium* biomass treatment (HU_1CV_2; 506.83 ± 249.10; t = 3.34, p = 0.0019), the high *Corophium* and low *Hydrobia* biomass treatment (CV_1HU_2; 550.25 ± 322.49; t = 3.01, p = 0.0046), and the three species mixed treatment (Mix_2; 458.33 ± 244.27; t = 2.77, p = 0.0085). The PAM measured F_o of the defaunated sediments was not significantly different to that of any of the species treatments. In some cases this is probably due to the variation of measurements among replicates of each species treatment. For example, PD and HDCV have mean F_os of 416.00 and 697.58 respectively, but are not significantly different to each other.

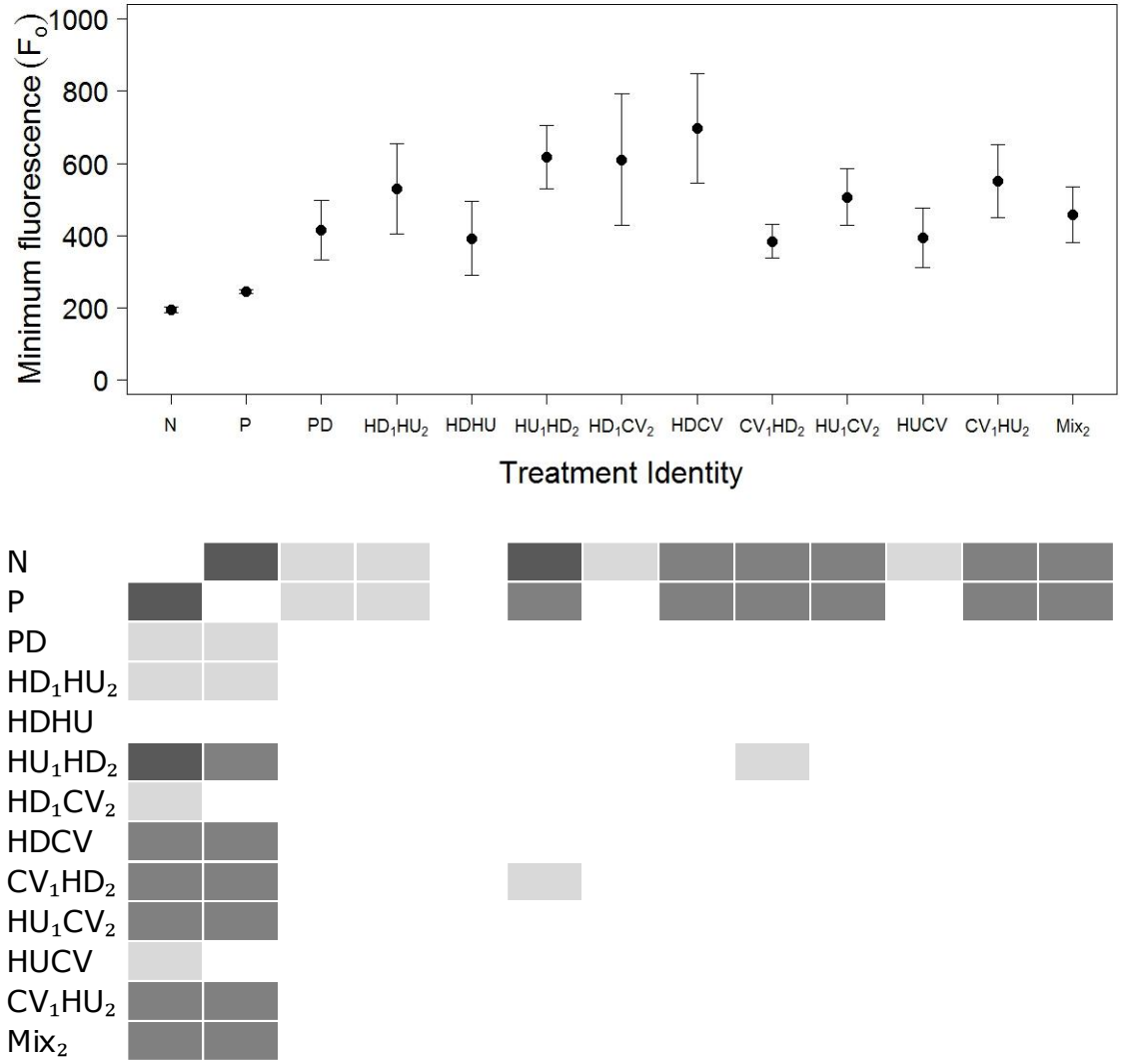

Figure 5.8 | Effect of defaunation, mesocosm presence and species biomass distribution on pulse amplitude modulated fluorometer measured minimum fluorescence (F_o; n = 4). Error bars are standard error. Treatment identity as in Figure 5.6. Significant differences are indicated in the accompanying table where darker shading indicates greater significant difference: 0.01 < p < 0.05; 0.0001 < p < 0.01; p < 0.0001.

There was no effect of mesocosm presence, defaunation or species treatment on the PAM measured maximum quantum yield (Figure 5.9; L-ratio = 17.16, d.f. = 26, p = 0.1436).

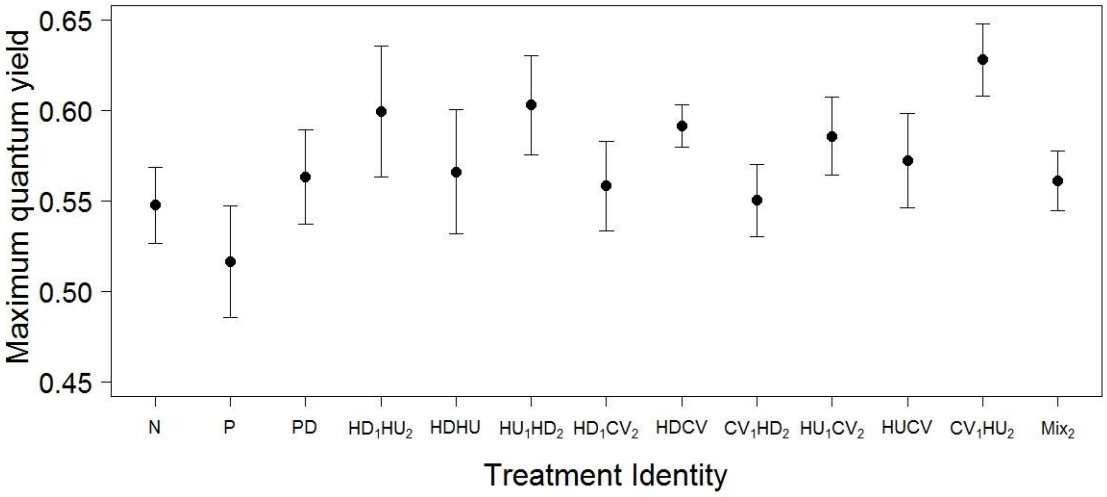

Figure 5.9 | Effect of defaunation, mesocosm presence and species biomass distribution on pulse amplitude modulated fluorometer measured maximum quantum yield (n = 4). Error bars are standard error. Treatment identity as in Figure 5.6.

5.3.4 | Minicore sediment properties

Minicore water content ranged between 46.22 and 60.83 %, however, there was no effect of mesocosm presence, defaunation or species treatment on minicore water content (%; Figure 5.10; L-ratio = 20.61, d.f. = 26, p = 0.0564), although the average water content of the natural sediments was larger than that of all the other treatments. It is probable that the mesocosms are preventing a build-up of a loose flocculent surface layer, possibly due to increased microphytobenthos biomass inside the mesocosms.

The minicore sediments were classified as very coarse silt under the GRADISTAT program scale (Blott and Pye 2001). There was no effect of mesocosm presence, defaunation or species treatment on minicore mean particle size (μm; Figure 5.11; L-ratio = 16.83, d.f. = 26, p = 0.1559).

Minicore mode particle size (μm) did not change between treatments and there was no effect of mesocosm presence or defaunation (Figure 5.12; F = 0.4525, d.f. = 12, p = 0.9300).

The minicore sediments were poorly sorted. Minicore particle sorting only ranged between 2.03 and 3.79 for all treatments and there was no effect of mesocosm presence, defaunation or species treatment on minicore particle sorting (Figure 5.13; L-ratio = 20.51734, d.f. = 26, p = 0.0579).

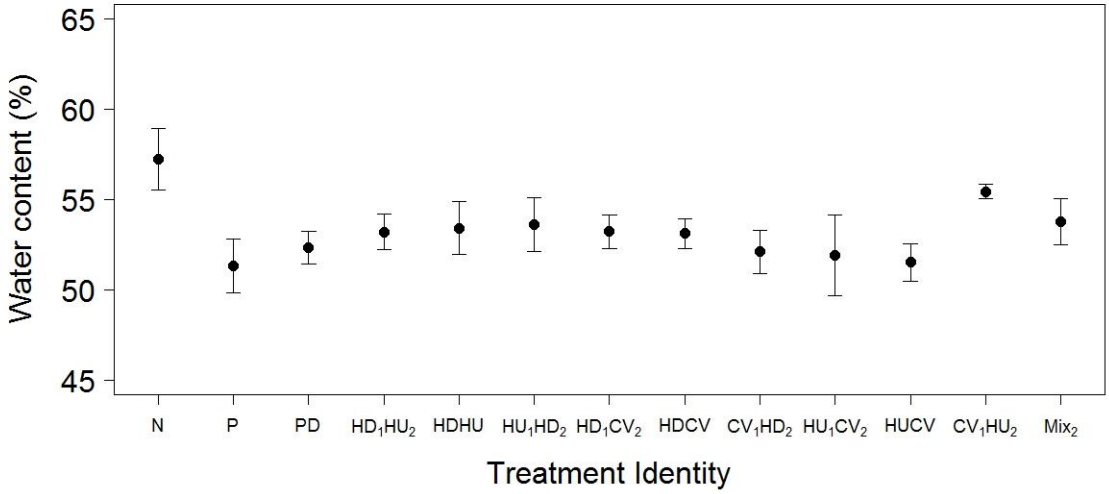

Figure 5.10 | Effect of defaunation, mesocosm presence and species biomass distribution on minicore water content (%; n = 4). Error bars are standard error. Treatment identity as in Figure 5.6.

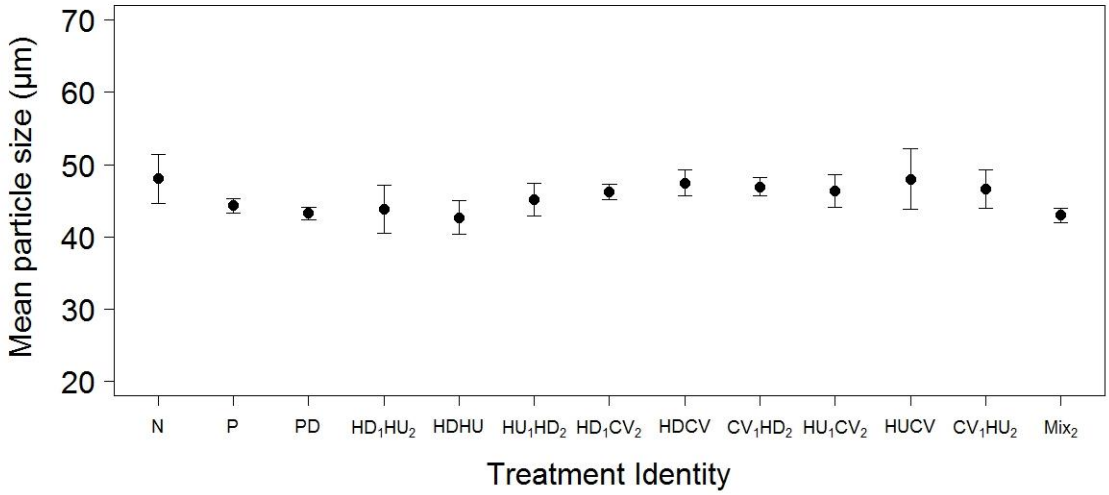

Figure 5.11 | Effect of defaunation, mesocosm presence and species biomass distribution on minicore mean particle size (µm; n = 4). Error bars are standard error. Treatment identity as in Figure 5.6.

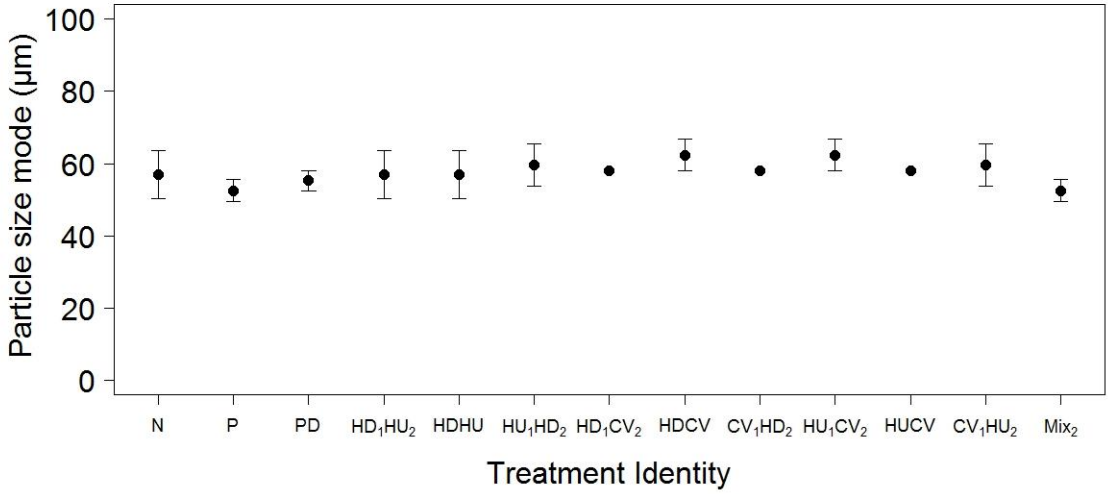

Figure 5.12 | Effect of defaunation, mesocosm presence and species biomass distribution on minicore particle size mode (µm; n = 4). Error bars are standard error. Treatment identity as in Figure 5.6.

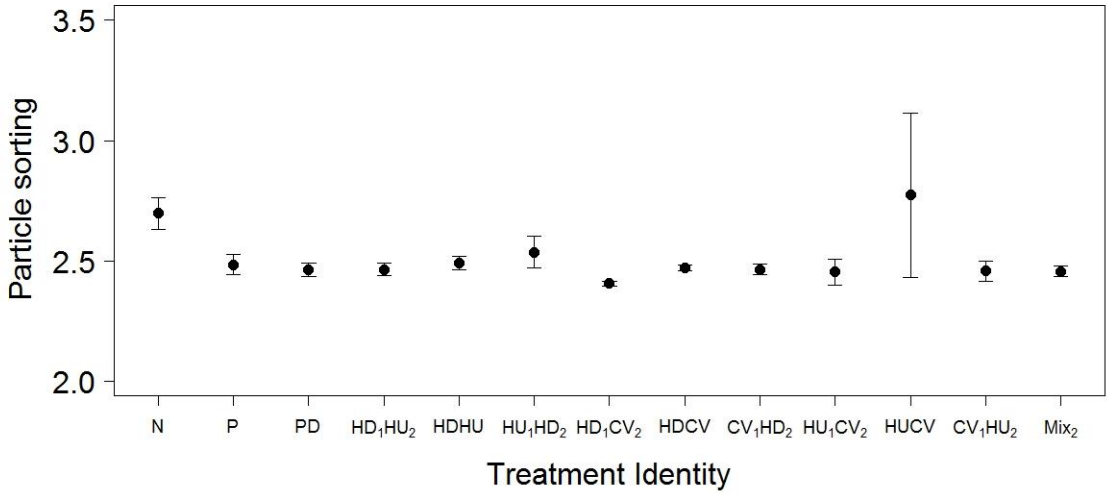

Figure 5.13 | Effect of defaunation, mesocosm presence and species biomass distribution on minicore particle sorting (n = 4). Error bars are standard error. Treatment identity as in Figure 5.6.

The minicore sediments were either skewed towards fine particles or symmetrical. Minicore particle skewness ranged between -0.90 and 0.60 for all treatments (Figure 5.14). There was a significant effect of sediment treatment on minicore particle skewness (L-ratio = 23.77, d.f. = 26, p = 0.0219). The procedural control (P; -0.53 ± 0.24) and the defaunated sediments (PD; -0.51 ± 0.20) had a smaller mean (± 95 % CI, n = 4) particle skewness than the natural sediments (N; -0.28 ± 0.29; t = -2.17, p

= 0.0364 and t = -2.08, p = 0.0446 respectively). The high *Hediste* and low *Corophium* biomass treatment (HD_1CV_2; -0.80 ± 0.12) had a smaller mean (± 95 % CI, n = 4) particle skewness than the procedural control (t = -3.15, p = 0.0031), the defaunated sediments (t = -3.90, p = 0.0004), the high *Corophium* and low *Hediste* biomass treatment (CV_1HD_2; -0.62 ± 0.14; t = -3.06, p = 0.0040) and the three species mixed treatment (Mix_2; -0.58 ± 0.20; t = -2.89, p = 0.0063).

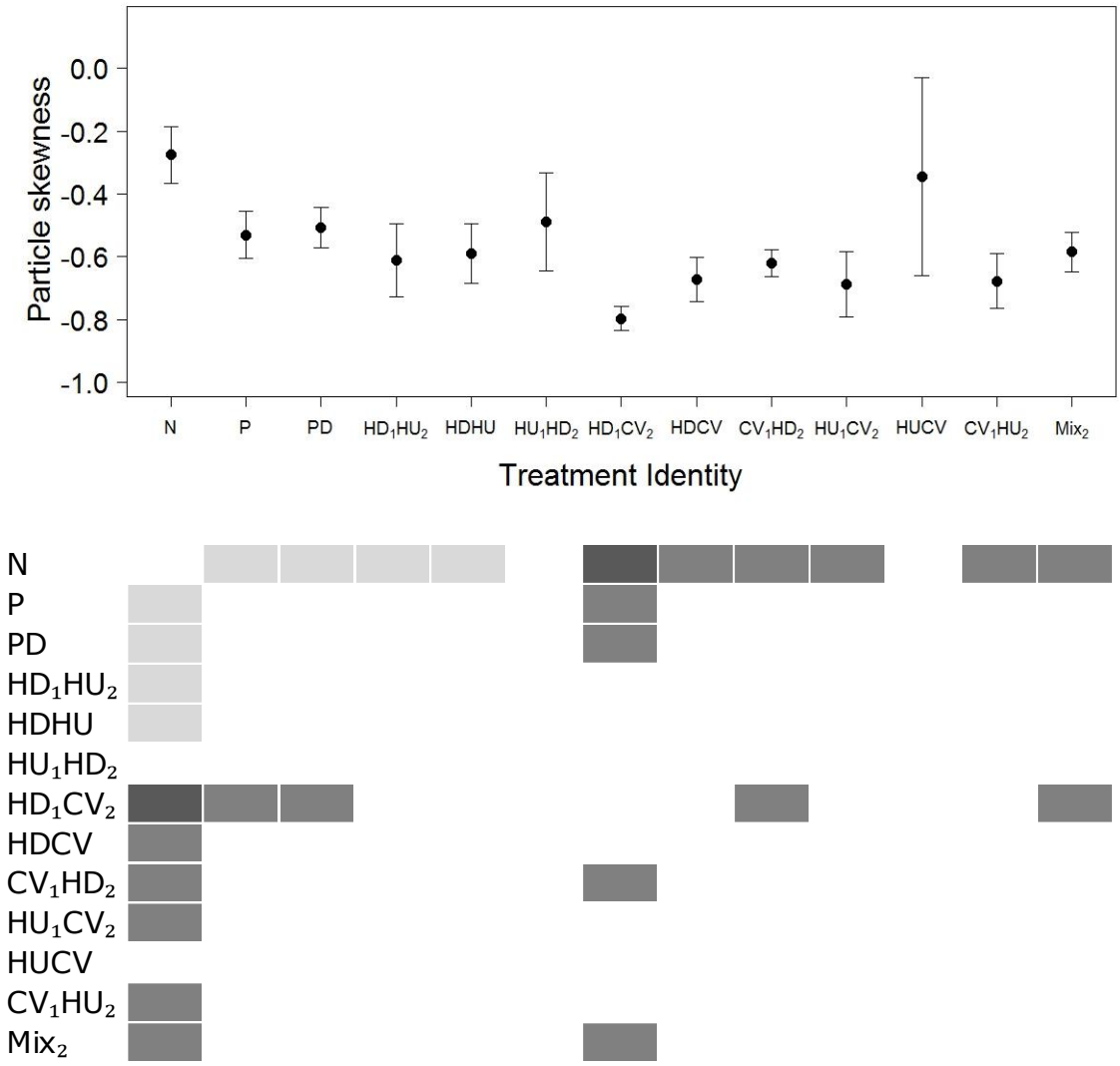

Figure 5.14 | Effect of defaunation, mesocosm presence and species biomass distribution on minicore particle skewness (n = 4). Error bars are standard error. Treatment identity as in Figure 5.6. Significant differences are indicated in the accompanying table where darker shading indicates greater significant difference: 0.01 < p < 0.05; 0.0001 < p < 0.01; p < 0.0001.

The minicore sediments showed either meso-kurtosis or lepto-kurtosis, meaning there was little spread of particle size in the samples. There was no effect of mesocosm presence, defaunation or species treatment on minicore particle kurtosis (Figure 5.15; L-ratio = 4.52, d.f. = 26, p = 0.9720).

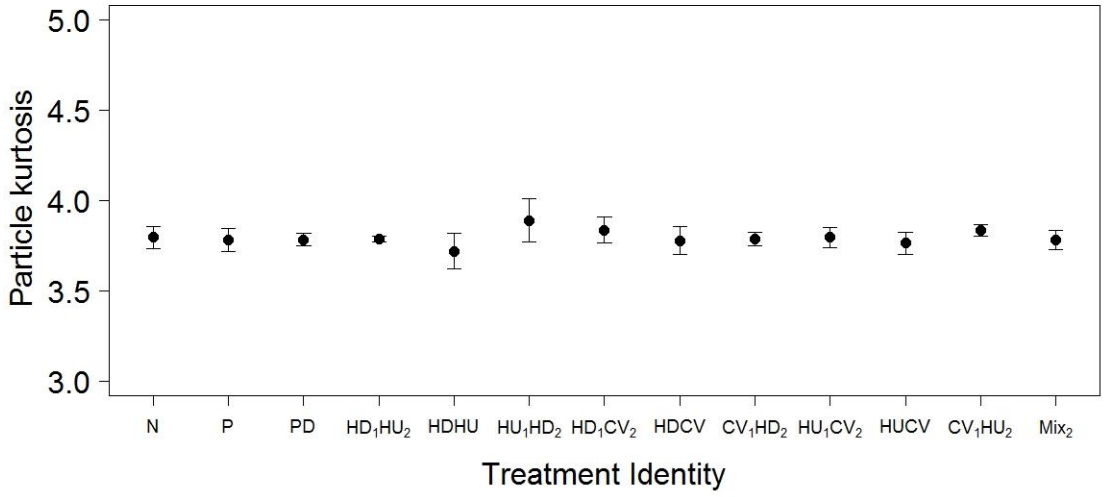

Figure 5.15 | Effect of defaunation, mesocosm presence and species biomass distribution on minicore particle kurtosis (n = 4). Error bars are standard error. Treatment identity as in Figure 5.6.

Minicore particle D_{10} ranged between 10.79 and 15.53 µm for all treatments. There was no effect of mesocosm presence, defaunation or species treatment on minicore particle D_{10} (µm; Figure 5.16; L-ratio =16.58, d.f. = 26, p = 0.1661).

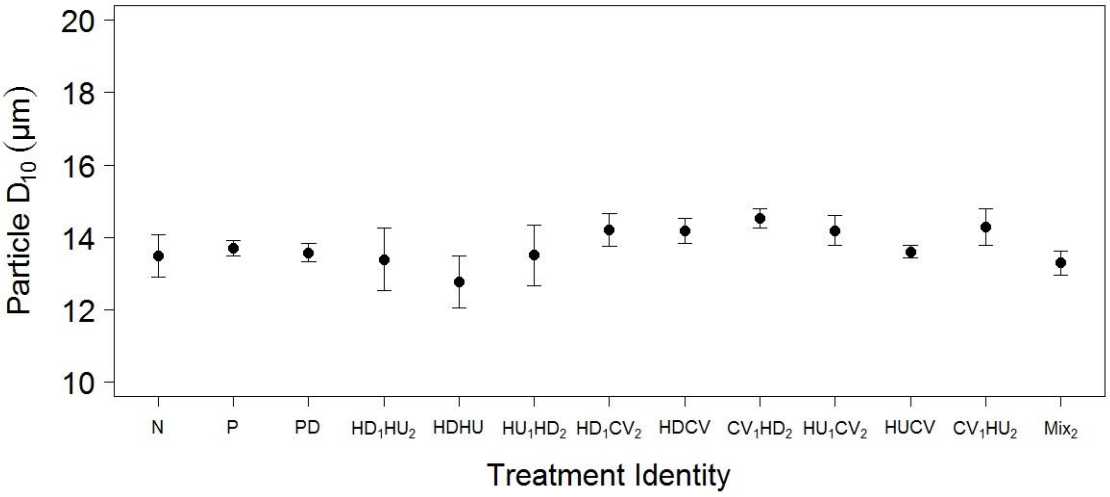

Figure 5.16 | Effect of defaunation, mesocosm presence and species biomass distribution on minicore particle D_{10} (µm; n = 4). Error bars are standard error. Treatment identity as in Figure 5.6.

There was no effect of mesocosm presence, defaunation or species treatment on minicore mud content (%; Figure 5.17; L-ratio = 16.24, d.f. = 26, p = 0.1807).

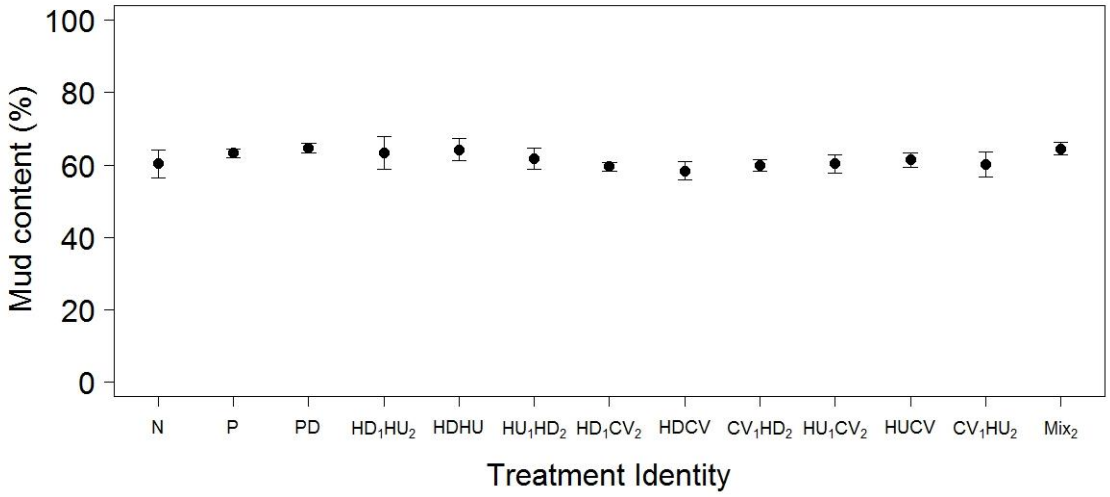

Figure 5.17 | Effect of defaunation, mesocosm presence and species biomass distribution on minicore mud content (%; n = 4). Error bars are standard error. Treatment identity as in Figure 5.6.

5.3.5 | Contact core sediment properties

There was no effect of mesocosm presence, defaunation or species treatment on contact core water concentration (gcm^{-3}; Figure 5.18; L-ratio = 16.24, d.f. = 26, p = 0.1807).

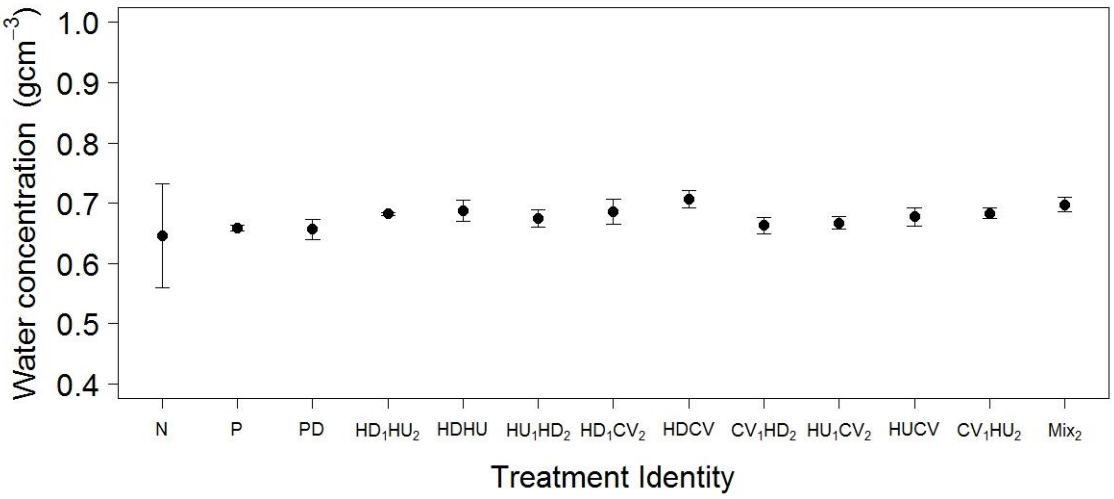

Figure 5.18 | Effect of defaunation, mesocosm presence and species biomass distribution on contact core water concentration (gcm^{-3}; n = 4). Error bars are standard error. Treatment identity as in Figure 5.6.

There was no effect of mesocosm presence, defaunation or species treatment on contact core colloidal carbohydrate concentration (μgcm^{-3}; Figure 5.19; L-ratio = 19.43, d.f. = 26, p = 0.0786).

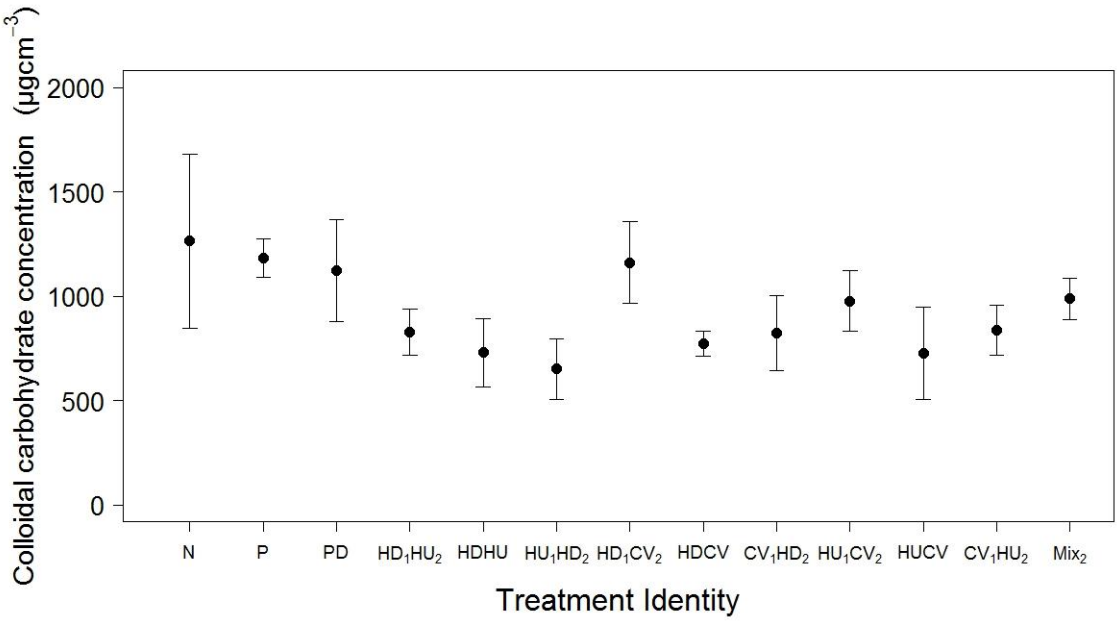

Figure 5.19 | Effect of defaunation, mesocosm presence and species biomass distribution on contact core colloidal carbohydrate concentration (μgcm^{-3}; n = 4). Error bars are standard error. Treatment identity as in Figure 5.6.

There was a significant effect of sediment treatment on contact core chlorophyll *a* concentration (μgcm^{-3}; Figure 5.20; L-ratio = 48.19, d.f. = 26, p < 0.0001). The procedural control (P; 22.64 ± 0.81 μgcm^{-3}) and the defaunated sediments (PD; 25.10 ± 6.34 μgcm^{-3}) had a larger mean (± 95 % CI, n = 4) contact core chlorophyll *a* concentration than the natural sediments (N; 15.84 ± 2.93 μgcm^{-3}; t = 7.12, p < 0.0001 and t = 4.22, p = 0.0001 respectively). The procedural control treatments (P) had a smaller mean (± 95 % CI, n = 4) chlorophyll *a* concentration than the high *Hediste* and low *Hydrobia* biomass treatment (HD_1HU_2; 27.81 ± 4.80 μgcm^{-3}; t = 3.38, p = 0.0017), the high *Hediste* and low *Corophium* biomass treatment (HD_1CV_2; 27.58 ± 5.08 μgcm^{-3}; t = 3.06, p = 0.0040), the equal *Hediste* and *Corophium* biomass treatment (HDCV; 27.70 ± 6.88 μgcm^{-3}; t = 2.32, p = 0.0255), and the high *Corophium* and low *Hydrobia* biomass treatment (CV_1HU_2; 25.33 ± 2.15 μgcm^{-3}; t = 3.74, p = 0.0006), and a larger chlorophyll *a* concentration than the equal *Hediste* and *Hydrobia* biomass treatment (HDHU; 20.74 ± 2.13 μgcm^{-3}; t = -2.66, p = 0.0114). The mean (± 95 % CI, n = 4) chlorophyll *a* concentration in the equal *Hediste* and

Hydrobia biomass treatment (HDHU) was also smaller than in the defaunated sediments (PD; t = -2.08, p = 0.0445), the high *Hediste* and low *Hydrobia* treatment (HD_1HU_2; 27.81 ± 4.80 µgcm^{-3}; t = -4.28, p = 0.0001), the high *Hydrobia* and low *Hediste* biomass treatment (HU_1HD_2; 24.01 ± 2.66 µgcm^{-3}; t = -3.06, p = 0.0040), the high *Hediste* and low *Corophium* biomass treatment (HD_1CV_2; 27.58 ± 5.08 µgcm^{-3}; t = -3.95, p = 0.0003), the equal *Hediste* and *Corophium* biomass treatment (HDCV; 27.70 ± 6.88 µgcm^{-3}; t = -3.07, p = 0.0039), the high *Corophium* and low *Hediste* biomass treatment (CV_1HD_2; 23.70 ± 3.11 µgcm^{-3}; t = -2.50, p = 0.0166), the high *Hydrobia* and low *Corophium* biomass treatment (HU_1CV_2; 24.94 ± 6.16 µgcm^{-3}; t = -2.05, p =0.0467), the high *Corophium* and low *Hydrobia* biomass treatment (CV_1HU_2; 25.33 ± 2.15 µgcm^{-3}; t = -4.83, p < 0.0001), and the three species mixed treatment (Mix_2; 25.33 ± 4.55 µgcm^{-3}; t = -2.91, p = 0.0060). Additionally, the high *Hediste* and low *Hydrobia* biomass treatment (HD_1HU_2; 27.81 ± 4.80 µgcm^{-3}) had a larger mean (± 95 % CI, n = 4) chlorophyll *a* concentration than the high *Corophium* and low *Hediste* biomass treatment (CV_1HD_2; 23.70 ± 3.11 µgcm^{-3}; t = 2.28, p = 0.0280) and the equal *Hydrobia* and *Corophium* biomass treatment (HUCV; 23.05 ± 5.38 µgcm^{-3}; t = 2.10, p = 0.0421). The high *Corophium* and low *Hediste* biomass treatment (CV_1HD_2; 23.70 ± 3.11 µgcm^{-3}) also had a smaller mean (± 95 % CI, n = 4) chlorophyll *a* concentration than the high *Hediste* and low *Corophium* biomass treatment (HD_1CV_2; 27.58 ± 5.08 µgcm^{-3}; t = -2.07, p = 0.0453).

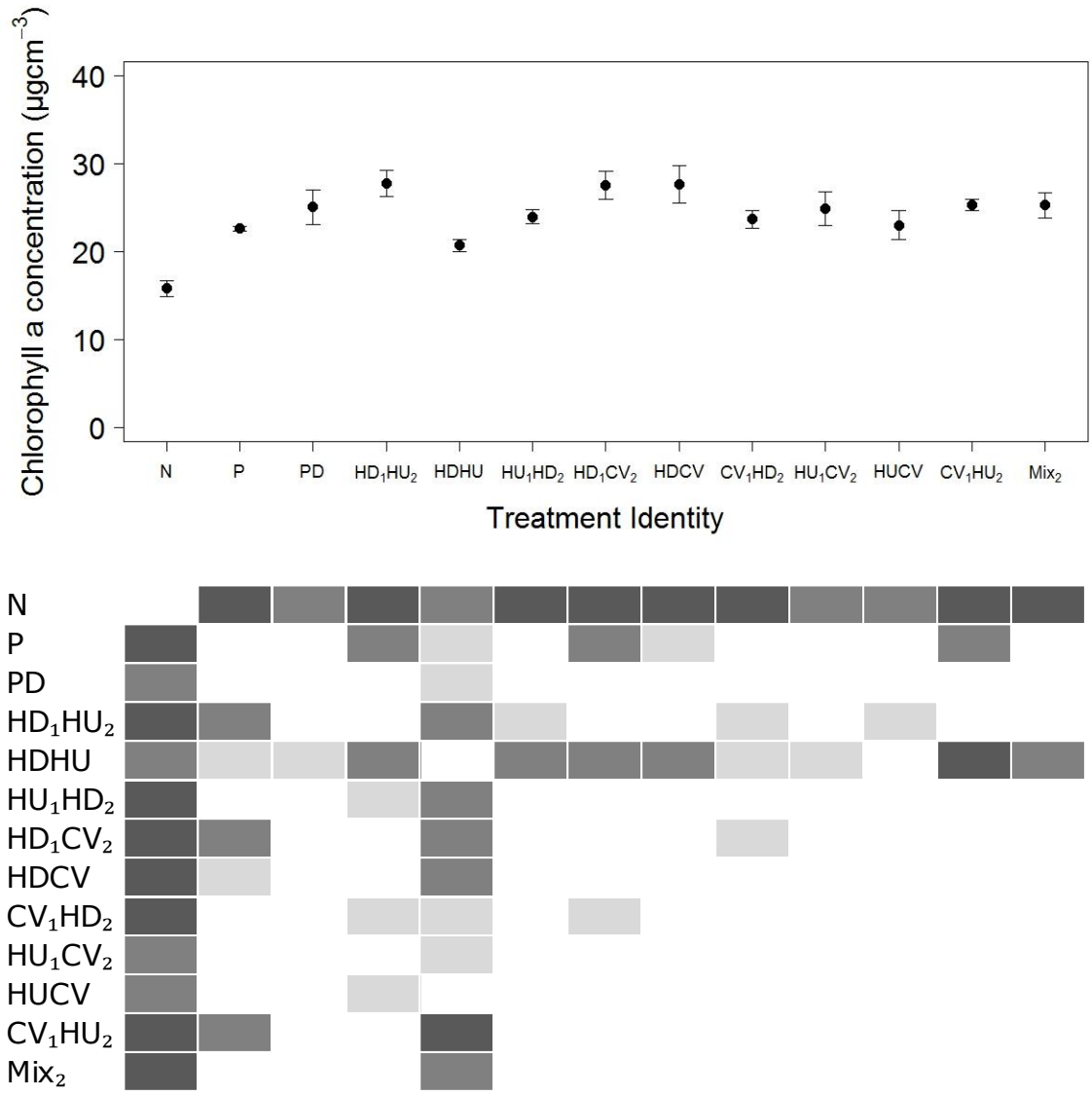

Figure 5.20 | Effect of defaunation, mesocosm presence and species biomass distribution on contact core chlorophyll *a* concentration (µgcm^{-3}; n = 4). Error bars are standard error. Treatment identity as in Figure 5.6. Significant differences are indicated in the accompanying table where darker shading indicates greater significant difference: 0.01 < p < 0.05; 0.0001 < p < 0.01; p < 0.0001.

There was also a significant effect of sediment treatment on contact core chlorophyll *b* concentration (µgcm^{-3}; Figure 5.21; L-ratio = 31.77, d.f. = 26, p = 0.0015). The procedural control (P; 4.64 ± 0.26 µgcm^{-3}) and the defaunated sediments (PD; 4.93 ± 1.27 µgcm^{-3}) had a larger mean (± 95 % CI, n = 4) contact core chlorophyll *b* concentration than the natural sediments (N; 3.75 ± 0.33 µgcm^{-3}; t = 6.75, p < 0.0001 and t = 2.87, p = 0.0066 respectively). The equal *Hediste* and *Hydrobia* biomass treatment had a smaller mean (± 95 % CI, n = 4) chlorophyll *b* concentration (HDHU; 4.22 ± 0.55 µgcm^{-3}) than the procedural control treatment (P; 4.64 ± 0.26 µgcm^{-3}; t = -2.19, p = 0.0345), the high *Hediste* and low *Hydrobia* biomass

treatment (HD_1HU_2; 5.04 ± 0.67 μgcm^{-3}; t = -3.03, p = 0.0043), the high *Hediste* and low *Corophium* biomass treatment (HD_1CV_2; 5.70 ± 1.93 μgcm^{-3}; t = -2.34, p = 0.0246), the equal *Hediste* and *Corophium* biomass treatment (HDCV; 5.11 ± 1.17 μgcm^{-3}; t = -2.21, p = 0.0333), and the three species mixed treatment (Mix_2; 5.22 ± 0.82 μgcm^{-3}; t = -3.22, p = 0.0026). The three species mixed treatment (Mix_2) also had a larger mean (± 95 % CI, n = 4) chlorophyll *b* concentration than the procedural control (P; 4.64 ± 0.26 μgcm^{-3}; t = 2.14, p = 0.0383).

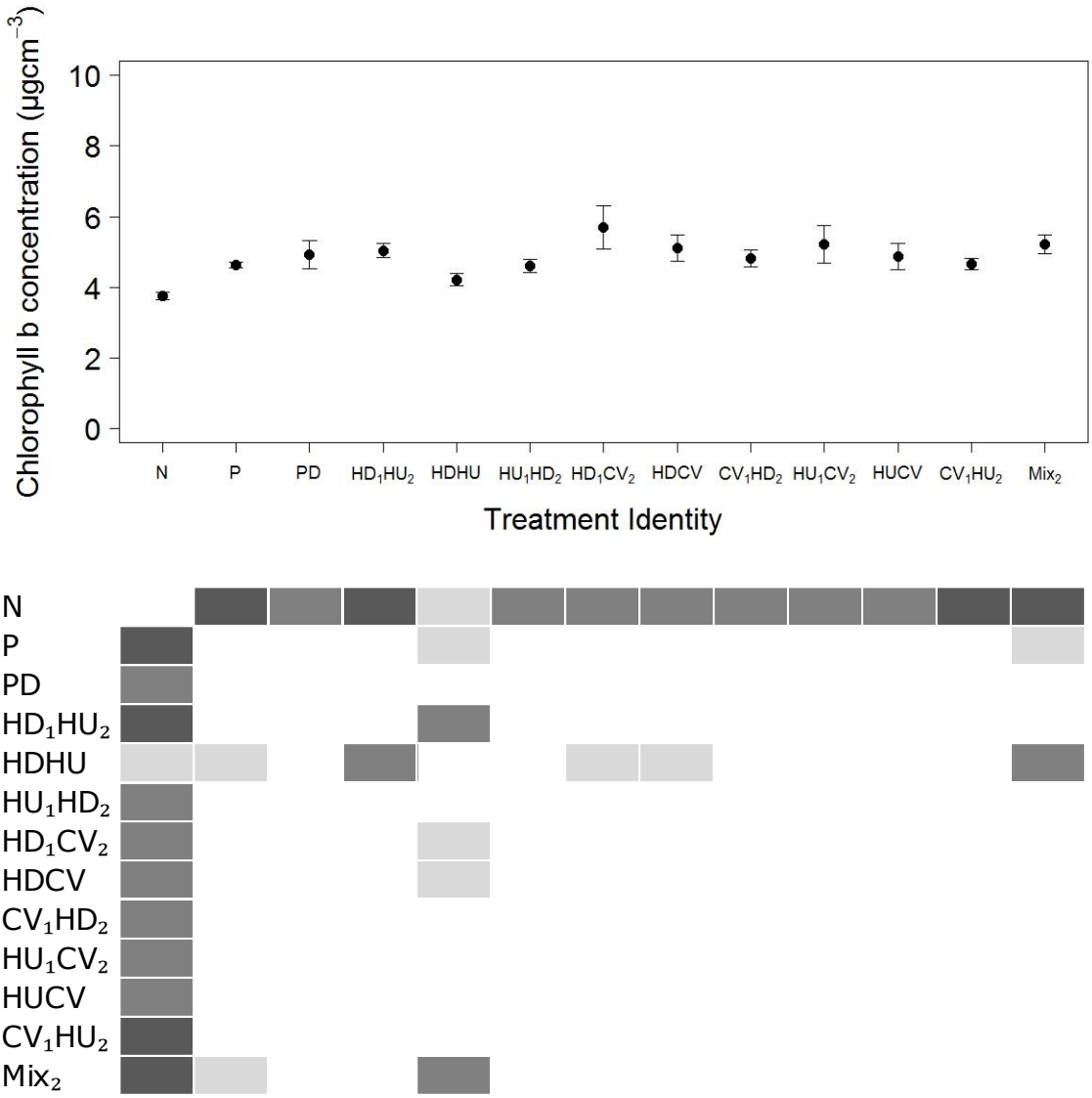

Figure 5.21 | Effect of defaunation, mesocosm presence and species biomass distribution on contact core chlorophyll *b* concentration (μgcm^{-3}; n = 4). Error bars are standard error. Treatment identity as in Figure 5.6. Significant differences are indicated in the accompanying table where darker shading indicates greater significant difference: 0.01 < p < 0.05; 0.0001 < p < 0.01; p < 0.0001.

The contact core sediments were classified as either very coarse silt or coarse silt under the GRADISTAT program scale (Blott and Pye 2001). Contact core sediment mean (± 95 % CI, n = 52) particle size (all treatments, 38.59 ± 0.87 µm) was smaller than that of the minicores (Figure 5.22; all treatments, 45.52 ± 1.26 µm). This is to be expected as the sediment surface layers generally include a fine, 'fluffy' layer (Gust and Morris 1989) and diatom cells, which are often in the silt range in size. There was a significant effect of sediment treatment on contact core mean particle size (µm; Figure 5.22; L-ratio = 36.43, d.f. = 26, p = 0.0001). There was no significant effect of mesocosm presence on the sediment mean (± 95 % CI, n =4) particle size (treatment N compared to treatment P; t = 1.59, p = 0.1210). The high *Hediste* and low *Hydrobia* biomass treatment (HD_1HU_2; 35.24 ± 2.16 µm) had a smaller mean (± 95 % CI, n = 4) particle size than the procedural control (P; 38.83 ± 3.78 µm; t = -2.62, p = 0.0125), the equal *Hediste* and Hydrobia biomass treatment (HDHU; 38.37 ± 2.10 µm; t = -3.30, p = 0.0021), the high *Hydrobia* and low *Hediste* biomass treatment (HU_1HD_2; 39.70 ± 4.40 µm; t = -2.89, p = 0.0062), the equal *Hediste* and *Corophium* biomass treatment (HDCV; 37.91 ± 1.00 µm; t = -3.56, p = 0.0010), the high *Corophium* and low *Hediste* biomass treatment (CV_1HD_2; 40.85 ± 1.77 µm; t = -6.39, p < 0.0001), the high *Corophium* and low *Hydrobia* treatment (CV_1HU_2; 40.64 ± 2.62 µm; t = -5.50, p < 0.0001), and the equal biomass mixed species treatment (Mix_2; 39.66 ± 1.61 µm; t = -5.21, p < 0.0001). The high *Corophium* and low *Hediste* biomass treatment (CV_1HD_2; 40.64 ± 2.62 µm) also had a larger mean (± 95 % CI, n = 4) particle size than the equal biomass *Hediste* and *Hydrobia* treatment (HDHU; 38.37 ± 2.10 µm; t = 2.88, p = 0.0065), the high *Hediste* and low *Corophium* biomass treatment (HD_1CV_2; 36.97 ± 5.00 µm; t = 2.33, p = 0.0250), the equal *Hediste* and *Corophium* biomass treatment (HDCV; 37.91 ± 1.00 µm; t = 4.61, p < 0.0001), and the high *Hydrobia* and low *Corophium* biomass treatment (HU_1CV_2; 34.93 ± 7.32 µm; t = 2.50, p = 0.0165). The high *Corophium* and low *Hydrobia* treatment (CV_1HU_2; 40.64 ± 2.62 µm) also had similarly large mean (± 95 % CI, n = 4) particle size, larger than the equal *Hediste* and *Hydrobia* biomass treatment (HDHU; 38.37 ± 2.10 µm; t = 2.15, p = 0.0378), the high *Hediste* and low *Corophium* biomass treatment (HD_1CV_2; 36.97 ± 5.00 µm; t = 2.07, p = 0.0451), the equal biomass *Hediste* and *Corophium* treatment (HDCV; 37.91 ± 1.00 µm; t = 3.10, p =

0.0036), and the high *Hydrobia* and low *Corophium* biomass treatment (HU_1CV_2; 34.93 ± 7.32 µm; t = 2.34, p = 0.0246). The three species mixed treatment (Mix_2; 39.66 ± 1.61) also had a larger mean (± 95 % CI, n = 4) particle size than the equal *Hediste* and *Corophium* biomass treatment (HDCV; 37.91 ± 1.00; t = 2.93, p = 0.0056).

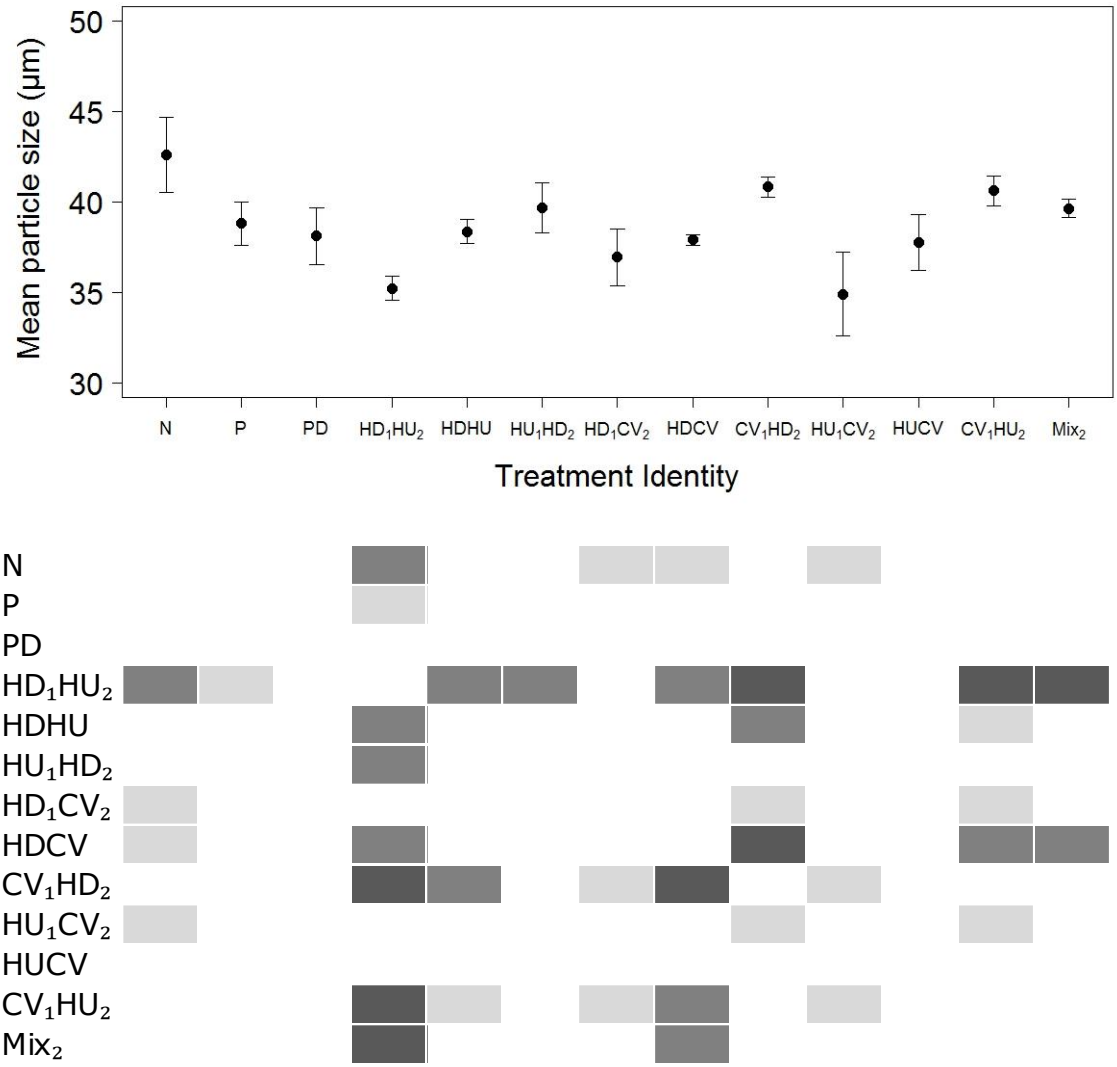

Figure 5.22 | Effect of defaunation, mesocosm presence and species biomass distribution on contact core mean particle size (µm; n = 4). Error bars are standard error. Treatment identity as in Figure 5.6. Significant differences are indicated in the accompanying table where darker shading indicates greater significant difference: 0.01 < p < 0.05; 0.0001 < p < 0.01; p < 0.0001.

Contact core mode particle size (μm) did not change between treatments and there was no effect of mesocosm presence or defaunation (Figure 5.23; F = 1.44, d.f. = 10, p = 0.1860).

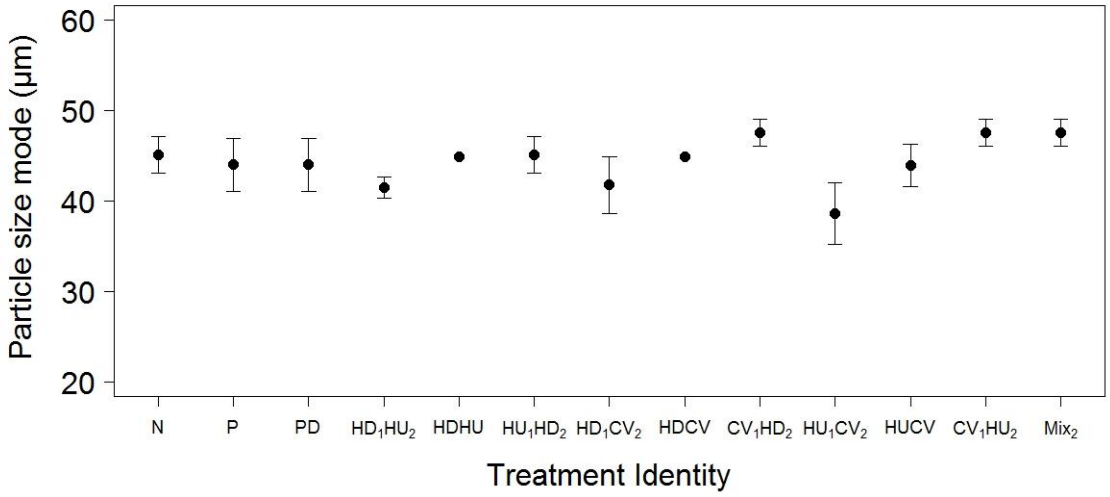

Figure 5.23 | Effect of defaunation, mesocosm presence and species biomass distribution on contact core particle size mode (μm; n = 4). Error bars are standard error. Treatment identity as in Figure 5.6.

The contact core sediments were poorly sorted. Contact core particle sorting ranged between 2.36 and 2.90 for all treatments. There was a significant effect of sediment treatment on contact core particle sorting (Figure 5.24; L-ratio = 37.37, d.f. = 26, p = 0.0002), however there was no significant difference in the mean (± 95 % CI, n = 4) particle sorting between those sediments held within a mesocosm and those not (treatment P compared to treatment N; t = -1.52, p = 0.1370). The high *Corophium* and low *Hediste* biomass treatment (Figure 5.24; CV_1HD_2; 2.57 ± 0.08) had a larger mean (± 95 % CI, n = 4) sorting value, i.e. they showed a greater variation of particle size around the mean, than the defaunated sediments (PD; 2.48 ± 0.09; t = 2.42, p = 0.0204), the high *Hediste* and low *Hydrobia* biomass treatment (HD_1HU_2; 2.45 ± 0.02; t = 4.56, p < 0.0001), the equal biomass *Hediste* and *Hydrobia* treatment (HDHU; 2.51 ± 0.05; t = 2.03, p = 0.0487), the equal *Hediste* and *Corophium* biomass treatment (HDCV; 2.46 ± 0.07; t = 3.28, p = 0.0022), and the three species mixed treatment (Mix_2; 2.49 ± 0.06; t = 2.39, p = 0.0216). The equal biomass *Hediste* and *Hydrobia* (HDHU; 2.51 ± 0.05) treatment had a larger mean (± 95 % CI, n = 4) particle sorting value than the high *Hediste* and low *Hydrobia* biomass treatment (HD_1HU_2; 2.45 ± 0.02; t = 3.21, p = 0.0026).

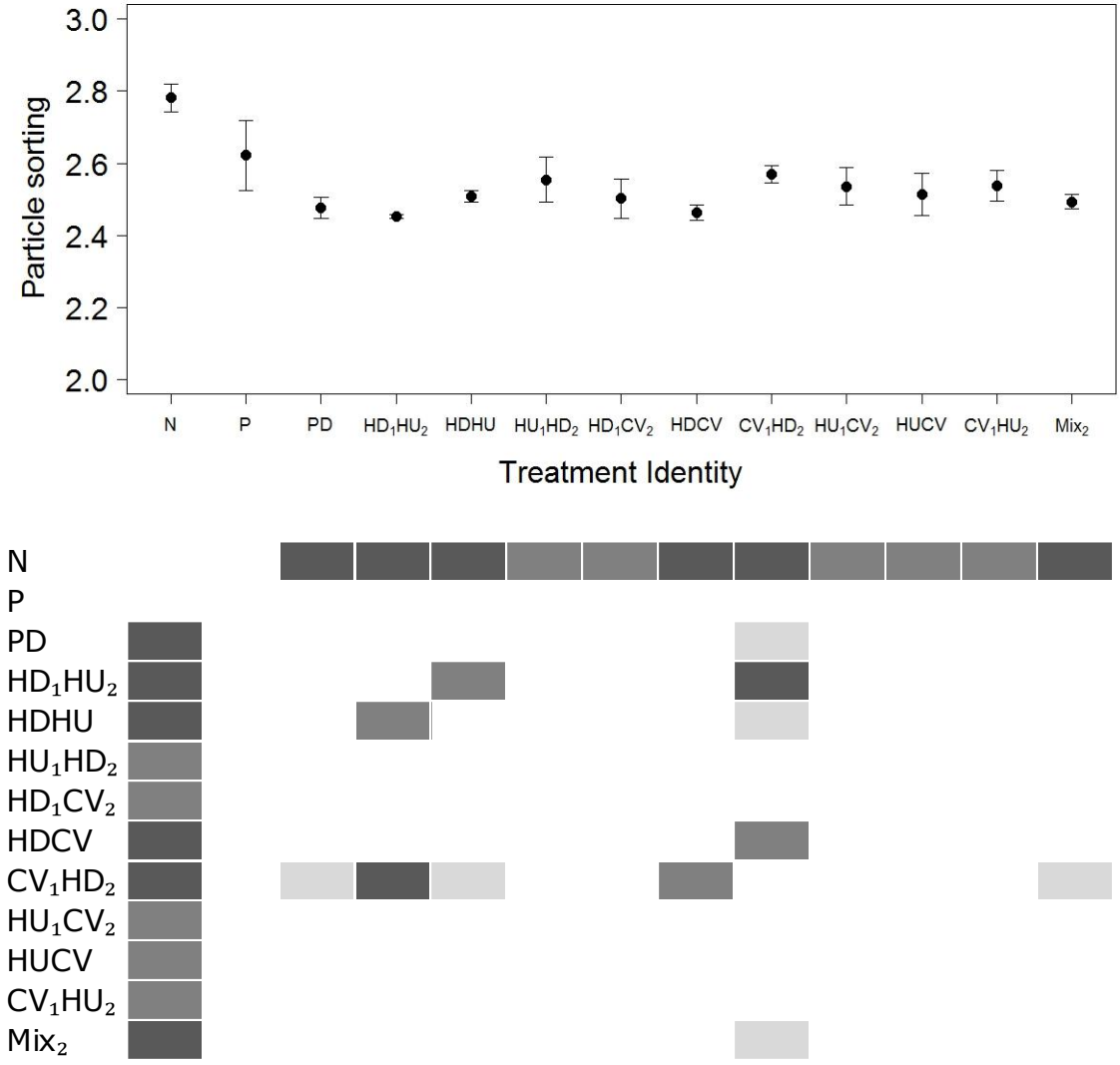

Figure 5.24 | Effect of defaunation, mesocosm presence and species biomass distribution on contact core particle sorting (n = 4). Error bars are standard error. Treatment identity as in Figure 5.6. Significant differences are indicated in the accompanying table where darker shading indicates greater significant difference: 0.01 < p < 0.05; 0.0001 < p < 0.01; p < 0.0001.

The contact core sediments were either finely skewed or symmetrical. Contact core skewness ranged between -0.38 and 0.36 for all treatments. The contact core sediments showed a smaller range than the minicore sediments. There was a significant effect of sediment treatment on contact core particle skewness (Figure 5.25; L-ratio = 22.90, d.f. = 26, p = 0.0286). However the only significant effect of particle skewness observed among the treatments was that between the natural sediments and the defaunated sediments and the defaunated species re-addition treatments, except for the high *Hydrobia* and low *Corophium* biomass treatment, which resulted in a significant fine skew of the particle sizes (t < - 2.03, p < 0.0489 for

significant treatments; see Figure 5.25 accompanying table) compared to the natural sediments.

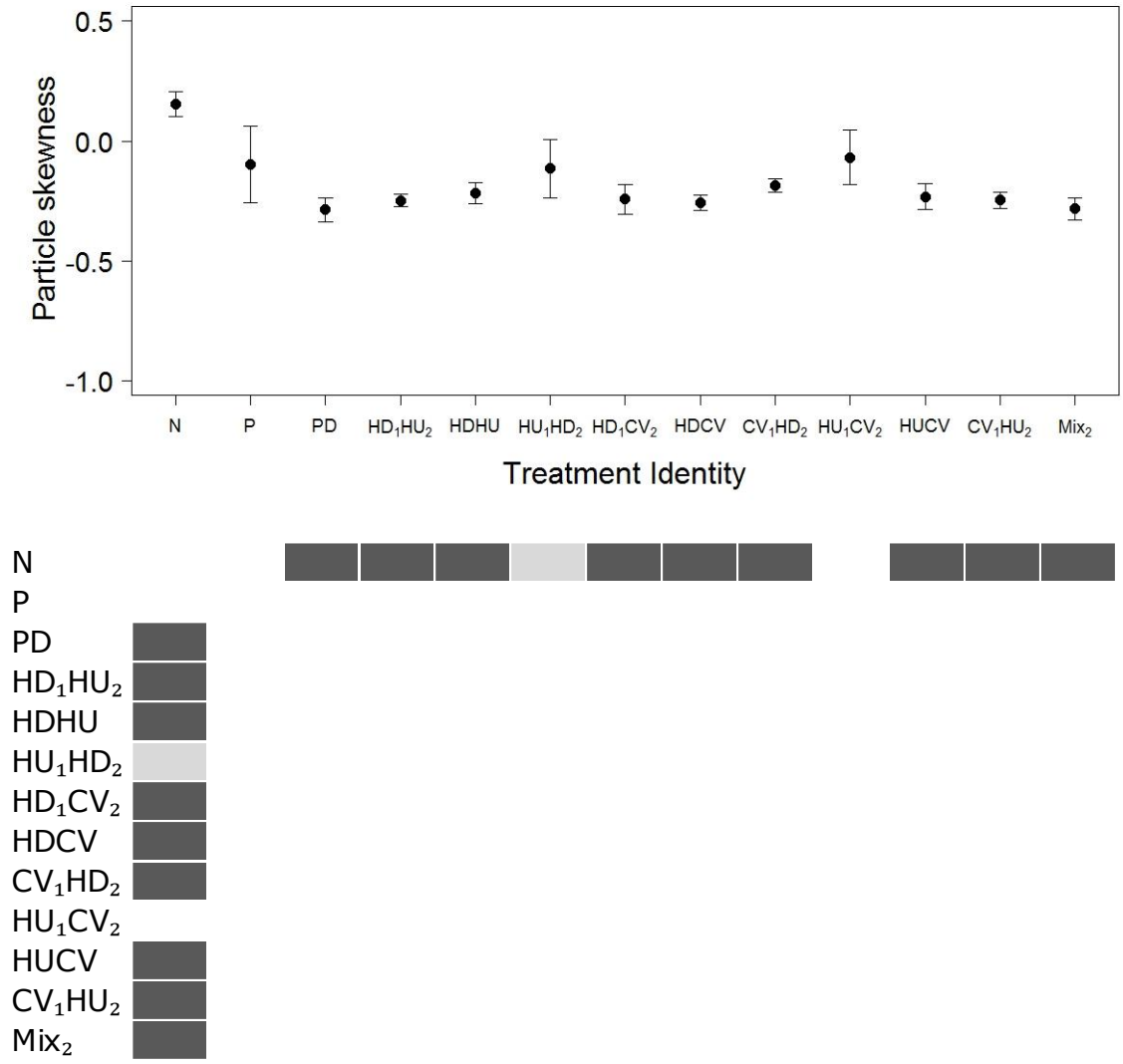

Figure 5.25 | Effect of defaunation, mesocosm presence and species biomass distribution on contact core particle skewness (n = 4). Error bars are standard error. Treatment identity as in Figure 5.6. Significant differences are indicated in the accompanying table where darker shading indicates greater significant difference: 0.01 < p < 0.05; 0.0001 < p < 0.01; p < 0.0001.

The contact core sediments showed mostly lepto-kurtosis, with some meso-kurtotis. There was no effect of mesocosm presence, defaunation or species treatment on contact core sediment particle skewness (Figure 5.26; L-ratio =15.99, d.f. = 26, p = 0.1915).

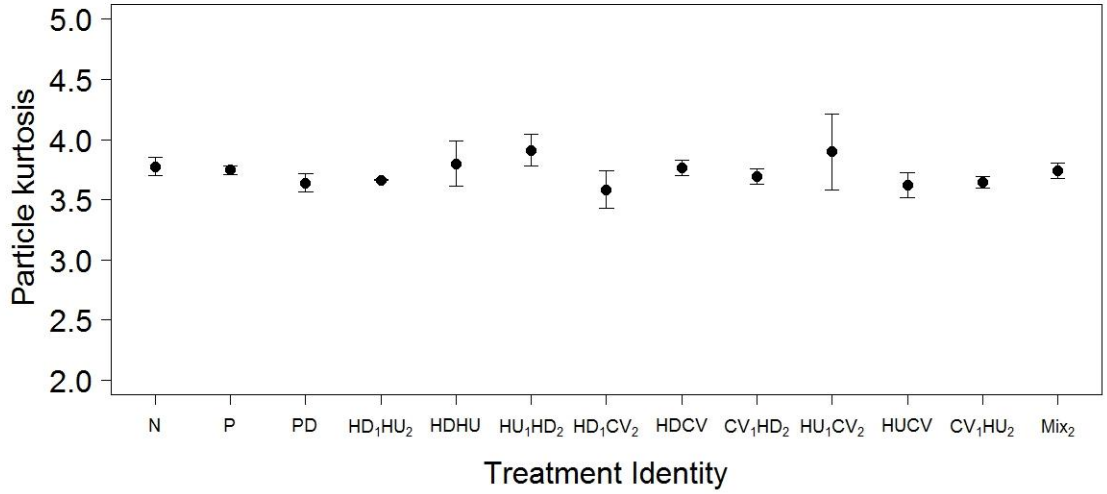

Figure 5.26 | Effect of defaunation, mesocosm presence and species biomass distribution on contact core particle skewness (n = 4). Error bars are standard error. Treatment identity as in Figure 5.6.

Contact core particle D_{10} ranged between 8.17 and 13.14 µm for all treatments and was lower than the minicore D_{10} (10.79 – 15.53 µm). There was no effect of mesocosm presence, defaunation or species treatment on contact core particle D_{10} (µm; Figure 5.27; L-ratio = 17.94, d.f. =26, p = 0.1175).

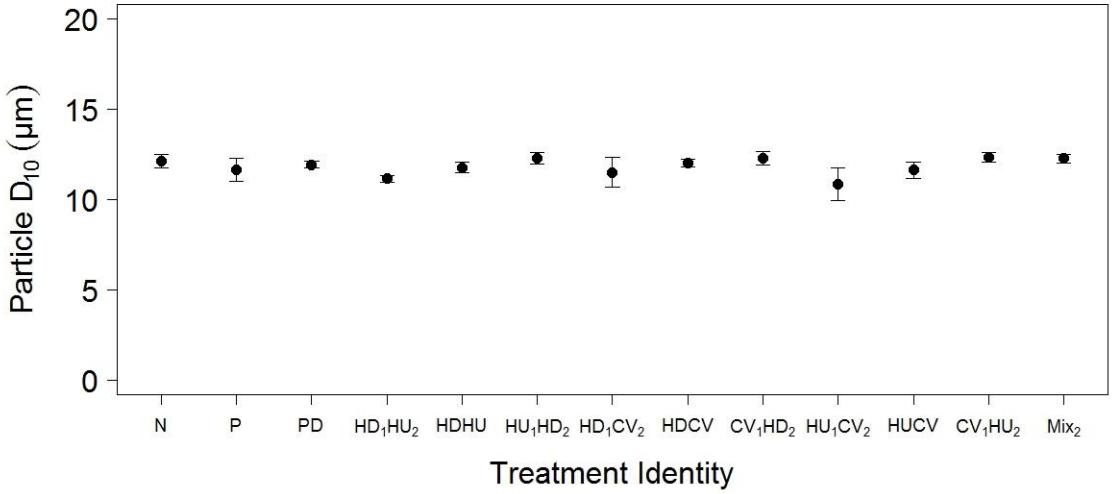

Figure 5.27 | Effect of defaunation, mesocosm presence and species biomass distribution on contact core particle D_{10} (µm; n = 4). Error bars are standard error. Treatment identity as in Figure 5.6.

There was a significant effect of sediment treatment on contact core sediment mud content (%; Figure 5.28; L-ratio = 34.75, d.f. = 26, p =

0.0005). The mean contact core sediment mud content was larger than that of the minicores. There was no effect of mesocosm presence (P; 70.54 ± 4.99 %; t = 1.01, p = 0.3180) or defaunation (PD; 71.51 ± 7.58 %; t = 1.14, p = 0.2605) on the mean (± 95 % CI, n = 4) contact core sediment mud content compared to the natural sediment (N; Figure 5.28; 67.73 ± 7.32 %). The high *Hediste* and low *Hydrobia* biomass treatment had a larger mean (± 95 % CI, n = 4) mud content (HD_1HU_2; 75.08 ± 2.97 %) than the procedural control (P; 70.54 ± 4.99 %; t = 2.49, p = 0.0173), the equal biomass *Hediste* and *Hydrobia* treatment (HDHU; 70.92 ± 2.84 %; t = 3.22, p = 0.0026), the high *Hydrobia* and low *Hediste* biomass treatment (HU_1HD_2; 70.20 ± 4.34 %; t = 2.95, p = 0.0053), the equal biomass *Hediste* and *Corophium* treatment (HDCV; 71.99 ± 1.59 %; t = 2.92, p = 0.0058), the high *Corophium* and low *Hediste* biomass treatment (CV_1HD_2; 68.10 ± 1.88 %; t = 6.33, p < 0.0001), the high *Corophium* and low *Hydrobia* biomass treatment (CV_1HU_2; 68.11 ± 4.29 %; t = 4.25, p = 0.0001), and the three species mixed treatment (Mix_2; 69.45 ± 2.34 %; t = 4.75, p < 0.0001). The high *Corophium* and low *Hediste* biomass treatment had a smaller mean (± 95 % CI, n = 4) mud content (CV_1HD_2; 68.10 ± 1.88 %) than the equal biomass *Hediste* and *Hydrobia* treatment (HDHU; 70.92 ± 2.84 %; t = -2.64, dp = 0.0120), the high *Hediste* and low *Corophium* treatment (HD_1CV_2; 72.31 ± 3.79 %; t = -3.17, p = 0.00.30), the equal biomass *Hediste* and *Corophium* treatment (HDCV; 71.99 ± 1.59 %; t = -5.05, p < 0.0001), and the high *Hydrobia* and low *Corophium* treatment (HU_1CV_2; 75.23 ± 7.35 %; t = -2.99, p = 0.0048). The high *Corophium* and low *Hydrobia* biomass treatment (CV_1HU_2; 68.11 ± 4.29 %) had a smaller mean (± 95 % CI, n = 4) mud content than the high *Hediste* and low *Corophium* biomass treatment (HD_1CV_2; 72.31 ± 3.79 %; t = -2.33, p = 0.0248), the equal biomass *Hediste* and *Corophium* treatment (HDCV; 71.99 ± 1.59 %; t = -2.70, p = 0.0101) and the high *Hydrobia* and low *Corophium* biomass treatment (HU_1CV_2; 75.23 ± 7.35 %; t = -2.66, p = 0.0113). Finally, the three species mixed treatment (Mix_2; 69.45 ± 2.34 %) had a smaller mean (± 95 % CI, n = 4) mud content than the equal biomass *Hediste* and *Corophium* treatment (HDCV; 71.99 ± 1.59 %; t = -2.87, p = 0.0066) and the high *Hydrobia* and low *Corophium* biomass treatment (HU_1CV_2; 75.23 ± 7.35 %; t = -2.38, p = 0.0221).

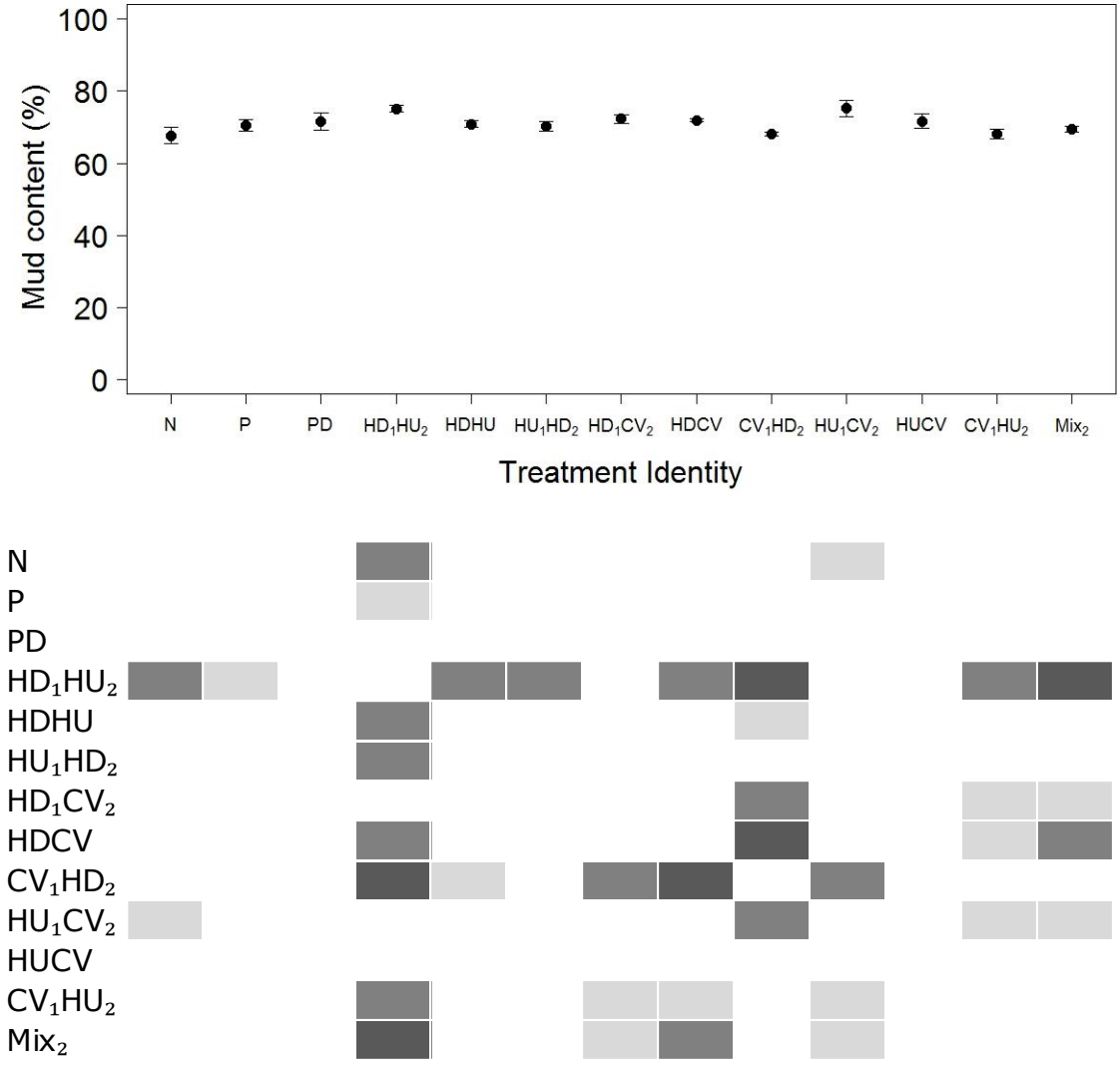

Figure 5.28 | Effect of defaunation, mesocosm presence and species biomass distribution on contact core mud content (%; n = 4). Error bars are standard error. Treatment identity as in Figure 5.6. Significant differences are indicated in the accompanying table where darker shading indicates greater significant difference: 0.01 < p < 0.05; 0.0001 < p < 0.01; p < 0.0001.

Table 5.2 | Summary table of effects of manipulating the density of benthic fauna on sediment characteristics compared with the control defaunated mesocosm (treatment PD). **+** or **–** indicate the direction of the effect where + represents a positive effect and – represents a negative effect compared to the control defaunated mesocosm. A single symbol indicates significance with $p < 0.05$, and a double symbol indicates significance with $p < 0.01$.

		***HEDISTE DIVERSICOLOR* DOMINATED**		***HYDROBIA ULVAE* DOMINATED**		***COROPHIUM VOLUTATOR* DOMINATED**		**MIXED SPECIES**			
	Sediment Characteristic	***Hediste diversicolor* dominated with *Hydrobia ulvae***	***Hediste diversicolor* dominated with *Corophium volutator***	***Hydrobia ulvae* dominated with *Hediste diversicolor***	***Hydrobia ulvae* dominated with *Corophium volutator***	***Corophium volutator* dominated with *Hediste diversicolor***	***Corophium volutator* dominated with *Hydrobia ulvae***	**Equal dominance of *Hediste diversicolor* and *Hydrobia ulvae***	**Equal dominance of *Hydrobia ulvae* and *Corophium volutator***	**Equal dominance of *Hediste diversicolor* and *Corophium volutator***	**Equal dominance of all three species**
Erosive properties	Erosion threshold										
	Suspension index										
MPB properties	Minimum fluorescence										
	Maxmimum quantum yield										
Minicore sediment properties	Water content										
	Mean particle size										
	Mode particle size										
	Particle sorting										
	Particle skewness		– –								
	Particle kurtosis										
	Particle D10										
	Mud content										
	Water concentration										
Contact core sediment properties	Colloidal carbohydrate concentration										
	Chlorophyll a concentration							–			
	Chlorophyll b concentration										
	Mean particle size										
	Mode particle size										
	Particle sorting					+					
	Particle skewness										
	Particle kurtosis										
	Particle D10										
	Mud content										

5.4 | Discussion

This experiment examined whether species density and biomass distribution affects mudflat stability and biogeochemical properties. The cryo-defaunation method resulted in sufficient reduction (85 %) in the abundance of the three species of interest, *Hediste diversicolor*, *Hydrobia ulvae*, and *Corophium volutator*, to provide a suitable method for assessing the effects of the individual species and the species mixtures on the stability and biogeochemistry of the sediment in the field.

5.4.1 | Use of mesocosms in the field and the effect of defaunation

As in Chapter 4, the mesocosms provided an effective way to ensure sediment defaunation and manipulations in species abundances were maintained for the length of the experiment, however similar experimental artefacts were observed to those presented in Section 4.4.1. Again, sediment held within the mesocosm had reduced species numbers of the three species of interest compared to the natural sediments, and there was a significant increase in the erosion threshold, the microphytobenthos minimum fluorescence, minicore particle size fine sediment skew, and contact core chlorophyll *a* and *b* concentration. There was also a significant decrease in the sediment suspension index. There are therefore a number of experimental artefacts associated with using a mesocosm, however the inclusion of a mesocosm only treatment as a procedural control as well as a defaunation control ensures there are comparable control treatments.

Cryo-defaunation caused a significant increase in the microphytobenthos minimum fluorescence (F_o). This likely due to a reduction in grazing pressure (Smith et al. 1996) as a result of the removal of the macrofauna.

5.4.2 | Interpreting species effects

When examining the species treatment data produced by this particular field experiment it becomes evident how complex the mudflat system is, even when the combined effects of only two or three macrofauna

species are investigated. To interpret the effects of species and their interactions on the mudflat it would be easy to cross into the realm of speculation. Based on my own experience and my reading of the published literature I present below a range of possible explanations for the patterns seen, however these discussions should not be considered exhaustive and there may be other behaviours, actions and interactions that result in the variations observed in the sediment properties. Due to the reduced replication in this experiment and variability between replicates within the same treatment, few of the variables exhibited significant changes in response to the species manipulations. Below I discuss changes in the sediment properties with reference to the observations made to determine the broad species effects and interactions that are occurring, however not all variation discussed is significantly so unless stated. When interpreting the effects of fauna on sediment stability, changes that are statistically significant may not necessarily be ecologically relevant. Low replicate variability, such as that seen in the sediment particle size measurements, means treatments might be statistically significantly different but only a small change has occurred in the particular sediment property. Whereas, overall some changes among treatments may be ecologically significant, resulting in a large change between the mean effects, but these are statistically insignificant due to high variability within treatments. Care should be taken therefore when interpreting data with high variability.

5.4.3 | Single species effects in mixed species treatments

As discussed in Section 4.4, the effect of *Hediste diversicolor*, *Hydrobia ulvae*, and *Corophium volutator* on sediment stability and biogeochemical properties can affect marine ecosystems through a number of mechanisms. Species are rarely found in monoculture in the natural environment and therefore the effect of species interactions, which can change the behaviours and actions of these species, are also, if not more, important. There are, however, a few effects that appear to be consistent with the species effects observed in single species dominated communities.

Those species treatments with a lower biomass of *Corophium volutator* (HD_1CV_2 and HU_1CV_2), although not those with no *Corophium* biomass

(HD_1HU_2, HDHU, and HU_1HD_2), had a significantly larger erosion threshold than the procedural control. Those treatments with a higher biomass of *Corophium volutator* (≥ 50 %; HDCV, HUCV, CV_1HD_2, and CV_1HU_2) had a smaller erosion threshold (on average < 2 Nm^{-2}) than many of the other treatments, although not significantly so. Additionally, one high biomass *Corophium* treatment (CV_1HU_2) had two replicates for which a much larger suspension index was measured, indicating that *Corophium* has the potential to greatly destabilise the sediment surface. *Corophium* has been shown to stabilise sediment through burrow stabilisation (Meadows and Tait 1989, Grant and Daborn 1994, Mouritsen et al. 1998) and destabilise the sediment due to high levels of bioturbation (de Deckere et al. 2000) and sediment ejection resulting in a surface layer of fine, easily re-suspendable particles (Grant and Daborn 1994) caused by burrow creation, maintenance and feeding. Low densities of *Corophium* may therefore result in increased sediment stability, whereas high densities of *Corophium* may result in decreased sediment stability. The species treatments containing *Corophium* also have a smaller measured microphytobenthos biomass, however not significantly so, which may be due to *Corophium* grazing (Smith et al. 1996, Mouritsen et al. 1998), and also contribute to the reduction in sediment stability (Paterson 1989, Underwood and Paterson 1993, Sutherland et al. 1998, Paterson and Black 1999, Black et al. 2002).

Corophium can also be seen to affect the sediment particle size distribution. Both species treatments containing the highest density of *Corophium* (CV_1HD_2 and CV_1HU_2) have significantly larger mean particle sizes than many of the other species treatments. *Corophium* has been shown to select preferentially a smaller particle size (4 to 60 μm) when grazing (Fenchel et al. 1975), potentially causing the loss of smaller particles from the sediment due to resuspension through ingestion and consequent incorporation of small particles into easily resuspendable fecal pellets (Grant and Daborn 1994), resulting in the loss of these particles from the sediment bed, or incorporation of these smaller particles into deeper sediment during burrow stabilisation (Meadows and Tait 1989).

In the treatments containing *Hediste diversicolor* (HD_1HU_2, HDHU, HU_1HD_2, HD_1CV_2, HDCV and CV_1HD_2), it appears to be the *Hediste*

diversicolor abundance controlling the sediment surface particle size distribution. Contact core mean particle size decreases with increasing *Hediste* abundance in these treatments. Riisgard (1991) showed that when filter feeding using a funnel shaped net-bag through which water was pumped by means of undulating movements by the body, *Hediste diversicolor* was 100 % efficient at removing particles larger than 7.5 µm from the water. The retention efficiency was much smaller for particles smaller than this, perhaps leading to the consumption of larger particles, reducing the average sediment surface particle size proportional to the Hediste biomass present in the treatment.

In the experiment presented in Chapter 4, when dominant in the community, *Hydrobia ulvae* resulted in reduced minimum fluorescence (F_o) and chlorophyll concentrations. In this experiment a number of mixtures containing *Hydrobia* (HDHU, HU_1CV_2, HUCV, CV_1HU_2 and Mix_2) also had a smaller average microphytobenthos biomass than the other species treatments (but not significantly so). *Hydrobia ulvae* has been shown to graze on microphytobenthos (Smith et al. 1996, Mouritsen et al. 1998, Austen et al. 1999, de Deckere et al. 2002, Hagerthey et al. 2002, Orvain et al. 2004) and the grazing pressure of *Hydrobia* may have reduced the microphytobenthos biomass and hence F_o and chlorophyll *a* and *b* concentrations.

5.4.4 | Density dependent effects and interactions in species mixtures

As discussed above, the large *Corophium* biomass treatment (CV_1HD_2) had a small F_o, however, two other species treatments containing *Hediste* and *Corophium* (HDCV, HD_1CV_2) had a larger minimum fluorescence, showing little or no effect of the presence of *Corophium*. Mixed species effects can be additive, or positively or negatively interactive (Statzner and Sagnes 2008). In the species treatments HD_1CV_2, HDCV, and CV_1HD_2 the net effect of the two species, *Corophium volutator* and *Hediste diversicolor*, changes depending on the distribution of species biomass. This indicates the effect of the two species in combination is ecologically context dependent due to interactive species effects. Among these treatments the changes in F_o observed could be due to interactive species effects, as suggested previously

by Petchey and Gaston (2002), caused by a reduction in *Corophium* biomass (see Table 5.1 for the post-experimental community core species biomass) as a result of predation by *Hediste* (Ronn et al. 1988) or increased predator avoidance behaviour causing a reduction in time spent grazing (as noted by Daborn et al., 1993, in response to bird predation). *Hediste diversicolor* has also been shown to cause the physical disturbance of *Corophium volutator* (Olafsson and Persson 1986) which usually results in *Corophium* migration (Bonsdorff et al. 1986, Jensen and Andre 1993) but in a confined area this may lead to mortality. Wilsey and Polley (2004) examined terrestrial treatment plots with varying plant species richness and evenness. They found that during the second year of the experiment species extinctions were not random but were greater in plots with low evenness (i.e. increased species rarity). Species extinction risk has been shown to be related to species population size (Pimm et al. 1988, Tracy and George 1992). Changes in species biomass distribution may therefore indirectly result in species extinctions and changes in species richness (Wilsey and Polley 2004)

The maximum quantum yield of the microphytobenthos varies among treatments, although not significantly so, however, the average maximum quantum yield of the high *Corophium* and low *Hydrobia* biomass treatment (CV_1HU_2) is noticeably higher than all the others (Figure 5.9), although not significantly so. This may be due to the strong regulatory influence of *Corophium* on epipelic diatoms as demonstrated by Hagerthey et al. (2002). *Corophium* has been shown to feed on certain dominant taxa, promoting epipelic diatom species richness and evenness (Hagerthey et al. 2002), perhaps resulting in the increased microphytobenthos 'health' measured in this study. A similar effect of *Corophium* is not observed, however, when a high biomass of *Corophium* is combined with *Hediste diversicolor*. This may again be as a result of reduced abundance, movement and grazing due to predator avoidance (Grant and Daborn 1994) and physical disruption (Olafsson and Persson 1986).

It may also be this interaction between *Corophium* and *Hediste* that meant a large suspension index was not measured in the high *Corophium* and low *Hediste* biomass treatments (CV_1HD_2). The high *Corophium* and low *Hydrobia* biomass treatments (CV_1HU_2) have a significantly larger suspension

index than many of the other treatments and the grazing action of both *Hydrobia* and *Corophium* has been found to be destabilising (Blanchard et al. 1997, Mouritsen et al. 1998, Austen et al. 1999, Andersen 2001, Orvain et al. 2004, Orvain et al. 2006), which should lead to a large suspension index. As the suspension index of the two high biomass *Hydrobia* treatments (HU_1HD_2, and HU_1CV_2), and the equal biomass *Hydrobia* and *Corophium* treatment (HUCV), are not significantly larger than any of the other treatments it can be hypothesised that it is predominantly the actions of *Corophium* that are destabilising the sediments, increasing the suspension index by the creation of a loose surface layer through sediment disruption while grazing (de Deckere et al. 2000) and the ejection of fine, easily re-suspendable, particles from burrows (Grant and Daborn 1994). The same large suspension index is not observed in the high *Corophium* and low *Hediste* biomass treatment (CV_1HD_2) even though the *Corophium* biomass in this treatment is comparable to that of the high *Corophium* and low *Hydrobia* treatment (CV_1HU_2; see Table 5.1). This is potentially another effect of an interaction between *Hediste* and *Corophium*, with the effect of the *Hediste* on *Corophium* causing a decrease in the *Corophium* behaviours that result in destabilised sediment, such as an increase in predation avoidance behaviour reducing surface browsing as seen by Daborn et al. (1993), or physical disruption by *Hediste* of *Corophium* burrowing processes as seen by Olafsson and Persson (1986).

The effect of combinations of the species on the erosion threshold appears to be variable. For example, the two treatments containing a large biomass of *Hydrobia* (HU_1HD_2 and HU_1CV_2) are significantly different. When combined with a small biomass of *Hediste diversicolor* the erosion threshold is lower, indicating that sediment is more unstable. When *Hydrobia ulvae* is combined with *Corophium volutator*, a species that has been shown to have a significant destabilising effect on intertidal sediment (see Chapter 4; Grant and Daborn, 1994, Smith et al., 1996, Mouritsen et al., 1998, De Deckere et al., 2000), the sediment has a significantly higher erosion threshold and is therefore more stable.

There is, therefore, a species interaction between *Hydrobia* and *Corophium*, and *Hydrobia* and *Hediste* resulting in changes to the sediment

erosion threshold. It is possible the presence of both *Corophium* and *Hydrobia* on the sediment surface results in changes to grazing or movement behaviour due to competition. Morrisey (1988) showed that *Hydrobia ulvae* will discriminate against sediment already grazed by *Corophium arenarium*, therefore when in combination with *Corophium volutator*, *Hydrobia* may reduce grazing activity, resulting in more stable sediment than would be expected. Whereas when *Hydrobia* is in combination with *Hediste*, the adaptable feeding behaviours of *Hediste* (Barnes 1994) may mean that surface sediment food resources are not limited and *Hydrobia* can graze freely, resulting in sediment destabilisation.

The patterns of chlorophyll *a* and *b* concentrations measured in the contact core samples approximately match those seen in the F_o. The reduction in chlorophyll *a* concentration in the equal *Hediste* and *Hydrobia* biomass treatment (HDHU) results in a significantly lower chlorophyll *a* and *b* concentration than in many of the other species treatments. This species treatment also has a smaller mean erosion threshold than the other *Hydrobia* and *Hediste* species treatments, however not significantly so. Reduced sediment surface chlorophyll concentration could be due to high grazing pressure exerted by the combination of *Hydrobia*, known to graze upon the microphytobenthos (Blanchard et al. 1997, Austen et al. 1999), and *Hediste*, which has multiple feeding strategies (Barnes 1994, Costa et al. 2006), one of which includes grazing upon benthic algae in shallow coastal areas (Engelsen and Pihl 2008). The other two treatments containing *Hydrobia ulvae* and *Hediste diversicolor* (HD_1HU_2 and HU_1HD_2), however, do not show a similar significant reduction in sediment chlorophyll concentrations. HD_1HU_2 actually has a significantly higher chlorophyll *a* concentration than the other *Hydrobia* and *Hediste* combination treatments. With this in mind, one might expect that the HU_1HD_2 treatment might have an even lower chlorophyll *a* concentration, which would indicate it is the increasing *Hydrobia* biomass (when combined with *Hediste*) that causes the reduction in chlorophyll *a* concentration. However the chlorophyll *a* concentration of the HU_1HD_2 treatment is not significantly different from that of the HDHU treatment but the mean chlorophyll *a* and *b* concentrations are actually larger. This indicates there is some form of interaction between *Hydrobia ulvae* and *Hediste diversicolor* causing these fluctuations in chlorophyll *a* and *b*,

concentrations. This effect may be due to the fact that the increased grazing caused by increased numbers of *Hydrobia* results in a reduction of grazing by *Hediste* and the effects of these species on sediment chlorophyll concentration observed are interactive, not additive.

With respect to the results observed regarding particle size distribution, the high *Hydrobia* and low *Corophium* biomass treatment (HU_1CV_2) has a significantly smaller contact core mean particle size than the two high *Corophium* biomass treatments. *Hydrobia* has been shown to select preferentially larger particle sizes (20 to 300 µm) when grazing (Fenchel et al. 1975), which may be ingested and excreted as readily suspendable fecal pellets, resulting in removal from the sediment surface. Conversely, the high *Hydrobia* and low *Hediste* treatment (HU_1HD_2) does not follow the same pattern and has a larger mean particle size than that of *Hydrobia* combined with *Corophium*, but not significantly so. While the *Hydrobia* biomass recorded in this treatment in the community composition cores is perhaps not as large as it should be, possibly due to unexpected mortality, it would be expected that *Hydrobia* would have a greater effect on particle size in this treatment and the equal biomass *Hediste* and *Hydrobia* treatment (HDHU) than observed. The fact it does not is perhaps due to a negative interaction between the *Hediste* and the *Hydrobia* causing an inhibition or alteration of grazing activity.

In an experiment examining ecosystem processes and evenness in a terrestrial field, total and belowground biomass production was found to increase with increasing evenness, but aboveground biomass was more dependent on the identity of the dominant species (Wilsey and Potvin 2000). In this study, those treatments with equal biomass allocations (HDHU, HDCV, and HUCV) did not show any significant patterns that would indicate that evenness of biomass results in increased sediment stability or instability or greater microphytobenthos productivity. It is the species present and the interactions occurring between these species that are the most important in determining the sediment erodibility and other biogeochemical properties. This has also been observed by other studies examining the effects of biodiversity on intertidal sediments. For example, the interaction between *Hediste diversicolor* and *Corophium volutator* observed during a two year

field study was so significant that Olafsson and Persson (1986) suggested that it may be a habitat structuring force in shallow brackish sediments.

Even though the combined effects of only three macrofauna species have been investigated here it is evident how complex the mudflat system is. Within the natural mudflat there are also many other species and environmental variables that change both temporally and spatially. Many of the effects examined in this chapter are caused by both direct and indirect effects on the macrofauna and the microphytobenthos. While the mudflat ecosystem must, to a certain extent, be the product of environmental variables, species effects, and the species and environmental interactions occurring at any moment, these interactions are complicated and it is likely that there are many that have not been investigated yet. This suggests that there are other important variables which require quantifying to enable improved understanding of the effects of biota on sediment erodibility. In addition, it may be that greater understanding of the underlying mechanisms and behaviours is needed. Our understanding of macrofaunal effects on sedimentary processes should then improve and what currently appear to be idiosyncratic responses could be elucidated. These issues are discussed in more detail in Chapters 7 and 8.

5.4.5 | Experimental limitations

As this experiment was carried out using *in situ* mesocosms it is potentially affected by a number of experimental artefacts discussed in the previous chapters, however the use of mesocosms to prevent colonisation of defaunated sediments and maintain the species biomass was necessary. The inclusion of a mesocosm only treatment ensured that the changes observed in the defaunated and the species treatments could be compared to a procedural control.

Species interactions, especially predation or disruption, within the cores may have changed the species biomass within, therefore the species biomass added at the start of the experiment may not have been maintained until the end of the experiments. As one of the aims of this experiment was to look at the effects of interspecific interactions this was not considered a

problem and measurement of core species biomass after the experiment ensured that all changes were documented.

5.4.6 | Future work

The two species biomass distribution treatments examined in this experiment are an initial assessment of the effects of individual species, biodiversity and species density on mudflat sediment properties. The effects of three, or more, common species on the mudflat in ecologically relevant combinations and densities should be investigated further. Studies focussing on the mechanisms of how these species interactions change with species density and richness, such as switching feeding and burrowing behaviours or time allocation will be of great importance in understanding the biological and sedimentary processes occurring.

5.4.7 | Chapter conclusions

1 | Due to the complex nature of the mudflat ecosystem including species multiple life strategies, species interactions, environmental interactions and indirect effects, interpretation of the observed data is difficult. Allocation of the variability observed to species activities will require a mechanism based approach, re-examination of previous studies and the use of novel analyses in the future.

2 | The individual effects of species are still discernible while in species combinations. Effects of *Hediste diversicolor*, *Hydrobia ulvae* and *Corophium volutator* on the sediment stability and other properties could still be discerned while in species mixture.

3 | Species densities within species mixtures had a significant effect on sediment stability and biogeochemical properties. Some species interactions were observed to be density dependent and at high species densities both inter- and intra-specific interactions may become important.

4 | Species interactions may be a habitat structuring force on the intertidal mudflat with variations in species densities and richness resulting in changes to mudflat sediment properties due to changes in species interactions.

Chapter 6 | Effects of Changes in Species Abundance on Mudflat Biogeochemical Properties

6.1 | Introduction

The experiments presented in the previous two chapters involved manipulating species biomass and abundances using defaunated *in situ* mesocosms. It was necessary to defaunate the mud cores before these experiments commenced so the effects of single and combinations of species on mudflat properties could be examined. This chapter also examines how changes in species biomass and abundance affect selected biogeochemical the properties of a mudflat, but instead of starting with a defaunated sediment core, species biomass was added on top of an already established community. Individuals of the species *Hediste diversicolor*, *Hydrobia ulvae* and *Corophium volutator*, were added to *in situ* mesocosms and the effect of species addition to the macrofaunal community on mudflat stability and biogeochemical properties was measured. This chapter specifically addresses Objectives 1, 2 and 4 presented in Section 1.7 when manipulations are made in an already established community:

Objective 1 | Investigate the effect of individual macrofauna species on mudflat sediment stability and biogeochemical properties *in situ*.

Objective 2 | Investigate the effect of macrofaunal species density on mudflat sediment stability and biogeochemical properties *in situ*.

Objective 4 | Investigate the effect of macrofaunal species biomass distribution on mudflat sediment stability and biogeochemical properties *in situ*.

Objective 5 | Investigate the effect of a macrofaunal species community on mudflat sediment stability and biogeochemical properties.

6.1.1 | Rationale

Chapter 4 examined how individual species when added to produce a single species dominated community affected sediment properties. Chapters 4 and 5 examined how the three species, *Hediste diversicolor*, *Hydrobia ulvae* and *Corophium volutator*, when added in combination in different abundances and biomass densities affected sediment properties. These experiments are useful in determining how species abundance and biomass distribution affects the sediment properties, however the natural ratio of species is lost and the activity of a species within a natural community cannot be examined in a sediment core that has been defaunated and the biomass replaced in pre-calculated ratios. Natural fluctuations in species abundances have been shown to result in changes in sediment topography and characteristics (Olafsson and Persson 1986, Mouritsen et al. 1998, Hagerthey et al. 2002, Kelaher et al. 2003). The interspecific interactions of *Hediste diversicolor* and *Corophium volutator* were hypothesised to be a structuring force in shallow brackish sediments, resulting in environmental patchiness on the south coast of Sweden (Olafsson and Persson 1986). Additionally, the interspecific interactions of the mud snail *Ilyanassa obsoleta* and the annelid species *Capitella* spp. and *Paranais litoralis* were also found to be important in structuring the benthic community on Long Island, NY, mudflats (Kelaher et al. 2003). Mass mortality of *Corophium* was found to result in a habitat shift from a mudflat with a mosaic of raised areas and tidal pools to a flatter, more homogenous environment (Mouritsen et al. 1998). These natural fluctuations can be informative when investigating the effects of changes of species abundance and density on the mudflat habitat, however the effect of known changes in species abundances cannot be studied in this way and only opportunistic observations, usually noticed while undertaking other investigations, can be made.

In this experiment, three treatments have been manipulated to alter the biomass distribution of the species *Hediste diversicolor*, *Hydrobia ulvae* and *Corophium volutator* within the community. Extra species biomass was added, changing which species was dominant within the community (i.e. had the greatest biomass), and increasing the abundance and biomass of each species of interest above the baseline.

6.2 | Materials and methods

Fieldwork was carried out at Breydon Water, Great Yarmouth, UK over the period 7th to 20th of August, 2012 adjacent to the area where the pilot experiment and the experiments presented in Chapters 4 and 5 were carried out. Five sediment cores to determine core species biomass were taken on the 7th of August following the method given in Section 2.2 for measurement of the macrofaunal biomass. These biomass measurements were used to determine the biomass required for the experimental treatments. The experiment was set up on the 13th of August, 2012. Biomass cores contained an average (± SE) of 0.57 ± 0.05 g of macrofaunal biomass, equivalent to 28.40 ± 2.40 g per m^2, consisting of predominantly *Corophium volutator* (45 %), *Macoma balthica* (20 %), *Hydrobia ulvae* (14 %), and *Hediste diversicolor* (6 %). Due to the difficulty of collecting and identifying live *Macoma balthica* with the resources available, *Macoma* density was not manipulated in this experiment.

6.2.1 | Experimental design

The experimental design consisted of 5 treatments (Figure 6.1; n = 6). There were two control treatments; natural sediment as a control baseline (N) and a pipe mesocosm only treatment as a procedural control (P). The three species treatments consisted of natural sediment with 50% additional biomass added as *Hediste diversicolor* held within a mesocosm (N_{HD}); natural sediment with 50% additional biomass added as *Hydrobia ulvae* held within a mesocosm (N_{HU}); and natural sediment with 50% additional biomass added as *Corophium volutator* held within a mesocosm (N_{CV}). The experimental procedure consisted of one day of mesocosm setup and species addition.

The 30 mesocosms were set up as detailed in Section 2.2. Treatments were representatively allocated to the treatment areas ensuring even allocation to each row (n = 7 or 8; Row1, Row2, Row3, Row4; where Row1 was highest on the shoreline).

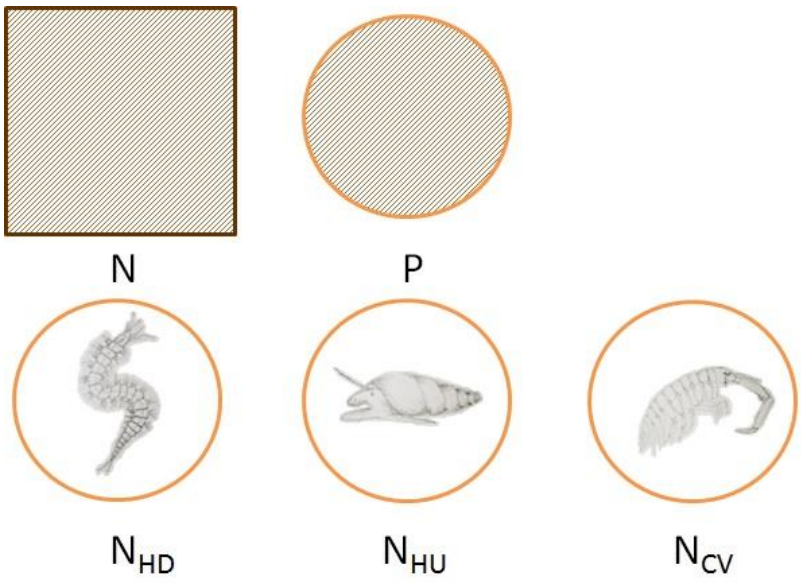

Figure 6.1 | The five experimental treatments represented visually. Shading represents the natural sediment. Each diagrammatic organism represents $^1/_2$ of the total core biomass. Where N is natural sediment as a mudflat baseline, P is a pipe mesocosm only treatment as a procedural control, N_{HD} is natural sediment held within a mesocosm with 50 % additional biomass added as *Hediste diversicolor*, N_{HU} is natural sediment held within a mesocosm with 50 % additional biomass added as *Hydrobia ulvae*, and N_{CV} is natural sediment held within a mesocosm with 50 % additional biomass added as *Corophium volutator*.

6.2.2 | Experimental data collection

Data collection occurred on the 20th of August 2012 following the protocols detailed in Section 2.3. In the field, data were collected using a cohesive strength meter (CSM; Section 2.3.1) and a pulse amplitude modulated fluorometer (PAM; Section 2.3.2). Minicores (Section 2.3.3) were collected and analysed for water content and particle size properties in the laboratory following the procedures described in Section 2.6.3. Contact cores (Section 2.3.4) were collected and analysed for water concentration, carbohydrates, chlorophyll *a* and *b* and particle size properties in the laboratory following the procedures presented in Section 2.6.4. Community composition cores were taken at the experiments end, on the 20th of August, and analysed to determine species biomass in the cores at the end of the experiment, following the methods presented in Section 2.6.5.

6.2.3 | Data analysis

Data obtained from the CSM was processed to obtain the sediment erosion threshold and suspension index following the procedures given in Section 2.6.1. Data obtained from the PAM provided the microphytobenthos minimum fluorescence and the maximum quantum yield (Section 2.6.2). The resulting data were analysed using a generalised least squares approach and a non-transgressive overyielding technique, as described in Section 2.7, to compare the species treatments and the procedural and experimental controls. All generalised least squares initial and final models used are presented in Appendix 4.

Non-trangressive overyielding techniques (Loreau 1998, Fridley 2001, Petchey 2003, Griffin et al. 2009) were used to compare the effects of the species in single species dominated communities (based on data presented in Chapter 4) to the effects of the species in a whole community (see also Section 2.7).

Using the data collected during the experiment presented in Chapter 4 the effect of each species when dominant was determined by subtracting the average value of a particular variable measured in the defaunated sediment treatment from that measured in the each species treatment where the whole of the defaunated biomass had been replaced by a single species (HD_1, HU_1, CV_1). This species effect can then be divided in half (to represent an addition of 50 % extra species biomass) and summed (whether a positive effect or a negative effect) with the procedural control (P) value obtained in this experiment to give an expected value for the variable of interest if the action of the species in a community was equivalent to the action of the species in the single species dominated community ('Effect (E)' in Equation 6.1). The comparative yield statistic (D_{sp}) can then be calculated to compare the expected effect against the observed effect obtained in this experiment ('Effect (O)' in Equation 6.1) for each species (Equation 6.1).

Equation 6.1 $$D_{sp} = \frac{\text{Effect (O)- Effect (E)}}{\text{Effect (E)}}$$

This was designed to highlight the differences between how the results of actions and behaviours of the species in the single species dominated communities affect the sediment properties in comparison with how the species actions and behaviours affect the sediment properties within a whole community. As the observed and expected values being compared are derived using two different experiments, carried out at different times of the year the statistics obtained may be temporally confounded, however by examining the effect of the species relative to the value measured in the defaunated sediment the influence of seasonal fluctuations can be minimised. This should, however, be taken into account when considering the data.

6.3 | Results

Addition of *Hediste diversicolor*, *Hydrobia ulvae* or *Corophium volutator* to the species treatments resulted in increased biomass of the three species above natural levels. The biomass of each species in the sediment cores was increased approximately four fold. The addition of the *Corophium* was not as successful as the addition of the other species, possibly due to the higher mobility of *Corophium* resulting in loss from the mesocosm through mesh, or through species interactions such as physical disturbance or predation. However, the individual species biomass in the treatment cores was increased above the levels found in the mesocosm control by approximately four fold (Table 6.1).

Table 6.1 | The mean biomass (g ± standard error; n = 5) of the three species of interest *Hediste diversicolor*, *Hydrobia ulvae* and *Corophium volutator*, in the community composition cores taken after the experimental cores had been in the field for two weeks.

Treatment	*Hediste*	*Hydrobia*	*Corophium*
Natural Sediments (N)	0.059 ± 0.013	0.117 ± 0.022	0.035 ± 0.006
Mesocosm Control (P)	0.053 ± 0.008	0.074 ± 0.008	0.024 ± 0.001
Hediste Added (N_{HD})	0.218 ± 0.042	0.080 ± 0.008	0.024 ± 0.003
Hydrobia Added (N_{HU})	0.068 ± 0.007	0.306 ± 0.027	0.019 ± 0.002
Corophium Added (N_{CV})	0.078 ± 0.014	0.074 ± 0.008	0.101 ± 0.012

6.3.1 | Row effects

The effect of the row the treatment was located in (n = 7 or 8; Row1, Row2, Row3, Row4; where Row1 was highest on the shoreline) was tested against two variables; the erosion threshold (ET, Nm^{-2}; Figure 6.2) and the PAM measured minimum fluorescence (F_o; Figure 6.3). The row location of the treatment did not affect the erosion threshold (Row; L-ratio = 1.84, d.f. = 8, p = 0.6057) or the pulse amplitude modulation (PAM) measured minimum fluorescence (Row; L-ratio = 1.01, d.f. = 8, p = 0.7991).

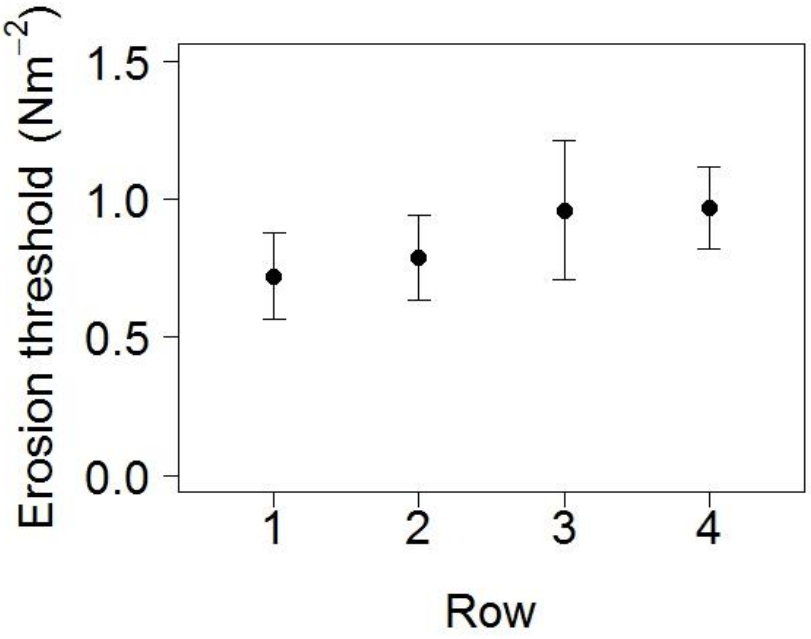

Figure 6.2 | Effect of mesocosm row location on the sediment erosion threshold (Nm^{-2}; n = 7). Error bars are standard error. 1, Row 1; 2, Row 2; 3, Row 3; 4, Row 4, where Row 1 was highest on the shoreline.

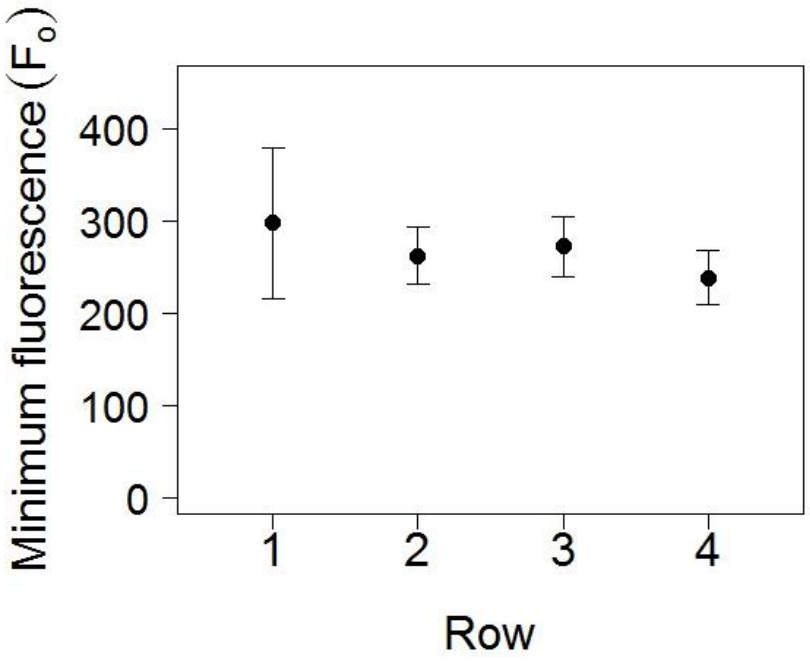

Figure 6.3 | Effect of mesocosm row location on the pulse amplitude modulated measured minimum fluorescence (F_o; n = 7). Error bars are standard error. 1, Row 1; 2, Row 2; 3, Row 3; 4, Row 4, where Row 1 was highest on the shoreline.

Many of the procedural control treatments (those sediments enclosed in a mesocosm on the mudflat but not defaunated; P) differed significantly from the natural sediments (no mesocosm; N). Thus, during the data statistical analysis and discussion all experimental treatments will be compared to the procedural control (P). The measurement of a natural mudflat baseline is interesting in its own right, but as the presence of the pipe mesocosm has a significant effect on some of the sediment properties the correct approach is to compare all species treatments with the procedural control. This approach will be adopted for all the following analyses in this chapter. See Appendix 4 for coefficients tables containing all p-values discussed in this chapter.

6.3.2 | Sediment erosion effects

Similarly to the results presented in Section 4.3.2 and 5.3.2, the natural mudflat at Breydon Water (treatment N) was found to have a small mean (± 95 % CI, n = 6) erosion threshold (Figure 6.4; 0.21 ± 0.11 Nm^{-2}) meaning it is easily erodible under low current speeds. There was a

significant effect of sediment treatment on the sediment erosion threshold (Nm^{-2}; L-ratio = 45.50, d.f. = 10, $p < 0.0001$). The procedural control (treatment P) had a larger mean (± 95 % CI, n = 6) erosion threshold (1.26 ± 0.64 Nm^{-2}; t = 1.05, $p < 0.0001$) than the natural sediments, indicating there is a significant effect on the mudflat sediments caused by using an experimental mesocosm *in situ*. Closer examination of the coefficient tables (Appendix 4) revealed that the erosion thresholds of the species treatments were not significantly different from the procedural control or each other.

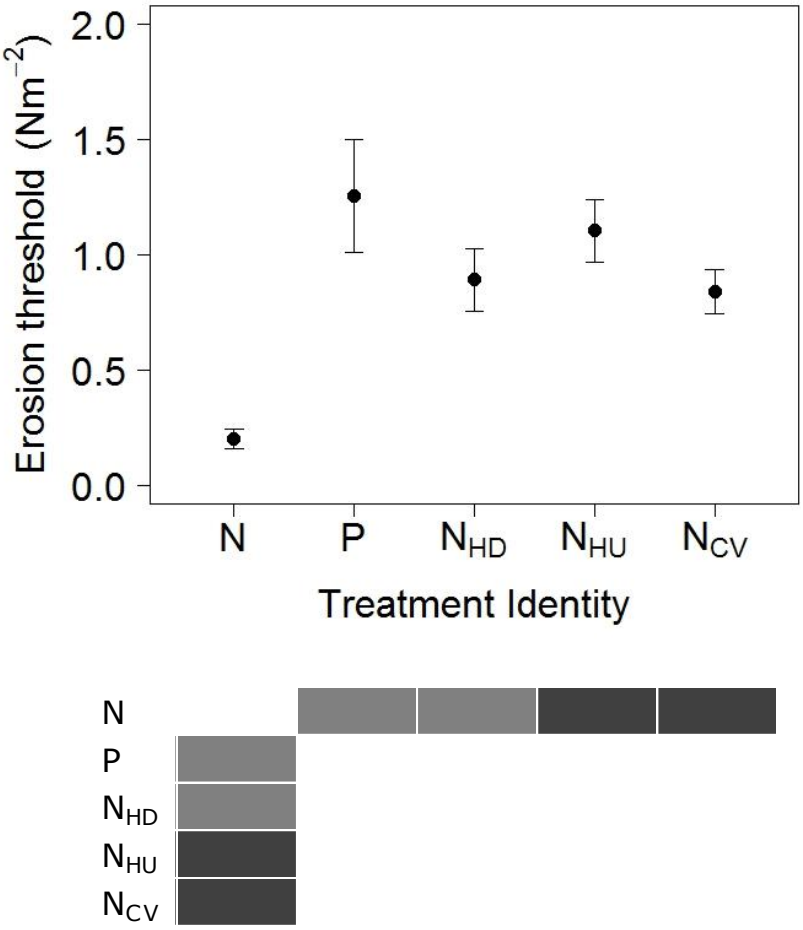

Figure 6.4 | Effect of mesocosm presence and species addition on sediment erosion threshold (Nm^{-2}; n = 6). Error bars are standard error. The species composition of each mixture is indicated on the x-axis, where treatment identity corresponds to: N, natural sediment as a mudflat baseline; P, a pipe mesocosm only treatment as a procedural control, N_{HD}, natural sediment with 50 % additional biomass added as *Hediste diversicolor*; N_{HU}, natural sediment with 50 % additional biomass added as *Hydrobia ulvae*; N_{CV}, natural sediment with 50 % additional biomass added as *Corophium volutator*. Significant differences are indicated in the accompanying table where darker shading indicates greater significant difference: ▫ $0.01 < p < 0.05$; ▪ $0.0001 < p < 0.01$; ■ $p < 0.0001$.

There was a significant effect of sediment treatment on the sediment suspension index (L-ratio = 16.64, d.f. = 10, p = 0.0023). The mean (± 95 % CI, n = 6) suspension index of the natural sediments (N; 32.46 ± 13.68) was larger than that of the procedural control treatments (Figure 6.5; P; 3.74 ± 2.54; t = -5.31, p < 0.0001), meaning the sediment has a larger erosion rate. The suspension indices of the species treatments were not significantly different from the procedural control or each other (see Appendix 4).

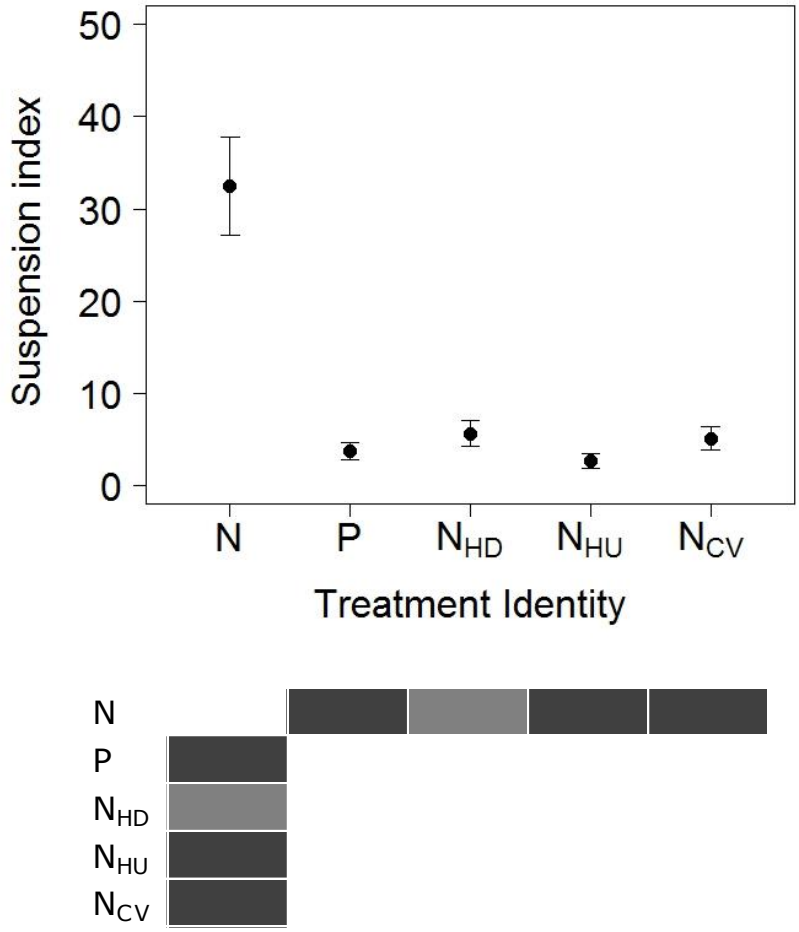

Figure 6.5 | Effect of mesocosm presence and species addition on sediment suspension index (n = 6). Error bars are standard error. Treatment identity as in Figure 6.4. Significant differences are indicated in the accompanying table where darker shading indicates greater significant difference: 0.01 < p < 0.05; 0.0001 < p < 0.01; p < 0.0001.

6.3.3 | Microphytobenthos biomass

There was a significant effect of sediment treatment on sediment microphytobenthos biomass (F_o; L-ratio = 25.69, d.f. = 10, p < 0.0001). The mean (± SE, n= 6) pulse amplitude modulated fluorometer measured

minimum fluorescence (F_o) of the natural sediments (N; 149.39 ± 20.67) was lower than the procedural control treatment (Figure 6.6; P; 378.06 ± 163.51; t = 3.57, p = 0.0015). The average minimum fluorescence values of the species treatments were smaller than that of the procedural control, however not significantly so (see Appendix 4).

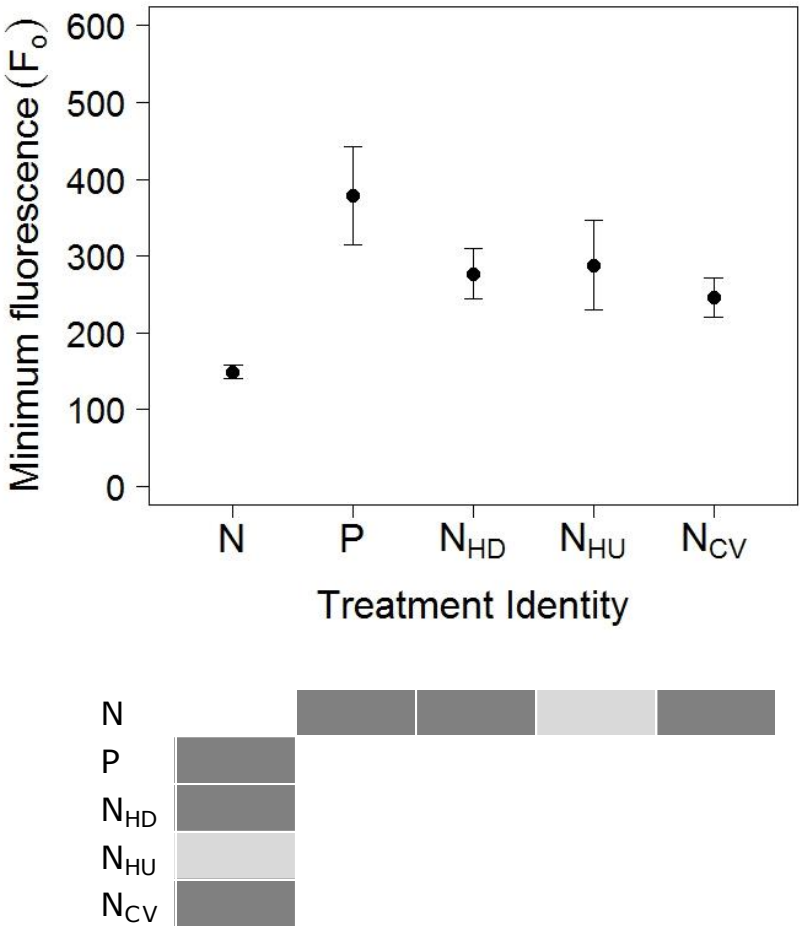

Figure 6.6 | Effect of mesocosm presence and species addition on the pulse amplitude modulated fluorometer measured minimum fluorescence (F_o; n = 6). Error bars are standard error. Treatment identity as in Figure 6.4. Significant differences are indicated in the accompanying table where darker shading indicates greater significant difference: 0.01 < p < 0.05; 0.0001 < p < 0.01; p < 0.0001.

There was a significant effect of sediment treatment on sediment microphytobenthos 'health' (L-ratio = 11.49, d.f. = 10, p = 0.0216). There was, however, no effect of mesocosm presence on the mean (± 95 % CI, n = 6) pulse amplitude modulated fluorometer measured maximum quantum yield (P; 0.62 ± 0.03) compared to that of the natural sediments (Figure 6.7; N; 0.60 ± 0.02; t = 1.73, p = 0.0953) and no difference observed between the species treatments and the procedural control.

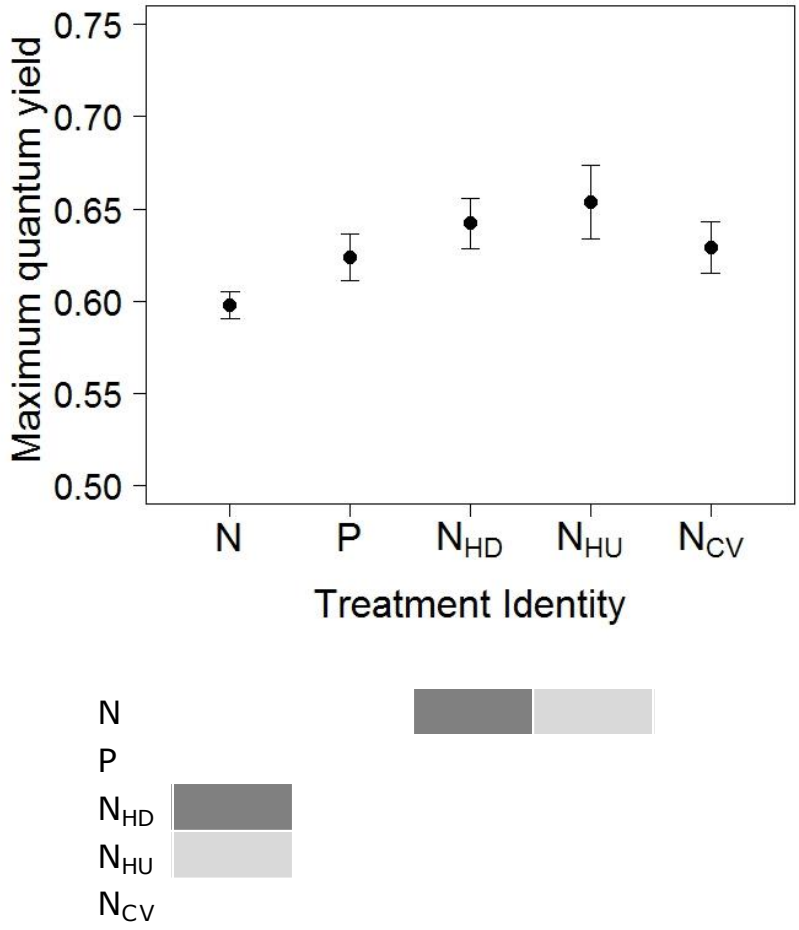

Figure 6.7 | Effect of mesocosm presence and species addition on the pulse amplitude modulated fluorometer measured maximum quantum yield (n = 6). Error bars are standard error. Treatment identity as in Figure 6.4. Significant differences are indicated in the accompanying table where darker shading indicates greater significant difference: 0.01 < p < 0.05; 0.0001 < p < 0.01; p < 0.0001.

6.3.4 | Minicore sediment properties

There was no effect of mesocosm addition or species addition on the minicore sediment water content (Figure 6.8; L-ratio = 20.61, d.f. = 10, p = 0.0564).

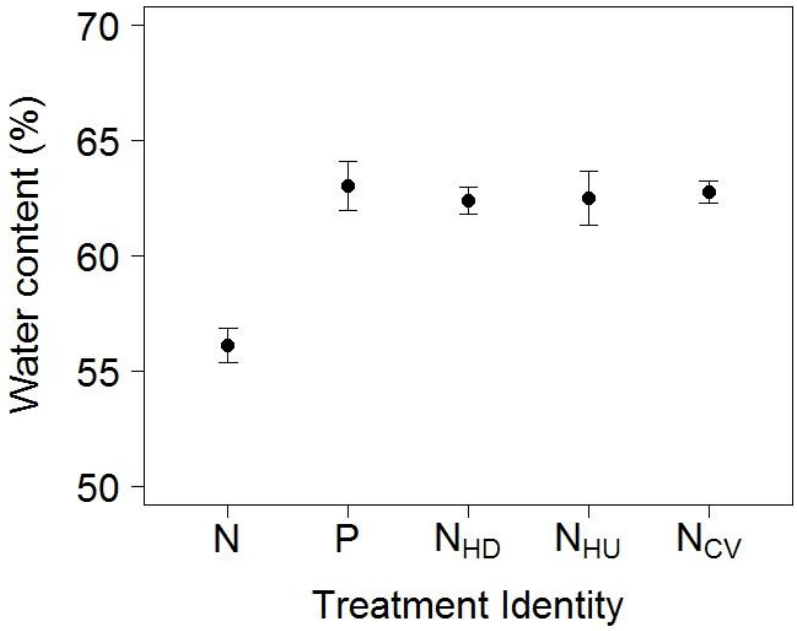

Figure 6.8 | Effect of mesocosm presence and species addition on minicore sediment water content (%; n = 6). Error bars are standard error. Treatment identity as in Figure 6.4.

The minicore sediments were classified as very coarse silt or very fine sand under the GRADISTAT program scale (Blott and Pye 2001). There was no effect of mesocosm addition or species addition on the minicore mean particle size (μm; Figure 6.9; L-ratio = 1.22, d.f. = 10, p = 0.8743).

There was no effect of mesocosm addition or species addition on minicore particle size mode (μm; Figure 6.10; F = 1.38, d.f. = 4, p = 0.2702).

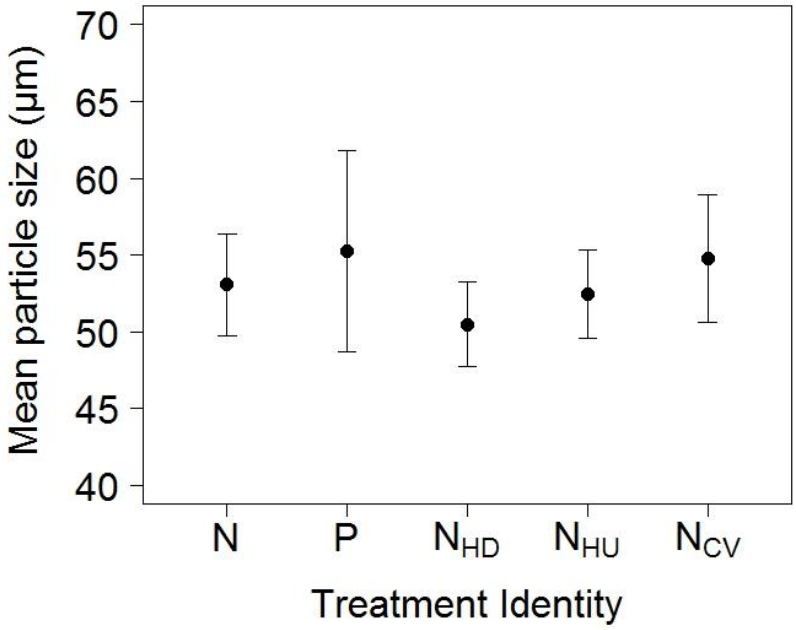

Figure 6.9 | Effect of mesocosm presence and species addition on minicore mean particle size (μm; n = 6). Error bars are standard error. Treatment identity as in Figure 6.4.

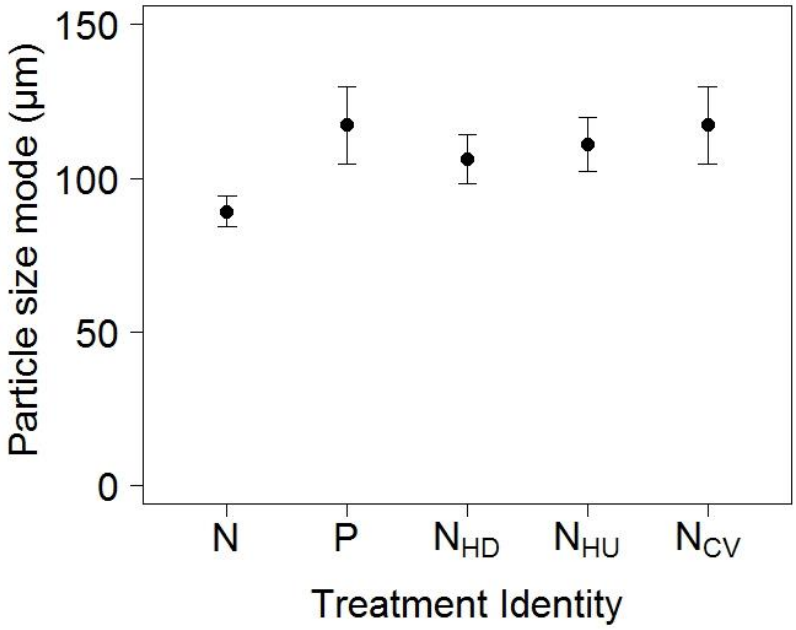

Figure 6.10 | Effect of mesocosm presence and species addition on minicore particle size mode (μm; n = 6). Error bars are standard error. Treatment identity as in Figure 6.4.

The minicore sediments were poorly sorted. There was no effect of mesocosm addition or species addition on minicore particle sorting (Figure 6.11; L-ratio = 1.10, d.f. =10, p = 0.8944).

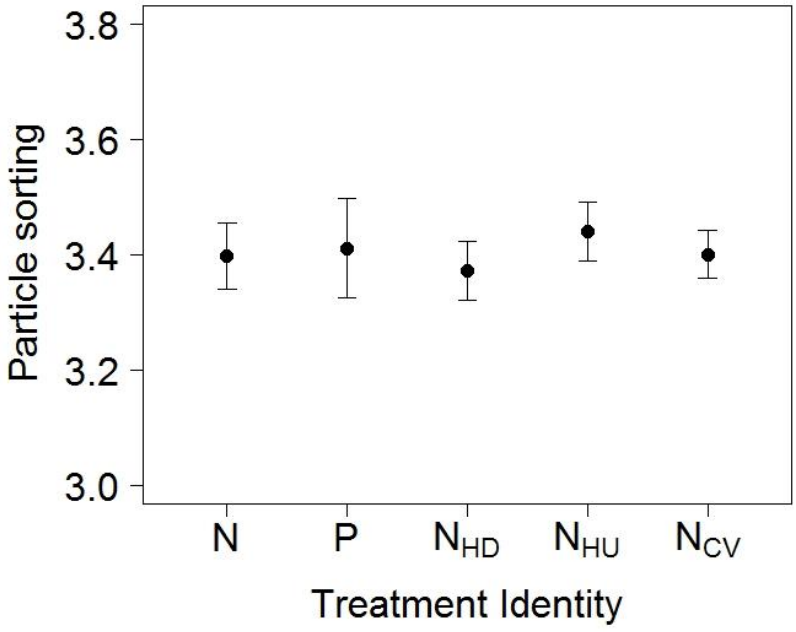

Figure 6.11 | Effect of mesocosm presence and species addition on minicore particle sorting (n = 6). Error bars are standard error. Treatment identity as in Figure 6.4.

The minicore sediments were fine skewed. There was no effect of mesocosm addition or species addition on minicore particle skewness (Figure 6.12; L-ratio = 7.71, d.f. =10, p = 0.1027).

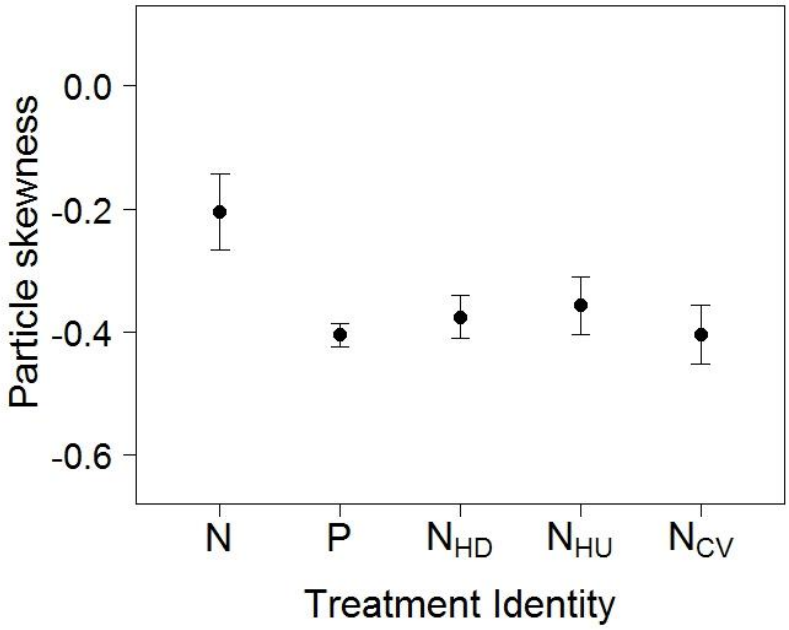

Figure 6.12 | Effect of mesocosm presence and species addition on minicore particle skewness (n = 6). Error bars are standard error. Treatment identity as in Figure 6.4.

There was a significant effect of sediment treatment on sediment particle kurtosis (L-ratio = 10.15, d.f. = 10, p = 0.0380). The minicore sediments were meso-kurtic, platy-kurtic or lepto-kurtic. Mesocosm addition (P; 2.49 ± 0.13) decreased the mean (± 95 % CI, n = 6) particle kurtosis compared to the natural sediments (Figure 6.13; N; 2.84 ± 0.21; t = -3.59, p = 0.0014), i.e. the particle sizes were more evenly distributed within the range of particle sizes, graphically this results in a flatter grain size curve. There was no effect of species addition on minicore particle kurtosis.

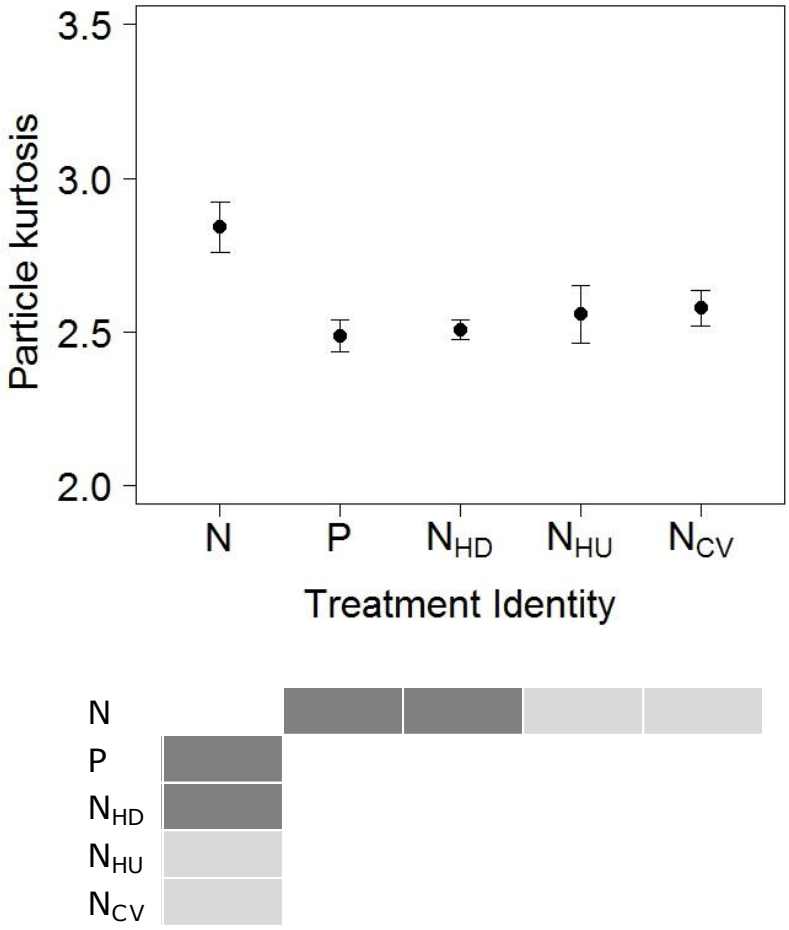

Figure 6.13 | Effect of mesocosm presence and species addition on minicore particle kurtosis (n = 6). Error bars are standard error. Treatment identity as in Figure 6.4. Significant differences are indicated in the accompanying table where darker shading indicates greater significant difference: 0.01 < p < 0.05; 0.0001 < p < 0.01; p < 0.0001.

Minicore particle D_{10} ranged between 7.56 and 12.40 µm for all treatments. There was no effect of mesocosm presence or species addition on minicore particle D_{10} (µm; Figure 6.14; L-ratio =2.42, d.f. = 10, p = 0.6587).

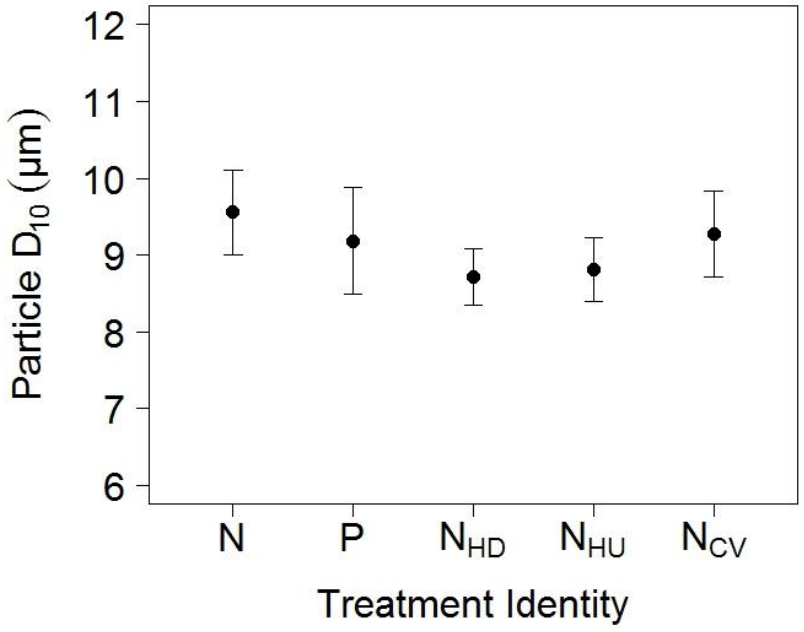

Figure 6.14 | Effect of mesocosm presence and species addition on minicore particle D_{10} (µm; n = 6). Error bars are standard error. Treatment identity as in Figure 6.4.

There was no effect of mesocosm presence or species addition on minicore mud content (%; Figure 6.15; L-ratio =1.20, d.f. = 10, p = 0.8775).

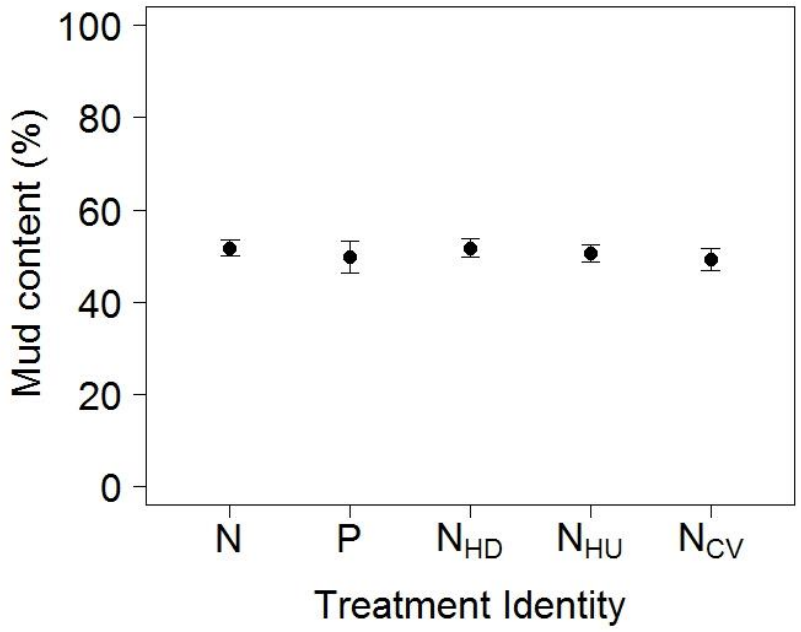

Figure 6.15 | Effect of mesocosm presence and species addition on minicore mud content (%; n = 6). Error bars are standard error. Treatment identity as in Figure 6.4.

6.3.5 | Contact core sediment properties

There was no effect of mesocosm presence or species addition on contact core water concentration (gcm^{-3}; Figure 6.16; L-ratio = 2.83, d.f. = 10, p = 0.5863).

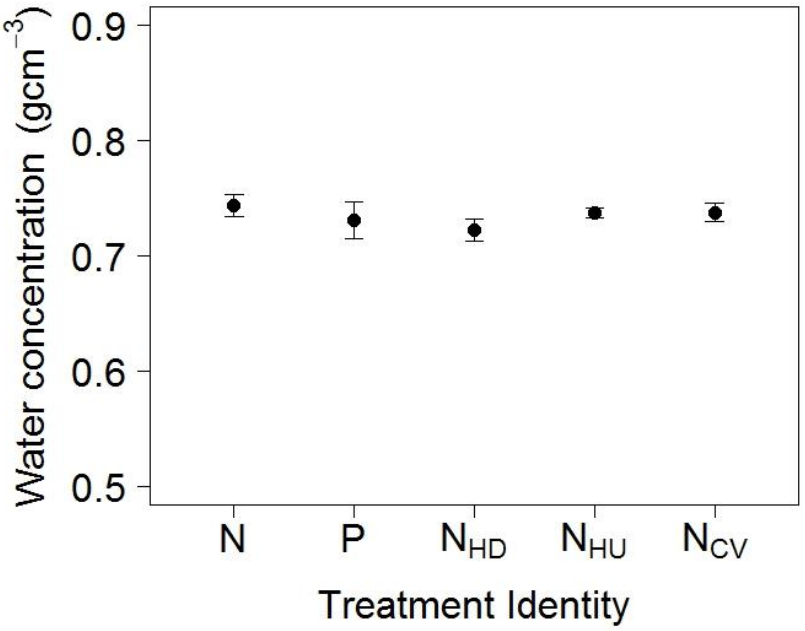

Figure 6.16 | Effect of mesocosm presence and species addition on contact core water concentration (gcm^{-3}; n = 6). Error bars are standard error. Treatment identity as in Figure 6.4.

There was a significant effect of sediment treatment on contact core colloidal carbohydrate concentration (μgcm^{-3}; L-ratio = 22.39, d.f. = 10, p < 0.0001). The procedural control had a larger mean (± 95 % CI, n = 6) contact core colloidal carbohydrate concentration (Figure 6.17; P; 685.37 ± 274.09 μgcm^{-3}) than the natural sediments (N; 310.49 ± 95.46 gcm^{-3}; t = 3.32, p = 0.0029). In addition to this, the treatment with *Hediste diversicolor* added had a larger mean (± 95 % CI, n = 6) colloidal carbohydrate concentration (N_{HD}; 875.95 ± 365.64 μgcm^{-3}) than the treatment with *Corophium volutator* added (N_{CV}; 482.15 ± 190.77 μgcm^{-3}; t = 2.45, p = 0.0217).

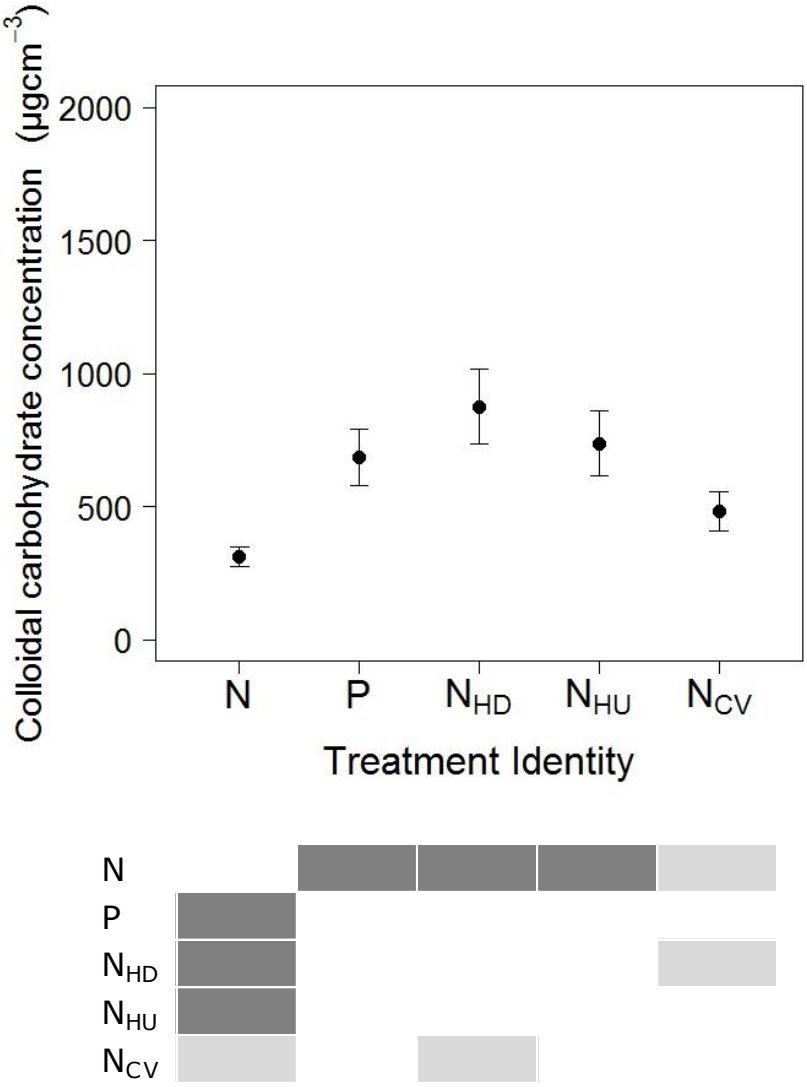

Figure 6.17 | Effect of mesocosm presence and species addition on contact core colloidal carbohydrate concentration (μgcm^{-3}; n = 6). Error bars are standard error. Treatment identity as in Figure 6.4. Significant differences are indicated in the accompanying table where darker shading indicates greater significant difference: ▒ 0.01 < p < 0.05; ▓ 0.0001 < p < 0.01; ■ p < 0.0001.

There was a significant effect of sediment treatment on contact core chlorophyll *a* concentration (gcm^{-3}; L-ratio = 32.85, d.f. = 10, $p < 0.0001$). The procedural control had a larger mean (± 95 % CI, n = 6) contact core chlorophyll *a* concentration (Figure 6.18; P; 20.81 ± 4.36 μgcm^{-3}) than the natural sediments (N; 12.64 ± 0.70 gcm^{-3}; t = 4.75, p = 0.0001). There was no effect of species addition on contact core chlorophyll *a* concentration.

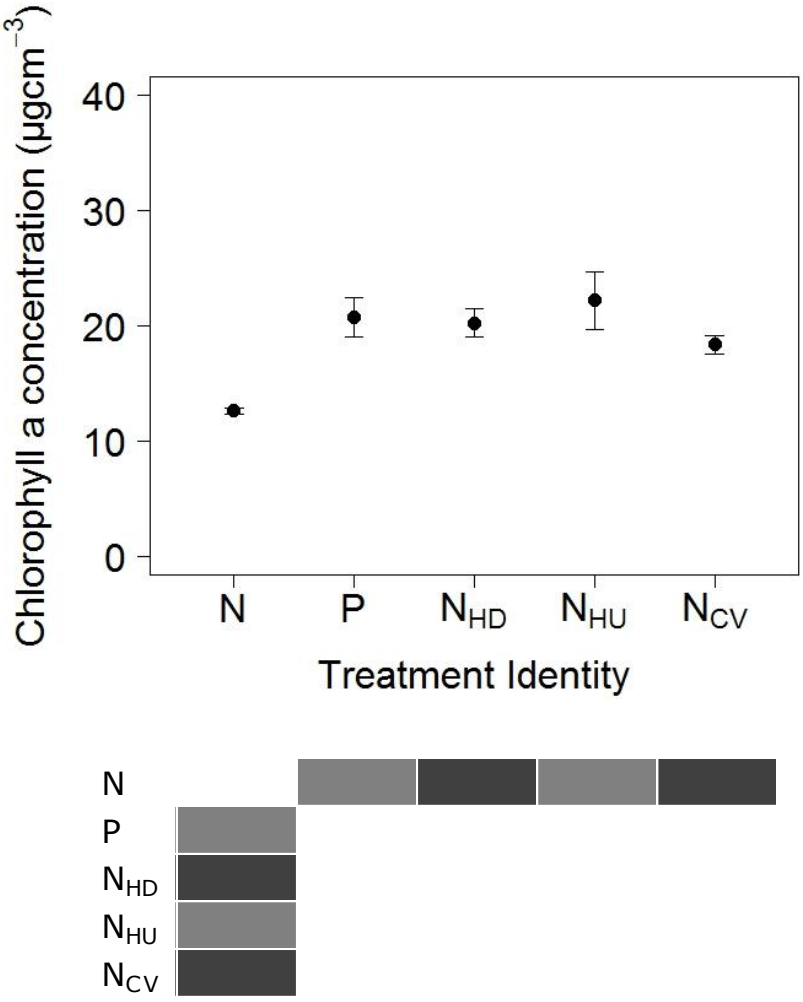

Figure 6.18 | Effect of mesocosm presence and species addition on contact core chlorophyll *a* concentration (μgcm^{-3}; n = 6). Error bars are standard error. Treatment identity as in Figure 6.4. Significant differences are indicated in the accompanying table where darker shading indicates greater significant difference: ▫ $0.01 < p < 0.05$; ▪ $0.0001 < p < 0.01$; ■ $p < 0.0001$.

There was a significant effect of sediment treatment on contact core chlorophyll *b* concentration (gcm^{-3}; L-ratio = 36.53, d.f. = 10, $p < 0.0001$). The procedural control had a larger mean (± 95 % CI, n = 6) contact core chlorophyll *b* concentration (Figure 6.19; P; 5.38 ± 1.35 μgcm^{-3}) than the natural sediments (N; 3.30 ± 0.13 gcm^{-3}; t = 3.93, p = 0.0006). There was no effect of species addition on contact core chlorophyll *b* concentration.

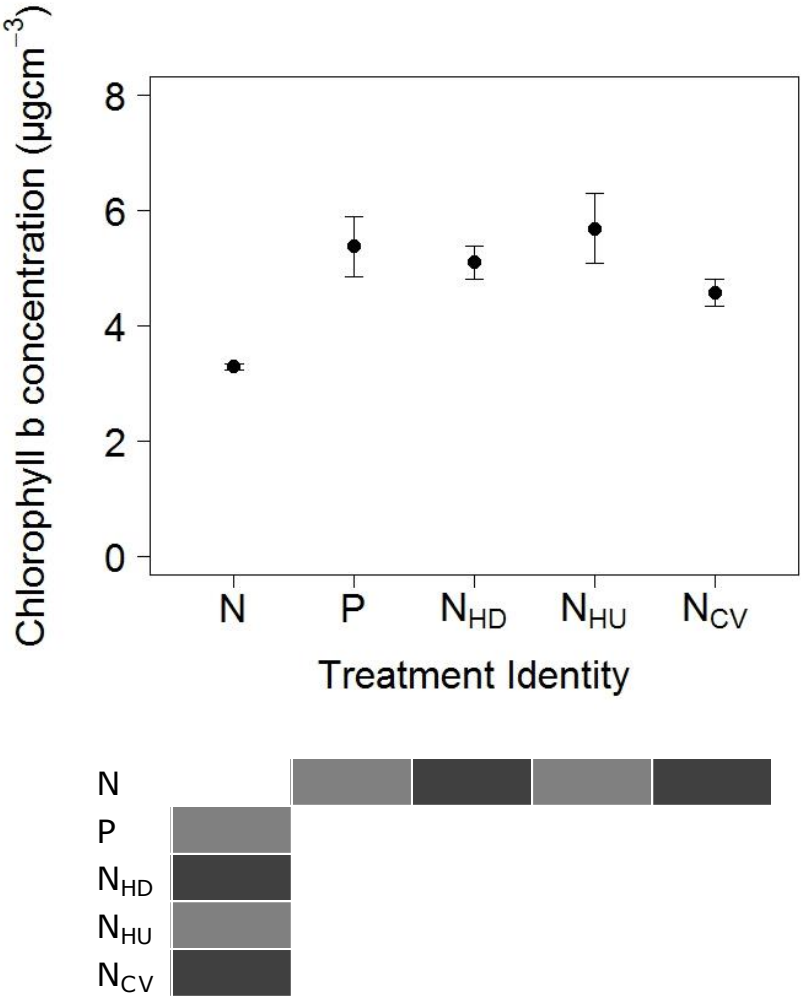

Figure 6.19 | Effect of mesocosm presence and species addition on contact core chlorophyll *b* concentration (μgcm^{-3}; n = 6). Error bars are standard error. Treatment identity as in Figure 6.4. Significant differences are indicated in the accompanying table where darker shading indicates greater significant difference: ▫ $0.01 < p < 0.05$; ▪ $0.0001 < p < 0.01$; ■ $p < 0.0001$.

The contact core sediments were classified as very coarse silt under the GRADISTAT program scale (Blott and Pye 2001). There was no effect of mesocosm presence or species addition on contact core mean particle size (μm; Figure 6.20; L-ratio = 9.40, d.f. = 10, p = 0.0518).

There was no effect of mesocosm presence or species addition on contact core particle size mode (μm; Figure 6.21; L-ratio = 1.93, d.f. = 10, p = 0.1388).

The contact core sediments were poorly sorted. There was a significant effect of sediment treatment on contact core particle sorting (L-ratio = 37.37, d.f. = 10, p < 0.0001). There was no effect of mesocosm presence on the mean (± 95 % CI, n = 6) contact core particle sorting (Figure 6.22; P; 2.58 ± 0.13) compared to the natural sediments (N; 2.65 ± 0.16; t = -0.93, p = 0.3601), however the treatment with *Corophium volutator* added (N_{CV}; 2.47 ± 0.03) had a lower mean (± 95 % CI, n = 6) particle sorting, i.e. was more well sorted, than the procedural control, mesocosm only treatment (P; t = -2.19, p = 0.0382).

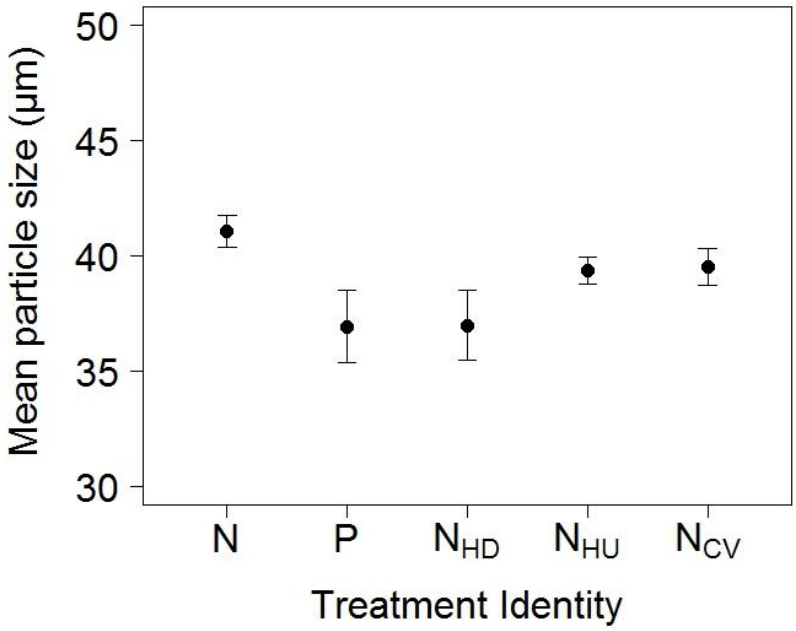

Figure 6.20 | Effect of mesocosm presence and species addition on contact core mean particle size (µm; n = 6). Error bars are standard error. Treatment identity as in Figure 6.4.

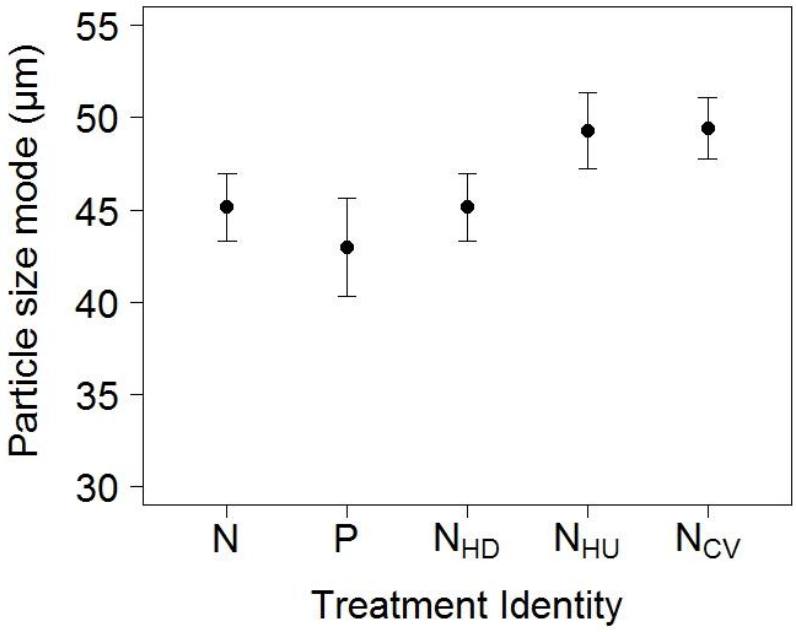

Figure 6.21 | Effect of mesocosm presence and species addition on contact core particle size mode (µm; n = 6). Error bars are standard error. Treatment identity as in Figure 6.4.

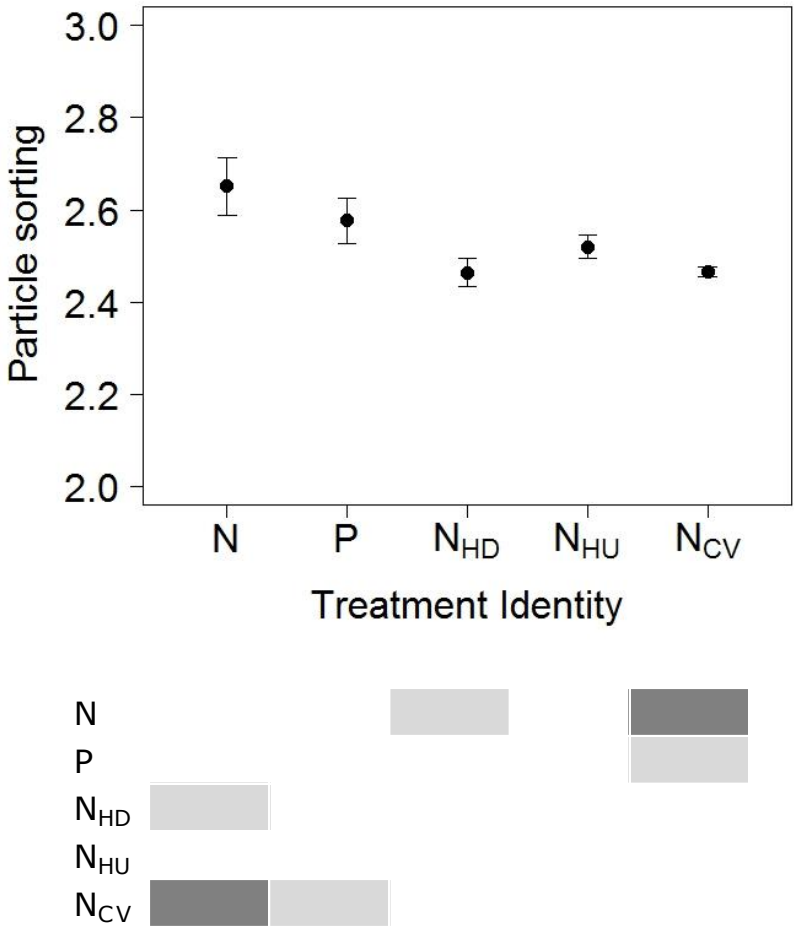

Figure 6.22 | Effect of mesocosm presence and species addition on contact core particle sorting (n = 6). Error bars are standard error. Treatment identity as in Figure 6.4. Significant differences are indicated in the accompanying table where darker shading indicates greater significant difference: 0.01 < p < 0.05; 0.0001 < p < 0.01; p < 0.0001.

The contact core sediments were finely skewed or symmetrical. There was a significant effect of sediment treatment on contact core particle distribution skewness (L-ratio = 13.86, d.f. = 10, p = 0.0077). There was no effect of mesocosm presence on the mean (± 95 % CI, n = 6) contact core particle skewness (Figure 6.23; P; -0.13 ± 0.21) compared to the natural sediments (N; 0.12 ± 0.25; t = -1.91, p = 0.0679), however the treatment with *Corophium volutator* added (N_{CV}; -0.34 ± 0.11) had a lower mean (± 95 % CI, n = 6) particle skewness, i.e. particle size was coarser, than the procedural control, mesocosm only treatment (P; t = -2.27, p = 0.0322).

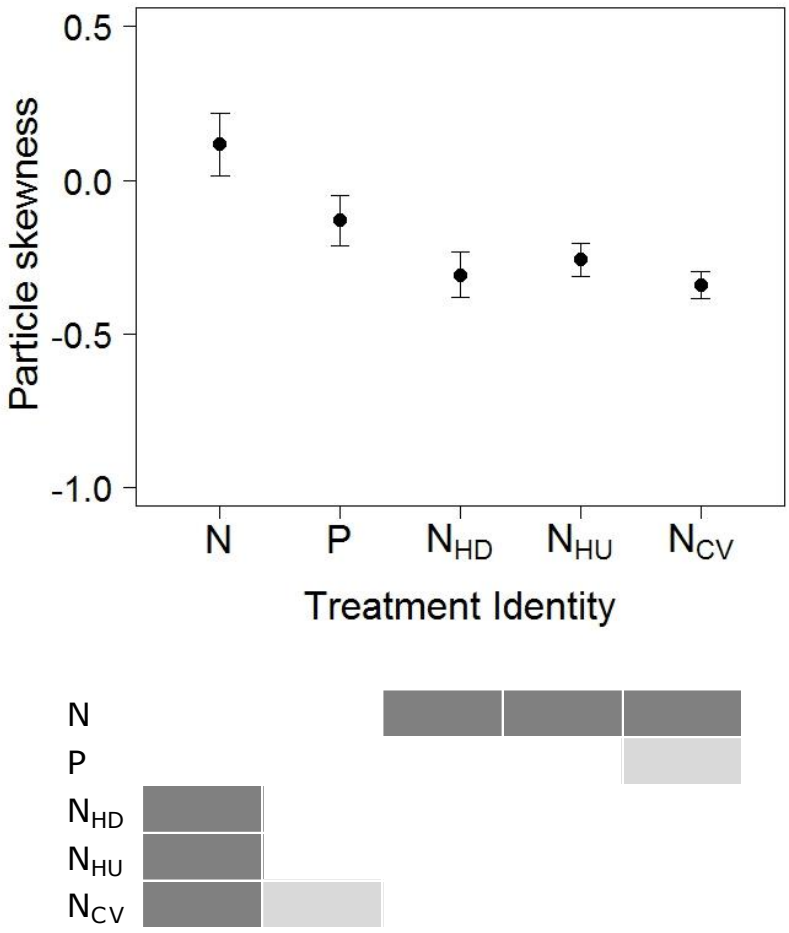

Figure 6.23 | Effect of mesocosm presence and species addition on contact core particle skewness (n = 6). Error bars are standard error. Treatment identity as in Figure 6.4. Significant differences are indicated in the accompanying table where darker shading indicates greater significant difference: 0.01 < p < 0.05; 0.0001 < p < 0.01; p < 0.0001.

The contact core sediments showed either meso-kurtosis or lepto-kurtosis. There was a significant effect of sediment treatment on contact core particle distribution kurtosis (L-ratio = 11.26, d.f. = 10, p = 0.0237). Mesocosm presence (P; 3.63 ± 0.40) caused a reduction in mean (± 95 % CI, n = 6) contact core particle kurtosis compared to that of the natural sediments (Figure 6.24; N; 4.10 ± 0.21; t = -2.67, p = 0.0135). Species addition had no effect on contact core particle kurtosis.

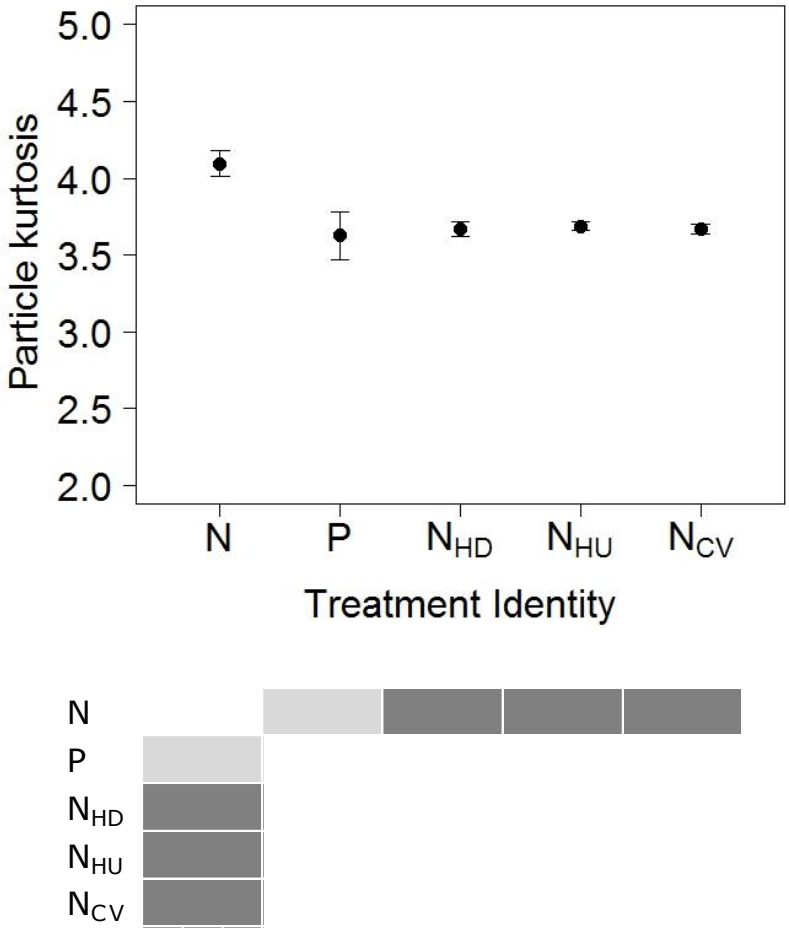

Figure 6.24 | Effect of mesocosm presence and species addition on contact core particle kurtosis (n = 6). Error bars are standard error. Treatment identity as in Figure 6.4. Significant differences are indicated in the accompanying table where darker shading indicates greater significant difference: 0.01 < p < 0.05; 0.0001 < p < 0.01; p < 0.0001.

There was a significant effect of sediment treatment on contact core particle D_{10} (µm; L-ratio = 9.88, d.f. = 10, p = 0.0425). Mesocosm presence (P; 10.89 ± 1.43 µm) caused a reduction in mean (± 95 % CI, n = 6) contact core particle D_{10} compared to the natural sediments (Figure 6.24; N; 12.54 ± 0.76 µm; t = -2.63, p = 0.0148). Species addition had no effect on contact core particle D_{10}.

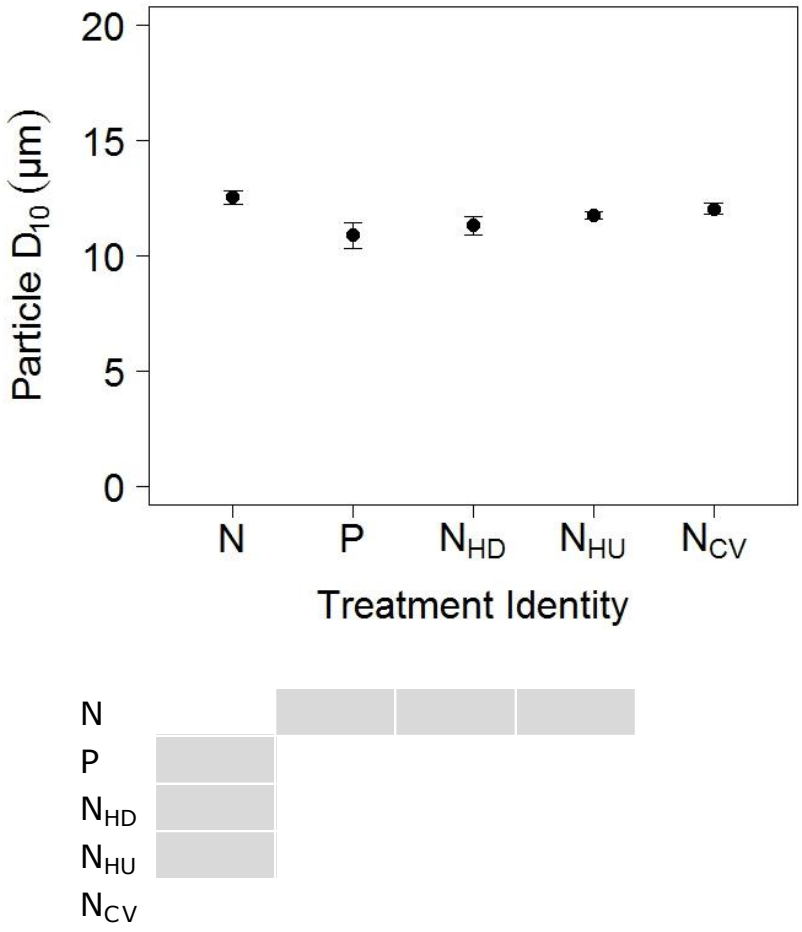

Figure 6.25 | Effect of mesocosm presence and species addition on contact core particle D_{10} (µm; n = 6). Error bars are standard error. Treatment identity as in Figure 6.4. Significant differences are indicated in the accompanying table where darker shading indicates greater significant difference: ▒ 0.01 < p < 0.05; ▓ 0.0001 < p < 0.01; ■ p < 0.0001.

Contact core mud content (%) was not affected by mesocosm presence or species addition (Figure 6.26; L-ratio = 4.27, d.f. = 10, p = 0.3703).

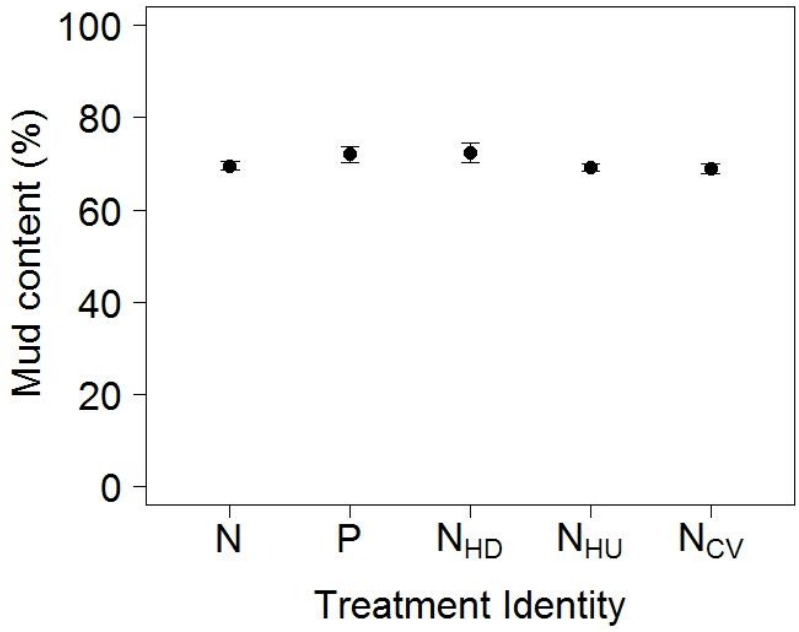

Figure 6.26 | Effect of mesocosm presence and species addition on contact core mud content (%; n = 6). Error bars are standard error. Treatment identity as in Figure 6.4.

In summary, the only significant effect of the three species compared to that of the procedural control treatments was a reduction in particle sorting and skewness in the treatments containing *Corophium volutator*.

6.3.6 | Species effects within a community

When examined using non-transgressive overyielding techniques, the treatments containing additional *Hediste diversicolor* (N_{HD}) had a smaller erosion threshold in natural sediment cores than would be expected based upon the effect of *Hediste diversicolor* observed in the single species dominated communities (Figure 6.27). Additionally, the suspension index is also higher than the expected value. This indicates that when in a community the action of *Hediste* on the sediment are more destabilising than would be expected.

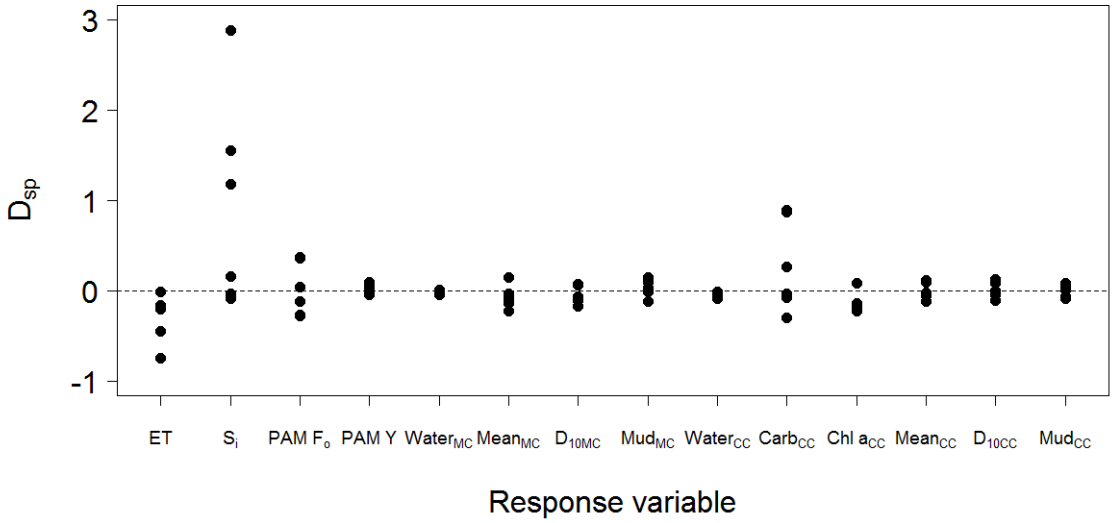

Figure 6.27 | Assessment of overyielding caused by *Hediste diversicolor* (n = 6). Where D_{sp} is negative, the values observed in the community with added *Hediste diversicolor* treatment are lower than would be expected and where D_{sp} is positive, the values are higher than would be expected compared to the effects of *Hediste diversicolor* in the single species dominated communities. (n = 6; ET = erosion threshold (Nm^{-2}), S_i = suspension index or relative erosion rate, PAM F_o = pulse amplitude modulation measured minimum fluorescence, PAM Y = pulse amplitude modulation measured maximum quantum yield, $Water_{MC}$ = minicore water content (%), $Mean_{MC}$ = minicore mean particle size (µm), D_{10MC} = minicore particle D_{10} (µm), Mud_{MC} = minicore mud content (%), $Water_{CC}$ = contact core water concentration (gcm^{-3}), $Carb_{CC}$ = contact core carbohydrate concentration (μgcm^{-3}), Chl a_{CC} = contact core chlorophyll *a* concentration (μgcm^{-3}), $Mean_{CC}$ = contact core mean particle size (µm), D_{10CC} = contact core particle D_{10} (µm), Mud_{CC} = contact core mud content (%).

The erosion threshold of the sediments containing a natural community to which *Hydrobia ulvae* (N_{HU}) had been added had a higher erosion threshold than expected, indicating that in a natural community, the sediment is more stable than expected (Figure 6.28). Additionally, the mean contact core sediment particle size and D_{10} is slightly larger than expected.

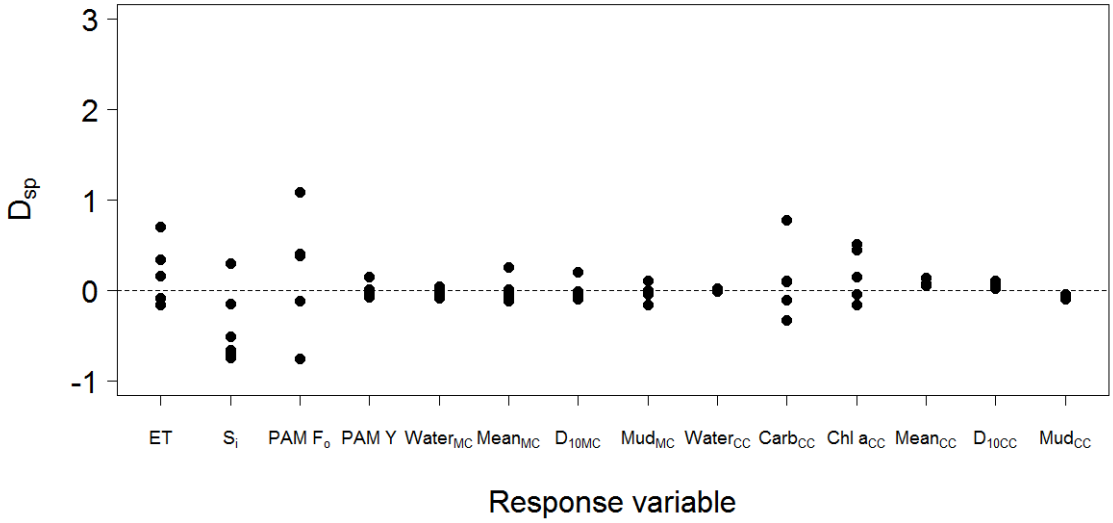

Figure 6.28 | Assessment of overyielding caused by *Hydrobia ulvae* (n = 6). Where D_{sp} is negative, the values observed in the community with added *Hydrobia ulvae* treatment are lower than would be expected and where D_{sp} is positive, the values are higher than would be expected compared to the effects of *Hydrobia ulvae* in the single species dominated communities. Response variables as in Figure 6.27.

The actions of *Corophium volutator* within a community are variable. On average the microphytobenthos minimum fluorescence and the surface sediment chlorophyll *a* concentration are lower than would be expected and the sediment mean particle size and D_{10} are slightly higher than would be expected (Figure 6.29).

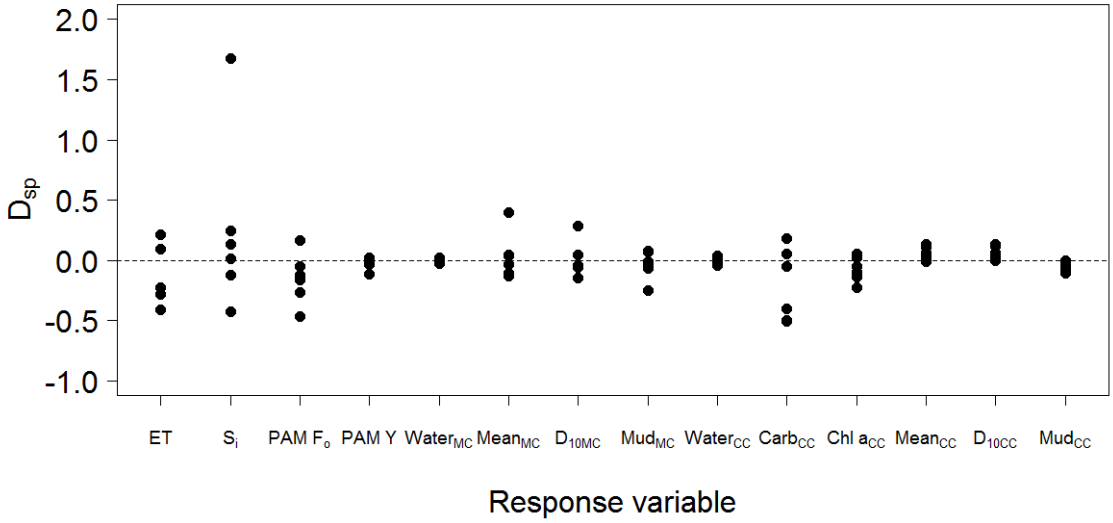

Figure 6.29 | Assessment of overyielding caused by *Corophium volutator* (n = 6). Where D_{sp} is negative, the values observed in the community with added *Corophium volutator* treatment are lower than would be expected and where D_{sp} is positive, the values are higher than would be expected compared to the effects of *Corophium volutator* in the single species dominated communities. Response variables as in Figure 6.27.

6.4 | Discussion

6.4.1 | Use of mesocosms in the field

The effect of the presence of the mesocosm was much greater in this experiment than it was in the pilot experiment and the experiments presented in Chapters 4 and 5. The placement of a mesocosm on the mudflat significantly affected many of the sediment properties measured. The procedural control treatment (P) had a significantly larger erosion threshold, microphytobenthos biomass, minicore water content, and contact core chlorophyll *a*, chlorophyll *b* and colloidal carbohydrate concentrations. The presence of the mesocosm also resulted in a significantly smaller suspension index and contact core particle D_{10}.

These effects are most likely caused by a decrease in species abundance (see Table 6.1) and an increase in the microphytobenthos biomass within the mesocosm. Similar changes in sediment properties have been seen in the laboratory (Tolhurst et al. 2008a) and the field when infaunal abundance is reduced and microphytobenthos biomass increases (Murphy and Tolhurst 2009). Such a large change in the above variables as a result of the placement of the mesocosm was unexpected and is a larger effect than any of the species effects observed in this experiment. It is possible that the use of a mesocosm for this experiment has masked any changes that might occur as a result of species addition. Before this experiment was started, pilot experiments were carried out adding extra species biomass to areas of the mudflat without mesocosms, but the mobility of the species of interest meant that when community cores were examined at the end of the experiments, species biomass levels had returned to that of the surrounding sediment. The use of a mesocosm was therefore determined to be the best method to enable addition of extra species biomass to a small area of mudflat and allow the experiment to be carried out *in situ*. Conducting experiments such as these *in situ* on the mudflat increases the relevance of the results to the natural world (Fridley 2001).

6.4.2 | Species addition effects

In comparison to the procedural control, the addition of an extra 50 % of the biomass of each species to an already diverse community, changing the species abundances and biomass distribution, did not significantly affect any of the parameters measured, indicating that the addition of extra species biomass to a community does not cumulatively add to the effect of the species on the mudflat. The addition of extra species, if not affected by the presence of the mesocosm, would be expected to cause changes in the sediment biogeochemical variables, based upon the data presented in Chapters 4 and 5. It is possible that the potential effects of the addition of extra species biomass are moderated by inter- and intra-specific interactions.

Such intra-specific effects have been observed in *Hydrobia ulvae*. This species has been shown to have reduced ingestion rate at high densities compared to low densities (Blanchard et al. 2000) and the closely related

species *Hydrobia ventrosa* and *Hydrobia totteni* were shown to move and feed less at higher densities (Levinton 1979). When *Hydrobia* is abundant, fecal excretions may enrich and fertilise diatom populations (Lopezfigueroa and Niell 1987, Plaganyi and Branch 2000), resulting in increased productivity and growth, buffering any effect of increased grazing on the F_o or chlorophyll concentrations. *Corophium* and *Hediste* have been found to have a strong inter-specific interaction. High densities of *Hediste diversicolor* were shown to reduce the density of *Corophium volutator* through physical disturbance (Olafsson and Persson 1986). Any effects on sediment variables seen in mesocosms to which *Hediste diversicolor* has been added may therefore be as a direct result of the addition of *Hediste* or the indirect result of the disturbance of *Corophium*.

6.4.3 | Species effects in single species dominated communities and within a natural community

The possible interactive effects outlined above were examined in more detail by comparing the effects of the three species observed in single species dominated communities in Chapter 4 to the effects of the species when added into an already established community using non-transgressive overyielding (Section 6.3.6). *Hediste diversicolor*, while not particularly stabilising or destabilising when dominant (see Section 4.3.2) appears to destabilise the sediments more than expected when there is an overabundance of the species in a natural community. At high densities, the burrowing activity of *Hediste diversicolor* has been shown to increase (Olafsson and Persson 1986), perhaps due to more competition for grazing, space, and other resources, requiring them to be more active grazers or hunters. In a natural community there may also be more prey available (i.e. the rest of the community, particularly meiofauna, has not been removed by defaunation) and the worms may be more actively hunting and therefore move on and within the sediment more. In addition to this, at high densities, *Hediste* have been shown to modify the shape and size of their burrows, to maintain adequate irrigation, enhancing the instability of the sediment at high worm and burrow densities (Luckenbach 1986, de Deckere et al. 2001). In a natural community, this increased *Hediste* burrow density is also combined with *Corophium* burrows and *Hydrobia* bioturbation. The resulting increase in food

seeking, burrow maintenance and consequent ventilation and irrigation results in more intensive sediment reworking occurring at high *Hediste diversicolor* abundances (Duport et al. 2006), perhaps leading to the greater sediment instability and larger sediment erosion rates observed in this experiment. The combative nature of *Hediste diversicolor* and their ability to defend their own territory results in an increase in aggressive behaviour at high species densities (Miron et al. 1992), which again may result in destabilisation of the sediment through increased movement and sediment disturbance during aggressive interactions between *Hediste* individuals.

Conversely, when there is an overabundance of *Hydrobia*, a species that has been shown to destabilise sediment significantly in the laboratory (Blanchard et al. 1997), in the field (Austen et al. 1999, Andersen 2001), and in the experiment presented in Chapter 4, the sediment is actually more stable than expected. Levinton (1979, 1985) noted that the closely related snails *Hydrobia ventrosa* and *Hydrobia totteni* reduced their feeding and crawling rates at high densities (above 1 snail per cm^2) and Barnes (2005) noted that *Hydrobia acuta* and *Hydrobia ventrosa* (although not *Hydrobia ulvae*) displayed intra-specific reduction in egestion at high densities (measured by the production of faecal pellets), an activity that has been shown to contribute to sediment destabilisation and reduced erosion threshold (Andersen 2001).

6.4.4 | Experimental limitations

The sediment properties measured in this experiment were all affected by the use of a mesocosm. This not only may have caused the changes observed but may also have affected the behaviour and interactions of the species of interest due to increased microphytobenthos biomass. The inclusion of a mesocosm only treatment ensured that the changes observed could be compared to a procedural control.

6.4.5 | Future work

Future work should consider repeating the experiment using a method that either does not require the use of a mesocosm or uses a mesocosm that

causes less of an effect on sediment properties. The effect of macrofaunal species density within mudflat communities on sediment properties should be further investigated using natural community observations or realistic species abundance manipulations based on future scenarios of climate change and species extinctions.

6.4.6 | Chapter conclusions

1 | Sediment stability, microphytobenthos biomass and productivity, and the physical characteristics of the mudflat appear robust to changes in species biomass distribution and abundance manipulated by species addition.

2 | In a natural community, the sediment erosion threshold appears to fluctuate more in response to changes in microphytobenthos biomass caused by the presence of the mesocosm, than changes in macrofaunal species abundance.

3 | When making predictions about whether macrofaunal species fluctuations will affect mudflats the effect of changes in individual species abundance in monoculture or when dominant cannot predict their effects in a community. Behavioural and activity modifications, as a result of inter- and intra-specific interactions, are perhaps more important than previously thought with respect to the effect of the species on sediment erosion, microphytobenthos biomass and productivity, and physical characteristics.

Chapter 7 | Effects of Single Species and Species Combinations on Bioturbation and Bioirrigation

7.1 | Introduction

This chapter investigates in greater detail the bioturbatory actions of the three species of interest: *Hediste diversicolor*, *Hydrobia ulvae* and *Corophium volutator*. The behaviours of these species were investigated using fluorescent sediment profile imaging (f-SPI), three-dimensional imaging analysis using computed tomography, and bioirrigation analysis using sodium bromide inoculation. This chapter examines the bioturbatory actions of the three species on the sediment to quantify the burrow structures created. This information can then be combined with that of the experiments in Chapters 4, 5 and 6 to determine the mechanisms of sediment destabilisation and address Objectives 1 and 3 in a laboratory and Objective 6 presented in Section 1.7:

Objective 1 | Investigate the effect of individual macrofauna species on mudflat sediment stability and biogeochemical properties.

Objective 3 | Investigate the effect of macrofaunal species richness on mudflat sediment stability and biogeochemical properties.

Objective 6 | Visualise the effect of *Hediste diversicolor*, *Hydrobia ulvae* and *Corophium volutator* on sediment particle mixing.

7.1.1 | Rationale

Intertidal sediment provides a three dimensional habitat for a wide range of organisms, including polychaetes, crustaceans and molluscs; to burrow, build permanent and semi-permanent tube structures and rework the sediment surface (Dufour et al. 2005). These biogenic structures are a record of the organismal activity within the sediment but are also important structures in themselves, which can have significant effects on sediment processes. Bioturbation has also been shown to be a key mechanism in

determining sediment stability (Rhoads and Young 1970, Rowe 1974, Meadows and Tait 1989, Grant and Daborn 1994, Mouritsen et al. 1998, Palomo and Iribarne 2000, de Deckere et al. 2001, Sgro et al. 2005, Widdows et al. 2009) and regulating ecosystem function in the marine benthos (Ieno et al. 2006, Solan et al. 2008). Widdows et al. (2009) showed that burrowing by *Hediste diversicolor* destabilised bed sediment, increasing sediment erodibility, and de Deckere et al. (2001) suggested that stabilisation of sediments after addition of formalin (which killed the infauna) was due to a reduction in bioturbation. It is hypothesised that the evolution of bioturbatory metazoans resulted in the transition of the sediment –water interface from a distinct and biogeochemically impermeable boundary to a diffuse layer more habitable to life (Seilacher and Pfluger 1994), leading to further evolution and macrofaunal succession (Bottjer et al. 2000, Dornbos et al. 2005, Solan et al. 2008, Bottjer 2010). Modern biogenic structures also provide surfaces for re-oxidation of subsurface sediment, biochemical activity and nutrient exchange, affecting the surrounding fauna (Rhoads et al. 1978a, Commito 1982, Flint and Kalke 1986, Tamaki 1988, Posey et al. 1991, Widdicombe et al. 2004) and microbial communities (Reise 1983, Alongi 1985, Austen and Widdicombe 1998).

Despite the importance of bioturbation, the architecture of biogenic structures has been historically difficult to visualise and quantify (Gerino and Stora 1991), meaning the most important surface area available for biogeochemical activity and nutrient exchange within the sediment is invisible to the researchers studying it. Resin or plaster casts can provide a low resolution and low definition method (Lee and Koh 1994, Dufour et al. 2005, Widdicombe and Needham 2007) to examine the length and shape of near surface burrows, but this is limited in the topography of the burrow it can show. For example, burrows with a high degree of complexity may not be accurately reflected in the cast produced and burrows that consist of small passages may clog with casting material preventing visualisation of the whole network.

By using fluorescent sediment profile imagery (f-SPI) two dimensional information on biogenic particle mixing can be obtained by photographing the activity on the edge of the sediment, either the sediment surface (Rhoads

and Cande 1971, Nilsson and Rosenberg 1997, Diaz and Cutter 2001) or the transparent wall of an aquarium (Solan et al. 2004b). Particle field optical holography (either in-line or off-axis) can be used to visualise sediments in three dimensions (Black et al. 2001), but this is limited by the penetration of the laser. These limitations make these methods unsuitable for visualising burrows in a whole sediment core accurately and completely.

X-ray Computed tomography (X-CT) offers a way of visualising the structure of a whole sediment core in three dimensions. X-CT was first used as a tool to visualise single slices of the human body and the first commercially viable scanner was introduced in 1971. Its uses have expanded rapidly and it is now regularly used in the environmental sciences. X-CT was used on modern biogenic structures in a non-destructive way to examine the underground architectural properties of earthworm burrows (Joschko et al. 1991, Daniel et al. 1997). Perez et al. (1999) used X-CT to examine biogenic structures in marine sediment to determine the percentage of tube and tunnel area of marine organisms along a pollution gradient, demonstrating the ease with which this novel technology could be applied to a new field. Since then this technique has been used to examine different aspects of organismal burrowing, such as burrow length, burrow width, burrow depth, burrow volume (Rosenberg et al. 2008, Hartmann 2011), and the vertical distribution of biogenic structures (Mermillod-Blondin et al. 2003), which can be easily determined from a three dimensional X-CT scan. Michaud et al. (2003) used the technique to examine recolonisation and the rapid formation of biogenic structures after a deposition event.

In this study, the combined techniques of f-SPI, bio-irrigation analysis and micro-focus X-CT were used to allow a holistic approach to examining the effects of community species composition on organismal sediment reworking activities.

7.2 | Materials and methods

7.2.1 | Sediment treatment and macrofauna collection

Sediment and macrofauna were collected from Breydon Water on the 26th of October 2012 and returned to the Biodiversity and Ecosystem Futures Facility at the National Oceanography Centre, Southampton, UK. Sediment was sieved (500 µm mesh) in a seawater (sand filtered, UV sterilized, salinity 33) bath to remove macrofauna, allowed to settle for 48 h to retain the fine fraction (less than 63 µm) and homogenized.

7.2.2 | Experimental design

Two different types of clear perspex core, circular and square, were used for different experimental analyses. The square cores (internal dimensions 8.86 × 8.86 cm, 15.0 cm tall, n = 20) were used for bioturbation analysis using f-SPI because this can only be done on cores with flat sides. The circular cores (internal diameter = 10.0 cm, 15.0 cm tall, n = 20) were required to facilitate rotational quantification of biogenic structures using 3-dimensional X-CT imaging because the circular shape prevents distortion in the resulting X-CT images. Bioirrigation analysis was done on both core types. When filled to the same height, both core types contain the same volume of sediment (1178 m^2). The cores were filled to approximately 8 cm depth with homogenised sediment and topped up to 14cm with seawater, taking care not to disturb the sediment surface. Overlying seawater was replaced after 24 hours to remove excess nutrients associated with core assembly. Cores were maintained at 12 ± 0.1°C under a 12:12h light cycle (Aqualine T5 Reef White 10 K fluorescent light tubes, Aqua Medic) and were continuously aerated.

Organisms were kept in aerated seawater until addition to the cores after 48 hours. Organisms were added to the cores on the 31st of October 2012. Replicate (n = 5) invertebrate communities (biomass fixed at 1g per core, equivalent to 127 g per m^2) were assembled in monoculture (*Hediste diversicolor*, HD; *Hydrobia ulvae*, HU; or *Corophium volutator*, CV) and in a mixture (Mix) of all three species in each of the two types of core (Figure 7.1).

Figure 7.2 shows the experimental setup in the Biodiversity and Ecosystem Futures Facility at the National Oceanography Centre.

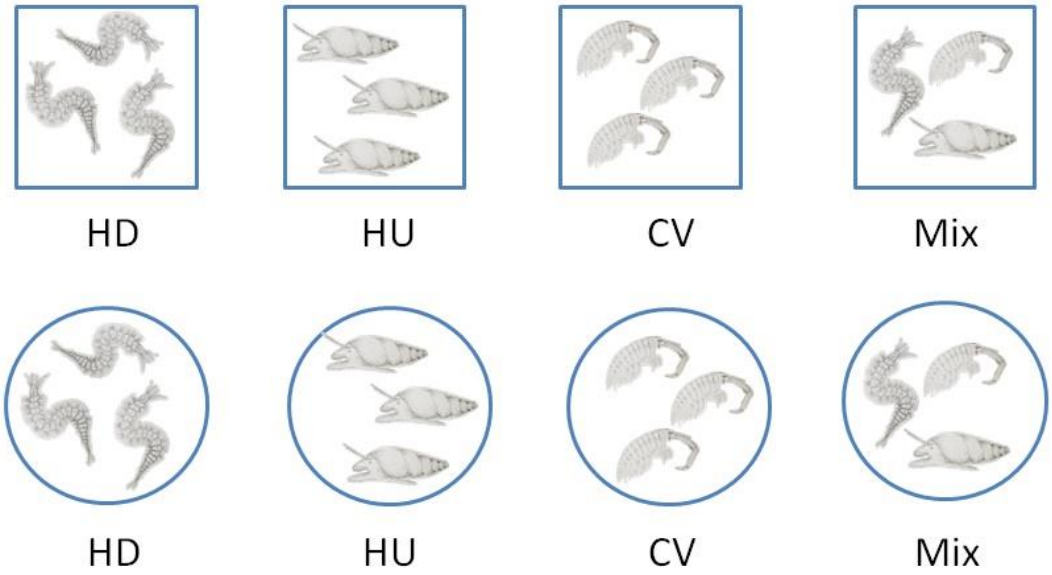

Figure 7.1 | The eight experimental treatments represented visually, showing the circular and square cores. Each diagrammatic organism represents 1/3 of the total core biomass. HD, both circular and square, contain 1 g of biomass consisting of *Hediste diversicolor*, HU, both circular and square, contain 1 g of biomass consisting of *Hydrobia ulvae*, CV, both circular and square, contain 1 g of biomass consisting of *Corophium volutator*, Mix, both circular and square, contain 1 g of biomass consisting of an equal mix of *Hediste diversicolor*, *Hydrobia ulvae* and *Corophium volutator*.

Figure 7.2 | The sediment cores in the Biodiversity and Ecosystem Futures Facility at the National Oceanography Centre, Southampton.

7.2.3 | Bioturbation analysis

To visualise particle movement and quantify bioturbation 15 g per core dry weight of luminophore tracers (pink colour that fluoresces under ultraviolet light, size class ≤125 µm; Brian Clegg Ltd., UK) were added to the square cores along the edges, ensuring 2-3 mm depth, 24 hours after adding the macrofauna (Figure 7.3) (Mahaut and Graf, 1987, Solan et al., 2004). The luminophores were pre-soaked 48 hours prior to distribution and vigorously shaken to prevent particle aggregation and flotation during application.

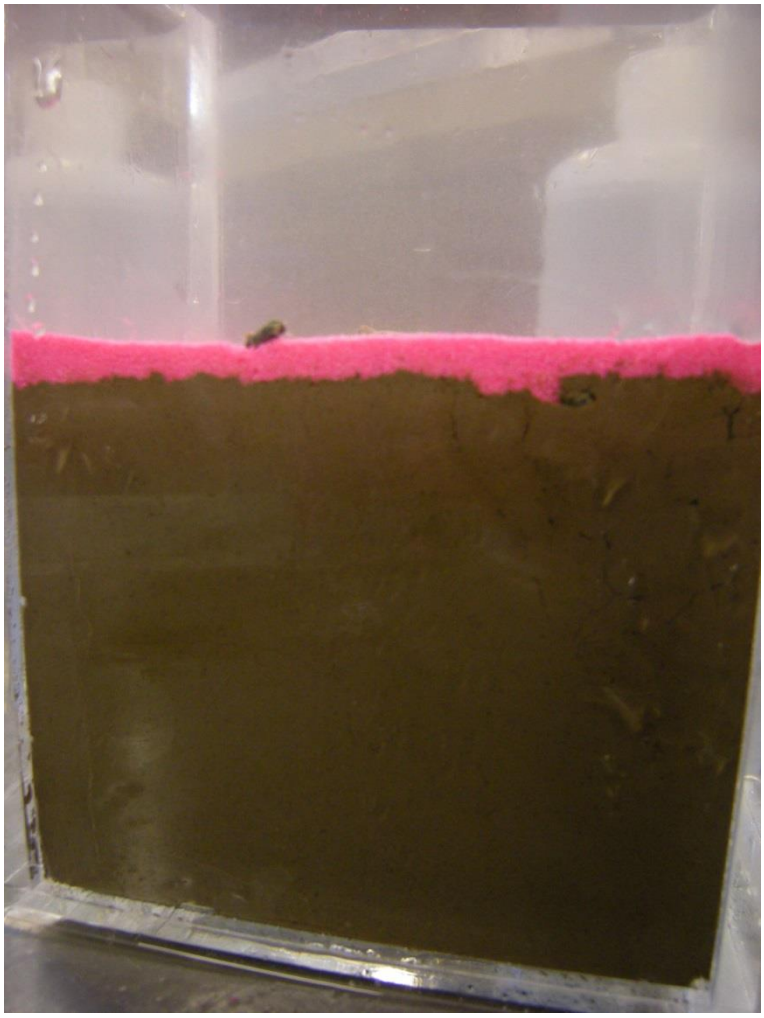

Figure 7.3 | Side view of a sediment core immediately after addition of luminophore tracers.

Six days after organism addition, faunal mediated sediment particle reworking in the square cores was estimated non-invasively using a sediment profile imaging camera (Canon 400D set to ISO 400, 10 second exposure, aperture f5.6; image size 3888 × 2592 pixels, i.e. 10.1 megapixels effective

resolution 56 × 56 µm per pixel). The camera was optically modified to allow preferential imaging of fluorescently labelled sand-based particulate tracers under UV light (f-SPI, Solan et al., 2004). Images of all four sides of each core were taken in a UV illuminated imaging box (Schiffers et al. 2011). The redistribution of the tracers was determined from stitched composite images (RGB colour, JPEG compression) using a custom-made semi-automated macro that runs within ImageJ (Version 1.47), a java-based public domain computer program developed at the US National Institutes of Health (available at http://rsb.info.nih.gov/ij/index.html). The macro returns a binary value depending on whether luminophores are present at each pixel (value = 1) or absent (value = 0) using the sediment water interface as the uppermost row. From these data, the total luminophores in each row are summed to obtain the vertical mixing profile. The median ($^{f\text{-}SPI}L_{med}$, typical short-term depth of mixing), maximum ($^{f\text{-}SPI}L_{max}$, maximum extent of mixing over the long-term), and mean ($^{f\text{-}SPI}L_{mean}$, time dependent indication of mixing) mixed depth of particle redistribution can then be calculated from this profile. In addition, the maximum vertical deviation of the sediment-water interface (upper – lower limit = surface boundary roughness, SBR) provided an indication of surficial activity.

7.2.4 | Burrow quantification using computed tomography

Quantification of biogenic structures in the circular cores was achieved using an X-ray computed tomography (X-CT) scanner housed within the µ-VIS imaging centre, University of Southampton. The CT suite at the University of Southampton consists of Nikon/Metris custom designed 20-225 kV and 100-450 kV x-ray sources capable of resolutions of approximately 3 µm at low kV and 50 µm at 450 kV with panel and line detectors, a panel shift system, with 1 m by 1 m by 1.5 m imaging volume taking weights of up to 100 kg in a temperature controlled environment. Batches of 5 cores were stacked and secured in a custom-made holding brace to ensure stability during scanning (Figure 7.4). The x-ray tube and detector array are installed on a gantry surrounding the scanning platform. During each acquisition, the cores were rotated through 360° whilst collecting 3142 projections averaging over 8 frames per 250 ms projection. X-ray conditions were set to 300 kV and 326 µA with a 3 mm Cu filter, and an XRD 1621 CN3 H5 PerkinElmer flat

panel detector was used to collect the images. The detector receives the x-ray photons after they have passed through the material and the images produced consist of pixels in greyscale relating to the x-ray attenuation. The variation in this attenuation is largely dependent on bulk density (Wellington and Vinegar 1987) and therefore the image that is produced can be interpreted using pixel brightness, with brighter pixels representing denser material and darker pixels representing less dense material. For our sediment cores, the sediment appeared lighter while any burrows appeared slightly darker. The x-ray takes raw image slices which can be stacked sequentially and reconstructed in three dimensions (3D) using 3D pixels called voxels. Scans produced 2000 slices with image size of 2000 by 2000 by 2000 voxels and an image resolution of 81 μm.

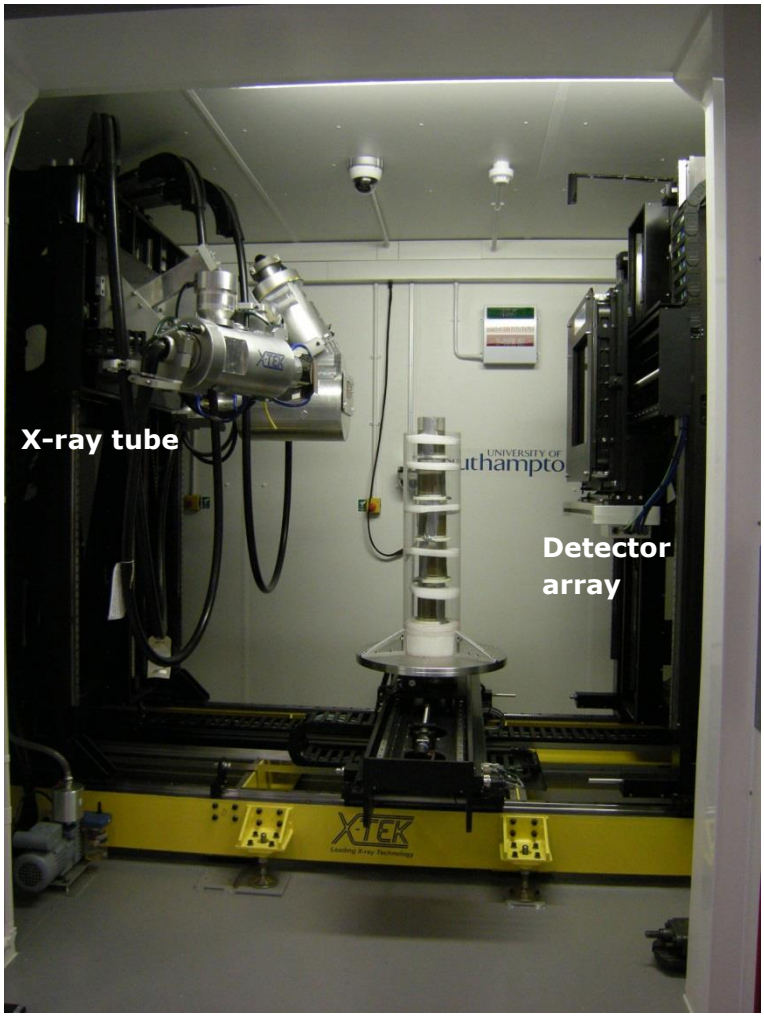

Figure 7.4 | The circular cores in the holding apparatus showing the x-ray tube (left) and the detector array (right).

The CT images were processed with four different software packages. CTPro3D (Version XT 2.2 service pack 10, MetrisNikon Metrology, UK) was used to determine the centre of rotation and reduce the beam hardening effect to produce a stack of 2 dimensional images. CTAgent (Version XT 2.2 service pack 10, Nikon Metrology, UK) was then used to reconstruct the images to enable them to be opened as a three dimensional image. Images were then converted from 32 bit '.vol' images to 8 bit '.raw' images to reduce processing time with minimal loss of image resolution using FIJI (Schindelin et al. 2012) reducing file size and computational loading. These images could then be opened as a 3D project in VGStudio (Version 2.1, Volume Graphics GmbH, Germany) enabling a three dimensional image to be produced using image segmentation. The noise in the 3D images was reduced using a median filter (Figure 7.5) to assist with edge detection in the final images. From these data, regions of interest were segmented using a threshold based seed point growing algorithm from which the burrow surface area ($^{CT}B_{SA}$, an important determinant of microbial-mediated biogeochemical cycling), volume ($^{CT}B_{vol}$, an indication of the extent of bioengineering and bioirrigation) and maximum depth of any biogenic features ($^{CT}B_{max}$) were calculated.

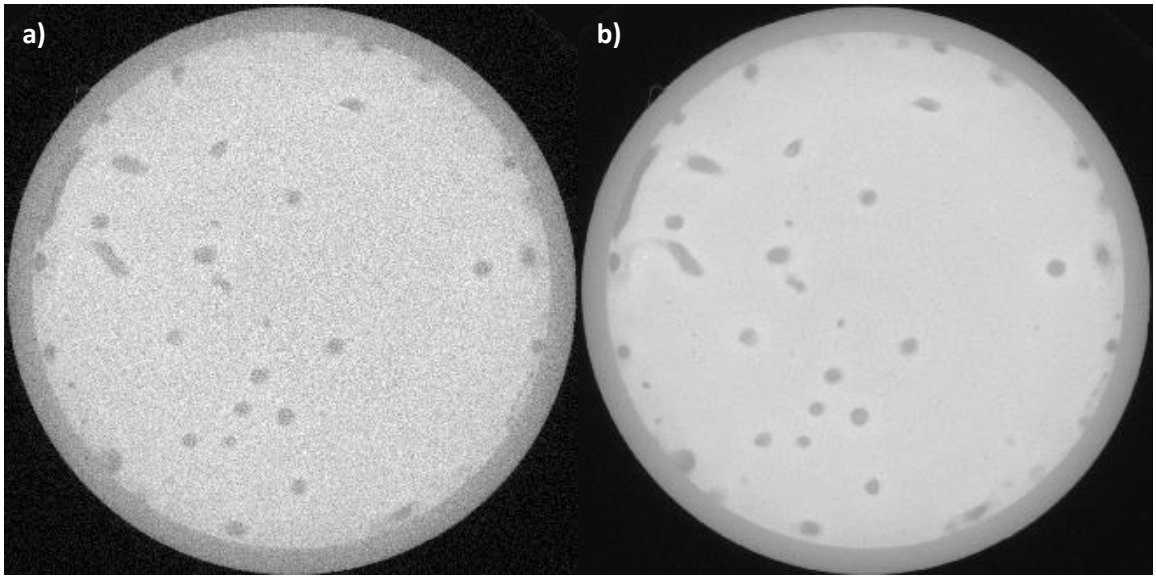

Figure 7.5 | Sediment core containing *Hediste diversicolor* burrows before (a) and after (b) median filter processing.

7.2.5 | Bioirrigation

Seven days after species addition, to determine the species and mixture bioirrigation rates, the circular and square cores were inoculated with 0.465g of sodium bromide dissolved in 6 ml of seawater to increase the Br^- concentration to approximately 0.66 gl^{-1} in the overlying water. Cores were incubated for 8 hours. The samples were analysed for the change in Br^- concentration ($\Delta[Br^-]$, mgl^{-1}) using a Tecator flow injection auto-analyser (FIA Star 5010 series).

7.2.6 | Data analysis

Data were analysed using a generalised least squares approach and models were developed for the dependent variables (${}^{f\text{-}SPI}L_{med}$, ${}^{f\text{-}SPI}L_{max}$, ${}^{f\text{-}SPI}L_{mean}$, SBR, ${}^{CT}B_{SA}$, ${}^{CT}B_{vol}$, ${}^{CT}B_{max}$, ($\Delta[Br^-]$) as described in Section 2.7, to compare the single and mixed species treatments. The independent nominal variable was species identity (SPID) or, for bioirrigation, the nominal variables SPID and core shape (square versus circular). All initial and final models used are presented in Appendix 5. To assess whether there were any effects of species interactions on the dependent variables the principles of transgressive and non-transgressive overyielding were used (Loreau 1998, Fridley 2001, Petchey 2003, Griffin et al. 2009). To determine if there was transgressive overyielding, the maximum performance of the species in monoculture ($V_{maximum\ in\ monoculture}$) was compared to the performance of the species in mixture (V_{mix}) using D_{max} (Loreau, 1998; Equation 7.1). Overyielding ($D_{max} > 0$) occurs when a mixture outperforms the corresponding monocultures.

Equation 7.1 $$D_{max} = \frac{V_{mix} - V_{maximum\ in\ monoculture}}{V_{maximum\ in\ monoculture}}$$

Non-transgressive overyielding techniques were used to determine whether the mixed species treatments had a greater effect on the variables than the species in monoculture in an additive model. These effects of the species in monoculture were summed and divided by three to produce an expected mixed species effect ('$V_{mix}(E)$'). This was compared to the observed

effect in the mixed species treatment ('$V_{mix}(O)$') using Equation 7.2. Again, overyielding ($D_T > 0$) occurs when a mixture outperforms the additive model mixture.

Equation 7.2 $$D_T = \frac{V_{mix}(O) - V_{mix}(E)}{V_{mix}(E)}$$

7.3 | Results

7.3.1 | Bioturbation

Figure 7.6 – 7.9 show the images for each species and the species mixture used to determine the sediment particle reworking profiles. These images show the luminophores (red) on the sediment surface and some burrows and sediment reworking can be seen. There was little intra-specific variation between replicates but a noticeable visual difference between cores containing different species.

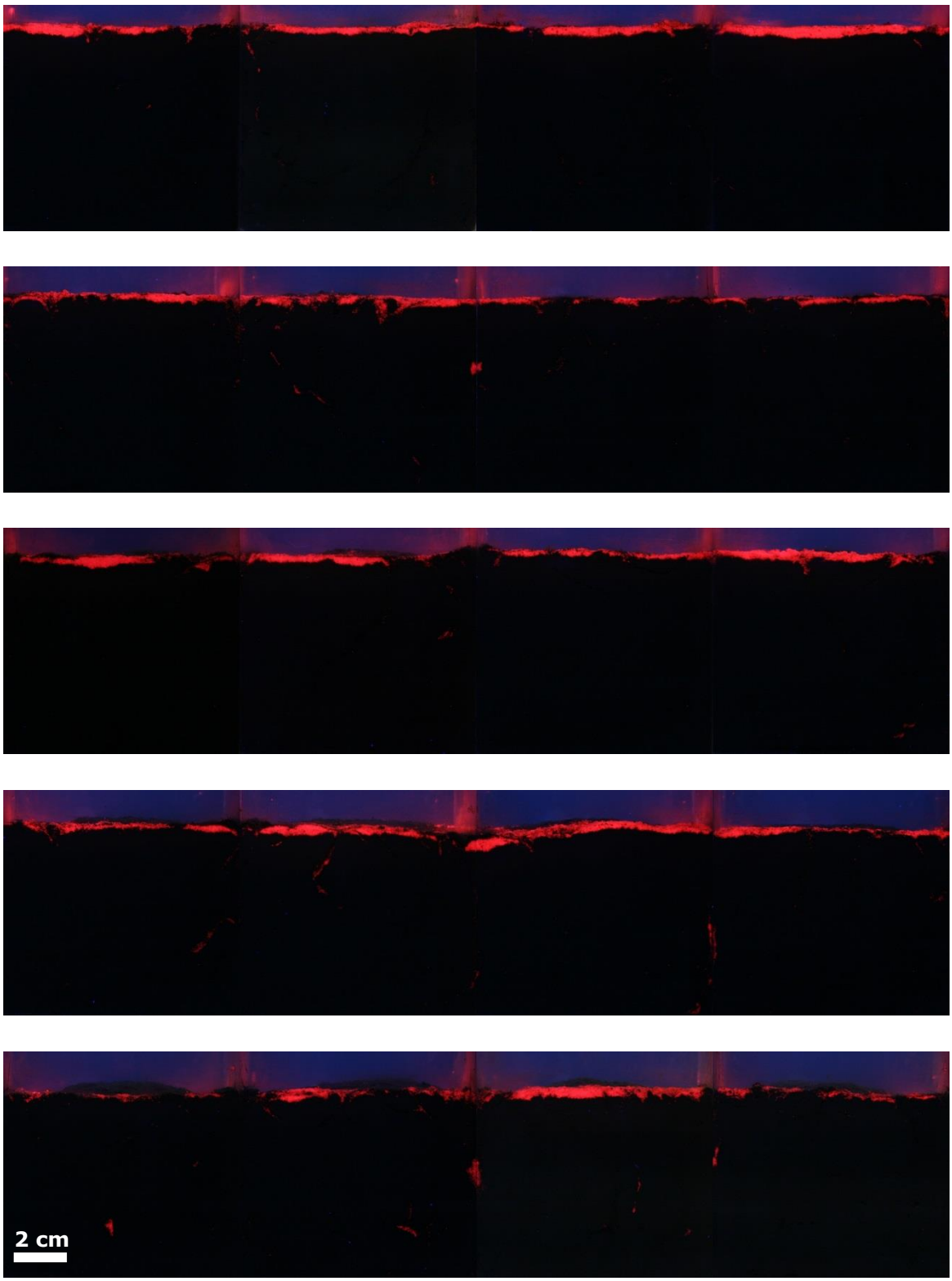

Figure 7.6 | Replicate (n=5) f-SPI images for *Hediste diversicolor*. Note that the light given off by the lumniophores is being reflected by the sealant used to keep the corners of the cores watertight.

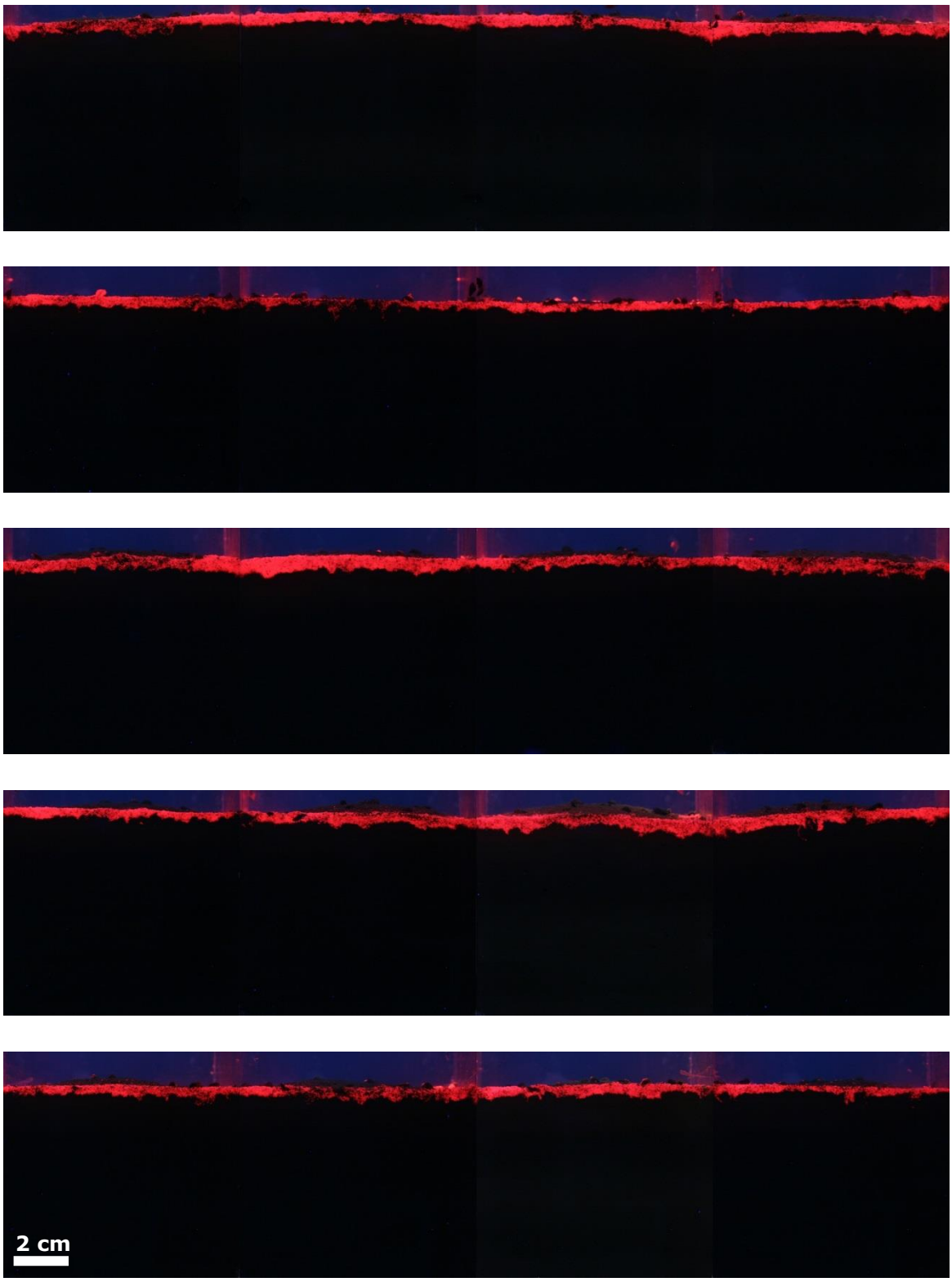

Figure 7.7 | Replicate (n=5) f-SPI images for *Hydrobia ulvae*. Note that the light given off by the lumniophores is being reflected by the sealant used to keep the corners of the cores watertight.

Figure 7.8 | Replicate (n=5) f-SPI images for *Corophium volutator*.

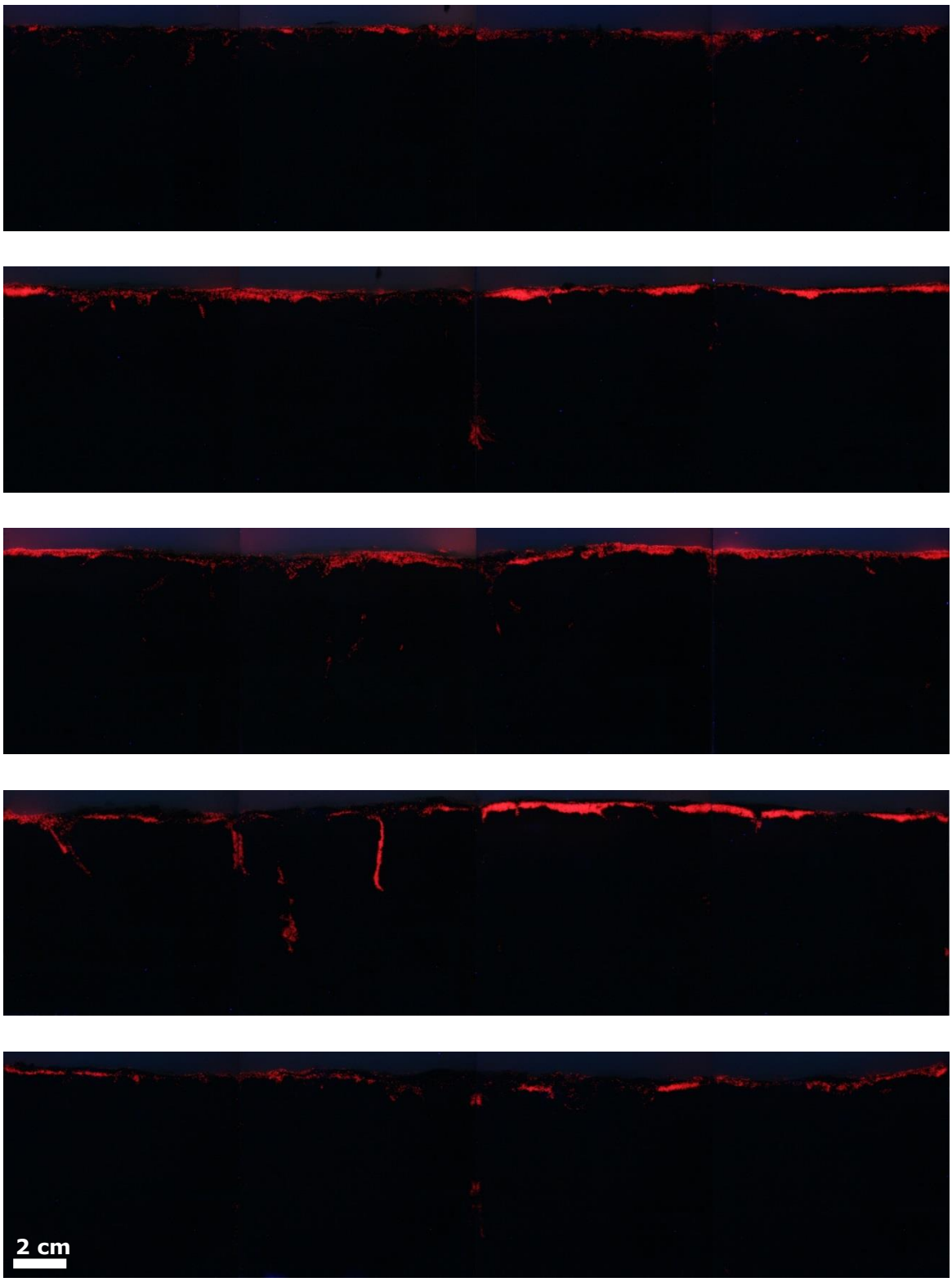

Figure 7.9 | Replicate (n=5) f-SPI images for the mixed treatment. Note that the light given off by the lumniophores is being reflected by the sealant used to keep the corners of the cores watertight.

These images were used to create sediment bioturbation profiles (Figure 7.10). Most luminophores are still located on or near the sediment surface, however the treatment containing *Hediste diversicolor* and the mixed species treatment show sediment reworking occurs down to the bottom of the cores (Figure 7.10a and 7.10d). The *Corophium volutator* and the mixed species treatments have a high level of sediment reworking occurring in the top 0.5 cm of the sediment (Figures 7.10c and 7.10d).

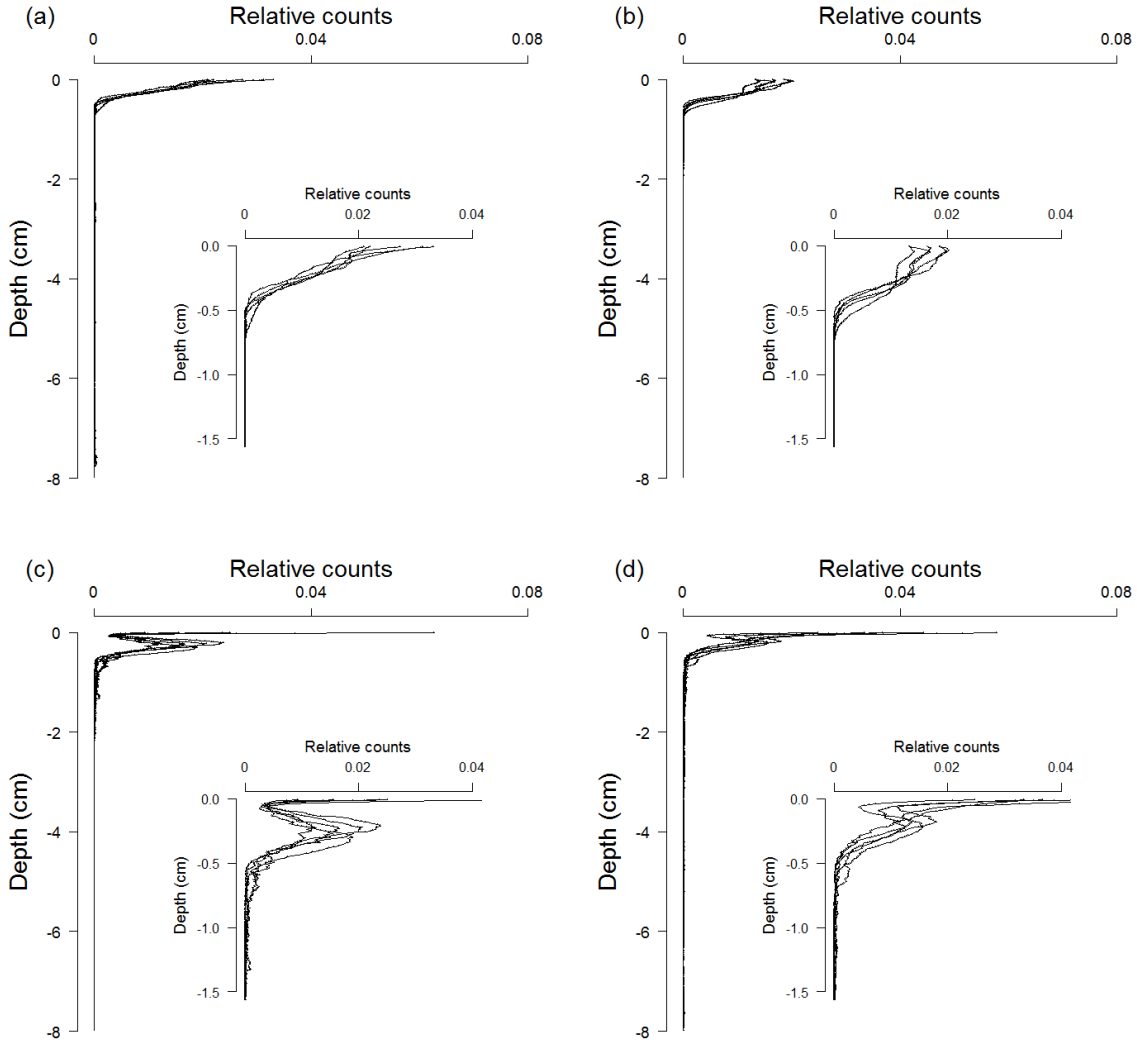

Figure 7.10 | Sediment particle reworking profiles (n = 5) derived from the f-SPI images for (a) *Hediste diversicolor*, (b) *Hydrobia ulvae*, (c) *Corophium volutator*, and (d) in species mixture. Insets show detail of main figure.

The average (± 95 % CI) mean maximum mixed depth ($^{f\text{-}SPI}L_{mean}$, cm) varied significantly with species identity (Figure 7.11; L-ratio = 19.18, d.f. = 8, $p < 0.0001$). The average (± 95 % CI) mean maximum mixed depth of the *Hediste diversicolor* treatment (HD; 0.87 ± 0.45 cm) was deeper than that of the *Hydrobia ulvae* treatment (HU; 0.37 ± 0.07 cm; t = -3.07, p = 0.0073) and the *Corophium volutator* treatment (CV; 0.29 ± 0.08 cm; t = -3.55, p = 0.0027). The average (± 95 % CI) mean maximum mixed depth of the mixed species treatment (Mix; 0.57 ± 0.14 cm) was also deeper than that of the *Hydrobia ulvae* treatment (t = -3.49, p = 0.0030) and the *Corophium volutator* treatment (t = -4.76, p = 0.0002).

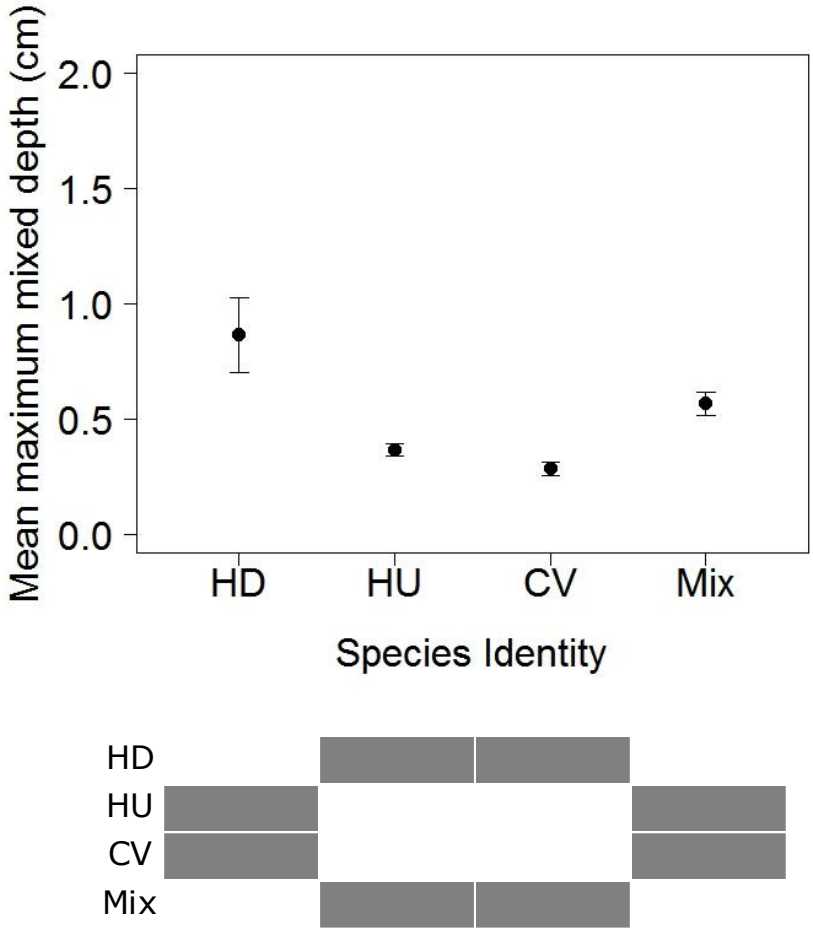

Figure 7.11 | The mean maximum mixed depth (cm) of the three species in monoculture and the mixed species treatment (n = 5). Error bars are standard error. The species composition of each mixture is indicated on the x-axis, where species identity corresponds to: HD, *Hediste diversicolor*; HU, *Hydrobia ulvae*; CV, *Corophium volutator*; Mix, mixed species treatment. Significant differences are indicated in the accompanying table where darker shading indicates greater significant difference: ▒ $0.01 < p < 0.05$; ▓ $0.0001 < p < 0.01$; ■ $p < 0.0001$.

The average (± 95 % CI) median maximum mixed depth ($^{f\text{-}SPI}L_{med}$, cm) varied significantly with species identity (Figure 7.12; L-ratio = 11.50, d.f. = 8, p = 0.0093). The average (± 95 % CI) median maximum mixed depth of the *Hydrobia ulvae* treatment (HU; 0.36 ± 0.08 cm) was the deepest. The average (± 95 % CI) median maximum mixed depth of the *Hydrobia ulvae* treatment was deeper than that of the *Hediste diversicolor* treatment (HD; 0.26 ± 0.06 cm; t = -2.77, p = 0.0136), the *Corophium volutator* treatment (CV; 0.23 ± 0.03 cm; t = -4.14, p = 0.0008) and the mixed species treatment (Mix; 0.27 ± 0.05 cm; t = -2.84, p = 0.0118).

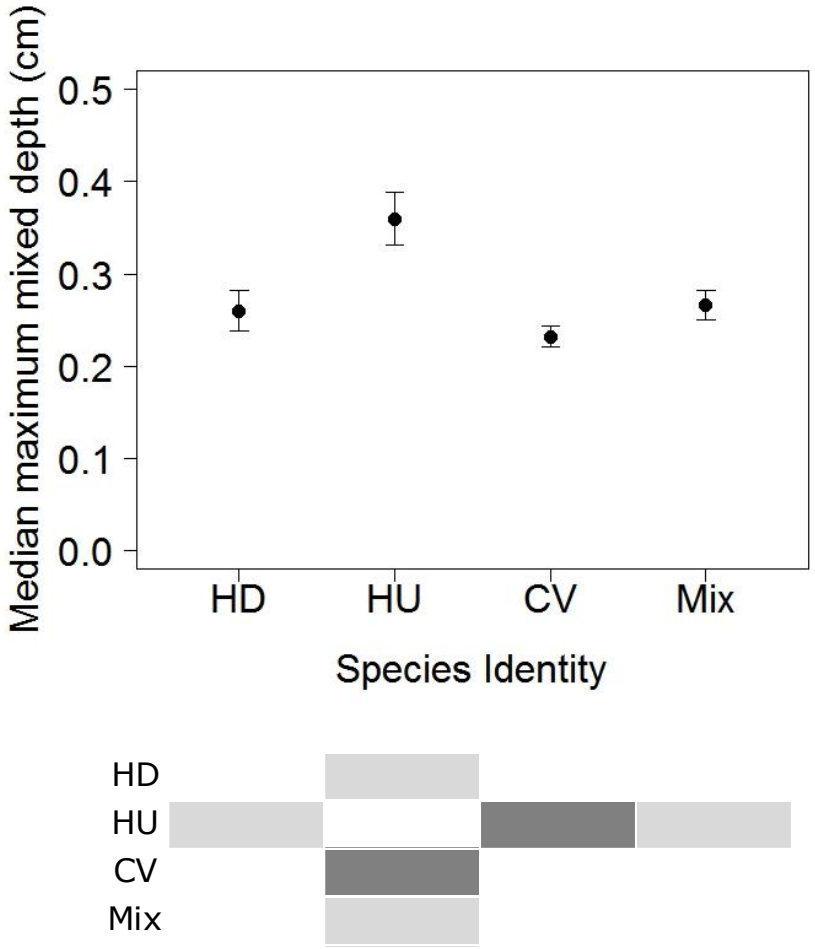

Figure 7.12 | The median maximum mixed depth (cm) of the three species in monoculture and the mixed species treatment (n = 5). Error bars are standard error. The species composition of each mixture is indicated on the x-axis, where species identity corresponds to: HD, *Hediste diversicolor*; HU, *Hydrobia ulvae*; CV, *Corophium volutator*; Mix, mixed species treatment. Significant differences are indicated in the accompanying table where darker shading indicates greater significant difference: ▒ 0.01 < p < 0.05; ▓ 0.0001 < p < 0.01; ■ p < 0.0001.

The average (± 95 % CI) maximum mixed depth ($^{f\text{-}SPI}L_{max}$, cm) varied significantly with species identity (Figure 7.13; L-ratio = 68.59, d.f. = 8, $p < 0.0001$). *Hediste diversicolor* and the mixed species treatment had a maximum mixed depth limited by the depth of the cores. The average (± 95 % CI) maximum mixed depth of the *Hediste diversicolor* treatment (HD; 7.38 ± 0.46 cm) was deeper than that of the *Hydrobia ulvae* treatment (HU; 1.55 ± 0.37 cm; $t = -27.19$, $p < 0.0001$) and the *Corophium volutator* treatment (CV; 1.98 ± 0.28 cm; $t = -27.66$, $p < 0.0001$) but shallower than the mixed species treatment (Mix; 7.79 ± 0.25 cm; $t = 2.17$, $p = 0.0454$). The *Hydrobia* treatment (HU) average (± 95 % CI) maximum mixed depth was shallower than that of the *Corophium* treatment (CV; $t = 2.56$, $p = 0.0209$) and the mixed species treatment (Mix; $t = 38.54$, $p < 0.0001$). The *Corophium* treatment (CV) has a shallower average (± 95 % CI) maximum mixed depth than the mixed species treatment (Mix; $t = 42.89$, $p < 0.0001$).

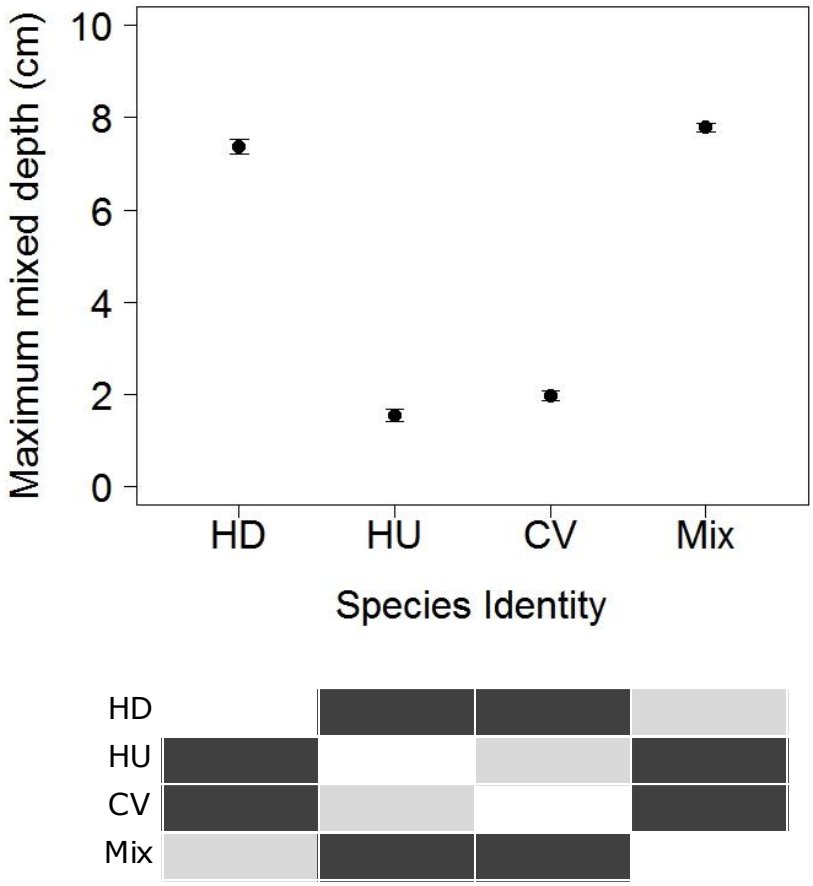

Figure 7.13 | The maximum mixed depth (cm) of the three species in monoculture and the mixed species treatment (n = 5). Error bars are standard error. The species composition of each mixture is indicated on the x-axis, where species identity corresponds to: HD, *Hediste diversicolor*; HU, *Hydrobia ulvae*; CV, *Corophium volutator*; Mix, mixed species treatment. Significant differences are indicated in the accompanying table where darker shading indicates greater significant difference: 0.01 < p < 0.05; 0.0001 < p < 0.01; p < 0.0001.

There was no significant effect of species or species mixture on the sediment surface boundary roughness (SBR, cm; Figure 7.14; $F = 0.3446$, d.f. = 3, $p = 0.7935$).

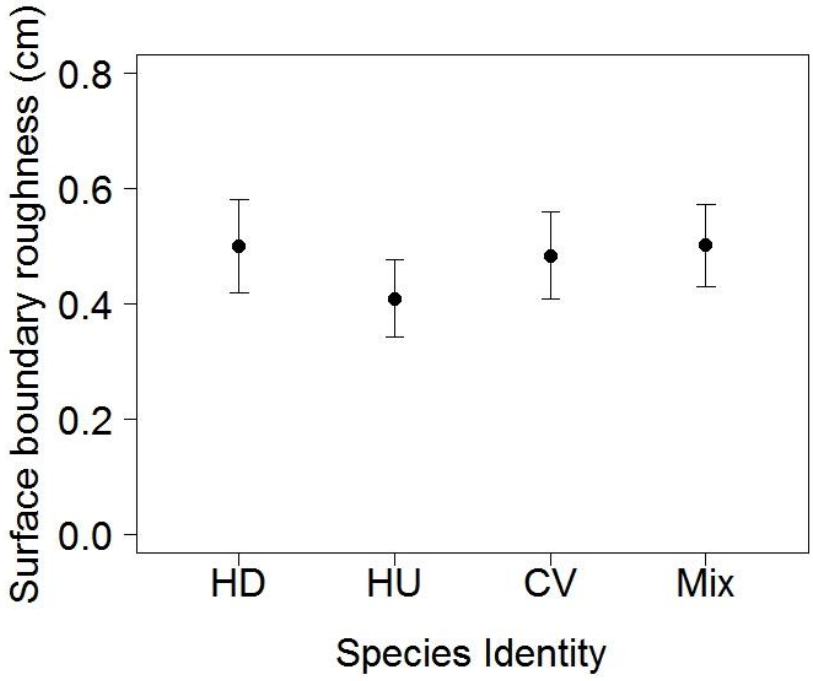

Figure 7.14 | The sediment surface boundary roughness (cm) of the three species in monoculture and the mixed species treatment (n = 5). Error bars are standard error. The species composition of each mixture is indicated on the x-axis, where species identity corresponds to: HD, *Hediste diversicolor*; HU, *Hydrobia ulvae*; CV, *Corophium volutator*; Mix, mixed species treatment.

7.3.2 | Three dimensional analysis

Replicate (n = 5) cross sectional images were reconstructed for the transverse plane 0.5 cm below the sediment-water interface (Figure 7.15a-d; additional images in Appendix 5) and the coronal plane through the rotational centre of the core (Figure 7.16a-d; additional images in Appendix 5). Three-dimensional models were created by segmentation of the burrows from the surrounding sediment (Figure 7.17a-d; additional images in Appendix 5).

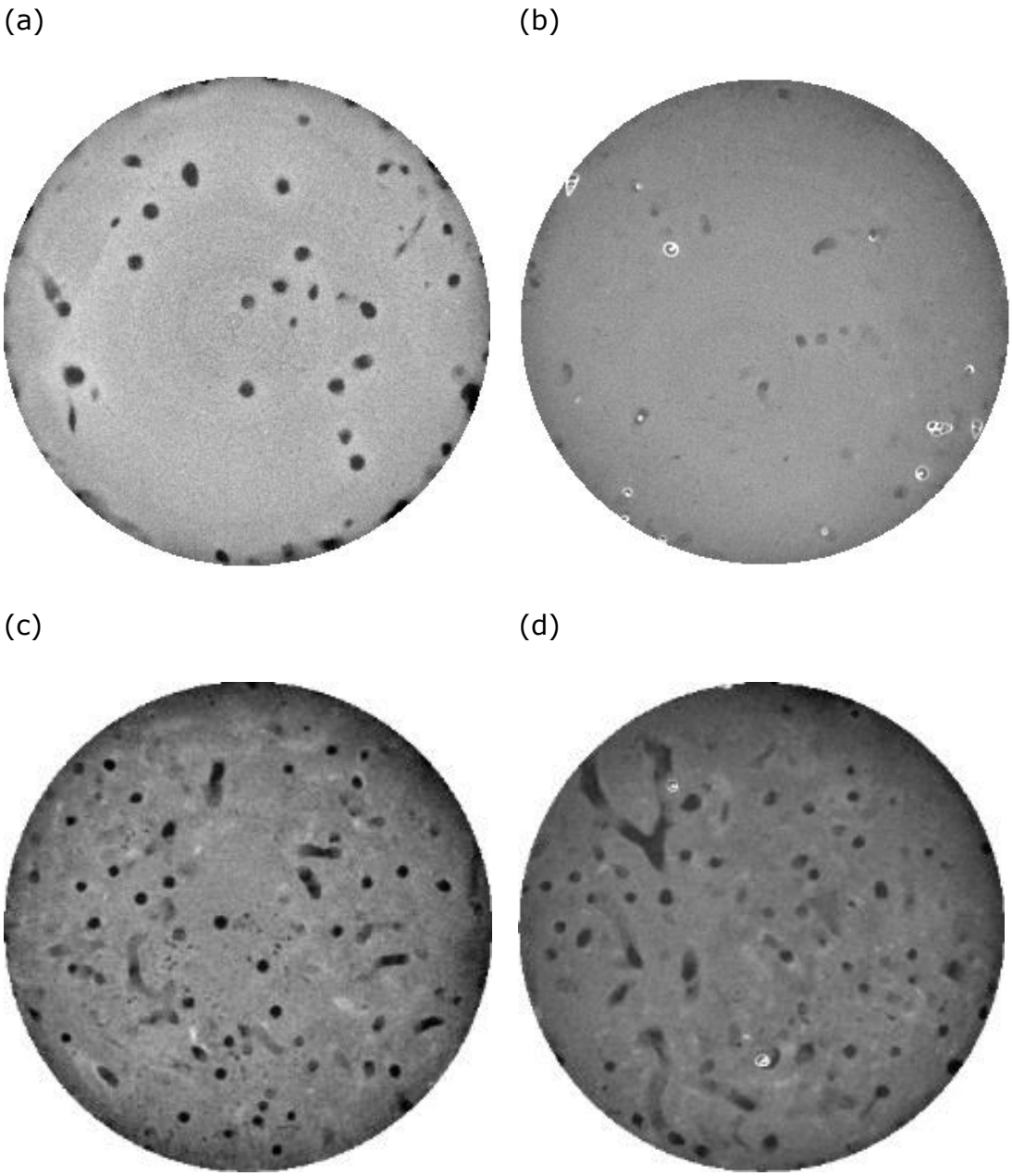

Figure 7.15 | Example transverse core slices taken at 0.5 cm below the sediment-water interface for (a) *Hediste diversicolor*, (b) *Hydrobia ulvae*, (c) *Corophium volutator*, and (d) in species mixture. All cores are 10 cm in diameter. Burrows appear as darker grey values. In (b) and (d), the detail (e.g. aperture, whorls and apex) of *H. ulvae* shells can be seen (white pixel values). Additional images (n = 5) in Appendix 5.

(a)

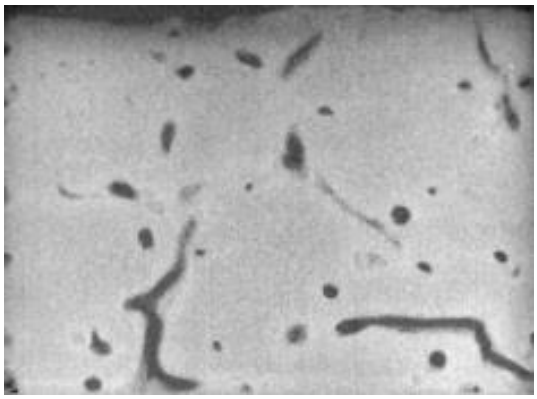

(b)

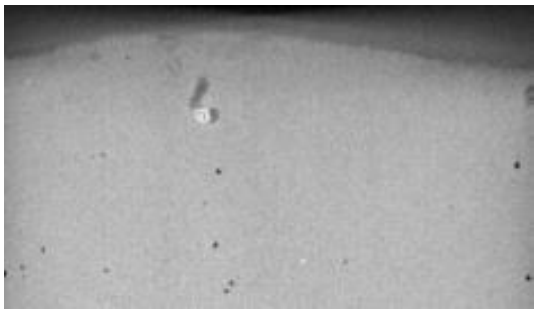

(c)

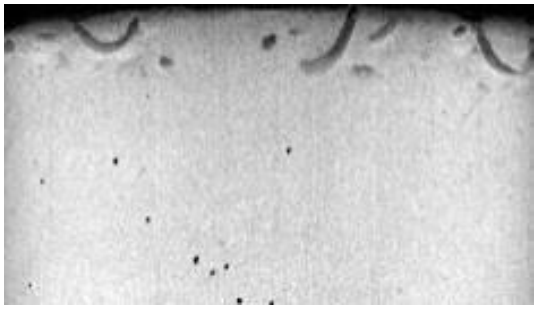

(d)

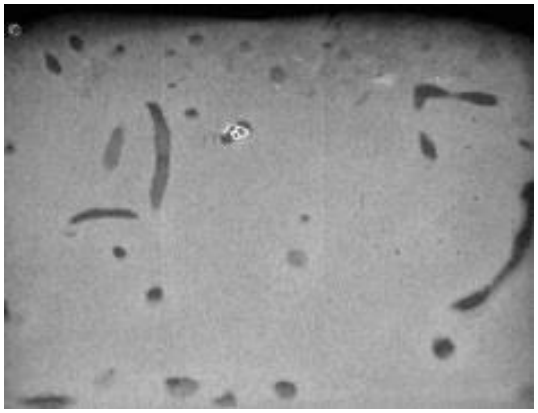

Figure 7.16 | Example coronal core slices for (a) *Hediste diversicolor*, (b) *Hydrobia ulvae*, (c) *Corophium volutator*, and (d) in species mixture. Burrows appear as darker grey values. In (b) and (d), the detail (e.g. aperture, whorls and apex) of *H. ulvae* shells can be seen (white pixel values). The sediment-water interface is at the top of the region of interest. Images are cropped immediately below the vertical extent of burrowing. All cores are 10 cm in diameter. Additional images (n = 5) in Appendix 5.

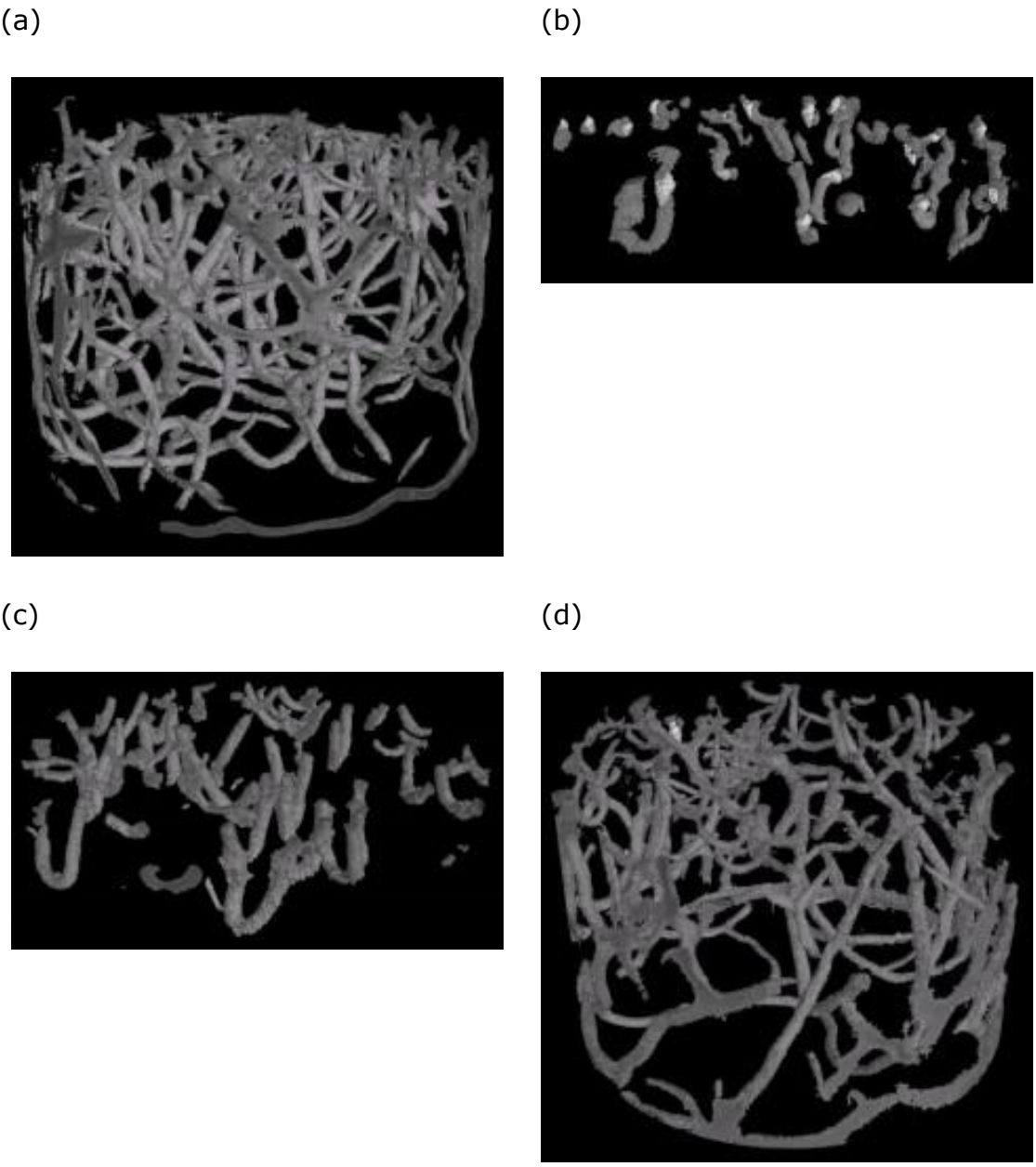

Figure 7.17 | Example reconstructed three-dimensional burrow models for (a) *Hediste diversicolor*, (b) *Hydrobia ulvae*, (c) *Corophium volutator*, and (d) in species mixture. In (b) and (d), *H. ulvae* shells can be seen (lighter pixel values). The sediment-water interface is at the top of the region of interest. Images are cropped immediately below the vertical extent of burrowing. All cores are 10 cm in diameter. Additional images (n = 5) in Appendix 5.

Average (± 95 % CI) maximum burrow depth calculated using CT ($^{CT}B_{max}$, cm) varied significantly between treatments (Figure 7.18; $F = 345.92$, d.f. = 16, $p < 0.0001$). *Hediste diversicolor* and the mixed species treatment had a maximum mixed depth limited by the depth of the cores. *Hediste diversicolor* (HD; 7.20 ± 0.35 cm) burrowed deeper (mean ± 95 % CI

maximum burrow depth) than both *Hydrobia ulvae* (HU; 2.66 ± 0.43 cm; t = -21.32, p < 0.0001) and *Corophium volutator* (CV; 2.11 ± 0.43 cm; t = -23.93, p < 0.0001). *Hydrobia ulvae* (HU) had a deeper average (± 95 % CI) maximum burrow depth than *Corophium volutator* (CV; t = -2.60, p = 0.0189). The mixed species treatment had a deeper average (± 95 % CI) maximum burrow depth than *Hydrobia ulvae* (HU; t =-21.48, p < 0.0001) and *Corophium volutator* (CV; t = -24.09, p < 0.0001).

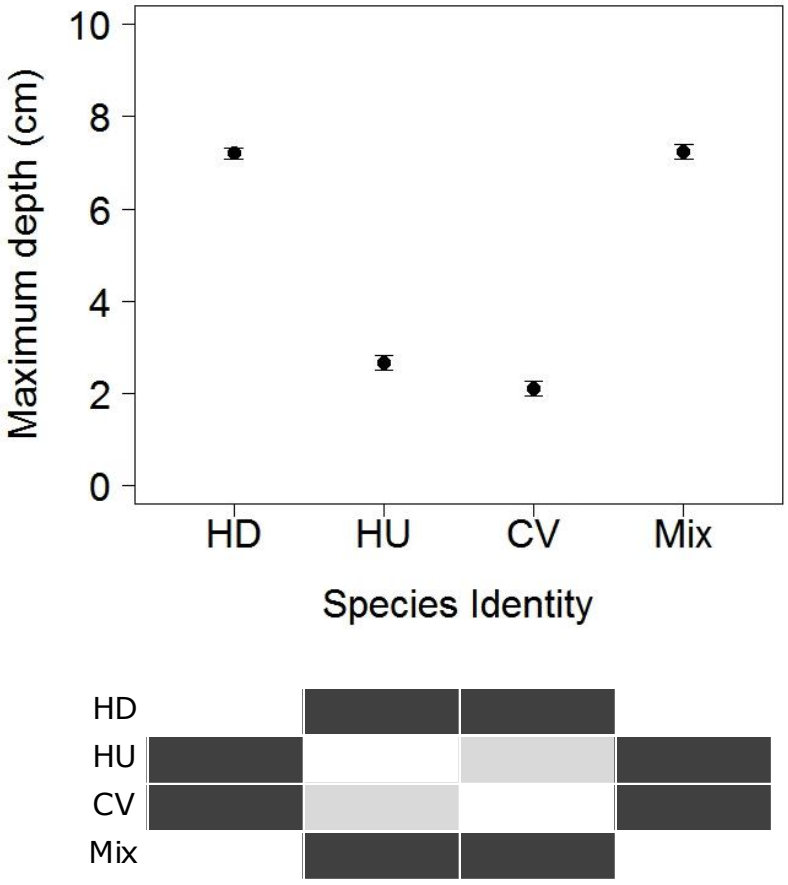

Figure 7.18 | The burrow maximum depth (cm), calculated using computed tomography, of the three species in monoculture and the mixed species treatment (n = 5). Error bars are standard error. The species composition of each mixture is indicated on the x-axis, where species identity corresponds to: HD, *Hediste diversicolor*; HU, *Hydrobia ulvae*; CV, *Corophium volutator*; Mix, mixed species treatment. Significant differences are indicated in the accompanying table where darker shading indicates greater significant difference: 0.01 < p < 0.05; 0.0001 < p < 0.01; p < 0.0001.

Average (± 95 % CI) burrow surface area calculated using CT ($^{CT}B_{SA}$, cm^2) varied significantly between treatments (Figure 7.19; L-ratio = 71.11, d.f. = 8, $p < 0.0001$). *Hediste diversicolor* (HD; 436.91 ± 84.92 cm^2) had a greater average (± 95 % CI) burrow surface area than both *Hydrobia ulvae* (HU; 33.17 ± 12.81 cm^2; t = -13.05, $p < 0.0001$), *Corophium volutator* (CV; 66.56 ± 19.37 cm^2; t = -11.81, $p < 0.0001$) and the mixed species treatment (Mix; 332.93 ± 80.62 cm^2; t = -2.47, p = 0.0254). *Corophium volutator* (CV) had a greater average burrow surface area than *Hydrobia ulvae* (HU; t = -3.99, p = 0.0010). The mixed species treatment had a greater average (± 95 % CI) burrow surface area than *Hydrobia ulvae* (HU; t = -10.20, $p < 0.0001$) and *Corophium volutator* (CV; t = -8.92, $p < 0.0001$).

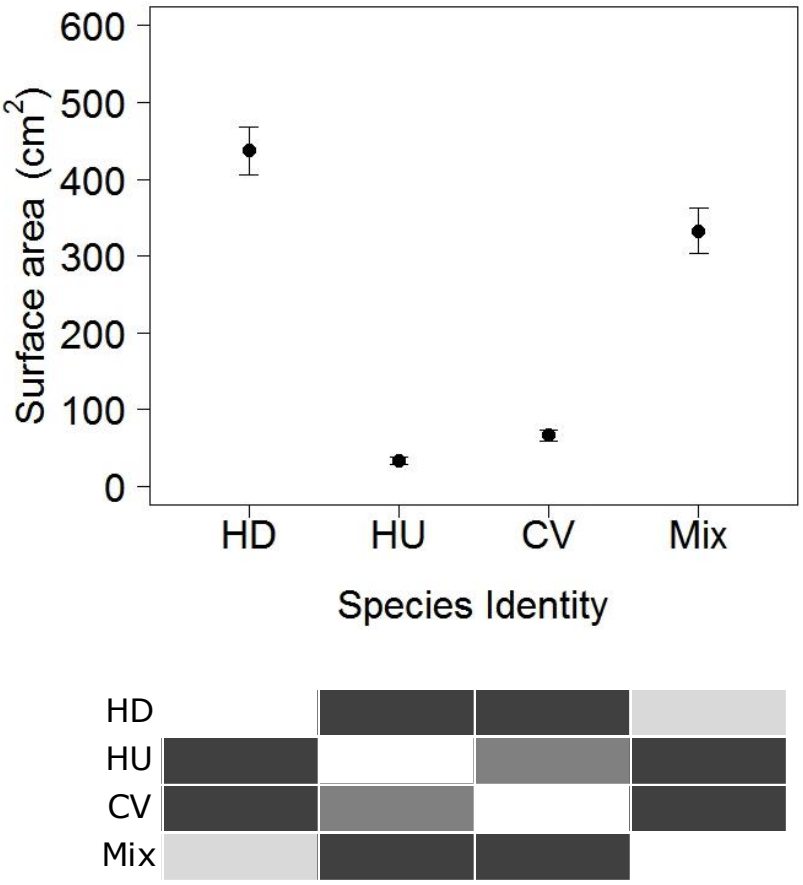

Figure 7.19 | The burrow surface area (cm^2), calculated using computed tomography, of the three species in monoculture and the mixed species treatment (n = 5). Error bars are standard error. The species composition of each mixture is indicated on the x-axis, where species identity corresponds to: HD, *Hediste diversicolor*; HU, *Hydrobia ulvae*; CV, *Corophium volutator*; Mix, mixed species treatment. Significant differences are indicated in the accompanying table where darker shading indicates greater significant difference: ▫ $0.01 < p < 0.05$; ▪ $0.0001 < p < 0.01$; ■ $p < 0.0001$.

Average (± 95 % CI) burrow volume calculated using CT ($^{CT}B_{vol}$, cm^3) varied significantly between treatments (Figure 7.20; L-ratio = 68.76, d.f. = 8, $p < 0.0001$). *Hediste diversicolor* (HD; 19.83 ± 4.99 cm^3) had a greater average (± 95 % CI) burrow volume than both *Hydrobia ulvae* (HU; 1.12 ± 0.43 cm^3; t = -10.38, $p < 0.0001$), *Corophium volutator* (CV; 2.43 ± 1.30 cm^3; t = -9.38, $p < 0.0001$) and the mixed species treatment (Mix; 13.92 ± 3.91 cm^3; t = -2.59, p = 0.0197). *Corophium volutator* (CV) had a average (± 95 % CI) greater burrow volume than *Hydrobia ulvae* (HU; t = -2.65, p = 0.0174). The mixed species treatment had a greater mean (± 95 % CI) burrow surface area than *Hydrobia ulvae* (HU; t = -9.03, $p < 0.0001$) and *Corophium volutator* (CV; t = -7.74, $p < 0.0001$).

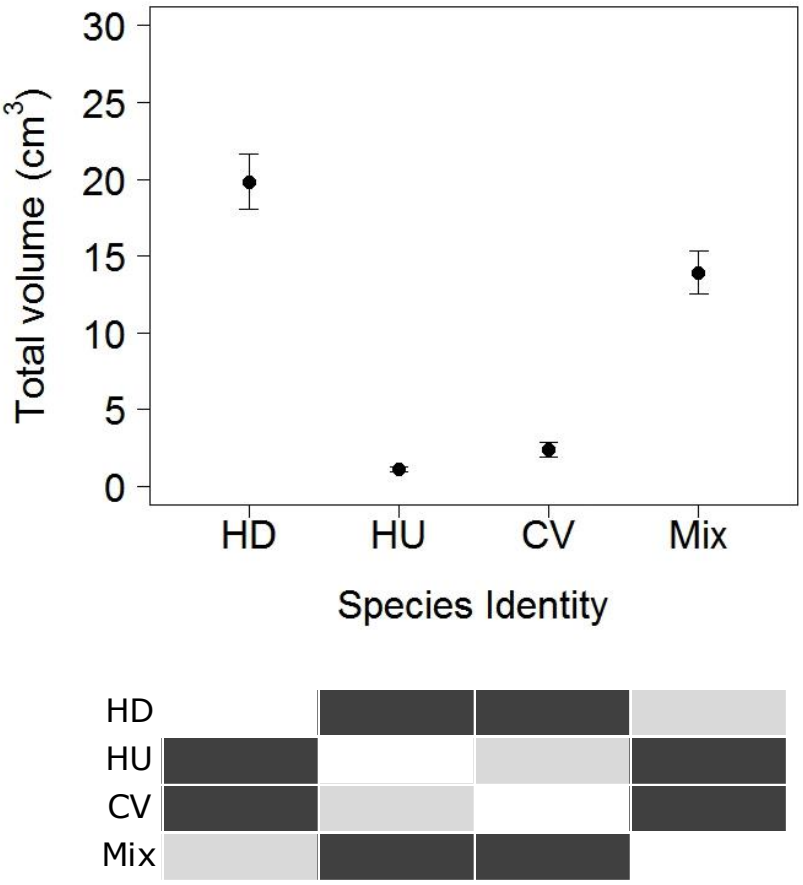

Figure 7.20 | The total burrow volume (cm^3), calculated using computed tomography, of the three species in monoculture and the mixed species treatment (n = 5). Error bars are standard error. The species composition of each mixture is indicated on the x-axis, where species identity corresponds to: HD, *Hediste diversicolor*; HU, *Hydrobia ulvae*; CV, *Corophium volutator*; Mix, mixed species treatment. Significant differences are indicated in the accompanying table where darker shading indicates greater significant difference: ▫ $0.01 < p < 0.05$; ▪ $0.0001 < p < 0.01$; ■ $p < 0.0001$.

7.3.3 | Bioirrigation

The individual effects of core shape (circular or square) and species identity (*Hediste diversicolor*, *Hydrobia ulvae*, *Corophium volutator* or mixed) significantly affected bioirrigation rates of the sediment (L-ratio = 21.56, d.f. = 13, p = 0.0104), however the core shape and species identity interaction did not and was removed from the generalised least squares model (see Appendix 5). The change in average (± 95 % CI) bromide concentration ($\triangle[Br^-]$, mgL^{-1}) after 8 hours incubation was greater in the circular cores (-546.15 ± 102.11 mgL^{-1}) than the square cores (-234.11 ± 43.79 mgL^{-1}; Figure 7.21; t = -7.77, p < 0.0001).

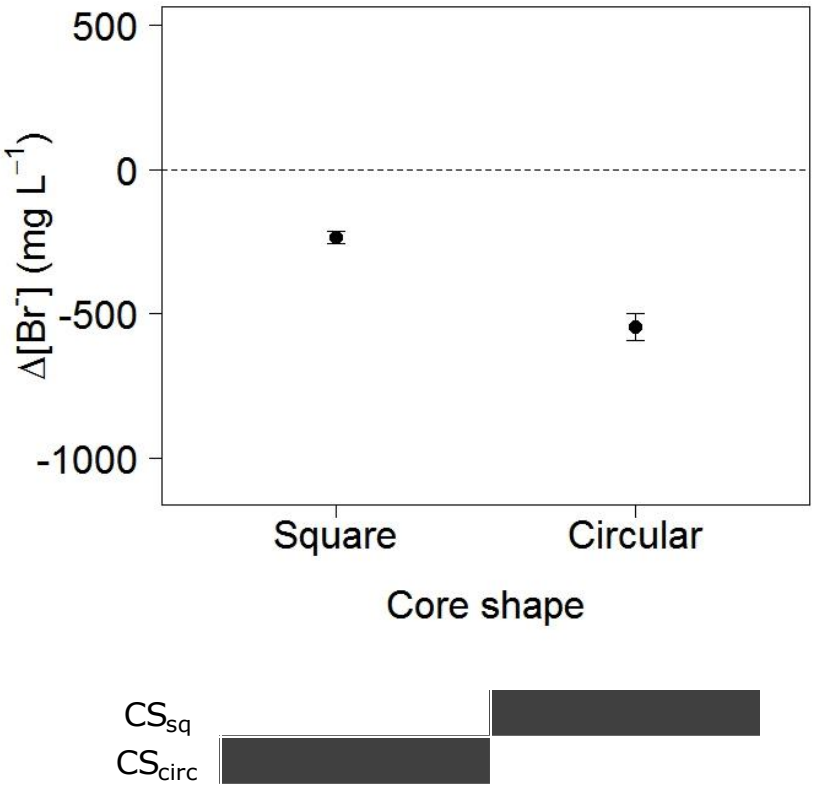

Figure 7.21 | Bioirrigation rates ($\triangle[Br^-]$, mgL^{-1}) in the two core shapes: square and circular (n = 20). Error bars are standard error. Significant differences are indicated in the accompanying table where darker shading indicates greater significant difference: 0.01 < p < 0.05; 0.0001 < p < 0.01; p < 0.0001.

The difference in average (± 95 % CI) bromide concentration after 8 hours incubation (△[Br^-], mgL^{-1}) was greater in the cores containing *Hediste diversicolor* (HD; -486.79 ± 162.92) than the cores containing *Hydrobia ulvae* (HD; -313.48 ± 199.91; Figure 7.22; t = 2.64, p = 0.0124) and the species mixture (Mix; -395.66 ± 170.22; t = 2.80, p = 0.0082).

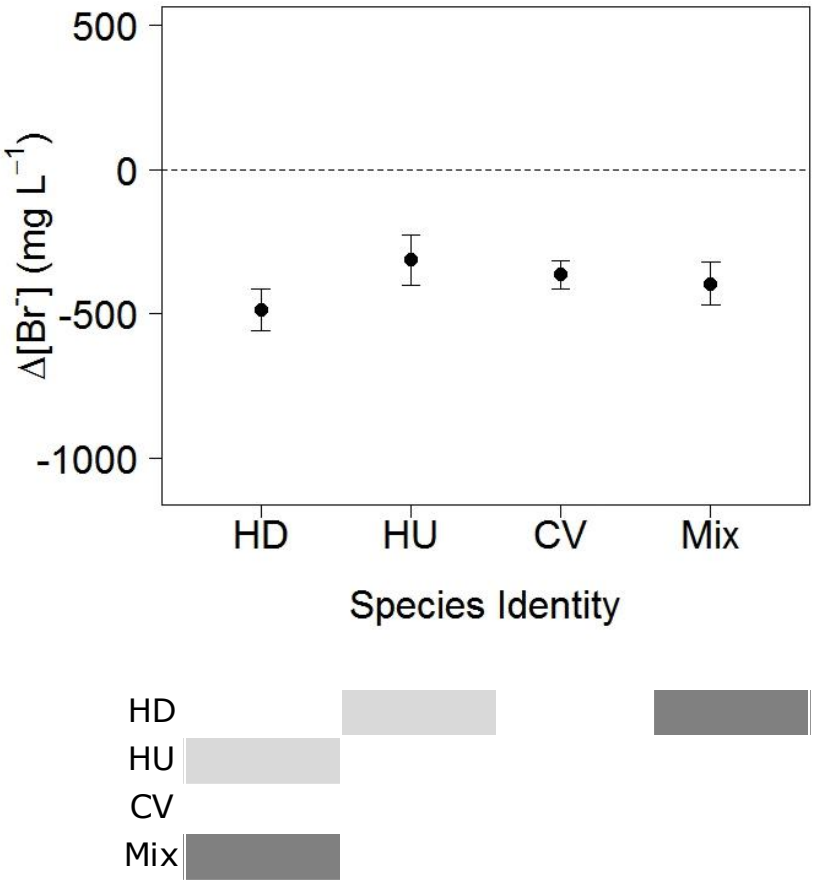

Figure 7.22 | The bioirrigation rates (△[Br^-], mgL^{-1}) of the three species in monoculture and the mixed species treatment (n = 5). Error bars are standard error. The species composition of each mixture is indicated on the x-axis, where species identity corresponds to: HD, *Hediste diversicolor*; HU, *Hydrobia ulvae*; CV, *Corophium volutator*; Mix, mixed species treatment. Significant differences are indicated in the accompanying table where darker shading indicates greater significant difference: 0.01 < p < 0.05; 0.0001 < p < 0.01; p < 0.0001.

7.3.4 | Species mixture effects

Compared to the maximum yield in monoculture the species mixture non-trangressively under-yielded for all variables (Figure 7.23), except the maximum mixing depth determined using f-SPI ($^{f\text{-}SPI}L_{max}$, cm) and the maximum burrow depth determined using CT ($^{CT}B_{max}$, cm). The maximum of both these variables is constrained by the depth of the sediment cores and in the CT scans *Hediste* was shown to burrow down to the bottom of the cores.

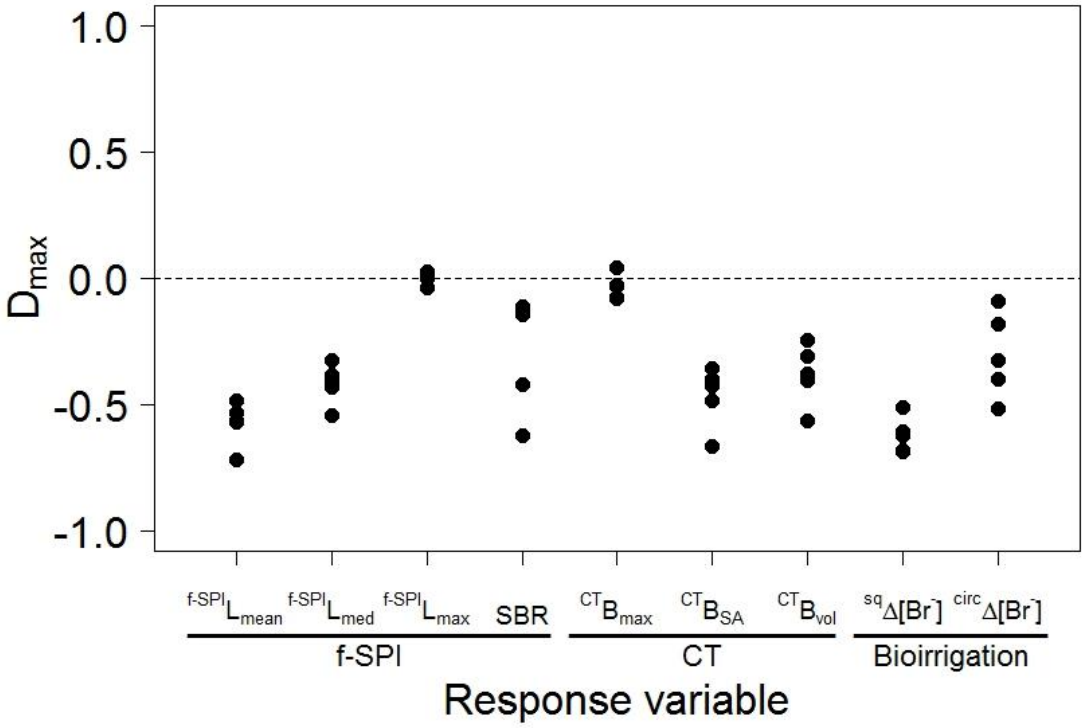

Figure 7.23 | Mixed species treatment yields compared to the maximum yield in monoculture for the mean maximum mixed depth ($^{f\text{-}SPI}L_{mean}$, cm), the median maximum mixed depth ($^{f\text{-}SPI}L_{med}$, cm) the maximum mixing depth ($^{f\text{-}SPI}L_{max}$, cm) and the surface boundary roughness (SBR, cm) measured using fluorescent sediment profile imaging (f-SPI), the maximum burrow depth ($^{CT}B_{max}$, cm), the burrow surface area ($^{CT}B_{SA}$, cm) and the burrow volume ($^{CT}B_{vol}$, cm) measured using computed tomography (CT) and the change caused in bromide concentration in the square ($^{sq}\triangle[Br^-]$) and circular ($^{circ}\triangle[Br^-]$) cores used to measure bioirrigation rates. Overyielding ($D_{max} > 0$) occurs when a mixture outperforms the corresponding monocultures.

When the expected yield in mixture is calculated using a non-transgressive model the species mixture overyields ($D_T > 0$) for three of the variables measured: the maximum mixing depth ($^{f\text{-}SPI}L_{max}$, cm) measured using fluorescent sediment profile imaging (f-SPI), and the maximum burrow depth ($^{CT}B_{max}$, cm) and the burrow volume ($^{CT}B_{vol}$, cm^3) measured using CT (Figure 7.24).

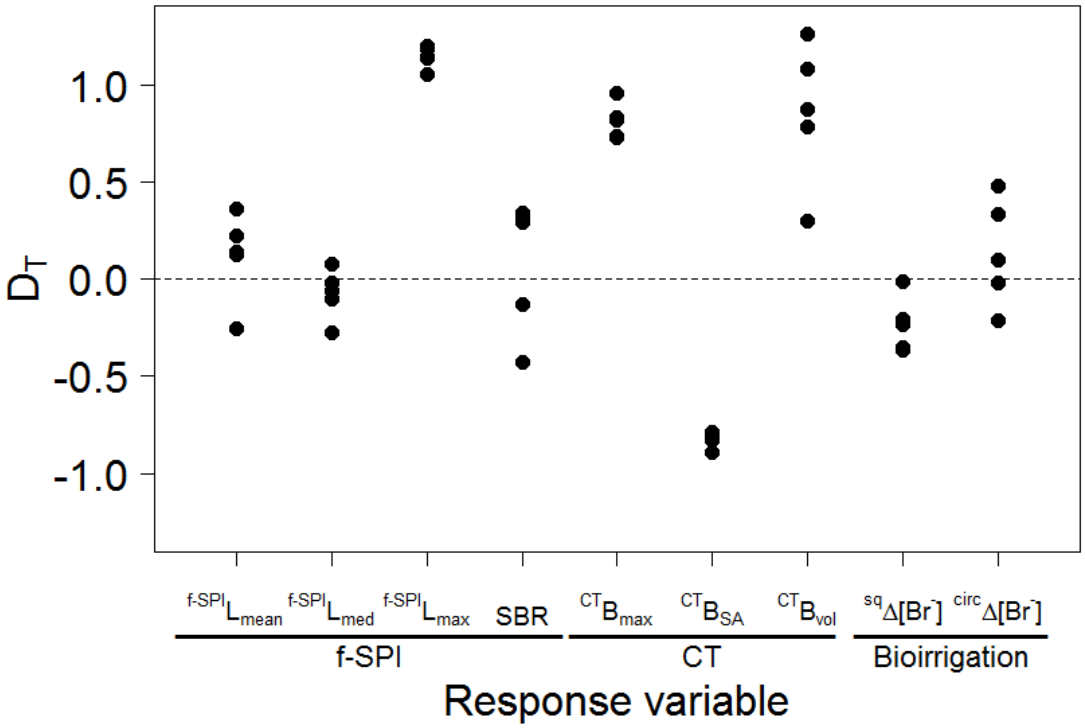

Figure 7.24 | Observed mixed species treatment yields compared to the expected yields for the mean maximum mixed depth ($^{f\text{-}SPI}L_{mean}$, cm), the median maximum mixed depth ($^{f\text{-}SPI}L_{med}$, cm) the maximum mixing depth ($^{f\text{-}SPI}L_{max}$, cm) and the surface boundary roughness (SBR, cm) measured using fluorescent sediment profile imaging (f-SPI), the maximum burrow depth ($^{CT}B_{max}$, cm), the burrow surface area ($^{CT}B_{SA}$, cm) and the burrow volume ($^{CT}B_{vol}$, cm) measured using computed tomography (CT) and the change caused in bromide concentration in the square ($^{sq}\triangle[Br^-]$) and circular ($^{circ}\triangle[Br^-]$) cores used to measure bioirrigation rates. Overyielding ($D_T > 0$) occurs when a mixture outperforms the corresponding monocultures.

7.4 | Discussion

The use of high-resolution two-dimensional measurements of the active transport of fluid and sediment particles with three-dimensional reconstructions of burrow geometry provided a comprehensive assessment and quantification of sediment bioturbation and bioirrigation caused by the

addition of *Hediste diversicolor*, *Hydrobia ulvae* and *Corophium volutator* to sediment cores. One unexpected finding regarding bioirrigation rates was that the core shape influences bioirrigation rate, with the circular cores (all species) having a greater rate of bioirrigation than the square cores. A similar effect was also seen by Lindqvist et al. (2013) who found that sediment reworking intensity differed between plexiglass cores and thin glass aquaria. This suggests that the f-SPI data (measured in square cores as the technique requires a flat side to photograph) are not directly comparable with the CT scan data (carried out on circular cores as the technique requires a round core to prevent x-ray distortion), however, valid comparisons may still be drawn. Lindqvist et al. (2013) attributed the variance between mesocosm types to the difference in species density between the treatments, however species density was constant between the two core shapes in this study. The study may have been confounded by edge effects. The square cores have a greater edge area (354.40 cm^2) than the circular cores (314.16 cm^2) and any burrow is therefore slightly more likely to touch a core edge within the square cores. Burrows that lie adjacent to an edge provide less surface area for bromide diffusion into the sediment, and in the circular core more burrows may be located wholly within the sediment where diffusion is maximised. This may result in the greater bioirrigation observed in the circular cores.

7.4.1 | Single species effects: *Hediste diversicolor*

Visually the f-SPI images and 3-dimensional core reconstructions show particle mixing and burrowing by *Hediste diversicolor* to occur at all depths within the sediment cores. Small burrows, fanning out up to the sediment surface, were revealed within the top 2 cm of the sediment. *Hediste diversicolor* burrowed the deepest of the three species, burrowing to the maximum depth possible in the sediment cores. Correspondingly, the treatments containing *Hediste diversicolor* in monoculture also had the deepest mean maximum mixed depth, a time dependent indicator of mixing depth, the greatest burrow surface area and the greatest burrow volume. *Hediste diversicolor* has been shown to play an important role in the destabilisation and erodibility of sediment as a result of high bioturbatory activity (Luckenbach 1986, de Deckere et al. 2001, Widdows et al. 2009). This bioturbation causes significant rates of sediment resuspension due to the

ejection of ingested sediment and the release of disturbed sediment (Widdows et al. 2009). De Deckere et al. (2001) noted that reduced infaunal abundance, especially that of *Hediste diversicolor*, caused a reduction in bioturbation and a corresponding increase in sediment stability.

7.4.2 | Single species effects: *Hydrobia ulvae*

Hydrobia ulvae were shown to be able to burrow to a maximum depth of 3.27 cm. Burrowing in *Hydrobia* has been observed previously (Newell 1962, Little and Nix 1976, Orvain and Sauriau 2002), however the characteristics of *Hydrobia* burrows have not been quantified. *Hydrobia* have been shown to contribute to sediment destabilisation through surface browsing and disruption (Blanchard et al. 1997, Orvain et al. 2004). However, bioturbation and burrowing by the snail may contribute to sediment destabilisation more than anticipated, especially at high sediment moisture contents, when *Hydrobia ulvae* bioturbation intensity has been shown to increase (Orvain et al. 2006). *Hydrobia* was actually shown to have a deeper average median and mean maximum mixing depth than *Corophium volutator*. This indicates that the short-term mixing and average depth of mixing over time of *Hydrobia* is deeper than that of *Corophium*. This could, however, just be an artefact of the fact that after 6 days in the treatment containing *Hydrobia* there was still a thick layer of luminophores over the surface of the sediment (i.e. there had been less reworking of the luminophores), artificially augmenting the depth of mixing observed due to the inclusion of the layer of luminophores in the top rows of the sediment profile analysis.

7.4.3 | Single species effects: *Corophium volutator*

CT scans of the circular sediment cores containing *Corophium volutator* showed the classic U- and J-shaped burrows (Meadows 1964, Pelegri et al. 1994, Riisgard 2007). The mean and median maximum mixed depths in the treatments containing *Corophium volutator* were the shallowest observed. The proximity of the majority of the bioturbatory action close to the surface is possibly why the actions of *Corophium* were observed to have a destabilising influence on the sediment in previous chapters due to near surface sediment disturbance (de Deckere et al. 2000). A number of studies, however, have

found that the creation and stabilisation of burrows actually increases sediment stability (Meadows and Tait 1989, Grant and Daborn 1994, Mouritsen et al. 1998).

7.4.4 | Mixed species effects

In the mixed species treatments the influence of the three species is visible in the sediment particle reworking profiles. The effect observed on maximum mixing depth ($^{f\text{-}SPI}L_{max}$) and maximum burrow depth ($^{CT}B_{max}$) in the mixed cores is controlled by the influence of *Hediste diversicolor*, which burrows to the bottom of the core whether in species mixture or monoculture.

The mixed species treatments were shown to under-yield compared to the maximum effect of species treatments in monoculture, indicating species interactions are moderating the maximum potential species effects in mixture. *Hediste* has been shown to destroy *Corophium* tubes through its own burrowing, forcing the animals to move around and construct new burrows (Olafsson and Persson 1986). This destruction of *Corophium* burrows may reduce *Corophium* bioirrigation rates when in species mixture. *Corophium volutator* has been shown to filter feed by producing a current through its tube to trap suspended particles (Hart 1930, Riisgard 2007). The disturbance of *Corophium* burrows may mean more time is allocated to burrow creation and pre-settlement activities rather than post-settlement feeding and burrow irrigation, resulting in a reduction in community bioirrigation.

When examining the data using a non-transgressive model, the mixed species cores had a smaller burrow surface area and a larger burrow volume than expected based on that observed in monoculture. Upon examination of the surface area to volume ratios, again it is the influence of the burrowing of *Hediste diversicolor* that resulted in a larger burrow volume with a smaller surface area. The individuals of *Hediste* in the mixed species cores have each produced a larger volume of burrows than each of those in the monoculture treatment. This may be due to the fact that in monoculture six worms are being held within the same volume as two in the mixed treatment. In a similar laboratory experiment, increased density was not shown to have an effect on *Hediste diversicolor* burrow size or complexity of structure at the

densities examined in this experiment (Duport et al. 2006). It is possible that at a low density (in the mixed species treatment) the worms are expanding to fill the available volume due to less competition for space, resulting in a greater number of burrow structures, with no change to burrow width or complexity.

7.4.5 | Experimental limitations

As a laboratory study, this experiment has a number of well characterised limitations. The experimental set up does not represent a natural situation (Skelly and Kiesecker 2001, Petersen et al. 2009, Hale et al. 2011). The sediment was removed from the mudflat, transported to the laboratory and sieved to defaunate it. Laboratory mesocosm experiments can be important in informing scientists about the nature of the organism-sediment interactions that occur (Stewart et al. 2013), however it should be accepted that a laboratory setting, such as was used, can never fully replicate the conditions and environmental variability of a habitat *in situ* (Hale et al. 2011).

The use of f-SPI, requiring a flat surface of which to take an image, has a number of limitations. There may be edge effects and the organisms may not behave the same way when burrowing against the edge of the core as in the centre. Additionally, each species may not be affected by the core edge in the same way. For example, the flexibility of *Hediste* may mean that it is able to move along the edge of the core with ease, whereas the hard shell of *Hydrobia* may prevent it from burrowing next to the cores edge.

A further limitation involves that of the reconstruction of the 3D burrows. Segmentation of the images required the differentiation of burrow from sediment. At the surface, the low density of the mud meant that this differentiation was harder to achieve using the tools in the VGStudio computer program. These burrows were segmented by eye, allowing subjective creation of the image. Some burrows, although discernible by eye, were not segmented and therefore not included in the final image as their inclusion would have required addition of the structure pixel by pixel due to the similarity in grey shade between the burrow and the surrounding

sediment. This would have been time consuming and of low accuracy. Approximately 80 % of all burrow structures identified were included in the final images. This issue affected the cores containing *Corophium volutator* burrows the most, due to the 'fluffy' layer created by the *Corophium*, resulting in a low density sediment surface layer and increased difficulty of sediment-burrow differentiation.

7.4.6 | Future work

Future work using multidisciplinary techniques should concentrate on linking new knowledge of burrow structure, depth, surface area and volume with other important sedimentary variables, such as sediment erodibility, microphytobenthos biomass, nutrient fluxes, sediment water content, and particle size distribution to establish the functional role of benthic biodiversity at regional and global scales. Experiments looking at changes in species density and different species combinations matching those carried out in the field in Chapters 4 and 5 could also be undertaken to develop a comprehensive picture of how these three (or more) macrofauna species interact in the sediment environment. Additionally, natural cores, upon which the erosion threshold, the microphytobenthos biomass and other sediment properties have been measured, could also be CT scanned to allow these variables to be correlated with bioturbation intensity and depth to determine the relative importance of benthic macrofaunal species in mediating ecosystem process.

7.4.7| Chapter conclusions

1 | X-ray computed tomography is an effective new technique to allow both qualitative and quantitative analysis of species sediment bioturbation. Its use in combination with other multidisciplinary techniques is a powerful application for the analysis of species activities within sediment and the mechanism of their effects on other ecosystem processes.

2 | *Hediste diversicolor*, *Hydrobia ulvae* and *Corophium volutator* each have a distinct burrowing pattern. *Hediste* create an interconnecting network of contiguous burrows throughout the sediment, resulting in the movement of sediment particles throughout the core. *Corophium* create individual U- or J-shaped burrows resulting in sediment bioturbation within the top 2 cm of the sediment. *Hydrobia* create individual burrows in the top 3 cm of the sediment.

3 | The contributions of sediment dwelling invertebrates to ecosystem-level processes are well known, but categorical descriptors of species functional effects tend to reference a limited number of biological traits and ignore the wider influence of organism-sediment interactions. Reliance on broad categorizations of species behaviour or activity without an appreciation of the more subtle aspects of organism-sediment interactions will be of limited value in determining the functional role of species. These findings suggest that present understanding of species contributions to ecosystem processes and functioning is inadequate and a detailed mechanistic approach is needed.

Chapter 8 | Discussion

The aim of this thesis was to use a series of progressive experiments employing interdisciplinary techniques and manipulative field and laboratory experiments to investigate the effects of species identity, richness, density and biomass distribution, on selected biogeochemical sedimentary properties related to mudflat sediment stability.

The effect of three species; *Hediste diversicolor*, *Hydrobia ulvae* and *Corophium volutator*, on erodibility and biogeochemical properties, in monoculture, single species dominated communities, two and three species combinations, and within an already established community was measured. Collecting data on a range of biogeochemical variables, including microphytobenthos biomass and health, sediment particle size and size distribution, sediment water content and concentration, chlorophyll *a* and *b* concentration, and colloidal carbohydrate concentration, enabled the examination of the effects of biodiversity changes on the sediment stability of an intertidal Norfolk mudflat. These experiments were specifically designed to address the objectives presented in Chapter 1, Section 1.7:

Objective 1 | Investigate the effect of individual macrofauna species on mudflat sediment stability and biogeochemical properties *in situ*.

Objective 2 | Investigate the effect of macrofaunal species density on mudflat sediment stability and biogeochemical properties *in situ*.

Objective 3 | Investigate the effect of macrofaunal species richness on mudflat sediment stability and biogeochemical properties *in situ*.

Objective 4 | Investigate the effect of macrofaunal species biomass distribution on mudflat sediment stability and biogeochemical properties *in situ*.

Objective 5 | Investigate the effect of a macrofaunal species community on mudflat sediment stability and biogeochemical properties.

Objective 6 | Visualise the effect of *Hediste diversicolor*, *Hydrobia ulvae* and *Corophium volutator* on sediment particle mixing.

8.1 | Examining Objective 1

The effect of individual macrofauna species in monoculture or single species dominated communities were examined in chapters 3, 4, and 7. Chapters 3 and 4 used *in situ* field experiments to determine the effect of the species *Hediste diversicolor*, *Hydrobia ulvae* and *Corophium volutator* in single species dominated communities on sediment stability and biogeochemical properties. When dominant, it is the functional traits and the interaction of the organism with the sediment that is the most important factor in structuring the biogeochemical processes of the mudflat. Species activities, such as tube building, bioturbation and grazing, may have potentially stabilising or destabilising effects on the sediment (Figure 8.1). All three species were revealed to cause significant destabilisation of the sediment; *Hediste diversicolor* in Chapter 3 and *Hydrobia ulvae* and *Corophium volutator* in Chapter 4 (Figure 8.1).

In Chapter 7, when the sediment mixing and burrowing of the three species was examined, the bioturbatory behaviours of each species were revealed to be different. *Hediste* created burrows throughout the whole sediment, however a network of thin burrows just below the surface may contribute to the destabilisation of the surface sediment. While *Hediste diversicolor* has previously been shown to increase the stability of mudflat sediments in the laboratory (Meadows and Tait 1989), other laboratory studies (Widdows et al. 2009) and field studies (de Deckere et al. 2001) have found that it destabilises sediments through the actions of bioturbation and microphytobenthos grazing (Smith et al. 1996). *Hydrobia ulvae* burrows sparsely and the greatest effect of this species on sediment stability is probably as a result of microphytobenthos grazing (Austen et al. 1999, Orvain et al. 2004), faecal pellet production (Andersen 2001), bioturbation (Orvain et al. 2006), and surface browsing (Blanchard et al. 1997), leading to the creation of tracks providing a focal point for erosion (Nowell et al. 1981). *Corophium volutator* creates U- and J-shaped burrows and from the sediment mixing profile it appears that the majority of bioturbation occurs 2-3 cm

below the sediment surface. The decreased sediment stability observed when *Corophium volutator* is added to sediment is probably indirect as a result of microphytobenthos grazing (Smith et al. 1996, Mouritsen et al. 1998), burrow creation and cleaning (Grant and Daborn 1994, de Deckere et al. 2000) or sediment disturbance from filter feeding currents created within the burrow (Riisgard and Schotge 2007).

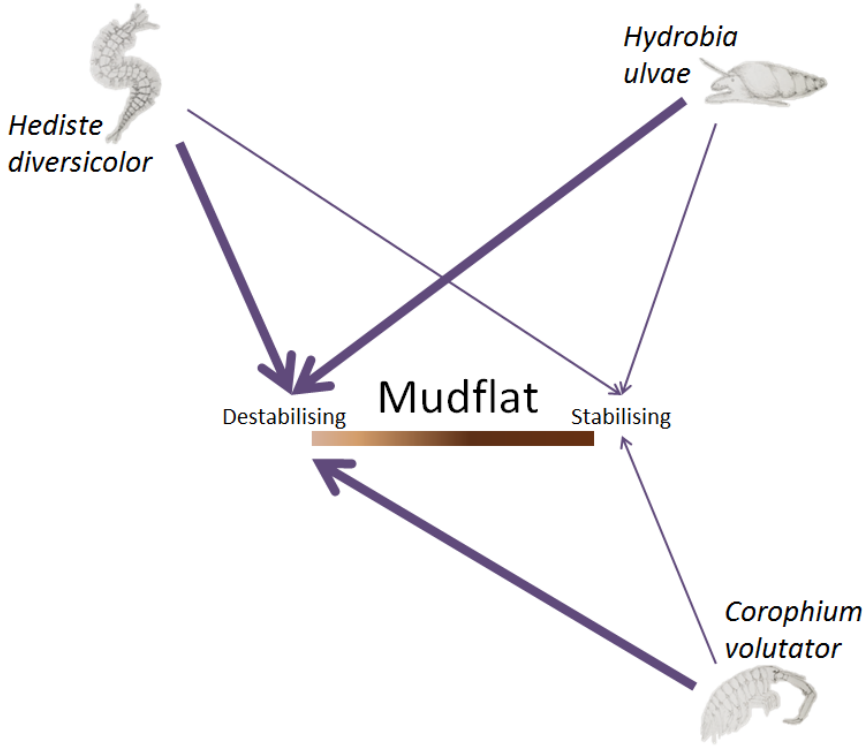

Figure 8.1 | *Hediste diversicolor*, *Hydrobia ulvae* and *Corophium volutator* may have potentially stabilising or destabilising effects on sediment properties (purple arrows). In Chapters 3 and 4, the net effects of *Hediste diversicolor*, *Hydrobia ulvae* and *Corophium volutator* were shown to be destabilising. Size of the effect on the sediment is represented by the thickness of the arrow with a greater effect shown by a thicker arrow.

8.2 | Examining Objective 2

The effect of individual macrofauna species at high and low densities in single species dominated communities was examined in Chapter 4. Increasing the species biomass density had a different effect depending on the species identity (Figure 8.2). At high species densities, intra-specific effects become important in structuring sediment properties. For example, at high densities of *Hydrobia ulvae* where intra-specific feeding rate inhibition, as observed by Levinton (1979) and Barnes (2005), may reduce the destabilising effect of the snails. In this study, *Corophium volutator* was

more destabilising (per biomass unit) at high densities than at low densities. This is perhaps due to a density dependent effect of the burrows, which at low densities may not cause significant destabilisation due to the distance between them, but at high densities the proximity of the burrows may weaken the sediment structure. Some types of intra-specific interaction may therefore only be obvious at high species densities, where interactions may be magnified (Griffin et al. 2008). In Chapter 4, *Hediste diversicolor* had no significant effect on sediment stability and there was no effect at either high or low densities. This is in contrast to an annular flume study by Widdows et al. (2009) who showed a density dependent response of sediment resuspension to *Hediste diversicolor* density.

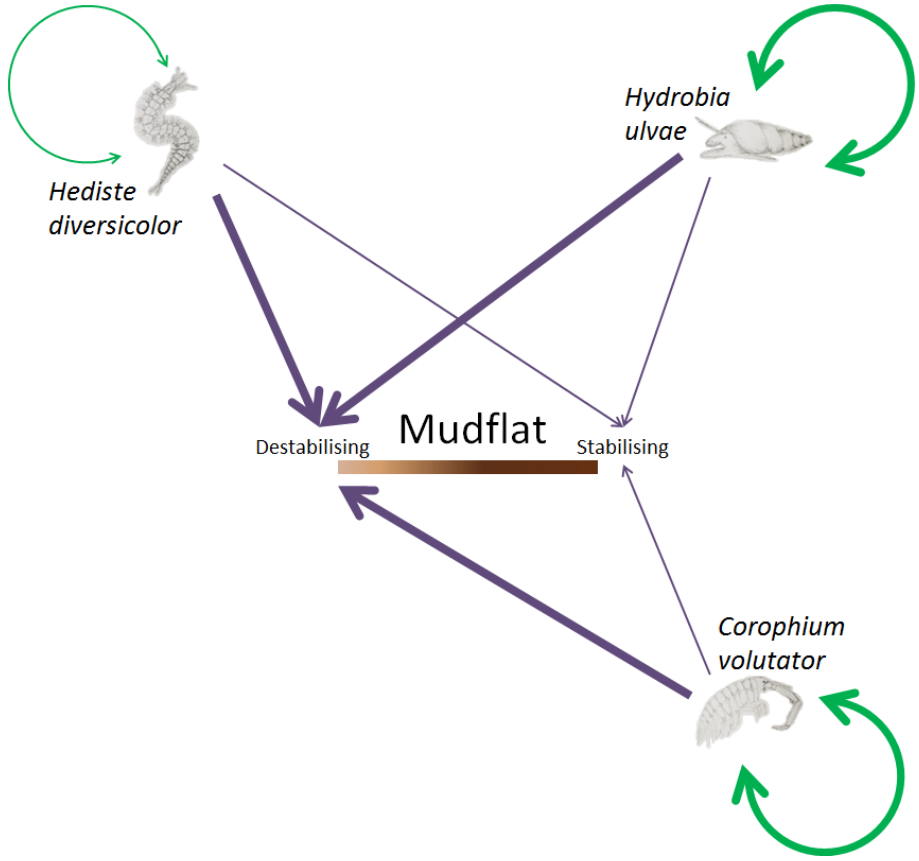

Figure 8.2 | *Hediste diversicolor*, *Hydrobia ulvae* and *Corophium volutator* may have potentially stabilising or destabilising effects on sediment properties (purple arrows) and intra-specific interactions (green arrows) moderate these effects. In Chapters 3 and 4, the net effects of *Hediste diversicolor*, *Hydrobia ulvae* and *Corophium volutator* were shown to be destabilising. In Chapter 4, the intra-specific interactions of *Hydrobia ulvae* and *Corophium volutator* were important in moderating their effect on the sediment, whereas the intra-specific interactions of *Hediste diversicolor* were less so. Size of the effect on the sediment is represented by the thickness of the arrow with a greater effect shown by a thicker arrow.

8.3 | Examining Objective 3

In terrestrial ecosystems, grassland plots with higher species richness were shown to be more productive (Tilman and Downing 1994, Tilman et al. 1996), which can occur through partitioning of the resource spectrum (Finke and Snyder 2008, Griffin et al. 2008). This has been observed in the mudflat species *Corophium volutator* and *Hydrobia ulvae* by Fenchel et al. (1975) through differential food particle size selection. Cardinale (2011) also observed similar resource partitioning in stream algal biofilms. Increased mudflat infaunal species diversity was shown to increase nutrient generation in a laboratory experiment (Ieno et al. 2006), however in a field experiment, species richness was not shown to have a significant effect on sediment shear strength, water content, particle size distribution, or nutrient flux (Bolam et al. 2002). Our results agree with the findings of Bolam et al. (2002) in that while dominant in the community, the three species examined in this thesis were shown to have different and distinct effects on sediment properties, however, when in combination, the species underperformed and had less of an effect on sediment biogeochemical properties compared to their dominant counterparts. This indicates that mudflat species interactions and indirect effects are more important as species richness increases, however the specific interactions occurring and the strength of these interactions are not obvious in the experiment in Chapter 4 when all three species are combined.

8.4 | Examining Objective 4

When the species of interest are held in two species combinations and the species biomass distribution is varied (as in Chapter 5), the species interactions occurring may be examined in more detail. In this study the effects of *Hydrobia ulvae* and *Corophium volutator* that were observed when these species were held in single species dominant communities could still be seen in the two species mixtures (Figure 8.3). It is the species present (Emmerson et al. 2001, Bolam et al. 2002, Ieno et al. 2006, Allen and Vaughn 2011) and the interactions occurring between them (Olafsson and Persson 1986) that are the most important in determining the sediment erodibility and other biogeochemical properties. In artificial streams in which mussel species and trait richness was manipulated, at high species densities,

certain combinations of species showed non-additive effects on erosion and the identity of the species in the mixture was important (Allen and Vaughn 2011). In a field experiment, Bolam et al. (2002) showed that in species mixtures, sediment properties may be controlled by the presence of a particular engineer organism. Olafsson and Persson (1986) showed the interaction between *Hediste diversicolor* and *Corophium volutator* was so significant that it may be a habitat structuring force in shallow brackish sediments. The effects observed in Chapter 5 were density dependent and variation between species biomass distribution treatments was observed. This indicates that for some species combinations there may be density dependent intra-specific effects occurring or a density threshold for the inter-specific interactions occurring (Figure 8.3; Sala and Knowlton 2006, Steneck et al. 2004). In an experiment examining ecosystem processes and evenness in a terrestrial field, total and belowground biomass production was found to increase with increasing evenness, but aboveground biomass was more dependent on the identity of the dominant species (Wilsey and Potvin 2000). In Chapter 5, those treatments with equal species biomass allocation (HDHU, HDCV, and HUCV) did not show any significant patterns that would indicate that evenness of biomass resulted in increased sediment stability or instability or greater microphytobenthos productivity.

8.5 | Examining Objective 5

The pilot experiment in Chapter 3 and the experiments in Chapters 4 and 5 showed that defaunation results in an increase in the biomass of the microphytobenthos and an increase in sediment stability. This supports previous manipulative defaunation work where Davis and Lee (1983) found that defaunation resulted in an increase in microphytobenthos biomass and De Deckere et al. (2001) showed that a reduction in infauna, and in particular *Hediste diversicolor* resulted in an increase in sediment stability. Van Colen et al. (2008) found that successional changes during benthic community recovery after induced hypoxia immediately resulted in a shift in functional group dominance from stabilising microphytobenthos in the early stages of recovery to biodestabilising macrofauna in the later stages.

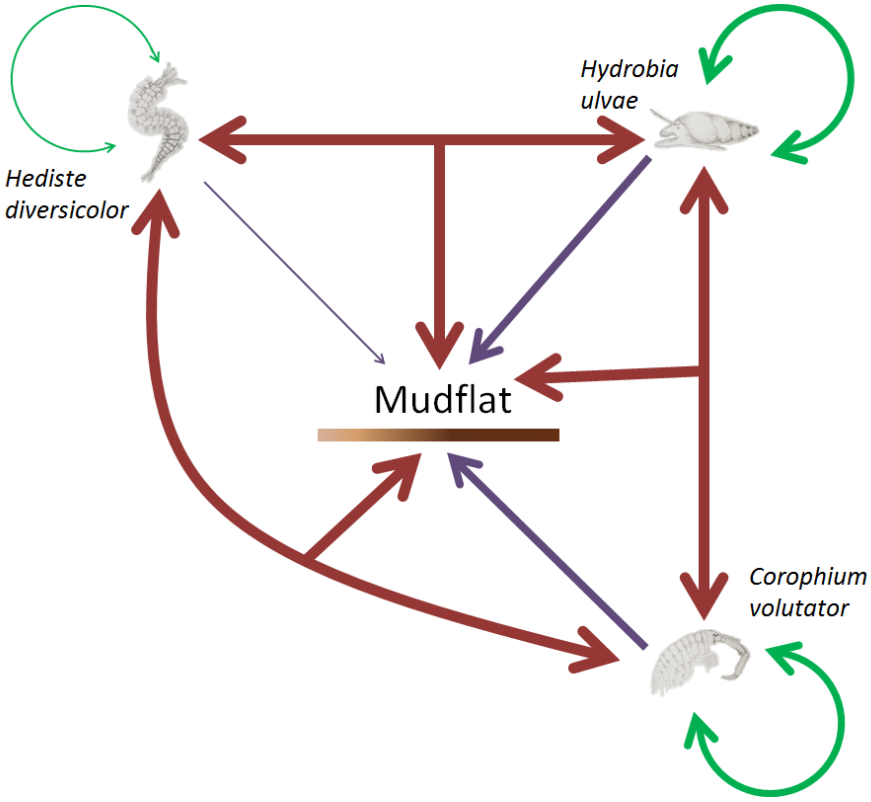

Figure 8.3 | Measurement of sediment properties using experimental treatments consisting of different species biomass distributions (Chapter 5) reveals that species specific effects (purple arrows), intra-specific density dependent effects (green arrows) and inter-specific density dependent effects (red arrows) are important in mudflat ecosystem structuring. In Chapters 3 and 4, the destabilising effects of *Hediste diversicolor*, *Hydrobia ulvae* and *Corophium volutator* were shown to be destabilising. The direct effects of *Hydrobia* and *Corophium* were still discernable on sediment properties in the two species mixtures, however those of *Hediste diversicolor* were not. In Chapter 4, the intra-specific interactions of *Hydrobia ulvae* and *Corophium volutator* were important in moderating their effect on the sediment and the intra-specific interactions of *Hediste diversicolor* were less so. These intra-specific density dependent effects were still important in multiple species mixtures. In Chapter 5, the interactions between the three species, when held in two species combinations, were the most important in structuring sediment processes. Size of the effect on the sediment is represented by the thickness of the arrow with a greater effect shown by a thicker arrow.

In Chapter 6, additional biomass of each species was added to a natural community. This experiment examined how fluctuations in species biomass distribution in a natural community might affect the sediment properties. Natural fluctuations in species abundances have previously been shown to result in changes in sediment topography and characteristics (Olafsson and Persson 1986, Mouritsen et al. 1998, Hagerthey et al. 2002, Kelaher et al. 2003). While the replacement of species biomass (in equal mixtures or with single species dominance) to defaunated sediment resulted

in significant changes to the biogeochemical properties of the sediment, the addition of an extra 50 % of the total biomass of a single species to a natural community resulted in few significant changes compared to the procedural control. Sediment stability, microphytobenthos biomass and health, and the physical characteristics of the mudflat appear robust to change when species biomass distribution and abundances are manipulated within an already functioning community. In Chapter 6, the sediment erosion threshold fluctuated more in response to changes in the microphytobenthos biomass unrelated to changes in macrofaunal species abundance. The effects of species abundance fluctuations may be regulated by their indirect inter- and intra-specific effects. Levinton (1979) and Barnes (2005) showed that *Hydrobia* species have a density dependent intra-specific dependent effect on feeding rates. When both *Hediste* and *Corophium* are present in an area of mudflat they will disturb each other resulting in reduced numbers of one or the other (Olafsson and Persson 1986). Fargione et al. (2003) found that when adding (as a seed) grassland perennials that are found locally but not present in the test area to an already established test area as an 'invasive' species the introduced species attained lower abundances even though they were functionally similar to species already prevalent in the community, indicating competitive inhibition of invaders. A similar action of competitive inhibition from already established species could be occurring in this experiment, preventing the added biomass from having a significant effect on sedimentary properties. Behavioural and activity moderation, as a result as inter- and intra-specific interactions, are perhaps more important than previously thought with respect to the effect of the species on sediment erosion, microphytobenthos biomass and health, and physical characteristics. In natural communities, there will also be environmental fluctuations, causing effects on species and potentially affecting their inter- and intra-specific interactions.

When making predictions about whether macrofaunal species density fluctuations will affect the mudflat, the effect of changes in individual species abundance when dominant cannot predict their effects in a community. Thus, the utility of laboratory or field studies on single species is limited.

8.6 | Examining Objective 6

In many previous studies, bioturbation has been shown to be a key factor in regulating sediment stability (Rhoads and Young 1970, Rowe 1974, Meadows and Tait 1989, Grant and Daborn 1994, Mouritsen et al. 1998, Palomo and Iribarne 2000, de Deckere et al. 2001, Sgro et al. 2005, Widdows et al. 2009) and ecosystem function in the marine benthos (Ieno et al. 2006, Solan et al. 2008). In the field experiments carried out in chapters 3, 4, 5 and 6, bioturbation through burrow creation, maintenance, grazing activities and sediment disturbance are significant factors in determining sediment stability.

Chapter 7 combined high-resolution two-dimensional measurements of the active transport of fluid and sediment particles with three-dimensional reconstructions of burrow geometry to examine the subtle aspects of organism-sediment interactions. *Hediste diversicolor* was revealed to have a more extensive burrow network than implied from the mixing profile determined using sediment profile imaging and *Hydrobia ulvae* had deeper burrows than expected from previous descriptions (see Newell 1962, Little and Nix 1976, Orvain and Sariau 2002). The data produced from these types of studies will be critical in determining the small scale relationships between organisms and their sediment habitat. Visualisation of subsurface sediment working by *Hediste diversicolor*, *Hydrobia ulvae*, *Corophium volutator* and other species is essential for establishing the functional role of benthic biodiversity at regional and global scales.

8.7 | Limitations

8.7.1 | Field study limitations

There were a number of limitations identified with the field experiments undertaken in this thesis:

1. Cryo-defaunation does not provide complete eradication of all living macro-fauna in the sediment cores.

As discussed in Chapter 3, this defaunation method is a compromise between defaunation effort, time, sediment disruption, cost and efficacy. After two weeks in the field a large reduction in abundance of the species of interest is maintained. Using cryo-defaunation was the most appropriate methodology for these experiments, where minimizing changes to the sediment properties was of paramount importance. When sediment defaunation is required, the methodology used will depend upon the experiment in question and there is no one 'correct' method of defaunation. There are numerous possible methods, each with a trade-off between efficacy, disruption, cost and time required (Tolhurst et al. 2012).

2. The mesocosm used had a sometimes significant and variable effect on sediment biogeochemical properties and always increased sediment stability.

The mesocosms were a necessary structure required to reduce, if not prevent, settling of fauna in the defaunated sediment cores, escape of the species biomass added, and migration into and/or out of the defaunated area. The addition of species to the mudflat without a mesocosm was trialled before undertaking these experiments. Unfortunately, due to the nature of the mudflats and the mobility of the species no increase in species abundance or species biomass was observed after species addition without a mesocosm. This series of manipulative experiments would not have been possible without the use of a mesocosm. The mesocosms used in this project were designed to cause minimum impact on sediment properties, however, in light of the fact that the use of a mesocosm affected some of the properties of the sediments inside, all experimental treatments were compared to a procedural

control consisting of mudflat sediments held within a mesocosm, rather than being compared to open mudflat sediments. When examining comparative effects of species treatments on sediment stability and biogeochemical properties the use of a procedural control as a baseline comparison, allowing experiments to take place *in situ,* is more representative of a natural situation than experiments carried out in a laboratory. Future *in situ* species manipulation experiments could benefit from the use of alternative mesocosms where the effect on sediment properties has been reduced further, or development of a method where a mesocosm is not required.

3. Temporal and spatial variation between experiments is not taken into account.

While temporal and spatial confounding of the experiments carried out was kept to a minimum, a number of issues were identified. *Hediste diversicolor* was observed to cause both significant destabilisation of the sediment in the pilot experiment (Chapter 3) and have no significant effect on stability (Chapter 4) when added to cryo-defaunated cores as a single dominant species. These two experiments had almost exactly the same setup procedures, however there were temporal and spatial differences between these studies that could have caused the change in results observed. Firstly, the experiments were carried out in different, but adjacent locations on the mudflat. All four field experiments were carried out in the same bay, with visually similar mudflat characteristics, containing the same species, however previous studies have shown that mudflats may have greater variation in sediment properties within the same bay than between bays (Chapman and Tolhurst 2007, Chapman et al. 2010). Secondly, the two experiments were carried out at different times of the year, with the pilot experiment (Chapter 3) carried out in April, whereas the experiment presented in Chapter 4 was carried out in August and September. This temporal variation in the effect of a species treatment could be due to natural seasonal changes in the mudflat and its flora and fauna resulting in changes in environmental, intra- and inter-specific interactions. The effect of this temporal variation was also observed in the varying effects of the presence of the mesocosm and defaunation (treatments P and PD) in Chapters 3, 4, 5,

and 6, and the two 3 species treatments (treatment Mix_2) in the experiments in Chapters 4 and 5.

The temporal variation between experiments means that the species effects between experiments cannot be directly compared, only their effects compared to the procedural or defaunation control, and even then only with caution. To interpret any spatial or temporal changes we need more information to describe the variability in the data, which could be due to a number of factors including nutrient distribution, tidal effects, or weather. Ideally, the full range of treatments would have been carried out throughout the year to provide a full picture of the effects of seasonal variation on species interactions and sediment properties (Raffaelli et al. 2003b).

4. The influence of only three species on sediment stability and biogeochemical properties was investigated.

As discussed in Section 2.1.1, Chapter 2, three species, *Hediste diversicolor*, *Hydrobia ulvae* and *Corophium volutator*, were used in this study. These species were primarily chosen on the basis of their abundance at the experimental site, the ease of collection *in situ* and their contrasting feeding and burrowing behaviours. An additional advantage of using these species was that many studies have already investigated their behaviours in the laboratory and *in situ*, meaning that the effect of these species on sediment stability, microphytobenthos biomass and sediment particle size can be attributed to species activities and behaviours already observed and studied (see for example Meadows and Tait 1989, Grant and Daborn 1994, Smith et al. 1996, Blanchard et al. 1997, Mouritsen et al. 1998, Austen et al. 1999, de Deckere et al. 2000, Andersen 2001, de Deckere et al. 2001, Biles et al. 2002, Orvain and Sauriau 2002, Orvain et al. 2004, Orvain et al. 2006, Widdows et al. 2009).

The mudflats at Breydon Water, Norfolk, UK contain a very limited number of species. The total species number found in all samples was 20; 6 species were found in most core benthic samples, another 5 were found frequently in the benthic samples, and the rest found rarely. Five species were found in only one sample. This series of experiments has identified that

even within this simple system, many complex interactions occur between the macrofauna studied, the microphytobenthos, and the environment, as well as other taxa not studied (such as bacteria, fungi, meiofauna, pelagic species).

Other common mudflat species, such as *Macoma balthica*, *Tubificoides* spp. and *Spio* spp., were numerous at the study site in some areas and contributed a substantial amount to the species biomass in that area (up to 20 %). These species were rejected for use in this study due to small body size meaning collection and identification in the field was difficult and time consuming. *Macoma balthica*, a species used commonly for similar mudflat biodiversity manipulative experiments, was rejected for use due to the small size of individuals found at the field site, indicating the specimens found were probably juveniles, and the difficulty of distinguishing live from dead individuals in the field. As well as these common species, in the benthic cores examined as part of this thesis I have identified a number of other meiofaunal and rare mudflat species. Meiofaunal species identified, whose effects on the sediment have not been assessed, included *Tubificoides benedii*, *Streblospio shrubsolii*, *Ampharete* sp. and the Nematoda. Rare macrofauna encountered included isopods, tanaids, gammarid shrimps, juvenile crabs and juvenile shrimp. The effect of these species at the field site remain unknown and future work should consider their effects. For example, even small biomasses of one of these species could cause significant changes in the behaviour of a more numerous species (Daborn et al. 1993) or support important ecosystem processes (Lyons and Schwartz 2001, Mouillot et al. 2013). The use of a limited pool of species, consisting of the most common at the experimental site, however, allowed characterisation of the effects of these species in greater detail.

Other limitations of this study include the inability to take account of any subtle effects that may cause changes in sediment stability and the other biogeochemical processes measured over longer timescales. This includes any community level effects caused by the direct and indirect effects of the species combinations investigated on larval recruitment or development and other factors not assessed.

8.7.2 | Laboratory study limitations

As a laboratory study, the experiment presented in Chapter 7 has a different range of limitations, in that is does not represent a natural situation (Skelly and Kiesecker 2001, Petersen et al. 2009, Hale et al. 2011). The use of replicated laboratory mesocosms in this case allowed the application of a novel investigative technique that is currently not possible in the intertidal environment.

8.7.3 | Equipment limitations

The cohesive strength meter (CSM) is a powerful portable device to determine sediment erosion threshold and potential sediment erosion rates (Tolhurst et al. 1999), however, due to the small portable design it is limited in the area of sediment it can analyse. The erosion chamber has an aperture diameter of 2.8 cm and can only determine the erosion characteristics of that area. The diameter of the mesocosms used was 16 cm and within that area it could be seen that there were variations in the sediment that would probably result in variations in the erosion characteristics. To standardise the measurements taken, cohesive strength tests were always taken in the same area of the mesocosm, to provide comparable erosion thresholds among treatments, however, this is not representative of the erosion characteristics of the whole mesocosm. A similar limitation was overcome when using the pulse amplitude modulated fluorometer (PAM), because its very rapid deployment time and very small footprint meant 3 replicate measurements could be taken in each mesocosm. This was not possible for the CSM due to the time needed to take measurements and the requirement of an area of undisturbed sediment to take a measurement.

8.8 | Future Work

There are a number of important points that can be taken from these studies that are relevant for future research in this area.

Selective laboratory experiments looking at a single aspect of actions of species or changing biotic or environmental variables can be informative in

deciphering the main effects of a species, but more realistic experiments in the field with environmental variation and the full range of species are needed. Field experiments in a natural setting are more ecologically relevant (Fridley 2001). The community composition as a whole, with the many inter- and intra- specific interactions occurring (Menge 1995), both direct and indirect, is a better determinant of the overall functioning of the ecosystem than the examination of a single species (Biles et al. 2002). While the effects of species in abstract situations, such as those in the lab and in unrealistic situations in the field, i.e. in monoculture, can provide valuable insights into the actions and behaviours of individual species, these behaviours may not be the same as those observed in a natural community setting. Future experiments should concentrate on teasing out the effects of individual species within a community, including environmental and biological variability in the field. Analysis using X-ray computed tomography could also be used on undisturbed natural sediment cores. Future work should also examine the effect of rare species within the community, not just common species.

8.9 | Interpreting biodiversity effects on mudflat sediment stability and biogeochemical processes

Contextual interpretation of these results requires careful attention to published data, especially as there have been many laboratory and field studies that have shown macrofaunal species to have antagonistic and contrasting effects on sediment stability and biogeochemical properties (even within the same study). For example, Mouritsen et al. (1998) concluded that *Corophium volutator* both stabilised the sediment by the creation of burrows and the stabilisation of these burrows, but also that diatom grazing by *Corophium* caused indirect destabilisation of the sediment. This study indicates that the effects of the three species studied on mudflat biogeochemical properties may be context dependent on species and environmental interactions, resulting in the variation of responses seen to the addition of species and species combinations.

In some cases it seems that a single organism can have as great an effect on selected ecosystem processes as a whole community (e.g. the effects of *Hediste diversicolor* in the experiment carried out in Chapter 3 and

Hydrobia ulvae in the experiment carried out in Chapter 4 on sediment stability) indicating that, under certain conditions, species identity rather than richness may be the key factor in delivering selected ecosystem processes. In the experiments examining the effects of species richness it even appears that species richness effects are negatively interactive with species rich treatments underyielding compared to their counterparts in single species dominant communities. It is likely additional subtle aspects of biodiversity, such as species density (Polley et al. 2003), species evenness (Wilsey and Potvin 2000, Wilsey and Polley 2004, Maestre et al. 2012), and spatial distribution of species biomass (Maestre et al. 2012) will prove to be key in the determination of the relationship between biodiversity and ecosystem processes. The importance of species density was emphasised in Chapter 4 where intra-specific interactions significantly changed the effect of some species on the measured sedimentary processes. Additionally, some species may exhibit a functional abundance threshold, below which they do not contribute significantly to ecosystem processes. Changes in the species biomass allocation resulted in significant changes to the effects of two species combinations on sediment processes in Chapter 5. Temporal and spatial variability observed in the experiments has emphasised the potential of environmental and abiotic factors to influence ecosystem processes. The effect of species biomass addition to established communities in Chapter 6 highlights the limitations of predicting ecosystem level responses using single species experiments because species were found to cause different effects when added to a community than when added to sediment as a dominant species. Finally, the visualisation of bioturbation in sediment cores in Chapter 7 showed that the three species, *Hediste diversicolor*, *Hydrobia ulvae* and *Corophium volutator* can cause significant sediment mixing, creating distinct networks of burrows and burrow structures. This suggests that there is a great deal of new information we can gain through the application of new techniques and methodologies to this field which will provide powerful tools for the analysis of biodiversity and ecosystem process relationships.

Interpretation of experimental data on the effect of biodiversity on ecosystem processes as an idiosyncratic relationship (Lawton 1994) is most likely due to the unknown influences of rare species and temporal and spatial environmental variability (Levin 1992). The allocation of variability in

ecosystem processes to currently unquantified variables may help to decode how species interact with their environment and each other.

With many interacting factors, and temporal and spatial variation, interpreting the changes observed in the mudflat ecosystem can be challenging. At some fundamental level the system must behave in a predictable way; it is not complete chaos. The presence and longevity of mudflats as a habitat is proof of that. While there is inherent variation in the mudflat ecosystem there must be a natural upper and lower limit for sediment stability. Barring extreme events, one does not usually observe the presence of a mudflat one day, only to find that it has been eroded and replaced by sand banks or open sea the next week. If the sediment got too unstable there would be no mudflat. If the mudflat got too stable there would be fewer or no burrowing organisms (e.g. *Hydrobia ulvae* does not burrow if the sediment is too hard, Little and Nix 1976), and the mudflat ecosystem as we know if would not exist. There must be an underlying ecosystem stability or a dynamic 'equilibrium' within the mudflat sediment stability continuum, with significant variability from this caused by physical, chemical and biological changes.

While it is possible all the variation observed in this study may be attributable to different factors present on the mudflat and their interactions, only a limited number of variables were measured in this project. To keep the discussion manageable and relevant I have considered some of the most likely factors affecting mudflat stability related to the changes observed in the measured sediment biogeochemical properties (based on my own experience and the published literature). There are, however, many other possible models that could explain the patterns seen in these experiments, so the discussions presented in this thesis should not be considered exhaustive.

What is striking is how different researchers find different things to be important that usually relate to their area of expertise, or what they are looking at, meaning important alternative interpretations of the data may be missed. Just because correlations or changes in some properties are observed when certain aspects are manipulated does not mean we can assume a direct relationship. It is quite likely that a lot of the changes

observed in this thesis are indirect. For example, many of the changes observed as a result of changing species identity or density in this study appear to be as a result of the effect of macrofauna species on the microphytobenthos. Many of these effects may, however, be mediated through something we are not even looking at, such as bacteria. Future effort needs to try and take a holistic approach, examining as many variables as possible, with no bias towards what is believed to be important, or the investigator's specialist area. This is slowly happening, as more data are collected and new insights will be provided by the novel application of new technologies such as remote sensing and computed tomography.

A Retrospective Reflection on the Thesis

Upon completion of this thesis and the viva examination a number of reflections on this work are worth consideration for those who may wish to use this thesis are a reference for future work.

Statistical Analyses

When selecting suitable statistical analyses for the data produced there were a number of options which may have provided a robust analysis. My data showed residual spread varying per treatment, violating the assumption of homogeneity of variance, one of the most important assumptions of linear regression. The distribution of the residuals of many of the variables showed skew (e.g. in Chapter 4 the erosion threshold data, sediment suspension index, minicore mean sediment particle size, contact core carbohydrate concentration, contact core chlorophyll *a* concentration, contact core chlorophyll *b* concentration) or a bimodal distribution (e.g. Chapter 4 the pulse amplitude modulated microphytobenthos minimum fluorescence, minicore water content). Ignoring these issues may result in statistical parameters with incorrect standard errors and a non-F-distributed F statistic, invalidating the ability of parametric statistics to assess statistical significance.

One solution to this problem is data transformation however to enable the incorporation of this heterogeneity into the statistical models I used the generalised least squares statistical method. The use of parametric ANOVAs and ANCOVAs with suitable post-hoc tests however would have provided a more powerful statistical method to analyse the data, giving sufficient degrees of freedom to explore two-way interactions. Transformations were applied to the data however many treatments still had greater variation between replicates than others after a range of transformations had been tested and a generalised least squares approach was chosen allowing for different variances.

There were some datasets where from the graphs produced with standard error bars it appeared that some treatments should be significantly

different from others. For example, on Chapter 4, Figure 4.14 shows the effect of sediment treatments on the skew in particle size distribution. The distribution skew of the natural sediment (N) is clearly larger than that of many of the other treatments and the standard error bars do not overlap. These data were retested using a linear model ANOVA with post hoc pairwise tests and Bonferroni's correction applied. In this case the sediment particle size distribution skew in the natural sediment is significantly different from that of the low biomass Corophium treatment ($p = 0.032$), but none of the other treatments.

When investigating the effects of Day (Chapters 4 and 5) and Row (Chapters 3, 4, 5 and 6) on sediment properties I did not carry out two-way analysis of treatment and either day or row due to the fact this would have reduced the replicates (degrees of freedom) for the interaction terms as there were 2 days, 4 rows and 6 replicates of each treatment. In retrospect the experiment could have been adapted to allow this to block for any effects of day or row by reducing the number of treatments and increasing the number of replicates for each treatment.

When analysing the change in sediment characteristics over sampling time during the pilot experiment presented in Chapter 3 (page 90) regressions were run on pooled data regardless of treatment. Any effect or lack of effect identified statistically may therefore be due to a masking effect in the pooled data hiding any significant effects within treatments. Due to the low replication of the majority of the treatments in this study ($n = 4$) it is difficult to discern any differences among treatments. On the preceding seven graphs each treatment type is represented by a different point type to enable examination of the effects of each treatment on the examined variables over the time elapsed. In some cases a non-linear regression would have been more appropriate. For example, in the treatments where *Hediste diversicolor* and *Hydrobia ulvae* were added, the erosion threshold is becoming smaller over time in an exponential manner. In the experiments carried out in Chapters 4, 5 and 6 data collection commenced over 45 minutes after tidal retreat from the experimental site. This was to ensure there was no effect on the erosion threshold from unequal drainage or variation in sediment stability in the initial dewatering period and no

consistent decline in sediment characteristics were observed after this period in the pilot experiment or the experiments in Chapters 4, 5 and 6.

With respect to the D_{sp}, D_T, D_{max} and D_{min} statistics I have chosen not to statistically test when the deviation of the observed value is significantly different from the calculated value expected. The expected statistic is generated using the maximum, minimum or mean values measured during experimentation. These expected values are therefore calculated from a subset of values within the actual potential range of the data. The mean values generated could also be expressed as a range based on calculations from the minimum and maximum values. Many users of this method do not statistically test the significance of the difference between the observed and expected values (Bruno et al. 2005, Wilkinson et al. 2010). Derived measures produced using similar calculations as in this thesis can be statistically analysed using general linear models (Roscher et al. 2005) however, they identify that these variables have more complicated theoretical distribution functions than the normal distribution assumed for general linear models.

Without using statistical analysis, it has been suggested the net biodiversity effect, the difference between the mixture and the average monoculture species, has to be at least as large as the difference between the best and average monoculture species to be considered to overyield (Schmid et al. 2008).

Thesis Structure

This thesis represents a large body of work carried out as 3 main field experiments and a single laboratory experiment. The field measurements, sediment samples and data analysis carried out during each experiment were similar. In retrospect, repetition of methodological descriptions and data interpretation, such as the effect of sediment defaunation, the use of mesocosms and the effect of the species treatments on each sediment characteristic could have been prevented if the thesis had been structured differently. With such a large body of work there are a number of ways that the thesis could have been structured. The chapters could have been based

around the effect of the treatments on different sediment characteristics e.g. those related to in situ sediment erosive properties (the sediment erosion threshold and the suspension index, sediment physical characteristics (sediment particle size and distribution), and microphytobenthos properties (PAM measurements and sediment carbohydrate and chlorophyll concentrations). The thesis could also have been structured so that each chapter focussed on the effects of each organism and the organisms in mixture.

The length of this thesis may have also been reduced by not including figures or where no statistically significant relationship was found (e.g. Figures 4.10, 4.11, 4.12, 4.13, and 4.14) or by combining figures such as these or those with similar legends (e.g. Figures 4.29, 4.30, and 4.31) into one figure.

The thesis would also have benefitted from being more hypothesis driven, leading to a structured piece of work with a deductive framework rather than being more lengthy and descriptive as it is. For example, when analysing Chapter 4, rather than referring to the objectives laid out in the Introduction chapter it would have been better to have a series of specific testable hypotheses.

Chapter 4 Objectives:
Objective 1 | Investigate the effect of individual macrofauna species on mudflat sediment stability and biogeochemical properties *in situ*.

Objective 2 | Investigate the effect of macrofaunal species density on mudflat sediment stability and biogeochemical properties *in situ*.

Objective 3 | Investigate the effect of macrofaunal species richness on mudflat sediment stability and biogeochemical properties *in situ*.

Chapter 4 Example Hypotheses:
The presence of *Hediste diversicolor* will reduce the sediment erosion threshold.

The presence of *Hediste diversicolor* will increase the sediment suspension index.
The presence of *Hediste diversicolor* will result in a reduction in microphytobenthos minimum fluorescence.
The presence of *Hediste diversicolor* will result in a reduction in microphytobenthos maximum yield.
The presence of *Hediste diversicolor* will result in a decrease in minicore sediment water content.
The presence of *Hediste diversicolor* will result in a decrease in minicore mean particle size.
The presence of *Hediste diversicolor* will result in a decrease in minicore mud content.
The presence of *Hediste diversicolor* will result in a decrease in contact core mean particle size.
The presence of *Hediste diversicolor* will result in a decrease in contact core sediment water concentration.
The presence of *Hediste diversicolor* will result in a decrease in contact core sediment colloidal carbohydrate concentration.
The presence of *Hediste diversicolor* will result in a decrease in sediment chlorophyll *a* concentration.
The presence of *Hediste diversicolor* will result in a decrease in contact core mud content.

These hypotheses relate to the effects of Hediste diversicolor on the sediment properties, however similar hypotheses could be drawn up for the other species of interest and the mixed species treatments. Each one of these is a statistically testable statement which can be either accepted or refuted using the data collected for this thesis.

Terminology

In the thesis I have referred to a number of sediment characteristics affecting ecosystem processes. On the Breydon Mudflat, these ecosystem processes include habitat provision for algal species, microfauna, meiofauna, macrofauna, fish and birds, facilitation of nutrient fluxes both as a sink and a source, primary production, and flood defence and storm protection of the

Norfolk coast. I have not identified which sediment characteristics affect which ecosystem processes in the text. The sediment erosion threshold and suspension index will affect nutrient fluxes in Breydon Water as resuspension of sediment is an important path of nutrient release from underlying sediments into the water column. The size of the sediment particles is also directly related to the erodability of the sediment with smaller particle more easily resuspended and has also been shown to be linked to the species diversity of mudflats with certain macrofauna species preferring sediments with particular particle size range and is therefore linked to habitat provision. Intertidal habitats are some of the most productive habitats in the world. The measurements made of microphytobenthos minimum fluorescence and maximum quantum yield give estimations of the primary productivity of the Breydon Water mudflat.

Appendix 1

Defaunation methodology 1 average dissimilarity matrix

			Control	Day 1		Day 7	
				1.5 litres	3 litres	1.5 litres	3 litres
			1	2	3	4	5
Control		1	-				
Day 1	1.5 litres	2	0.0805	-			
	3 litres	3	0.3162	0.3358	-		
Day 7	1.5 litres	4	0.1118	0.0417	0.3308	-	
	3 litres	5	0.4426	0.4583	0.1829	0.4569	-

Defaunation methodology 2 average dissimilarity matrix

		Control	Mesocosm	Cryo-defaunated
		1	2	3
Control	1	-		
Mesocosm	2	0.1772806	-	
Cryo-defaunated	3	0.6487805	0.5423197	-

Statistical model summary

Summary of statistical analysis for the 23 statistical models. For each model the initial linear regression model, the minimal adequate model with GLS estimation and a summary of the coefficient table is given. The coefficients indicate the relative performance of each treatment level relative to the relevelled baseline (as indicated). Coefficients ± SE and t-values are presented alongside corresponding significance values (in parentheses). Abbreviations: N, natural sediment as a mudflat baseline; D, cryo-defaunation treatment as a procedural control; PD, defaunated mesocosm treatment as an experimental control; HD, original biomass replacement with

equal biomass of *Hediste diversicolor*; HU, original biomass replacement with equal biomass of *Hydrobia ulvae*; Row, row location of pipe mesocosm; Treat, species treatment code [N, D, PD, HD, HU].

Model Summary 1 | Erosion Threshold (ET, Nm^{-2}) by row location of mesocosm (Row)

Initial linear regression model:

lm(ET ~ as.factor(Row))

No minimal adequate model, intercept only (Row, L-ratio = 2.363626, d.f. = 6, p = 0.3067).

Model Summary 2 | Average pulse amplitude modulated measured minimum fluorescence (PAMFAv) by row location of mesocosm (Row)

Initial linear regression model:

lm(PAMFAv ~ as.factor(Row))

No minimal adequate model, intercept only (Row, L-ratio = 0.1699412, d.f. = 6, p = 0.9185).

Model Summary 3 | Minicore D_{10} (D_{10}, µm) by row location of mesocosm (Row)

Initial linear regression model:

lm(D_{10} ~ as.factor(Row))

No minimal adequate model, intercept only (Row, L-ratio = 0.692956, d.f. = 6, p = 0.7072).

Model Summary 4 | Erosion Threshold (ET, Nm^{-2}) by species treatment (Treat)

Initial linear regression model:

lm(ET ~ as.factor(Treat))

Minimal adequate model:

gls(ET ~ as.factor(Treat),

weights = varIdent(form = ~1|as.factor(Treat)),

method = 'REML')

Coefficient Table

Intercept ± SE (when baseline is for N): 0.29 ± 0.06, t = 4.56, p = 0.0003.

	N	D	PD	HD	HU
N	-	0.50 ± 0.41 1.21 0.2425	1.08 ± 0.34 3.18 **0.0055**	0.18 ± 0.10 1.69 0.1099	0.39 ± 0.19 2.04 0.0571
D	-0.50 ± 0.41 -1.21 0.2425	-	0.58 ± 0.53 1.10 0.2854	-0.32 ± 0.41 -0.78 0.4477	-0.11 ± 0.45 -0.24 0.8165
PD	-1.08 ± 0.34 -3.18 **0.0055**	-0.58 ± 0.53 -1.10 0.2854	-	-0.90 ± 0.34 -2.63 **0.0176**	-0.69 ± 0.38 -1.80 0.0890
HD	-0.18 ± 0.10 -1.69 0.1099	0.32 ± 0.41 0.78 0.4477	0.90 ± 0.34 2.63 **0.0176**	-	0.22 ± 0.20 1.09 0.2918
HU	-0.39 ± 0.19 -2.04 0.0571	0.11 ± 0.45 0.24 0.8165	0.69 ± 0.38 1.80 0.0890	-0.22 ± 0.20 -1.09 0.2918	-

Model Summary 5 | Suspension index (SI) by species treatment (Treat)

Initial linear regression model:

lm(SI ~ as.factor(Treat))

Minimal adequate model:

gls(SI ~ as.factor(Treat),

weights = varIdent(form = ~1|as.factor(Treat)),

method = 'REML')

Coefficient Table

Intercept ± SE (when baseline is for N): 15.57 ± 1.34, t = 11.66, p < 0.0001.

	N	D	PD	HD	HU
N	-	-2.92 ± 3.49 -0.84 0.4143	-9.03 ± 2.43 -3.72 **0.0017**	-0.56 ± 1.72 -0.33 0.7476	-7.69 ± 2.54 -3.02 **0.0077**
D	2.92 ± 3.49 0.84 0.4143	-	-6.11 ± 3.81 -1.61 0.1267	2.36 ± 3.40 0.69 0.4971	-4.77 ± 3.88 -1.23 0.2361
PD	9.03 ± 2.43 3.72 **0.0017**	6.11 ± 3.81 1.61 0.1267	-	8.47 ± 2.30 3.69 **0.0018**	1.35 ± 2.97 0.45 0.6556
HD	0.56 ± 1.72 0.33 0.7476	-2.36 ± 3.40 -0.69 0.4971	-8.47 ± 2.30 -3.69 **0.0018**	-	-7.13 ± 2.42 -2.95 **0.0090**
HU	7.69 ± 2.54 3.02 **0.0077**	4.77 ± 3.88 1.23 0.2361	-1.35 ± 2.97 -0.45 0.6556	7.13 ± 2.42 2.95 **0.0090**	-

Model Summary 6 | Average pulse amplitude modulated measured minimum fluorescence (PAMFAv) by species treatment (Treat)

Initial linear regression model:

```
lm(PAMFAv ~ as.factor(Treat))
```

Minimal adequate model:

```
gls(PAMFAv ~ as.factor(Treat),
    weights = varIdent(form = ~1|as.factor(Treat)),
    method = 'REML')
```

Coefficient Table

Intercept ± SE (when baseline is for N): 413.94 ± 31.97, t = 12.94, p < 0.0001.

	N	D	PD	HD	HU
N	-	213.14 ± 104.37 2.04 0.0570	808.06 ± 167.53 4.82 **0.0002**	399.97 ± 172.29 2.32 **0.0329**	701.64 ± 192.37 3.65 **0.0020**
D	-213.14 ± 104.37 -2.04 0.0570	-	594.92 ± 192.13 3.10 **0.0066**	186.83 ± 196.29 0.95 0.3545	488.50 ± 214.13 2.28 **0.0357**
PD	-808.06 ± 167.53 -4.82 **0.0002**	-594.92 ± 192.13 -3.10 **0.0066**	-	-408.08 ± 236.02 -1.73 0.1019	-106.42 ± 251.05 -0.42 0.6770
HD	-399.97 ± 172.29 -2.32 **0.0329**	-186.83 ± 196.29 -0.95 0.3545	408.08 ± 236.02 1.73 0.1019	-	301.67 ± 254.25 1.19 0.2517
HU	-701.64 ± 192.37 -3.65 **0.0020**	-488.50 ± 214.13 -2.28 **0.0357**	106.42 ± 251.05 0.42 0.6770	-301.67 ± 254.25 -1.19 0.2517	-

Model Summary 7 | Average pulse amplitude modulated measured maximum quantum yield (PAMYAv) by species treatment (Treat)

Initial linear regression model:

lm(PAMYAv ~ as.factor(Treat))

No minimal adequate model, intercept only (Treat, L-ratio = 1.771441, d.f. = 4, p = 0.7777).

Model Summary 8 | Minicore mean particle size (MCMean, µm) by species treatment (Treat)

Initial linear regression model:

lm(MCMean ~ as.factor(Treat))

No minimal adequate model, intercept only (Treat, L-ratio =7.772078, d.f. = 6, p = 0.1003).

Model Summary 9 | Minicore D_{10} (D_{10}, µm) by species treatment (Treat)

Initial linear regression model:

lm(D_{10} ~ as.factor(Treat))

Minimal adequate model:

gls(D_{10} ~ as.factor(Treat),
weights = varIdent(form = ~1|as.factor(Treat)),
method = 'REML')

Coefficient Table

Intercept ± SE (when baseline is for N): 8.96 ± 0.34, t = 26.11, p < 0.0001.

	N	D	PD	HD	HU
N	-	-0.15 ± 0.69 -0.22 0.8300	1.50 ± 0.41 3.63 **0.0021**	1.26 ± 0.76 1.66 0.1156	1.42 ± 0.51 2.78 **0.0128**
D	0.15 ± 0.69 0.22 0.8300	-	1.65 ± 0.65 2.56 **0.0204**	1.41 ± 0.91 1.55 0.1387	1.57 ± 0.71 2.20 **0.0416**
PD	-1.50 ± 0.41 -3.63 **0.0021**	-1.65 ± 0.65 -2.56 **0.0204**	-	-0.25 ± 0.71 -0.34 0.7348	-0.08 ± 0.44 -0.19 0.8510
HD	-1.26 ± 0.76 -1.66 0.1156	-1.41 ± 0.91 -1.55 0.1387	0.25 ± 0.71 0.34 0.7348	-	0.16 ± 0.77 0.21 0.8370
HU	-1.42 ± 0.51 -2.78 **0.0128**	-1.57 ± 0.71 -2.20 **0.0416**	0.08 ± 0.44 0.19 0.8510	-0.16 ± 0.77 -0.21 0.8370	-

Model Summary 10 | Minicore mud content (MCMud%, %) by species treatment (Treat)

Initial linear regression model:

lm(MCMud% ~ as.factor(Treat))

No minimal adequate model, intercept only (Treat, L-ratio = 6.841376, d.f. = 6, p = 0.1445).

Appendix 2

Statistical model summary

Summary of the statistical analysis for the 23 statistical models. For each model the initial linear regression model, the minimal adequate model with GLS estimation and a summary of the coefficient table is given. The coefficients indicate the relative performance of each treatment level relative to the relevelled baseline (as indicated). Coefficients ± SE and t-values are presented alongside corresponding significance values (in parentheses). Abbreviations: N, natural sediment as a mudflat baseline; P, pipe mesocosm only treatment as a procedural control; PD, defaunated mesocosm treatment as an experimental control; HD_1, original biomass replaced with *Hediste diversicolor*; HD_2, $^1/_3$ original biomass replaced with *Hediste diversicolor*; HU_1, original biomass replaced with *Hydrobia ulvae*; HU_2, $^1/_3$ original biomass replaced with *Hydrobia ulvae*; CV_1, original biomass replaced with *Corophium volutator*; CV_2, $^1/_3$ original biomass replaced with *Corophium volutator*; Mix_1, biomass replaced with an equal mix of HD, HU and CV to three times the original biomass; Mix_2, biomass replaced with an equal mix of HD, HU and CV to the original biomass; Day, day of data collection; Row, row location of pipe mesocosm; Tcode, species treatment code [N, P, PF, HD_1, HD_2, HU_1, HU_2, CV_1, CV_2, Mix_1, Mix_2].

Model Summary 1 | Erosion Threshold (ET, Nm^{-2}) by day of data collection (Day)

Initial linear regression model:

lm(ET ~ as.factor(Day))

No minimal adequate model, intercept only (Day, L-ratio = 1.511836, d.f. = 3, p = 0.2189).

Model Summary 2 | Average pulse amplitude modulated (PAM) measured minimum fluorescence (PAMFAv) by day of data collection (Day)

Initial linear regression model:

lm(PAMFmAv ~ as.factor(Day))

No minimal adequate model, intercept only (Day, L-ratio = 3.784608, d.f. = 2, p = 0.0517).

Model Summary 3 | Erosion Threshold (ET, Nm^{-2}) by row location of mesocosm (Row)

Initial linear regression model:

lm(ET ~ as.factor(Row))

No minimal adequate model, intercept only (Day, L-ratio = 3.863222, d.f. = 8, p = 0.2766).

Model Summary 4 | Average pulse amplitude modulated (PAM) measured minimum fluorescence (PAMFAv) by row location of mesocosm (Row)

Initial linear regression model:

lm(PAMFmAv ~ as.factor(Row))

Linear regression was suitable for analysis of this data, but no minimal adequate model, intercept only (Day, L-ratio = 5.629328, d.f. = 8, p = 0.1311).

Model Summary 5 | Erosion threshold (ET, Nm^{-2}) by species treatment (Tcode)

Initial linear regression model:

lm(ET ~ as.factor(Tcode))

Minimal adequate model:

```
gls(ET~ as.factor(Tcode),
        weights = varIdent(form = ~1|as.factor(Tcode)),
        method = 'REML')
```

Coefficient Table

Intercept ± SE (when baseline is for N): 2.41 ± 0.53, t = 4.58, p < 0.0001.

	N	P	PD	HD_1	HD_2	HU_1	HU_2	CV_1	CV_2	Mix_1	Mix_2
N	-	5.06 ± 2.02 2.51 **0.0151**	12.41 ± 2.82 4.40 **< 0.0001**	12.76 ± 4.00 3.19 **0.0023**	11.15 ± 3.42 3.26 **0.0019**	5.86 ± 1.92 3.05 **0.0035**	4.71 ± 1.59 2.97 **0.0044**	5.98 ± 1.97 3.04 **0.0037**	16.09 ± 4.24 3.79 **0.0004**	8.96 ± 2.41 3.72 **0.0005**	8.62 ± 4.45 1.94 0.0579
P	-5.06 ± 2.02 -2.51 **0.0151**	-	7.35 ± 3.38 2.17 **0.0340**	7.70 ± 4.41 1.74 0.0866	6.09 ± 3.90 1.56 0.1242	0.80 ± 2.68 0.30 0.7656	-0.34 ± 2.45 -0.14 0.8888	0.92 ± 2.72 0.34 0.7363	11.03 ± 4.64 2.38 **0.0208**	3.91 ± 3.05 1.28 0.2061	3.56 ± 4.83 0.74 0.4637
PD	-12.41 ± 2.82 -4.40 **< 0.0001**	-7.35 ± 3.38 -2.17 **0.0340**	-	0.34 ± 4.83 0.07 0.9434	-1.26 ± 4.37 -0.29 0.7734	-6.55 ± 3.33 -1.97 0.0542	-7.70 ± 3.15 -2.45 **0.0176**	-6.44 ± 3.36 -1.92 0.0603	3.68 ± 5.04 0.73 0.4684	-3.45 ± 3.63 -0.95 0.3468	-3.79 ± 5.21 -0.73 0.4701
HD_1	-12.76 ± 4.00 -3.19 **0.0023**	-7.70 ± 4.41 -1.74 0.0866	-0.34 ± 4.83 -0.07 0.9434	-	-1.61 ± 5.21 -0.31 0.7585	-6.90 ± 4.37 -1.58 0.1205	-8.04 ± 4.23 -1.90 0.0627	-6.78 ± 4.39 -1.54 0.1283	3.33 ± 5.78 0.58 0.5665	-3.79 ± 4.61 -0.82 0.4140	-4.14 ± 5.93 -0.70 0.4886
HD_2	-11.15 ± 3.42 -3.26 **0.0019**	-6.09 ± 3.90 -1.56 0.1242	1.26 ± 4.37 0.29 0.7734	1.61 ± 5.21 0.31 0.7585	-	-5.29 ± 3.85 -1.37 0.1758	-6.44 ± 3.70 -1.74 0.0874	-5.17 ± 3.88 -1.33 0.1877	4.94 ± 5.40 0.92 0.3639	-2.18 ± 4.12 -0.53 0.5982	-2.53 ± 5.56 -0.45 0.6513
HU_1	-5.86 ± 1.92 -3.05 **0.0035**	-0.80 ± 2.68 -0.30 0.7656	6.55 ± 3.33 1.97 0.0542	6.90 ± 4.37 1.58 0.1205	5.29 ± 3.85 1.37 0.1758	-	-1.15 ± 2.38 -0.48 0.6311	0.11 ± 2.65 0.04 0.9656	10.23 ± 4.60 2.23 **0.0302**	3.10 ± 2.99 1.04 0.3045	2.76 ± 4.79 0.58 0.5671
HU_2	-4.71 ± 1.59 -2.97 **0.0044**	0.34 ± 2.45 0.14 0.8888	7.70 ± 3.15 2.45 **0.0176**	8.04 ± 4.23 1.90 0.0627	6.44 ± 3.70 1.74 0.0874	1.15 ± 2.38 0.48 0.6311	-	1.26 ± 2.42 0.52 0.6028	11.38 ± 4.47 2.55 **0.0137**	4.25 ± 2.79 1.52 0.1331	3.91 ± 4.67 0.84 0.4059
CV_1	-5.98 ± 1.97 -3.04 **0.0037**	0.92 ± 2.72 -0.34 0.7363	6.44 ± 3.36 1.92 0.0603	6.78 ± 4.39 1.54 0.1283	5.17 ± 3.88 1.33 0.1877	-0.11 ± 2.65 -0.04 0.9656	-1.26 ± 2.42 -0.52 0.6028	-	10.11 ± 4.61 2.19 **0.0327**	2.99 ± 3.02 0.99 0.3272	2.64 ± 4.81 0.55 0.5847
CV_2	-16.09 ± 4.24 -3.79 **0.0004**	-11.03 ± 4.64 -2.38 0.0208	-3.68 ± 5.04 -0.73 0.4684	-3.33 ± 5.78 -0.58 0.5665	-4.94 ± 5.40 -0.92 0.3639	-10.23 ± 4.60 -2.23 **0.0302**	-11.38 ± 4.47 -2.55 **0.0137**	-10.11 ± 4.61 -2.19 **0.0327**	-	-7.12 ± 4.82 -1.48 0.1451	-7.47 ± 6.10 -1.22 0.2260
Mix_1	-8.96 ± 2.41 -3.72 **0.0005**	-3.91 ± 3.05 -1.28 0.2061	3.45 ± 3.63 0.95 0.3468	3.79 ± 4.61 0.82 0.4140	2.18 ± 4.12 0.53 0.5982	-3.10 ± 2.99 -1.04 0.3045	-4.25 ± 2.79 -1.52 0.1331	-2.99 ± 3.02 -0.99 0.3272	7.12 ± 4.82 1.48 0.1451	-	-0.34 ± 5.01 -0.07 0.9453
Mix_2	-8.62 ± 4.45 -1.94 0.0579	-3.56 ± 4.83 -0.74 0.4637	3.79 ± 5.21 0.73 0.4701	4.14 ± 5.93 0.70 0.4886	2.53 ± 5.56 0.45 0.6513	-2.76 ± 4.79 -0.58 0.5671	-3.91 ± 4.67 -0.84 0.4059	-2.64 ± 4.81 -0.55 0.5847	7.47 ± 6.10 1.22 0.2260	0.34 ± 5.01 0.07 0.9453	-

Model Summary 6 | Suspension index (SI) by species treatment (Tcode)

Initial linear regression model:

```
lm(SI ~ as.factor(Tcode))
```

Minimal adequate model:

```
gls(SI ~ as.factor(Tcode),
    weights = varIdent(form = ~1|as.factor(Tcode)),
    method = 'REML')
```

Coefficient Table

Intercept ± SE (when baseline is for N): 21.19 ± 2.58, t = 8.22, p < 0.0001.

	N	P	PD	HD_1	HD_2	HU_1	HU_2	CV_1	CV_2	Mix_1	Mix_2
N	-	-10.79 ± 5.16 -2.09 **0.0411**	-14.06 ± 3.40 -4.14 **0.0001**	-15.74 ± 2.90 -5.42 **< 0.0001**	-13.40 ± 4.92 -2.72 **0.0087**	-12.38 ± 4.67 -2.65 **0.0104**	-15.84 ± 2.77 -5.71 **< 0.0001**	-13.39 ± 3.22 -4.16 **0.0001**	-18.30 ± 2.66 -6.89 **< 0.0001**	-9.43 ± 6.53 -1.45 0.1541	-13.50 ± 4.30 -3.14 **0.0027**
P	10.79 ± 5.16 2.09 **0.0411**	-	-3.27 ± 4.98 -0.66 0.5140	-4.96 ± 4.66 -1.06 0.2924	-2.61 ± 6.13 -0.43 0.6715	-1.59 ± 5.92 -0.27 0.7889	-5.06 ± 4.58 -1.10 0.2747	-2.60 ± 4.87 -0.53 0.5955	-7.51 ± 4.51 -1.66 0.1016	1.35 ± 7.48 0.18 0.8571	-2.71 ± 5.64 -0.48 0.6332
PD	14.06 ± 3.40 4.14 **0.0001**	3.27 ± 4.98 0.66 0.5140	-	-1.682 ± 2.5838 -0.650891 0.5178	0.6625 ± 4.7392 0.139791 0.8893	1.6806 ± 4.4746 0.375575 0.7087	-1.782 ± 2.4367 -0.731146 0.4678	0.6767 ± 2.9334 0.23069 0.8184	-4.24 ± 2.3033 -1.840707 0.0711	4.6273 ± 6.3921 0.723906 0.4722	0.5671 ± 4.0936 0.13853 0.8903
HD_1	15.74 ± 2.90 5.42 **< 0.0001**	4.96 ± 4.66 1.06 0.2924	1.68 ± 2.58 0.65 0.5178	-	2.34 ± 4.40 0.53 0.5962	3.36 ± 4.11 0.82 0.4171	-0.10 ± 1.68 -0.06 0.9529	2.36 ± 2.34 1.01 0.3188	-2.56 ± 1.48 -1.73 0.0900	6.31 ± 6.14 1.03 0.3090	2.25 ± 3.69 0.61 0.5452
HD_2	13.40 ± 4.92 2.72 **0.0087**	2.61 ± 6.13 0.43 0.6715	-0.66 ± 4.74 -0.14 0.8893	-2.34 ± 4.40 -0.53 0.5962	-	1.02 ± 5.72 0.18 0.8593	-2.44 ± 4.31 -0.57 0.5734	0.01 ± 4.61 0.00 0.9976	-4.90 ± 4.24 -1.16 0.2526	3.96 ± 7.32 0.54 0.5901	-0.10 ± 5.43 -0.02 0.9860
HU_1	12.38 ± 4.67 2.65 **0.0104**	1.59 ± 5.92 0.27 0.7889	-1.68 ± 4.47 -0.38 0.7087	-3.36 ± 4.11 -0.82 0.4171	-1.02 ± 5.72 -0.18 0.8593	-	-3.46 ± 4.02 -0.86 0.3931	-1.00 ± 4.34 -0.23 0.8180	-5.92 ± 3.94 -1.50 0.1389	2.95 ± 7.15 0.41 0.6818	-1.11 ± 5.20 -0.21 0.8311
HU_2	15.84 ± 2.77 5.71 **< 0.0001**	5.06 ± 4.58 1.10 0.2747	1.78 ± 2.44 0.73 0.4678	0.10 ± 1.68 0.06 0.9529	2.44 ± 4.31 0.57 0.5734	3.46 ± 4.02 0.86 0.3931	-	2.46 ± 2.18 1.13 0.2646	-2.46 ± 1.21 -2.04 **0.0466**	6.41 ± 6.08 1.05 0.2967	2.35 ± 3.59 0.65 0.5160
CV_1	13.39 ± 3.22 4.16 **0.0001**	-2.60 ± 4.87 0.53 0.5955	-0.68 ± 2.93 -0.23 0.8184	-2.36 ± 2.34 -1.01 0.3188	-0.01 ± 4.61 0.00 0.9976	1.00 ± 4.34 0.23 0.8180	-2.46 ± 2.18 -1.13 0.2646	-	-4.92 ± 2.03 -2.42 **0.0188**	3.95 ± 6.30 0.63 0.5331	-0.11 ± 3.95 -0.03 0.9779
CV_2	18.30 ± 2.66 6.89 **< 0.0001**	7.51 ± 4.51 1.66 0.1016	4.24 ± 2.30 1.84 0.0711	2.56 ± 1.48 1.73 0.0900	4.90 ± 4.24 1.16 0.2526	5.92 ± 3.94 1.50 0.1389	2.46 ± 1.21 2.04 **0.0466**	4.92 ± 2.03 2.42 **0.0188**	-	8.87 ± 6.03 1.47 0.1472	4.81 ± 3.50 1.37 0.1757
Mix_1	9.43 ± 6.53 1.45 0.1541	-1.35 ± 7.48 -0.18 0.8571	-4.63 ± 6.39 -0.72 0.4722	-6.31 ± 6.14 -1.03 0.3090	-3.96 ± 7.32 -0.54 0.5901	-2.95 ± 7.15 -0.41 0.6818	-6.41 ± 6.08 -1.05 0.2967	-3.95 ± 6.30 -0.63 0.5331	-8.87 ± 6.03 -1.47 0.1472	-	-4.06 ± 6.92 -0.59 0.5596
Mix_2	13.50 ± 4.30 3.14 **0.0027**	2.71 ± 5.64 0.48 0.6332	-0.57 ± 4.09 -0.14 0.8903	-2.25 ± 3.69 -0.61 0.5452	0.10 ± 5.43 0.02 0.9860	1.11 ± 5.20 0.21 0.8311	-2.35 ± 3.59 -0.65 0.5160	0.11 ± 3.95 0.03 0.9779	-4.81 ± 3.50 -1.37 0.1757	4.06 ± 6.92 0.59 0.5596	-

Model Summary 7 | Average pulse amplitude modulated (PAM) measured minimum fluorescence (PAMFAv) by species treatment (Tcode)

Initial linear regression model:

```
lm(PAMFAv ~ as.factor(Tcode))
```

Minimal adequate model:

```
gls(PAMFAv ~ as.factor(Tcode),
    weights = varIdent(form = ~1|as.factor(Tcode)),
    method = 'REML')
```

Coefficient Table

Intercept ± SE (when baseline is for N): 230.00 ± 20.93, t = 10.99, p < 0.0001.

	N	P	PD	HD_1	HD_2	HU_1	HU_2	CV_1	CV_2	Mix_1	Mix_2
N	-	214.00 ± 70.50 3.04 **0.0037**	632.22 ± 85.67 7.38 **< 0.0001**	419.22 ± 77.68 5.40 **< 0.0001**	572.11 ± 156.96 3.64 **0.0006**	343.67 ± 59.18 5.81 **< 0.0001**	551.94 ± 143.41 3.85 **0.0003**	453.28 ± 107.00 4.24 **0.0001**	559.78 ± 58.89 9.51 **< 0.0001**	221.28 ± 55.47 3.99 **0.0002**	414.56 ± 75.71 5.48 **< 0.0001**
P	-214.00 ± 70.50 -3.04 **0.0037**	-	418.22 ± 106.93 3.91 **0.0003**	205.22 ± 100.64 2.04 **0.0463**	358.11 ± 169.50 2.11 **0.0392**	129.67 ± 87.16 1.49 0.1426	337.94 ± 157.04 2.15 **0.0358**	239.28 ± 124.68 1.92 0.0602	345.78 ± 86.97 3.98 **0.0002**	7.28 ± 84.69 0.09 0.9318	200.56 ± 99.13 2.02 **0.0479**
PD	-632.22 ± 85.67 -7.38 **< 0.0001**	-418.22 ± 106.93 -3.91 **0.0003**	-	-213.00 ± 111.79 -1.91 0.0620	-60.11 ± 176.35 -0.34 0.7345	-288.56 ± 99.83 -2.89 **0.0055**	-80.28 ± 164.41 -0.49 0.6273	-178.94 ± 133.84 -1.34 0.1867	-72.44 ± 99.66 -0.73 0.4703	-410.94 ± 97.67 -4.21 **0.0001**	-217.67 ± 110.43 -1.97 0.0538
HD_1	-419.22 ± 77.68 -5.40 **< 0.0001**	-205.22 ± 100.64 -2.04 **0.0463**	213.00 ± 111.79 1.91 0.0620	-	152.89 ± 172.61 0.89 0.3796	-75.56 ± 93.06 -0.81 0.4203	132.72 ± 160.39 0.83 0.4115	34.06 ± 128.87 0.26 0.7926	140.56 ± 92.88 1.51 0.1359	-197.94 ± 90.75 -2.18 **0.0335**	-4.67 ± 104.35 -0.04 0.9645
HD_2	-572.11 ± 156.96 -3.64 **0.0006**	-358.11 ± 169.50 -2.11 **0.0392**	60.11 ± 176.35 0.34 0.7345	-152.89 ± 172.61 -0.89 0.3796	-	-228.44 ± 165.11 -1.38 0.1721	-20.17 ± 210.54 -0.10 0.9240	-118.83 ± 187.65 -0.63 0.5292	-12.33 ± 165.01 -0.07 0.9407	-350.83 ± 163.82 -2.14 **0.0367**	-157.56 ± 171.73 -0.92 0.3629
HU_1	-343.67 ± 59.18 -5.81 **< 0.0001**	-129.67 ± 87.16 -1.49 0.1426	288.56 ± 99.83 2.89 **0.0055**	75.56 ± 93.06 0.81 0.4203	228.44 ± 165.11 1.38 0.1721	-	208.28 ± 152.29 1.37 0.1770	109.61 ± 118.64 0.92 0.3596	216.11 ± 78.07 2.77 **0.0077**	-122.39 ± 75.52 -1.62 0.1108	70.89 ± 91.42 0.78 0.4414
HU_2	-551.94 ± 143.41 -3.85 **0.0003**	-337.94 ± 157.04 -2.15 **0.0358**	80.28 ± 164.41 0.49 0.6273	-132.72 ± 160.39 -0.83 0.4115	20.17 ± 210.54 0.10 0.9240	-208.28 ± 152.29 -1.37 0.1770	-	-98.67 ± 176.47 -0.56 0.5784	7.83 ± 152.18 0.05 0.9591	-330.67 ± 150.89 -2.19 **0.0327**	-137.39 ± 159.45 -0.86 0.3926
CV_1	-453.28 ± 107.00 -4.24 **0.0001**	239.28 ± 124.68 1.92 0.0602	178.94 ± 133.84 1.34 0.1867	-34.06 ± 128.87 -0.26 0.7926	118.83 ± 187.65 0.63 0.5292	-109.61 ± 118.64 -0.92 0.3596	98.67 ± 176.47 0.56 0.5784	-	106.50 ± 118.50 0.90 0.3727	-232.00 ± 116.84 -1.99 0.0521	-38.72 ± 127.70 -0.30 0.7629
CV_2	-559.78 ± 58.89 -9.51 **< 0.0001**	-345.78 ± 86.97 -3.98 **0.0002**	72.44 ± 99.66 0.73 0.4703	-140.56 ± 92.88 -1.51 0.1359	12.33 ± 165.01 0.07 0.9407	-216.11 ± 78.07 -2.77 **0.0077**	-7.83 ± 152.18 -0.05 0.9591	-106.50 ± 118.50 -0.90 0.3727	-	-338.50 ± 75.29 -4.50 **< 0.0001**	-145.22 ± 91.24 -1.59 0.1172
Mix_1	-221.28 ± 55.47 -3.99 **0.0002**	-7.28 ± 84.69 -0.09 0.9318	410.94 ± 97.67 4.21 **0.0001**	197.94 ± 90.75 2.18 **0.0335**	350.83 ± 163.82 2.14 **0.0367**	122.39 ± 75.52 1.62 0.1108	330.67 ± 150.89 2.19 **0.0327**	232.00 ± 116.84 1.99 0.0521	338.50 ± 75.29 4.50 **< 0.0001**	-	193.28 ± 89.07 2.17 **0.0343**
Mix_2	-414.56 ± 75.71 -5.48 **< 0.0001**	-200.56 ± 99.13 -2.02 **0.0479**	217.67 ± 110.43 1.97 0.0538	4.67 ± 104.35 0.04 0.9645	157.56 ± 171.73 0.92 0.3629	-70.89 ± 91.42 -0.78 0.4414	137.39 ± 159.45 0.86 0.3926	38.72 ± 127.70 0.30 0.7629	145.22 ± 91.24 1.59 0.1172	-193.28 ± 89.07 -2.17 **0.0343**	-

Model Summary 8 | Average pulse amplitude modulated (PAM) measured maximum quantum yield (PAMYAv) by species treatment (Tcode)

Initial linear regression model:

lm(PAMYAv ~ as.factor(Tcode))

Minimal adequate model:

gls(PAMFYAv ~ as.factor(Tcode),
method = 'REML')

Coefficient Table

Intercept ± SE (when baseline is for N): 0.58 ± 0.02, t = 26.42, p < 0.0001.

	N	P	PD	HD_1	HD_2	HU_1	HU_2	CV_1	CV_2	Mix_1	Mix_2
N	-	-0.02 ± 0.03 -0.68 0.4967	-0.08 ± 0.03 -2.73 **0.0086**	-0.07 ± 0.03 -2.11 **0.0392**	-0.05 ± 0.03 -1.56 0.1254	-0.02 ± 0.03 -0.85 0.3982	-0.05 ± 0.03 -1.68 0.0996	-0.05 ± 0.02 -1.94 0.0573	-0.06 ± 0.03 -1.88 0.0652	0.00 ± 0.03 0.03 0.9789	-0.05 ± 0.03 -1.68 0.0996
P	0.02 ± 0.03 0.68 0.4967	-	-0.06 ± 0.02 -2.71 **0.0090**	-0.05 ± 0.03 -1.89 0.0641	-0.03 ± 0.03 -1.23 0.2253	-0.01 ± 0.02 -0.33 0.7461	-0.03 ± 0.02 -1.37 0.1758	-0.03 ± 0.02 -1.86 0.0680	-0.04 ± 0.03 -1.62 0.1117	0.02 ± 0.02 1.03 0.3061	-0.03 ± 0.02 -1.38 0.1726
PD	0.08 ± 0.03 2.73 **0.0086**	0.06 ± 0.02 2.71 **0.0090**	-	0.01 ± 0.03 0.29 0.7748	0.03 ± 0.03 0.92 0.3605	0.05 ± 0.03 2.01 **0.0491**	0.03 ± 0.03 1.17 0.2460	0.03 ± 0.02 1.61 0.1126	0.02 ± 0.03 0.62 0.5355	0.08 ± 0.02 3.56 **0.0008**	0.03 ± 0.02 1.39 0.1707
HD_1	0.07 ± 0.03 2.11 **0.0392**	0.05 ± 0.03 1.89 0.0641	-0.01 ± 0.03 -0.29 0.7748	-	0.02 ± 0.03 0.56 0.5799	0.05 ± 0.03 1.44 0.1554	0.02 ± 0.03 0.71 0.4802	0.02 ± 0.03 0.93 0.3567	0.01 ± 0.03 0.29 0.7759	0.07 ± 0.03 2.56 **0.0131**	0.03 ± 0.03 0.85 0.3975
HD_2	0.05 ± 0.03 1.56 0.1254	0.03 ± 0.03 1.23 0.2253	-0.03 ± 0.03 -0.92 0.3605	-0.02 ± 0.03 -0.56 0.5799	-	0.03 ± 0.03 0.84 0.4038	0.00 ± 0.03 0.09 0.9291	0.01 ± 0.03 0.20 0.8426	-0.01 ± 0.03 -0.28 0.7775	0.05 ± 0.03 1.91 0.0614	0.01 ± 0.03 0.20 0.8431
HU_1	0.02 ± 0.03 0.85 0.3982	0.01 ± 0.02 0.33 0.7461	-0.05 ± 0.03 -2.01 **0.0491**	-0.05 ± 0.03 -1.44 0.1554	-0.03 ± 0.03 -0.84 0.4038	-	-0.02 ± 0.03 -0.87 0.3868	-0.02 ± 0.02 -0.99 0.3242	-0.04 ± 0.03 -1.17 0.2456	0.03 ± 0.02 1.13 0.2645	-0.02 ± 0.02 -0.82 0.4161
HU_2	0.05 ± 0.03 1.68 0.0996	0.03 ± 0.02 1.37 0.1758	-0.03 ± 0.03 -1.17 0.2460	-0.02 ± 0.03 -0.71 0.4802	0.00 ± 0.03 -0.09 0.9291	0.02 ± 0.03 0.87 0.3868	-	0.00 ± 0.02 0.12 0.9069	-0.01 ± 0.03 -0.41 0.6823	0.05 ± 0.02 2.21 **0.0309**	0.00 ± 0.02 0.12 0.9017
CV_1	0.05 ± 0.02 1.94 0.0573	-0.03 ± 0.02 1.86 0.0680	-0.03 ± 0.02 -1.61 0.1126	-0.02 ± 0.03 -0.93 0.3567	-0.01 ± 0.03 -0.20 0.8426	0.02 ± 0.02 0.99 0.3242	0.00 ± 0.02 -0.12 0.9069	-	-0.01 ± 0.02 -0.59 0.5579	0.05 ± 0.01 3.17 **0.0025**	0.00 ± 0.02 0.03 0.9726
CV_2	0.06 ± 0.03 1.88 0.0652	0.04 ± 0.03 1.62 0.1117	-0.02 ± 0.03 -0.62 0.5355	-0.01 ± 0.03 -0.29 0.7759	0.01 ± 0.03 0.28 0.7775	0.04 ± 0.03 1.17 0.2456	0.01 ± 0.03 0.41 0.6823	0.01 ± 0.02 0.59 0.5579	-	0.06 ± 0.03 2.32 **0.0239**	0.02 ± 0.03 0.54 0.5890
Mix_1	0.00 ± 0.03 -0.03 0.9789	-0.02 ± 0.02 -1.03 0.3061	-0.08 ± 0.02 -3.56 **0.0008**	-0.07 ± 0.03 -2.56 **0.0131**	-0.05 ± 0.03 -1.91 0.0614	-0.03 ± 0.02 -1.13 0.2645	-0.05 ± 0.02 -2.21 **0.0309**	-0.05 ± 0.01 -3.17 **0.0025**	-0.06 ± 0.03 -2.32 **0.0239**	-	-0.05 ± 0.02 -2.33 **0.0234**
Mix_2	0.05 ± 0.03 1.68 0.0996	0.03 ± 0.02 1.38 0.1726	-0.03 ± 0.02 -1.39 0.1707	-0.03 ± 0.03 -0.85 0.3975	-0.01 ± 0.03 -0.20 0.8431	0.02 ± 0.02 0.82 0.4161	0.00 ± 0.02 -0.12 0.9017	0.00 ± 0.02 -0.03 0.9726	-0.02 ± 0.03 -0.54 0.5890	0.05 ± 0.02 2.33 **0.0234**	-

Model Summary 9 | Minicore water content (MCWater, %) by species treatment (Tcode)

Initial linear regression model:

lm(MCWater% ~ as.factor(Tcode))

No minimal adequate model, intercept only (Tcode, L-ratio = 12.35444, d.f. = 22, p = 0.2620).

Model Summary 10 | Minicore mean particle size (MCMean, µm) by species treatment (Tcode)

Initial linear regression model:

lm(MCMean ~ as.factor(Tcode))

No minimal adequate model, intercept only (Tcode, L-ratio = 6.70592, d.f. = 22, p = 0.7529).

Model Summary 11 | Minicore mode particle size (MCMode, µm) by species treatment (Tcode)

Initial linear regression model:

lm(MCMode ~ as.factor(Tcode))

No minimal adequate model, intercept only (Tcode, F = 0.4533, d.f. = 10, p = 0.9124).

Model Summary 12 | Minicore particle sorting (MCSort) by species treatment (Tcode)

Initial linear regression model:

lm(MCSort ~ as.factor(Tcode))

No minimal adequate model, intercept only (Tcode, L-ratio = 17.57463, d.f. = 22, p = 0.0626).

Model Summary 13 | Minicore particle skewness (MCSkew) by species treatment (Tcode)

Initial linear regression model:

lm(MCSkew ~ as.factor(Tcode))

No minimal adequate model, intercept only (Tcode, L-ratio = 17.5279, d.f. = 22, p = 0.0635).

Model Summary 14 | Minicore particle kurtosis (MCKurt) by species treatment (Tcode)

Initial linear regression model:

lm(MCKurt ~ as.factor(Tcode))

Minimal adequate model:

gls(MCKurt ~ as.factor(Tcode),
weights = varIdent(form = ~1|as.factor(Tcode)),
method = 'REML')

Coefficient Table

Intercept ± SE (when baseline is for N): 3.77 ± 0.07, t =50.93, p < 0.0001.

	N	P	PD	HD_1	HD_2	HU_1	HU_2	CV_1	CV_2	Mix_1	Mix_2
N	-	-0.15 ± 0.09 -1.67 0.1013	-0.07 ± 0.11 -0.64 0.5269	-0.13 ± 0.09 -1.47 0.1464	-0.18 ± 0.09 -2.15 **0.0362**	-0.15 ± 0.08 -1.89 0.0634	-0.05 ± 0.07 -0.68 0.5016	-0.07 ± 0.08 -0.90 0.3711	-0.20 ± 0.10 -2.04 **0.0460**	0.17 ± 0.16 1.08 0.2863	-0.07 ± 0.10 -0.67 0.5038
P	0.15 ± 0.09 1.67 0.1013	-	0.08 ± 0.10 0.83 0.4080	0.02 ± 0.07 0.24 0.8145	-0.03 ± 0.07 -0.49 0.6236	0.00 ± 0.06 0.00 0.9989	0.10 ± 0.05 1.88 0.0652	0.08 ± 0.06 1.23 0.2243	-0.05 ± 0.08 -0.58 0.5615	0.32 ± 0.15 2.17 **0.0341**	0.08 ± 0.08 1.02 0.3144
PD	0.07 ± 0.11 0.64 0.5269	-0.08 ± 0.10 -0.83 0.4080	-	-0.06 ± 0.10 -0.65 0.5160	-0.11 ± 0.09 -1.24 0.2220	-0.08 ± 0.09 -0.93 0.3556	0.02 ± 0.08 0.24 0.8140	0.00 ± 0.09 -0.04 0.9670	-0.13 ± 0.10 -1.25 0.2183	0.24 ± 0.16 1.49 0.1415	0.00 ± 0.10 0.04 0.9707
HD_1	0.13 ± 0.09 1.47 0.1464	-0.02 ± 0.07 -0.24 0.8145	0.06 ± 0.10 0.65 0.5160	-	-0.05 ± 0.07 -0.75 0.4571	-0.02 ± 0.06 -0.29 0.7716	0.08 ± 0.05 1.55 0.1267	0.06 ± 0.06 0.95 0.3463	-0.06 ± 0.08 -0.80 0.4297	0.30 ± 0.15 2.05 **0.0447**	0.07 ± 0.08 0.81 0.4239
HD_2	0.18 ± 0.09 2.15 **0.0362**	0.03 ± 0.07 0.49 0.6236	0.11 ± 0.09 1.24 0.2220	0.05 ± 0.07 0.75 0.4571	-	0.03 ± 0.05 0.64 0.5264	0.13 ± 0.04 2.99 **0.0042**	0.11 ± 0.06 1.99 0.0521	-0.01 ± 0.08 -0.19 0.8517	0.35 ± 0.14 2.45 **0.0175**	0.12 ± 0.08 1.51 0.1368
HU_1	0.15 ± 0.08 1.89 0.0634	0.00 ± 0.06 0.00 0.9989	0.08 ± 0.09 0.93 0.3556	0.02 ± 0.06 0.29 0.7716	-0.03 ± 0.05 -0.64 0.5264	-	0.10 ± 0.03 3.19 **0.0024**	0.08 ± 0.05 1.69 0.0965	-0.05 ± 0.07 -0.69 0.4959	0.32 ± 0.14 2.27 **0.0269**	0.08 ± 0.07 1.19 0.2405
HU_2	0.05 ± 0.07 0.68 0.5016	-0.10 ± 0.05 -1.88 0.0652	-0.02 ± 0.08 -0.24 0.8140	-0.08 ± 0.05 -1.55 0.1267	-0.13 ± 0.04 -2.99 **0.0042**	-0.10 ± 0.03 -3.19 **0.0024**	-	-0.02 ± 0.04 -0.63 0.5309	-0.15 ± 0.06 -2.31 **0.0248**	0.22 ± 0.14 1.59 0.1179	-0.02 ± 0.07 -0.24 0.8137
CV_1	0.07 ± 0.08 0.90 0.3711	0.08 ± 0.06 -1.23 0.2243	0.00 ± 0.09 0.04 0.9670	-0.06 ± 0.06 -0.95 0.3463	-0.11 ± 0.06 -1.99 0.0521	-0.08 ± 0.05 -1.69 0.0965	0.02 ± 0.04 0.63 0.5309	-	-0.12 ± 0.07 -1.73 0.0892	0.24 ± 0.14 1.71 0.0932	0.01 ± 0.07 0.10 0.9191
CV_2	0.20 ± 0.10 2.04 **0.0460**	0.05 ± 0.08 0.58 0.5615	0.13 ± 0.10 1.25 0.2183	0.06 ± 0.08 0.80 0.4297	0.01 ± 0.08 0.19 0.8517	0.05 ± 0.07 0.69 0.4959	0.15 ± 0.06 2.31 **0.0248**	0.12 ± 0.07 1.73 0.0892	-	0.37 ± 0.15 2.43 **0.0185**	0.13 ± 0.09 1.46 0.1499
Mix_1	-0.17 ± 0.16 -1.08 0.2863	-0.32 ± 0.15 -2.17 **0.0341**	-0.24 ± 0.16 -1.49 0.1415	-0.30 ± 0.15 -2.05 **0.0447**	-0.35 ± 0.14 -2.45 **0.0175**	-0.32 ± 0.14 -2.27 **0.0269**	-0.22 ± 0.14 -1.59 0.1179	-0.24 ± 0.14 -1.71 0.0932	-0.37 ± 0.15 -2.43 **0.0185**	-	-0.23 ± 0.15 -1.54 0.1285
Mix_2	0.07 ± 0.10 0.67 0.5038	-0.08 ± 0.08 -1.02 0.3144	0.00 ± 0.10 -0.04 0.9707	-0.07 ± 0.08 -0.81 0.4239	-0.12 ± 0.08 -1.51 0.1368	-0.08 ± 0.07 -1.19 0.2405	0.02 ± 0.07 0.24 0.8137	-0.01 ± 0.07 -0.10 0.9191	-0.13 ± 0.09 -1.46 0.1499	0.23 ± 0.15 1.54 0.1285	-

Model Summary 15 | Minicore D_{10} (MCD_{10}, µm) by species treatment (Tcode)

Initial linear regression model:

lm(MCD_{10} ~ as.factor(Tcode))

No minimal adequate model, intercept only (Tcode, L-ratio = 7.703501, d.f. = 22, p = 0.6578).

Model Summary 16 | Minicore mud content (MCPCMud, %) by species treatment (Tcode)

Initial linear regression model:

lm(MCPCMud% ~ as.factor(Tcode))

No minimal adequate model, intercept only (Tcode, L-ratio = 6.226999, d.f. = 22, p = 0.7958).

Model Summary 17 | Contact core water concentration (CCWat, gcm^{-3}) by species treatment (Tcode)

Initial linear regression model:

lm(CCWCpV ~ as.factor(Tcode))

Minimal adequate model:

gls(CCWCpV ~ as.factor(Tcode),
weights = varIdent(form = ~1|as.factor(Tcode)),
method = 'REML')

Coefficient Table

Intercept ± SE (when baseline is for N): 0.77 ± 0.01, t = 62.65, p < 0.0001.

	N	P	PD	HD_1	HD_2	HU_1	HU_2	CV_1	CV_2	Mix_1	Mix_2
N	-	-0.05 ± 0.02 -2.70 **0.0091**	-0.05 ± 0.02 -2.75 **0.0081**	-0.01 ± 0.02 -0.51 0.6089	-0.03 ± 0.02 -1.94 0.0576	-0.05 ± 0.02 -3.39 **0.0013**	-0.06 ± 0.02 -3.30 **0.0017**	-0.03 ± 0.02 -1.61 0.1134	0.00 ± 0.02 -0.21 0.8359	-0.05 ± 0.01 -3.63 **0.0006**	-0.04 ± 0.02 -2.14 **0.0370**
P	0.05 ± 0.02 2.70 **0.0091**	-	0.00 ± 0.02 0.07 0.9424	0.04 ± 0.02 2.42 **0.0191**	0.02 ± 0.02 0.87 0.3884	0.00 ± 0.02 -0.03 0.9745	-0.01 ± 0.02 -0.62 0.5354	0.02 ± 0.02 1.08 0.2851	0.05 ± 0.02 2.62 **0.0114**	0.00 ± 0.02 0.28 0.7782	0.01 ± 0.02 0.76 0.4477
PD	0.05 ± 0.02 2.75 **0.0081**	0.00 ± 0.02 -0.07 0.9424	-	0.04 ± 0.02 2.45 **0.0173**	0.02 ± 0.02 0.83 0.4104	0.00 ± 0.02 -0.12 0.9033	-0.01 ± 0.02 -0.72 0.4765	0.02 ± 0.02 1.05 0.2992	0.05 ± 0.02 2.66 **0.0101**	0.00 ± 0.01 0.20 0.8407	0.01 ± 0.02 0.72 0.4746
HD_1	0.01 ± 0.02 0.51 0.6089	-0.04 ± 0.02 -2.42 **0.0191**	-0.04 ± 0.02 -2.45 **0.0173**	-	-0.03 ± 0.02 -1.58 0.1189	-0.04 ± 0.01 -3.15 **0.0027**	-0.06 ± 0.02 -3.05 **0.0035**	-0.02 ± 0.02 -1.24 0.2199	0.00 ± 0.02 0.32 0.7529	-0.04 ± 0.01 -3.46 **0.0010**	-0.03 ± 0.02 -1.79 0.0787
HD_2	0.03 ± 0.02 1.94 0.0576	-0.02 ± 0.02 -0.87 0.3884	-0.02 ± 0.02 -0.83 0.4104	0.03 ± 0.02 1.58 0.1189	-	-0.02 ± 0.02 -1.10 0.2759	-0.03 ± 0.02 -1.50 0.1383	0.00 ± 0.02 0.25 0.8020	0.03 ± 0.02 1.82 0.0739	-0.01 ± 0.01 -0.93 0.3571	0.00 ± 0.02 -0.14 0.8925
HU_1	0.05 ± 0.02 3.39 **0.0013**	0.00 ± 0.02 0.03 0.9745	0.00 ± 0.02 0.12 0.9033	0.04 ± 0.01 3.15 **0.0027**	0.02 ± 0.02 1.10 0.2759	-	-0.01 ± 0.02 -0.71 0.4828	0.02 ± 0.02 1.34 0.1870	0.05 ± 0.01 3.35 **0.0015**	0.00 ± 0.01 0.48 0.6350	0.02 ± 0.02 0.99 0.3283
HU_2	0.06 ± 0.02 3.30 **0.0017**	0.01 ± 0.02 0.62 0.5354	0.01 ± 0.02 0.72 0.4765	0.06 ± 0.02 3.05 **0.0035**	0.03 ± 0.02 1.50 0.1383	0.01 ± 0.02 0.71 0.4828	-	0.03 ± 0.02 1.69 0.0966	0.06 ± 0.02 3.24 **0.0020**	0.02 ± 0.02 1.10 0.2754	0.03 ± 0.02 1.42 0.1620
CV_1	0.03 ± 0.02 1.61 0.1134	0.02 ± 0.02 -1.08 0.2851	-0.02 ± 0.02 -1.05 0.2992	0.02 ± 0.02 1.24 0.2199	0.00 ± 0.02 -0.25 0.8020	-0.02 ± 0.02 -1.34 0.1870	-0.03 ± 0.02 -1.69 0.0966	-	0.03 ± 0.02 1.48 0.1447	-0.02 ± 0.01 -1.20 0.2351	-0.01 ± 0.02 -0.39 0.6984
CV_2	0.00 ± 0.02 0.21 0.8359	-0.05 ± 0.02 -2.62 **0.0114**	-0.05 ± 0.02 -2.66 **0.0101**	0.00 ± 0.02 -0.32 0.7529	-0.03 ± 0.02 -1.82 0.0739	-0.05 ± 0.01 -3.35 **0.0015**	-0.06 ± 0.02 -3.24 **0.0020**	-0.03 ± 0.02 -1.48 0.1447	-	-0.04 ± 0.01 -3.66 **0.0006**	-0.03 ± 0.02 -2.03 **0.0473**
Mix_1	0.05 ± 0.01 3.63 **0.0006**	0.00 ± 0.02 -0.28 0.7782	0.00 ± 0.01 -0.20 0.8407	0.04 ± 0.01 3.46 **0.0010**	0.01 ± 0.01 0.93 0.3571	0.00 ± 0.01 -0.48 0.6350	-0.02 ± 0.02 -1.10 0.2754	0.02 ± 0.01 1.20 0.2351	0.04 ± 0.01 3.66 **0.0006**	-	0.01 ± 0.01 0.79 0.4313
Mix_2	0.04 ± 0.02 2.14 **0.0370**	-0.01 ± 0.02 -0.76 0.4477	-0.01 ± 0.02 -0.72 0.4746	0.03 ± 0.02 1.79 0.0787	0.00 ± 0.02 0.14 0.8925	-0.02 ± 0.02 -0.99 0.3283	-0.03 ± 0.02 -1.42 0.1620	0.01 ± 0.02 0.39 0.6984	0.03 ± 0.02 2.03 **0.0473**	-0.01 ± 0.01 -0.79 0.4313	-

Model Summary 18 | Contact core carbohydrate concentration (CCCarb, glucose µgcm^{-3}) by species treatment (Tcode)

Initial linear regression model:

lm(CCCarb ~ as.factor(Tcode))

Minimal adequate model:

gls(CCCarb ~ as.factor(Tcode),
weights = varIdent(form = ~1|as.factor(Tcode)),
method = 'REML')

Coefficient Table

Intercept ± SE (when baseline is for N): 561.84 ± 23.84, t = 23.57, p < 0.0001.

	N	P	PD	HD_1	HD_2	HU_1	HU_2	CV_1	CV_2	Mix_1	Mix_2
N	-	403.37 ± 126.60 3.19 **0.0024**	525.49 ± 170.85 3.08 **0.0033**	531.48 ± 161.56 3.29 **0.0018**	73.02 ± 88.15 0.83 0.4111	482.89 ± 168.18 2.87 **0.0058**	382.41 ± 159.24 2.40 **0.0197**	361.67 ± 94.45 3.83 **0.0003**	558.31 ± 202.39 2.76 **0.0079**	184.45 ± 49.39 3.73 **0.0004**	457.08 ± 109.96 4.16 **0.0001**
P	-403.37 ± 126.60 -3.19 **0.0024**	-	122.11 ± 209.95 0.58 0.5632	128.11 ± 202.46 0.63 0.5295	-330.36 ± 150.54 -2.19 **0.0324**	79.52 ± 207.78 0.38 0.7034	-20.97 ± 200.62 -0.10 0.9171	-41.70 ± 154.30 -0.27 0.7880	154.94 ± 236.33 0.66 0.5148	-218.92 ± 131.64 -1.66 0.1020	53.71 ± 164.26 0.33 0.7449
PD	-525.49 ± 170.85 -3.08 **0.0033**	-122.11 ± 209.95 -0.58 0.5632	-	5.99 ± 232.71 0.03 0.9796	-452.47 ± 189.28 -2.39 **0.0203**	-42.60 ± 237.36 -0.18 0.8582	-143.08 ± 231.11 -0.62 0.5384	-163.81 ± 192.29 -0.85 0.3979	32.82 ± 262.71 0.12 0.9010	-341.04 ± 174.62 -1.95 0.0559	-68.40 ± 200.36 -0.34 0.7341
HD_1	-531.48 ± 161.56 -3.29 **0.0018**	-128.11 ± 202.46 -0.63 0.5295	-5.99 ± 232.71 -0.03 0.9796	-	-458.46 ± 180.93 -2.53 **0.0142**	-48.59 ± 230.75 -0.21 0.8340	-149.07 ± 224.32 -0.66 0.5091	-169.80 ± 184.07 -0.92 0.3603	26.83 ± 256.76 0.10 0.9172	-347.03 ± 165.54 -2.10 **0.0407**	-74.39 ± 192.49 -0.39 0.7006
HD_2	-73.02 ± 88.15 -0.83 0.4111	330.36 ± 150.54 2.19 **0.0324**	452.47 ± 189.28 2.39 **0.0203**	458.46 ± 180.93 2.53 **0.0142**	-	409.88 ± 186.86 2.19 **0.0325**	309.39 ± 178.86 1.73 0.0893	288.66 ± 124.72 2.31 **0.0244**	485.30 ± 218.17 2.22 **0.0302**	111.43 ± 95.26 1.17 0.2471	384.07 ± 136.84 2.81 **0.0069**
HU_1	-482.89 ± 168.18 -2.87 **0.0058**	-79.52 ± 207.78 -0.38 0.7034	42.60 ± 237.36 0.18 0.8582	48.59 ± 230.75 0.21 0.8340	-409.88 ± 186.86 -2.19 **0.0325**	-	-100.48 ± 229.14 -0.44 0.6627	-121.22 ± 189.91 -0.64 0.5259	75.42 ± 260.98 0.29 0.7737	-298.44 ± 172.01 -1.74 0.0883	-25.81 ± 198.09 -0.13 0.8968
HU_2	-382.41 ± 159.24 -2.40 **0.0197**	20.97 ± 200.62 0.10 0.9171	143.08 ± 231.11 0.62 0.5384	149.07 ± 224.32 0.66 0.5091	-309.39 ± 178.86 -1.73 0.0893	100.48 ± 229.14 0.44 0.6627	-	-20.73 ± 182.05 -0.11 0.9097	175.90 ± 255.31 0.69 0.4937	-197.96 ± 163.28 -1.21 0.2306	74.68 ± 190.55 0.39 0.6966
CV_1	-361.67 ± 94.45 -3.83 **0.0003**	-41.70 ± 154.30 0.27 0.7880	163.81 ± 192.29 0.85 0.3979	169.80 ± 184.07 0.92 0.3603	-288.66 ± 124.72 -2.31 **0.0244**	121.22 ± 189.91 0.64 0.5259	20.73 ± 182.05 0.11 0.9097	-	196.64 ± 220.79 0.89 0.3770	-177.22 ± 101.11 -1.75 0.0852	95.41 ± 140.97 0.68 0.5014
CV_2	-558.31 ± 202.39 -2.76 **0.0079**	-154.94 ± 236.33 -0.66 0.5148	-32.82 ± 262.71 -0.12 0.9010	-26.83 ± 256.76 -0.10 0.9172	-485.30 ± 218.17 -2.22 **0.0302**	-75.42 ± 260.98 -0.29 0.7737	-175.90 ± 255.31 -0.69 0.4937	-196.64 ± 220.79 -0.89 0.3770	-	-373.86 ± 205.59 -1.82 0.0744	-101.23 ± 227.85 -0.44 0.6586
Mix_1	-184.45 ± 49.39 -3.73 **0.0004**	218.92 ± 131.64 1.66 0.1020	341.04 ± 174.62 1.95 0.0559	347.03 ± 165.54 2.10 **0.0407**	-111.43 ± 95.26 -1.17 0.2471	298.44 ± 172.01 1.74 0.0883	197.96 ± 163.28 1.21 0.2306	177.22 ± 101.11 1.75 0.0852	373.86 ± 205.59 1.82 0.0744	-	272.64 ± 115.73 2.36 **0.0221**
Mix_2	-457.08 ± 109.96 -4.16 **0.0001**	-53.71 ± 164.26 -0.33 0.7449	68.40 ± 200.36 0.34 0.7341	74.39 ± 192.49 0.39 0.7006	-384.07 ± 136.84 -2.81 **0.0069**	25.81 ± 198.09 0.13 0.8968	-74.68 ± 190.55 -0.39 0.6966	-95.41 ± 140.97 -0.68 0.5014	101.23 ± 227.85 0.44 0.6586	-272.64 ± 115.73 -2.36 **0.0221**	-

Model Summary 19 | Contact core chlorophyll *a* concentration (CCChl*a*, µgcm^{-3}) by species treatment (Tcode)

Initial linear regression model:

lm(CCChl*a* ~ as.factor(Tcode))

Minimal adequate model:

gls(CCChl*a* ~ as.factor(Tcode),
weights = varIdent(form = ~1|as.factor(Tcode)),
method = 'REML')

Coefficient Table

Intercept ± SE (when baseline is for N): 18.05 ± 0.68, t = 26.68, p < 0.0001.

	N	P	PD	HD_1	HD_2	HU_1	HU_2	CV_1	CV_2	Mix_1	Mix_2
N	-	4.29 ± 1.43 3.01 **0.0039**	9.68 ± 1.77 5.47 **< 0.0001**	12.46 ± 2.70 4.61 **< 0.0001**	10.25 ± 2.69 3.81 **0.0004**	5.62 ± 1.36 4.12 **0.0001**	8.57 ± 1.79 4.79 **< 0.0001**	7.74 ± 2.24 3.46 **0.0010**	11.35 ± 2.34 4.85 **< 0.0001**	6.47 ± 2.02 3.21 **0.0022**	7.64 ± 1.62 4.73 **< 0.0001**
P	-4.29 ± 1.43 -3.01 **0.0039**	-	5.39 ± 2.06 2.61 **0.0115**	8.16 ± 2.90 2.81 **0.0068**	5.95 ± 2.89 2.06 **0.0441**	1.32 ± 1.73 0.77 0.4470	4.28 ± 2.08 2.06 **0.0446**	3.45 ± 2.47 1.39 0.1688	7.06 ± 2.57 2.75 **0.0081**	2.18 ± 2.28 0.96 0.3430	3.35 ± 1.93 1.73 0.0886
PD	-9.68 ± 1.77 -5.47 **< 0.0001**	-5.39 ± 2.06 -2.61 **0.0115**	-	2.77 ± 3.08 0.90 0.3722	0.57 ± 3.07 0.18 0.8545	-4.07 ± 2.02 -2.02 **0.0488**	-1.11 ± 2.33 -0.48 0.6344	-1.94 ± 2.69 -0.72 0.4732	1.67 ± 2.77 0.60 0.5500	-3.21 ± 2.51 -1.28 0.2053	-2.04 ± 2.20 -0.93 0.3567
HD_1	-12.46 ± 2.70 -4.61 **< 0.0001**	-8.16 ± 2.90 -2.81 **0.0068**	-2.77 ± 3.08 -0.90 0.3722	-	-2.21 ± 3.69 -0.60 0.5521	-6.84 ± 2.87 -2.38 **0.0206**	-3.89 ± 3.10 -1.26 0.2146	-4.71 ± 3.37 -1.40 0.1679	-1.10 ± 3.44 -0.32 0.7496	-5.98 ± 3.23 -1.85 0.0693	-4.81 ± 3.00 -1.61 0.1139
HD_2	-10.25 ± 2.69 -3.81 **0.0004**	-5.95 ± 2.89 -2.06 **0.0441**	-0.57 ± 3.07 -0.18 0.8545	2.21 ± 3.69 0.60 0.5521	-	-4.63 ± 2.86 -1.62 0.1109	-1.68 ± 3.09 -0.54 0.5885	-2.51 ± 3.36 -0.74 0.4595	1.10 ± 3.44 0.32 0.7495	-3.78 ± 3.22 -1.17 0.2461	-2.61 ± 2.99 -0.87 0.3867
HU_1	-5.62 ± 1.36 -4.12 **0.0001**	-1.32 ± 1.73 -0.77 0.4470	4.07 ± 2.02 2.02 **0.0488**	6.84 ± 2.87 2.38 **0.0206**	4.63 ± 2.86 1.62 0.1109	-	2.95 ± 2.04 1.45 0.1528	2.13 ± 2.44 0.87 0.3866	5.74 ± 2.54 2.26 **0.0276**	0.86 ± 2.24 0.38 0.7036	2.03 ± 1.88 1.07 0.2871
HU_2	-8.57 ± 1.79 -4.79 **< 0.0001**	-4.28 ± 2.08 -2.06 **0.0446**	1.11 ± 2.33 0.48 0.6344	3.89 ± 3.10 1.26 0.2146	1.68 ± 3.09 0.54 0.5885	-2.95 ± 2.04 -1.45 0.1528	-	-0.83 ± 2.70 -0.31 0.7607	2.78 ± 2.79 1.00 0.3228	-2.10 ± 2.52 -0.83 0.4088	-0.93 ± 2.21 -0.42 0.6767
CV_1	-7.74 ± 2.24 -3.46 **0.0010**	3.45 ± 2.47 -1.39 0.1688	1.94 ± 2.69 0.72 0.4732	4.71 ± 3.37 1.40 0.1679	2.51 ± 3.36 0.74 0.4595	-2.13 ± 2.44 -0.87 0.3866	0.83 ± 2.70 0.31 0.7607	-	3.61 ± 3.09 1.17 0.2484	-1.27 ± 2.85 -0.45 0.6577	-0.10 ± 2.59 -0.04 0.9688
CV_2	-11.35 ± 2.34 -4.85 **< 0.0001**	-7.06 ± 2.57 -2.75 **0.0081**	-1.67 ± 2.77 -0.60 0.5500	1.10 ± 3.44 0.32 0.7496	-1.10 ± 3.44 -0.32 0.7495	-5.74 ± 2.54 -2.26 **0.0276**	-2.78 ± 2.79 -1.00 0.3228	-3.61 ± 3.09 -1.17 0.2484	-	-4.88 ± 2.94 -1.66 0.1024	-3.71 ± 2.68 -1.38 0.1717
Mix_1	-6.47 ± 2.02 -3.21 **0.0022**	-2.18 ± 2.28 -0.96 0.3430	3.21 ± 2.51 1.28 0.2053	5.98 ± 3.23 1.85 0.0693	3.78 ± 3.22 1.17 0.2461	-0.86 ± 2.24 -0.38 0.7036	2.10 ± 2.52 0.83 0.4088	1.27 ± 2.85 0.45 0.6577	4.88 ± 2.94 1.66 0.1024	-	1.17 ± 2.40 0.49 0.6277
Mix_2	-7.64 ± 1.62 -4.73 **< 0.0001**	-3.35 ± 1.93 -1.73 0.0886	2.04 ± 2.20 0.93 0.3567	4.81 ± 3.00 1.61 0.1139	2.61 ± 2.99 0.87 0.3867	-2.03 ± 1.88 -1.07 0.2871	0.93 ± 2.21 0.42 0.6767	0.10 ± 2.59 0.04 0.9688	3.71 ± 2.68 1.38 0.1717	-1.17 ± 2.40 -0.49 0.6277	-

Model Summary 20 | Contact core chlorophyll *b* concentration (CCChl*b*, µgcm^{-3}) by species treatment (Tcode)

Initial linear regression model:

lm(CCChl*b* ~ as.factor(Tcode))

Minimal adequate model:

gls(CCChl*b* ~ as.factor(Tcode),
weights = varIdent(form = ~1|as.factor(Tcode)),
method = 'REML')

Coefficient Table

Intercept ± SE (when baseline is for N): 3.87 ± 0.19, t = 20.41, p < 0.0001.

	N	P	PD	HD_1	HD_2	HU_1	HU_2	CV_1	CV_2	Mix_1	Mix_2
N	-	1.17 ± 0.29 4.05 **0.0002**	2.82 ± 0.58 4.87 **< 0.0001**	3.52 ± 0.87 4.04 **0.0002**	3.32 ± 0.83 3.98 **0.0002**	1.95 ± 0.47 4.15 **0.0001**	2.57 ± 0.48 5.33 **< 0.0001**	2.37 ± 0.65 3.63 **0.0006**	2.83 ± 0.36 7.88 **< 0.0001**	1.56 ± 0.41 3.82 **0.0003**	1.94 ± 0.40 4.90 **< 0.0001**
P	-1.17 ± 0.29 -4.05 **0.0002**	-	1.65 ± 0.59 2.81 **0.0068**	2.36 ± 0.88 2.68 **0.0097**	2.15 ± 0.84 2.56 **0.0133**	0.78 ± 0.48 1.62 0.1099	1.40 ± 0.49 2.85 **0.0062**	1.20 ± 0.66 1.82 0.0741	1.67 ± 0.37 4.45 **< 0.0001**	0.40 ± 0.42 0.94 0.3522	0.77 ± 0.41 1.89 0.0644
PD	-2.82 ± 0.58 -4.87 **< 0.0001**	-1.65 ± 0.59 -2.81 **0.0068**	-	0.70 ± 1.01 0.69 0.4905	0.49 ± 0.98 0.51 0.6153	-0.87 ± 0.70 -1.25 0.2154	-0.25 ± 0.70 -0.36 0.7215	-0.45 ± 0.83 -0.54 0.5909	0.01 ± 0.63 0.02 0.9849	-1.26 ± 0.66 -1.92 0.0604	-0.88 ± 0.65 -1.36 0.1799
HD_1	-3.52 ± 0.87 -4.04 **0.0002**	-2.36 ± 0.88 -2.68 **0.0097**	-0.70 ± 1.01 -0.69 0.4905	-	-0.21 ± 1.18 -0.18 0.8601	-1.58 ± 0.95 -1.65 0.1046	-0.96 ± 0.96 -0.99 0.3242	-1.15 ± 1.06 -1.09 0.2804	-0.69 ± 0.91 -0.76 0.4484	-1.96 ± 0.93 -2.12 **0.0387**	-1.58 ± 0.92 -1.72 0.0910
HD_2	-3.32 ± 0.83 -3.98 **0.0002**	-2.15 ± 0.84 -2.56 **0.0133**	-0.49 ± 0.98 -0.51 0.6153	0.21 ± 1.18 0.18 0.8601	-	-1.37 ± 0.92 -1.49 0.1424	-0.75 ± 0.92 -0.81 0.4226	-0.94 ± 1.02 -0.92 0.3609	-0.48 ± 0.87 -0.56 0.5799	-1.75 ± 0.89 -1.97 0.0536	-1.38 ± 0.88 -1.56 0.1250
HU_1	-1.95 ± 0.47 -4.15 **0.0001**	-0.78 ± 0.48 -1.62 0.1099	0.87 ± 0.70 1.25 0.2154	1.58 ± 0.95 1.65 0.1046	1.37 ± 0.92 1.49 0.1424	-	0.62 ± 0.62 1.01 0.3193	0.42 ± 0.76 0.56 0.5796	0.88 ± 0.53 1.68 0.0991	-0.39 ± 0.56 -0.69 0.4950	-0.01 ± 0.55 -0.02 0.9875
HU_2	-2.57 ± 0.48 -5.33 **< 0.0001**	-1.40 ± 0.49 -2.85 **0.0062**	0.25 ± 0.70 0.36 0.7215	0.96 ± 0.96 0.99 0.3242	0.75 ± 0.92 0.81 0.4226	-0.62 ± 0.62 -1.01 0.3193	-	-0.20 ± 0.77 -0.26 0.7979	0.26 ± 0.54 0.49 0.6251	-1.01 ± 0.57 -1.76 0.0841	-0.63 ± 0.56 -1.12 0.2689
CV_1	-2.37 ± 0.65 -3.63 **0.0006**	1.20 ± 0.66 -1.82 0.0741	0.45 ± 0.83 0.54 0.5909	1.15 ± 1.06 1.09 0.2804	0.94 ± 1.02 0.92 0.3609	-0.42 ± 0.76 -0.56 0.5796	0.20 ± 0.77 0.26 0.7979	-	0.46 ± 0.70 0.66 0.5102	-0.81 ± 0.72 -1.12 0.2678	-0.43 ± 0.72 -0.60 0.5489
CV_2	-2.83 ± 0.36 -7.88 **< 0.0001**	-1.67 ± 0.37 -4.45 **< 0.0001**	-0.01 ± 0.63 -0.02 0.9849	0.69 ± 0.91 0.76 0.4484	0.48 ± 0.87 0.56 0.5799	-0.88 ± 0.53 -1.68 0.0991	-0.26 ± 0.54 -0.49 0.6251	-0.46 ± 0.70 -0.66 0.5102	-	-1.27 ± 0.47 -2.68 **0.0096**	-0.89 ± 0.46 -1.93 0.0588
Mix_1	-1.56 ± 0.41 -3.82 **0.0003**	-0.40 ± 0.42 -0.94 0.3522	1.26 ± 0.66 1.92 0.0604	1.96 ± 0.93 2.12 **0.0387**	1.75 ± 0.89 1.97 0.0536	0.39 ± 0.56 0.69 0.4950	1.01 ± 0.57 1.76 0.0841	0.81 ± 0.72 1.12 0.2678	1.27 ± 0.47 2.68 **0.0096**	-	0.38 ± 0.50 0.75 0.4556
Mix_2	-1.94 ± 0.40 -4.90 **< 0.0001**	-0.77 ± 0.41 -1.89 0.0644	0.88 ± 0.65 1.36 0.1799	1.58 ± 0.92 1.72 0.0910	1.38 ± 0.88 1.56 0.1250	0.01 ± 0.55 0.02 0.9875	0.63 ± 0.56 1.12 0.2689	0.43 ± 0.72 0.60 0.5489	0.89 ± 0.46 1.93 0.0588	-0.38 ± 0.50 -0.75 0.4556	-

Model Summary 21 | Contact core mean particle size (CCMean, µm) by species treatment (Tcode)

Initial linear regression model:

lm(CCMean ~ as.factor(Tcode))

No minimal adequate model, intercept only (Tcode, L-ratio = 6.308949, d.f. = 22, p = 0.7887).

Model Summary 22 | Contact core particle size mode (CCMode, µm) by species treatment (Tcode)

Initial linear regression model:

lm(CCMode ~ as.factor(Tcode))

No minimal adequate model, intercept only (Tcode, F = 0.8261, d.f. = 10, p = 0.6054).

Model Summary 23 | Contact core particle sorting (CCSort) by species treatment (Tcode)

Initial linear regression model:

lm(CCSort ~ as.factor(Tcode))

No minimal adequate model, intercept only (Tcode, L-ratio = 16.51317, d.f. = 22, p = 0.0859).

Model Summary 24 | Contact core particle skewness (CCSkew) by species treatment (Tcode)

Initial linear regression model:

lm(CCSkew ~ as.factor(Tcode))

No minimal adequate model, intercept only (Tcode, L-ratio = 18.00562, d.f. = 22, p = 0.0549).

Model Summary 25 | Contact core particle kurtosis (CCKurt) by species treatment (Tcode)

Initial linear regression model:

lm(CCKurt ~ as.factor(Tcode))

Minimal adequate model:

gls(CCKurt ~ as.factor(Tcode),
weights = varIdent(form = ~1|as.factor(Tcode)),
method = 'REML')

Coefficient Table

Intercept ± SE (when baseline is for N): 4.35 ± 0.15, t = 28.78, p < 0.0001.

	N	P	PD	HD_1	HD_2	HU_1	HU_2	CV_1	CV_2	Mix_1	Mix_2
N	-	-0.65 ± 0.16 -3.99 **0.0002**	-0.88 ± 0.22 -4.07 **0.0002**	-0.71 ± 0.17 -4.12 **0.0001**	-1.27 ± 0.22 -5.77 **< 0.0001**	-0.76 ± 0.17 -4.47 **< 0.0001**	-0.77 ± 0.39 -1.99 0.0516	-0.74 ± 0.18 -4.22 **0.0001**	-0.82 ± 0.16 -5.10 **< 0.0001**	-0.61 ± 0.21 -2.87 **0.0059**	-0.77 ± 0.15 -5.01 **< 0.0001**
P	0.65 ± 0.16 3.99 **0.0002**	-	-0.23 ± 0.17 -1.35 0.1820	-0.05 ± 0.10 -0.52 0.6065	-0.61 ± 0.17 -3.58 **0.0007**	-0.11 ± 0.10 -1.07 0.2913	-0.11 ± 0.36 -0.31 0.7554	-0.09 ± 0.11 -0.82 0.4170	-0.17 ± 0.08 -1.99 0.0514	0.05 ± 0.16 0.30 0.7639	-0.12 ± 0.07 -1.69 0.0971
PD	0.88 ± 0.22 4.07 **0.0002**	0.23 ± 0.17 1.35 0.1820	-	0.17 ± 0.17 0.99 0.3272	-0.39 ± 0.22 -1.74 0.0869	0.12 ± 0.17 0.69 0.4949	0.11 ± 0.39 0.29 0.7702	0.14 ± 0.18 0.75 0.4539	0.06 ± 0.16 0.37 0.7146	0.27 ± 0.21 1.28 0.2044	0.11 ± 0.16 0.71 0.4835
HD_1	0.71 ± 0.17 4.12 **0.0001**	0.05 ± 0.10 0.52 0.6065	-0.17 ± 0.17 -0.99 0.3272	-	-0.56 ± 0.18 -3.13 **0.0028**	-0.05 ± 0.11 -0.48 0.6351	-0.06 ± 0.36 -0.16 0.8709	-0.04 ± 0.12 -0.31 0.7605	-0.11 ± 0.10 -1.15 0.2533	0.10 ± 0.17 0.60 0.5478	-0.06 ± 0.09 -0.73 0.4688
HD_2	1.27 ± 0.22 5.77 **< 0.0001**	0.61 ± 0.17 3.58 **0.0007**	0.39 ± 0.22 1.74 0.0869	0.56 ± 0.18 3.13 **0.0028**	-	0.51 ± 0.18 2.85 **0.0061**	0.50 ± 0.39 1.29 0.2027	0.52 ± 0.18 2.85 **0.0062**	0.45 ± 0.17 2.66 **0.0102**	0.66 ± 0.22 3.05 **0.0035**	0.50 ± 0.16 3.09 **0.0032**
HU_1	0.76 ± 0.17 4.47 **< 0.0001**	0.11 ± 0.10 1.07 0.2913	-0.12 ± 0.17 -0.69 0.4949	0.05 ± 0.11 0.48 0.6351	-0.51 ± 0.18 -2.85 **0.0061**	-	-0.01 ± 0.36 -0.02 0.9877	0.02 ± 0.12 0.14 0.8919	-0.06 ± 0.09 -0.62 0.5373	0.16 ± 0.17 0.93 0.3552	-0.01 ± 0.08 -0.10 0.9188
HU_2	0.77 ± 0.39 1.99 0.0516	0.11 ± 0.36 0.31 0.7554	-0.11 ± 0.39 -0.29 0.7702	0.06 ± 0.36 0.16 0.8709	-0.50 ± 0.39 -1.29 0.2027	0.01 ± 0.36 0.02 0.9877	-	0.02 ± 0.37 0.06 0.9523	-0.05 ± 0.36 -0.15 0.8824	0.16 ± 0.38 0.42 0.6762	0.00 ± 0.36 -0.01 0.9938
CV_1	0.74 ± 0.18 4.22 **0.0001**	-0.09 ± 0.11 0.82 0.4170	-0.14 ± 0.18 -0.75 0.4539	0.04 ± 0.12 0.31 0.7605	-0.52 ± 0.18 -2.85 **0.0062**	-0.02 ± 0.12 -0.14 0.8919	-0.02 ± 0.37 -0.06 0.9523	-	-0.08 ± 0.11 -0.71 0.4802	0.14 ± 0.17 0.80 0.4254	-0.02 ± 0.09 -0.26 0.7944
CV_2	0.82 ± 0.16 5.10 **< 0.0001**	0.17 ± 0.08 1.99 0.0514	-0.06 ± 0.16 -0.37 0.7146	0.11 ± 0.10 1.15 0.2533	-0.45 ± 0.17 -2.66 **0.0102**	0.06 ± 0.09 0.62 0.5373	0.05 ± 0.36 0.15 0.8824	0.08 ± 0.11 0.71 0.4802	-	0.21 ± 0.16 1.37 0.1778	0.05 ± 0.06 0.84 0.4024
Mix_1	0.61 ± 0.21 2.87 **0.0059**	-0.05 ± 0.16 -0.30 0.7639	-0.27 ± 0.21 -1.28 0.2044	-0.10 ± 0.17 -0.60 0.5478	-0.66 ± 0.22 -3.05 **0.0035**	-0.16 ± 0.17 -0.93 0.3552	-0.16 ± 0.38 -0.42 0.6762	-0.14 ± 0.17 -0.80 0.4254	-0.21 ± 0.16 -1.36 0.1778	-	-0.16 ± 0.15 -1.10 0.2783
Mix_2	0.77 ± 0.15 5.01 **< 0.0001**	0.12 ± 0.07 1.69 0.0971	-0.11 ± 0.16 -0.71 0.4835	0.06 ± 0.09 0.73 0.4688	-0.50 ± 0.16 -3.09 **0.0032**	0.01 ± 0.08 0.10 0.9188	0.00 ± 0.36 0.01 0.9938	0.02 ± 0.09 0.26 0.7944	-0.05 ± 0.06 -0.84 0.4024	0.16 ± 0.15 1.10 0.2783	-

Model Summary 26 | Contact core D_{10} (CCD_{10}, µm) by species treatment (Tcode)

Initial linear regression model:

lm(CCD_{10} ~ as.factor(Tcode))

No minimal adequate model, intercept only (Tcode, L-ratio = 13.6147, d.f. = 22, p = 0.1913).

Model Summary 27 | Contact core mud content (CCPCMud, %) by species treatment (Tcode)

Initial linear regression model:

lm(CCPCMud% ~ as.factor(Tcode))

No minimal adequate model, intercept only (Tcode, L-ratio = 7.814853, d.f. = 22, p = 0.6469).

Appendix 3

Statistical model summary

Summary of the statistical analysis for the 27 statistical models. For each model the initial linear regression model, the minimal adequate model with GLS estimation and a summary of the coefficient table is given. The coefficients indicate the relative performance of each treatment level relative to the relevelled baseline (as indicated). Coefficients ± SE and t-values are presented alongside corresponding significance values (in parentheses). Abbreviations: N, natural sediment as a mudflat baseline; P, pipe mesocosm only treatment as a procedural control; PD, defaunated mesocosm treatment as an experimental control; HD_1HU_2 $^2/_3$ original biomass replaced with *Hediste diversicolor*, $^1/_3$ original biomass replaced with *Hydrobia ulvae*; HDHU, $^1/_2$ original biomass replaced with *Hediste diversicolor*, $^1/_2$ original biomass replaced with *Hydrobia ulvae*; HU_1HD_2, $^2/_3$ original biomass replaced with *Hydrobia ulvae*, $^1/_3$ original biomass replaced with *Hediste diversicolor*; HD_1CV_2 $^2/_3$ original biomass replaced with *Hediste diversicolor*, $^1/_3$ original biomass replaced with *Corophium volutator*; HDCV, $^1/_2$ original biomass replaced with *Hediste diversicolor*, $^1/_2$ original biomass replaced with *Corophium volutator*; CV_1HD_2, $^2/_3$ original biomass replaced with *Corophium volutator*, $^1/_3$ original biomass replaced with *Hediste diversicolor*; HU_1CV_2 $^2/_3$ original biomass replaced with *Hydrobia ulvae*, $^1/_3$ original biomass replaced with *Corophium volutator*; HUCV, $^1/_2$ original biomass replaced with *Hydrobia ulvae*, $^1/_2$ original biomass replaced with *Corophium volutator*; CV_1HU_2, $^2/_3$ original biomass replaced with *Corophium volutator*, $^1/_3$ original biomass replaced with *Hydrobia ulvae*; Mix_2, mix of HD, HU and CV, each species replacing a $^1/_3$ of the original biomass, as in Chapter 4; Day, day of data collection; Row, row location of pipe mesocosm; Tcode, species treatment code [N, P, PF, HD_1HU_2, HDHU, HU_1HD_2, HD_1CV_2, HDCV, CV_1HD_2, HU_1CV_2, HUCV, CV_1HU_2, Mix_2].

Model Summary 1 | Erosion threshold (ET, Nm^{-2}) by day of data collection (Day)

Initial linear regression model:

lm(ET ~ as.factor(Day))

No minimal adequate model, intercept only (Day, L-ratio = 1.523347, d.f. = 4, p = 0.2171).

Model Summary 2 | Average pulse amplitude modulated (PAM) measured minimum fluorescence (PAMFAv) by day of data collection (Day)

Initial linear regression model:

lm(PAMFmAv ~ as.factor(Day))

Minimal adequate model:

gls(PAMFAv~ as.factor(Day),
method = 'REML')

Coefficient Table

Intercept ± SE (when baseline is for N): 368.54 ± 36.83, t = 10.01, p < 0.0001.

	1	2
1	-	185.85 ± 56.77 3.27 **0.0019**
2	-185.85 ± -56.77 -3.27 **0.0019**	-

Model Summary 3 | Erosion threshold (ET, Nm^{-2}) by row location of mesocosm (Row)

Initial linear regression model:

lm(ET ~ as.factor(Row))

No minimal adequate model, intercept only (Day, L-ratio = 0.1673436, d.f. = 5, p = 0.9827).

Model Summary 4 | Average pulse amplitude modulated (PAM) measured minimum fluorescence (PAMFAv) by row location of mesocosm (Row)

Initial linear regression model:

lm(PAMFmAv ~ as.factor(Row))

Minimal adequate model:

gls(PAMFAv~ as.factor(Row),
weights = varIdent(form = ~1|as.factor(Row)),
method = 'REML')

Coefficient Table

Intercept ± SE (when baseline is for N): 613.38 ± 79.59, t = 7.71, p < 0.0001.

	1	2	3	4
1	-	-138.18 ± 93.92 -1.47 0.1478	-241.55 ± 94.33 -2.56 **0.0137**	-251.82 ± 87.80 -2.87 **0.0061**
2	138.18 ± 93.92 1.47 0.1478	-	-103.38 ± 71.08 -1.45 0.1523	-113.6 ± 62.15 -1.83 0.0737
3	241.55 ± 94.33 2.56 **0.0137**	103.38 ± 71.08 1.45 0.1523	-	-10.27 ± 62.77 -0.16 0.8707
4	251.82 ± 87.80 2.87 **0.0061**	113.64 ± 62.15 1.83 0.0737	10.27 ± 62.77 0.16 0.8707	-

Model Summary 5 | Erosion threshold (ET, Nm^{-2}) by species treatment (Tcode)

Initial linear regression model:

```
lm(ET ~ as.factor(Tcode))
```

Minimal adequate model:

```
gls(ET~ as.factor(Tcode),
    weights = varIdent(form = ~1|as.factor(Tcode)),
    method = 'REML')
```

Coefficient Table

Intercept ± SE (when baseline is for N): 0.32 ± 0.04, t = 7.20, p < 0.0001.

	N	P	PD	HD_1HU_2	HDHU	HU_1HD_2	HD_1CV_2	HDCV	CV_1HD_2	HU_1CV_2	HUCV	CV_1HU_2	Mix_2
N	-	1.39 ± 0.22 6.30 **< 0.0001**	2.66 ± 0.79 3.37 **0.0017**	1.91 ± 0.46 4.18 **0.0002**	1.00 ± 0.35 2.86 **0.0067**	1.48 ± 0.29 5.05 **< 0.0001**	2.44 ± 0.27 8.92 **< 0.0001**	1.60 ± 0.26 6.23 **< 0.0001**	1.46 ± 0.26 5.54 **< 0.0001**	2.32 ± 0.22 10.37 **< 0.0001**	1.70 ± 0.39 4.34 **0.0001**	1.36 ± 0.63 2.17 **0.0363**	2.75 ± 0.76 3.60 **0.0009**
P	-1.39 ± 0.22 -6.30 **< 0.0001**	-	1.28 ± 0.82 1.56 0.1261	0.53 ± 0.50 1.04 0.3029	-0.38 ± 0.41 -0.94 0.3549	0.10 ± 0.36 0.27 0.7886	1.05 ± 0.34 3.05 **0.0041**	0.21 ± 0.33 0.64 0.5255	0.07 ± 0.34 0.21 0.8363	0.94 ± 0.31 3.04 **0.0042**	0.31 ± 0.44 0.70 0.4855	-0.03 ± 0.66 -0.04 0.9670	1.36 ± 0.79 1.72 0.0934
PD	-2.66 ± 0.79 -3.37 **0.0017**	-1.28 ± 0.82 -1.56 0.1261	-	-0.75 ± 0.91 -0.83 0.4133	-1.66 ± 0.86 -1.93 0.0613	-1.18 ± 0.84 -1.40 0.1680	-0.23 ± 0.83 -0.27 0.7862	-1.07 ± 0.83 -1.29 0.2058	-1.21 ± 0.83 -1.46 0.1536	-0.34 ± 0.82 -0.42 0.6778	-0.97 ± 0.88 -1.10 0.2789	-1.31 ± 1.01 -1.30 0.2020	0.08 ± 1.10 0.08 0.9404
HD_1HU_2	-1.91 ± 0.46 -4.18 **0.0002**	-0.53 ± 0.50 -1.04 0.3029	0.75 ± 0.91 0.83 0.4133	-	-0.91 ± 0.57 -1.59 0.1207	-0.43 ± 0.54 -0.79 0.4327	0.53 ± 0.53 0.99 0.3265	-0.31 ± 0.52 -0.60 0.5513	-0.46 ± 0.52 -0.87 0.3897	0.41 ± 0.50 0.81 0.4214	-0.21 ± 0.60 -0.36 0.7241	-0.55 ± 0.77 -0.72 0.4786	0.84 ± 0.89 0.94 0.3519
HDHU	-1.00 ± 0.35 -2.86 **0.0067**	0.38 ± 0.41 0.94 0.3549	1.66 ± 0.86 1.93 0.0613	0.91 ± 0.57 1.59 0.1207	-	0.48 ± 0.45 1.06 0.2954	1.43 ± 0.44 3.26 **0.0023**	0.60 ± 0.43 1.39 0.1737	0.45 ± 0.43 1.04 0.3027	1.32 ± 0.41 3.21 **0.0027**	0.70 ± 0.52 1.33 0.1899	0.36 ± 0.71 0.50 0.6220	1.74 ± 0.84 2.08 **0.0438**
HU_1HD_2	-1.48 ± 0.29 -5.05 **< 0.0001**	-0.10 ± 0.36 -0.27 0.7886	1.18 ± 0.84 1.40 0.1680	0.43 ± 0.54 0.79 0.4327	-0.48 ± 0.45 -1.06 0.2954	-	0.95 ± 0.40 2.41 **0.0210**	0.12 ± 0.38 0.30 0.7666	-0.03 ± 0.39 -0.07 0.9440	0.84 ± 0.36 2.30 **0.0267**	0.22 ± 0.48 0.44 0.6598	-0.13 ± 0.69 -0.18 0.8569	1.26 ± 0.81 1.55 0.1291
HD_1CV_2	-2.44 ± 0.27 -8.92 **< 0.0001**	-1.05 ± 0.34 -3.05 **0.0041**	0.23 ± 0.83 0.27 0.7862	-0.53 ± 0.53 -0.99 0.3265	-1.43 ± 0.44 -3.26 **0.0023**	-0.95 ± 0.40 -2.41 **0.0210**	-	-0.84 ± 0.37 -2.27 **0.0289**	-0.98 ± 0.37 -2.62 **0.0124**	-0.12 ± 0.35 -0.3312 0.7423	-0.74 ± 0.47 -1.5611 0.1266	-1.08 ± 0.68 -1.58 0.1211	0.31 ± 0.81 0.38 0.7030
HDCV	-1.60 ± 0.26 -6.23 **< 0.0001**	0.21 ± 0.33 -0.64 0.5255	1.07 ± 0.83 1.29 0.2058	0.31 ± 0.52 0.60 0.5513	-0.60 ± 0.43 -1.39 0.1737	-0.12 ± 0.38 -0.30 0.7666	0.84 ± 0.37 2.27 **0.0289**	-	-0.14 ± 0.36 -0.39 0.6957	0.72 ± 0.33 2.16 **0.0369**	0.10 ± 0.46 0.22 0.8302	-0.24 ± 0.67 -0.36 0.7235	1.15 ± 0.80 1.43 0.1603
CV_1HD_2	-1.46 ± 0.26 -5.54 **< 0.0001**	-0.07 ± 0.34 -0.21 0.8363	1.21 ± 0.83 1.46 0.1536	0.46 ± 0.52 0.87 0.3897	-0.45 ± 0.43 -1.04 0.3027	0.03 ± 0.39 0.07 0.9440	0.98 ± 0.37 2.62 **0.0124**	0.14 ± 0.36 0.39 0.6957	-	0.87 ± 0.34 2.55 **0.0148**	0.24 ± 0.47 0.52 0.6062	-0.10 ± 0.68 -0.14 0.8860	1.29 ± 0.80 1.61 0.1166
HU_1CV_2	-2.32 ± 0.22 -10.37 **< 0.0001**	-0.94 ± 0.31 -3.04 **0.0042**	0.34 ± 0.82 0.42 0.6778	-0.41 ± 0.50 -0.81 0.4214	-1.32 ± 0.41 -3.21 **0.0027**	-0.84 ± 0.36 -2.30 **0.0267**	0.12 ± 0.35 0.33 0.7423	-0.72 ± 0.33 -2.16075 **0.0369**	-0.87 ± 0.34 -2.55 **0.0148**	-	-0.62 ± 0.45 -1.40 0.1705	-0.96 ± 0.66 -1.45 0.1538	0.43 ± 0.79 0.54 0.5945
HUCV	-1.70 ± 0.39 -4.34 **0.0001**	-0.31 ± 0.44 -0.70 0.4855	0.97 ± 0.88 1.10 0.2789	0.21 ± 0.60 0.36 0.7241	-0.70 ± 0.52 -1.33 0.1899	-0.22 ± 0.48 -0.44 0.6598	0.74 ± 0.47 1.56 0.1266	-0.10 ± 0.46 -0.22 0.8302	-0.24 ± 0.47 -0.52 0.6062	0.62 ± 0.45 1.40 0.1705	-	-0.34 ± 0.74 -0.46 0.6463	1.05 ± 0.85 1.23 0.2274
CV_1HU_2	-1.36 ± 0.63 -2.17 **0.0363**	0.03 ± 0.66 0.04 0.9670	1.31 ± 1.01 1.30 0.2020	0.55 ± 0.77 0.72 0.4786	-0.36 ± 0.71 -0.50 0.6220	0.13 ± 0.69 0.18 0.8569	1.08 ± 0.68 1.58 0.1211	0.24 ± 0.67 0.36 0.7235	0.10 ± 0.68 0.14 0.8860	0.96 ± 0.66 1.45 0.1538	0.34 ± 0.74 0.46 0.6463	-	1.39 ± 0.98 1.41 0.1665
Mix_2	-2.75 ± 0.76 -3.60 **0.0009**	-1.36 ± 0.79 -1.72 0.0934	-0.08 ± 1.10 -0.08 0.9404	-0.84 ± 0.89 -0.94 0.3519	-1.74 ± 0.84 -2.08 **0.0438**	-1.26 ± 0.81 -1.55 0.1291	-0.31 ± 0.81 -0.38 0.7030	-1.15 ± 0.80 -1.43 0.1603	-1.29 ± 0.80 -1.61 0.1166	-0.43 ± 0.79 -0.54 0.5945	-1.05 ± 0.85 -1.23 0.2274	-1.39 ± 0.98 -1.41 0.1665	-

Model Summary 6 | Suspension index (SI) by species treatment (Tcode)

Initial linear regression model:

```
lm(SI ~ as.factor(Tcode))
```

Minimal adequate model:

```
gls(SI ~ as.factor(Tcode),
    weights = varIdent(form = ~1|as.factor(Tcode)),
    method = 'REML')
```

Coefficient Table

Intercept ± SE (when baseline is for N): 10.40 ± 1.81, t = 5.76, p < 0.0001.

	N	P	PD	HD_1HU_2	HDHU	HU_1HD_2	HD_1CV_2	HDCV	CV_1HD_2	HU_1CV_2	HUCV	CV_1HU_2	Mix_2
N	-	-8.35 ± 2.19 -3.81 **0.0005**	-8.33 ± 1.94 -4.30 **0.0001**	-8.06 ± 1.94 -4.16 **0.0002**	-7.52 ± 2.24 -3.36 **0.0018**	-9.49 ± 1.82 -5.21 **< 0.0001**	-8.28 ± 2.05 -4.03 **0.0002**	-9.12 ± 1.84 -4.95 **< 0.0001**	-8.93 ± 1.86 -4.82 **< 0.0001**	-9.03 ± 1.96 -4.60 **< 0.0001**	-9.14 ± 1.98 -4.61 **< 0.0001**	0.47 ± 5.05 0.09 0.9255	-9.18 ± 1.83 -5.03 **< 0.0001**
P	8.35 ± 2.19 3.81 **0.0005**	-	0.02 ± 1.43 0.01 0.9903	0.29 ± 1.43 0.20 0.8399	0.84 ± 1.81 0.46 0.6474	-1.13 ± 1.26 -0.90 0.3739	0.08 ± 1.58 0.05 0.9623	-0.77 ± 1.29 -0.60 0.5542	-0.58 ± 1.31 -0.44 0.6591	-0.67 ± 1.46 -0.46 0.6461	-0.79 ± 1.49 -0.53 0.6006	8.83 ± 4.88 1.81 0.0780	-0.83 ± 1.27 -0.65 0.5195
PD	8.33 ± 1.94 4.30 **0.0001**	-0.02 ± 1.43 -0.01 0.9903	-	0.27 ± 1.00 0.27 0.7860	0.82 ± 1.50 0.55 0.5882	-1.15 ± 0.74 -1.55 0.1291	0.06 ± 1.21 0.05 0.9621	-0.79 ± 0.80 -0.99 0.3279	-0.60 ± 0.83 -0.73 0.4718	-0.69 ± 1.04 -0.66 0.5103	-0.80 ± 1.08 -0.74 0.4630	8.81 ± 4.77 1.85 0.0723	-0.84 ± 0.76 -1.11 0.2729
HD_1HU_2	8.06 ± 1.94 4.16 **0.0002**	-0.29 ± 1.43 -0.20 0.8399	-0.27 ± 1.00 -0.27 0.7860	-	0.55 ± 1.50 0.36 0.7175	-1.43 ± 0.74 -1.93 0.0608	-0.22 ± 1.20 -0.18 0.8591	-1.06 ± 0.79 -1.34 0.1876	-0.87 ± 0.82 -1.06 0.2946	-0.96 ± 1.04 -0.93 0.3582	-1.08 ± 1.08 -1.00 0.3252	8.54 ± 4.77 1.79 0.0812	-1.12 ± 0.75 -1.48 0.1465
HDHU	7.52 ± 2.24 3.36 **0.0018**	-0.84 ± 1.81 -0.46 0.6474	-0.82 ± 1.50 -0.55 0.5882	-0.55 ± 1.50 -0.36 0.7175	-	-1.97 ± 1.34 -1.47 0.1494	-0.76 ± 1.64 -0.46 0.6460	-1.61 ± 1.37 -1.17 0.2478	-1.42 ± 1.39 -1.02 0.3128	-1.51 ± 1.53 -0.99 0.3283	-1.62 ± 1.55 -1.04 0.3034	7.99 ± 4.90 1.63 0.1108	-1.66 ± 1.35 -1.23 0.2252
HU_1HD_2	9.49 ± 1.82 5.21 **< 0.0001**	1.13 ± 1.26 0.90 0.3739	1.15 ± 0.74 1.55 0.1291	1.43 ± 0.74 1.93 0.0608	1.97 ± 1.34 1.47 0.1494	-	1.21 ± 1.00 1.21 0.2349	0.36 ± 0.43 0.85 0.4013	0.55 ± 0.48 1.14 0.2600	0.46 ± 0.80 0.58 0.5660	0.35 ± 0.85 0.41 0.6826	9.96 ± 4.72 2.11 **0.0413**	0.31 ± 0.35 0.88 0.3844
HD_1CV_2	8.28 ± 2.05 4.03 **0.0002**	-0.08 ± 1.58 -0.05 0.9623	-0.06 ± 1.21 -0.05 0.9621	0.22 ± 1.20 0.18 0.8591	0.76 ± 1.64 0.46 0.6460	-1.21 ± 1.00 -1.21 0.2349	-	-0.85 ± 1.04 -0.81 0.4217	-0.66 ± 1.07 -0.62 0.5404	-0.75 ± 1.24 -0.6044 0.5491	-0.86 ± 1.28 -0.6746 0.5039	8.75 ± 4.82 1.82 0.0769	-0.90 ± 1.01 -0.89 0.3798
HDCV	9.12 ± 1.84 4.95 **< 0.0001**	-0.77 ± 1.29 0.60 0.5542	0.79 ± 0.80 0.99 0.3279	1.06 ± 0.79 1.34 0.1876	1.61 ± 1.37 1.17 0.2478	-0.36 ± 0.43 -0.85 0.4013	0.85 ± 1.04 0.81 0.4217	-	0.19 ± 0.56 0.34 0.7391	0.10 ± 0.85 0.12 0.9088	-0.01 ± 0.90 -0.01 0.9884	9.60 ± 4.73 2.03 **0.0493**	-0.05 ± 0.45 -0.12 0.9060
CV_1HD_2	8.93 ± 1.86 4.82 **< 0.0001**	0.58 ± 1.31 0.44 0.6591	0.60 ± 0.83 0.73 0.4718	0.87 ± 0.82 1.06 0.2946	1.42 ± 1.39 1.02 0.3128	-0.55 ± 0.48 -1.14 0.2600	0.66 ± 1.07 0.62 0.5404	-0.19 ± 0.56 -0.34 0.7391	-	-0.09 ± 0.87 -0.10 0.9179	-0.20 ± 0.92 -0.22 0.8285	9.41 ± 4.74 1.99 0.0539	-0.24 ± 0.51 -0.48 0.6344
HU_1CV_2	9.03 ± 1.96 4.60 **< 0.0001**	0.67 ± 1.46 0.46 0.6461	0.69 ± 1.04 0.66 0.5103	0.96 ± 1.04 0.93 0.3582	1.51 ± 1.53 0.99 0.3283	-0.46 ± 0.80 -0.58 0.5660	0.75 ± 1.24 0.60 0.5491	-0.10 ± 0.85 -0.115291 0.9088	0.09 ± 0.87 0.10 0.9179	-	-0.11 ± 1.12 -0.10 0.9218	9.50 ± 4.78 1.99 0.0538	-0.15 ± 0.81 -0.19 0.8526
HUCV	9.14 ± 1.98 4.61 **< 0.0001**	0.79 ± 1.49 0.53 0.6006	0.80 ± 1.08 0.74 0.4630	1.08 ± 1.08 1.00 0.3252	1.62 ± 1.55 1.04 0.3034	-0.35 ± 0.85 -0.41 0.6826	0.86 ± 1.28 0.67 0.5039	0.01 ± 0.90 0.01 0.9884	0.20 ± 0.92 0.22 0.8285	0.11 ± 1.12 0.10 0.9218	-	9.61 ± 4.79 2.01 0.0516	-0.04 ± 0.86 -0.05 0.9625
CV_1HU_2	-0.47 ± 5.05 -0.09 0.9255	-8.83 ± 4.88 -1.81 0.0780	-8.81 ± 4.77 -1.85 0.0723	-8.54 ± 4.77 -1.79 0.0812	-7.99 ± 4.90 -1.63 0.1108	-9.96 ± 4.72 -2.11 **0.0413**	-8.75 ± 4.82 -1.82 0.0769	-9.60 ± 4.73 -2.03 **0.0493**	-9.41 ± 4.74 -1.99 0.0539	-9.50 ± 4.78 -1.99 0.0538	-9.61 ± 4.79 -2.01 0.0516	-	-9.65 ± 4.72 -2.04 **0.0478**
Mix_2	9.18 ± 1.83 5.03 **< 0.0001**	0.83 ± 1.27 0.65 0.5195	0.84 ± 0.76 1.11 0.2729	1.12 ± 0.75 1.48 0.1465	1.66 ± 1.35 1.23 0.2252	-0.31 ± 0.35 -0.88 0.3844	0.90 ± 1.01 0.89 0.3798	0.05 ± 0.45 0.12 0.9060	0.24 ± 0.51 0.48 0.6344	0.15 ± 0.81 0.19 0.8526	0.04 ± 0.86 0.05 0.9625	9.65 ± 4.72 2.04 **0.0478**	-

Model Summary 7 | Average pulse amplitude modulated (PAM) measured minimum fluorescence (PAMFAv) by species treatment (Tcode)

Initial linear regression model:

```
lm(PAMFAv ~ as.factor(Tcode))
```

Minimal adequate model:

```
gls(PAMFAv ~ as.factor(Tcode),
    weights = varIdent(form = ~1|as.factor(Tcode)),
    method = 'REML')
```

Coefficient Table

Intercept ± SE (when baseline is for N): 195.50 ± 8.05, t = 24.30, p < 0.0001.

	N	P	PD	HD_1HU_2	HDHU	HU_1HD_2	HD_1CV_2	HDCV	CV_1HD_2	HU_1CV_2	HUCV	CV_1HU_2	Mix_2
N	-	49.67 ± 9.23 5.38 **< 0.0001**	220.50 ± 83.57 2.64 **0.0119**	333.92 ± 125.85 2.65 **0.0115**	196.58 ± 102.40 1.92 0.0622	422.25 ± 89.24 4.73 **< 0.0001**	415.42 ± 181.71 2.29 **0.0278**	502.08 ± 151.55 3.31 **0.0020**	189.25 ± 46.58 4.06 **0.0002**	311.33 ± 78.69 3.96 **0.0003**	198.92 ± 82.05 2.42 **0.0201**	354.75 ± 101.65 3.49 **0.0012**	262.83 ± 77.18 3.41 **0.0015**
P	-49.67 ± 9.23 -5.38 **< 0.0001**	-	170.83 ± 83.30 2.05 **0.0470**	284.25 ± 125.67 2.26 **0.0294**	146.92 ± 102.18 1.44 0.1585	372.58 ± 88.99 4.19 **0.0002**	365.75 ± 181.58 2.01 0.0509	452.42 ± 151.41 2.99 **0.0048**	139.58 ± 46.10 3.03 **0.0044**	261.67 ± 78.40 3.34 **0.0019**	149.25 ± 81.78 1.83 0.0757	305.08 ± 101.44 3.01 **0.0046**	213.17 ± 76.89 2.77 **0.0085**
PD	-220.50 ± 83.57 -2.64 **0.0119**	-170.83 ± 83.30 -2.05 **0.0470**	-	113.42 ± 150.63 0.75 0.4560	-23.92 ± 131.68 -0.18 0.8568	201.75 ± 121.73 1.66 0.1055	194.92 ± 199.68 0.98 0.3350	281.58 ± 172.69 1.63 0.1110	-31.25 ± 94.99 -0.33 0.7439	90.83 ± 114.22 0.80 0.4313	-21.58 ± 116.56 -0.19 0.8541	134.25 ± 131.10 1.02 0.3121	42.33 ± 113.18 0.37 0.7104
HD_1HU_2	-333.92 ± 125.85 -2.65 **0.0115**	-284.25 ± 125.67 -2.26 **0.0294**	-113.42 ± 150.63 -0.75 0.4560	-	-137.33 ± 161.84 -0.85 0.4013	88.33 ± 153.85 0.57 0.5692	81.50 ± 220.74 0.37 0.7140	168.17 ± 196.66 0.86 0.3977	-144.67 ± 133.71 -1.08 0.2859	-22.58 ± 147.98 -0.15 0.8795	-135.00 ± 149.80 -0.90 0.3730	20.83 ± 161.37 0.13 0.8979	-71.08 ± 147.19 -0.48 0.6318
HDHU	-196.58 ± 102.40 -1.92 0.0622	-146.92 ± 102.18 -1.44 0.1585	23.92 ± 131.68 0.18 0.8568	137.33 ± 161.84 0.85 0.4013	-	225.67 ± 135.35 1.67 0.1035	218.83 ± 208.26 1.05 0.2998	305.50 ± 182.55 1.67 0.1022	-7.33 ± 111.92 -0.07 0.9481	114.75 ± 128.63 0.89 0.3778	2.33 ± 130.72 0.02 0.9858	158.17 ± 143.84 1.10 0.2782	66.25 ± 127.72 0.52 0.6069
HU_1HD_2	-422.25 ± 89.24 -4.73 **< 0.0001**	-372.58 ± 88.99 -4.19 **0.0002**	-201.75 ± 121.73 -1.66 0.1055	-88.33 ± 153.85 -0.57 0.5692	-225.67 ± 135.35 -1.67 0.1035	-	-6.83 ± 202.12 -0.03 0.9732	79.83 ± 175.51 0.45 0.6517	-233.00 ± 100.02 -2.33 0.0251	-110.92 ± 118.43 -0.94 0.3547	-223.33 ± 120.69 -1.85 0.0718	-67.50 ± 134.79 -0.50 0.6193	-159.42 ± 117.43 -1.36 0.1824
HD_1CV_2	-415.42 ± 181.71 -2.29 **0.0278**	-365.75 ± 181.58 -2.01 0.0509	-194.92 ± 199.68 -0.98 0.3350	-81.50 ± 220.74 -0.37 0.7140	-218.83 ± 208.26 -1.05 0.2998	6.83 ± 202.12 0.03 0.9732	-	86.67 ± 236.34 0.37 0.7158	-226.17 ± 187.24 -1.21 0.2344	-104.08 ± 197.68 -0.5265 0.6015	-216.50 ± 199.05 -1.0877 0.2834	-60.67 ± 207.90 -0.29 0.7720	-152.58 ± 197.09 -0.77 0.4435
HDCV	-502.08 ± 151.55 -3.31 **0.0020**	452.42 ± 151.41 -2.99 **0.0048**	-281.58 ± 172.69 -1.63 0.1110	-168.17 ± 196.66 -0.86 0.3977	-305.50 ± 182.55 -1.67 0.1022	-79.83 ± 175.51 -0.45 0.6517	-86.67 ± 236.34 -0.37 0.7158	-	-312.83 ± 158.14 -1.98 0.0550	-190.75 ± 170.38 -1.12 0.2698	-303.17 ± 171.96 -1.76 0.0857	-147.33 ± 182.13 -0.81 0.4235	-239.25 ± 169.69 -1.41 0.1665
CV_1HD_2	-189.25 ± 46.58 -4.06 **0.0002**	-139.58 ± 46.10 -3.03 **0.0044**	31.25 ± 94.99 0.33 0.7439	144.67 ± 133.71 1.08 0.2859	7.33 ± 111.92 0.07 0.9481	233.00 ± 100.02 2.33 0.0251	226.17 ± 187.24 1.21 0.2344	312.83 ± 158.14 1.98 0.0550	-	122.08 ± 90.73 1.35 0.1862	9.67 ± 93.66 0.10 0.9183	165.50 ± 111.24 1.49 0.1448	73.58 ± 89.42 0.82 0.4156
HU_1CV_2	-311.33 ± 78.69 -3.96 **0.0003**	-261.67 ± 78.40 -3.34 **0.0019**	-90.83 ± 114.22 -0.80 0.4313	22.58 ± 147.98 0.15 0.8795	-114.75 ± 128.63 -0.89 0.3778	110.92 ± 118.43 0.94 0.3547	104.08 ± 197.68 0.53 0.6015	190.75 ± 170.38 1.119536 0.2698	-122.08 ± 90.73 -1.35 0.1862	-	-112.42 ± 113.11 -0.99 0.3264	43.42 ± 128.04 0.34 0.7364	-48.50 ± 109.63 -0.44 0.6606
HUCV	-198.92 ± 82.05 -2.42 **0.0201**	-149.25 ± 81.78 -1.83 0.0757	21.58 ± 116.56 0.19 0.8541	135.00 ± 149.80 0.90 0.3730	-2.33 ± 130.72 -0.02 0.9858	223.33 ± 120.69 1.85 0.0718	216.50 ± 199.05 1.09 0.2834	303.17 ± 171.96 1.76 0.0857	-9.67 ± 93.66 -0.10 0.9183	112.42 ± 113.11 0.99 0.3264	-	155.83 ± 130.14 1.20 0.2384	63.92 ± 112.07 0.57 0.5717
CV_1HU_2	-354.75 ± 101.65 -3.49 **0.0012**	-305.08 ± 101.44 -3.01 **0.0046**	-134.25 ± 131.10 -1.02 0.3121	-20.83 ± 161.37 -0.13 0.8979	-158.17 ± 143.84 -1.10 0.2782	67.50 ± 134.79 0.50 0.6193	60.67 ± 207.90 0.29 0.7720	147.33 ± 182.13 0.81 0.4235	-165.50 ± 111.24 -1.49 0.1448	-43.42 ± 128.04 -0.34 0.7364	-155.83 ± 130.14 -1.20 0.2384	-	-91.92 ± 127.12 -0.72 0.4740
Mix_2	-262.83 ± 77.18 -3.41 **0.0015**	-213.17 ± 76.89 -2.77 **0.0085**	-42.33 ± 113.18 -0.37 0.7104	71.08 ± 147.19 0.48 0.6318	-66.25 ± 127.72 -0.52 0.6069	159.42 ± 117.43 1.36 0.1824	152.58 ± 197.09 0.77 0.4435	239.25 ± 169.69 1.41 0.1665	-73.58 ± 89.42 -0.82 0.4156	48.50 ± 109.63 0.44 0.6606	-63.92 ± 112.07 -0.57 0.5717	91.92 ± 127.12 0.72 0.4740	-

Model Summary 8 | Average pulse amplitude modulated (PAM) measured maximum quantum yield (PAMYAv) by species treatment (Tcode)

Initial linear regression model:

lm(PAMYAv ~ as.factor(Tcode))

No minimal adequate model, intercept only (Tcode, L-ratio = 17.16329, d.f. = 26, p = 0.1436).

Model Summary 9 | Minicore water content (MCWater%, %) by species treatment (Tcode)

Initial linear regression model:

lm(MCWater% ~ as.factor(Tcode))

No minimal adequate model, intercept only (Tcode, L-ratio = 20.60921, d.f. = 26, p = 0.0564).

Model Summary 10 | Minicore mean particle size (MCMean, µm) by species treatment (Tcode)

Initial linear regression model:

lm(MCMean ~ as.factor(Tcode))

No minimal adequate model, intercept only (Tcode, L-ratio = 16.83424, d.f. = 26, p = 0.1559).

Model Summary 11 | Minicore mode particle size (MCMode, µm) by species treatment (Tcode)

Initial linear regression model:

lm(MCMode ~ as.factor(Tcode))

No minimal adequate model, intercept only (Tcode, F = 0.4525, d.f. = 12, p = 0.9300).

Model Summary 12 | Minicore particle sorting (MCSort) by species treatment (Tcode)

Initial linear regression model:

lm(MCSort ~ as.factor(Tcode))

No minimal adequate model, intercept only (Tcode, L-ratio = 20.51734, d.f. = 26, p = 0.0579).

Model Summary 13 | Minicore particle skewness (MCSkew) by species treatment (Tcode)

Initial linear regression model:

lm(MCSkew ~ as.factor(Tcode))

Minimal adequate model:

gls(MCSkew ~ as.factor(Tcode),
weights = varIdent(form = ~1|as.factor(Tcode)),
method = 'REML')

Coefficient Table

Intercept ± SE (when baseline is for N): -0.28 ± 0.09, t = -3.03, p = 0.0043.

	N	P	PD	HD_1HU_2	HDHU	HU_1HD_2	HD_1CV_2	HDCV	CV_1HD_2	HU_1CV_2	HUCV	CV_1HU_2	Mix_2
N	-	-0.26 ± 0.12 -2.17 **0.0364**	-0.23 ± 0.11 -2.08 **0.0446**	-0.34 ± 0.15 -2.27 **0.0286**	-0.31 ± 0.13 -2.39 **0.0220**	-0.21 ± 0.18 -1.17 0.2472	-0.52 ± 0.10 -5.31 **< 0.0001**	-0.40 ± 0.11 -3.47 **0.0013**	-0.35 ± 0.10 -3.44 **0.0014**	-0.41 ± 0.14 -2.99 **0.0049**	-0.07 ± 0.33 -0.21 0.8321	-0.40 ± 0.13 -3.21 **0.0027**	-0.31 ± 0.11 -2.79 **0.0080**
P	0.26 ± 0.12 2.17 **0.0364**	-	0.03 ± 0.10 0.25 0.8021	-0.1 ± 0.14 -0.58 0.5678	-0.06 ± 0.12 -0.48 0.6311	0.04 ± 0.17 0.25 0.8074	-0.27 ± 0.08 -3.15 **0.0031**	-0.14 ± 0.10 -1.38 0.1768	-0.09 ± 0.09 -1.03 0.3088	-0.16 ± 0.13 -1.22 0.2300	0.19 ± 0.32 0.57 0.5698	-0.15 ± 0.11 -1.27 0.2101	-0.05 ± 0.10 -0.54 0.5917
PD	0.23 ± 0.11 2.08 **0.0446**	-0.03 ± 0.10 -0.25 0.8021	-	-0.11 ± 0.13 -0.79 0.4348	-0.08 ± 0.12 -0.73 0.4704	0.02 ± 0.17 0.10 0.9172	-0.29 ± 0.07 -3.90 **0.0004**	-0.17 ± 0.10 -1.75 0.0873	-0.11 ± 0.08 -1.48 0.1465	-0.18 ± 0.12 -1.49 0.1453	0.16 ± 0.32 0.50 0.6200	-0.17 ± 0.11 -1.59 0.1199	-0.08 ± 0.09 -0.87 0.3904
HD_1HU_2	0.34 ± 0.15 2.27 **0.0286**	0.08 ± 0.14 0.58 0.5678	0.11 ± 0.13 0.79 0.4348	-	0.02 ± 0.15 0.14 0.8900	0.12 ± 0.20 0.63 0.5337	-0.19 ± 0.12 -1.51 0.1379	-0.06 ± 0.14 -0.45 0.6524	-0.01 ± 0.12 -0.08 0.9379	-0.08 ± 0.16 -0.49 0.6252	0.27 ± 0.34 0.79 0.4338	-0.07 ± 0.15 -0.46 0.6506	0.03 ± 0.13 0.20 0.8412
HDHU	0.31 ± 0.13 2.39 **0.0220**	0.06 ± 0.12 0.48 0.6311	0.08 ± 0.12 0.73 0.4704	-0.02 ± 0.15 -0.14 0.8900	-	0.10 ± 0.18 0.55 0.5831	-0.21 ± 0.10 -2.01 0.0516	-0.08 ± 0.12 -0.70 0.4897	-0.03 ± 0.11 -0.29 0.7713	-0.10 ± 0.14 -0.69 0.4928	0.24 ± 0.33 0.74 0.4619	-0.09 ± 0.13 -0.68 0.5027	0.01 ± 0.11 0.05 0.9603
HU_1HD_2	0.21 ± 0.18 1.17 0.2472	-0.04 ± 0.17 -0.25 0.8074	-0.02 ± 0.17 -0.10 0.9172	-0.12 ± 0.20 -0.63 0.5337	-0.10 ± 0.18 -0.55 0.5831	-	-0.31 ± 0.16 -1.91 0.0635	-0.18 ± 0.17 -1.07 0.2898	-0.13 ± 0.16 -0.81 0.4207	-0.20 ± 0.19 -1.06 0.2957	0.14 ± 0.35 0.41 0.6869	-0.19 ± 0.18 -1.05 0.2981	-0.10 ± 0.17 -0.57 0.5737
HD_1CV_2	0.52 ± 0.10 5.31 **< 0.0001**	0.27 ± 0.08 3.15 **0.0031**	0.29 ± 0.07 3.90 **0.0004**	0.19 ± 0.12 1.51 0.1379	0.21 ± 0.10 2.01 0.0516	0.31 ± 0.16 1.91 0.0635	-	0.12 ± 0.08 1.55 0.1281	0.18 ± 0.06 3.06 **0.0040**	0.11 ± 0.11 0.9786 0.3338	0.45 ± 0.32 1.4217 0.1631	0.12 ± 0.09 1.26 0.2135	0.21 ± 0.07 2.89 **0.0063**
HDCV	0.40 ± 0.11 3.47 **0.0013**	-0.14 ± 0.10 1.38 0.1768	0.17 ± 0.10 1.75 0.0873	0.06 ± 0.14 0.45 0.6524	0.08 ± 0.12 0.70 0.4897	0.18 ± 0.17 1.07 0.2898	-0.12 ± 0.08 -1.55 0.1281	-	0.05 ± 0.08 0.63 0.5319	-0.02 ± 0.13 -0.12 0.9040	0.33 ± 0.32 1.01 0.3167	0.00 ± 0.11 -0.04 0.9680	0.09 ± 0.09 0.94 0.3544
CV_1HD_2	0.35 ± 0.10 3.44 **0.0014**	0.09 ± 0.09 1.03 0.3088	0.11 ± 0.08 1.48 0.1465	0.01 ± 0.12 0.08 0.9379	0.03 ± 0.11 0.29 0.7713	0.13 ± 0.16 0.81 0.4207	-0.18 ± 0.06 -3.06 **0.0040**	-0.05 ± 0.08 -0.63 0.5319	-	-0.07 ± 0.11 -0.60 0.5549	0.28 ± 0.32 0.87 0.3918	-0.06 ± 0.10 -0.58 0.5624	0.04 ± 0.08 0.48 0.6365
HU_1CV_2	0.41 ± 0.14 2.99 **0.0049**	0.16 ± 0.13 1.22 0.2300	0.18 ± 0.12 1.49 0.1453	0.08 ± 0.16 0.49 0.6252	0.10 ± 0.14 0.69 0.4928	0.20 ± 0.19 1.06 0.2957	-0.11 ± 0.11 -0.98 0.3338	0.02 ± 0.13 0.121341 0.9040	0.07 ± 0.11 0.60 0.5549	-	0.34 ± 0.33 1.03 0.3082	0.01 ± 0.14 0.08 0.9372	0.10 ± 0.12 0.85 0.4001
HUCV	0.07 ± 0.33 0.21 0.8321	-0.19 ± 0.32 -0.57 0.5698	-0.16 ± 0.32 -0.50 0.6200	-0.27 ± 0.34 -0.79 0.4338	-0.24 ± 0.33 -0.74 0.4619	-0.14 ± 0.35 -0.41 0.6869	-0.45 ± 0.32 -1.42 0.1631	-0.33 ± 0.32 -1.01 0.3167	-0.28 ± 0.32 -0.87 0.3918	-0.34 ± 0.33 -1.03 0.3082	-	-0.33 ± 0.33 -1.02 0.3159	-0.24 ± 0.32 -0.74 0.4616
CV_1HU_2	0.40 ± 0.13 3.21 **0.0027**	0.15 ± 0.11 1.27 0.2101	0.17 ± 0.11 1.59 0.1199	0.07 ± 0.15 0.46 0.6506	0.09 ± 0.13 0.68 0.5027	0.19 ± 0.18 1.05 0.2981	-0.12 ± 0.09 -1.26 0.2135	0.00 ± 0.11 0.04 0.9680	0.06 ± 0.10 0.58 0.5624	-0.01 ± 0.14 -0.08 0.9372	0.33 ± 0.33 1.02 0.3159	-	0.09 ± 0.11 0.87 0.3905
Mix_2	0.31 ± 0.11 2.79 **0.0080**	0.05 ± 0.10 0.54 0.5917	0.08 ± 0.09 0.87 0.3904	-0.03 ± 0.13 -0.20 0.8412	-0.01 ± 0.11 -0.05 0.9603	0.10 ± 0.17 0.57 0.5737	-0.21 ± 0.07 -2.89 **0.0063**	-0.09 ± 0.09 -0.94 0.3544	-0.04 ± 0.08 -0.48 0.6365	-0.10 ± 0.12 -0.85 0.4001	0.24 ± 0.32 0.74 0.4616	-0.09 ± 0.11 -0.87 0.3905	-

Model Summary 14 | Minicore particle kurtosis (MCKurt) by species treatment (Tcode)

Initial linear regression model:

lm(MCKurt ~ as.factor(Tcode))

No minimal adequate model, intercept only (Tcode, L-ratio = 4.523799, d.f. = 26, p = 0.9720).

Model Summary 15 | Minicore D_{10} (MCD_{10}, µm) by species treatment (Tcode)

Initial linear regression model:

lm(MCD_{10} ~ as.factor(Tcode))

No minimal adequate model, intercept only (Tcode, L-ratio = 16.57876, d.f. = 26, p = 0.1661).

Model Summary 16 | Minicore mud content (MCPCMud, %) by species treatment (Tcode)

Initial linear regression model:

lm(MCPCMud% ~ as.factor(Tcode))

No minimal adequate model, intercept only (Tcode, L-ratio = 16.23516, d.f. = 26, p = 0.1807).

Model Summary 17 | Contact core water concentration (CCWat, gcm^{-3}) by species treatment (Tcode)

Initial linear regression model:

lm(CCWat ~ as.factor(Tcode))

No minimal adequate model, intercept only (Tcode, L-ratio = 20.31593, d.f. = 26, p = 0.0613).

Model Summary 18 | Contact core carbohydrate concentration (CCCarb, glucose µgcm^{-3}) by species treatment (Tcode)

Initial linear regression model:

lm(CCCarb ~ as.factor(Tcode))

No minimal adequate model, intercept only (Tcode, L-ratio = 19.43181, d.f. = 26, p = 0.0786).

Model Summary 19 | Contact core chlorophyll *a* concentration (CCChl*a*, µgcm^{-3}) by species treatment (Tcode)

Initial linear regression model:

lm(CCChl*a* ~ as.factor(Tcode))

Minimal adequate model:

gls(CCChl*a* ~ as.factor(Tcode),
weights = varIdent(form = ~1|as.factor(Tcode)),
method = 'REML')

Coefficient Table

Intercept ± SE (when baseline is for N): 15.84 ± 0.92, t = 17.21, p < 0.0001.

	N	P	PD	HD_1HU_2	HDHU	HU_1HD_2	HD_1CV_2	HDCV	CV_1HD_2	HU_1CV_2	HUCV	CV_1HU_2	Mix_2
N	-	6.79 ± 0.95 7.12 **< 0.0001**	9.26 ± 2.19 4.22 **0.0001**	11.97 ± 1.77 6.77 **< 0.0001**	4.89 ± 1.14 4.30 **0.0001**	8.17 ± 1.24 6.57 **< 0.0001**	11.73 ± 1.84 6.37 **< 0.0001**	11.85 ± 2.35 5.04 **< 0.0001**	7.86 ± 1.34 5.85 **< 0.0001**	9.10 ± 2.14 4.25 **0.0001**	7.20 ± 1.92 3.74 **0.0006**	9.48 ± 1.14 8.31 **< 0.0001**	9.48 ± 1.70 5.57 **< 0.0001**
P	-6.79 ± 0.95 -7.12 **< 0.0001**	-	2.47 ± 2.01 1.23 0.2270	5.174 ± 1.53 3.38 **0.0017**	-1.90 ± 0.71 -2.66 **0.0114**	1.38 ± 0.87 1.58 0.1228	4.94 ± 1.62 3.06 **0.0040**	5.06 ± 2.18 2.32 **0.0255**	1.07 ± 1.01 1.06 0.2971	2.31 ± 1.95 1.18 0.2441	0.41 ± 1.71 0.24 0.8116	2.69 ± 0.72 3.74 **0.0006**	2.69 ± 1.45 1.85 0.0716
PD	-9.26 ± 2.19 -4.22 **0.0001**	-2.47 ± 2.01 -1.23 0.2270	-	2.71 ± 2.50 1.08 0.2852	-4.36 ± 2.10 -2.08 **0.0445**	-1.09 ± 2.16 -0.50 0.6168	2.47 ± 2.55 0.97 0.3385	2.59 ± 2.94 0.88 0.3831	-1.40 ± 2.22 -0.63 0.5325	-0.16 ± 2.78 -0.06 0.9550	-2.06 ± 2.61 -0.79 0.4363	0.23 ± 2.10 0.11 0.9149	0.23 ± 2.45 0.09 0.9273
HD_1HU_2	-11.97 ± 1.77 -6.77 **< 0.0001**	-5.17 ± 1.53 -3.38 **0.0017**	-2.71 ± 2.50 -1.08 0.2852	-	-7.07 ± 1.65 -4.28 **0.0001**	-3.80 ± 1.72 -2.20 **0.0336**	-0.23 ± 2.20 -0.11 0.9154	-0.11 ± 2.64 -0.04 0.9656	-4.11 ± 1.80 -2.28 **0.0280**	-2.87 ± 2.45 -1.17 0.2499	-4.76 ± 2.27 -2.10 **0.0421**	-2.48 ± 1.65 -1.50 0.1413	-2.48 ± 2.08 -1.19 0.2396
HDHU	-4.89 ± 1.14 -4.30 **0.0001**	1.90 ± 0.71 2.66 **0.0114**	4.36 ± 2.10 2.08 **0.0445**	7.07 ± 1.65 4.28 **0.0001**	-	3.27 ± 1.07 3.06 **0.0040**	6.84 ± 1.73 3.95 **0.0003**	6.96 ± 2.26 3.07 **0.0039**	2.97 ± 1.18 2.50 **0.0166**	4.21 ± 2.05 2.05 **0.0467**	2.31 ± 1.82 1.27 0.2116	4.59 ± 0.95 4.83 **< 0.0001**	4.59 ± 1.58 2.91 **0.0060**
HU_1HD_2	-8.17 ± 1.24 -6.57 **< 0.0001**	-1.38 ± 0.87 -1.58 0.1228	1.09 ± 2.16 0.50 0.6168	3.80 ± 1.72 2.20 **0.0336**	-3.27 ± 1.07 -3.06 **0.0040**	-	3.56 ± 1.80 1.98 0.0550	3.68 ± 2.32 1.59 0.1202	-0.31 ± 1.29 -0.24 0.8119	0.93 ± 2.11 0.44 0.6607	-0.97 ± 1.89 -0.51 0.6114	1.32 ± 1.07 1.23 0.2275	1.31 ± 1.66 0.79 0.4321
HD_1CV_2	-11.73 ± 1.84 -6.37 **< 0.0001**	-4.94 ± 1.62 -3.06 **0.0040**	-2.47 ± 2.55 -0.97 0.3385	0.23 ± 2.20 0.11 0.9154	-6.84 ± 1.73 -3.95 **0.0003**	-3.56 ± 1.80 -1.98 0.0550	-	0.12 ± 2.69 0.04 0.9646	-3.87 ± 1.87 -2.07 **0.0453**	-2.63 ± 2.51 -1.0491 0.3006	-4.53 ± 2.32 -1.9481 0.0586	-2.25 ± 1.73 -1.30 0.2022	-2.25 ± 2.14 -1.05 0.3006
HDCV	-11.85 ± 2.35 -5.04 **< 0.0001**	5.06 ± 2.18 -2.32 **0.0255**	-2.59 ± 2.94 -0.88 0.3831	0.11 ± 2.64 0.04 0.9656	-6.96 ± 2.26 -3.07 **0.0039**	-3.68 ± 2.32 -1.59 0.1202	-0.12 ± 2.69 -0.04 0.9646	-	-3.99 ± 2.37 -1.68 0.1007	-2.75 ± 2.90 -0.95 0.3489	-4.65 ± 2.75 -1.69 0.0983	-2.37 ± 2.27 -1.05 0.3024	-2.37 ± 2.59 -0.91 0.3666
CV_1HD_2	-7.86 ± 1.34 -5.85 **< 0.0001**	-1.07 ± 1.01 -1.06 0.2971	1.40 ± 2.22 0.63 0.5325	4.11 ± 1.80 2.28 **0.0280**	-2.97 ± 1.18 -2.50 **0.0166**	0.31 ± 1.29 0.24 0.8119	3.87 ± 1.87 2.07 **0.0453**	3.99 ± 2.37 1.68 0.1007	-	1.24 ± 2.17 0.57 0.5706	-0.66 ± 1.95 -0.34 0.7382	1.62 ± 1.19 1.37 0.1795	1.62 ± 1.73 0.94 0.3548
HU_1CV_2	-9.10 ± 2.14 -4.25 **0.0001**	-2.31 ± 1.95 -1.18 0.2441	0.16 ± 2.78 0.06 0.9550	2.87 ± 2.45 1.17 0.2499	-4.21 ± 2.05 -2.05 **0.0467**	-0.93 ± 2.11 -0.44 0.6607	2.63 ± 2.51 1.05 0.3006	2.75 ± 2.90 0.948107 0.3489	-1.24 ± 2.17 -0.57 0.5706	-	-1.90 ± 2.57 -0.74 0.4646	0.38 ± 2.05 0.19 0.8524	0.38 ± 2.41 0.16 0.8745
HUCV	-7.20 ± 1.92 -3.74 **0.0006**	-0.41 ± 1.71 -0.24 0.8116	2.06 ± 2.61 0.79 0.4363	4.76 ± 2.27 2.10 **0.0421**	-2.31 ± 1.82 -1.27 0.2116	0.97 ± 1.89 0.51 0.6114	4.53 ± 2.32 1.95 0.0586	4.65 ± 2.75 1.69 0.0983	0.66 ± 1.95 0.34 0.7382	1.90 ± 2.57 0.74 0.4646	-	2.28 ± 1.82 1.25 0.2175	2.28 ± 2.21 1.03 0.3095
CV_1HU_2	-9.48 ± 1.14 -8.31 **< 0.0001**	-2.69 ± 0.72 -3.74 **0.0006**	-0.23 ± 2.10 -0.11 0.9149	2.48 ± 1.65 1.50 0.1413	-4.59 ± 0.95 -4.83 **< 0.0001**	-1.32 ± 1.07 -1.23 0.2275	2.25 ± 1.73 1.30 0.2022	2.37 ± 2.27 1.05 0.3024	-1.62 ± 1.19 -1.37 0.1795	-0.38 ± 2.05 -0.19 0.8524	-2.28 ± 1.82 -1.25 0.2175	-	0.00 ± 1.58 0.00 0.9995
Mix_2	-9.48 ± 1.70 -5.57 **< 0.0001**	-2.69 ± 1.45 -1.85 0.0716	-0.23 ± 2.45 -0.09 0.9273	2.48 ± 2.08 1.19 0.2396	-4.59 ± 1.58 -2.91 **0.0060**	-1.31 ± 1.66 -0.79 0.4321	2.25 ± 2.14 1.05 0.3006	2.37 ± 2.59 0.91 0.3666	-1.62 ± 1.73 -0.94 0.3548	-0.38 ± 2.41 -0.16 0.8745	-2.28 ± 2.21 -1.03 0.3095	0.00 ± 1.58 0.00 0.9995	-

Model Summary 20 | Contact core chlorophyll *b* concentration (CCChl*b*, µgcm^{-3}) by species treatment (Tcode)

Initial linear regression model:

lm(CCChl*b* ~ as.factor(Tcode))

Minimal adequate model:

gls(CCChl*b* ~ as.factor(Tcode),
weights = varIdent(form = ~1|as.factor(Tcode)),
method = 'REML')

Coefficient Table

Intercept ± SE (when baseline is for N): 3.75 ± 0.10, t = 36.50, p < 0.0001.

	N	P	PD	HD_1HU_2	HDHU	HU_1HD_2	HD_1CV_2	HDCV	CV_1HD_2	HU_1CV_2	HUCV	CV_1HU_2	Mix_2
N	-	0.89 ± 0.13 6.75 **< 0.0001**	1.18 ± 0.41 2.87 **0.0066**	1.29 ± 0.23 5.53 **< 0.0001**	0.47 ± 0.20 2.33 **0.0248**	0.85 ± 0.21 4.00 **0.0003**	1.95 ± 0.62 3.16 **0.0031**	1.36 ± 0.38 3.58 **0.0009**	1.06 ± 0.26 4.10 **0.0002**	1.46 ± 0.53 2.75 **0.0091**	1.12 ± 0.39 2.85 **0.0070**	0.91 ± 0.20 4.64 **< 0.0001**	1.47 ± 0.28 5.29 **< 0.0001**
P	-0.89 ± 0.13 -6.75 **< 0.0001**	-	0.29 ± 0.41 0.72 0.4735	0.41 ± 0.23 1.80 0.0796	-0.42 ± 0.19 -2.19 **0.0345**	-0.04 ± 0.20 -0.19 0.8521	1.06 ± 0.61 1.73 0.0921	0.48 ± 0.38 1.27 0.2129	0.18 ± 0.25 0.70 0.4909	0.58 ± 0.53 1.09 0.2830	0.23 ± 0.39 0.60 0.5547	0.02 ± 0.19 0.10 0.9187	0.58 ± 0.27 2.14 **0.0383**
PD	-1.18 ± 0.41 -2.87 **0.0066**	-0.29 ± 0.41 -0.72 0.4735	-	0.11 ± 0.45 0.25 0.8055	-0.71 ± 0.43 -1.64 0.1087	-0.33 ± 0.44 -0.76 0.4540	0.76 ± 0.73 1.05 0.2993	0.18 ± 0.54 0.33 0.7395	-0.12 ± 0.46 -0.26 0.7983	0.28 ± 0.66 0.43 0.6708	-0.06 ± 0.55 -0.12 0.9084	-0.28 ± 0.43 -0.64 0.5272	0.29 ± 0.47 0.60 0.5505
HD_1HU_2	-1.29 ± 0.23 -5.53 **< 0.0001**	-0.41 ± 0.23 -1.80 0.0796	-0.11 ± 0.45 -0.25 0.8055	-	-0.82 ± 0.27 -3.03 **0.0043**	-0.44 ± 0.28 -1.58 0.1214	0.65 ± 0.64 1.02 0.3163	0.07 ± 0.42 0.16 0.8699	-0.23 ± 0.32 -0.73 0.4711	0.17 ± 0.56 0.30 0.7647	-0.18 ± 0.43 -0.40 0.6878	-0.39 ± 0.27 -1.44 0.1565	0.17 ± 0.33 0.52 0.6036
HDHU	-0.47 ± 0.20 -2.33 **0.0248**	0.42 ± 0.19 2.19 **0.0345**	0.71 ± 0.43 1.64 0.1087	0.82 ± 0.27 3.03 **0.0043**	-	0.38 ± 0.25 1.50 0.1416	1.48 ± 0.63 2.34 **0.0246**	0.89 ± 0.41 2.21 **0.0333**	0.59 ± 0.29 2.02 0.0504	0.99 ± 0.55 1.81 0.0786	0.65 ± 0.42 1.56 0.1267	0.44 ± 0.24 1.83 0.0754	1.00 ± 0.31 3.22 **0.0026**
HU_1HD_2	-0.85 ± 0.21 -4.00 **0.0003**	0.04 ± 0.20 0.19 0.8521	0.33 ± 0.44 0.76 0.4540	0.44 ± 0.28 1.58 0.1214	-0.38 ± 0.25 -1.50 0.1416	-	1.10 ± 0.64 1.73 0.0922	0.51 ± 0.41 1.25 0.2187	0.21 ± 0.30 0.71 0.4844	0.61 ± 0.56 1.11 0.2751	0.27 ± 0.42 0.64 0.5275	0.06 ± 0.25 0.23 0.8199	0.62 ± 0.32 1.95 0.0589
HD_1CV_2	-1.95 ± 0.62 -3.16 **0.0031**	-1.06 ± 0.61 -1.73 0.0921	-0.76 ± 0.73 -1.05 0.2993	-0.65 ± 0.64 -1.02 0.3163	-1.48 ± 0.63 -2.34 **0.0246**	-1.10 ± 0.64 -1.73 0.0922	-	-0.58 ± 0.71 -0.82 0.4164	-0.88 ± 0.65 -1.35 0.1834	-0.48 ± 0.80 -0.6023 0.5504	-0.83 ± 0.72 -1.1566 0.2545	-1.04 ± 0.63 -1.65 0.1068	-0.48 ± 0.66 -0.72 0.4728
HDCV	-1.36 ± 0.38 -3.58 **0.0009**	0.48 ± 0.38 -1.27 0.2129	-0.18 ± 0.54 -0.33 0.7395	-0.07 ± 0.42 -0.16 0.8699	-0.89 ± 0.41 -2.21 **0.0333**	-0.51 ± 0.41 -1.25 0.2187	0.58 ± 0.71 0.82 0.4164	-	-0.30 ± 0.44 -0.69 0.4955	0.10 ± 0.64 0.16 0.8761	-0.25 ± 0.53 -0.46 0.6446	-0.46 ± 0.40 -1.13 0.2634	0.10 ± 0.45 0.23 0.8169
CV_1HD_2	-1.06 ± 0.26 -4.10 **0.0002**	-0.18 ± 0.25 -0.70 0.4909	0.12 ± 0.46 0.26 0.7983	0.23 ± 0.32 0.73 0.4711	-0.59 ± 0.29 -2.02 0.0504	-0.21 ± 0.30 -0.71 0.4844	0.88 ± 0.65 1.35 0.1834	0.30 ± 0.44 0.69 0.4955	-	0.40 ± 0.57 0.70 0.4893	0.06 ± 0.45 0.12 0.9014	-0.16 ± 0.29 -0.54 0.5939	0.41 ± 0.35 1.15 0.2552
HU_1CV_2	-1.46 ± 0.53 -2.75 **0.0091**	-0.58 ± 0.53 -1.09 0.2830	-0.28 ± 0.66 -0.43 0.6708	-0.17 ± 0.56 -0.30 0.7647	-0.99 ± 0.55 -1.81 0.0786	-0.61 ± 0.56 -1.11 0.2751	0.48 ± 0.80 0.60 0.5504	-0.10 ± 0.64 -0.156906 0.8761	-0.40 ± 0.57 -0.70 0.4893	-	-0.35 ± 0.65 -0.53 0.5958	-0.56 ± 0.55 -1.02 0.3161	0.00 ± 0.58 0.01 0.9941
HUCV	-1.12 ± 0.39 -2.85 **0.0070**	-0.23 ± 0.39 -0.60 0.5547	0.06 ± 0.55 0.12 0.9084	0.18 ± 0.43 0.40 0.6878	-0.65 ± 0.42 -1.56 0.1267	-0.27 ± 0.42 -0.64 0.5275	0.83 ± 0.72 1.16 0.2545	0.25 ± 0.53 0.46 0.6446	-0.06 ± 0.45 -0.12 0.9014	0.35 ± 0.65 0.53 0.5958	-	-0.21 ± 0.41 -0.51 0.6114	0.35 ± 0.46 0.76 0.4501
CV_1HU_2	-0.91 ± 0.20 -4.64 **< 0.0001**	-0.02 ± 0.19 -0.10 0.9187	0.28 ± 0.43 0.64 0.5272	0.39 ± 0.27 1.44 0.1565	-0.44 ± 0.24 -1.83 0.0754	-0.06 ± 0.25 -0.23 0.8199	1.04 ± 0.63 1.65 0.1068	0.46 ± 0.40 1.13 0.2634	0.16 ± 0.29 0.54 0.5939	0.56 ± 0.55 1.02 0.3161	0.21 ± 0.41 0.51 0.6114	-	0.56 ± 0.31 1.83 0.0749
Mix_2	-1.47 ± 0.28 -5.29 **< 0.0001**	-0.58 ± 0.27 -2.14 **0.0383**	-0.29 ± 0.47 -0.60 0.5505	-0.17 ± 0.33 -0.52 0.6036	-1.00 ± 0.31 -3.22 **0.0026**	-0.62 ± 0.32 -1.95 0.0589	0.48 ± 0.66 0.72 0.4728	-0.10 ± 0.45 -0.23 0.8169	-0.41 ± 0.35 -1.15 0.2552	0.00 ± 0.58 -0.01 0.9941	-0.35 ± 0.46 -0.76 0.4501	-0.56 ± 0.31 -1.83 0.0749	-

Model Summary 21 | Contact core mean particle size (CCMean, µm) by species treatment (Tcode)

Initial linear regression model:

```
lm(CCMean ~ as.factor(Tcode))
```

Minimal adequate model:

```
gls(CCMean ~ as.factor(Tcode),
    weights = varIdent(form = ~1|as.factor(Tcode)),
    method = 'REML')
```

Coefficient Table

Intercept ± SE (when baseline is for N): 42.63 ± 2.09, t = 20.42, p < 0.0001.

	N	P	PD	HD_1HU_2	HDHU	HU_1HD_2	HD_1CV_2	HDCV	CV_1HD_2	HU_1CV_2	HUCV	CV_1HU_2	Mix_2
N	-	-3.81 ± 2.40 -1.59 0.1210	-4.51 ± 2.62 -1.72 0.0929	-7.39 ± 2.20 -3.37 **0.0017**	-4.26 ± 2.19 -1.95 0.0588	-2.93 ± 2.50 -1.17 0.2486	-5.67 ± 2.61 -2.17 **0.0362**	-4.72 ± 2.11 -2.24 **0.0311**	-1.78 ± 2.16 -0.82 0.4150	-7.71 ± 3.11 -2.48 **0.0175**	-4.85 ± 2.60 -1.87 0.0694	-2.00 ± 2.24 -0.89 0.3794	-2.98 ± 2.15 -1.39 0.1736
P	3.81 ± 2.40 1.59 0.1210	-	-0.70 ± 1.97 -0.35 0.7249	-3.6 ± 1.37 -2.62 **0.0125**	-0.46 ± 1.36 -0.33 0.7394	0.88 ± 1.82 0.48 0.6338	-1.86 ± 1.97 -0.94 0.3508	-0.92 ± 1.23 -0.75 0.4607	2.03 ± 1.31 1.55 0.1302	-3.90 ± 2.59 -1.51 0.1400	-1.04 ± 1.95 -0.54 0.5957	1.81 ± 1.44 1.25 0.2171	0.83 ± 1.29 0.64 0.5241
PD	4.51 ± 2.62 1.72 0.0929	0.70 ± 1.97 0.35 0.7249	-	-2.88 ± 1.72 -1.68 0.1014	0.25 ± 1.71 0.14 0.8868	1.58 ± 2.10 0.75 0.4572	-1.16 ± 2.23 -0.52 0.6054	-0.22 ± 1.61 -0.13 0.8943	2.73 ± 1.67 1.63 0.1110	-3.20 ± 2.79 -1.15 0.2583	-0.34 ± 2.21 -0.16 0.8775	2.51 ± 1.78 1.41 0.1659	1.53 ± 1.66 0.92 0.3615
HD_1HU_2	7.39 ± 2.20 3.37 **0.0017**	3.58 ± 1.37 2.62 **0.0125**	2.88 ± 1.72 1.68 0.1014	-	3.13 ± 0.95 3.30 **0.0021**	4.46 ± 1.54 2.89 **0.0062**	1.72 ± 1.71 1.01 0.3206	2.67 ± 0.75 3.56 **0.0010**	5.61 ± 0.88 6.39 **< 0.0001**	-0.32 ± 2.40 -0.13 0.8954	2.54 ± 1.69 1.50 0.1404	5.40 ± 1.07 5.05 **< 0.0001**	4.41 ± 0.85 5.21 **< 0.0001**
HDHU	4.26 ± 2.19 1.95 0.0588	0.46 ± 1.36 0.33 0.7394	-0.25 ± 1.71 -0.14 0.8868	-3.13 ± 0.95 -3.30 **0.0021**	-	1.33 ± 1.53 0.87 0.3903	-1.41 ± 1.70 -0.82 0.4147	-0.46 ± 0.73 -0.63 0.5321	2.48 ± 0.86 2.88 **0.0065**	-3.45 ± 2.39 -1.44 0.1579	-0.59 ± 1.68 -0.35 0.7284	2.27 ± 1.05 2.15 **0.0378**	1.29 ± 0.83 1.55 0.1302
HU_1HD_2	2.93 ± 2.50 1.17 0.2486	-0.88 ± 1.82 -0.48 0.6338	-1.58 ± 2.10 -0.75 0.4572	-4.46 ± 1.54 -2.89 **0.0062**	-1.33 ± 1.53 -0.87 0.3903	-	-2.74 ± 2.09 -1.31 0.1989	-1.79 ± 1.42 -1.26 0.2140	1.15 ± 1.49 0.77 0.4438	-4.78 ± 2.68 -1.78 0.0830	-1.92 ± 2.07 -0.93 0.3606	0.94 ± 1.61 0.58 0.5633	-0.05 ± 1.47 -0.03 0.9758
HD_1CV_2	5.67 ± 2.61 2.17 **0.0362**	1.86 ± 1.97 0.94 0.3508	1.16 ± 2.23 0.52 0.6054	-1.72 ± 1.71 -1.01 0.3206	1.41 ± 1.70 0.82 0.4147	2.74 ± 2.09 1.31 0.1989	-	0.95 ± 1.60 0.59 0.5587	3.89 ± 1.67 2.33 **0.0250**	-2.04 ± 2.79 -0.7323 0.4684	0.82 ± 2.20 0.3710 0.7127	3.67 ± 1.77 2.07 **0.0451**	2.69 ± 1.65 1.63 0.1113
HDCV	4.72 ± 2.11 2.24 **0.0311**	-0.92 ± 1.23 0.75 0.4607	0.22 ± 1.61 0.13 0.8943	-2.67 ± 0.75 -3.56 **0.0010**	0.46 ± 0.73 0.63 0.5321	1.79 ± 1.42 1.26 0.2140	-0.95 ± 1.60 -0.59 0.5587	-	2.94 ± 0.64 4.61 **< 0.0001**	-2.99 ± 2.32 -1.29 0.2061	-0.13 ± 1.58 -0.08 0.9359	2.73 ± 0.88 3.10 **0.0036**	1.75 ± 0.60 2.93 **0.0056**
CV_1HD_2	1.78 ± 2.16 0.82 0.4150	-2.03 ± 1.31 -1.55 0.1302	-2.73 ± 1.67 -1.63 0.1110	-5.61 ± 0.88 -6.39 **< 0.0001**	-2.48 ± 0.86 -2.88 **0.0065**	-1.15 ± 1.49 -0.77 0.4438	-3.89 ± 1.67 -2.33 **0.0250**	-2.94 ± 0.64 -4.61 **< 0.0001**	-	-5.93 ± 2.37 -2.50 **0.0165**	-3.07 ± 1.64 -1.87 0.0690	-0.22 ± 0.99 -0.22 0.8297	-1.20 ± 0.75 -1.59 0.1194
HU_1CV_2	7.71 ± 3.11 2.48 **0.0175**	3.90 ± 2.59 1.51 0.1400	3.20 ± 2.79 1.15 0.2583	0.32 ± 2.40 0.13 0.8954	3.45 ± 2.39 1.44 0.1579	4.78 ± 2.68 1.78 0.0830	2.04 ± 2.79 0.73 0.4684	2.99 ± 2.32 1.285856 0.2061	5.93 ± 2.37 2.50 **0.0165**	-	2.86 ± 2.77 1.03 0.3088	5.71 ± 2.44 2.34 **0.0246**	4.73 ± 2.36 2.01 0.0516
HUCV	4.85 ± 2.60 1.87 0.0694	1.04 ± 1.95 0.54 0.5957	0.34 ± 2.21 0.16 0.8775	-2.54 ± 1.69 -1.50 0.1404	0.59 ± 1.68 0.35 0.7284	1.92 ± 2.07 0.93 0.3606	-0.82 ± 2.20 -0.37 0.7127	0.13 ± 1.58 0.08 0.9359	3.07 ± 1.64 1.87 0.0690	-2.86 ± 2.77 -1.03 0.3088	-	2.86 ± 1.75 1.63 0.1109	1.87 ± 1.63 1.15 0.2564
CV_1HU_2	2.00 ± 2.24 0.89 0.3794	-1.81 ± 1.44 -1.25 0.2171	-2.51 ± 1.78 -1.41 0.1659	-5.40 ± 1.07 -5.05 **< 0.0001**	-2.27 ± 1.05 -2.15 **0.0378**	-0.94 ± 1.61 -0.58 0.5633	-3.67 ± 1.77 -2.07 **0.0451**	-2.73 ± 0.88 -3.10 **0.0036**	0.22 ± 0.99 0.22 0.8297	-5.71 ± 2.44 -2.34 **0.0246**	-2.86 ± 1.75 -1.63 0.1109	-	-0.98 ± 0.97 -1.02 0.3154
Mix_2	2.98 ± 2.15 1.39 0.1736	-0.83 ± 1.29 -0.64 0.5241	-1.53 ± 1.66 -0.92 0.3615	-4.41 ± 0.85 -5.21 **< 0.0001**	-1.29 ± 0.83 -1.55 0.1302	0.05 ± 1.47 0.03 0.9758	-2.69 ± 1.65 -1.63 0.1113	-1.75 ± 0.60 -2.93 **0.0056**	1.20 ± 0.75 1.59 0.1194	-4.73 ± 2.36 -2.01 0.0516	-1.87 ± 1.63 -1.15 0.2564	0.98 ± 0.97 1.02 0.3154	-

Model Summary 22 | Contact core particle size mode (CCMode, µm) by species treatment (Tcode)

Initial linear regression model:

lm(CCMode ~ as.factor(Tcode))

No minimal adequate model, intercept only (Tcode, F = 1.4489, d.f. = 12, p = 0.1860).

Model Summary 23 | Contact core particle sorting (CCSort) by species treatment (Tcode)

Initial linear regression model:

lm(CCSort ~ as.factor(Tcode))

Minimal adequate model:

gls(CCMean ~ as.factor(Tcode),
weights = varIdent(form = ~1|as.factor(Tcode)),
method = 'REML')

Coefficient Table

Intercept ± SE (when baseline is for N): 2.78 ± 0.04, t = 71.62, p < 0.0001.

	N	P	PD	HD_1HU_2	HDHU	HU_1HD_2	HD_1CV_2	HDCV	CV_1HD_2	HU_1CV_2	HUCV	CV_1HU_2	Mix_2
N	-	-0.16 ± 0.11 -1.52 0.1370	-0.31 ± 0.05 -6.26 **< 0.0001**	-0.33 ± 0.04 -8.38 **< 0.0001**	-0.27 ± 0.04 -6.47 **< 0.0001**	-0.23 ± 0.07 -3.08 **0.0037**	-0.28 ± 0.07 -4.18 **0.0002**	-0.32 ± 0.04 -7.23 **< 0.0001**	-0.21 ± 0.05 -4.59 **< 0.0001**	-0.25 ± 0.06 -3.81 **0.0005**	-0.27 ± 0.07 -3.81 **0.0005**	-0.24 ± 0.06 -4.23 **0.0001**	-0.29 ± 0.04 -6.61 **< 0.0001**
P	0.16 ± 0.11 1.52 0.1370	-	-0.15 ± 0.10 -1.43 0.1610	-0.2 ± 0.10 -1.73 0.0911	-0.11 ± 0.10 -1.14 0.2605	-0.07 ± 0.12 -0.58 0.5644	-0.12 ± 0.11 -1.07 0.2913	-0.16 ± 0.10 -1.60 0.1184	-0.05 ± 0.10 -0.52 0.6077	-0.09 ± 0.11 -0.78 0.4411	-0.11 ± 0.11 -0.95 0.3482	-0.09 ± 0.11 -0.80 0.4308	-0.13 ± 0.10 -1.29 0.2046
PD	0.31 ± 0.05 6.26 **< 0.0001**	0.15 ± 0.10 1.43 0.1610	-	-0.02 ± 0.03 -0.79 0.4371	0.03 ± 0.03 0.97 0.3402	0.08 ± 0.07 1.13 0.2640	0.03 ± 0.06 0.42 0.6744	-0.01 ± 0.04 -0.38 0.7075	0.09 ± 0.04 2.42 **0.0204**	0.06 ± 0.06 1.01 0.3185	0.04 ± 0.07 0.58 0.5685	0.06 ± 0.05 1.17 0.2488	0.02 ± 0.04 0.48 0.6314
HD_1HU_2	0.33 ± 0.04 8.38 **< 0.0001**	0.17 ± 0.10 1.73 0.0911	0.02 ± 0.03 0.79 0.4371	-	0.06 ± 0.02 3.21 **0.0026**	0.10 ± 0.06 1.63 0.1120	0.05 ± 0.05 0.91 0.3672	0.01 ± 0.02 0.46 0.6512	0.12 ± 0.03 4.56 **< 0.0001**	0.08 ± 0.05 1.62 0.1140	0.06 ± 0.06 1.04 0.3027	0.08 ± 0.04 1.96 0.0574	0.04 ± 0.02 1.97 0.0555
HDHU	0.27 ± 0.04 6.47 **< 0.0001**	0.11 ± 0.10 1.14 0.2605	-0.03 ± 0.03 -0.97 0.3402	-0.06 ± 0.02 -3.21 **0.0026**	-	0.05 ± 0.06 0.71 0.4840	-0.01 ± 0.06 -0.11 0.9097	-0.05 ± 0.03 -1.74 0.0904	0.06 ± 0.03 2.03 **0.0487**	0.03 ± 0.05 0.50 0.6169	0.01 ± 0.06 0.08 0.9349	0.03 ± 0.05 0.62 0.5421	-0.02 ± 0.03 -0.60 0.5519
HU_1HD_2	0.23 ± 0.07 3.08 **0.0037**	0.07 ± 0.12 0.58 0.5644	-0.08 ± 0.07 -1.13 0.2640	-0.10 ± 0.06 -1.63 0.1120	-0.05 ± 0.06 -0.71 0.4840	-	-0.05 ± 0.08 -0.63 0.5326	-0.09 ± 0.07 -1.40 0.1705	0.02 ± 0.07 0.23 0.8222	-0.02 ± 0.08 -0.23 0.8206	-0.04 ± 0.09 -0.48 0.6372	-0.02 ± 0.08 -0.23 0.8188	-0.06 ± 0.07 -0.93 0.3568
HD_1CV_2	0.28 ± 0.07 4.18 **0.0002**	0.12 ± 0.11 1.07 0.2913	-0.03 ± 0.06 -0.42 0.6744	-0.05 ± 0.05 -0.91 0.3672	0.01 ± 0.06 0.11 0.9097	0.05 ± 0.08 0.63 0.5326	-	-0.04 ± 0.06 -0.68 0.4975	0.07 ± 0.06 1.13 0.2670	0.03 ± 0.07 0.4504 0.6549	0.01 ± 0.08 0.1438 0.8864	0.03 ± 0.07 0.50 0.6189	-0.01 ± 0.06 -0.16 0.8774
HDCV	0.32 ± 0.04 7.23 **< 0.0001**	-0.16 ± 0.10 1.60 0.1184	0.01 ± 0.04 0.38 0.7075	-0.01 ± 0.02 -0.46 0.6512	0.05 ± 0.03 1.74 0.0904	0.09 ± 0.07 1.40 0.1705	0.04 ± 0.06 0.68 0.4975	-	0.11 ± 0.03 3.28 **0.0022**	0.07 ± 0.06 1.33 0.1925	0.05 ± 0.06 0.83 0.4131	0.07 ± 0.05 1.56 0.1257	0.03 ± 0.03 1.07 0.2912
CV_1HD_2	0.21 ± 0.05 4.59 **< 0.0001**	0.05 ± 0.10 0.52 0.6077	-0.09 ± 0.04 -2.42 **0.0204**	-0.12 ± 0.03 -4.56 **< 0.0001**	-0.06 ± 0.03 -2.03 **0.0487**	-0.02 ± 0.07 -0.23 0.8222	-0.07 ± 0.06 -1.13 0.2670	-0.11 ± 0.03 -3.28 **0.0022**	-	-0.03 ± 0.06 -0.59 0.5587	-0.06 ± 0.06 -0.88 0.3847	-0.03 ± 0.05 -0.66 0.5132	-0.08 ± 0.03 -2.39 **0.0216**
HU_1CV_2	0.25 ± 0.06 3.81 **0.0005**	0.09 ± 0.11 0.78 0.4411	-0.06 ± 0.06 -1.01 0.3185	-0.08 ± 0.05 -1.62 0.1140	-0.03 ± 0.05 -0.50 0.6169	0.02 ± 0.08 0.23 0.8206	-0.03 ± 0.07 -0.45 0.6549	-0.07 ± 0.06 -1.32622 0.1925	0.03 ± 0.06 0.59 0.5587	-	-0.02 ± 0.08 -0.29 0.7769	0.00 ± 0.07 0.01 0.9882	-0.04 ± 0.06 -0.78 0.4430
HUCV	0.27 ± 0.07 3.81 **0.0005**	0.11 ± 0.11 0.95 0.3482	-0.04 ± 0.07 -0.58 0.5685	-0.06 ± 0.06 -1.04 0.3027	-0.01 ± 0.06 -0.08 0.9349	0.04 ± 0.09 0.48 0.6372	-0.01 ± 0.08 -0.14 0.8864	-0.05 ± 0.06 -0.83 0.4131	0.06 ± 0.06 0.88 0.3847	0.02 ± 0.08 0.29 0.7769	-	0.02 ± 0.07 0.32 0.7504	-0.02 ± 0.06 -0.33 0.7421
CV_1HU_2	0.24 ± 0.06 4.23 **0.0001**	0.09 ± 0.11 0.80 0.4308	-0.06 ± 0.05 -1.17 0.2488	-0.08 ± 0.04 -1.96 0.0574	-0.03 ± 0.05 -0.62 0.5421	0.02 ± 0.08 0.23 0.8188	-0.03 ± 0.07 -0.50 0.6189	-0.07 ± 0.05 -1.56 0.1257	0.03 ± 0.05 0.66 0.5132	0.00 ± 0.07 -0.01 0.9882	-0.02 ± 0.07 -0.32 0.7504	-	-0.04 ± 0.05 -0.93 0.3601
Mix_2	0.29 ± 0.04 6.61 **< 0.0001**	0.13 ± 0.10 1.29 0.2046	-0.02 ± 0.04 -0.48 0.6314	-0.04 ± 0.02 -1.97 0.0555	0.02 ± 0.03 0.60 0.5519	0.06 ± 0.07 0.93 0.3568	0.01 ± 0.06 0.16 0.8774	-0.03 ± 0.03 -1.07 0.2912	0.08 ± 0.03 2.39 **0.0216**	0.04 ± 0.06 0.78 0.4430	0.02 ± 0.06 0.33 0.7421	0.04 ± 0.05 0.93 0.3601	-

Model Summary 24 | Contact core particle skewness (CCSkew) by species treatment (Tcode)

Initial linear regression model:

```
lm(CCSkew ~ as.factor(Tcode))
```

Minimal adequate model:

```
gls(CCSkew ~ as.factor(Tcode),
    weights = varIdent(form = ~1|as.factor(Tcode)),
    method = 'REML')
```

Coefficient Table

Intercept ± SE (when baseline is for N): 0.15 ± 0.05, t = 2.97, p = 0.0051.

	N	P	PD	HD_1HU_2	HDHU	HU_1HD_2	HD_1CV_2	HDCV	CV_1HD_2	HU_1CV_2	HUCV	CV_1HU_2	Mix_2
N	-	-0.25 ± 0.17 -1.48 0.1467	-0.44 ± 0.07 -6.10 **< 0.0001**	-0.40 ± 0.06 -7.00 **< 0.0001**	-0.37 ± 0.07 -5.52 **< 0.0001**	-0.27 ± 0.13 -2.03 **0.0489**	-0.40 ± 0.08 -4.88 **< 0.0001**	-0.41 ± 0.06 -6.84 **< 0.0001**	-0.34 ± 0.06 -5.74 **< 0.0001**	-0.22 ± 0.13 -1.77 0.0846	-0.39 ± 0.07 -5.19 **< 0.0001**	-0.40 ± 0.06 -6.48 **< 0.0001**	-0.44 ± 0.07 -6.40 **< 0.0001**
P	0.25 ± 0.17 1.48 0.1467	-	-0.19 ± 0.17 -1.12 0.2679	-0.2 ± 0.16 -0.92 0.3630	-0.12 ± 0.17 -0.72 0.4742	-0.02 ± 0.20 -0.09 0.9322	-0.14 ± 0.17 -0.84 0.4073	-0.16 ± 0.16 -0.98 0.3352	-0.09 ± 0.16 -0.53 0.6008	0.03 ± 0.20 0.14 0.8860	-0.14 ± 0.17 -0.80 0.4296	-0.15 ± 0.16 -0.90 0.3724	-0.19 ± 0.17 -1.11 0.2739
PD	0.44 ± 0.07 6.10 **< 0.0001**	0.19 ± 0.17 1.12 0.2679	-	0.04 ± 0.06 0.71 0.4830	0.07 ± 0.07 1.04 0.3026	0.17 ± 0.13 1.31 0.1964	0.05 ± 0.08 0.56 0.5783	0.03 ± 0.06 0.50 0.6170	0.10 ± 0.06 1.80 0.0802	0.22 ± 0.12 1.75 0.0886	0.05 ± 0.07 0.74 0.4649	0.04 ± 0.06 0.68 0.4998	0.00 ± 0.07 0.06 0.9499
HD_1HU_2	0.40 ± 0.06 7.00 **< 0.0001**	0.15 ± 0.16 0.92 0.3630	-0.04 ± 0.06 -0.71 0.4830	-	0.03 ± 0.05 0.60 0.5548	0.13 ± 0.12 1.07 0.2895	0.01 ± 0.07 0.08 0.9380	-0.01 ± 0.04 -0.25 0.8002	0.06 ± 0.04 1.72 0.0938	0.18 ± 0.12 1.53 0.1350	0.01 ± 0.06 0.25 0.8066	0.00 ± 0.04 0.04 0.9714	-0.04 ± 0.05 -0.70 0.4889
HDHU	0.37 ± 0.07 5.52 **< 0.0001**	0.12 ± 0.17 0.72 0.4742	-0.07 ± 0.07 -1.04 0.3026	-0.03 ± 0.05 -0.60 0.5548	-	0.10 ± 0.13 0.80 0.4268	-0.02 ± 0.08 -0.32 0.7508	-0.04 ± 0.05 -0.75 0.4587	0.03 ± 0.05 0.67 0.5076	0.15 ± 0.12 1.22 0.2299	-0.02 ± 0.07 -0.22 0.8280	-0.03 ± 0.05 -0.51 0.6103	-0.07 ± 0.06 -1.05 0.2999
HU_1HD_2	0.27 ± 0.13 2.03 **0.0489**	0.02 ± 0.20 0.09 0.9322	-0.17 ± 0.13 -1.31 0.1964	-0.13 ± 0.12 -1.07 0.2895	-0.10 ± 0.13 -0.80 0.4268	-	-0.13 ± 0.14 -0.94 0.3553	-0.14 ± 0.12 -1.14 0.2603	-0.07 ± 0.12 -0.56 0.5820	0.05 ± 0.17 0.27 0.7850	-0.12 ± 0.13 -0.89 0.3774	-0.13 ± 0.13 -1.04 0.3028	-0.17 ± 0.13 -1.30 0.2000
HD_1CV_2	0.40 ± 0.08 4.88 **< 0.0001**	0.14 ± 0.17 0.84 0.4073	-0.05 ± 0.08 -0.56 0.5783	-0.01 ± 0.07 -0.08 0.9380	0.02 ± 0.08 0.32 0.7508	0.13 ± 0.14 0.94 0.3553	-	-0.02 ± 0.07 -0.22 0.8276	0.06 ± 0.07 0.86 0.3974	0.17 ± 0.13 1.3299 0.1913	0.01 ± 0.08 0.1125 0.9110	0.00 ± 0.07 -0.05 0.9581	-0.04 ± 0.08 -0.53 0.5981
HDCV	0.41 ± 0.06 6.84 **< 0.0001**	-0.16 ± 0.16 0.98 0.3352	-0.03 ± 0.06 -0.50 0.6170	0.01 ± 0.04 0.25 0.8002	0.04 ± 0.05 0.75 0.4587	0.14 ± 0.12 1.14 0.2603	0.02 ± 0.07 0.22 0.8276	-	0.07 ± 0.04 1.78 0.0824	0.19 ± 0.12 1.59 0.1193	0.02 ± 0.06 0.40 0.6930	0.01 ± 0.05 0.25 0.8012	-0.03 ± 0.05 -0.47 0.6394
CV_1HD_2	0.34 ± 0.06 5.74 **< 0.0001**	0.09 ± 0.16 0.53 0.6008	-0.10 ± 0.06 -1.80 0.0802	-0.06 ± 0.04 -1.72 0.0938	-0.03 ± 0.05 -0.67 0.5076	0.07 ± 0.12 0.56 0.5820	-0.06 ± 0.07 -0.86 0.3974	-0.07 ± 0.04 -1.78 0.0824	-	0.11 ± 0.12 0.98 0.3355	-0.05 ± 0.06 -0.82 0.4187	-0.06 ± 0.04 -1.43 0.1607	-0.10 ± 0.05 -1.89 0.0660
HU_1CV_2	0.22 ± 0.13 1.77 0.0846	-0.03 ± 0.20 -0.14 0.8860	-0.22 ± 0.12 -1.75 0.0886	-0.18 ± 0.12 -1.53 0.1350	-0.15 ± 0.12 -1.22 0.2299	-0.05 ± 0.17 -0.27 0.7850	-0.17 ± 0.13 -1.33 0.1913	-0.19 ± 0.12 -1.5926632 0.1193	-0.11 ± 0.12 -0.98 0.3355	-	-0.16 ± 0.13 -1.30 0.2014	-0.18 ± 0.12 -1.49 0.1454	-0.21 ± 0.12 -1.74 0.0890
HUCV	0.39 ± 0.07 5.19 **< 0.0001**	0.14 ± 0.17 0.80 0.4296	-0.05 ± 0.07 -0.74 0.4649	-0.01 ± 0.06 -0.25 0.8066	0.02 ± 0.07 0.22 0.8280	0.12 ± 0.13 0.89 0.3774	-0.01 ± 0.08 -0.11 0.9110	-0.02 ± 0.06 -0.40 0.6930	0.05 ± 0.06 0.82 0.4187	0.16 ± 0.13 1.30 0.2014	-	-0.01 ± 0.06 -0.21 0.8378	-0.05 ± 0.07 -0.72 0.4764
CV_1HU_2	0.40 ± 0.06 6.48 **< 0.0001**	0.15 ± 0.16 0.90 0.3724	-0.04 ± 0.06 -0.68 0.4998	0.00 ± 0.04 -0.04 0.9714	0.03 ± 0.05 0.51 0.6103	0.13 ± 0.13 1.04 0.3028	0.00 ± 0.07 0.05 0.9581	-0.01 ± 0.05 -0.25 0.8012	0.06 ± 0.04 1.43 0.1607	0.18 ± 0.12 1.49 0.1454	0.01 ± 0.06 0.21 0.8378	-	-0.04 ± 0.06 -0.66 0.5102
Mix_2	0.44 ± 0.07 6.40 **< 0.0001**	0.19 ± 0.17 1.11 0.2739	0.00 ± 0.07 -0.06 0.9499	0.04 ± 0.05 0.70 0.4889	0.07 ± 0.06 1.05 0.2999	0.17 ± 0.13 1.30 0.2000	0.04 ± 0.08 0.53 0.5981	0.03 ± 0.05 0.47 0.6394	0.10 ± 0.05 1.89 0.0660	0.21 ± 0.12 1.74 0.0890	0.05 ± 0.07 0.72 0.4764	0.04 ± 0.06 0.66 0.5102	-

Model Summary 25 | Contact core particle kurtosis (CCKurt) by species treatment (Tcode)

Initial linear regression model:

lm(CCKurt ~ as.factor(Tcode))

No minimal adequate model, intercept only (Tcode, L-ratio = 15.99337, d.f. = 26, p = 0.1915).

Model Summary 26 | Contact core D_{10} (CCD_{10}, µm) by species treatment (Tcode)

Initial linear regression model:

lm(CCD_{10} ~ as.factor(Tcode))

No minimal adequate model, intercept only (Tcode, L-ratio = 17.94011, d.f. = 26, p = 1175).

Model Summary 27 | Contact core mud content (CCPCMud, %) by species treatment (Tcode)

Initial linear regression model:

lm(CCMud% ~ as.factor(Tcode))

Minimal adequate model:

gls(CCMud% ~ as.factor(Tcode),
weights = varIdent(form = ~1|as.factor(Tcode)),
method = 'REML')

Coefficient Table

Intercept ± SE (when baseline is for N): 67.73 ± 2.30, t = 29.46, p < 0.0001.

	N	P	PD	HD_1HU_2	HDHU	HU_1HD_2	HD_1CV_2	HDCV	CV_1HD_2	HU_1CV_2	HUCV	CV_1HU_2	Mix_2
N	-	2.82 ± 2.78 1.01 0.3180	3.78 ± 3.31 1.14 0.2605	7.35 ± 2.48 2.96 **0.0052**	3.19 ± 2.47 1.29 0.2035	2.48 ± 2.67 0.93 0.3601	4.58 ± 2.59 1.77 0.0847	4.27 ± 2.35 1.81 0.0776	0.37 ± 2.37 0.15 0.8778	7.50 ± 3.26 2.30 **0.0269**	3.97 ± 3.03 1.31 0.1982	0.38 ± 2.66 0.14 0.8866	1.72 ± 2.41 0.71 0.4810
P	-2.82 ± 2.78 -1.01 0.3180	-	0.97 ± 2.85 0.34 0.7369	4.54 ± 1.82 2.49 **0.0173**	0.38 ± 1.80 0.21 0.8364	-0.34 ± 2.08 -0.16 0.8708	1.77 ± 1.97 0.90 0.3754	1.45 ± 1.64 0.88 0.3834	-2.45 ± 1.67 -1.46 0.1519	4.68 ± 2.79 1.68 0.1015	1.15 ± 2.52 0.46 0.6502	-2.43 ± 2.07 -1.18 0.2463	-1.10 ± 1.73 -0.63 0.5297
PD	-3.78 ± 3.31 -1.14 0.2605	-0.97 ± 2.85 -0.34 0.7369	-	3.57 ± 2.56 1.40 0.1707	-0.59 ± 2.54 -0.23 0.8178	-1.31 ± 2.74 -0.48 0.6370	0.80 ± 2.66 0.30 0.7654	0.49 ± 2.43 0.20 0.8431	-3.41 ± 2.45 -1.39 0.1722	3.72 ± 3.32 1.12 0.2695	0.19 ± 3.09 0.06 0.9520	-3.40 ± 2.74 -1.24 0.2218	-2.06 ± 2.49 -0.83 0.4130
HD_1HU_2	-7.35 ± 2.48 -2.96 **0.0052**	-4.54 ± 1.82 -2.49 **0.0173**	-3.57 ± 2.56 -1.40 0.1707	-	-4.16 ± 1.29 -3.22 **0.0026**	-4.88 ± 1.65 -2.95 **0.0053**	-2.77 ± 1.51 -1.83 0.0746	-3.09 ± 1.06 -2.92 **0.0058**	-6.98 ± 1.10 -6.33 **< 0.0001**	0.15 ± 2.49 0.06 0.9531	-3.38 ± 2.18 -1.55 0.1295	-6.97 ± 1.64 -4.25 **0.0001**	-5.63 ± 1.19 -4.75 **< 0.0001**
HDHU	-3.19 ± 2.47 -1.29 0.2035	-0.38 ± 1.80 -0.21 0.8364	0.59 ± 2.54 0.23 0.8178	4.16 ± 1.29 3.22 **0.0026**	-	-0.72 ± 1.63 -0.44 0.6631	1.39 ± 1.49 0.93 0.3561	1.08 ± 1.02 1.05 0.2998	-2.82 ± 1.07 -2.64 **0.0120**	4.31 ± 2.48 1.74 0.0899	0.78 ± 2.17 0.36 0.7218	-2.81 ± 1.62 -1.74 0.0903	-1.47 ± 1.16 -1.27 0.2103
HU_1HD_2	-2.48 ± 2.67 -0.93 0.3601	0.34 ± 2.08 0.16 0.8708	1.31 ± 2.74 0.48 0.6370	4.88 ± 1.65 2.95 **0.0053**	0.72 ± 1.63 0.44 0.6631	-	2.11 ± 1.81 1.16 0.2517	1.79 ± 1.45 1.23 0.2246	-2.11 ± 1.48 -1.42 0.1636	5.02 ± 2.68 1.87 0.0686	1.49 ± 2.40 0.62 0.5375	-2.09 ± 1.92 -1.09 0.2814	-0.76 ± 1.55 -0.49 0.6272
HD_1CV_2	-4.58 ± 2.59 -1.77 0.0847	-1.77 ± 1.97 -0.90 0.3754	-0.80 ± 2.66 -0.30 0.7654	2.77 ± 1.51 1.83 0.0746	-1.39 ± 1.49 -0.93 0.3561	-2.11 ± 1.81 -1.16 0.2517	-	-0.32 ± 1.29 -0.24 0.8085	-4.21 ± 1.33 -3.17 **0.0030**	2.92 ± 2.60 1.1225 0.2685	-0.61 ± 2.31 -0.2656 0.7920	-4.20 ± 1.80 -2.33 **0.0248**	-2.86 ± 1.40 -2.05 0.0475
HDCV	-4.27 ± 2.35 -1.81 0.0776	1.45 ± 1.64 -0.88 0.3834	-0.49 ± 2.43 -0.20 0.8431	3.09 ± 1.06 2.92 **0.0058**	-1.08 ± 1.02 -1.05 0.2998	-1.79 ± 1.45 -1.23 0.2246	0.32 ± 1.29 0.24 0.8085	-	-3.90 ± 0.77 -5.05 **< 0.0001**	3.23 ± 2.36 1.37 0.1793	-0.30 ± 2.04 -0.15 0.8847	-3.88 ± 1.44 -2.70 **0.0101**	-2.55 ± 0.89 -2.87 **0.0066**
CV_1HD_2	-0.37 ± 2.37 -0.15 0.8778	2.45 ± 1.67 1.46 0.1519	3.41 ± 2.45 1.39 0.1722	6.98 ± 1.10 6.33 **< 0.0001**	2.82 ± 1.07 2.64 **0.0120**	2.11 ± 1.48 1.42 0.1636	4.21 ± 1.33 3.17 **0.0030**	3.90 ± 0.77 5.05 **< 0.0001**	-	7.13 ± 2.38 2.99 **0.0048**	3.60 ± 2.06 1.75 0.0886	0.02 ± 1.47 0.01 0.9919	1.35 ± 0.94 1.43 0.1597
HU_1CV_2	-7.50 ± 3.26 -2.30 **0.0269**	-4.68 ± 2.79 -1.68 0.1015	-3.72 ± 3.32 -1.12 0.2695	-0.15 ± 2.49 -0.06 0.9531	-4.31 ± 2.48 -1.74 0.0899	-5.02 ± 2.68 -1.87 0.0686	-2.92 ± 2.60 -1.12 0.2685	-3.23 ± 2.36 -1.36761 0.1793	-7.13 ± 2.38 -2.99 **0.0048**	-	-3.53 ± 3.04 -1.16 0.2526	-7.12 ± 2.67 -2.66 **0.0113**	-5.78 ± 2.42 -2.38 **0.0221**
HUCV	-3.97 ± 3.03 -1.31 0.1982	-1.15 ± 2.52 -0.46 0.6502	-0.19 ± 3.09 -0.06 0.9520	3.38 ± 2.18 1.55 0.1295	-0.78 ± 2.17 -0.36 0.7218	-1.49 ± 2.40 -0.62 0.5375	0.61 ± 2.31 0.27 0.7920	0.30 ± 2.04 0.15 0.8847	-3.60 ± 2.06 -1.75 0.0886	3.53 ± 3.04 1.16 0.2526	-	-3.59 ± 2.39 -1.50 0.1418	-2.25 ± 2.11 -1.07 0.2922
CV_1HU_2	-0.38 ± 2.66 -0.14 0.8866	2.43 ± 2.07 1.18 0.2463	3.40 ± 2.74 1.24 0.2218	6.97 ± 1.64 4.25 **0.0001**	2.81 ± 1.62 1.74 0.0903	2.09 ± 1.92 1.09 0.2814	4.20 ± 1.80 2.33 **0.0248**	3.88 ± 1.44 2.70 **0.0101**	-0.02 ± 1.47 -0.01 0.9919	7.12 ± 2.67 2.66 **0.0113**	3.59 ± 2.39 1.50 0.1418	-	1.34 ± 1.53 0.87 0.3895
Mix_2	-1.72 ± 2.41 -0.71 0.4810	1.10 ± 1.73 0.63 0.5297	2.06 ± 2.49 0.83 0.4130	5.63 ± 1.19 4.75 **< 0.0001**	1.47 ± 1.16 1.27 0.2103	0.76 ± 1.55 0.49 0.6272	2.86 ± 1.40 2.05 0.0475	2.55 ± 0.89 2.87 **0.0066**	-1.35 ± 0.94 -1.43 0.1597	5.78 ± 2.42 2.38 **0.0221**	2.25 ± 2.11 1.07 0.2922	-1.34 ± 1.53 -0.87 0.3895	-

Appendix 4

Statistical model summary

Summary of the statistical analysis for the 27 statistical models. For each model the initial linear regression model, the minimal adequate model with GLS estimation and a summary of the coefficient table is given. The coefficients indicate the relative performance of each treatment level relative to the relevelled baseline (as indicated). Coefficients ± SE and t-values are presented alongside corresponding significance values (in parentheses). Abbreviations: N, natural sediment as a mudflat baseline; P, pipe mesocosm only treatment as a procedural control; N_{HD}, natural sediment with 50 % additional biomass added as Hediste diversicolor, N_{HU}, natural sediment with 50 % additional biomass added as Hydrobia ulvae, N_{CV}, natural sediment with 50 % additional biomass added as Corophium volutator; Day, day of data collection; Row, row location of pipe mesocosm; Tcode, species treatment code [N, P, N_{HD}, N_{HU}, H_{CV}].

Model Summary 1 | Erosion threshold (ET, Nm^{-2}) by row location of mesocosm (Row)

Initial linear regression model:

lm(ET ~ as.factor(Row))

No minimal adequate model, intercept only (Day, L-ratio = 1.842856, d.f. = 5, p = 0.6057).

Model Summary 2 | Average pulse amplitude modulated (PAM) measured minimum fluorescence (PAMFAv) by row location of mesocosm (Row)

Initial linear regression model:

lm(PAMFmAv ~ as.factor(Row))

No minimal adequate model, intercept only (Day, L-ratio = 1.008963, d.f. = 5, p = 0.7991).

Model Summary 3 | Erosion threshold (ET, Nm^{-2}) by species treatment (Tcode)

Initial linear regression model:

lm(ET ~ as.factor(Tcode))

Minimal adequate model:

gls(ET~ as.factor(Tcode),
weights = varIdent(form = ~1|as.factor(Tcode)),
method = 'REML')

Coefficient Table

Intercept ± SE (when baseline is for N): 0.21 ± 0.04, t = 4.82, p = 0.0001.

	N	P	N_{HD}	N_{HU}	N_{CV}
N	-	1.05 ± 0.25 4.19 **0.0003**	0.69 ± 0.14 4.84 **0.0001**	0.90 ± 0.14 6.29 **< 0.0001**	0.64 ± 0.10 6.09 **< 0.0001**
P	-1.05 ± 0.25 -4.19 **0.0003**	-	-0.36 ± 0.28 -1.29 0.2093	-0.2 ± 0.28 -0.54 0.5959	-0.41 ± 0.27 -1.56 0.1315
N_{HD}	-0.69 ± 0.14 -4.84 **0.0001**	0.36 ± 0.28 1.29 0.2093	-	0.21 ± 0.19 1.10 0.2819	-0.05 ± 0.17 -0.30 0.7658
N_{HU}	-0.90 ± 0.14 -6.29 **< 0.0001**	0.15 ± 0.28 0.54 0.5959	-0.21 ± 0.19 -1.10 0.2819	-	-0.26 ± 0.17 -1.57 0.1293
N_{CV}	-0.64 ± 0.10 -6.09 **< 0.0001**	0.41 ± 0.27 1.56 0.1315	0.05 ± 0.17 0.30 0.7658	0.26 ± 0.17 1.57 0.1293	-

Model Summary 4 | Suspension index (SI) by species treatment (Tcode)

Initial linear regression model:

lm(SI ~ as.factor(Tcode))

Minimal adequate model:

gls(SI ~ as.factor(Tcode),
weights = varIdent(form = ~1|as.factor(Tcode)),
method = 'REML')

Coefficient Table

Intercept ± SE (when baseline is for N): 32.46 ± 5.32, t = 6.10, p < 0.0001.

	N	P	N_{HD}	N_{HU}	N_{CV}
N	-	-28.72 ± 5.41 -5.31 **< 0.0001**	-26.81 ± 5.50 -4.88 **0.0001**	-29.76 ± 5.38 -5.54 **< 0.0001**	-27.34 ± 5.46 -5.01 **< 0.0001**
P	28.72 ± 5.41 5.31 **< 0.0001**	-	1.91 ± 1.70 1.12 0.2727	-1.04 ± 1.25 -0.83 0.4126	1.38 ± 1.57 0.88 0.3898
N_{HD}	26.81 ± 5.50 4.88 **0.0001**	-1.91 ± 1.70 -1.12 0.2727	-	-2.95 ± 1.58 -1.87 0.0739	-0.53 ± 1.85 -0.29 0.7765
N_{HU}	29.76 ± 5.38 5.54 **< 0.0001**	1.04 ± 1.25 0.83 0.4126	2.95 ± 1.58 1.87 0.0739	-	2.42 ± 1.44 1.68 0.1062
N_{CV}	27.34 ± 5.46 5.01 **< 0.0001**	-1.38 ± 1.57 -0.88 0.3898	0.53 ± 1.85 0.29 0.7765	-2.42 ± 1.44 -1.68 0.1062	-

Model Summary 5 | Average pulse amplitude modulated (PAM) measured minimum fluorescence (PAMFAv) by species treatment (Tcode)

Initial linear regression model:

lm(PAMFAv ~ as.factor(Tcode))

Minimal adequate model:

gls(PAMFAv ~ as.factor(Tcode),
weights = varIdent(form = ~1|as.factor(Tcode)),
method = 'REML')

Coefficient Table

Intercept ± SE (when baseline is for N): 149.39 ± 8.04, t = 18.58, p < 0.0001.

	N	P	N_{HD}	N_{HU}	N_{CV}
N	-	228.67 ± 64.11 3.57 **0.0015**	127.61 ± 33.56 3.80 **0.0008**	138.83 ± 59.32 2.34 **0.0275**	96.67 ± 26.12 3.70 **0.0011**
P	-228.67 ± 64.11 -3.57 **0.0015**	-	-101.06 ± 71.47 -1.41 0.1697	-89.83 ± 86.60 -1.04 0.3095	-132.00 ± 68.29 -1.93 0.0646
N_{HD}	-127.61 ± 33.56 -3.80 **0.0008**	101.06 ± 71.47 1.41 0.1697	-	11.22 ± 67.20 0.17 0.8687	-30.94 ± 40.98 -0.76 0.4572
N_{HU}	-138.83 ± 59.32 -2.34 **0.0275**	89.83 ± 86.60 1.04 0.3095	-11.22 ± 67.20 -0.17 0.8687	-	-42.17 ± 63.81 -0.66 0.5148
N_{CV}	-96.67 ± 26.12 -3.70 **0.0011**	132.00 ± 68.29 1.93 0.0646	30.94 ± 40.98 0.76 0.4572	42.17 ± 63.81 0.66 0.5148	-

Model Summary 6 | Average pulse amplitude modulated (PAM) measured maximum quantum yield (PAMYAv) by species treatment (Tcode)

Initial linear regression model:

lm(PAMYAv ~ as.factor(Tcode))

Minimal adequate model:

gls(PAMYAv ~ as.factor(Tcode),
weights = varIdent(form = ~1|as.factor(Tcode)),
method = 'REML')

Coefficient Table

Intercept ± SE (when baseline is for N): 0.60 ± 0.01, t = 79.95, p < 0.0001.

	N	P	N_{HD}	N_{HU}	N_{CV}
N	-	0.03 ± 0.01 1.73 0.0953	0.04 ± 0.02 2.80 **0.0096**	0.06 ± 0.02 2.61 **0.0152**	0.03 ± 0.02 1.99 0.0575
P	-0.03 ± 0.01 -1.73 0.0953	-	0.02 ± 0.02 0.97 0.3411	0.03 ± 0.02 1.26 0.2188	0.01 ± 0.02 0.28 0.7790
N_{HD}	-0.04 ± 0.02 -2.80 **0.0096**	-0.02 ± 0.02 -0.97 0.3411	-	0.01 ± 0.02 0.48 0.6348	-0.01 ± 0.02 -0.67 0.5109
N_{HU}	-0.06 ± 0.02 -2.61 **0.0152**	-0.03 ± 0.02 -1.26 0.2188	-0.01 ± 0.02 -0.48 0.6348	-	-0.02 ± 0.02 -1.02 0.3188
N_{CV}	-0.03 ± 0.02 -1.99 0.0575	-0.01 ± 0.02 -0.28 0.7790	0.01 ± 0.02 0.67 0.5109	0.02 ± 0.02 1.02 0.3188	-

Model Summary 7 | Minicore water content (MCWater%, %) by species treatment (Tcode)

Initial linear regression model:

lm(MCWater% ~ as.factor(Tcode))

Minimal adequate model:

gls(MCWater% ~ as.factor(Tcode),
weights = varIdent(form = ~1|as.factor(Tcode)),
method = 'REML')

Coefficient Table

Intercept ± SE (when baseline is for N): 56.12 ± 0.75, t = 74.62, p < 0.0001.

	N	P	N_{HD}	N_{HU}	N_{CV}
N	-	6.93 ± 1.31 5.31 **< 0.0001**	6.28 ± 0.94 6.67 **< 0.0001**	6.38 ± 1.39 4.58 **0.0001**	6.67 ± 0.89 7.47 **< 0.0001**
P	-6.93 ± 1.31 -5.31 **< 0.0001**	-	-0.65 ± 1.21 -0.54 0.5971	-0.5 ± 1.58 -0.35 0.7314	-0.26 ± 1.17 -0.22 0.8287
N_{HD}	-6.28 ± 0.94 -6.67 **< 0.0001**	0.65 ± 1.21 0.54 0.5971	-	0.10 ± 1.30 0.07 0.9409	0.39 ± 0.74 0.53 0.6039
N_{HU}	-6.38 ± 1.39 -4.58 **0.0001**	0.55 ± 1.58 0.35 0.7314	-0.10 ± 1.30 -0.07 0.9409	-	0.29 ± 1.27 0.23 0.8184
N_{CV}	-6.67 ± 0.89 -7.47 **< 0.0001**	0.26 ± 1.17 0.22 0.8287	-0.39 ± 0.74 -0.53 0.6039	-0.29 ± 1.27 -0.23 0.8184	-

Model Summary 8 | Minicore mean particle size (MCMean, µm) by species treatment (Tcode)

Initial linear regression model:

lm(MCMean ~ as.factor(Tcode))

No minimal adequate model, intercept only (Tcode, L-ratio = 1.223021, d.f. = 10, p = 0.8743).

Model Summary 9 | Minicore mode particle size (MCMode, µm) by species treatment (Tcode)

Initial linear regression model:

lm(MCMode ~ as.factor(Tcode))

No minimal adequate model, intercept only (Tcode, F = 1.3773, d.f. = 4, p = 0.2702).

Model Summary 10 | Minicore particle sorting (MCSort) by species treatment (Tcode)

Initial linear regression model:

lm(MCSort ~ as.factor(Tcode))

No minimal adequate model, intercept only (Tcode, L-ratio = 1.099348, d.f. = 10, p = 0.8944).

Model Summary 11 | Minicore particle skewness (MCSkew) by species treatment (Tcode)

Initial linear regression model:

lm(MCSkew ~ as.factor(Tcode))

No minimal adequate model, intercept only (Tcode, L-ratio = 7.713462, d.f. = 10, p = 0.1027).

Model Summary 12 | Minicore particle kurtosis (MCKurt) by species treatment (Tcode)

Initial linear regression model:

lm(MCKurt ~ as.factor(Tcode))

Minimal adequate model:

gls(MCKurt ~ as.factor(Tcode),
weights = varIdent(form = ~1|as.factor(Tcode)),
method = 'REML')

Coefficient Table

Intercept ± SE (when baseline is for N): 2.84 ± 0.08, t = 33.99, p < 0.0001.

	N	P	N_{HD}	N_{HU}	N_{CV}
N	-	-0.35 ± 0.10 -3.59 **0.0014**	-0.33 ± 0.09 -3.74 **0.0010**	-0.28 ± 0.12 -2.26 **0.0325**	-0.26 ± 0.10 -2.59 **0.0156**
P	0.35 ± 0.10 3.59 **0.0014**	-	0.02 ± 0.06 0.32 0.7511	0.07 ± 0.11 0.66 0.5168	0.09 ± 0.08 1.17 0.2544
N_{HD}	0.33 ± 0.09 3.74 **0.0010**	-0.02 ± 0.06 -0.32 0.7511	-	0.05 ± 0.10 0.52 0.6109	0.07 ± 0.07 1.08 0.2903
N_{HU}	0.28 ± 0.12 2.26 **0.0325**	-0.07 ± 0.11 -0.66 0.5168	-0.05 ± 0.10 -0.52 0.6109	-	0.02 ± 0.11 0.18 0.8560
N_{CV}	0.26 ± 0.10 2.59 **0.0156**	-0.09 ± 0.08 -1.17 0.2544	-0.07 ± 0.07 -1.08 0.2903	-0.02 ± 0.11 -0.18 0.8560	-

Model Summary 13 | Minicore D_{10} (MCD_{10}, µm) by species treatment (Tcode)

Initial linear regression model:

lm(MCD_{10} ~ as.factor(Tcode))

No minimal adequate model, intercept only (Tcode, L-ratio = 2.421743, d.f. = 10, p = 0.6587).

Model Summary 14 | Minicore mud content (MCPCMud, %) by species treatment (Tcode)

Initial linear regression model:

lm(MCPCMud% ~ as.factor(Tcode))

No minimal adequate model, intercept only (Tcode, L-ratio = 1.203632, d.f. = 10, p = 0.8775).

Model Summary 15 | Contact core water concentration (CCWat, gcm^{-3}) by species treatment (Tcode)

Initial linear regression model:

lm(CCWat ~ as.factor(Tcode))

No minimal adequate model, intercept only (Tcode, L-ratio = 2.832344, d.f. = 10, p = 0.5863).

Model Summary 16 | Contact core carbohydrate concentration (CCCarb, glucose µgcm^{-3}) by species treatment (Tcode)

Initial linear regression model:

lm(CCCarb ~ as.factor(Tcode))

Minimal adequate model:

gls(CCCarb ~ as.factor(Tcode),
weights = varIdent(form = ~1|as.factor(Tcode)),
method = 'REML')

Coefficient Table

Intercept ± SE (when baseline is for N): 310.49 ± 37.14, t = 8.36, p < 0.0001.

	N	P	N_{HD}	N_{HU}	N_{CV}
N	-	374.88 ± 112.91 3.32 **0.0029**	565.46 ± 147.01 3.85 **0.0008**	427.28 ± 128.59 3.32 **0.0028**	171.66 ± 82.99 2.07 **0.0495**
P	-374.88 ± 112.91 -3.32 **0.0029**	-	190.58 ± 177.77 1.07 0.2944	52.395 ± 162.87 0.32 0.7505	-203.22 ± 129.91 -1.56 0.1308
N_{HD}	-565.46 ± 147.01 -3.85 **0.0008**	-190.58 ± 177.77 -1.07 0.2944	-	-138.18 ± 188.12 -0.73 0.4697	-393.80 ± 160.44 -2.45 **0.0217**
N_{HU}	-427.28 ± 128.59 -3.32 **0.0028**	-52.39 ± 162.87 -0.32 0.7505	138.18 ± 188.12 0.73 0.4697	-	-255.62 ± 143.75 -1.78 0.0880
N_{CV}	-171.66 ± 82.99 -2.07 **0.0495**	203.22 ± 129.91 1.56 0.1308	393.80 ± 160.44 2.45 **0.0217**	255.62 ± 143.75 1.78 0.0880	-

Model Summary 17 | Contact core chlorophyll *a* concentration (CCChl*a*, µgcm^{-3}) by species treatment (Tcode)

Initial linear regression model:

lm(CCChl*a* ~ as.factor(Tcode))

Minimal adequate model:

gls(CCChl*a* ~ as.factor(Tcode),
weights = varIdent(form = ~1|as.factor(Tcode)),
method = 'REML')

Coefficient Table

Intercept ± SE (when baseline is for N): 12.64 ± 0.27, t = 46.09, p < 0.0001.

	N	P	N_{HD}	N_{HU}	N_{CV}
N	-	8.17 ± 1.72 4.75 **0.0001**	7.63 ± 1.28 5.96 **< 0.0001**	9.58 ± 2.51 3.82 **0.0008**	5.74 ± 0.88 6.51 **< 0.0001**
P	-8.17 ± 1.72 -4.75 **0.0001**	-	-0.54 ± 2.11 -0.26 0.8007	1.41 ± 3.02 0.47 0.6456	-2.43 ± 1.89 -1.28 0.2114
N_{HD}	-7.63 ± 1.28 -5.96 **< 0.0001**	0.54 ± 2.11 0.26 0.8007	-	1.94 ± 2.79 0.70 0.4929	-1.89 ± 1.51 -1.26 0.2211
N_{HU}	-9.58 ± 2.51 -3.82 **0.0008**	-1.41 ± 3.02 -0.47 0.6456	-1.94 ± 2.79 -0.70 0.4929	-	-3.83 ± 2.63 -1.46 0.1580
N_{CV}	-5.74 ± 0.88 -6.51 **< 0.0001**	2.43 ± 1.89 1.28 0.2114	1.89 ± 1.51 1.26 0.2211	3.83 ± 2.63 1.46 0.1580	-

Model Summary 18 | Contact core chlorophyll *b* concentration (CCChl*b*, µgcm^{-3}) by species treatment (Tcode)

Initial linear regression model:

lm(CCChl*b* ~ as.factor(Tcode))

Minimal adequate model:

gls(CCChl*b* ~ as.factor(Tcode),
weights = varIdent(form = ~1|as.factor(Tcode)),
method = 'REML')

Coefficient Table

Intercept ± SE (when baseline is for N): 3.30 ± 0.05, t = 64.46, p < 0.0001.

	N	P	N_{HD}	N_{HU}	N_{CV}
N	-	2.08 ± 0.53 3.93 **0.0006**	1.81 ± 0.29 6.23 **< 0.0001**	2.39 ± 0.61 3.92 **0.0006**	1.29 ± 0.24 5.32 **< 0.0001**
P	-2.08 ± 0.53 -3.93 **0.0006**	-	-0.27 ± 0.60 -0.45 0.6557	0.31 ± 0.80 0.38 0.7053	-0.79 ± 0.58 -1.38 0.1817
N_{HD}	-1.81 ± 0.29 -6.23 **< 0.0001**	0.27 ± 0.60 0.45 0.6557	-	0.58 ± 0.67 0.86 0.3975	-0.52 ± 0.37 -1.41 0.1715
N_{HU}	-2.39 ± 0.61 -3.92 **0.0006**	-0.31 ± 0.80 -0.38 0.7053	-0.58 ± 0.67 -0.86 0.3975	-	-1.10 ± 0.65 -1.69 0.1038
N_{CV}	-1.29 ± 0.24 -5.32 **< 0.0001**	0.79 ± 0.58 1.38 0.1817	0.52 ± 0.37 1.41 0.1715	1.10 ± 0.65 1.69 0.1038	-

Model Summary 19 | Contact core mean particle size (CCMean, µm) by species treatment (Tcode)

Initial linear regression model:

lm(CCMean ~ as.factor(Tcode))

No minimal adequate model, intercept only (Tcode, L-ratio = 9.404243, d.f. = 10, p = 0.0518).

Model Summary 20 | Contact core particle size mode (CCMode, µm) by species treatment (Tcode)

Initial linear regression model:

lm(CCMode ~ as.factor(Tcode))

No minimal adequate model, intercept only (Tcode, F = 1.9255, d.f. = 4, p = 0.1388).

Model Summary 21 | Contact core particle sorting (CCSort) by species treatment (Tcode)

Initial linear regression model:

lm(CCSort ~ as.factor(Tcode))

Minimal adequate model:

gls(CCMean ~ as.factor(Tcode),
weights = varIdent(form = ~1|as.factor(Tcode)),
method = 'REML')

Coefficient Table

Intercept ± SE (when baseline is for N): 2.65 ± 0.06, t = 42.80, p < 0.0001.

	N	P	N_{HD}	N_{HU}	N_{CV}
N	-	-0.07 ± 0.08 -0.93 0.3601	-0.19 ± 0.07 -2.70 **0.0126**	-0.13 ± 0.07 -1.97 0.0608	-0.18 ± 0.06 -2.93 **0.0073**
P	0.07 ± 0.08 0.93 0.3601	-	-0.11 ± 0.06 -1.94 0.0639	-0.1 ± 0.05 -1.04 0.3088	-0.11 ± 0.05 -2.19 **0.0382**
N_{HD}	0.19 ± 0.07 2.70 **0.0126**	0.11 ± 0.06 1.94 0.0639	-	0.06 ± 0.04 1.42 0.1689	0.00 ± 0.03 0.07 0.9444
N_{HU}	0.13 ± 0.07 1.97 0.0608	0.06 ± 0.05 1.04 0.3088	-0.06 ± 0.04 -1.42 0.1689	-	-0.05 ± 0.03 -2.00 0.0570
N_{CV}	0.18 ± 0.06 2.93 **0.0073**	0.11 ± 0.05 2.19 **0.0382**	0.00 ± 0.03 -0.07 0.9444	0.05 ± 0.03 2.00 0.0570	-

Model Summary 22 | Contact core particle skewness (CCSkew) by species treatment (Tcode)

Initial linear regression model:

lm(CCSkew ~ as.factor(Tcode))

Minimal adequate model:

gls(CCSkew ~ as.factor(Tcode),
weights = varIdent(form = ~1|as.factor(Tcode)),
method = 'REML')

Coefficient Table

Intercept ± SE (when baseline is for N): 0.12 ± 0.10, t = 1.16, p = 0.2581.

	N	P	N_{HD}	N_{HU}	N_{CV}
N	-	-0.25 ± 0.13 -1.91 0.0679	-0.42 ± 0.12 -3.42 **0.0023**	-0.38 ± 0.11 -3.27 **0.0033**	-0.46 ± 0.11 -4.17 **0.0003**
P	0.25 ± 0.13 1.91 0.0679	-	-0.18 ± 0.11 -1.62 0.1182	-0.1 ± 0.10 -1.30 0.2064	-0.21 ± 0.09 -2.27 **0.0322**
N_{HD}	0.42 ± 0.12 3.42 **0.0023**	0.18 ± 0.11 1.62 0.1182	-	0.05 ± 0.09 0.54 0.5955	-0.03 ± 0.08 -0.40 0.6932
N_{HU}	0.38 ± 0.11 3.27 **0.0033**	0.13 ± 0.10 1.30 0.2064	-0.05 ± 0.09 -0.54 0.5955	-	-0.08 ± 0.07 -1.17 0.2517
N_{CV}	0.46 ± 0.11 4.17 **0.0003**	0.21 ± 0.09 2.27 **0.0322**	0.03 ± 0.08 0.40 0.6932	0.08 ± 0.07 1.17 0.2517	-

Model Summary 23 | Contact core particle kurtosis (CCKurt) by species treatment (Tcode)

Initial linear regression model:

lm(CCKurt ~ as.factor(Tcode))

Minimal adequate model:

gls(CCKurt ~ as.factor(Tcode),
weights = varIdent(form = ~1|as.factor(Tcode)),
method = 'REML')

Coefficient Table

Intercept ± SE (when baseline is for N): 4.10 ± 0.08, t = 50.19, p < 0.0001.

	N	P	N_{HD}	N_{HU}	N_{CV}
N	-	-0.47 ± 0.17 -2.67 **0.0135**	-0.43 ± 0.09 -4.54 **0.0001**	-0.41 ± 0.09 -4.75 **0.0001**	-0.42 ± 0.09 -4.82 **0.0001**
P	0.47 ± 0.17 2.67 **0.0135**	-	0.04 ± 0.16 0.25 0.8075	0.06 ± 0.16 0.37 0.7171	0.04 ± 0.16 0.27 0.7857
N_{HD}	0.43 ± 0.09 4.54 **0.0001**	-0.04 ± 0.16 -0.25 0.8075	-	0.02 ± 0.05 0.33 0.7457	0.00 ± 0.06 0.06 0.9493
N_{HU}	0.41 ± 0.09 4.75 **0.0001**	-0.06 ± 0.16 -0.37 0.7171	-0.02 ± 0.05 -0.33 0.7457	-	-0.01 ± 0.04 -0.33 0.7429
N_{CV}	0.42 ± 0.09 4.82 **0.0001**	-0.04 ± 0.16 -0.28 0.7857	0.00 ± 0.06 -0.06 0.9493	0.01 ± 0.04 0.33 0.7429	-

Model Summary 24 | Contact core D_{10} (CCD_{10}, µm) by species treatment (Tcode)

Initial linear regression model:

lm(CCD_{10} ~ as.factor(Tcode))

Minimal adequate model:

gls(CCD_{10} ~ as.factor(Tcode),
weights = varIdent(form = ~1|as.factor(Tcode)),
method = 'REML')

Coefficient Table

Intercept ± SE (when baseline is for N): 12.54 ± 0.29, t = 42.68, p < 0.0001.

	N	P	N_{HD}	N_{HU}	N_{CV}
N	-	-1.65 ± 0.63 -2.63 **0.0148**	-1.21 ± 0.50 -2.41 **0.0239**	-0.76 ± 0.34 -2.26 **0.0331**	-0.51 ± 0.38 -1.33 0.1950
P	1.65 ± 0.63 2.63 **0.0148**	-	0.44 ± 0.69 0.64 0.5284	0.89 ± 0.58 1.53 0.1395	1.14 ± 0.60 1.89 0.0704
N_{HD}	1.21 ± 0.50 2.41 **0.0239**	-0.44 ± 0.69 -0.64 0.5284	-	0.45 ± 0.44 1.01 0.3203	0.70 ± 0.47 1.49 0.1482
N_{HU}	0.76 ± 0.34 2.26 **0.0331**	-0.89 ± 0.58 -1.53 0.1395	-0.45 ± 0.44 -1.01 0.3203	-	0.26 ± 0.29 0.89 0.3835
N_{CV}	0.51 ± 0.38 1.33 0.1950	-1.14 ± 0.60 -1.89 0.0704	-0.70 ± 0.47 -1.49 0.1482	-0.26 ± 0.29 -0.89 0.3835	-

Model Summary 25 | Contact core mud content (CCPCMud, %) by species treatment (Tcode)

Initial linear regression model:

lm(CCMud% ~ as.factor(Tcode))

No minimal adequate model, intercept only (Tcode, L-ratio = 4.273412, d.f. = 10, p = 0.3703).

Appendix 5

Statistical model summary

Summary of the statistical analyses for our 8 statistical models (Models S1 to S8). For each model, we list the initial linear regression model, the minimal adequate model with GLS estimation, and a summary of the coefficient table. The coefficients indicate the relative performance of each treatment level relative to the relevelled baseline (as indicated). Coefficients ± SE and t-values are presented alongside corresponding significance values (in parentheses). Abbreviations: HD, *Hediste diversicolor*; HU, *Hydrobia ulvae*; CV, *Corophium volutator*; Mix, 1:1:1 mix of HD, HU and CV; SPID, Species identity [HD, HU, CV, Mix]; CS, core shape [square or round].

Model Summary 1| Mean maximum mixed depth of particle reworking ($^{f\text{-}SPI}L_{mean}$, cm)

Initial linear regression model:

lm($^{f\text{-}SPI}L_{mean}$ ~ as.factor(SPID))

Minimal adequate model:

gls($^{f\text{-}SPI}L_{mean}$ ~ as.factor(SPID),
weights = varIdent(form = ~1|as.factor(SPID)), method = 'REML')

Coefficient Table

Intercept ± SE (when baseline is for HD): 0.866 ± 0.1607047, t = 5.388766, p = 0.0001.

	HD	HU	CV	Mix
HD	-	-0.50 ± 0.16 -3.07 **0.0073**	-0.58 ± 0.16 -3.55 **0.0027**	-0.30 ± 0.17 -1.77 0.0965
HU	0.50 ± 0.16 3.07 **0.0073**	-	-0.08 ± 0.04 -2.03 0.0592	0.20 ± 0.06 3.49 **0.0030**
CV	0.58 ± 0.16 3.55 **0.0027**	0.08 ± 0.04 2.03 0.0592	-	0.28 ± 0.06 4.76 **0.0002**
Mix	0.30 ± 0.17 1.77 0.0965	-0.20 ± 0.06 -3.49 **0.0030**	-0.28 ± 0.06 -4.76 **0.0002**	-

Model Summary 2 | Median maximum mixed depth of particle reworking ($^{f\text{-}SPI}L_{med}$, cm)

Initial linear regression model:

lm($^{f\text{-}SPI}L_{med}$ ~ as.factor(SPID))

Minimal adequate model:

gls($^{f\text{-}SPI}L_{med}$ ~ as.factor(SPID),

weights = varIdent(form = ~1|as.factor(SPID)), method = 'REML')

Coefficient Table

Intercept ± SE (when baseline is for HD): 0.260 ± 0.02167948, t = 11.992906, p = 0.0000.

	HD	HU	CV	Mix
HD	-	0.10 ± 0.04 2.77 **0.0136**	-0.03 ± 0.02 -1.15 0.2675	0.01 ± 0.03 0.22 0.8278
HU	-0.10 ± 0.04 -2.77 **0.0136**	-	-0.13 ± 0.03 -4.14 **0.0008**	-0.09 ± 0.03 -2.84 **0.0118**
CV	0.03 ± 0.02 1.15 0.2675	0.13 ± 0.03 4.14 **0.0008**	-	0.03 ± 0.02 1.72 0.1044
Mix	-0.01 ± 0.03 -0.22 0.8278	0.09 ± 0.03 2.84 **0.0118**	-0.03 ± 0.02 -1.72 0.1044	-

Model Summary 3 | Maximum mixed depth of particle reworking ($^{f\text{-}SPI}L_{max}$, cm)

Initial linear regression model:

lm($^{f\text{-}SPI}L_{max}$ ~ as.factor(SPID))

Minimal adequate model:

gls($^{f\text{-}SPI}L_{max}$ ~ as.factor(SPID),
weights = varIdent(form = ~1|as.factor(SPID)), method = 'REML')

Coefficient Table
Intercept ± SE (when baseline is for HD): 7.37668 ± 0.1667988, t = 44.22501, p = 0.0000.

	HD	HU	CV	Mix
HD	-	-5.83 ± 0.21 -27.19 **< 0.0001**	-5.40 ± 0.20 -27.66 **< 0.0001**	0.41 ± 0.19 2.17 **0.0454**
HU	5.83 ± 0.21 27.19 **< 0.0001**	-	0.43 ± 0.17 2.56 **0.0209**	6.24 ± 0.16 38.54 **< 0.0001**
CV	5.40 ± 0.20 27.66 **< 0.0001**	-0.43 ± 0.17 -2.56 **0.0209**	-	5.81 ± 0.14 42.89 **< 0.0001**
Mix	-0.41 ± 0.19 -2.17 **0.0454**	-6.24 ± 0.16 -38.54 **< 0.0001**	-5.81 ± 0.14 -42.89 **< 0.0001**	-

Model Summary 4 | Surface boundary roughness (SBR, cm)

Initial linear regression model:

lm(SBR ~ as.factor(SPID))

No minimal adequate model, intercept only (SPID, F = 0.3446, d.f. = 3, p = 0.7935).

Model Summary 5 | Maximum burrow depth ($^{CT}B_{max}$, cm)

Initial linear regression model:

lm($^{CT}B_{max}$ ~ as.factor(SPID))

Minimal adequate model:

lm($^{CT}B_{max}$ ~ as.factor(SPID))

Coefficient Table

Intercept ± SE (when baseline is for HD): 7.2020 ± 0.1505, t = 47.85, p = 0.0000.

	HD	HU	CV	Mix
HD	-	-4.54 ± 0.21 -21.32 **< 0.0001**	-5.09 ± 0.21 -23.93 **< 0.0001**	0.03 ± 0.21 0.16 0.0875
HU	4.54 ± 0.21 21.32 **< 0.0001**	-	-0.56 ± 0.21 -2.61 **0.0189**	4.57 ± 0.21 21.48 **< 0.0001**
CV	5.09 ± 0.21 23.93 **< 0.0001**	0.56 ± 0.21 2.61 **0.0189**	-	5.13 ± 0.21 24.09 **< 0.0001**
Mix	-0.03 ± 0.21 -0.16 0.0875	-4.57 ± 0.21 -21.48 **< 0.0001**	-5.13 ± 0.21 -24.09 **< 0.0001**	-

Model Summary 6 | Burrow surface area ($^{CT}B_{SA}$, cm^2)

Initial linear regression model:

lm($^{CT}B_{SA}$ ~ as.factor(SPID))

Minimal adequate model:

gls($^{CT}B_{SA}$ ~ as.factor(SPID),

weights = varIdent(form = ~1|as.factor(SPID)), method = 'REML')

Coefficient Table

Intercept ± SE (when baseline is for HD): 436.9088 ± 30.58431, t = 14.285389, p = 0.0000.

	HD	HU	CV	Mix
HD	-	-403.74 ± 30.93 -13.05 **< 0.0001**	-370.35 ± 31.37 -11.81 **< 0.0001**	-103.98 ± 42.17 -2.47 **0.0254**
HU	403.74 ± 30.93 13.05 **< 0.0001**	-	33.39 ± 8.36 3.99 **0.0010**	299.76 ± 29.40 10.20 **< 0.0001**
CV	370.35 ± 31.37 11.81 **< 0.0001**	-33.39 ± 8.36 -3.99 **0.0010**	-	266.37 ± 29.86 8.92 **< 0.0001**
Mix	103.98 ± 42.17 2.47 **0.0254**	-299.76 ± 29.40 -10.20 **< 0.0001**	-266.37 ± 29.86 -8.92 **< 0.0001**	-

Model Summary 7 | Burrow volume ($^{CT}B_{vol}$, cm^3)

Initial linear regression model:

lm($^{CT}B_{vol}$ ~ as.factor(SPID))

Minimal adequate model:

gls($^{CT}B_{vol}$ ~ as.factor(SPID),

weights = varIdent(form = ~1|as.factor(SPID)), method = 'REML')

Coefficient Table

Intercept ± SE (when baseline is for HD): 19.829278 ± 1.796173, t = 11.039737, p = 0.0000.

	HD	HU	CV	Mix
HD	-	-18.71 ± 1.08 -10.38 **< 0.0001**	-17.40 ± 1.86 -9.38 **< 0.0001**	-2.59 ± 2.28 -2.59 **0.0197**
HU	18.71 ± 1.08 10.38 **< 0.0001**	-	1.31 ± 0.49 2.65 **0.0174**	12.80 ± 1.42 9.03 **< 0.0001**
CV	17.40 ± 1.86 9.38 **< 0.0001**	-1.31 ± 0.49 -2.65 **0.0174**	-	11.49 ± 1.48 7.74 **< 0.0001**
Mix	2.59 ± 2.28 2.59 **0.0197**	-12.80 ± 1.42 -9.03 **< 0.0001**	-11.49 ± 1.48 -7.74 **< 0.0001**	-

Model Summary 8 | Bioirrigation ($\Delta[Br^-]$, mg L^{-1})

Initial linear regression model:

lm($\Delta[Br^-]$ ~ as.factor(SPID)* as.factor(CS))

Minimal adequate model:

gls($\Delta[Br^-]$ ~ as.factor(SPID) + as.factor(CS),
weights = varIdent(form = ~ 1|as.factor(SPID) * as.factor(CS)),
method = 'REML')

Coefficient Tables

Intercept ± SE (when baseline is for HD in square cores): -321.8755 ± 43.33559, t = -7.427508, p = 0.0000. Core shape (CS) is denoted by subscripted text (circ = circular, sq = square).

	HD	HU	CV	Mix
HD	-	139.89 ± 53.03 2.64 **0.0124**	103.37 ± 53.16 -1.94 0.0599	126.97 ± 45.27 2.80 **0.0082**
HU	-139.89 ± 53.03 -2.64 **0.0124**	-	-36.52 ± 49.41 -0.74 0.4647	-12.93 ± 35.25 -0.37 0.7160
CV	-103.37 ± 53.16 -1.94 0.0599	36.52 ± 49.41 0.74 0.4647	-	23.59 ± 40.98 0.58 0.5684
Mix	-126.96 ± 45.27 -2.80 **0.0082**	12.93 ± 35.25 0.37 0.7160	23.59 ± 40.98 0.58 0.5684	-

	CS_{sq}	CS_{circ}
CS_{sq}	-	-325.20 ± 41.88 -7.77 **< 0.0001**
CS_{circ}	325.20 ± 41.88 7.77 **< 0.0001**	-

Additional computed tomography images

Transverse core slices (n = 5) taken at 0.5 cm below the sediment-water interface for (a) *Hediste diversicolor*, (b) *Hydrobia ulvae*, (c) *Corophium volutator*, and (d) in species mixture. All cores are 10 cm in diameter. Burrows appear as darker grey values. In (b) and (d), the detail (e.g. aperture, whorls and apex) of *H. ulvae* shells can be seen (white pixel values).

(a)

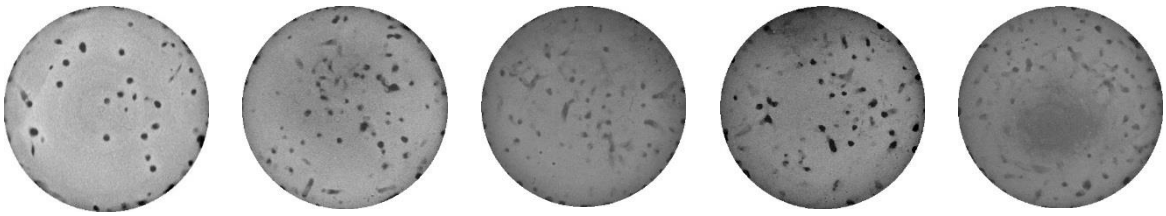

(b)

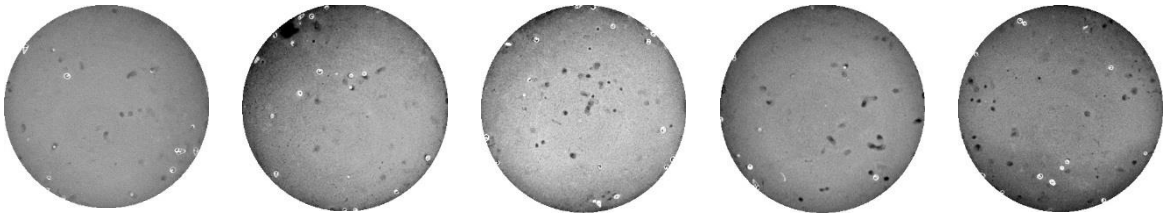

(c)

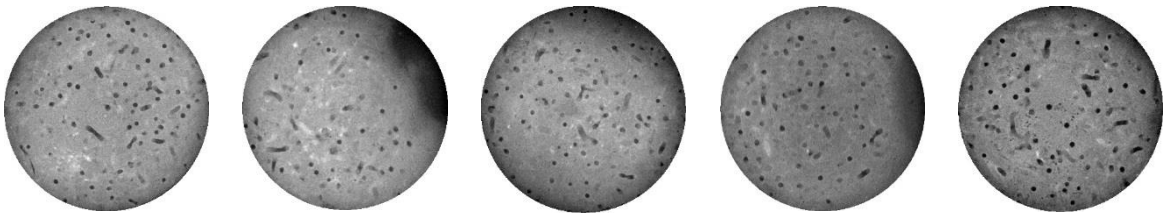

(d)

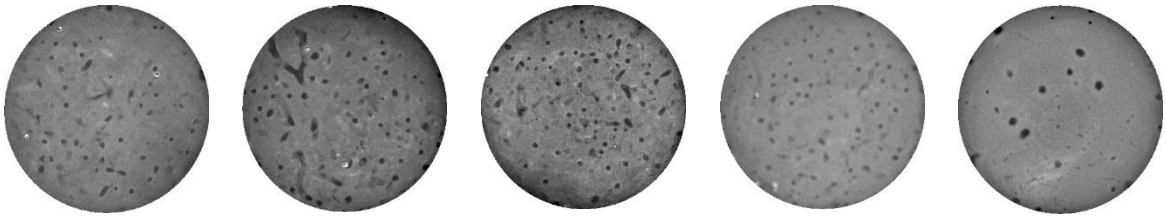

Coronal core slices (n = 5) for (a) *Hediste diversicolor*, (b) *Hydrobia ulvae*, (c) *Corophium volutator*, and (d) in species mixture. Burrows appear as darker grey values. In (b) and (d), the detail (e.g. aperture, whorls and apex) of *H. ulvae* shells can be seen (white pixel values). The sediment-water interface is at the top of the region of interest. Images are cropped immediately below the vertical extent of burrowing. All cores are 10 cm in diameter.

(a)

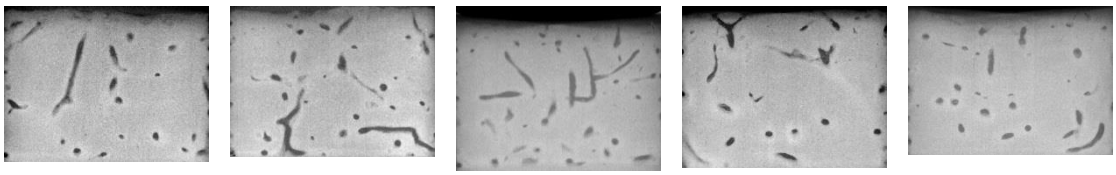

(b)

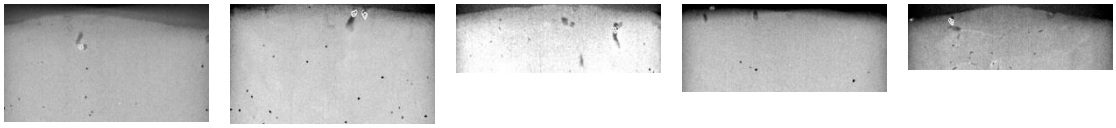

(c)

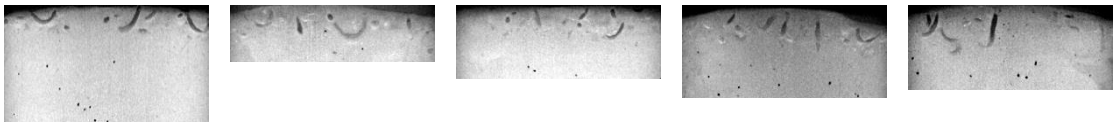

(d)

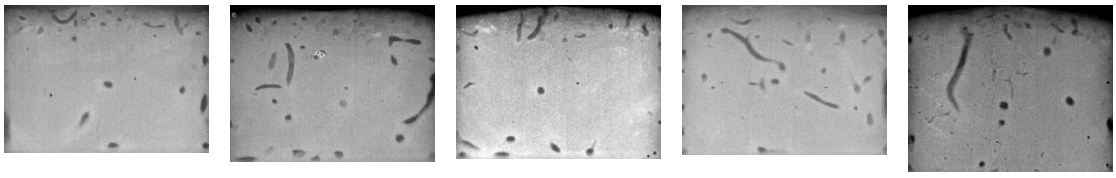

Reconstructed three-dimensional burrow models (n = 5) for (a) *Hediste diversicolor*, (b) *Hydrobia ulvae*, (c) *Corophium volutator*, and (d) in species mixture. In (b) and (d), *H. ulvae* shells can be seen (lighter pixel values). The sediment-water interface is at the top of the region of interest. Images are cropped immediately below the vertical extent of burrowing. All cores are 10 cm in diameter. All cores are 10 cm in diameter.

(a)

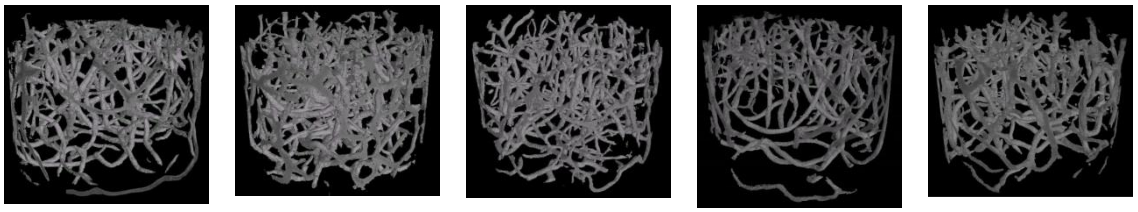

(b)

(c)

(d)

References

Allen, D. C., and C. C. Vaughn. 2011. Density-dependent biodiversity effects on physical habitat modification by freshwater bivalves. Ecology **92**:1013-1019.

Alongi, D. M. 1985. Effect of physical disturbance on population-dynamics and trophic interactions among microbes and meiofauna. Journal of Marine Research **43**:351-364.

Amos, C. L., M. Brylinsky, T. F. Sutherland, D. O'Brien, S. Lee, and A. Cramp. 1998. The stability of a mudflat in the Humber Estuary, South Yorkshire, UK.*in* K. S. Black, D. M. Paterson, and A. Cramp, editors. Sedimentary Processes in the Intertidal Zone. Geological Society, London, UK.

Amos, C. L., G. R. Daborn, H. A. Christian, A. Atkinson, and A. Robertson. 1992. *In situ* erosion measurements on fine-grained sediments from the bay of fundy. Marine Geology **108**:175-196.

Amos, C. L., T. Feeney, T. F. Sutherland, and J. L. Luternauer. 1997. The stability of fine-grained sediments from the Fraser River delta. Estuarine Coastal and Shelf Science **45**:507-524.

Andersen, T. J. 2001. Seasonal variation in erodibility of two temperate, microtidal mudflats. Estuarine Coastal and Shelf Science **53**:1-12.

Anderson, A. 1971. Intertidal activity, breeding and floating habit of *Hydrobia ulvae* in Ythan Estuary. Journal of the Marine Biological Association of the United Kingdom **51**:423-&.

Anderson, F. E., and L. F. Black. 1980. A method for sampling fine-grained surface sediments in inter-tidal areas. Journal of Sedimentary Petrology **50**:637-638.

Arkema, K. K., G. Guannel, G. Verutes, S. A. Wood, A. Guerry, M. Ruckelshaus, P. Kareiva, M. Lacayo, and J. M. Silver. 2013. Coastal habitats shield people and property from sea-level rise and storms. Nature Climate Change **advance online publication**.

Arroyo, N. L., K. Aarnio, and E. Bonsdorff. 2006. Drifting algae as a means of re-colonizing defaunated sediments in the Baltic Sea. A short-term microcosm study. Hydrobiologia **554**:83-95.

Asmus, R. M., and H. Asmus. 1991. Mussel beds - Limiting or promoting phytoplankton. Journal of Experimental Marine Biology and Ecology **148**:215-232.

Austen, I., T. J. Andersen, and K. Edelvang. 1999. The influence of benthic diatoms and invertebrates on the erodibility of an intertidal mudflat, the Danish Wadden Sea. Estuarine, Coastal and Shelf Science **49**:99-111.

Austen, M. C., P. J. D. Lambshead, P. A. Hutchings, G. Boucher, P. V. R. Snelgrove, C. Heip, G. King, I. Koike, and C. Smith. 2002. Biodiversity links above and below the marine sediment-water interface that may influence community stability. Biodiversity and Conservation **11**:113-136.

Austen, M. C., and S. Widdicombe. 1998. Experimental evidence of effects of the heart urchin *Brissopsis lyrifera* on associated subtidal meiobenthic nematode communities. Journal of Experimental Marine Biology and Ecology **222**:219-238.

Baban, S. M. J. 1997. Environmental monitoring of estuaries estimating and mapping various environmental indicators in Breydon Water Estuary, UK, using Landsat TM imagery. Estuarine Coastal and Shelf Science **44**:589-598.

Bale, A. J., J. A. Stephens, and C. B. Harris. 2007. Critical erosion profiles in macro-tidal estuary sediments: Implications for the stability of intertidal mud and the slope of mud banks. Continental Shelf Research **27**:2303-2312.

Barbier, E. B., I. Y. Georgiou, B. Enchelmeyer, and D. J. Reed. 2013. The value of wetlands in protecting southeast Louisiana from hurricane storm surges. Plos One **8**.

Barnes, R. S. K. 1981. Behavioural activities and ecological strategies in the intertidal gastropod *Hydrobia ulvae*. Pages 79-90 *in* N. V. Jones and W. J. Wolff, editors. Feeding and Survival Strategies of Estuarine Organisms. Springer US, New York.

Barnes, R. S. K. 1994. The Brackish-Water Fauna of Northwestern Europe. Cambridge University Press, Cambridge.

Barnes, R. S. K. 2005. Interspecific competition and rarity in mudsnails: feeding interactions between and within *Hydrobia acuta neglecta* and sympatric *Hydrobia* species. Aquatic Conservation-Marine and Freshwater Ecosystems **15**:485-493.

Baumgartner, S. 2007. The insurance value of biodiversity in the provision of ecosystem services. Natural Resource Modeling **20**:87-127.

Bell, S. S., and D. J. Devlin. 1983. Short-term macrofaunal recolonization of sediment and epibenthic habitats in Tampa Bay, florida. Bulletin of Marine Science **33**:102-108.

Bender, K., and W. R. Davis. 1984. The effect of feeding by *Yoldia limatula* on bioturbation. Ophelia **23**:91-100.

Berge, J. A. 1990. Macrofauna recolonization on defaunated sediment contaminated with crude-oil in 2 Norwegian fjords with unequal eutrophication status, 1. Community responses. Marine Ecology Progress Series **66**:103-115.

Berlamont, J., M. Ockenden, E. Toorman, and J. Winterwerp. 1993. The characterisation of cohesive sediment properties. Coastal Engineering **21**:105-128.

Beukema, J. J., E. C. Flach, R. Dekker, and M. Starink. 1999. A long-term study of the recovery of the macrozoobenthos on large defaunated plots on a tidal flat in the Wadden Sea. Journal of Sea Research **42**:235-254.

Biles, C. L., D. M. Paterson, R. B. Ford, M. Solan, and D. G. Raffaelli. 2002. Bioturbation, ecosystem functioning and community structure. Hydrology and Earth System Sciences **6**:999-1005.

Biles, C. L., M. Solan, I. Isaksson, D. M. Paterson, C. Emes, and D. G. Raffaelli. 2003. Flow modifies the effect of biodiversity on ecosystem functioning: an *in situ* study of estuarine sediments. Journal of Experimental Marine Biology and Ecology **285**:165-177.

Black, K. S., H. Y. Sun, G. Craig, D. M. Paterson, J. Watson, and T. Tolhurst. 2001. Incipient erosion of biostabilized sediments examined using particle-field optical holography. Environmental Science & Technology **35**:2275-2281.

Black, K. S., T. J. Tolhurst, D. M. Paterson, and S. E. Hagerthey. 2002. Working with natural cohesive sediments. Journal of Hydraulic Engineering-Asce **128**:2-8.

Blanchard, G. F., T. Agion, J.-M. Guarini, O. Herlory, and P. Richard. 2003. Analysis of the short-term dynamics of microphytobenthos biomass on intertidal mudflats. Pages 85-98 *in* Functioning of micrphytobenthos in estuaries. Royal Netherlands Academy of Arts and Sciences, Amsterdam.

Blanchard, G. F., J. M. Guarini, L. Provot, P. Richard, and P. G. Sauriau. 2000. Measurement of ingestion rate of *Hydrobia ulvae* (Pennant) on intertidal epipelic microalgae: the effect of mud snail density. Journal of Experimental Marine Biology and Ecology **255**:247-260.

Blanchard, G. F., P. G. Sauriau, V. C. L. Gall, D. Gouleau, M. J. Garet, and F. Olivier. 1997. Kinetics of tidal resuspension of microbiota: Testing the effects of sediment cohesiveness and bioturbation using flume experiments. Marine Ecology Progress Series **151**:17-25.

Blott, S. J., and K. Pye. 2001. GRADISTAT: A grain size distribution and statistics package for the analysis of unconsolidated sediments. Earth Surface Processes and Landforms **26**:1237-1248.

Bolam, S. G., T. F. Fernandes, and M. Huxham. 2002. Diversity, biomass, and ecosystem processes in the marine benthos. Ecological Monographs **72**:599-615.

Bolam, S. G., P. Whomersley, and M. Schratzberger. 2004. Macrofaunal recolonization on intertidal mudflats: effect of sediment organic and sand content. Journal of Experimental Marine Biology and Ecology **306**:157-180.

Bonsdorff, E., J. Mattila, C. Ronn, and C. S. Osterman. 1986. Multidimensional interactions in shallow soft-bottom ecosystems - testing the competitive-exclusion principle. Ophelia:37-44.

Boogert, N. J., D. M. Paterson, and K. N. Laland. 2006. The implications of niche construction and ecosystem engineering for conservation biology. Bioscience **56**:570-578.

Bostrom, C., and E. Bonsdorff. 2000. Zoobenthic community establishment and habitat complexity - the importance of seagrass shoot-density, morphology and physical disturbance for faunal recruitment. Marine Ecology Progress Series **205**:123-138.

Bottjer, D. J. 2010. The Cambrian substrate revolution and early evolution of the phyla. Journal of Earth Science **21**:21-24.

Bottjer, D. J., J. W. Hagadorn, and S. Q. Dornbos. 2000. The Cambrian substrate revolution. GSA Today **10**:1-7.

Braeckman, U., P. Provoost, B. Gribsholt, D. Van Gansbeke, J. J. Middelburg, K. Soetaert, M. Vincx, and J. Vanaverbeke. 2010. Role of macrofauna functional traits and density in biogeochemical fluxes and bioturbation. Marine Ecology Progress Series **399**:173-186.

Bruno, J. F., K. E. Boyer, J. E. Duffy, S. C. Lee, and J. S. Kertesz. 2005. Effects of macroalgal species identity and richness on primary production in benthic marine communities. Ecology Letters **8**(11):1165-1174.

Budd, G. 2008. *Hediste diversicolor*. Ragworm. Marine life information network: Biology and sensitivity key information sub-programme.*in* P. M. B. A. o. t. U. Kingdom, editor., http://www.marlin.ac.uk/speciesfullreview.php?speciesID=3470.

Bulling, M., M. Solan, K. Dyson, G. Hernandez-Milian, P. Luque, G. Pierce, D. Raffaelli, D. Paterson, and P. White. 2008. Species effects on ecosystem processes are modified by faunal responses to habitat composition. Oecologia **158**:511-520.

Button, K. S., J. P. A. Ioannidis, C. Mokrysz, B. A. Nosek, J. Flint, E. S. J. Robinson, and M. R. Munafo. 2013. Power failure: why small sample size undermines the reliability of neuroscience. Nature Reviews Neuroscience **14**:365-376.

Caldeira, K., and M. E. Wickett. 2003. Anthropogenic carbon and ocean pH. Nature **425**:365-365.

Cardinale, B. J. 2011. Biodiversity improves water quality through niche partitioning. Nature **472**:86-U113.

Carey, D. A. 1983. Particle resuspension in the benthic boundary-layer induced by flow around polychaete tubes. Canadian Journal of Fisheries and Aquatic Sciences **40**:301-308.

Chandler, G. T., and J. W. Fleeger. 1983. Meiofaunal colonization of azoic estuarine sediment in Louisiana - Mechanisms of dispersal. Journal of Experimental Marine Biology and Ecology **69**:175-188.

Chapin, F. S., E. S. Zavaleta, V. T. Eviner, R. L. Naylor, P. M. Vitousek, H. L. Reynolds, D. U. Hooper, S. Lavorel, O. E. Sala, S. E. Hobbie, M. C. Mack, and S. Diaz. 2000. Consequences of changing biodiversity. Nature **405**:234-242.

Chapman, M. G., and T. J. Tolhurst. 2007. Relationships between benthic macrofauna and biogeochemical properties of sediments at different spatial scales and among different habitats in mangrove forests. Journal of Experimental Marine Biology and Ecology **343**:96-109.

Chapman, M. G., T. J. Tolhurst, R. J. Murphy, and A. J. Underwood. 2010. Complex and inconsistent patterns of variation in benthos, micro-algae and sediment over multiple spatial scales. Marine Ecology Progress Series **398**:33-47.

Christensen, B., A. Vedel, and E. Kristensen. 2000. Carbon and nitrogen fluxes in sediment inhabited by suspension-feeding (*Nereis diversicolor*) and non-suspension-feeding (*N-virens*) polychaetes. Marine Ecology Progress Series **192**:203-217.

Christiansen, T., P. L. Wiberg, and T. G. Milligan. 2000. Flow and sediment transport on a tidal salt marsh surface. Estuarine Coastal and Shelf Science **50**:315-331.

Ciutat, A., J. Widdows, and J. W. Readman. 2006. Influence of cockle *Cerastoderma edule* bioturbation and tidal-current cycles on resuspension of sediment and polycyclic aromatic hydrocarbons. Marine Ecology Progress Series **328**:51-64.

Commito, J. A. 1982. Importance of predation by infaunal polychaetes in controlling the structure of a soft-bottom community in Maine, USA. Marine Biology **68**:77-81.

Condit, R., S. P. Hubbell, and R. B. Foster. 1996. Changes in tree species abundance in a neotropical forest: Impact of climate change. Journal of Tropical Ecology **12**:231-256.

Consalvey, M., B. Jesus, R. G. Perkins, V. Brotas, G. J. C. Underwood, and D. M. Paterson. 2004a. Monitoring migration and measuring biomass in benthic biofilms: the effects of dark/far-red adaptation and vertical migration on fluorescence measurements. Photosynthesis Research **81**:91-101.

Consalvey, M., D. M. Paterson, and G. J. C. Underwood. 2004b. The ups and downs of life in a benthic biofilm: Migration of benthic diatoms. Diatom Research **19**:181-202.

Costa, P., R. F. Oliveira, and L. C. D. Fonseca. 2006. Feeding ecology of *Nereis diversicolor* (OF Müller)(Annelida, Polychaeta) on estuarine and lagoon environments in the southwest coast of Portugal. Pan-American Journal of Aquatic Sciences **1**:104-113.

Costanza, R., R. dArge, R. deGroot, S. Farber, M. Grasso, B. Hannon, K. Limburg, S. Naeem, R. V. ONeill, J. Paruelo, R. G. Raskin, P. Sutton, and M. vandenBelt. 1997. The value of the world's ecosystem services and natural capital. Nature **387**:253-260.

Countryside Access. 2013. Norfolk long distance paths. http://www.countrysideaccess.norfolk.gov.uk/walk.aspx?section=1&id=71.

Covich, A. P., M. C. Austen, F. Barlocher, E. Chauvet, B. J. Cardinale, C. L. Biles, P. Inchausti, O. Dangles, M. Solan, M. O. Gessner, B. Statzner, and B. Moss. 2004. The role of biodiversity in the functioning of freshwater and marine benthic ecosystems. Bioscience **54**:767-775.

Croel, R. C., and J. M. Kneitel. 2011. Ecosystem-level effects of bioturbation by the tadpole shrimp *Lepidurus packardi* in temporary pond mesocosms. Hydrobiologia **665**:169-181.

Crooks, S., and R. K. Turner. 1999. Integrated coastal management: Sustaining estuarine natural resources. Advances in Ecological Research **29**:241-289.

Crowe, W. A., A. B. Josefson, and I. Svane. 1987. Influence of adult density on recruitment into soft sediments - A short-term *in situ* sublittoral experiment. Marine Ecology Progress Series **41**:61-69.

Daborn, G. R., C. L. Amos, M. Brylinsky, H. Christian, G. Drapeau, R. W. Faas, J. Grant, B. Long, D. M. Paterson, G. M. E. Perillo, and M. C. Piccolo. 1993. An ecological cascade effect - Migratory birds affect stability of intertidal sediments. Limnology and Oceanography **38**:225-231.

Dade, W. B., J. D. Davis, P. D. Nichols, A. R. M. Nowell, D. Thistle, M. B. Trexler, and D. C. White. 1990. Effects of bacterial exopolymer adhesion on the entrainment of sand. Geomicrobiology Journal **8**:1-16.

Dade, W. B., A. R. M. Nowell, and P. A. Jumars. 1992. Predicting erosion resistance of muds. Marine Geology **105**:285-297.

Daniel, O., A. Kretzschmar, Y. Capowiez, L. Kohli, and J. Zeyer. 1997. Computer-assisted tomography of macroporosity and its application to study the activity of the earthworm *Aporrectodea nocturna*. European Journal of Soil Science **48**:727-737.

Davidson, I. C., A. C. Crook, and D. K. A. Barnes. 2004. Quantifying spatial patterns of intertidal biodiversity: Is movement important? Marine Ecology-Pubblicazioni Della Stazione Zoologica Di Napoli I **25**:15-34.

Davis, M. B., and R. G. Shaw. 2001. Range shifts and adaptive responses to Quaternary climate change. Science **292**:673-679.

Davis, M. W., and H. Lee. 1983. Recolonization of sediment-associated microalgae and effects of estuarine infauna on microalgal production. Marine Ecology Progress Series **11**:227-232.

Davis, W. R. 1993. The role of bioturbation in sediment resuspension and its interaction with physical shearing. Journal of Experimental Marine Biology and Ecology **171**:187-200.

De Backer, A., F. Van Coillie, F. Montserrat, P. Provoost, C. Van Colen, M. Vincx, and S. Degraer. 2011. Bioturbation effects of *Corophium volutator*: Importance of density and behavioural activity. Estuarine Coastal and Shelf Science **91**:306-313.

de Brouwer, J. F. C., S. Bjelic, E. M. G. T. de Deckere, and L. J. Stal. 2000. Interplay between biology and sedimentology in a mudflat (Biezelingse Ham, Westerschelde, The Netherlands). Continental Shelf Research **20**:1159-1177.

de Brouwer, J. F. C., T. R. Neu, and L. J. Stal. 2003. On the function of secretion of extracellular polymeric substances by benthic diatoms and their role in intertidal mudflats: A review

of recent insights and views. Pages 45-64 *in* Functioning of Microphytobenthos in Estuaries. Royal Netherlands Academy of Arts and Sciences, Amsterdam.

de Brouwer, J. F. C., and L. J. Stal. 2002. Daily fluctuations of exopolymers in cultures of the benthic diatoms *Cylindrotheca closterium* and *Nitzschia* sp. (Bacillariophyceae). Journal of Phycology **38**:464-472.

de Deckere, E. M. G. T., B. A. Kornman, N. Staats, G. R. Termaat, B. de Winder, L. J. Stal, and C. H. R. Heip. 2002. The seasonal dynamics of benthic (micro) organisms and extracellular carbohydrates in an Intertidal mudflat and their effect on the concentration of suspended sediment. Fine Sediment Dynamics in the Marine Environment **5**:429-440.

de Deckere, E. M. G. T., T. J. Tolhurst, and J. F. C. de Brouwer. 2001. Destabilization of cohesive intertidal sediments by infauna. Estuarine Coastal and Shelf Science **53**:665-669.

de Deckere, E. M. G. T., J. van de Koppel, and C. H. R. Heip. 2000. The influence of *Corophium volutator* abundance on resuspension. Hydrobiologia **426**:37-42.

De Jonge, V. N., and J. Van Den Berg. 1987. Experiments on the resuspension of estuarine sediments containing benthic diatoms. Estuarine and Coastal Shelf Science **24**:725-740.

Decho, A. W. 2000. Microbial biofilms in intertidal systems: an overview. Continental Shelf Research **20**:1257-1273.

Defew, E. C., T. J. Tolhurst, and D. M. Paterson. 2002. Site-specific features influence sediment stability of intertidal flats. Hydrology and Earth System Sciences **6**:971-981.

Delgado, M., V. N. Dejonge, and H. Peletier. 1991. Experiments on resuspension of natural microphytobenthos populations. Marine Biology **108**:321-328.

Diaz, R. J., and G. R. Cutter. 2001. *In situ* measurement of organism-sediment interaction: Rates of burrow formation, abandonment and sediment oxidation, reduction. Organism-Sediment Interactions:19-32.

Diaz, S., J. Fargione, F. S. Chapin, and D. Tilman. 2006. Biodiversity loss threatens human well-being. Plos Biology **4**:1300-1305.

Diggle, P. J., P. Heagerty, K. Y. Liang, and S. L. Zeger. 2002. Analysis of Longitudinal Data. Oxford University Press, Oxford, UK.

Dornbos, S. Q., D. J. Bottjer, and J. Y. Chen. 2005. Paleoecology of benthic metazoans in the Early Cambrian Maotianshan Shale biota and the Middle Cambrian Burgess Shale biota: evidence for the Cambrian substrate revolution. Palaeogeography Palaeoclimatology Palaeoecology **220**:47-67.

Dubois, J. 1956. Un cas de presentation primitive de la face. Presse Medicale **64**:96-96.

Dufour, S. C., G. Desrosiers, B. Long, P. Lajeunesse, M. Gagnoud, J. Labrie, P. Archambault, and G. Stora. 2005. A new method for three-dimensional visualization and quantification of biogenic structures in aquatic sediments using axial tomodensitometry. Limnology and Oceanography-Methods **3**:372-380.

Duncan, E. 2013. All creatures great and small. The Economist. The Economist Group.

Duport, E., G. Stora, P. Tremblay, and F. Gilbert. 2006. Effects of population density on the sediment mixing induced by the gallery-diffusor *Hediste* (*Nereis*) *diversicolor* O.F. Muller, 1776. Journal of Experimental Marine Biology and Ecology **336**:33-41.

Dyson, K. E., M. T. Bulling, M. Solan, G. Hernandez-Milian, D. G. Raffaelli, P. C. L. White, and D. M. Paterson. 2007. Influence of macrofaunal assemblages and environmental heterogeneity on microphytobenthic production in experimental systems. Proceedings of the Royal Society B-Biological Sciences **274**:2547-2554.

Eckman, J. E., and A. R. M. Nowell. 1984. Boundary skin friction and sediment transport about an animal-tube mimic. Sedimentology **31**:851-862.

Eckman, J. E., A. R. M. Nowell, and P. A. Jumars. 1981. Sediment destabilization by animal tubes. Journal of Marine Research **39**:361-374.

Edgar, L. A., and J. D. Pickettheaps. 1984. Valve morphogenesis in the pennate diatom *Navicula cuspidata*. Journal of Phycology **20**:47-61.

Eggert, A., N. Haubner, S. Klausch, U. Karsten, and R. Schumann. 2006. Quantification of algal biofilms colonising building materials: chlorophyll *a* measured by PAM-fluorometry as a biomass parameter. Biofouling **22**:79-90.

Ehrlich, P. R., and A. H. Ehrlich. 1981. Extinction: The Causes and Consequenes of the Disappearance of Species. Random House, New York, US.

Emmerson, M. C., M. Solan, C. Emes, D. M. Paterson, and D. Raffaelli. 2001. Consistent patterns and the idiosyncratic effects of biodiversity in marine ecosystems. Nature **411**:73-77.

Engelsen, A., and L. Pihl. 2008. Grazing effects by *Nereis diversicolor* on development and growth of green algal mats. Journal of Sea Research **59**:228-236.

Escapa, M., G. M. E. Perillo, and O. Iribarne. 2008. Sediment dynamics modulated by burrowing crab activities in contrasting SW Atlantic intertidal habitats. Estuarine Coastal and Shelf Science **80**:365-373.

Esnault, G., C. Retiere, and R. Lambert. 1990. Food resource partitioning in a population of *Nereis diversicolor* (Annelida, Polychaeta) under experimental conditions. Pages 453-476 *in* M. Barnes and R. N. Gibson, editors. Trophic relationships in the marine environment. Proceedings of the 24th European Marine Biology Symposium, Oban, United Kingdom. Aberdeen University Press, Aberdeen.

Fager, E. W. 1964. Marine sediments - Effects of tube-building polychaete. Science **143**:356-&.

Faraco, L. F. D., and P. D. Lana. 2003. Response of polychaetes to oil spills in natural and defaunated subtropical mangrove sediments from Paranagua bay (SE Brazil). Hydrobiologia **496**:321-328.

Fargione, J., C. S. Brown, and D. Tilman. 2003. Community assembly and invasion: An experimental test of neutral versus niche processes. Proceedings of the National Academy of Sciences of the United States of America **100**:8916-8920.

Fauchald, J., and P. A. Jumars. 1979. The diet of worms: a study of polychaete feedings guilds. Oceanography and Marine Biology: An Annual Review **17**:193-284.

Feely, R. A., C. L. Sabine, K. Lee, W. Berelson, J. Kleypas, V. J. Fabry, and F. J. Millero. 2004. Impact of anthropogenic CO_2 on the $CaCO_3$ system in the oceans. Science **305**:362-366.

Fegley, S. R. 1988. A comparison of meiofaunal settlement onto the sediment surface and recolonization of defaunated sandy sediment. Journal of Experimental Marine Biology and Ecology **123**:97-113.

Fenchel, T., L. H. Kofoed, and A. Lappalainen. 1975. Particle size selection of 2 deposit feeders - Amphipod *Corophium volutator* and Prosobranch *Hydrobia ulvae*. Marine Biology **30**:119-128.

Filho Negrello, O. A., A. J. Underwood, and M. G. Chapman. 2006. Recolonization of infauna on a tidal flat: An experimental analysis of modes of dispersal. Journal of Experimental Marine Biology and Ecology **328**:240-250.

Finke, D. L., and W. E. Snyder. 2008. Niche partitioning increases resource exploitation by diverse communities. Science **321**:1488-1490.

Flemer, D. A., J. R. Clark, R. S. Stanley, C. M. Bundrick, and G. R. Plaia. 1993. The importance of physical scaling factors to benthic marine invertebrate recolonization of laboratory microcosms. International Journal of Environmental Studies **44**:161-179.

Flemer, D. A., B. F. Ruth, and C. M. Bundrick. 2002. Effects of sediment type on macrobenthic infaunal colonization of laboratory microcosms. Hydrobiologia **485**:83-96.

Flemming, B. W., and M. T. Delafontaine. 2000. Mass physical properties of muddy intertidal sediments: some applications, misapplications and non-applications. Continental Shelf Research **20**:1179-1197.

Flint, R. W., and R. D. Kalke. 1986. Biological enhancement of estuarine benthic community structure. Marine Ecology Progress Series **31**:23-33.

Ford, R. B., S. F. Thrush, and P. K. Probert. 1999. Macrobenthic colonisation of disturbances on an intertidal sandflat: the influence of season and buried algae. Marine Ecology Progress Series **191**:163-174.

Frey, R. W., and P. B. Basan. 1985. Coastal salt marshes.*in* R. A. Davis, editor. Coastal Sedimentary Environments. Springer, New York, USA.

Fridley, J. D. 2001. The influence of species diversity on ecosystem productivity: How, where, and why? Oikos **93**:514-526.

Friend, P. L., P. Ciavola, S. Cappucci, and R. Santos. 2003a. Bio-dependent bed parameters as a proxy tool for sediment stability in mixed habitat intertidal areas. Continental Shelf Research **23**:1899-1917.

Friend, P. L., M. B. Collins, and P. M. Holligan. 2003b. Day-night variation of intertidal flat sediment properties in relation to sediment stability. Estuarine Coastal and Shelf Science **58**:663-675.

Frithsen, J. B., and P. H. Doering. 1986. Active enhancement of particle removal from the water column by tentaculate benthic polychaetes. Ophelia **25**:169-182.

Gall, V. C. L., and G. F. Blanchard. 1995. Monthly HPLC Measurements of Pigment Concentration from an Intertidal Muddy Sediment of Marennes-Oleron Bay, France. Marine Ecology Progress Series **121**:171-179.

Gallagher, E. D., P. A. Jumars, and D. D. Trueblood. 1983. Facilitation of soft-bottom benthic succession by tube builders. Ecology **64**:1200-1216.

Gamenick, I., A. Jahn, K. Vopel, and O. Giere. 1996. Hypoxia and sulphide as structuring factors in a macrozoobenthic community on the Baltic Sea shore: Colonisation studies and tolerance experiments. Marine Ecology Progress Series **144**:73-85.

Geider, R. J., T. Platt, and J. A. Raven. 1986. Size dependence of growth and photosynthesis in diatoms - A synthesis. Marine Ecology Progress Series **30**:93-104.

Gerdol, V., and R. G. Hughes. 1994. Feeding-behavior and diet of *Corophium volutator* in an estuary in southeastern England. Marine Ecology Progress Series **114**:103-108.

Gerino, M., and G. Stora. 1991. *In vitro* quantitative-analysis of the bioturbation induced by the polychaete *Nereis diversicolor*. Comptes Rendus De L'Academie Des Sciences Serie III-Sciences De La Vie-Life Sciences **313**:489-494.

Gilbert, F., G. Stora, and J. C. Bertrand. 1996. *In situ* bioturbation and hydrocarbon fate in an experimental contaminated Mediterranean coastal ecosystem. Chemosphere **33**:1449-1458.

Godbold, J. A., M. Solan, and K. Killham. 2009. Consumer and resource diversity effects on marine macroalgal decomposition. Oikos **118**:77-86.

Gooday, A. J. 2002. Biological responses to seasonally varying fluxes of organic matter to the ocean floor: A review. Journal of Oceanography **58**:305-332.

Graf, G., and R. Rosenberg. 1997. Bioresuspension and biodeposition: A review. Journal of Marine Systems **11**:269-278.

Grant, J. 1988. Intertidal bedforms, sediment transport, and stabilization by benthic macroalgae.*in* P. L. Deboer, A. Van Gelder, and N. D. Nio, editors. Tide-Influenced Sedimentary Environments and Facies. D. Reidel, Amsterdam, Netherlands.

Grant, J., and U. V. Bathmann. 1987. Swept away - resuspension of bacterial mats regulates benthic-pelagic exchange of sulfur. Science **236**:1472-1474.

Grant, J., and G. Daborn. 1994. The effects of bioturbation on sediment transport on an intertidal mudflat. Netherlands Journal of Sea Research **32**:63-72.

Green, J. 1968. Biology of Estuarine Animals. University of Washington Press, Seattle, Washington, US.

Griffin, J. N., K. L. De la Haye, S. J. Hawkins, R. C. Thompson, and S. R. Jenkins. 2008. Predator diversity and ecosystem functioning: Density modifies the effect of resource partitioning. Ecology **89**:298-305.

Griffin, J. N., V. Mendez, A. F. Johnson, S. R. Jenkins, and A. Foggo. 2009. Functional diversity predicts overyielding effect of species combination on primary productivity. Oikos **118**:37-44.

Grigulis, K., S. Lavorel, I. D. Davies, A. Dossantos, F. Lloret, and M. Vila. 2005. Landscape-scale positive feedbacks between fire and expansion of the large tussock grass, *Ampelodesmos mauritanica* in Catalan shrublands. Global Change Biology **11**:1042-1053.

Gross, K., and B. J. Cardinale. 2005. The functional consequences of random vs. ordered species extinctions. Ecology Letters **8**:409-418.

Guerra-Garcia, J. M., and J. C. Garcia-Gomez. 2006. Recolonization of defaunated sediments: Fine versus gross sand and dredging versus experimental trays. Estuarine Coastal and Shelf Science **68**:328-342.

Guerra-Garcia, J. M., and J. C. Garcia-Gomez. 2009. Recolonization of macrofauna in unpolluted sands placed in a polluted yachting harbour: A field approach using experimental trays. Estuarine Coastal and Shelf Science **81**:49-58.

Gust, G., and M. J. Morris. 1989. Erosion thresholds and entrainment rates of undisturbed *in situ* sediments. Journal of Coastal Research **5**:87-99.

Hagerthey, S. E., E. C. Defew, and D. M. Paterson. 2002. Influence of *Corophium volutator* and *Hydrobia ulvae* on intertidal benthic diatom assemblages under different nutrient and temperature regimes. Marine Ecology Progress Series **245**:47-59.

Hale, R., P. Calosi, L. McNeill, N. Mieszkowska, and S. Widdicombe. 2011. Predicted levels of future ocean acidification and temperature rise could alter community structure and biodiversity in marine benthic communities. Oikos **120**:661-674.

Hall, J. A., and C. L. J. Frid. 1997. Colonisation patterns of adult macrobenthos in a polluted North Sea estuary. Aquatic Ecology **31**:333-340.

Hall, S. J., D. Raffaelli, and W. R. Turrell. 1990. Predator-caging experiments in marine systems - A reexamination of their value. American Naturalist **136**:657-672.

Hansen, K., and E. Kristensen. 1997. Impact of macrofaunal recolonization on benthic metabolism and nutrient fluxes in a shallow marine sediment previously overgrown with macroalgal mats. Estuarine Coastal and Shelf Science **45**:613-628.

Hansen, L. S., and T. H. Blackburn. 1991. Aerobic and anaerobic mineralization of organic material in marine sediment microcosms. Marine Ecology Progress Series **75**:283-291.

Hart, T. J. 1930. Preliminary notes on the bionomics of the amphipod *Corophium volutator* Pallas. Journal of the Marine Biological Association of the United Kingdom **16**:761-789.

Hartmann, V. A. 2011. The use of computer tomography to measure biogenic structures in recently hypoxic and normoxic sediments on the Louisiana continental shelf. University of Southern Mississippi.

Hector, A., B. Schmid, C. Beierkuhnlein, M. C. Caldeira, M. Diemer, P. G. Dimitrakopoulos, J. A. Finn, H. Freitas, P. S. Giller, J. Good, R. Harris, P. Hogberg, K. Huss-Danell, J. Joshi, A. Jumpponen, C. Korner, P. W. Leadley, M. Loreau, A. Minns, C. P. H. Mulder, G. O'Donovan, S. J. Otway, J. S. Pereira, A. Prinz, D. J. Read, M. Scherer-Lorenzen, E. D. Schulze, A. S. D. Siamantziouras, E. M. Spehn, A. C. Terry, A. Y. Troumbis, F. I. Woodward, S. Yachi, and J. H. Lawton. 1999. Plant diversity and productivity experiments in European grasslands. Science **286**:1123-1127.

Heilskov, A. C., and M. Holmer. 2001. Effects of benthic fauna on organic matter mineralization in fish-farm sediments: importance of size and abundance. Ices Journal of Marine Science **58**:427-434.

Heinz Walz GmbH. 1998. Underwater Fluorometer Diving-PAM. Walz, Effeltrich, Germany.

Hoagland, K. D., J. R. Rosowski, M. R. Gretz, and S. C. Roemer. 1993. Diatom extracellular polymeric substances - Function, fine-structure, chemistry, and physiology. Journal of Phycology **29**:537-566.

Honeywill, C., D. N. Paterson, and S. E. Hagerthey. 2002. Determination of microphytobenthic biomass using pulse-amplitude modulated minimum fluorescence. European Journal of Phycology **37**:485-492.

Hsieh, H. L., and C. F. Hsu. 1999. Differential recruitment of annelids onto tidal elevations in an estuarine mud flat. Marine Ecology Progress Series **177**:93-102.

Hughes, R. G. 1988. Dispersal by benthic invertebrates - the i*n situ* Swimming behavior of the amphipod *Corophium Volutator*. Journal of the Marine Biological Association of the United Kingdom **68**:565-579.

Hughes, R. G., and O. A. L. Paramor. 2004. On the loss of saltmarshes in south-east England and methods for their restoration. Journal of Applied Ecology **41**:440-448.

Ieno, E. N., M. Solan, P. Batty, and G. J. Pierce. 2006. How biodiversity affects ecosystem functioning: Roles of infaunal species richness, identity and density in the marine benthos. Marine Ecology Progress Series **311**:263-271.

Jensen, K. T., and C. Andre. 1993. Field and laboratory experiments on interactions among an infaunal polychaete, *Nereis diversicolor*, and 2 amphipods, *Corophium volutator* and *C.arenarium* - Effects on survival, recruitment and migration. Journal of Experimental Marine Biology and Ecology **168**:259-278.

Jesus, B., V. Brotas, M. Marani, and D. M. Paterson. 2005. Spatial dynamics of microphytobenthos determined by PAM fluorescence. Estuarine Coastal and Shelf Science **65**:30-42.

Jesus, B., R. G. Perkins, C. R. Mendes, V. Brotas, and D. M. Paterson. 2006. Chlorophyll fluorescence as a proxy for microphytobenthic biomass: alternatives to the current methodology. Marine Biology **150**:17-28.

Joint Nature Conservation Committee. 2001. SPA description Breydon Water. http://jncc.defra.gov.uk/page-2015.

Joint Nature Conservation Committee. 2004. Designated and proposed Ramsar sites in England. http://jncc.defra.gov.uk/page-1390.

Jones, S. E., and C. F. Jago. 1993. *In situ* assessment of modification of sediment properties by burrowing invertebrates. Marine Biology **115**:133-142.

Joschko, M., O. Graff, P. C. Muller, K. Kotzke, P. Lindner, D. P. Pretschner, and O. Larink. 1991. A nondestructive method for the morphological assessment of earthworm burrow systems in 3 dimensions by X-ray computed-tomography. Biology and Fertility of Soils **11**:88-92.

Kelaher, B. P., J. S. Levinton, and J. M. Hoch. 2003. Foraging by the mud snail, *Ilyanassa obsoleta* (Say), modulates spatial variation in benthic community structure. Journal of Experimental Marine Biology and Ecology **292**:139-157.

Kern, J. C. 1990. Active and passive aspects of meiobenthic copepod dispersal at 2 sites near Mustang Island, Texas. Marine Ecology Progress Series **60**:211-223.

Kirby, R. R., G. Beaugrand, J. A. Lindley, A. J. Richardson, M. Edwards, and P. C. Reid. 2007. Climate effects and benthic-pelagic coupling in the North Sea. Marine Ecology Progress Series **330**:31-38.

Kirwan, M. L., G. R. Guntenspergen, A. D'Alpaos, J. T. Morris, S. M. Mudd, and S. Temmerman. 2010. Limits on the adaptability of coastal marshes to rising sea level. Geophysical Research Letters **37**.

Kline, E. R., and M. S. Stekoll. 2001. Colonization of mine tailings by marine invertebrates. Marine Environmental Research **51**:301-325.

Kling, G. W., G. W. Kipphut, M. M. Miller, and W. J. O'Brien. 2000. Integration of lakes and streams in a landscape perspective: The importance of material processing on spatial patterns and temporal coherence. Freshwater Biology **43**:477-497.

Krumbein, W. C., and F. J. Pettijohn. 1938. Manual of Sedimentary petrography. Appleton Century Crofts, Inc., New York, USA.

Lawton, J. 1994. What do species do in ecosystems? Oikos **71**:367-374.

Lee, S. Y. 1999. The effect of mangrove leaf litter enrichment on macrobenthic colonization of defaunated sandy substrates. Estuarine Coastal and Shelf Science **49**:703-712.

Lee, Y. H., and C. H. Koh. 1994. Biogenic sedimentary structures on a Korean mud flat - Spring-neap variations. Netherlands Journal of Sea Research **32**:81-90.

Levin, L. A. 1984. Life-history and dispersal patterns in a dense infaunal polychaete assemblage - Community structure and response to disturbance. Ecology **65**:1185-1200.

Levin, S. A. 1992. The problem of pattern and scale in ecology. Ecology **73**:1943-1967.

Levinton, J. S. 1979. Effect of density upon deposit-feeding populations - Movement, feeding and floating of *Hydrobia ventrosa* Montagu (Gastropoda, Prosobranchia). Oecologia **43**:27-39.

Levinton, J. S. 1985. Complex interactions of a deposit feeder with its resources - Roles of density, a competitor, and detrital addition in the growth and survival of the mudsnail *Hydrobia totteni*. Marine Ecology Progress Series **22**:31-40.

Lindqvist, S., F. Gilbert, S. Eriksson, and S. Hulth. 2013. Activities by *Hediste diversicolor* under different light regimes: Experimental quantification of particle reworking using time-resolved imaging. Journal of Experimental Marine Biology and Ecology **448**:240-249.

Linke, O. 1939. Die biota des jadebusenwattes. Pages 201-348 Helgolander Wissenschaftliche Meeresuntersuchungen I.

Liquete, C., G. Zulian, I. Delgado, A. Stips, and J. Maes. 2013. Assessment of coastal protection as an ecosystem service in Europe. Ecological Indicators **30**:205-217.

Little, C., and W. Nix. 1976. Burrowing and floating behavior of Gastropod *Hydrobia ulvae*. Estuarine and Coastal Marine Science **4**:537-544.

Loo, L. O., and R. Rosenberg. 1989. Bivalve suspension-feeding dynamics and benthic pelagic coupling in an eutrophicated marine bay. Journal of Experimental Marine Biology and Ecology **130**:253-276.

Lopezfigueroa, F., and F. X. Niell. 1987. Feeding-behavior of *Hydrobia ulvae* (Pennant) in microcosms. Journal of Experimental Marine Biology and Ecology **114**:153-167.

Loreau, M. 1998. Separating sampling and other effects in biodiversity experiments. Oikos **82**:600-602.

Lu, L., and R. S. S. Wu. 2000. An experimental study on recolonization and succession of marine macrobenthos in defaunated sediment. Marine Biology **136**:291-302.

Lucas, C. H., J. Widdows, and L. Wall. 2003. Relating spatial and temporal variability in sediment chlorophyll *a* and carbohydrate distribution with erodibility of a tidal flat. Estuaries **26**:885-893.

Luckenbach, M. W. 1986. Sediment stability around animal tubes - The roles of hydrodynamic processes and biotic activity. Limnology and Oceanography **31**:779-787.

Lyons, K. G., and M. W. Schwartz. 2001. Rare species loss alters ecosystem function - invasion resistance. Ecology Letters **4**:358-365.

Macarthur, R. 1955. Fluctuations of animal populations, and a measure of community stability. Ecology **36**:533-536.

MacIntyre, H. L., R. J. Geider, and D. C. Miller. 1996. Microphytobenthos: The ecological role of the "Secret Garden" of unvegetated, shallow-water marine habitats. I. Distribution, abundance and primary production. Estuaries **19**:186-201.

Madsen, K. N., P. Nilsson, and K. Sundback. 1993. The influence of benthic microalgae on the stability of a subtidal shallow water sediment. Journal of Experimental Marine Biology and Ecology **170**:159-177.

Maestre, F. T., A. P. Castillo-Monroy, M. A. Bowker, and R. Ochoa-Hueso. 2012. Species richness effects on ecosystem multifunctionality depend on evenness, composition and spatial pattern. Journal of Ecology **100**:317-330.

Mahaut, M. L., and G. Graf. 1987. A luminophore tracer technique for bioturbation studies. Oceanologica Acta **10**:323-328.

Marcus, N. H., and F. Boero. 1998. Minireview: The importance of benthic-pelagic coupling and the forgotten role of life cycles in coastal aquatic systems. Limnology and Oceanography **43**:763-768.

Mason, C. 2011. NMBAQC's best practice guidance. Particle size analysis (PSA) for supporting biological analysis. Page 72 *in* N. M. B. A. C. Committee, editor.

Maxwell, K., and G. N. Johnson. 2000. Chlorophyll fluorescence - a practical guide. Journal of Experimental Botany **51**:659-668.

Mccormick, P. V., and R. J. Stevenson. 1991. Grazer control of nutrient availability in the periphyton. Oecologia **86**:287-291.

McKinney, M. L. 1997. Extinction vulnerability and selectivity: Combining ecological and paleontological views. Annual Review of Ecology and Systematics **28**:495-516.

Mcquaid, C. D., and P. W. Froneman. 1993. Mutualism between the territorial intertidal limpet *Patella longicosta* and the crustose alga *Ralfsia verrucosa*. Oecologia **96**:128-133.

Meadows, P. S. 1964. Experiments on substrate selection by *Corophium volutator* (Pallas) - Depth selection and population density. Journal of Experimental Biology **41**:677-&.

Meadows, P. S., and A. Reid. 1966. Behaviour of *Corophium volutator* (Crustacea - Amphipoda). Journal of Zoology **150**:387-399.

Meadows, P. S., and J. Tait. 1989. Modification of sediment permeability and shear-strength by 2 burrowing invertebrates. Marine Biology **101**:75-82.

Mehta, A. J., E. J. Hayter, W. R. Parker, R. B. Krone, and A. M. Teeter. 1989. Cohesive sediment transport .1. Process description. Journal of Hydraulic Engineering-Asce **115**:1076-1093.

Menge, B. A. 1995. Indirect effects in marine rocky intertidal interaction webs - Patterns and importance. Ecological Monographs **65**:21-74.

Mermillod-Blondin, F., S. Marie, G. Desrosiers, B. Long, L. de Montety, E. Michaud, and G. Stora. 2003. Assessment of the spatial variability of intertidal benthic communities by axial tomodensitometry: importance of fine-scale heterogeneity. Journal of Experimental Marine Biology and Ecology **287**:193-208.

Michaud, E., G. Desrosiers, B. Long, L. de Montety, J. F. Cremer, E. Pelletier, J. Locat, F. Gilbert, and G. Stora. 2003. Use of axial tomography to follow temporal changes of benthic communities in an unstable sedimentary environment (Baie des Ha! Ha!, Saguenay Fjord). Journal of Experimental Marine Biology and Ecology **285**:265-282.

Mieszkowska, N., M. A. Kendall, S. J. Hawkins, R. Leaper, P. Williamson, N. J. Hardman-Mountford, and A. J. Southward. 2006. Changes in the range of some common rocky shore species in Britain - a response to climate change? Hydrobiologia **555**:241-251.

Mills, L. S., M. E. Soule, and D. F. Doak. 1993. The keystone-species concept in ecology and conservation. Bioscience **43**:219-224.

Mimura, M. 1993. Rates of erosion and deposition of cohesive sediments under wave action.*in* A. J. Mehta, editor. Nearshore and Estuarine Cohesive Sediment Transport. American Geophysical Union, Washington, DC, USA.

Miron, G., G. Desrosiers, C. Retiere, and S. Masson. 1992. Variations in time budget of the polychaete Nereis virens as a function of density and acclimation after introduction to a new burrow. Marine Biology **114**:41-48.

Montague, C. L. 1986. Influence of biota on erodibility of sediments.*in* A. J. Mehta, editor. Estuarine Cohesive Sediment Dynamics. Springer, Berlin, Germnay.

Montserrat, F., C. Van Colen, S. Degraer, T. Ysebaert, and P. M. J. Herman. 2008. Benthic community-mediated sediment dynamics. Marine Ecology Progress Series **372**:43-59.

Morrisey, D. J. 1988. Differences in effects of grazing by deposit-feeders *Hydrobia ulvae* (Pennant) (Gastropoda, Prosobranchia) and *Corophium arenarium* Crawford (Amphipoda) on sediment microalgal populations .1. Qualitative differences. Journal of Experimental Marine Biology and Ecology **118**:33-42.

Mouillot, D., D. R. Bellwood, C. Baraloto, J. Chave, R. Galzin, M. Harmelin-Vivien, M. Kulbicki, S. Lavergne, S. Lavorel, N. Mouquet, C. E. T. Paine, J. Renaud, and W. Thuiller. 2013. Rare species support vulnerable functions in high-diversity ecosystems. Plos Biology **11**.

Mouritsen, K. N., L. T. Mouritsen, and K. T. Jensen. 1998. Change of topography and sediment characteristics on an intertidal mud-flat following mass-mortality of the amphipod *Corophium volutator*. Journal of the Marine Biological Association of the United Kingdom **78**:1167-1180.

Muller, O. F. 1776. Zoologica danicae prodromus seu animalium daniae et Norvegiae indigenarum characters, nomine, et synonyma imprimis popularium. Havniae. XXXII.

Murphy, R. J., and T. J. Tolhurst. 2009. Effects of experimental manipulation of algae and fauna on the properties of intertidal soft sediments. Journal of Experimental Marine Biology and Ecology **379**:77-84.

Murphy, R. J., A. J. Underwood, T. J. Tolhurst, and M. G. Chapman. 2008. Field-based remote-sensing for experimental intertidal ecology: Case studies using hyperspatial and hyperspectral data for New South Wales (Australia). Remote Sensing of Environment **112**:3353-3365.

Muschenheim, D. K., and C. R. Newell. 1992. Utilization of seston flux over a mussel bed. Marine Ecology Progress Series **85**:131-136.

Mwamba, M. J., and R. Torres. 2002. Rainfall effects on marsh sediment redistribution, North Inlet, South Carolina, USA. Marine Geology **189**:267-287.

Naeem, S. 1998. Species redundancy and ecosystem reliability. Conservation Biology **12**:39-45.

Naeem, S. 2006. Expanding scales in biodiversity-based reseach : Challenges and solutions for marine systems. Marine Ecology Progress Series **311**:273-283.

Naeem, S., K. Hakansson, J. H. Lawton, M. J. Crawley, and L. J. Thompson. 1996. Biodiversity and plant productivity in a model assemblage of plant species. Oikos **76**:259-264.

Naeem, S., M. Loreau, and P. Inchausti. 2002. Biodiversity and ecosystem functioning: the emergence of a synthetic ecological framework. Page 308 *in* M. Loreau, S. Naeem, and P. Inchausti, editors. Biodiversity and Ecosystem Functioning: Synthesis and Perspectives. Oxford University Press, Oxford.

Naeem, S., L. J. Thompson, S. P. Lawler, J. H. Lawton, and R. M. Woodfin. 1995. Empirical-evidence that declining species-diversity may alter the performance of terrestrial ecosystems. Philosophical Transactions of the Royal Society of London Series B-Biological Sciences **347**:249-262.

Natural England. 2013. SSSI units for Breydon Water. Natural England, http://www.sssi.naturalengland.org.uk/Special/sssi/unitlist.cfm?sssi_id=1000454.

Nature Editorial. 2012. Social dimensions to biodiversity. Nature **488**:E9-E9.

Neumeier, U., C. H. Lucas, and M. Collins. 2006. Erodibility and erosion patterns of mudflat sediments investigated using an annular flume. Aquatic Ecology **40**:543-554.

Newell, R. 1961. Behavioural aspects of the ecology of *Peringia* (=*Hydrobia*) *ulvae* (Pennant) (Gasteropoda, Prosobranchia). Proceedings of the Zoological Society of London **138**:49-74.

Newell, R. 1962. Behavioural aspects of the ecology of *Peringia* (=*Hydrobia*) *ulvae* (Pennant) (Gastropoda, Prosobranchia). Proceedings of the Zoological Society of London **138**:49-75.

Nilsson, H. C., and R. Rosenberg. 1997. Benthic habitat quality assessment of an oxygen stressed fjord by surface and sediment profile images. Journal of Marine Systems **11**:249-264.

Nixon, S. W., C. A. Oviatt, J. Frithsen, and B. Sullivan. 1986. Nutrients and the productivity of estuarine and coastal marine ecosystems. Journal of the Limnological Society of Southern Africa **12**:43-71.

Norkko, A., R. Rosenberg, S. F. Thrush, and R. B. Whitlatch. 2006. Scale- and intensity-dependent disturbance determines the magnitude of opportunistic response. Journal of Experimental Marine Biology and Ecology **330**:195-207.

Nowell, A. R. M., P. A. Jumars, and J. E. Eckman. 1981. Effects of biological-activity on the entrainment of marine-sediments. Marine Geology **42**:133-153.

Noyes, P. D., M. K. McElwee, H. D. Miller, B. W. Clark, L. A. Van Tiem, K. C. Walcott, K. N. Erwin, and E. D. Levin. 2009. The toxicology of climate change: Environmental contaminants in a warming world. Environment International **35**:971-986.

Nunes, P. A. L. D., H. Ding, B. Boteler, P. ten Brink, E. Cottee-Jones, M. Davis, A. Ghermandi, T. Kaphengst, M. Lago, A. J. McConville, N. S., M. Pieterse, M. Rayment, and A. Varma. 2011. The Social Dimension of Biodiversity Policy: Final Report for the European Commission, DG Environment under contract: ENV.G.1/FRA/2006/0073. Fondazione Eni Enrico Mattei, GHK Ecologic Institute, Institute for European Environmental Policy,, Venice/Brussels.

Olafsson, E., and C. G. Moore. 1990. Control of meiobenthic abundance by macroepifauna in a subtidal muddy habitat. Marine Ecology Progress Series **65**:241-249.

Olafsson, E., and C. G. Moore. 1992. Effects of macroepifauna on developing Nematode and Harpacticoid assemblages in a subtidal muddy habitat. Marine Ecology Progress Series **84**:161-171.

Olafsson, E. B., and L. E. Persson. 1986. The interaction between *Nereis diversicolor* Muller,O.F. And *Corophium volutator* Pallas as a structuring force in a shallow brackish sediment. Journal of Experimental Marine Biology and Ecology **103**:103-117.

Olivier, M., G. Desrosiers, A. Caron, C. Retière, and A. Caillou. 1995. Résponses comportementales des polychètes *Nereis diversicolor* (O.F. Müller) et *Nereis virens* (Sars) aux stimuli d'ordre alimentaire: utilisation de la matière organique particulaire (algues et halophytes). Canadian Journal of Zoology **73**:2307-2317.

Ordnance Survey. 2013. OS OpenData - driving growth and innovation. http://www.ordnancesurvey.co.uk/oswebsite/products/os-opendata.html.

Orvain, F., R. Galois, C. Barnard, A. Sylvestre, G. Blanchard, and P. G. Sauriau. 2003. Carbohydrate production in relation to microphytobenthic biofilm development: An integrated approach in a tidal mesocosm. Microbial Ecology **45**:237-251.

Orvain, F., and P. G. Sauriau. 2002. Environmental and behavioural factors affecting activity in the intertidal gastropod *Hydrobia ulvae*. Journal of Experimental Marine Biology and Ecology **272**:191-216.

Orvain, F., P. G. Sauriau, C. Bacher, and M. Prineau. 2006. The influence of sediment cohesiveness on bioturbation effects due to *Hydrobia ulvae* on the initial erosion of intertidal sediments: A study combining flume and model approaches. Journal of Sea Research **55**:54-73.

Orvain, F., P. G. Sauriau, A. Sygut, L. Joassard, and P. Le Hir. 2004. Interacting effects of *Hydrobia ulvae* bioturbation and microphytobenthos on the erodibility of mudflat sediments. Marine Ecology Progress Series **278**:205-223.

Pallas, P. S. 1766. Miscellanea Zoologica Quibus Novæ Imprimis Atque Obscuræ Animalium Species Describuntur et Observationibus Iconibusque Illustrantur. - pp. I-XIJ [= 1-12], 1-224, Tab. I-XIV [= 1-14]. Hagae Comitum. (Van Cleef).

Palomo, G., and O. Iribarne. 2000. Sediment bioturbation by polychaete feeding may promote sediment stability. Bulletin of Marine Science **67**:249-257.

Paramor, O. A. L., and R. G. Hughes. 2004. The effects of bioturbation and herbivory by the polychaete *Nereis diversicolor* on loss of saltmarsh in south-east England. Journal of Applied Ecology **41**:449-463.

Parmesan, C., N. Ryrholm, C. Stefanescu, J. K. Hill, C. D. Thomas, H. Descimon, B. Huntley, L. Kaila, J. Kullberg, T. Tammaru, W. J. Tennent, J. A. Thomas, and M. Warren. 1999. Poleward shifts in geographical ranges of butterfly species associated with regional warming. Nature **399**:579-583.

Passarelli, C., C. Hubas, A. N. Segui, J. Grange, and T. Meziane. 2012. Surface adhesion of microphytobenthic biofilms is enhanced under *Hediste diversicolor* (O.F. Muller) trophic pressure. Journal of Experimental Marine Biology and Ecology **438**:52-60.

Paterson, D. M. 1989. Short-term changes in the erodibility of intertidal cohesive sediments related to the migratory behavior of epipelic diatoms. Limnology and Oceanography **34**:223-234.

Paterson, D. M. 1997. Biological mediation of sediment erodibility: Ecological and physical dynamics.*in* A. J. Mehta, editor. Nearshore and Estuarine Cohesive Sediment Transport. American Geophysical Union, Washington, DC, USA.

Paterson, D. M., and K. S. Black. 1999. Water flow, sediment dynamics and benthic biology. Advances in Ecological Research, Vol 29 **29**:155-193.

Paterson, D. M., R. M. Crawford, and C. Little. 1990. Subaerial exposure and changes in the stability of intertidal estuarine sediments. Estuarine Coastal and Shelf Science **30**:541-556.

Paterson, D. M., T. J. Tolhurst, J. A. Kelly, C. Honeywill, E. M. G. T. de Deckere, V. Huet, S. A. Shayler, K. S. Black, J. de Brouwer, and I. Davidson. 2000. Variations in sediment

properties, Skeffling mudflat, Humber Estuary, UK. Continental Shelf Research **20**:1373-1396.

Pechenik, J. A., and T. R. Cerulli. 1991. Influence of delayed metamorphosis on survival, growth and reproduction of the marine polychate *Capitella* sp. I. Journal of Experimental Marine Biology and Ecology **151**:17-27.

Pelegri, S. P., L. P. Nielsen, and T. H. Blackburn. 1994. Denitrification in estuarine sediment stimulated by the irrigation activity of the Amphipod *Corophium volutator*. Marine Ecology Progress Series **105**:285-290.

Pennant, T. 1777. British Zoology Volume IV. Crustacea, Mollusca, Testacea. B. White, London.

Perez, K. T., E. W. Davey, R. H. Moore, P. R. Burn, M. S. Rosol, J. A. Cardin, R. L. Johnson, and D. N. Kopans. 1999. Application of computer-aided tomography (CT) to the study of estuarine benthic communities. Ecological Appilcations **9**:1050-1058.

Perkins, R. G., C. Honeywill, M. Consalvey, H. A. Austin, T. J. Tolhurst, and D. M. Paterson. 2003. Changes in microphytobenthic chlorophyll *a* and EPS resulting from sediment compaction due to de-watering: opposing patterns in concentration and content. Continental Shelf Research **23**:575-586.

Perrings, C., K.-G. Maler, C. Folke, C. S. Holling, and B.-O. Jansson. 1995. Biodiversity Loss: Economic and Ecological Issues. Cambridge University Press, Cambridge, UK.

Petchey, O. L. 2003. Integrating methods that investigate how complementarity influences ecosystem functioning. Oikos **101**:323-330.

Petchey, O. L., and K. J. Gaston. 2002. Extinction and the loss of functional diversity. Proceedings of the Royal Society B-Biological Sciences **269**:1721-1727.

Petchey, O. L., P. T. McPhearson, T. M. Casey, and P. J. Morin. 1999. Environmental warming alters food-web structure and ecosystem function. Nature **402**:69-72.

Petersen, J. E., V. S. Kennedy, W. C. Dennison, and W. M. Kemp. 2009. Enclosed Experimental Ecosystems and Scale Tools for Understanging and Managing Coastal ecosystems. Springer, New York, US.

Pilditch, C. A., J. Widdows, N. J. Kuhn, N. D. Pope, and M. D. Brinsley. 2008. Effects of low tide rainfall on the erodibility of intertidal cohesive sediments. Continental Shelf Research **28**:1854-1865.

Pimm, S. L., H. L. Jones, and J. Diamond. 1988. On the risk of extinction. American Naturalist **132**:757-785.

Pinheiro, J., D. Bates, S. DebRoy, D. Sarkar, and R Development Core Team. 2013. nlme: Linear and nonlinear mixed effects models. R package version 3.1-108.

Pinheiro, J. C., and D. M. Bates. 2000. Mixed-effects Models in S and S-plus. Springer, New York, NY, United States of America.

Plaganyi, E. E., and G. M. Branch. 2000. Does the limpet *Patella cochlear* fertilize its own algal garden? Marine Ecology Progress Series **194**:113-122.

Polley, H. W., B. J. Wilsey, and J. D. Derner. 2003. Do species evenness and plant density influence the magnitude of selection and complementarity effects in annual plant species mixtures? Ecology Letters **6**:248-256.

Porra, R. J., W. A. Thompson, and P. E. Kriedemann. 1989. Determination of accurate extinction coefficients and simultaneous-equations for assaying chlorophyll-*a* and chlorophyll-*b* extracted with 4 different solvents - Verification of the concentration of chlorophyll standards by atomic-absorption spectroscopy. Biochimica Et Biophysica Acta **975**:384-394.

Portner, H. O. 2008. Ecosystem effects of ocean acidification in times of ocean warming: a physiologist's view. Marine Ecology Progress Series **373**:203-217.

Posey, M. H., B. R. Dumbauld, and D. A. Armstrong. 1991. Effects of a burrowing mud shrimp, *Upogebia pugettensis* (Dana), on abundances of macro-infauna. Journal of Experimental Marine Biology and Ecology **148**:283-294.

Raffaelli, D., E. Bell, G. Weithoff, A. Matsumoto, J. J. Cruz-Motta, P. Kershaw, R. Parker, D. Parry, and M. Jones. 2003a. The ups and downs of benthic ecology: considerations of scale,

heterogeneity and surveillance for benthic-pelagic coupling. Journal of Experimental Marine Biology and Ecology **285**:191-203.

Raffaelli, D., A. Conacher, H. Mclachlan, and C. Emes. 1989. The role of epibenthic crustacean predators in an estuarine food web. Estuarine Coastal and Shelf Science **28**:149-160.

Raffaelli, D., M. Emmerson, M. Solan, C. Biles, and D. Paterson. 2003b. Biodiversity and ecosystem processes in shallow coastal waters: an experimental approach. Journal of Sea Research **49**:133-141.

Reaka-Kudla, M. L., D. E. Wilson, and E. O. Wilson. 1997. Biodiversity II: Understanding and Protecting our Biological Resources. Joseph Henry Press, Washington, D.C., USA.

Reise, K. 1978. Experiments on epibenthic predation in the Wadden Sea. Helgolander Wissenschaftliche Meeresuntersuchungen **31**:55-101.

Reise, K. 1983. Experimental removal of lugworms from marine sand affects small zoobenthos. Marine Biology **74**:327-332.

Reise, K. 1985. Tidal Flat Ecology. An Experimental Approach to Species Interactions. Springer-Verlag, Berlin.

Reise, K. 1992. Grazing on sediment shores. Pages 133-145 *in* D. M. John, S. J. Hawkins, and J. H. Price, editors. Plant-animal interactions in the marine benthos. Clarendon Press, Oxford, UK.

Rhoads, D. C., and S. Cande. 1971. Sediment profile camera for *in-situ* study of organism-sediment relations. Limnology and Oceanography **16**:110-&.

Rhoads, D. C., P. L. Mccall, and J. Y. Yingst. 1978a. Disturbance and production on estuarine seafloor. American Scientist **66**:577-586.

Rhoads, D. C., J. Y. Yingst, and W. J. Ulman. 1978b. Seafloor stability in Central Long Island Sound: Part I. Temporal changes in erodibility of fine grained sediments.*in* M. L. Wiley, editor. Estuarine Interactions. Academic Press, New Yrok, USA.

Rhoads, D. C., and D. K. Young. 1970. Influence of deposit-feeding organisms on sediment stability and community trophic structure. Journal of Marine Research **28**:150-&.

Riethmuller, R., M. Heineke, H. Kuhl, and R. Keuker-Rudiger. 2000. Chlorophyll alpha concentration as an index of sediment surface stabilisation by microphytobenthos? Continental Shelf Research **20**:1351-1372.

Riisgard, H. U. 1991. Suspension feeding in the polychaete *Nereis diversicolor*. Marine Ecology Progress Series **70**:29-37.

Riisgard, H. U. 2007. Biomechanics and energy cost of the amphipod *Corophium volutator* filter-pump. Biological Bulletin **212**:104-114.

Riisgard, H. U., and P. Schotge. 2007. Surface deposit feeding versus filter feeding in the amphipod *Corophium volutator*. Marine Biology Research **3**:421-427.

Ronn, C., E. Bonsdorff, and W. G. Nelson. 1988. Predation as a mechanism of interference within infauna in shallow brackish water soft bottoms - Experiments with an infauna predator, *Nereis diversicolor* Muller,O.F. Journal of Experimental Marine Biology and Ecology **116**:143-157.

Rosenberg, R., E. Davey, J. Gunnarsson, K. Norling, and M. Frank. 2007. Application of computer-aided tomography to visualize and quantify biogenic structures in marine sediments. Marine Ecology Progress Series **331**:23-34.

Rosenberg, R., A. Gremare, J. C. Duchene, E. Davey, and M. Frank. 2008. Visualization and quantification of marine benthic biogenic structures and particle transport utilizing computer-aided tomography. Marine Ecology Progress Series **363**:171-182.

Roscher, C., V. M. Temperton, M. Scherer-Lorenzen, M. Schmitz, J. Schumacher, B. Schmid, N. Buchmann, W. W. Weisser, and E.-D. Schulze. 2005. Overyielding in experimental grassland communities – irrespective of species pool or spatial scale. Ecology Letters **8**:419-429.

Rowden, A. A., and M. B. Jones. 1994. Contribution to the biology of the burrowing mud shrimp, *Callianassa subterranea* (Decapoda, Thalassinidea). Journal of the Marine Biological Association of the United Kingdom **74**:623-635.

Rowden, A. A., and M. B. Jones. 1995. The burrow structure of the mud shrimp *Callianassa subterranea* (Decapoda, Thalassinidea) from the North Sea. Journal of Natural History **29**:1155-1165.

Rowe, G. T. 1974. The effects of the benthic fauna on the physical properties of deep-sea sediments. Pages 381-400 *in* A. L. Inderbitzen, editor. Deep-Sea Sediments: Physical and Mechanical Properties. Springer, New York, US.

Royal Society for the Protection of Birds. 2013. Berney Marshes and Breydon Water. http://www.rspb.org.uk/reserves/guide/b/berneybreydon/index.aspx.

Ruddy, G., C. M. Turley, and T. E. R. Jones. 1998. Ecological interaction and sediment transport on an intertidal mudflat I. Evidence for a biologically mediated sediment-water interface. Pages 135-148 *in* K. S. Black, D. M. Paterson, and A. Cramp, editors. Sedimentary Processes in the Intertidal Zone. Geological Society, London.

Ruth, B. F., D. A. Flemer, and C. M. Bundrick. 1994. Recolonization of estuarine sediments by macroinvertebrates - Does microcosm size matter. Estuaries **17**:606-613.

Sabri, A. 1977. Phosphate Flux in Breydon Water Estuary. University of East Anglia, Norwich.

Sala, E., and N. Knowlton. 2006. Global marine biodiversity trends. Annual Review of Environment and Resources **31**:93-122.

Sandnes, J., T. Forbes, R. Hansen, and B. Sandnes. 2000. Influence of particle type and faunal activity on mixing of di(2-ethylhexyl)phthalate (DEHP) in natural sediments. Marine Ecology Progress Series **197**:151-167.

Saunders, J., K. Dyson, and D. Paterson. 2005. The influence of the lugworm *Arenicola marina* on biodiversity and ecosystem functioning in an intertidal mudflat. MarBEF Newsletter **3**:17.

Sauriau, P. G., V. Mouret, and J. P. Rince. 1989. Trophic system of wild soft-bottom mollusks in the Marennes-Oleron oyster-farming bay. Oceanologica Acta **12**:193-204.

Savidge, W. B., and G. L. Taghon. 1988. Passive and active components of colonization following 2 types of disturbance on intertidal sandflat. Journal of Experimental Marine Biology and Ecology **115**:137-155.

Schaffner, L. C., R. M. Dickhut, S. Mitra, P. W. Lay, and C. BrouwerRiel. 1997. Effects of physical chemistry and bioturbation by estuarine macrofauna on the transport of hydrophobic organic contaminants in the benthos. Environmental Science & Technology **31**:3120-3125.

Schiffers, K., L. R. Teal, J. M. J. Travis, and M. Solan. 2011. An open source simulation model for soil and sediment bioturbation. Plos One **6**:e28028.

Schindelin, J., I. Arganda-Carreras, E. Frise, V. Kaynig, M. Longair, T. Pietzsch, S. Preibisch, C. Rueden, S. Saalfeld, B. Schmid, J.-Y. Tinevez, D. J. White, V. Hartenstein, K. Eliceiri, P. Tomancak, and A. Cardona. 2012. Fiji: an open-source platform for biological-image analysis. Nature Methods **9**:676-682.

Schmid, B., A. Hector, P. Saha, and M. Loreau. 2008. Biodiversity effects and transgressive overyielding. Journal of Plant Ecology **1(2)**:95-102.

Schreiber, U., U. Schliwa, and W. Bilger. 1986. Continuous recording of photochemical and nonphotochemical chlorophyll fluorescence quenching with a new type of modulation fluorometer. Photosynthesis Research **10**:51-62.

Schunemann, M., and H. Kuhl. 1993. Experimental investigations of the erosional behavior of naturally formed mud from the Elbe Estuary and adjacent Wadden Sea, Germany. Nearshore and Estuarine Cohesive Sediment Transport **42**:314-330.

Schwartz, M. W., C. A. Brigham, J. D. Hoeksema, K. G. Lyons, M. H. Mills, and P. J. van Mantgem. 2000. Linking biodiversity to ecosystem function: implications for conservation ecology. Oecologia **122**:297-305.

Seilacher, A., and F. Pfluger. 1994. From biomats to benthic agriculture: a biohistoric revolution. Pages 97-105 *in* W. E. Krumbein, editor. Biostabilization of Sediments. Bibliotheks and Informationsystem del Carl von Ossietzky Universitat, Oldenburg.

Self, R. F. L., A. R. M. Nowell, and P. A. Jumars. 1989. Factors controlling critical shears for deposition and erosion of individual grains. Marine Geology **86**:181-199.

Service, S. K., and S. S. Bell. 1987. Density-influenced active dispersal of harpaticoid copepods. Journal of Experimental Marine Biology and Ecology **114**:49-62.

Sgro, L., M. Mistri, and J. Widdows. 2005. Impact of the infaunal Manila clam, *Ruditapes philippinarum*, on sediment stability. Hydrobiologia **550**:175-182.

Shi, Z., J. S. Pethick, F. Burd, and B. Murphy. 1996. Velocity profiles in a salt marsh canopy. Geo-Marine Letters **16**:319-323.

Skelly, D. K., and J. M. Kiesecker. 2001. Venue and outcome in ecological experiments: manipulations of larval anurans. Oikos **94**:198-208.

Smith, D., R. G. Hughes, and E. J. Cox. 1996. Predation of epipelic diatoms by the amphipod *Corophium volutator* and the polychaete *Nereis diversicolor*. Marine Ecology Progress Series **145**:53-61.

Snelgrove, P. V. R., J. Grant, and C. A. Pilditch. 1999. Habitat selection and adult-larvae interactions in settling larvae of soft-shell clam *Mya arenaria*. Marine Ecology Progress Series **182**:149-159.

Solan, M., P. Batty, M. T. Bulling, and J. A. Godbold. 2008. How biodiversity affects ecosystem processes: implications for ecological revolutions and benthic ecosystem function. Aquatic Biology **2**:289-301.

Solan, M., B. J. Cardinale, A. L. Downing, K. A. M. Engelhardt, J. L. Ruesink, and D. S. Srivastava. 2004a. Extinction and ecosystem function in the marine benthos. Science **306**:1177-1180.

Solan, M., D. G. Raffaelli, D. M. Paterson, P. C. L. White, and G. J. Pierce. 2006. Marine biodiversity and ecosystem function: Empirical approaches and future research needs. Marine Ecology Progress Series **311**.

Solan, M., B. D. Wigham, I. R. Hudson, R. Kennedy, C. H. Coulon, K. Norling, H. C. Nilsson, and R. Rosenberg. 2004b. *In situ* quantification of bioturbation using time-lapse fluorescent sediment profile imaging (f-SPI), luminophore tracers and model simulation. Marine Ecology Progress Series **27**:1-12.

Solomon, S., D. Qin, M. Manning, R. B. Alley, T. Berntsen, N. L. Bindoff, Z. Chen, A. Chidthaisong, J. M. Gregory, G. C. Hegerl, M. Heimann, B. Hewitson, B. J. Hoskins, F. Joos, J. Jouzel, V. Kattsov, U. Lohmann, T. Matsuno, M. Molina, N. Nicholls, J. Overpeck, G. Raga, V. Ramaswamy, J. Ren, M. Rusticucci, R. Somerville, T. F. Stocker, P. Whetton, R. A. Wood, and D. Wratt. 2007. Technical summary.*in* S. Solomon, D. Qin, M. Manning, Z. Chen, M. Marquis, K. B. Averyt, M. Tignor, and H. L. Miller, editors. Climate Change 2007: The Physical Science Basis. Contribution of Working Group I to the Fourth Assessment Report of the Intergovernmental Panel on Climate Change. Cambridge University Press, United Kingdom and New York, NY, USA.

Stal, L. J. 2003. Microphytobenthos, their extracellular polymeric substances, and the morphogenesis of intertidal sediments. Geomicrobiology Journal **20**:463-478.

Statzner, B., and P. Sagnes. 2008. Crayfish and fish as bioturbators of streambed sediments: Assessing joint effects of species with different mechanistic abilities. Geomorphology **93**:267-287.

Steneck, R. S., J. Vavrinec, and A. V. Leland. 2004. Accelerating trophic-level dysfunction in kelp forest ecosystems of the western North Atlantic. Ecosystems **7**:323-332.

Stewart, R. I. A., M. Dossena, D. A. Bohan, E. Jeppesen, R. L. Kordas, M. E. Ledger, M. Meerhoff, B. Moss, C. Mulder, J. B. Shurin, B. Suttle, R. Thompson, M. Trimmer, and G. Woodward. 2013. Mesocosm experiments as a tool for ecological climate-change research. Advances in Ecological Research: Global Change in Multispecies Systems, Pt 3 **48**:71-181.

Stimson, J. 1973. Role of territory in the ecology of the intertidal limpet *Lottia gigantea* (Gray). Ecology **54**:1020-1030.

Stocks, K. I., and J. F. Grassle. 2001. Effects of microalgae and food limitation on the recolonization of benthic macrofauna into *in situ* saltmarsh-pond mesocosms. Marine Ecology Progress Series **221**:93-104.

Stolzenbach, K. D. 1989. Particle transport and attachment.*in* W. H. Characklis and P. A. Wilderer, editors. Structure and Function of Biofilms. Wiley, New York, USA.

Stolzenbach, K. D., K. A. Newman, and C. S. Wong. 1992. Aggregation of fine particles at the sediment-water interface. Journal of Geophysical Research-Oceans **97**:17889-17898.

Sutherland, T. F., C. L. Amos, and J. Grant. 1998. The erosion threshold of biotic sediments: a comparison of methods. Pages 295-307 Special Publication. Geological Society, London.

Tamaki, A. 1988. Effects of the bioturbating activity of the ghost shrimp *Callianassa japonica* Ortmann on migration of a mobile polychaete. Journal of Experimental Marine Biology and Ecology **120**:81-95.

Taylor, I. S., and D. M. Paterson. 1998. Microspatial variation in carbohydrate concentrations with depth in the upper millimetres of intertidal cohesive sediments. Estuarine Coastal and Shelf Science **46**:359-370.

Teisson, C., M. Ockenden, P. Lehir, C. Kranenburg, and L. Hamm. 1993. Cohesive sediment transport processes. Coastal Engineering **21**:129-162.

The Wherryman's Way. 2013. Discover the Heart of the Broads. http://www.wherrymansway.net/.

Thomas, C. D., A. Cameron, R. E. Green, M. Bakkenes, L. J. Beaumont, Y. C. Collingham, B. F. N. Erasmus, M. F. de Siqueira, A. Grainger, L. Hannah, L. Hughes, B. Huntley, A. S. van Jaarsveld, G. F. Midgley, L. Miles, M. A. Ortega-Huerta, A. T. Peterson, O. L. Phillips, and S. E. Williams. 2004. Extinction risk from climate change. Nature **427**:145-148.

Thrush, S. F., R. D. Pridmore, J. E. Hewitt, and V. J. Cummings. 1992. Adult infauna as facilitators of colonization on intertidal sandflats. Journal of Experimental Marine Biology and Ecology **159**:253-265.

Thrush, S. F., and D. S. Roper. 1988. Merits of macrofaunal colonization of intertidal mudflats for pollution monitoring - Preliminary study. Journal of Experimental Marine Biology and Ecology **116**:219-233.

Thrush, S. F., R. B. Whitlatch, R. D. Pridmore, J. E. Hewitt, V. J. Cummings, and M. R. Wilkinson. 1996. Scale-dependent recolonization: The role of sediment stability in a dynamic sandflat habitat. Ecology **77**:2472-2487.

Tilman, D. 1999. The ecological consequences of changes in biodiversity: A search for general principles. Ecology **80**:1455-1474.

Tilman, D., and J. A. Downing. 1994. Biodiversity and stability in grasslands. Nature **367**:363-365.

Tilman, D., D. Wedin, and J. Knops. 1996. Productivity and sustainability influenced by biodiversity in grassland ecosystems. Nature **379**:718-720.

Tolhurst, J., E. C. Defew, R. G. Perkins, A. Sharples, and D. M. Paterson. 2006a. The effects of tidally-driven temporal variation on measuring intertidal cohesive sediment erosion threshold. Aquatic Ecology **40**:521-531.

Tolhurst, T. J., K. S. Black, and D. M. Paterson. 2009. Muddy sediment erosion: Insights from field studies. Journal of Hydraulic Engineering-Asce **135**:73-87.

Tolhurst, T. J., K. S. Black, D. M. Paterson, H. J. Mitchener, G. R. Termaat, and S. A. Shayler. 2000a. A comparison and measurement standardisation of four *in situ* devices for determining the erosion shear stress of intertidal sediments. Continental Shelf Research **20**:1397-1418.

Tolhurst, T. J., K. S. Black, S. A. Shayler, S. Mather, I. Black, K. Baker, and D. M. Paterson. 1999. Measuring the *in situ* erosion shear stress of intertidal sediments with the Cohesive Strength Meter (CSM). Estuarine Coastal and Shelf Science **49**:281-294.

Tolhurst, T. J., and M. G. Chapman. 2005. Spatial and temporal variation in the sediment properties of an intertidal mangrove forest: implications for sampling. Journal of Experimental Marine Biology and Ecology **317**:213-222.

Tolhurst, T. J., M. G. Chapman, A. J. Underwood, and J. J. Cruz. 2012. Technical Note: The effects of five different defaunation methods on biogeochemical properties of intertidal sediment. Biogeosciences **9**:3647-3661.

Tolhurst, T. J., M. Consalvey, and D. M. Paterson. 2008a. Changes in cohesive sediment properties associated with the growth of a diatom biofilm. Hydrobiologia **596**:225-239.

Tolhurst, T. J., E. C. Defew, J. F. C. de Brouwer, K. Wolfstein, L. J. Stal, and D. M. Paterson. 2006b. Small-scale temporal and spatial variability in the erosion threshold and properties of cohesive intertidal sediments. Continental Shelf Research **26**:351-362.

Tolhurst, T. J., P. L. Friend, C. Watts, R. Wakefield, K. S. Black, and D. M. Paterson. 2006c. The effects of rain on the erosion threshold of intertidal cohesive sediments. Aquatic Ecology **40**:533-541.

Tolhurst, T. J., G. Gust, and D. M. Paterson. 2002. The influence of an extracellular polymeric substance (EPS) on cohesive sediment stability. Fine Sediment Dynamics in the Marine Environment **5**:409-425.

Tolhurst, T. J., B. Jesus, V. Brotas, and D. M. Paterson. 2003. Diatom migration and sediment armouring - an example from the Tagus Estuary, Portugal. Hydrobiologia **503**:183-193.

Tolhurst, T. J., R. Riethmuller, and D. M. Paterson. 2000b. *In situ* versus laboratory analysis of sediment stability from intertidal mudflats. Continental Shelf Research **20**:1317-1334.

Tolhurst, T. J., A. J. Underwood, R. G. Perkins, and M. G. Chapman. 2005. Content versus concentration: Effects of units on measuring the biogeochemical properties of soft sediments. Estuarine Coastal and Shelf Science **63**:665-673.

Tolhurst, T. J., C. W. Watts, S. Vardy, J. E. Saunders, M. C. Consalvey, and D. M. Paterson. 2008b. The effects of simulated rain on the erosion threshold and biogeochemical properties of intertidal sediments. Continental Shelf Research **28**:1217-1230.

Torres, R., M. J. Mwamba, and M. A. Goni. 2003. Properties of intertidal marsh sediment mobilized by rainfall. Limnology and Oceanography **48**:1245-1253.

Tracy, C. R., and T. L. George. 1992. On the determinants of extinction. American Naturalist **139**:102-122.

Turner, S. J., J. Grant, R. D. Pridmore, J. E. Hewitt, M. R. Wilkinson, T. M. Hume, and D. J. Morrisey. 1997. Bedload and water-column transport and colonization processes by post-settlement benthic macrofauna: Does infaunal density matter? Journal of Experimental Marine Biology and Ecology **216**:51-75.

Turnhout, E., B. Bloomfield, M. Hulme, J. Vogel, and B. Wynne. 2012. Listen to the voices of experience. Nature **488**:454-455.

Underwood, G. J. C., and D. M. Paterson. 1993. Seasonal-changes in diatom biomass, sediment stability and biogenic stabilization in the Severn Estuary. Journal of the Marine Biological Association of the United Kingdom **73**:871-887.

Underwood, G. J. C., D. M. Paterson, and R. J. Parkes. 1995. The measurement of microbial carbohydrate exopolymers from intertidal sediments. Limnology and Oceanography **40**:1243-1253.

Van Colen, C., F. Montserrat, M. Vincx, P. M. J. Herman, T. Ysebaert, and S. Degraer. 2008. Macrobenthic recovery from hypoxia in an estuarine tidal mudflat. Marine Ecology Progress Series **372**:31-42.

Vardy, S., J. E. Saunders, T. J. Tolhurst, P. A. Davies, and D. M. Paterson. 2007. Calibration of the high-pressure cohesive strength meter (CSM). Continental Shelf Research **27**:1190-1199.

Verreet, G., J. V. Goethem, W. Viaene, J. Berlamonte, R. Holthuis, and E. Berleur. 1986. Relations between physicochemical and rheological properties of fine grained muds. Pages 1637-1646 *in* 3rd International Symposium on River Sedimentation, Mississippi, USA.

Verwey, J. 1952. On the ecology of distribution of cockle and mussel in the Dutch Waddenzee, their role in sedimentation, and source of their food supply, with a short review of the feeding behaviour of bivalve mollusks. Archives Neerlandaises de Zoologie **10**:172-239.

Virnstein, R. W. 1978. Predator Caging Experiments In Soft Sediments: Caution Advised. Pages 261-273 *in* M. L. Wiley, editor. Estuarine Interactions. Academic Press, New York.

Waide, R. B., M. R. Willig, C. F. Steiner, G. Mittelbach, L. Gough, S. I. Dodson, G. P. Juday, and R. Parmenter. 1999. The relationship between productivity and species richness. Annual Review of Ecology and Systematics **30**:257-300.

Walker, B. H. 1992. Biodiversity and ecological redundancy. Conservation Biology **6**:18-23.

Walther, G. R., E. Post, P. Convey, A. Menzel, C. Parmesan, T. J. C. Beebee, J. M. Fromentin, O. Hoegh-Guldberg, and F. Bairlein. 2002. Ecological responses to recent climate change. Nature **416**:389-395.

Wedin, D. A., and D. Tilman. 1996. Influence of nitrogen loading and species composition on the carbon balance of grasslands. Science **274**:1720-1723.

Wellington, S. L., and H. J. Vinegar. 1987. X-ray computerized tomography. Journal of Petroleum **39**:885-898.

West, B. T., K. B. Welch, and A. T. Galecki. 2006. Linear Mixed Model: A Practical Guide to Using Statistical Software. Chapman & Hall, London, United Kingdom.

Whitlach, R. B., and R. N. Zajac. 1985. Biotic interactions among estuarine infaunal opportunistic species. Marine Ecology Progress Series **21**:299-211.

Widdicombe, S., M. C. Austen, M. A. Kendall, F. Olsgard, M. T. Schaanning, S. L. Dashfield, and H. R. Needham. 2004. Importance of bioturbators for biodiversity maintenance: indirect effects of fishing disturbance. Marine Ecology Progress Series **275**:1-10.

Widdicombe, S., and H. R. Needham. 2007. Impact of CO_2-induced seawater acidification on the burrowing activity of *Nereis virens* and sediment nutrient flux. Marine Ecology Progress Series **341**:111-122.

Widdows, J., and M. Brinsley. 2002. Impact of biotic and abiotic processes on sediment dynamics and the consequences to the structure and functioning of the intertidal zone. Journal of Sea Research **48**:143-156.

Widdows, J., M. Brinsley, and M. Elliott. 1998a. Use of *in situ* flume to quantify particle flux (biodeposition rates and sediment erosion) for an intertidal mudflat in relation to changes in current velocity and benthic macrofauna.*in* K. S. Black, D. M. Paterson, and A. Cramp, editors. Sedimentary Processes in the Intertidal Zone. Geological Society, London.

Widdows, J., M. D. Brinsley, N. Bowley, and C. Barrett. 1998b. A benthic annular flume for *in situ* measurement of suspension feeding/biodeposition rates and erosion potential of intertidal cohesive sediments. Estuarine Coastal and Shelf Science **46**:27-38.

Widdows, J., M. D. Brinsley, and N. D. Pope. 2009. Effect of *Nereis diversicolor* density on the erodibility of estuarine sediment. Marine Ecology Progress Series **378**:135-143.

Widdows, J., M. D. Brinsley, P. N. Salkeld, and M. Elliott. 1998c. Use of annular flumes to determine the influence of current velocity and bivalves on material flux at the sediment-water interface. Estuaries **21**:552-559.

Widdows, J., M. D. Brinsley, P. N. Salkeld, and C. H. Lucas. 2000a. Influence of biota on spatial and temporal variation in sediment erodibility and material flux on a tidal flat (Westerschelde, The Netherlands). Marine Ecology Progress Series **194**:23-37.

Widdows, J., S. Brown, M. D. Brinsley, P. N. Salkeld, and M. Elliott. 2000b. Temporal changes in intertidal sediment erodibility: influence of biological and climatic factors. Continental Shelf Research **20**:1275-1289.

Widdows, J., J. S. Lucas, M. D. Brinsley, P. N. Salkeld, and F. J. Staff. 2002. Investigation of the effects of current velocity on mussel feeding and mussel bed stability using an annular flume. Helgoland Marine Research **56**:3-12.

Wilkinson A., M. Solan, A. F. S. Taylor, I. J. Alexander and D. Johnson. 2010. Intraspecific diversity regulates fungal productivity and respiration. PLoS ONE **5(9)**:e12604.

Williams, S. L., and R. C. Carpenter. 1988. Nitrogen-limited primary productivity of coral-reef algal turfs - Potential contribution of ammonium excreted by *Diadema antillarum*. Marine Ecology Progress Series **47**:145-152.

Wilsey, B. J., and H. W. Polley. 2004. Realistically low species evenness does not alter grassland species-richness-productivity relationships. Ecology **85**:2693-2700.

Wilsey, B. J., and C. Potvin. 2000. Biodiversity and ecosystem functioning: Importance of species evenness in an old field. Ecology **81**:887-892.

Wood, R., and J. Widdows. 2002. A model of sediment transport over an intertidal transect, comparing the influences of biological and physical factors. Limnology and Oceanography **47**:848-855.

Woodin, S. A. 1977. Algal gardening behavior by nereid polychaetes - Effects on soft-bottom community structure. Marine Biology **44**:39-42.

Worm, B., E. B. Barbier, N. Beaumont, J. E. Duffy, C. Folke, B. S. Halpern, J. B. C. Jackson, H. K. Lotze, F. Micheli, S. R. Palumbi, E. Sala, K. A. Selkoe, J. J. Stachowicz, and R. Watson. 2006. Impacts of biodiversity loss on ocean ecosystem services. Science **314**:787-790.

Wu, R. S. S., and P. K. S. Shinn. 1997. Sediment characteristics and colonization of soft bottom benthos - a field manipulation experiment. Marine Biology **128**:475-487.

Yachi, S., and M. Loreau. 1999. Biodiversity and ecosystem productivity in a fluctuating environment: The insurance hypothesis. Proceedings of the National Academy of Sciences of the United States of America **96**:1463-1468.

Yager, P. L., A. R. M. Nowell, and P. A. Jumars. 1993. Enhanced deposition to pits - a local food source for benthos. Journal of Marine Research **51**:209-236.

Yallop, M. L., D. M. Paterson, and P. Wellsbury. 2000. Interrelationships between rates of microbial production, exopolymer production, microbial biomass, and sediment stability in biofilms of intertidal sediments. Microbial Ecology **39**:116-127.

Zhou, H. 2001. Effects of leaf litter addition on meiofaunal colonization of azoic sediments in a subtropical mangrove in Hong Kong. Journal of Experimental Marine Biology and Ecology **256**:99-121.

Zuur, A. F., E. N. Ieno, and C. S. Elphick. 2009a. A protocol for data ecploration to avoid common statistical problems. Methods in Ecology and Evolution **1**:3-14.

Zuur, A. F., E. N. Ieno, and G. M. Smith. 2007. Analysing Ecological Data. Springer, New York, NY, United States of America.

Zuur, A. F., E. N. Ieno, N. J. Walker, A. A. Saveliev, and G. M. Smith. 2009b. Mixed Effects Models and Extensions in Ecology with R. Springer Science+Business Media, New York, NY, United States of America.